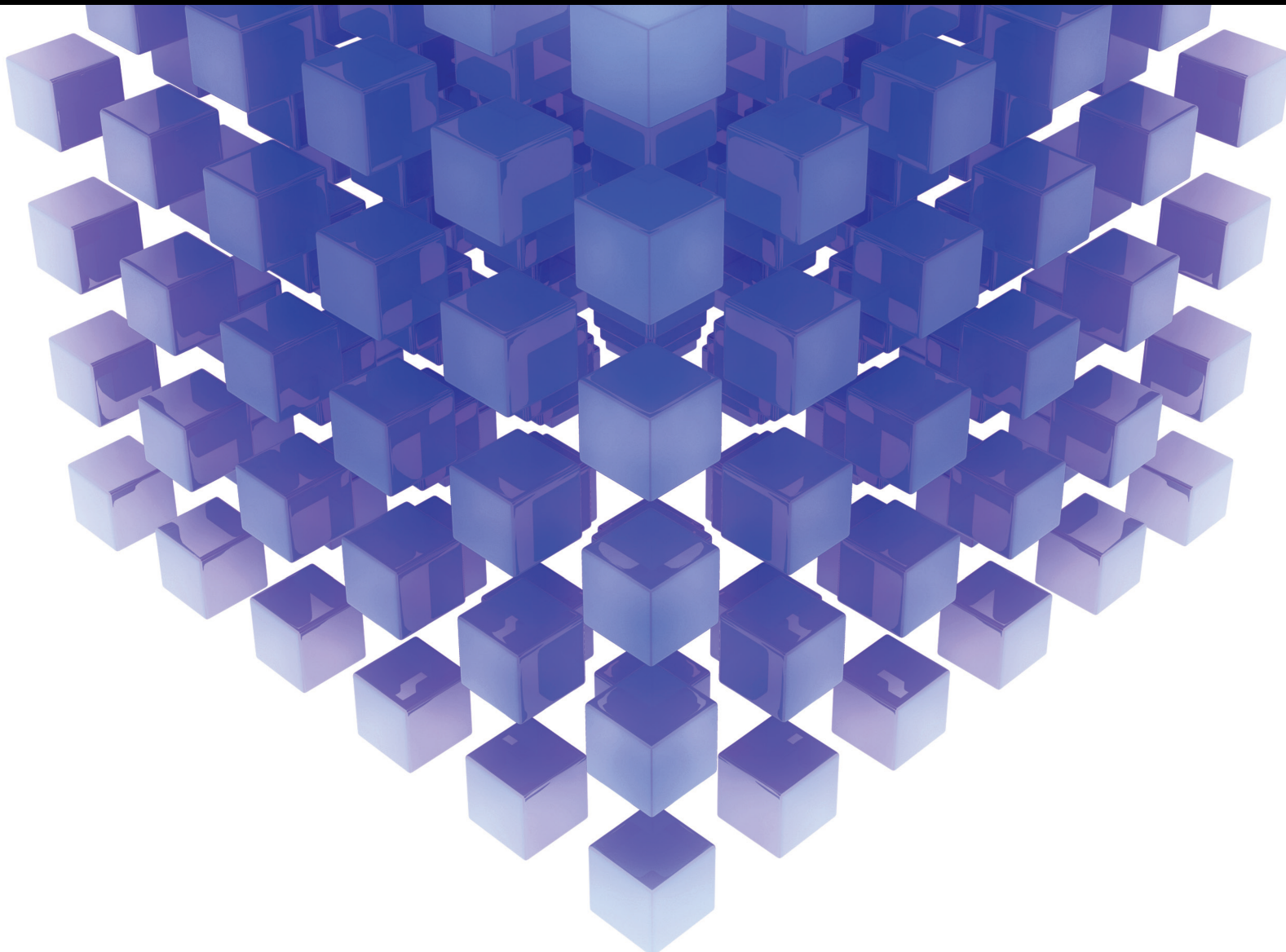


# Computational Intelligence and Fuzzy Modeling for Sustainable Decision-Making in Engineering Processes

Lead Guest Editor: Dragan Pamučar

Guest Editors: Dragan Z. Marinkovic and Muhammet Devenci





---

**Computational Intelligence and Fuzzy  
Modeling for Sustainable Decision-Making in  
Engineering Processes**

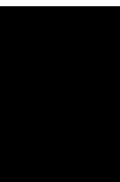
Mathematical Problems in Engineering

---

**Computational Intelligence and Fuzzy  
Modeling for Sustainable Decision-  
Making in Engineering Processes**

Lead Guest Editor: Dragan Pamučar

Guest Editors: Dragan Z. Marinkovic and  
Muhammet Deveci




---

Copyright © 2022 Hindawi Limited. All rights reserved.

This is a special issue published in “Mathematical Problems in Engineering.” All articles are open access articles distributed under the Creative Commons Attribution License, which permits unrestricted use, distribution, and reproduction in any medium, provided the original work is properly cited.

# Chief Editor

Guangming Xie , China

## Academic Editors

Kumaravel A , India  
Waqas Abbasi, Pakistan  
Mohamed Abd El Aziz , Egypt  
Mahmoud Abdel-Aty , Egypt  
Mohammed S. Abdo, Yemen  
Mohammad Yaghoub Abdollahzadeh  
Jamalabadi , Republic of Korea  
Rahib Abiyev , Turkey  
Leonardo Acho , Spain  
Daniela Addessi , Italy  
Arooj Adeel , Pakistan  
Waleed Adel , Egypt  
Ramesh Agarwal , USA  
Francesco Aggogeri , Italy  
Ricardo Aguilar-Lopez , Mexico  
Afaq Ahmad , Pakistan  
Naveed Ahmed , Pakistan  
Elias Aifantis , USA  
Akif Akgul , Turkey  
Tareq Al-shami , Yemen  
Guido Ala, Italy  
Andrea Alaimo , Italy  
Reza Alam, USA  
Osamah Albahri , Malaysia  
Nicholas Alexander , United Kingdom  
Salvatore Alfonzetti, Italy  
Ghous Ali , Pakistan  
Nouman Ali , Pakistan  
Mohammad D. Aliyu , Canada  
Juan A. Almendral , Spain  
A.K. Alomari, Jordan  
José Domingo Álvarez , Spain  
Cláudio Alves , Portugal  
Juan P. Amezcua-Sanchez, Mexico  
Mukherjee Amitava, India  
Lionel Amodeo, France  
Sebastian Anita, Romania  
Costanza Arico , Italy  
Sabri Arik, Turkey  
Fausto Arpino , Italy  
Rashad Asharabi , Saudi Arabia  
Farhad Aslani , Australia  
Mohsen Asle Zaem , USA

Andrea Avanzini , Italy  
Richard I. Avery , USA  
Viktor Avrutin , Germany  
Mohammed A. Awadallah , Malaysia  
Francesco Aymerich , Italy  
Sajad Azizi , Belgium  
Michele Bacciocchi , Italy  
Seungik Baek , USA  
Khaled Bahlali, France  
M.V.A Raju Bahubalendruni, India  
Pedro Balaguer , Spain  
P. Balasubramaniam, India  
Stefan Balint , Romania  
Ines Tejado Balsera , Spain  
Alfonso Banos , Spain  
Jerzy Baranowski , Poland  
Tudor Barbu , Romania  
Andrzej Bartoszewicz , Poland  
Sergio Baselga , Spain  
S. Caglar Baslamisli , Turkey  
David Bassir , France  
Chiara Bedon , Italy  
Azeddine Beghdadi, France  
Andriette Bekker , South Africa  
Francisco Beltran-Carbajal , Mexico  
Abdellatif Ben Makhlof , Saudi Arabia  
Denis Benasciutti , Italy  
Ivano Benedetti , Italy  
Rosa M. Benito , Spain  
Elena Benvenuti , Italy  
Giovanni Berselli, Italy  
Michele Betti , Italy  
Pietro Bia , Italy  
Carlo Bianca , France  
Simone Bianco , Italy  
Vincenzo Bianco, Italy  
Vittorio Bianco, Italy  
David Bigaud , France  
Sardar Muhammad Bilal , Pakistan  
Antonio Bilotta , Italy  
Sylvio R. Bistafa, Brazil  
Chiara Boccaletti , Italy  
Rodolfo Bontempo , Italy  
Alberto Borboni , Italy  
Marco Bortolini, Italy

Paolo Boscariol, Italy  
Daniela Boso , Italy  
Guillermo Botella-Juan, Spain  
Abdesselem Boulkroune , Algeria  
Boulaïd Boulkroune, Belgium  
Fabio Bovenga , Italy  
Francesco Braghin , Italy  
Ricardo Branco, Portugal  
Julien Bruchon , France  
Matteo Bruggi , Italy  
Michele Brun , Italy  
Maria Elena Bruni, Italy  
Maria Angela Butturi , Italy  
Bartłomiej Błachowski , Poland  
Dhanamjayulu C , India  
Raquel Caballero-Águila , Spain  
Filippo Cacace , Italy  
Salvatore Caddemi , Italy  
Zuowei Cai , China  
Roberto Caldelli , Italy  
Francesco Cannizzaro , Italy  
Maosen Cao , China  
Ana Carpio, Spain  
Rodrigo Carvajal , Chile  
Caterina Casavola, Italy  
Sara Casciati, Italy  
Federica Caselli , Italy  
Carmen Castillo , Spain  
Inmaculada T. Castro , Spain  
Miguel Castro , Portugal  
Giuseppe Catalanotti , United Kingdom  
Alberto Cavallo , Italy  
Gabriele Cazzulani , Italy  
Fatih Vehbi Celebi, Turkey  
Miguel Cerrolaza , Venezuela  
Gregory Chagnon , France  
Ching-Ter Chang , Taiwan  
Kuei-Lun Chang , Taiwan  
Qing Chang , USA  
Xiaoheng Chang , China  
Prasenjit Chatterjee , Lithuania  
Kacem Chehdi, France  
Peter N. Cheimets, USA  
Chih-Chiang Chen , Taiwan  
He Chen , China

Kebing Chen , China  
Mengxin Chen , China  
Shyi-Ming Chen , Taiwan  
Xizhong Chen , Ireland  
Xue-Bo Chen , China  
Zhiwen Chen , China  
Qiang Cheng, USA  
Zeyang Cheng, China  
Luca Chiapponi , Italy  
Francisco Chicano , Spain  
Tirivanhu Chinyoka , South Africa  
Adrian Chmielewski , Poland  
Seongim Choi , USA  
Gautam Choubey , India  
Hung-Yuan Chung , Taiwan  
Yusheng Ci, China  
Simone Cinquemani , Italy  
Roberto G. Citarella , Italy  
Joaquim Ciurana , Spain  
John D. Clayton , USA  
Piero Colajanni , Italy  
Giuseppina Colicchio, Italy  
Vassilios Constantoudis , Greece  
Enrico Conte, Italy  
Alessandro Contento , USA  
Mario Cools , Belgium  
Gino Cortellessa, Italy  
Carlo Cosentino , Italy  
Paolo Crippa , Italy  
Erik Cuevas , Mexico  
Guozeng Cui , China  
Mehmet Cunkas , Turkey  
Giuseppe D'Aniello , Italy  
Peter Dabnichki, Australia  
Weizhong Dai , USA  
Zhifeng Dai , China  
Purushothaman Damodaran , USA  
Sergey Dashkovskiy, Germany  
Adiel T. De Almeida-Filho , Brazil  
Fabio De Angelis , Italy  
Samuele De Bartolo , Italy  
Stefano De Miranda , Italy  
Filippo De Monte , Italy



























José António Fonseca De Oliveira  
Correia , Portugal  
Jose Renato De Sousa , Brazil  
Michael Defoort, France  
Alessandro Della Corte, Italy  
Laurent Dewasme , Belgium  
Sanku Dey , India  
Gianpaolo Di Bona , Italy  
Roberta Di Pace , Italy  
Francesca Di Puccio , Italy  
Ramón I. Diego , Spain  
Yannis Dimakopoulos , Greece  
Hasan Dinçer , Turkey  
José M. Domínguez , Spain  
Georgios Dounias, Greece  
Bo Du , China  
Emil Dumic, Croatia  
Madalina Dumitriu , United Kingdom  
Premraj Durairaj , India  
Saeed Eftekhari Azam, USA  
Said El Kafhali , Morocco  
Antonio Elipse , Spain  
R. Emre Erkmen, Canada  
John Escobar , Colombia  
Leandro F. F. Miguel , Brazil  
FRANCESCO FOTI , Italy  
Andrea L. Facci , Italy  
Shahla Faisal , Pakistan  
Giovanni Falsone , Italy  
Hua Fan, China  
Jianguang Fang, Australia  
Nicholas Fantuzzi , Italy  
Muhammad Shahid Farid , Pakistan  
Hamed Faruqi, Iran  
Yann Favennec, France  
Fiorenzo A. Fazzolari , United Kingdom  
Giuseppe Fedele , Italy  
Roberto Fedele , Italy  
Baowei Feng , China  
Mohammad Ferdows , Bangladesh  
Arturo J. Fernández , Spain  
Jesus M. Fernandez Oro, Spain  
Francesco Ferrise, Italy  
Eric Feulvarch , France  
Thierry Floquet, France

Eric Florentin , France  
Gerardo Flores, Mexico  
Antonio Forcina , Italy  
Alessandro Formisano, Italy  
Francesco Franco , Italy  
Elisa Francomano , Italy  
Juan Frausto-Solis, Mexico  
Shujun Fu , China  
Juan C. G. Prada , Spain  
HECTOR GOMEZ , Chile  
Matteo Gaeta , Italy  
Mauro Gaggero , Italy  
Zoran Gajic , USA  
Jaime Gallardo-Alvarado , Mexico  
Mosè Gallo , Italy  
Akemi Gálvez , Spain  
Maria L. Gandarias , Spain  
Hao Gao , Hong Kong  
Xingbao Gao , China  
Yan Gao , China  
Zhiwei Gao , United Kingdom  
Giovanni Garcea , Italy  
José García , Chile  
Harish Garg , India  
Alessandro Gasparetto , Italy  
Stylianos Georgantzinou, Greece  
Fotios Georgiades , India  
Parviz Ghadimi , Iran  
Ştefan Cristian Gherghina , Romania  
Georgios I. Giannopoulos , Greece  
Agathoklis Giaralis , United Kingdom  
Anna M. Gil-Lafuente , Spain  
Ivan Giorgio , Italy  
Gaetano Giunta , Luxembourg  
Jefferson L.M.A. Gomes , United Kingdom  
Emilio Gómez-Déniz , Spain  
Antonio M. Gonçalves de Lima , Brazil  
Qunxi Gong , China  
Chris Goodrich, USA  
Rama S. R. Gorla, USA  
Veena Goswami , India  
Xunjie Gou , Spain  
Jakub Grabski , Poland

















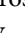







Antoine Grall , France  
George A. Gravvanis , Greece  
Fabrizio Greco , Italy  
David Greiner , Spain  
Jason Gu , Canada  
Federico Guarracino , Italy  
Michele Guida , Italy  
Muhammet Gul , Turkey  
Dong-Sheng Guo , China  
Hu Guo , China  
Zhaoxia Guo, China  
Yusuf Gurefe, Turkey  
Salim HEDDAM , Algeria  
ABID HUSSANAN, China  
Quang Phuc Ha, Australia  
Li Haitao , China  
Petr Hájek , Czech Republic  
Mohamed Hamdy , Egypt  
Muhammad Hamid , United Kingdom  
Renke Han , United Kingdom  
Weimin Han , USA  
Xingsi Han, China  
Zhen-Lai Han , China  
Thomas Hanne , Switzerland  
Xinan Hao , China  
Mohammad A. Hariri-Ardebili , USA  
Khalid Hattaf , Morocco  
Defeng He , China  
Xiao-Qiao He, China  
Yanchao He, China  
Yu-Ling He , China  
Ramdane Hedjar , Saudi Arabia  
Jude Hemanth , India  
Reza Hemmati, Iran  
Nicolae Herisanu , Romania  
Alfredo G. Hernández-Díaz , Spain  
M.I. Herreros , Spain  
Eckhard Hitzer , Japan  
Paul Honeine , France  
Jaromir Horacek , Czech Republic  
Lei Hou , China  
Yingkun Hou , China  
Yu-Chen Hu , Taiwan  
Yunfeng Hu, China  
Can Huang , China  
Gordon Huang , Canada  
Linsheng Huo , China  
Sajid Hussain, Canada  
Asier Ibeas , Spain  
Orest V. Iftime , The Netherlands  
Przemyslaw Ignaciuk , Poland  
Giacomo Innocenti , Italy  
Emilio Insfran Pelozo , Spain  
Azeem Irshad, Pakistan  
Alessio Ishizaka, France  
Benjamin Ivorra , Spain  
Breno Jacob , Brazil  
Reema Jain , India  
Tushar Jain , India  
Amin Jajarmi , Iran  
Chiranjibe Jana , India  
Łukasz Jankowski , Poland  
Samuel N. Jator , USA  
Juan Carlos Jáuregui-Correa , Mexico  
Kandasamy Jayakrishna, India  
Reza Jazar, Australia  
Khalide Jbilou, France  
Isabel S. Jesus , Portugal  
Chao Ji , China  
Qing-Chao Jiang , China  
Peng-fei Jiao , China  
Ricardo Fabricio Escobar Jiménez , Mexico  
Emilio Jiménez Macías , Spain  
Maolin Jin, Republic of Korea  
Zhuo Jin, Australia  
Ramash Kumar K , India  
BHABEN KALITA , USA  
MOHAMMAD REZA KHEDMATI , Iran  
Viacheslav Kalashnikov , Mexico  
Mathiyalagan Kalidass , India  
Tamas Kalmar-Nagy , Hungary  
Rajesh Kaluri , India  
Jyotheeswara Reddy Kalvakurthi, India  
Zhao Kang , China  
Ramani Kannan , Malaysia  
Tomasz Kapitaniak , Poland  
Julius Kaplunov, United Kingdom  
Konstantinos Karamanos, Belgium  
Michal Kawulok, Poland



Irfan Kaymaz , Turkey  
Vahid Kayvanfar , Qatar  
Krzysztof Kecik , Poland  
Mohamed Khader , Egypt  
Chaudry M. Khalique , South Africa  
Mukhtaj Khan , Pakistan  
Shahid Khan , Pakistan  
Nam-Il Kim, Republic of Korea  
Philipp V. Kiryukhantsev-Korneev ,  
Russia  
P.V.V Kishore , India  
Jan Koci , Czech Republic  
Ioannis Kostavelis , Greece  
Sotiris B. Kotsiantis , Greece  
Frederic Kratz , France  
Vamsi Krishna , India  
Edyta Kucharska, Poland  
Krzysztof S. Kulpa , Poland  
Kamal Kumar, India  
Prof. Ashwani Kumar , India  
Michal Kunicki , Poland  
Cedrick A. K. Kwuimy , USA  
Kyandoghere Kyamakya, Austria  
Ivan Kyrchei , Ukraine  
Márcio J. Lacerda , Brazil  
Eduardo Lalla , The Netherlands  
Giovanni Lancioni , Italy  
Jaroslaw Latalski , Poland  
Hervé Laurent , France  
Agostino Lauria , Italy  
Aimé Lay-Ekuakille , Italy  
Nicolas J. Leconte , France  
Kun-Chou Lee , Taiwan  
Dimitri Lefebvre , France  
Eric Lefevre , France  
Marek Lefik, Poland  
Yaguo Lei , China  
Kauko Leiviskä , Finland  
Ervin Lenzi , Brazil  
ChenFeng Li , China  
Jian Li , USA  
Jun Li , China  
Yueyang Li , China  
Zhao Li , China






























Zhen Li , China  
En-Qiang Lin, USA  
Jian Lin , China  
Qibin Lin, China  
Yao-Jin Lin, China  
Zhiyun Lin , China  
Bin Liu , China  
Bo Liu , China  
Heng Liu , China  
Jianxu Liu , Thailand  
Lei Liu , China  
Sixin Liu , China  
Wanquan Liu , China  
Yu Liu , China  
Yuanchang Liu , United Kingdom  
Bonifacio Llamazares , Spain  
Alessandro Lo Schiavo , Italy  
Jean Jacques Loiseau , France  
Francesco Lolli , Italy  
Paolo Lonetti , Italy  
António M. Lopes , Portugal  
Sebastian López, Spain  
Luis M. López-Ochoa , Spain  
Vassilios C. Loukopoulos, Greece  
Gabriele Maria Lozito , Italy  
Zhiguo Luo , China  
Gabriel Luque , Spain  
Valentin Lychagin, Norway  
YUE MEI, China  
Junwei Ma , China  
Xuanlong Ma , China  
Antonio Madeo , Italy  
Alessandro Magnani , Belgium  
Toqeer Mahmood , Pakistan  
Fazal M. Mahomed , South Africa  
Arunava Majumder , India  
Sarfranz Nawaz Malik, Pakistan  
Paolo Manfredi , Italy  
Adnan Maqsood , Pakistan  
Muazzam Maqsood, Pakistan  
Giuseppe Carlo Marano , Italy  
Damijan Markovic, France  
Filipe J. Marques , Portugal  
Luca Martinelli , Italy  
Denizar Cruz Martins, Brazil

Francisco J. Martos , Spain  
Elio Masciari , Italy  
Paolo Massioni , France  
Alessandro Mauro , Italy  
Jonathan Mayo-Maldonado , Mexico  
Pier Luigi Mazzeo , Italy  
Laura Mazzola, Italy  
Driss Mehdi , France  
Zahid Mehmood , Pakistan  
Roderick Melnik , Canada  
Xiangyu Meng , USA  
Jose Merodio , Spain  
Alessio Merola , Italy  
Mahmoud Mesbah , Iran  
Luciano Mescia , Italy  
Laurent Mevel , France  
Constantine Michailides , Cyprus  
Mariusz Michta , Poland  
Prankul Middha, Norway  
Aki Mikkola , Finland  
Giovanni Minafò , Italy  
Edmondo Minisci , United Kingdom  
Hiroyuki Mino , Japan  
Dimitrios Mitsotakis , New Zealand  
Ardashir Mohammadzadeh , Iran  
Francisco J. Montáns , Spain  
Francesco Montefusco , Italy  
Gisele Mophou , France  
Rafael Morales , Spain  
Marco Morandini , Italy  
Javier Moreno-Valenzuela , Mexico  
Simone Morganti , Italy  
Caroline Mota , Brazil  
Aziz Moukrim , France  
Shen Mouquan , China  
Dimitris Mourtzis , Greece  
Emiliano Mucchi , Italy  
Taseer Muhammad, Saudi Arabia  
Ghulam Muhiuddin, Saudi Arabia  
Amitava Mukherjee , India  
Josefa Mula , Spain  
Jose J. Muñoz , Spain  
Giuseppe Muscolino, Italy  
Marco Mussetta , Italy

Hariharan Muthusamy, India  
Alessandro Naddeo , Italy  
Raj Nandkeolyar, India  
Keivan Navaie , United Kingdom  
Soumya Nayak, India  
Adrian Neagu , USA  
Erivelton Geraldo Nepomuceno , Brazil  
AMA Neves, Portugal  
Ha Quang Thinh Ngo , Vietnam  
Nhon Nguyen-Thanh, Singapore  
Papakostas Nikolaos , Ireland  
Jelena Nikolic , Serbia  
Tatsushi Nishi, Japan  
Shanzhou Niu , China  
Ben T. Nohara , Japan  
Mohammed Nouari , France  
Mustapha Nourelfath, Canada  
Kazem Nouri , Iran  
Ciro Núñez-Gutiérrez , Mexico  
Włodzimierz Ogryczak, Poland  
Roger Ohayon, France  
Krzysztof Okarma , Poland  
Mitsuhiro Okayasu, Japan  
Murat Olgun , Turkey  
Diego Oliva, Mexico  
Alberto Olivares , Spain  
Enrique Onieva , Spain  
Calogero Orlando , Italy  
Susana Ortega-Cisneros , Mexico  
Sergio Ortobelli, Italy  
Naohisa Otsuka , Japan  
Sid Ahmed Ould Ahmed Mahmoud , Saudi Arabia  
Taoreed Owolabi , Nigeria  
EUGENIA PETROPOULOU , Greece  
Arturo Pagano, Italy  
Madhumangal Pal, India  
Pasquale Palumbo , Italy  
Dragan Pamučar, Serbia  
Weifeng Pan , China  
Chandan Pandey, India  
Rui Pang, United Kingdom  
Jürgen Pannek , Germany  
Elena Panteley, France  
Achille Paolone, Italy

George A. Papakostas , Greece  
Xosé M. Pardo , Spain  
You-Jin Park, Taiwan  
Manuel Pastor, Spain  
Pubudu N. Pathirana , Australia  
Surajit Kumar Paul , India  
Luis Payá , Spain  
Igor Pažanin , Croatia  
Libor Pekař , Czech Republic  
Francesco Pellicano , Italy  
Marcello Pellicciari , Italy  
Jian Peng , China  
Mingshu Peng, China  
Xiang Peng , China  
Xindong Peng, China  
Yuexing Peng, China  
Marzio Pennisi , Italy  
Maria Patrizia Pera , Italy  
Matjaz Perc , Slovenia  
A. M. Bastos Pereira , Portugal  
Wesley Peres, Brazil  
F. Javier Pérez-Pinal , Mexico  
Michele Perrella, Italy  
Francesco Pesavento , Italy  
Francesco Petrini , Italy  
Hoang Vu Phan, Republic of Korea  
Lukasz Pieczonka , Poland  
Dario Piga , Switzerland  
Marco Pizzarelli , Italy  
Javier Plaza , Spain  
Goutam Pohit , India  
Dragan Poljak , Croatia  
Jorge Pomares , Spain  
Hiram Ponce , Mexico  
Sébastien Poncet , Canada  
Volodymyr Ponomaryov , Mexico  
Jean-Christophe Ponsart , France  
Mauro Pontani , Italy  
Sivakumar Poruran, India  
Francesc Pozo , Spain  
Aditya Rio Prabowo , Indonesia  
Anchasa Pramuanjaroenkij , Thailand  
Leonardo Primavera , Italy  
B Rajanarayan Prusty, India

Krzysztof Puszynski , Poland  
Chuan Qin , China  
Dongdong Qin, China  
Jianlong Qiu , China  
Giuseppe Quaranta , Italy  
DR. RITU RAJ , India  
Vitomir Racic , Italy  
Carlo Rainieri , Italy  
Kumbakonam Ramamani Rajagopal, USA  
Ali Ramazani , USA  
Angel Manuel Ramos , Spain  
Higinio Ramos , Spain  
Muhammad Afzal Rana , Pakistan  
Muhammad Rashid, Saudi Arabia  
Manoj Rastogi, India  
Alessandro Rasulo , Italy  
S.S. Ravindran , USA  
Abdolrahman Razani , Iran  
Alessandro Reali , Italy  
Jose A. Reinoso , Spain  
Oscar Reinoso , Spain  
Haijun Ren , China  
Carlo Renno , Italy  
Fabrizio Renno , Italy  
Shahram Rezapour , Iran  
Ricardo Rianza , Spain  
Francesco Riganti-Fulginei , Italy  
Gerasimos Rigatos , Greece  
Francesco Ripamonti , Italy  
Jorge Rivera , Mexico  
Eugenio Roanes-Lozano , Spain  
Ana Maria A. C. Rocha , Portugal  
Luigi Rodino , Italy  
Francisco Rodríguez , Spain  
Rosana Rodríguez López, Spain  
Francisco Rossomando , Argentina  
Jose de Jesus Rubio , Mexico  
Weiguo Rui , China  
Rubén Ruiz , Spain  
Ivan D. Rukhlenko , Australia  
Dr. Eswaramoorthi S. , India  
Weichao SHI , United Kingdom  
Chaman Lal Sabharwal , USA  
Andrés Sáez , Spain

Bekir Sahin, Turkey  
Laxminarayan Sahoo , India  
John S. Sakellariou , Greece  
Michael Sakellariou , Greece  
Salvatore Salamone, USA  
Jose Vicente Salcedo , Spain  
Alejandro Salcido , Mexico  
Alejandro Salcido, Mexico  
Nunzio Salerno , Italy  
Rohit Salgotra , India  
Miguel A. Salido , Spain  
Sinan Salih , Iraq  
Alessandro Salvini , Italy  
Abdus Samad , India  
Sovan Samanta, India  
Nikolaos Samaras , Greece  
Ramon Sancibrian , Spain  
Giuseppe Sanfilippo , Italy  
Omar-Jacobo Santos, Mexico  
J Santos-Reyes , Mexico  
José A. Sanz-Herrera , Spain  
Musavarah Sarwar, Pakistan  
Shahzad Sarwar, Saudi Arabia  
Marcelo A. Savi , Brazil  
Andrey V. Savkin, Australia  
Tadeusz Sawik , Poland  
Roberta Sburlati, Italy  
Gustavo Scaglia , Argentina  
Thomas Schuster , Germany  
Hamid M. Sedighi , Iran  
Mijanur Rahaman Seikh, India  
Tapan Senapati , China  
Lotfi Senhadji , France  
Junwon Seo, USA  
Michele Serpilli, Italy  
Silvestar Šesnić , Croatia  
Gerardo Severino, Italy  
Ruben Sevilla , United Kingdom  
Stefano Sfarra , Italy  
Dr. Ismail Shah , Pakistan  
Leonid Shaikhet , Israel  
Vimal Shanmuganathan , India  
Prayas Sharma, India  
Bo Shen , Germany  
Hang Shen, China

Xin Pu Shen, China  
Dimitri O. Shepelsky, Ukraine  
Jian Shi , China  
Amin Shokrollahi, Australia  
Suzanne M. Shontz , USA  
Babak Shotorban , USA  
Zhan Shu , Canada  
Angelo Sifaleras , Greece  
Nuno Simões , Portugal  
Mehakpreet Singh , Ireland  
Piyush Pratap Singh , India  
Rajiv Singh, India  
Seralathan Sivamani , India  
S. Sivasankaran , Malaysia  
Christos H. Skiadas, Greece  
Konstantina Skouri , Greece  
Neale R. Smith , Mexico  
Bogdan Smolka, Poland  
Delfim Soares Jr. , Brazil  
Alba Sofi , Italy  
Francesco Soldovieri , Italy  
Raffaele Solimene , Italy  
Yang Song , Norway  
Jussi Sopanen , Finland  
Marco Spadini , Italy  
Paolo Spagnolo , Italy  
Ruben Specogna , Italy  
Vasilios Spitas , Greece  
Ivanka Stamova , USA  
Rafał Stanisławski , Poland  
Miladin Stefanović , Serbia  
Salvatore Strano , Italy  
Yakov Strelniker, Israel  
Kangkang Sun , China  
Qiuqin Sun , China  
Shuaishuai Sun, Australia  
Yanchao Sun , China  
Zong-Yao Sun , China  
Kumarasamy Suresh , India  
Sergey A. Suslov , Australia  
D.L. Suthar, Ethiopia  
D.L. Suthar , Ethiopia  
Andrzej Swierniak, Poland  
Andras Szekrenyes , Hungary  
Kumar K. Tamma, USA

Yong (Aaron) Tan, United Kingdom  
Marco Antonio Taneco-Hernández , Mexico  
Lu Tang , China  
Tianyou Tao, China  
Hafez Tari , USA  
Alessandro Tasora , Italy  
Sergio Teggi , Italy  
Adriana del Carmen Téllez-Anguiano , Mexico  
Ana C. Teodoro , Portugal  
Efstathios E. Theotokoglou , Greece  
Jing-Feng Tian, China  
Alexander Timokha , Norway  
Stefania Tomasiello , Italy  
Gisella Tomasini , Italy  
Isabella Torcicollo , Italy  
Francesco Tornabene , Italy  
Mariano Torrisi , Italy  
Thang nguyen Trung, Vietnam  
George Tsiatas , Greece  
Le Anh Tuan , Vietnam  
Nerio Tullini , Italy  
Emilio Turco , Italy  
Ilhan Tuzcu , USA  
Efstratios Tzirtzilakis , Greece  
FRANCISCO UREÑA , Spain  
Filippo Ubertini , Italy  
Mohammad Uddin , Australia  
Mohammad Safi Ullah , Bangladesh  
Serdar Ulubeyli , Turkey  
Mati Ur Rahman , Pakistan  
Panayiotis Vafeas , Greece  
Giuseppe Vairo , Italy  
Jesus Valdez-Resendiz , Mexico  
Eusebio Valero, Spain  
Stefano Valvano , Italy  
Carlos-Renato Vázquez , Mexico  
Martin Velasco Villa , Mexico  
Franck J. Vernerey, USA  
Georgios Veronis , USA  
Vincenzo Vespri , Italy  
Renato Vidoni , Italy  
Venkatesh Vijayaraghavan, Australia

Anna Vila, Spain  
Francisco R. Villatoro , Spain  
Francesca Vipiana , Italy  
Stanislav Vitek , Czech Republic  
Jan Vorel , Czech Republic  
Michael Vynnycky , Sweden  
Mohammad W. Alomari, Jordan  
Roman Wan-Wendner , Austria  
Bingchang Wang, China  
C. H. Wang , Taiwan  
Dagang Wang, China  
Guoqiang Wang , China  
Huaiyu Wang, China  
Hui Wang , China  
J.G. Wang, China  
Ji Wang , China  
Kang-Jia Wang , China  
Lei Wang , China  
Qiang Wang, China  
Qingling Wang , China  
Weiwei Wang , China  
Xinyu Wang , China  
Yong Wang , China  
Yung-Chung Wang , Taiwan  
Zhenbo Wang , USA  
Zhibo Wang, China  
Waldemar T. Wójcik, Poland  
Chi Wu , Australia  
Qihong Wu, China  
Yuqiang Wu, China  
Zhibin Wu , China  
Zhizheng Wu , China  
Michalis Xenos , Greece  
Hao Xiao , China  
Xiao Ping Xie , China  
Qingzheng Xu , China  
Binghan Xue , China  
Yi Xue , China  
Joseph J. Yame , France  
Chuanliang Yan , China  
Xinggang Yan , United Kingdom  
Hongtai Yang , China  
Jixiang Yang , China  
Mijia Yang, USA  
Ray-Yeng Yang, Taiwan

Zaoli Yang , China  
Jun Ye , China  
Min Ye , China  
Luis J. Yebra , Spain  
Peng-Yeng Yin , Taiwan  
Muhammad Haroon Yousaf , Pakistan  
Yuan Yuan, United Kingdom  
Qin Yuming, China  
Elena Zaitseva , Slovakia  
Arkadiusz Zak , Poland  
Mohammad Zakwan , India  
Ernesto Zambrano-Serrano , Mexico  
Francesco Zammori , Italy  
Jessica Zangari , Italy  
Rafal Zdunek , Poland  
Ibrahim Zeid, USA  
Nianyin Zeng , China  
Junyong Zhai , China  
Hao Zhang , China  
Haopeng Zhang , USA  
Jian Zhang , China  
Kai Zhang, China  
Lingfan Zhang , China  
Mingjie Zhang , Norway  
Qian Zhang , China  
Tianwei Zhang , China  
Tongqian Zhang , China  
Wenyu Zhang , China  
Xianming Zhang , Australia  
Xuping Zhang , Denmark  
Yinyan Zhang, China  
Yifan Zhao , United Kingdom  
Debao Zhou, USA  
Heng Zhou , China  
Jian G. Zhou , United Kingdom  
Junyong Zhou , China  
Xueqian Zhou , United Kingdom  
Zhe Zhou , China  
Wu-Le Zhu, China  
Gaetano Zizzo , Italy  
Mingcheng Zuo, China




## Contents

### **Study of Third-Grade Fluid under the Fuzzy Environment with Couette and Poiseuille Flows**

Muhammad Nadeem, Imran Siddique, Rifaqat Ali , Nawa Alshammari , Raja Noshad Jamil , Nawaf Hamadneh , Ilyas Khan , and Mulugeta Andualem 



Research Article (19 pages), Article ID 2458253, Volume 2022 (2022)

### **Decision-Making Approach Based on Generalized Aggregation Operators with Complex Single-Valued Neutrosophic Hesitant Fuzzy Set Information**

Harish Garg , Zeeshan Ali, Ibrahim M. Hezam , and Jeonghwan Gwak 

Research Article (20 pages), Article ID 9164735, Volume 2022 (2022)

### **Inertia Theory Frequency Dynamic Analysis and Control of Power System with High Proportion of Renewable Source**

Badar ul Islam , Zuhairi Baharudin, and Parameshwari Kattel 

Research Article (16 pages), Article ID 9472957, Volume 2021 (2021)

### **Analysis and Implementation of Thermal Heat Exchanger Tube Performance with Helically Pierced Twisted Tape Inserts Using ANFIS Model**

Faisal Altarazi, Sunil Kumar , Gaurav Gupta , Muhammad Gulzar , Yaé Ulrich Gaba , Anil Kumar, and Rajesh Maithani 



Research Article (13 pages), Article ID 1734909, Volume 2021 (2021)

### **Measuring the Return on Investment of Training Modules of Electrical Protection and Uninterruptible Power Supply (UPS) Using the Corrective and AHP Approaches**

Farhad Salimian 

Research Article (10 pages), Article ID 2635761, Volume 2021 (2021)

### **A New TOPSIS Approach Using Cosine Similarity Measures and Cubic Bipolar Fuzzy Information for Sustainable Plastic Recycling Process**

Muhammad Riaz , Dragan Pamucar , Anam Habib, and Mishal Riaz



Research Article (18 pages), Article ID 4309544, Volume 2021 (2021)

### **Pythagorean Fuzzy Soft Einstein Ordered Weighted Average Operator in Sustainable Supplier Selection Problem**

Rana Muhammad Zulqarnain , Imran Siddique , Shahzad Ahmad, Aiyared Iampan , Goran Jovanov , Đorđe Vranješ , and Jovica Vasiljević

Research Article (16 pages), Article ID 2559979, Volume 2021 (2021)

### **Weak Hopf Algebra and Its Quiver Representation**

Muhammad Naseer Khan, Ahmed Munir, Muhammad Arshad, Ahmed Alsanad , and Suheer Al-Hadhrami 



Research Article (8 pages), Article ID 1483371, Volume 2021 (2021)

### **Computer-Based Fuzzy Numerical Method for Solving Engineering and Real-World Applications**

Naila Rafiq , Naveed Yaqoob , Nasreen Kausar , Mudassir Shams , Nazir Ahmad Mir , Yaé Ulrich Gaba , and Naveed Khan

Research Article (13 pages), Article ID 6916282, Volume 2021 (2021)

**Novel Technique for Group Decision-Making under Fuzzy Parameterized  $q$ -Rung Orthopair Fuzzy Soft Expert Framework**

Ghous Ali  and Musavarah Sarwar 

Research Article (22 pages), Article ID 5449403, Volume 2021 (2021)

**Numerical Study of MHD Third-Grade Fluid Flow through an Inclined Channel with Ohmic Heating under Fuzzy Environment**

Muhammad Nadeem, Imran Siddique , Fahd Jarad , and Raja Noshad Jamil 

Research Article (17 pages), Article ID 9137479, Volume 2021 (2021)



## Research Article

# Study of Third-Grade Fluid under the Fuzzy Environment with Couette and Poiseuille Flows

Muhammad Nadeem,<sup>1</sup> Imran Siddique,<sup>1</sup> Rifaqat Ali ,<sup>2</sup> Nawa Alshammari ,<sup>3</sup>  
Raja Noshad Jamil ,<sup>1</sup> Nawaf Hamadneh ,<sup>3</sup> Ilyas Khan ,<sup>4</sup> and Mulugeta Andualem ,<sup>5</sup>

<sup>1</sup>Department of Mathematics, University of Management and Technology, Lahore 54770, Pakistan

<sup>2</sup>Department of Mathematics, College of Science and Arts, King Khalid University, Muhayil, Abha 61413, Saudi Arabia

<sup>3</sup>Department of Basic Sciences, College of Science and Theoretical Studies, Saudi Electronic University, Riyadh 11673, Saudi Arabia

<sup>4</sup>Department of Mathematics, College of Science Al-Zulfi, Majmaah University, Al Majma'ah 11952, Saudi Arabia

<sup>5</sup>Department of Mathematics, Bonga University, Bonga, Ethiopia

Correspondence should be addressed to Nawa Alshammari; [n.alshammari@seu.edu.sa](mailto:n.alshammari@seu.edu.sa), Ilyas Khan; [i.said@mu.edu.sa](mailto:i.said@mu.edu.sa), and Mulugeta Andualem; [mulugetaandualem4@gmail.com](mailto:mulugetaandualem4@gmail.com)

Received 3 September 2021; Revised 1 November 2021; Accepted 20 November 2021; Published 17 January 2022

Academic Editor: Arunava Majumder

Copyright © 2022 Muhammad Nadeem et al. This is an open access article distributed under the Creative Commons Attribution License, which permits unrestricted use, distribution, and reproduction in any medium, provided the original work is properly cited.

In this work, fundamental flow problems, namely, Couette flow, fully developed plane Poiseuille flow, and plane Couette–Poiseuille flow of a third-grade non-Newtonian fluid between two horizontal parallel plates separated by a finite distance in a fuzzy environment are considered. The governing nonlinear differential equations (DEs) are converted into fuzzy differential equations (FDEs) and explain our approach with the help of the membership function (MF) of triangular fuzzy numbers (TFNs). Adomian decomposition method (ADM) is used to solve fundamental flow problems based on FDEs. In a crisp environment, the current findings are in good accord with their previous numerical and analytical results. Finally, the effect of the  $\alpha$ -cut ( $\alpha \in [0, 1]$ ) and other engineering constants on fuzzy velocity profile are invested in graphically and tabular forms. Also, the variability of the uncertainty is studied through the triangular MF.

## 1. Introduction

The non-Newtonian fluids have gained considerable attention from scientists because of extensive applications in engineering, science, and industry. Various industrial ingredients fall into this bunch, such as biological solutions, soap, paints, cosmetics, tars, shampoos, mayonnaise, blood, yoghurt, syrups, and glues, etc. Due to the intricate nature of non-Newtonian fluids, it is very hard to establish a single model that can describe the characteristics of all non-Newtonian fluids. So, the fluids of differential type [1] have received superior consideration by researchers. Here, we will consider the third-grade fluids (differential type by a subclass), which have been studied effectively in numerous types of flow mechanisms [2–9]. In fluid dynamics, the study of

three fundamental flows specifically (Couette, Poiseuille, and generalized Couette flow) attracts the researchers by various non-Newtonian fluids, due to their uses in science, engineering, and industry. The unidirectional flows are used in polymer engineering, for instance, die flow, injection moulding, extrusion, plastic forming, continuous casting, and asthenosphere flows [10–13]. ADM was introduced by Adomian [14–16]. ADM is a reliable, effective, and powerful technique to calculate linear and nonlinear DEs. It gives analytical solutions in the form of an infinite convergent series. The ADM has various imperative points of interest over other scientific techniques just as mathematical strategies, no linearization, discretization, perturbation, and spatial transformation. Siddiqui et al., [17] deliberated parallel plate flow of a third-grade fluid using ADM and

compare the results with numerical technique.” Pirzada and Vakaskar [18] calculated the solution of the fuzzy heat equation with the help of fuzzy ADM. Paripour et al. [19] studied the analytical solution of hybrid FDEs by using the fuzzy ADM and predictor-corrector method, which shows ADM is better than the predictor-corrector method. “Also, Siddiqui et al., [20] provided a comparison of ADM and Homotopy perturbation method (HPM) in terms of squeezing flow between two circular plates. Their analysis shows that ADM is better than HPM. In the review of literature, third-grade fluid problems are studied only for crisp cases.”

Fluid flow plays the main role in the field of science and engineering. The rise is in an extensive range of problems like chemical diffusion, magnetic effect, and heat transfer, etc. After governing these physical problems convert into linear or nonlinear DEs. In general, the physical problems with involved geometry, coefficients, parameters, initial and boundary conditions greatly affect the solution of DEs. Then the coefficients, parameters, initial and boundary conditions are not crisp due to the mechanical defects, experimental and measurement errors, etc. So in this situation, fuzzy sets theory (FST) is an effective tool for a better understanding of the considered phenomena and it is more accurate than assuming the crisp physical problems. More precisely, the FDEs play a major role to reduce the uncertainty and proper way to describe the physical problem which arises in uncertain parameters, initial and boundary conditions.

Zadeh [21] established the FST in 1965. FST is an extremely useful technique for defining situations in which information is ambiguous, hazy, or uncertain. FST is entirely defined by its MF or sense of belonging. In FST, the MF allocates a number between 0 and 1 to each element in the discourse universe. On the other hand, the degree of non-belongingness is a complement to “one” of the membership degree. The fuzzy number (FN) is a generalization of the classical real number (which uses absolute 0 and 1 only, and nothing in between) with additional properties. FN can be expected as a function whose domain is specified zero to one. This domain is called an MF. Every numerical value in the domain is allocated a definite grade of MF where 0 signifies the minimum possible grade and 1 is the maximum possible grade. FNs are competent in modelling epistemic uncertainty and its circulation. FNs are a very useful tool for FDEs, fuzzy analysis and other applications in fuzzy logic. Arithmetic operations on FNs were developed by Dubois and Prade [22]. The impreciseness or vagueness can be defined mathematically using FNs. The information of dynamical systems modelled by ODEs or PEDs is commonly incomplete, vague, or uncertain, while FDEs represent a proper way to model the dynamical systems under vagueness or uncertainty. Seikala [23] introduced the fuzzy differentiability concept. Later on, Kaleva [24] presented fuzzy differentiation and integration. Kandel and Byatt [25] introduced the FDEs in 1987. Buckley et al. [26] used two methods extension principle and FNs for the solution of FDEs. Nieto [27] studied the Cauchy problem for continuous FDEs. Lakshmikantham and Mohapatra studied the initial value problems for FDEs that have been commenced

in [28]. Park and Han [29] used successive approximation methods for the existence and uniqueness solution of FDE. Hashemi et al. [30] used HAM (Homotopyanalysis method) to calculate the analytical solutions for the system of fuzzy differential equations (SFDEs). Mosleh [31] used universal approximation and fuzzy neural network methods to solve the SFDEs. Gasilov et al. [32] developed the geometric method to solve SFDEs. Khasan and Nieto [33] used a generalized differentiability concept to solve the second-order FDE. A few decades ago, there have been many studies revolving around the concept of FDEs. [34–47] Biswal et al. [48] studied the Natural convection of nanofluid flow between two parallel plates using HPM in a fuzzy environment. The volume fraction of nanoparticles is considered as TFN and also shows the fuzzy result is better than a crisp result. Borah et al. [49] discussed the MHD flow of second-grade fluids in a fuzzy environment using fractional derivatives Atangana-Baleanu and Caputo-Fabrizio. The nondimensional governing equations convert into fuzzified governing equations with the help of the Zadeh extension principle and triangular fuzzy number. MHD and ohmic heating on the third-grade fluid in an inclined channel in a fuzzy environment was investigated by Nadeem et al. [50]. To discuss the uncertainty, the triangle membership function was used, as shown in Figure 1. Furthermore, FST has been employed by several researchers to accomplish well-known scientific and engineering conclusions [51–59].

The above-mentioned works motivated us to develop a model to describe the fuzzy\uncertain analysis for fundamental flow problems, namely, plane Couette, fully developed plane Poiseuille, and plane Couette–Poiseuille flow of the third-grade fluid between two parallel plates. The basic purpose of this article is to show the uncertain flow mechanism through FDEs and the generalization to the work of Siddiqui et al. [17] in the circumstance of fuzzy environment.

The article is structured as follows. Basic preliminaries are given in Section 2. In Section 3, the governing equations of the proposed study and changed governing equations in the fuzzy form for solving by a fuzzy ADM are developed. Results and discussion in graphical and tabular forms are presented in Section 4. In Section 5, some conclusions are given.

## 2. Preliminaries about FST

*Definition 1* (see [21, 50]). Fuzzy set  $\bar{Z}$  is defined as a set of ordered pairs such that  $\bar{Z} = \{x, \mu_{\bar{Z}}(x) : x \in U, \mu_{\bar{Z}}(x) \in [0, 1]\}$ ; here  $U$  is the universal set,  $\mu_{\bar{Z}}(x)$  is MF of  $\bar{Z}$  and mapping defined as  $\mu_{\bar{Z}}(x) : U \rightarrow [0, 1]$ .

*Definition 2* (see [22, 50]).  $\alpha$ -cut or  $\alpha$ -level of a fuzzy set  $\bar{Z}$ , defined by  $0 \leq \alpha \leq 1$ ,  $Z_\alpha = \{x / \mu_{\bar{Z}}(x) \geq \alpha\}$ , where  $Z_\alpha$  is crisp set and  $0 \leq \alpha \leq 1$ .

*Definition 3* (see [22, 50]). Let  $\bar{Z} = (\delta, \chi, \eta)$  with MF  $\mu_{\bar{Z}}(x)$  called a TFNs if

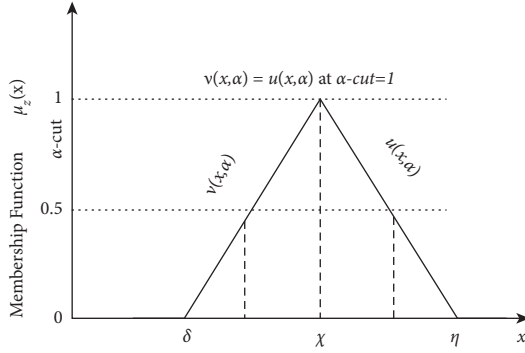


FIGURE 1: Triangular membership function.

$$\mu_{\bar{z}}(x) = \begin{cases} 1 - \frac{x - \chi}{\delta - \chi}, & x \in [\delta, \chi], \\ 1 - \frac{x - \chi}{\eta - \chi}, & x \in [\chi, \eta], \\ 0, & \text{otherwise.} \end{cases} \quad (1)$$

The TFNs with peak (center)  $\chi$ , right width  $\eta - \chi > 0$ , left width  $\chi - \delta > 0$ , and representation of ordered pair functions through  $\alpha$ -cut approach is written as  $\bar{z} = [v(x; \alpha), u(x; \alpha)] = [\delta + \alpha(\chi - \delta), \eta - \alpha(\eta - \chi)]$ , where  $0 \leq \alpha \leq 1$ . TFNs satisfy the following conditions: (i)  $v(x; \alpha)$  is non-decreasing on  $[0, 1]$ . (ii)  $u(x; \alpha)$  is nonincreasing on  $[0, 1]$ . (iii)  $u(x; \alpha) = v(x; \alpha)$  on  $[0, 1]$ . (iv)  $v(x; \alpha)$  and  $u(x; \alpha)$  are bounded on left continuous and right continuous at  $[0, 1]$ , respectively. (v) If  $v(x; \alpha) = u(x; \alpha)$  then it is called a crisp solution.

*Definition 4* (see [23, 50]). Let  $I^{\bar{z}}$  be an interval such that  $I^{\bar{z}} \subseteq R$ . A mapping  $\bar{u}: I^{\bar{z}} \rightarrow F^*$  is called a fuzzy process, defined as  $\bar{u}(x; \alpha) = [v(x; \alpha), u(x; \alpha)]$ ,  $x \in I^{\bar{z}}$  and  $0 \leq \alpha \leq 1$ . The derivative  $d\bar{u}(x; \alpha)/dx \in F^*$  of a fuzzy process  $\bar{u}(x; \alpha)$  is defined as  $d\bar{u}(x; \alpha)/dx = [(dv(x; \alpha)/dx), (du(x; \alpha)/dx)]$ .

*Definition 5* (see [23, 50]). Let  $I^{\bar{z}} \subseteq R$  and  $\bar{u}(x; \alpha)$  be a fuzzy valued function define on  $I^{\bar{z}}$ . Let  $\bar{u}(x; \alpha) = [v(x; \alpha), u(x; \alpha)]$  for all  $\alpha$ -cut. Assume that  $v(x; \alpha)$  and  $u(x; \alpha)$  have continuous derivatives or differentiable, for all  $x \in I^{\bar{z}}$  and  $0 \leq \alpha \leq 1$  then  $[d\bar{u}(x; \alpha)/dx]_{\alpha} = [(dv(x; \alpha)/dx), (du(x; \alpha)/dx)]_{\alpha}$ . Similarly, the higher-order derivatives can be defined in the same way. Then  $[d\bar{u}(x; \alpha)/dx]$  satisfy the following conditions: (i)  $dv(x; \alpha)/dx$  is nondecreasing on  $[0, 1]$ . (ii)  $du(x; \alpha)/dx$  is nonincreasing on  $[0, 1]$ . (iii)  $du(x; \alpha)/dx \geq dv(x; \alpha)/dx$  on  $[0, 1]$ .

### 3. Basic Equations

The basic equations which govern the flow of an incompressible fluid ignoring the thermal effects are as follows [17]:

$$\nabla \cdot \mathbf{V} = 0, \quad (2)$$

$$\rho \frac{d\mathbf{V}}{dt} = \rho \mathbf{f} + \nabla \cdot \boldsymbol{\tau}, \quad (3)$$

$$\boldsymbol{\tau} = -p_1 \mathbf{I} + \boldsymbol{\tau}_1, \quad (4)$$

where  $f$  is the body force,  $p_1$  is the pressure,  $\rho$  is the density of fluid,  $\mathbf{V}$  is velocity vector,  $d/dt$  is the material derivative,  $\mathbf{I}$  is the unit tensor,  $\boldsymbol{\tau}$  is the stress tensor, and  $\boldsymbol{\tau}_1$  is the extra stress defined as follows:

$$\boldsymbol{\tau}_1 = \boldsymbol{\tau}_2 + \varepsilon_1 \boldsymbol{\tau}_3 + \kappa_1 \boldsymbol{\tau}_4 + \kappa_2 (\boldsymbol{\tau}_2 \boldsymbol{\tau}_3 + \boldsymbol{\tau}_3 \boldsymbol{\tau}_2) + \kappa_3 (tr \boldsymbol{\tau}_2^2) \boldsymbol{\tau}_2. \quad (5)$$

Here,  $\mu$  represents the coefficient of shear viscosity,  $\kappa_1$ ,  $\kappa_2$ ,  $\kappa_3$ ,  $\varepsilon_1$  and  $\varepsilon_2$  are material constants. The tensors  $\boldsymbol{\tau}_2$ ,  $\boldsymbol{\tau}_3$  and  $\boldsymbol{\tau}_4$  are, respectively, given by the following:

$$\begin{aligned} \boldsymbol{\tau}_2 &= \nabla \mathbf{V} + (\nabla \mathbf{V})^T, \\ \boldsymbol{\tau}_3 &= \frac{d\boldsymbol{\tau}_2}{dt} + \boldsymbol{\tau}_2 [(\nabla \mathbf{V})^T + (\nabla \mathbf{V})], \\ \boldsymbol{\tau}_4 &= \frac{d\boldsymbol{\tau}_3}{dt} + \boldsymbol{\tau}_3 [(\nabla \mathbf{V}) + (\nabla \mathbf{V})^T]. \end{aligned} \quad (6)$$

“For the problem under consideration, we assume a velocity profile for one-dimensional flow and stress tensor of the form.”

$$\begin{aligned} \mathbf{V} &= (u(x), 0, 0), \\ \boldsymbol{\tau}_1 &= \boldsymbol{\tau}_1(x). \end{aligned} \quad (7)$$

By utilizing equation (7), the continuity equation (2) is indistinguishably fulfilled and the equation of motion (3), without gravitational impact, becomes as follows:

$$\mu \frac{d^2 u}{dx^2} + 6(\kappa_2 + \kappa_3) \left( \frac{du}{dx} \right)^2 \left( \frac{d^2 u}{dx^2} - \frac{dp_1}{dy} \right) = 0, \quad (8)$$

$$-\frac{dp_1}{dx} + (2\varepsilon_1 + \varepsilon_2) \left( \frac{d}{dx} \right) \left( \frac{du}{dx} \right)^2 = 0, \quad (9)$$

On introducing the modified pressure  $p^{\bar{z}}$ ,

$$p^{\bar{z}} = -p_1(x, y) + (2\varepsilon_1 + \varepsilon_2) \left( \frac{du}{dx} \right)^2. \quad (10)$$

Using equation (10) in (9), we find that

$$\frac{dp^{\bar{z}}}{dx} = 0. \quad (11)$$

From equation (11)  $p^{\bar{z}} = p^{\bar{z}}(x)$  and as a result, equation (8) becomes as follows:

$$\mu \left( \frac{d^2 u}{dx^2} \right) + 6\beta \left( \frac{du}{dx} \right)^2 \left( \frac{d^2 u}{dx^2} - \frac{dp^{\bar{z}}}{dy} \right) = 0, \quad (12)$$

where for simplicity we have introduced  $\beta = \kappa_2 + \kappa_3$ .

“Equation (12) is a second-order nonlinear ordinary differential equation. This equation governs the

unidirectional flow of a non-Newtonian third-grade fluid between two horizontal infinite parallel plates.”

**3.1. The Adomian Decomposition Method (ADM).** In this section, we briefly outline the decomposition method [14]. To clarify the basic idea, we write the underlying nonlinear differential equation as follows:

$$L_1 u^{\mp}(x) + N_1 u^{\mp}(x) = q(x), \quad (13)$$

where  $L_1$  and  $N_1$  are linear and nonlinear operators, respectively, and  $q$  is the source term.

In general, the operator  $L_1$  can be written in the form

$$L_1 = \widehat{L} + R_1, \quad (14)$$

where  $\widehat{L}$  is the highest order derivative in  $L_1$  and is assumed to be easily invertible,  $R_1$  is the remaining operator in  $L_1$  whose order is less than the order of  $\widehat{L}$ .

Using equation (14) in (13), we have the following:

$$\widehat{L}u^{\mp}(x) = q(x) - R_1u^{\mp}(x) - N_1u^{\mp}(x). \quad (15)$$

Applying  $\widehat{L}^{-1}$  on the above equation, we have the following:

$$u^{\mp}(x) = -\widehat{L}^{-1}R_1u^{\mp}(x) - \widehat{L}^{-1}N_1u^{\mp}(x) + g(x), \quad (16)$$

where  $g(x)$  signifies the terms arising after integration of  $q(x)$  and calculate the constants of integration with the help of initial/boundary conditions. According to Adomian [14–16],  $u^{\mp}(x)$  and  $N_1u^{\mp}(x)$  can be uttered individually in the form

$$u^{\mp}(x) = \sum_{n=0}^{\infty} u_n^{\mp}(x), \quad (17)$$

$$N_1u^{\mp}(x) = \sum_{n=0}^{\infty} A_n^*(x). \quad (18)$$

where  $A_n^*, s$  are called Adomian polynomials [14, 15].

The algorithm of the general ADM can be communicated as follows:

$$u_0^{\mp}(x) = g(x), \quad (19)$$

$$u_{n+1}^{\mp}(x) = -\widehat{L}^{-1}A_n^*(x) - \widehat{L}^{-1}R_1u_n^{\mp}(x), \quad n \geq 0. \quad (20)$$

Thus, by calculating all components of  $u^{\mp}(x)$ , the solution can be written as follows:

$$u^{\mp}(x) = \sum_{k=1}^{\infty} u_k^{\mp}(x). \quad (21)$$

Many researchers have established the convergence of this method [16]. In this continuation, we apply the ADM in the fuzzy sense to three flow problems  $d$  problems.

**3.2. Plane Couette Flow.** Let us consider the steady laminar flow of an incompressible third-grade fluid between two infinite horizontal parallel plates. The lower plate is fixed while the upper plate at a distance  $x = d$  is moving with unvarying speed  $U$ . Also assume that  $x$  – axis is normal to the flow while  $y$  – axis is taken in the direction of flow as shown in Figure 2. In the absence of pressure gradient, the resultant differential equation (12) for such flow with boundary conditions reduces to the following:

$$\mu \frac{d^2u}{dx^2} + 6\beta \left( \frac{du}{dx} \right)^2 \left( \frac{d^2u}{dx^2} \right) = 0, \quad (22)$$

$$u(x) = 0 \text{ at } x = 0, \quad (23)$$

$$u(x) = U \text{ at } x = d. \quad (24)$$

Introduce the following dimensionless parameters

$$x^{\mp} = \frac{x}{d}, \quad (25)$$

$$u^{\mp} = \frac{u}{U},$$

$$\beta^{\mp} = \frac{\beta U^2}{\mu d^2}.$$

The boundary value problem (22) and (24) after dropping “ $\mp$ ” becomes

$$\frac{d^2u}{dx^2} + 6\beta \left( \frac{du}{dx} \right)^2 \left( \frac{d^2u}{dx^2} \right) = 0, \quad (26)$$

$$u(x) = 0 \text{ at } x = 0, \quad (27)$$

$$u(x) = 1 \text{ at } x = 1. \quad (28)$$

**3.2.1. Solution of the Problem in Fuzzy Environment.** To handle these problems, we have taken TFNs and discretization in the form of  $(\delta, \chi, \eta)$  and  $(d, e, f)$  for the fuzzy parameters. This discretization is used in the boundary of the parallel plates for certain flow behavior because the boundary is taken as fuzzified. In above, the governing equation (26) is taken as FDE

$$\frac{d^2\bar{u}(x; \alpha)}{dx^2} + 6 \odot \beta \odot \frac{d^2\bar{u}(x; \alpha)}{dx^2} \odot \left( \frac{d\bar{u}(x; \alpha)}{dx} \right)^2 = 0. \quad (29)$$

Subject to fuzzy boundary conditions by using the  $\alpha$ -cut approach, the fuzzy boundary conditions can be decomposed into an interval form regarding the  $\alpha$ -cut. Therefore, under the  $\alpha$ -cut, the interval boundary conditions can be written as follows:

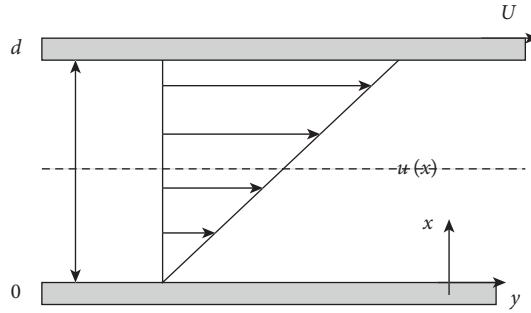


FIGURE 2: Geometry of the pure Couette flow.

$$\bar{u}(0; \alpha) = [\delta + \alpha(\chi - \delta), \eta - \alpha(\eta - \chi)],$$

$$\bar{u}(1; \alpha) = [\alpha(e - d) + d, f\alpha(f - e)],$$

$$\bar{u}(x; \alpha) = \left[ \frac{\alpha - 1}{100}, \frac{1 - \alpha}{100} \right] \text{ at } x \tag{30}$$

$$\bar{u}(x; \alpha) = \left[ \frac{2\alpha - 2}{100}, \frac{2 - 2\alpha}{100} \right] \text{ at } x$$

where operator  $\odot$  defines the multiplication of fuzzy numbers with a real number and  $\bar{u}(x; \alpha) = [v(x; \alpha), u(x; \alpha)]$ ,  $0 \leq \alpha \leq 1$ , is a fuzzy valued function [23]. Also  $\bar{u}(x; \alpha)$ , say, is the fuzzy velocity profile,  $d\bar{u}(x; \alpha)/dx$  and  $d^2\bar{u}(x; \alpha)/dx^2$  represent the fuzzy first and second-order derivatives. Then  $v(x; \alpha)$  and  $u(x; \alpha)$  are the lower and upper bounds of fuzzy velocity profiles, respectively, while (30) are the fuzzy boundary conditions. So, equation (29) with fuzzy boundary conditions becomes

$$\frac{d^2v(x; \alpha)}{dx^2} + 6\beta \left( \frac{dv(x; \alpha)}{dx} \right)^2 \frac{d^2v(x; \alpha)}{dx^2} = 0, \tag{31}$$

$$v(x; \alpha) = \frac{\alpha - 1}{100} \text{ at } x = 0, \tag{32}$$

$$v(x; \alpha) = \frac{2\alpha - 2}{100} \text{ at } x = 1.$$

$$\frac{d^2u(x; \alpha)}{dx^2} + 6\beta \left( \frac{du(x; \alpha)}{dx} \right)^2 \frac{d^2u(x; \alpha)}{dx^2} = 0, \tag{33}$$

$$u(x; \alpha) = \frac{1 - \alpha}{100} \text{ at } x = 0, \tag{34}$$

$$u(x; \alpha) = \frac{2 - 2\alpha}{100} \text{ at } x = 1.$$

For lower bound of velocity profile, we apply the ADM to equation (31) with the fuzzified boundary conditions (32) as follows:

$$L_1 v(x; \alpha) = -6\beta \left( \frac{dv(x; \alpha)}{dx} \right)^2 \left( \frac{d^2v(x; \alpha)}{dx^2} \right), \tag{35}$$

where  $L_1 = d^2/dx^2$  and inverse operator is  $\hat{L}^{-1} = \iint (\cdot) dx dx$ . Applying  $\hat{L}^{-1}$  on both sides of equation (35), we have the following:

$$v(x; \alpha) = c_1 x + c_2 - 6\beta \hat{L}^{-1} \left[ \left( \frac{dv(x; \alpha)}{dx} \right)^2 \frac{d^2v(x; \alpha)}{dx^2} \right], \tag{36}$$

where the constants of integration are  $c_1$  and  $c_2$ .

To solve equation (36) by the ADM, we let

$$v(x; \alpha) = \sum_{n=0}^{\infty} v_n(x; \alpha), \tag{37}$$

$$N_1 v(x; \alpha) = \sum_{n=0}^{\infty} A_n^*(x; \alpha), \tag{38}$$

where

$$N_1 v(x; \alpha) = \left( \frac{dv(x; \alpha)}{dx} \right)^2 \frac{d^2v(x; \alpha)}{dx^2}. \tag{39}$$

In view of equations (37)–(39), equation (36) provides the following:

$$\sum_{n=0}^{\infty} v_n(x; \alpha) = c_1 x + c_2 - 6\beta \hat{L}^{-1} [A_n^*(x; \alpha)]. \tag{40}$$

We identify the zeroth-order component as follows:

$$v_0(x; \alpha) = c_1 x + c_2. \tag{41}$$

And the remaining components as the recurrence relation,

$$v_{n+1}(x; \alpha) = -6\beta \hat{L}^{-1} [A_n^*(x; \alpha)], \tag{42}$$

where  $A_n^*$  are the Adomian polynomials that represent the nonlinear term in (39). The first few Adomian polynomials are as follows:

$$\begin{aligned}
A_0^*(x; \alpha) &= \frac{d^2 v_0(x; \alpha)}{dx^2} \left( \frac{dv_0(x; \alpha)}{dx} \right)^2, \\
A_1^*(x; \alpha) &= \left( \frac{dv_0(x; \alpha)}{dx} \right)^2 \left( \frac{d^2 v_1(x; \alpha)}{dx^2} \right) + \left( 2 \frac{dv_0(x; \alpha)}{dx} \frac{dv_1(x; \alpha)}{dx} \frac{d^2 v_0(x; \alpha)}{dx^2} \right), \\
A_2^*(x; \alpha) &= \left( \frac{dv_1(x; \alpha)}{dx} \right)^2 \left( \frac{d^2 v_0(x; \alpha)}{dx^2} \right) + \left( 2 \frac{dv_0(x; \alpha)}{dx} \frac{dv_2(x; \alpha)}{dx} \frac{d^2 v_0(x; \alpha)}{dx^2} \right), \\
&\quad + \left( 2 \frac{dv_0(x; \alpha)}{dx} \frac{dv_1(x; \alpha)}{dx} \frac{d^2 v_1(x; \alpha)}{dx^2} \right) + \left( \frac{dv_0(x; \alpha)}{dx} \right)^2 \left( \frac{d^2 v_2(x; \alpha)}{dx^2} \right). \\
&\quad \vdots
\end{aligned} \tag{43}$$

The corresponding fuzzy boundary conditions, after using (37) in (32), become as follows:

$$\begin{aligned}
v_0(x; \alpha) &= \frac{\alpha - 1}{100} \text{ at } x = 0, \\
v_0(x; \alpha) &= \frac{2\alpha - 2}{100} \text{ at } x = 1.
\end{aligned} \tag{44}$$

And

$$\begin{aligned}
v_n(x; \alpha) &= 0 \text{ at } x = 0, \\
v_n(x; \alpha) &= 0 \text{ at } x = 1, n \geq 1.
\end{aligned} \tag{45}$$

Solving equations (41) and (44), we obtain the zeroth-order solution as follows:

$$v_0(x; \alpha) = \frac{(\alpha - 1)(x + 1)}{100}. \tag{46}$$

Using polynomial (43) into (42), with the boundary conditions (45), we obtain the following:

$$\begin{aligned}
v_1(x; \alpha) &= v_2(x; \alpha) \\
&= v_3(x; \alpha) = 0, \text{ and } v_n(x; \alpha) = 0, n \geq 1.
\end{aligned} \tag{47}$$

Inserting equations (46) and (47) in (37), the solution of the differential equation (31) takes the form

$$v(x; \alpha) = \frac{1}{100} (\alpha - 1)(x + 1). \tag{48}$$

Similarly, the upper bound of velocity profile is as follows:

$$u(x; \alpha) = \frac{1}{100} (1 - \alpha)(x + 1). \tag{49}$$

Equations (48) and (49) represent the solutions of the fuzzy velocity profile for the flow of a fuzzified third-grade fluid between two parallel plates. In these solutions, the non-Newtonian parameter  $\beta$  does not appear. Hence, solutions of fuzzy velocity profile give the same solution as for a Newtonian fluid.

**3.3. Fully Developed Plane Poiseuille Flow.** We consider the steady laminar flow of a third-grade fluid between two stationary infinite parallel plates under a constant pressure gradient. Assume that distance between two plates is  $2d$  and origin of the rectangular coordinates in between the plates as shown in Figure 3.

Thus, the resulting differential equation for the problem under consideration takes the form of equation (12) with the following boundary conditions  $2d$

$$\frac{du(x)}{dx} = 0 \text{ at } x = 0, \tag{50}$$

$$u(x) = 0 \text{ at } x = d. \tag{51}$$

Introducing the dimensionless parameters

$$\begin{aligned}
y^{\bar{}} &= \frac{y}{d}, \\
x^{\bar{}} &= \frac{x}{d}, \\
u^{\bar{}} &= \frac{u}{U}, \\
\beta^{\bar{}} &= \frac{\beta U^2}{\mu d^2}, \\
p^{\bar{}} &= \frac{p d}{\mu U}.
\end{aligned} \tag{52}$$

Equations (12) and (51) after dropping “ $\bar{}$ ” take the following form:

$$\frac{d^2 u}{dx^2} + \beta \left( \frac{du}{dx} \right)^2 \left( \frac{d^2 u}{dx^2} - \frac{dp}{dy} \right) = 0, \tag{53}$$

$$\frac{du(x)}{dx} = 0 \text{ at } x = 0, \tag{54}$$

$$u(x) = 0 \text{ at } x = 1. \tag{55}$$

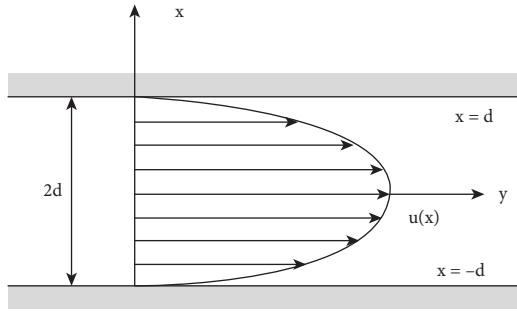


FIGURE 3: Velocity profile of the fluid flow between two parallel plates.

Now, convert equations (53) and (55) into the form of FDE as follows:

$$\frac{d^2 \bar{u}(x; \alpha)}{dx^2} + 6 \odot \beta \odot \frac{d^2 \bar{u}(x; \alpha)}{dx^2} \odot \left( \frac{d\bar{u}(x; \alpha)}{dx} \right)^2 = \frac{dp}{dy}, \quad (56)$$

$$\begin{aligned} \frac{d\bar{u}(x; \alpha)}{dx} &= \left[ \frac{\alpha - 1}{100}, \frac{1 - \alpha}{100} \right] \text{ at } x = 0, \\ \bar{u}(x; \alpha) &= \left[ \frac{2\alpha - 2}{100}, \frac{2 - 2\alpha}{100} \right] \text{ at } x = 1. \end{aligned} \quad (57)$$

Lower and upper bounds of velocity profile are as follows:

$$\frac{d^2 v(x; \alpha)}{dx^2} + 6\beta \left( \frac{dv(x; \alpha)}{dx} \right)^2 \frac{d^2 v(x; \alpha)}{dx^2} = \frac{dp}{dy}, \quad (58)$$

$$\begin{aligned} \frac{dv(x; \alpha)}{dx} &= \frac{1}{100} (-1 + \alpha) \text{ at } x = 0, \\ v(x; \alpha) &= \frac{1}{50} (\alpha - 1) \text{ at } x = 1. \end{aligned} \quad (59)$$

$$\frac{d^2 u(x; \alpha)}{dx^2} + 6\beta \frac{d^2 u(x; \alpha)}{dx^2} \left( \frac{du(x; \alpha)}{dx} \right)^2 = \frac{dp}{dy}, \quad (60)$$

$$\begin{aligned} \frac{du(x; \alpha)}{dx} &= \frac{1 - \alpha}{100} \text{ at } x = 0, \\ u(x; \alpha) &= \frac{1 - \alpha}{50} \text{ at } x = 1. \end{aligned} \quad (61)$$

For lower bound of velocity profile, we apply the ADM to equation (58) as we have applied in Section 3.2.1, with the fuzzified boundary conditions (59)

$$L_1 v(x; \alpha) = \frac{dp}{dy} - 6\beta \left( \frac{dv(x; \alpha)}{dx} \right)^2 \left( \frac{d^2 v(x; \alpha)}{dx^2} \right), \quad (62)$$

where  $L_1 = d^2/dx^2$ . Applying the inverse operator  $\widehat{L}^{-1} = \iint (\cdot) dx dx$  on both sides of equation (62) yields the following:

$$v(x; \alpha) = c_1 x + c_2 + \widehat{L}^{-1} \frac{dp}{dy} - 6\beta \widehat{L}^{-1} \left( \frac{dv(x; \alpha)}{dx} \right)^2 \left( \frac{d^2 v(x; \alpha)}{dx^2} \right), \quad (63)$$

where the constants of integration are  $c_1$  and  $c_2$ .

Given equations (37) and (38), equation (63) is provided as follows:

$$\sum_{n=0}^{\infty} v_n(x; \alpha) = c_1 x + c_2 + \widehat{L}^{-1} \left( \frac{dp}{dy} \right) - 6\beta \widehat{L}^{-1} [A_n^*(x; \alpha)], \quad (64)$$

Consequently, the decomposition method yields the recurrence relation,

$$v_0(x; \alpha) = c_1 x + c_2 + \widehat{L}^{-1} \left( \frac{dp}{dy} \right), \quad (65)$$

$$v_{n+1}(x; \alpha) = -6\beta \widehat{L}^{-1} [A_n^*(x; \alpha)], \quad (66)$$

where the first few terms of the Adomian polynomial that represent the nonlinear term are defined in (43). Insight of expressions (66), we know that

$$\begin{aligned} v_1(x; \alpha) &= -6\beta \widehat{L}^{-1} [A_0^*(x; \alpha)], \\ v_2(x; \alpha) &= -6\beta \widehat{L}^{-1} [A_1^*(x; \alpha)], \\ v_3(x; \alpha) &= -6\beta \widehat{L}^{-1} [A_2^*(x; \alpha)], \\ &\vdots \end{aligned} \quad (67)$$

The corresponding fuzzy boundary conditions become as follows:

$$\frac{dv_0(x; \alpha)}{dx} = \frac{1 - \alpha}{100} \text{ at } x = 0, \quad (68)$$

$$v_0(x; \alpha) = \frac{\alpha - 1}{50} \text{ at } x = 1,$$

And so on

$$\frac{dv_n(x; \alpha)}{dx} = 0 \text{ at } x = 0, \quad (69)$$

$$v_n(x; \alpha) = 0 \text{ at } x = 1, n \geq 1.$$

By solving equations (65) and (66) with the fuzzified boundary conditions (68) and (69), using expression of adomian polynomials (43), equation (63) gives the solution of lower bound of velocity profile as follows:

$$\begin{aligned}
 v(x; \alpha) = & \frac{1}{2} [px^2 + 2F(x + 1) - p] + \frac{\beta}{2p} [E^4 - (px + F)^4 + 8pF^3(x - 1)] + \frac{2\beta^2}{p} (px + F)^6 \\
 & - 4\beta^2 F^3 (px + F)^3 + \frac{9\beta^2 E^5 F^3}{p} - 12\beta^2 F^5 + 6\beta^2 F^6 + \frac{2(FE)^3 - E^6}{3p} (2\beta^2) \\
 & - 6\beta^3 \left[ 2(px + F)^8 - \frac{24pF^3 + 15F^3}{10p} (px + F)^5 - 2pF^2 + x \left( 12pF^7 - \frac{112F^7}{7} \right) \right. \\
 & \left. - 2pF^6 - \frac{2E^8}{p} - \frac{12E^5 F^3}{5} + \frac{112F^3}{7} - 12pF^7 - \frac{15F^7}{2} \right],
 \end{aligned} \tag{70}$$

where  $F = (\alpha - 1)(p + 1)/100$  and  $E = 100p + (\alpha - 1)(1 + p)/100$ .

Equation (70) is the approximate solution of the fully developed plan Poiseuille flow and  $\beta$  is a non-Newtonian

parameter. By setting  $\beta = 0$ , we have the solution for a viscous fluid.

Similarly, we can find the solution of the upper bound of velocity profile as follows:

$$\begin{aligned}
 u(x; \alpha) = & \frac{1}{2} [-p + 2A_1(x + 1) + px^2] + \frac{\beta}{2p} [A_2^4 - (px + A_1)^4 + 8pA_1^3(x - 1)] + \frac{2\beta^2}{p} (px + A_1)^6 \\
 & - 4\beta^2 A_1^3 (px + A_1)^3 + \frac{9\beta^2 A_2^5 A_1^3}{p} - 12\beta^2 A_1^5 + 6\beta^2 A_1^6 + \frac{2(A_1 A_2)^3 - A_2^6}{3p} (2\beta^2) \\
 & - 6\beta^3 \left[ 2(px + A_1)^8 - \frac{24pA_1^3 + 15A_1^3}{10p} (px + A_1)^5 - 2pA_1^2 + x \left( 12pA_1^7 - \frac{112A_1^7}{7} \right) \right. \\
 & \left. - 2pA_1^6 - \frac{2A_2^8}{p} - \frac{12A_2^5 A_1^3}{5} + \frac{112A_1^3}{7} - 12pA_1^7 - \frac{15A_1^7}{2} \right],
 \end{aligned} \tag{71}$$

where  $A_1 = (p + 1)(1 - \alpha)/100$  and  $A_2 = 100p + (1 - \alpha)(p + 1)/100$ .

**3.4. Plane Couette–Poiseuille flow.** Again consider the steady laminar flow of a third-grade fluid between two infinite horizontal parallel plates at a distance  $d$  apart. The upper plate is moving with constant speed  $U$  while the lower plate is stationary. We choose  $y$ –axis along with the lower plate and  $x$ –axis perpendicular to it as shown in Figure 4. The resulting differential equation in dimensionless form is (53) and the corresponding dimensionless form boundary conditions for this flow are given as follows.

$$\begin{aligned}
 u(x) = 0 & \text{ at } x = 0, \\
 u(x) = 1 & \text{ at } x = 1.
 \end{aligned} \tag{72}$$

Now we convert equations (53) and (72) into the form of FDE as follows:

$$\begin{aligned}
 \frac{d^2 \bar{u}(x; \alpha)}{dx^2} + 6\odot\beta \frac{d^2 \bar{u}(x; \alpha)}{dx^2} \\
 \left( \frac{d\bar{u}(x; \alpha)}{dx} \right)^2 = \frac{dp}{dy},
 \end{aligned} \tag{73}$$

$$\begin{aligned}
 \bar{u}(x; \alpha) = & \left[ \frac{\alpha - 1}{100}, \frac{1 - \alpha}{100} \right] \text{ at } x = 0, \\
 \bar{u}(x; \alpha) = & \left[ \frac{\alpha - 1}{50}, \frac{1 - \alpha}{50} \right] \text{ at } x = 1.
 \end{aligned} \tag{74}$$

Lower and upper bounds of velocity profiles with fuzzy boundary conditions are as follows:

$$\frac{d^2 v(x; \alpha)}{dx^2} + 6\beta \frac{d^2 v(x; \alpha)}{dx^2} \left( \frac{dv(x; \alpha)}{dx} \right)^2 = \frac{dp}{dy}, \tag{75}$$

$$\begin{aligned}
 v(x; \alpha) = & \frac{\alpha - 1}{100} \text{ at } x = 0, \\
 v(x; \alpha) = & \frac{\alpha - 1}{50} \text{ at } x = 1.
 \end{aligned} \tag{76}$$

$$\frac{d^2 u(x; \alpha)}{dx^2} + 6\beta \left( \frac{du(x; \alpha)}{dx} \right)^2 \frac{d^2 u(x; \alpha)}{dx^2} = \frac{dp}{dy}, \tag{77}$$

$$\begin{aligned}
 u(x; \alpha) = & \frac{1 - \alpha}{100} \text{ at } x = 0, \\
 u(x; \alpha) = & \frac{1 - \alpha}{50} \text{ at } x = 1.
 \end{aligned} \tag{78}$$

Following the same process as in previous sections and applying ADM to equation (75) with the fuzzified boundary conditions (76), we find the solution of lower bound of velocity profile as follows:



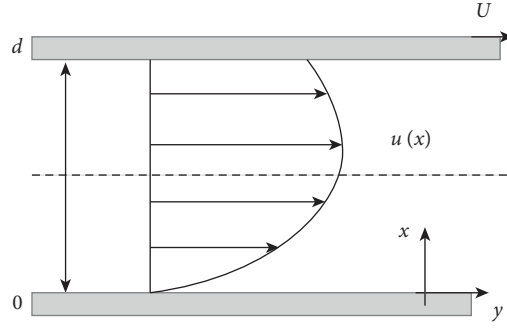


FIGURE 4: Geometry of the Couette–Poiseuille flow.

$$\begin{aligned}
 v(x; \alpha) = & A(x+1) + p\left(\frac{x^2}{2} + Dx + A\right) - p\beta\left[\frac{p^2(x+D)^4}{2} + 3A^2x^2 + p(2D+1)(x+D)^3 - \frac{p^2D^4}{2}\right. \\
 & - x\left\{\frac{p^2D^4}{2} + pD^3(2D+1) + 3A^2 + \frac{p(D+1)}{2} + p(2D+1)(D+1)^3\right\} - pD^3(2D+1)] \\
 & - 6\beta^2\left[Ap^3(x^4 + 2Dx^3) + \frac{4p^5(x+D)^6}{15} - \frac{A^2p^3(x+D)^4}{4} - \left(Ap^2x^2 + \frac{p^3x^3}{3} + Dp^3x^2\right)\right. \\
 & \times \left.\left\{\frac{p^2D^4}{2} + pD^3(2D+1) + 3A^2 + \frac{p(D+1)}{2} + p(2D+1)(D+1)^3\right\} - 3pA^2x^2(A+2pD)\right. \\
 & - \frac{p^2(p+A)(x+D)^4}{2} - \frac{3p^4A(x+D)^5}{5} - \frac{p^2A^3(x+D)^3}{2} + x\left\{6p^2A^2D + \frac{p^4}{5}(D+1)^5(3A-1)\right. \\
 & \left. - \frac{p^4}{15}(D+1)^6 + \frac{p^2A}{4}(D+1)^4(2p+Ap+2) + \frac{p^2A^3}{2}(D+1)^3 + 3pA^3 - Ap^3 - 2DAp^3\right\}\left. \right], \tag{79}
 \end{aligned}$$

where  $A = \alpha - 1/100$ ,  $D = \alpha - 51/100$ . Similarly, the solution of an upper bound of the velocity profile is as follows:

$$\begin{aligned}
 u(x; \alpha) = & B(x+1) + p\left(\frac{x^2}{2} + B_1x + B\right) - p\beta\left[\frac{p^2(x+B_1)^4}{2} + 3B^2p^2 + p(2B_1+1)(x+B_1)^3\right. \\
 & - x\left\{\frac{p^2B_1^4}{2} + pB_1^3(2B_1+1) + 3B^2 + \frac{p(1+B_1)}{2} + p(1+2B_1)(1+B_1)^3\right\} - \frac{p^2B_1^4}{2} \\
 & - pB_1^3(2B_1+1)] - 6\beta^2\left[Bp^3(x^4 + 2B_1x^3) + \frac{4p^5(x+B_1)^6}{15} - \frac{B^2p^3(x+B_1)^4}{4} - \left(\begin{array}{c} Bp^2x^2 \\ + \frac{p^3x^3}{3} + B_1p^3x^2 \end{array}\right)\right. \\
 & \left.\left\{\frac{p^2B_1^4}{2} + pB_1^3(2B_1+1) + 3B^2 + \frac{p(1+B_1)}{2} + p(1+2B_1)(B_1+1)^3\right\}\right. \\
 & - 3pB^2x^2(B+2pB_1) - \frac{p^2(p+B)(B_1+x)^4}{2} - \frac{3p^4B(B_1+x)^5}{5} - \frac{p^2B^3(B_1+x)^3}{2} \\
 & + x\left\{6p^2B^2B_1 + \frac{p^4}{5}(B_1+1)^5(3B-1) - \frac{p^4}{15}(B_1+1)^6 + \frac{p^2B}{4}(B_1+1)^4(2p+Bp+2)\right. \\
 & \left. + \frac{p^2B^3}{2}(B_1+1)^3 + 3pB^3 - Bp^3 - 2BB_1p^3\right\}\left. \right], \tag{80}
 \end{aligned}$$

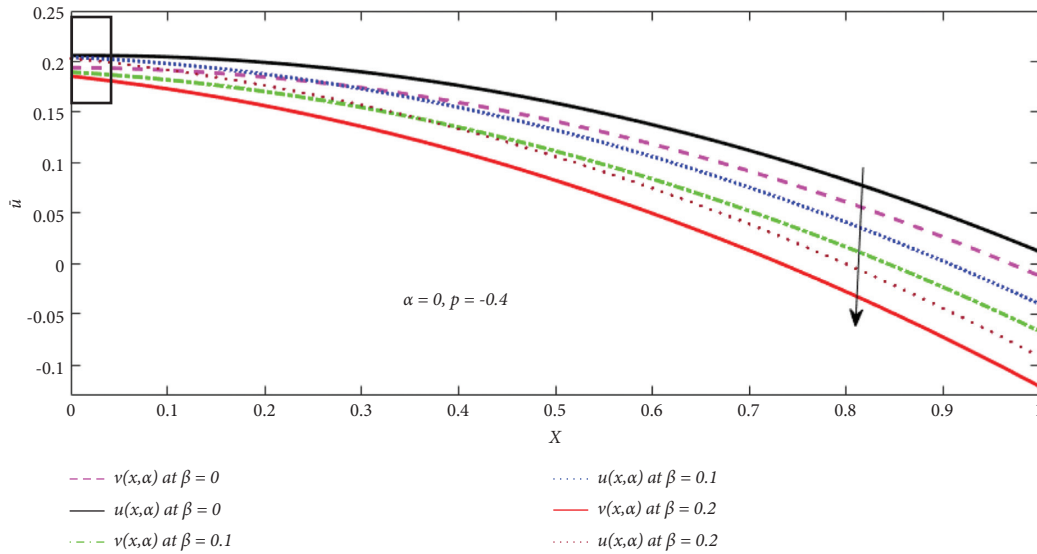


FIGURE 5: Fuzzy velocity profiles for influence of  $\beta$ .

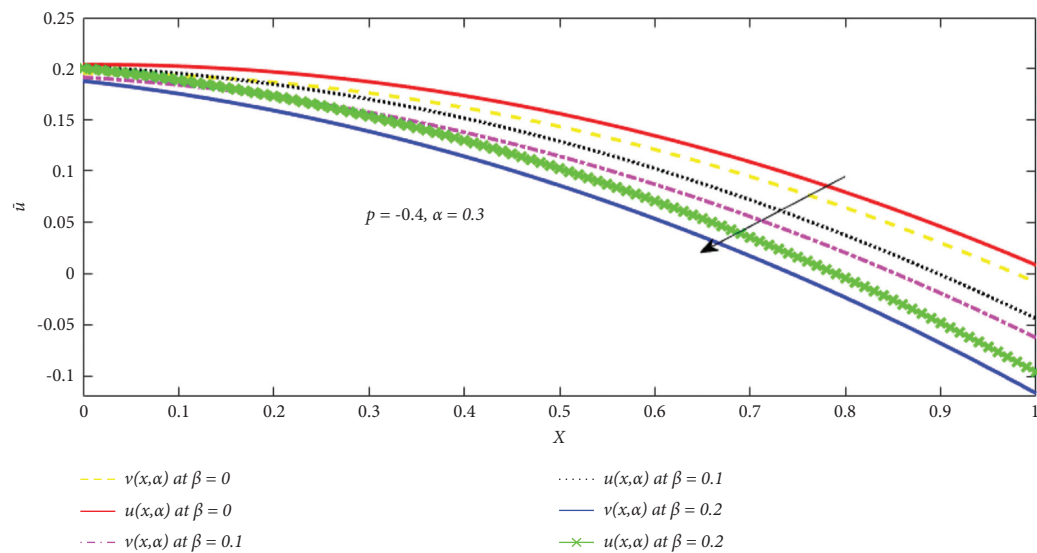


FIGURE 6: Fuzzy velocity profiles for influence of  $\beta$ .

where  $B = 1 - \alpha/100$  and  $B_1 = -(\alpha + 49/100)$ .

### 4. Results and Discussion

In this section, we present a numerical solution of Plane Couette flow, fully developed plane Poiseuille flow, and plane Couette–Poiseuille flow for the third-grade non-Newtonian fluid with fuzzified boundary conditions. Firstly, convert the governing equations of these problems into FDEs, then find the solutions for fuzzy velocity profiles by using ADM. Achieved fuzzy velocity profiles are plotted in Figures 5–17 for different values of  $\alpha$ -cut ( $\alpha = 0, 0.3, 0.7, 1$ ). It can be observed that as  $\alpha$  increases from 0 to 1, we have a narrow width of fuzzy velocity profiles and uncertainty decreases drastically, which finally provide crisp results for  $\alpha = 1$ .

Tables 1–3 show the comparison of the crisp velocity profile with Siddiqui et al. [4] and Yürüsoy [9]. The validation of the present study findings was determined to be in excellent agreement.

4.1. For Plane Couette Flow. The non-Newtonian parameter  $\beta$  does not exist in this solution. As a result, solutions for fuzzy velocity profiles are the same as for a Newtonian fluid.

4.2. For Fully Developed Plane Poiseuille Flow. Figures 5–8 show the effect of non-Newtonian parameter  $\beta$  on the fuzzy velocity profiles with constant pressure gradient  $p = dp/dy$  at different values of fuzzy parameter  $\alpha$ . It is observed that the lower and upper bounds of velocity profiles decrease with increasing non-Newtonian parameter

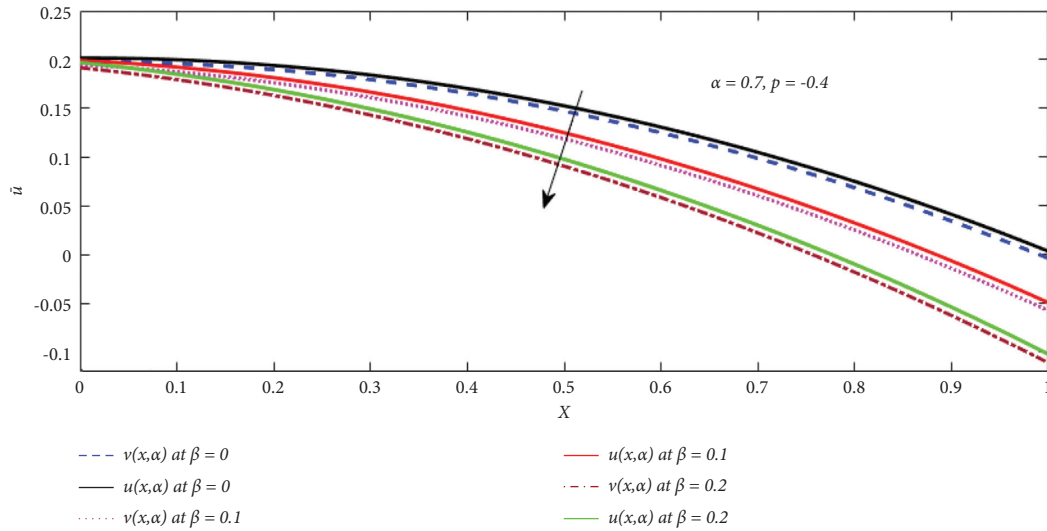


FIGURE 7: Fuzzy velocity profiles for influence of  $\beta$ .

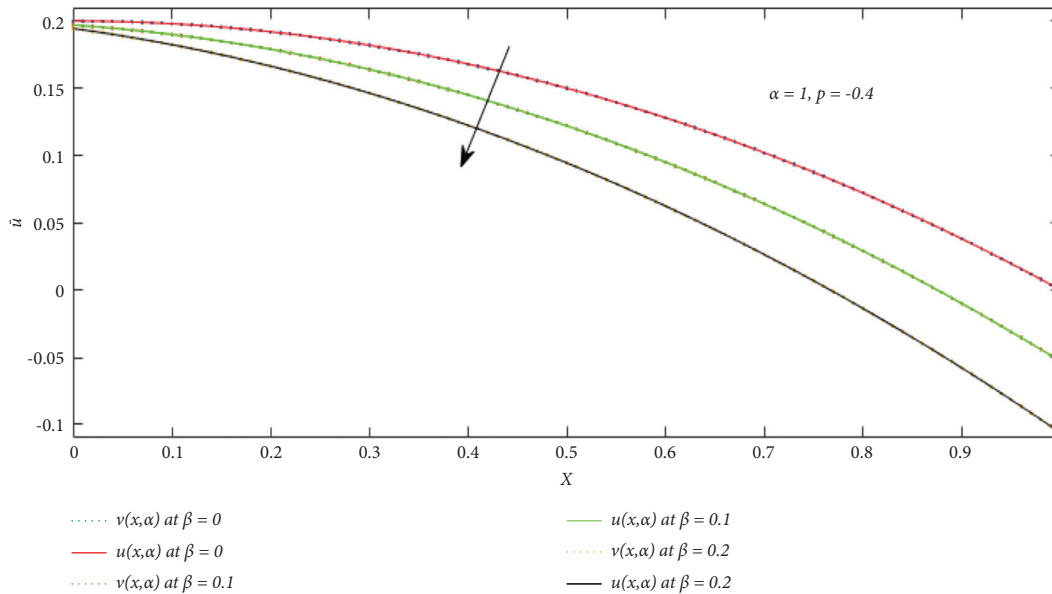


FIGURE 8: Fuzzy velocity profiles for influence of  $\beta$ .

$\beta$  as well fuzzy parameter  $\alpha$ . Figure 8 shows the good agreement of crisp solution or classical solution that lower and upper bounds of velocity profiles are the same at  $\alpha = 1$ . Figure 9 describes the lower and upper bounds of fuzzy velocity profiles at the different values of  $\alpha$ . So, for  $\alpha = 1$  the fuzzy velocity profile falls into classical velocity profile, which shows the present problem is a generalization of Siddiqui et al. [17]. Figure 10 shows the uncertain behavior in terms of the triangular fuzzy plot by fixing the values of  $x$  and  $p = dp/dy$ . The horizontal axis display the velocity profile and the vertical axis expresses the  $\alpha$  – cut which range from 0 to 1. In this figure, uncertain width gradually decreases with increasing  $\alpha$ -cut. We observed that  $v(x; \alpha)$  increases and  $u(x; \alpha)$  decreases with increasing of  $\alpha$ -cut, so the solution is strong. When  $\alpha$  increases the width between

lower and upper bounds of fuzzy velocity profiles decreases and when  $\alpha = 1$  they concur with one another. Also, the width between  $v(x; \alpha)$  and  $u(x; \alpha)$  for different values of beta is the same. This means that the uncertainty of fuzzy velocity is minimum. Table 4 shows the analysis of lower, mid and upper bounds of velocity profiles at different values of  $x$  with constant pressure gradient  $p = -0.4$ . The mid-value of a TFN concurs with the crisp or classical value of the original problem.

4.3. For Plane Couette–Poiseuille Flow. Figures 11–14 shows the effect of non-Newtonian parameter  $\beta$  on the fuzzy velocity profiles with constant pressure gradient at different values of fuzzy parameter  $\alpha$ . The fuzzy velocity profiles

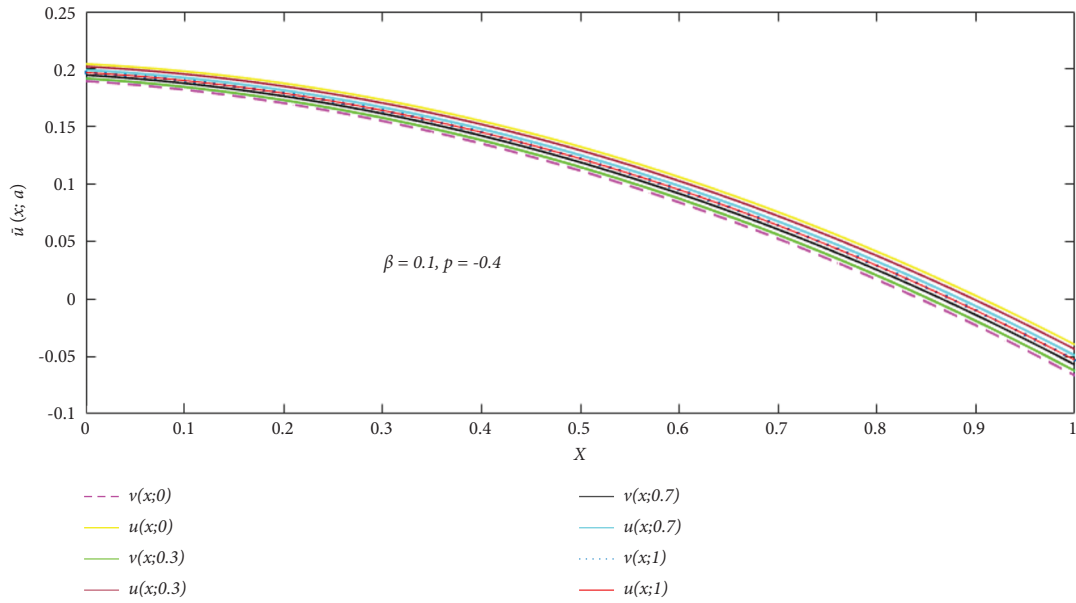


FIGURE 9: Fuzzy velocity profiles for different values of  $\alpha$ -cut ( $0 \leq \alpha \leq 1$ ).

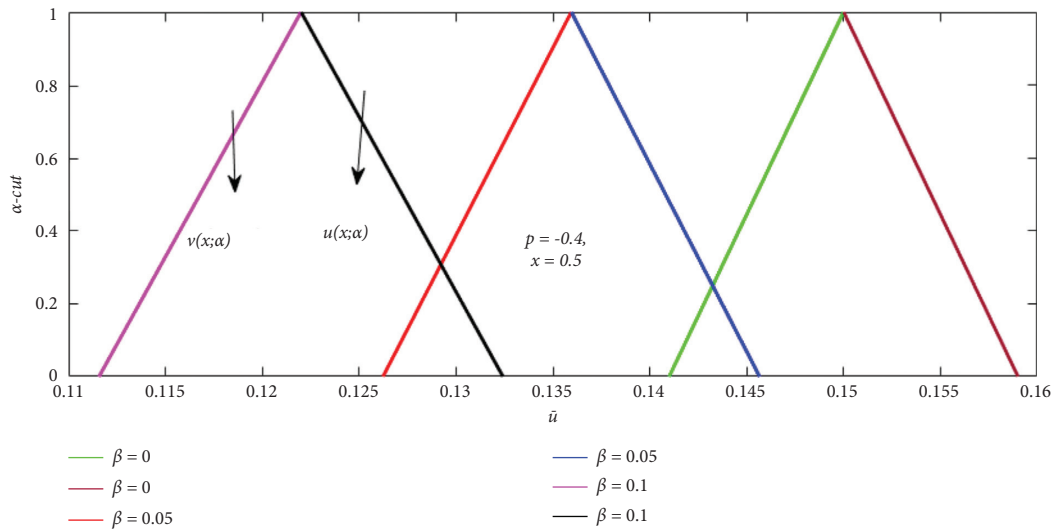


FIGURE 10: Triangular membership function of fuzzy velocity profiles for influence of  $\beta$ .

increases with increasing non-Newtonian parameter  $\beta$  and fuzzy parameter  $\alpha$ . Figure 14, shows the good agreement of crisp solution or classical solution for  $v(x; \alpha)$  and  $u(x; \alpha)$  of velocity profiles at  $\alpha = 1$ . Figure 15 describes the lower and upper bounds of fuzzy velocity profiles at the different values of  $\alpha$ . So, for  $\alpha = 1$  the fuzzy velocity profile fall into classical velocity profile, which shows the present problem is a generalization of Siddiqui et al. [17]. Figure 16 represents the fuzzy velocity profile for different ranges of the imposed pressure gradient. Figure 17 shows the uncertain behavior in terms of a triangular fuzzy plot by fixing the values of  $x = 0.1$  and  $p = -0.6$ . We observed that  $v(x; \alpha)$  increases and  $u(x; \alpha)$  decreases with increasing  $\alpha$ , so the solution is strong. The crisp or classical solution lies among the fuzzy solutions

when  $\alpha$  increases the width between lower and upper bounds of fuzzy velocity profiles decreases and at  $\alpha = 1$  the coherent with one another. Since the boundary conditions are fuzzy, the uncertain width gradually decreases with increasing  $\alpha$  and non-Newtonian parameter  $\beta$ . Table 5 shows the analysis of lower, mid, and upper bounds of velocity profiles at different values of  $x$  with constant pressure gradient  $p = -0.6$ . The mid-value of a TFN concurs with the crisp or classical value of the original problem. Furthermore, fuzzy velocity profiles always change with a certain range for any fixed  $\alpha$ -cut and the range gradually decreases with increasing the values of  $\alpha$ - cut.

This whole discussion concludes that the fuzzy velocity profile of the fluid is a better option as compared to the crisp

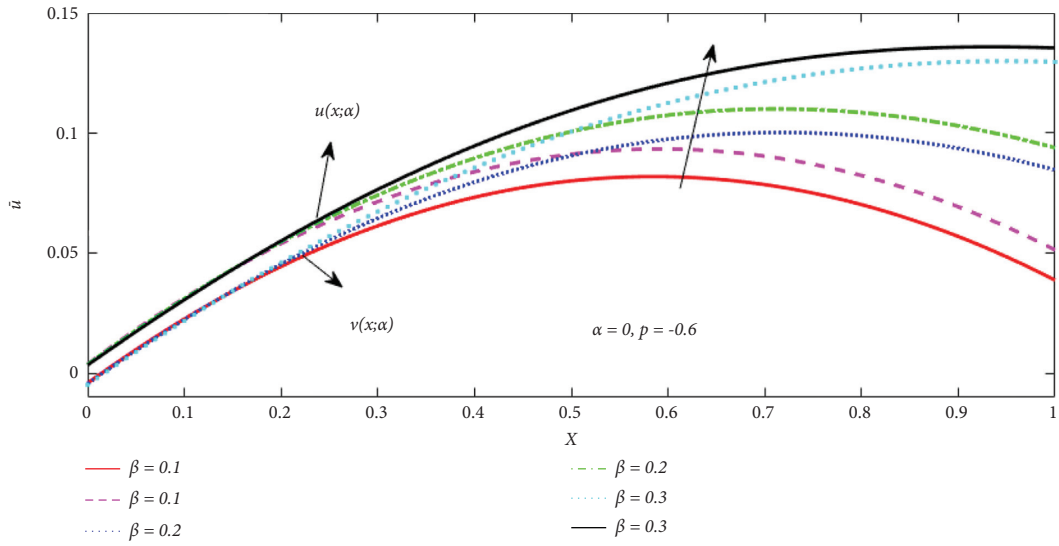


FIGURE 11: Fuzzy velocity profiles for influence of  $\beta$ .

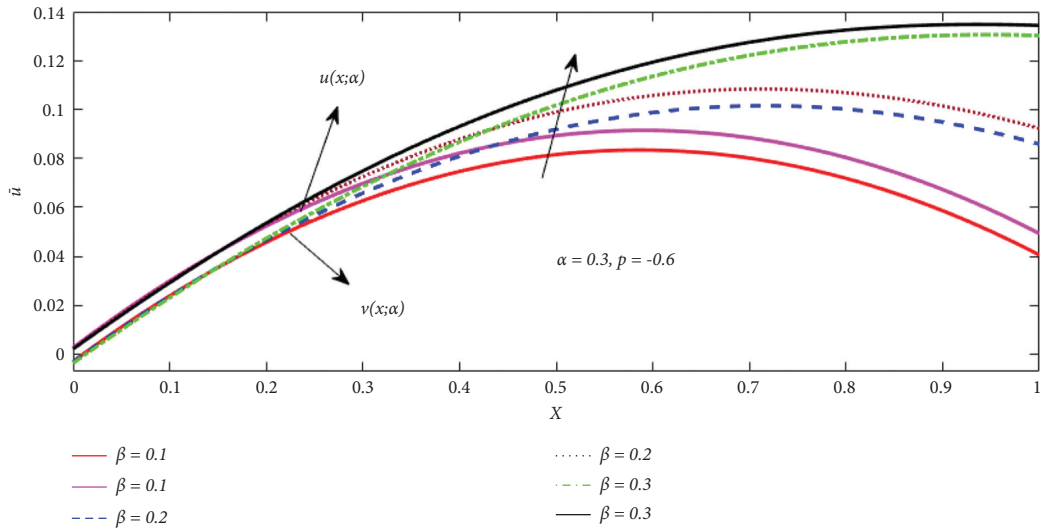


FIGURE 12: Fuzzy velocity profiles for influence of  $\beta$ .

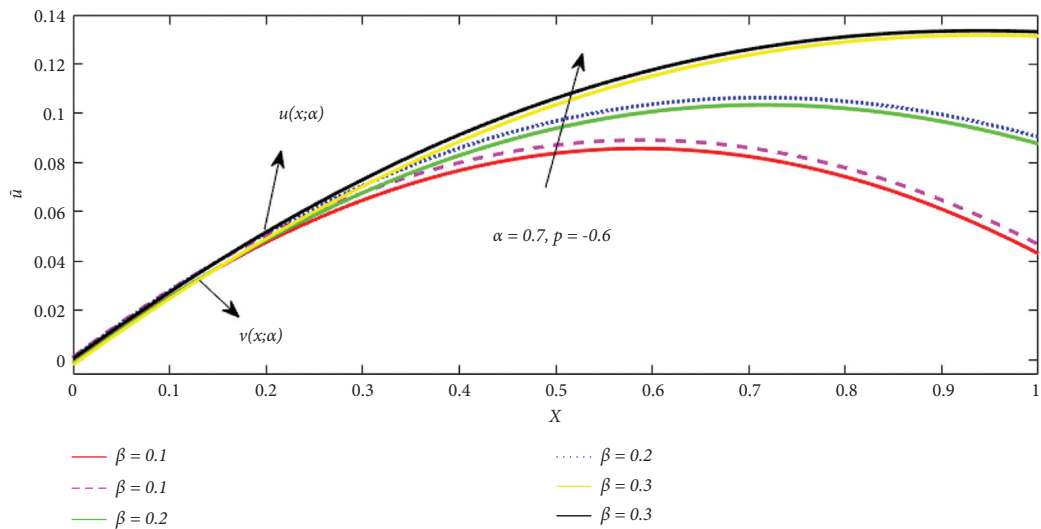


FIGURE 13: Fuzzy velocity profiles for influence of  $\beta$ .

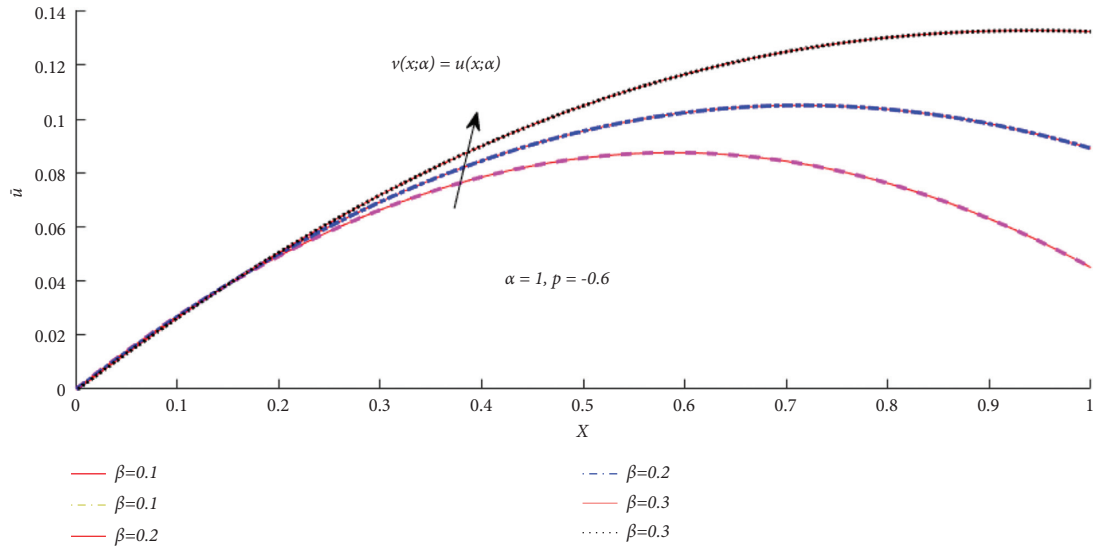


FIGURE 14: Fuzzy velocity profiles for influence of  $\beta$ .

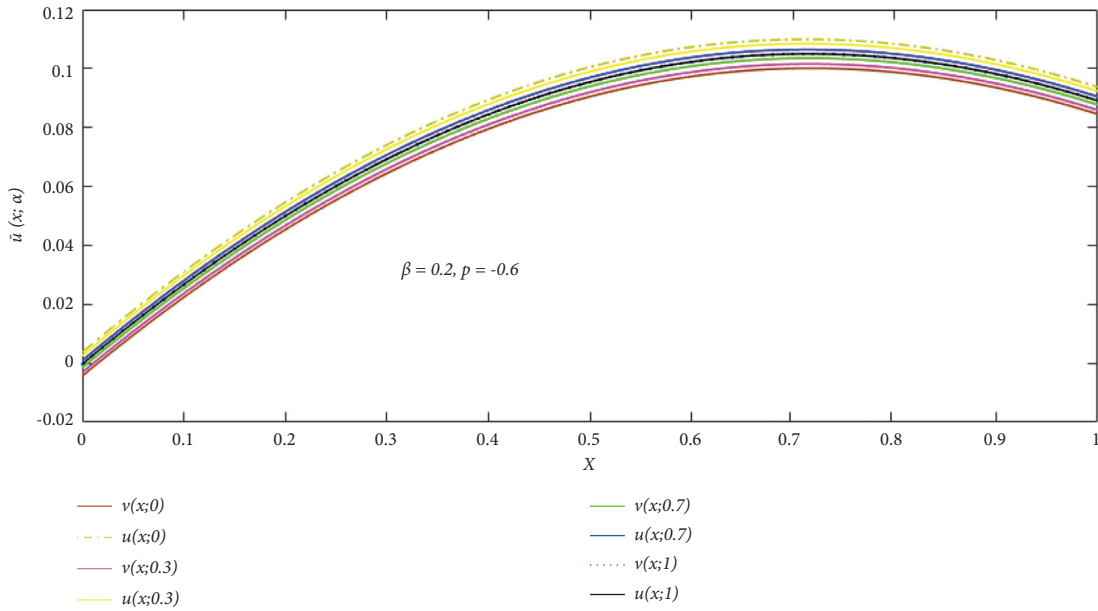


FIGURE 15: Fuzzy velocity profiles for different values of  $\alpha$ - cut ( $0 \leq \alpha \leq 1$ ).

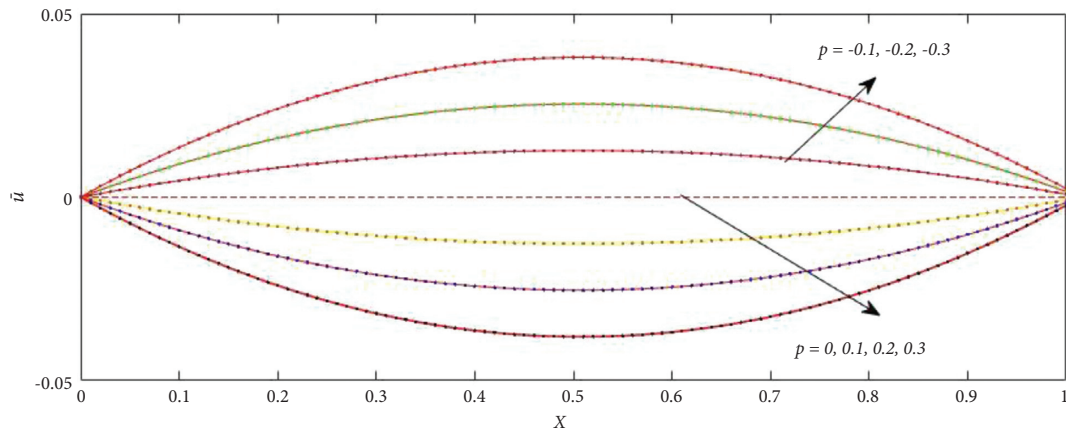


FIGURE 16: Influence of pressure gradient  $dp/dy = p$ .

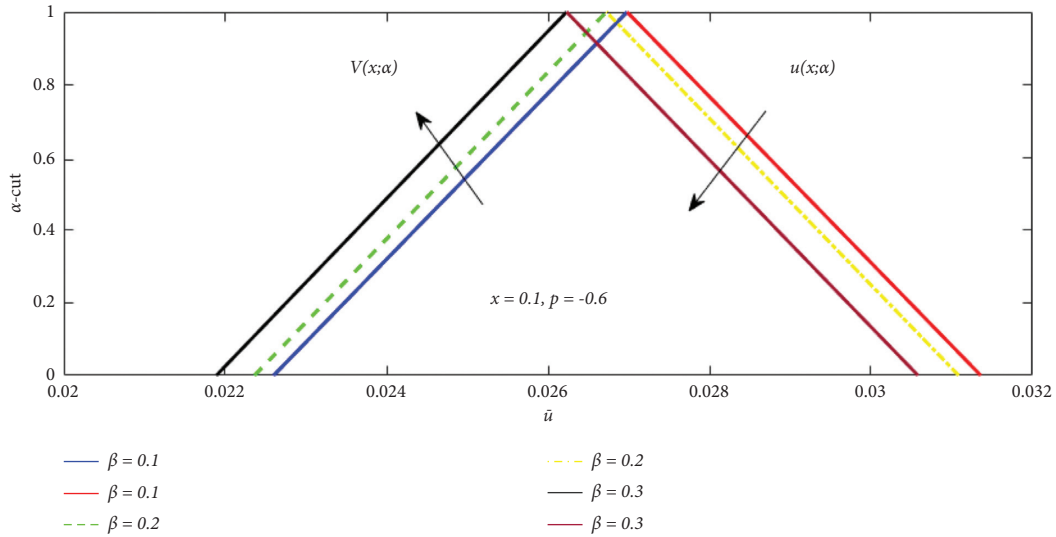


FIGURE 17: Triangular MFs of fuzzy velocity profiles for influence of  $\beta$ .

TABLE 1: Comparison of analytical results for the crisp velocity profile of Couette flow when  $\beta = 0.1$ ,  $p = -0.5$ , and  $\alpha = 1$ .

$x$	HPM [4]	PM [9]	ADM present results
0	0	0	0
0.1	0.0814178	0.091211	0.076017
0.2	0.1618119	0.181128	0.151478
0.3	0.2618251	0.301241	0.249145
0.4	0.3410156	0.374915	0.330151
0.5	0.4721819	0.467189	0.476182
0.6	0.5215171	0.572820	0.518251
0.7	0.6214168	0.667189	0.610425
0.8	0.7514268	0.771810	0.741516
0.9	0.8810148	0.882185	0.871816
1	1	1	1

TABLE 2: Comparison of analytical results for the crisp velocity profile of Poiseuille flow when  $\beta = 0.1$ ,  $p = -0.5$ , and  $\alpha = 1$ .

$x$	HPM [4]	PM [9]	ADM present results
0	0.049141	0.049792	0.048812
0.1	0.048818	0.049211	0.048314
0.2	0.046718	0.047801	0.045140
0.3	0.045168	0.045314	0.044141
0.4	0.041015	0.041830	0.040019
0.5	0.037180	0.037351	0.036124
0.6	0.031417	0.031876	0.031109
0.7	0.025001	0.025404	0.024914
0.8	0.017912	0.017934	0.017819
0.9	0.009214	0.009466	0.009164
1	0	0	0

TABLE 3: Comparison of analytical results for the crisp velocity profile of Couette–Poiseuille flow when  $\beta = 0.1$ ,  $p = -0.5$ , and  $\alpha = 1$ .

$x$	HPM [4]	PM [9]	ADM present results
0	0	0	0
0.1	0.081018	0.091401	0.044181
0.2	0.121481	0.020762	0.109168
0.3	0.194415	0.300141	0.191620
0.4	0.281510	0.411359	0.266405
0.5	0.380151	0.521415	0.361791
0.6	0.481141	0.591618	0.471819
0.7	0.601486	0.691619	0.599160
0.8	0.721412	0.791819	0.714991
0.9	0.881514	0.900410	0.871680
1	1	1	1

TABLE 4: Fuzzy solution of lower, mid and upper bounds of velocity profiles at different values of  $x$  with constant pressure gradient  $p = -0.4$ .

$x$	$v(x; \alpha)$	Mid-value	$u(x; \alpha)$
0	0.1895776184	0.1970011712	0.2044247240
0.1	0.1819776137	0.1900011710	0.1980247283
0.2	0.1703775897	0.1790011570	0.1876247244
0.3	0.1547774055	0.1640010163	0.1732246271
0.4	0.13517655524	0.1450003147	0.1548240742
0.5	0.11157377629	0.1219979280	0.1324220798
0.6	0.08396651205	0.0949915265	0.1060165410
0.7	0.05235022580	0.0639769107	0.0756035957
0.8	0.01671756767	0.0289472010	0.0411768343
0.9	-0.0229426059	-0.0101081214	0.0027263631
1	-0.0666463604	-0.0532043200	-0.0397622795

TABLE 5: Fuzzy solution of lower, mid and upper bounds of velocity profiles at different values of  $x$  with constant pressure gradient  $p = -0.6$ .

$x$	$v(x; \alpha)$	Mid value	$u(x; \alpha)$
0	-0.0043186926	-0.0002926560	0.0037333806
0.1	0.0223634776	0.0267255366	0.0310875957
0.2	0.0453558474	0.0499846994	0.0546135514
0.3	0.0644547391	0.0692807804	0.0741068218
0.4	0.0795257286	0.0844783261	0.0894309236
0.5	0.0904934414	0.0955015114	0.100509581
0.6	0.0973341525	0.1023287586	0.1073233647
0.7	0.1000709293	0.1049909429	0.1099109565
0.8	0.0987710557	0.1035731870	0.1083753183
0.9	0.0935454754	0.0982202415	0.1028950076
1	0.0845499956	0.0891454549	0.0937409143

or classical velocity profile of the fluid. Crisp or classical velocity profile of fluid gives the single flow situation of the fluid while fuzzy velocity profile of fluid gives the interval flow situation like lower and upper bounds of the velocity profile.

4.3.1. *Fully Developed Plane Poiseuille Flow.* Fuzzy velocity profiles are provided in Figures 5–10.

4.3.2. *Plane Couette–Poiseuille Flow.* Fuzzy velocity profiles, influence of pressure gradient, and triangular MFs of fuzzy velocity profiles are shown in Figures 11–17, respectively.

### 5. Conclusions

In this work, we have studied the three basic fundamental flow problems in a fuzzy environment. The dimensionless nonlinear governing equations are converted into FDEs with fuzzified boundary conditions and find their solutions using ADM. For the case of a plane Couette flow, we find the same solution as in the incident of viscous fluid. For plane Poiseuille and generalized Couette flows, triangular fuzzy numbers are used for uncertainty on the dynamic behavior of fuzzy velocity profiles. The most important findings are presented below:



- (i) Fuzzy velocity profiles increases with increasing the non-Newtonian fluid parameter  $\beta$  and fuzzy parameter ( $\alpha \in [0, 1]$ ).
- (ii) The results are indicated that the range of calculated lower and upper-velocity profiles depends upon a fuzzy parameter.
- (iii) The results are always an envelope of solutions with a crisp solution between the upper and lower bounds of the solutions. So fuzzy velocity profiles are the generalization of the crisp velocity profile for third-grade fluid between two parallel plates.
- (iv) Furthermore, it is observed that, in triangular MFs, if the width of fuzzy or uncertain velocity becomes more, then the boundary conditions are more sensitive, while for less width of fuzzy or uncertain velocity, the assumed boundary conditions are less sensitive.
- (v) The present crisp results obtained from ADM are found to be in excellent agreement as compared to existing results.
- (vi) In future work, for easier comprehension, the TFN is visualized. As a result, TFNs may be used to a variety of heat transfer challenges.

## Data Availability

No data were used to perform this research.

## Conflicts of Interest

The authors declare that they have no conflicts of interest.

## References

- [1] C. Truesdell and W. Noll, *The nonlinear field's theories of mechanics*, Springer, Heidelberg, Germany, third edition, 2004.
- [2] K. R. Rajagopal, "On the stability of third grade fluids," *Arch Mech*, vol. 32, no. 6, pp. 867–875, 1980.
- [3] K. R. Rajagopal, "Thermodynamics and stability of fluids of third grade," *Pros R Soc Lond A*, vol. 339, pp. 351–377, 1980.
- [4] A. M. Siddiqui, A. Zeb, Q. K. Ghori, and A. M. Benharbit, "Homotopy perturbation method for heat transfer flow of a third grade fluid between parallel plates," *Chaos, Solitons & Fractals*, vol. 36, no. 1, pp. 182–192, 2008.
- [5] T. Hayat, R. Ellahi, and F. M. Mahomed, "Exact solutions for thin film flow of a third grade fluid down an inclined plane," *Chaos, Solitons & Fractals*, vol. 38, no. 5, pp. 1336–1341, 2008.
- [6] M. Sajid and T. Hayat, "The application of homotopy analysis method to thin film flows of a third order fluid," *Chaos, Solitons & Fractals*, vol. 38, no. 2, pp. 506–515, 2008.
- [7] R. A. Shah, S. Islam, M. Zeb, and I. Ali, "Optimal homotopy asymptotic method for thin-film flows of a third-order fluid," *J. of Adv. Research in Scientific Computing*, vol. 2, pp. 1–14, 2011.
- [8] A. M. Siddiqui, A. A. Farooq, T. Haroon, M. A. Rana, and B. S. Babcock, "Application of he's variational iterative method for solving thin film flow problem arising in non-newtonian fluid mechanics," *World Journal of Mechanics*, vol. 02, no. 03, pp. 138–142, 2012.
- [9] M. Yürüsoy, M. Pakdemirli, and B. S. Yilbas, "Perturbation solution for a third-grade fluid flowing between parallel plates," *Proceedings of the Institution of Mechanical Engineers, Part C: Journal of Mechanical Engineering Science*, vol. 222, no. 4, pp. 653–656, 2008.
- [10] S. I. Natarov and C. P. Conrad, "The role of Poiseuille flow in creating depth-variation of asthenospheric shear," *Geophysical Journal International*, vol. 190, no. 3, pp. 1297–1310, 2012.
- [11] T. Hayat, M. Khan, and M. Ayub, "Couette and Poiseuille flows of an Oldroyd 6-constant fluid with magnetic field," *Journal of Mathematical Analysis and Applications*, vol. 298, no. 1, pp. 225–244, 2004.
- [12] T. Hayat, R. Naz, and M. Sajid, "On the homotopy solution for Poiseuille flow of a fourth grade fluid," *Communications in Nonlinear Science and Numerical Simulation*, vol. 15, no. 3, pp. 581–589, 2010.
- [13] T. Chinyoka and O. D. Makinde, "Analysis of transient generalized Couette flow of a reactive variable viscosity third-grade liquid with asymmetric convective cooling," *Math. Comput. Model*, vol. 54, no. 1, pp. 160–174, 2011.
- [14] G. Adomian, "A review of the decomposition method and some recent results for nonlinear equations," *Math Comput Model*, vol. 13, no. 7, pp. 287–99, 1992.
- [15] G. Adomian, *Solving frontier problems of physics: the decomposition method*, Kluwer, Dordrecht, Netherland, 1994.
- [16] Y. Cherruault and G. Adomian, "Decomposition methods: a new proof of convergence," *Mathematical and Computer Modelling*, vol. 18, no. 12, pp. 103–106, 1993.
- [17] A. M. Siddiqui, M. Hameed, B. M. Siddiqui, and Q. K. Ghori, "Use of Adomian decomposition method in the study of parallel plate flow of a third grade fluid," *Communications in Nonlinear Science and Numerical Simulation*, vol. 15, no. 9, pp. 2388–2399, 2010.
- [18] U. M. Pirzada and D. C. Vakaskar, "Solution of fuzzy heat equations using adomian decomposition method," *Int. J. Adv. Appl. Math. Mech.* vol. 3, no. 1, pp. 87–91, 2015.
- [19] M. Paripour, E. Hajilou, and H. Heidari, "Application of Adomian decomposition method to solve hybrid fuzzy differential equations," *J. of Taibah Uni. for Sci.* vol. 57, pp. 1658–3655, 2014.
- [20] A. M. Siddiqui, T. Haroon, S. Bhatti, and A. R. Ansari, "A comparison of the adomian and homotopy perturbation methods in solving the problem of squeezing flow between two circular plates," *Mathematical Modelling and Analysis*, vol. 15, no. 4, pp. 491–504, 2010.
- [21] L. A. Zadeh, "Fuzzy Sets," *Information and Control*, vol. 8, no. 3, pp. 338–353, 1965.
- [22] D. Dubois and H. Prade, "Operations on fuzzy numbers," *International Journal of Systems Science*, vol. 9, no. 6, pp. 613–626, 1978.
- [23] S. Seikala, "On the fuzzy initial value problem," *Fuzzy Sets and Systems*, vol. 24, no. 3, pp. 319–330, 1987.
- [24] O. Kaleva, "Fuzzy differential equations," *Fuzzy Sets and Systems*, vol. 24, no. 3, pp. 301–317, 1987.
- [25] A. Kandel and W. J. Byatt, "Fuzzy differential equations," in *Proceedings of International Conference Cybernetics and Society*, vol. 1, pp. 1213–1216, Tokyo, Japan, November 1978.
- [26] J. J. Buckley, T. Feuring, and Y. Hayashi, "Linear systems of first order ordinary differential equations: fuzzy initial conditions," *Soft Computing - A Fusion of Foundations, Methodologies and Applications*, vol. 6, no. 6, pp. 415–421, 2002.

- [27] J. J. Nieto, "The Cauchy problem for continuous fuzzy differential equations," *Fuzzy Sets and Systems*, vol. 102, no. 2, pp. 259–262, 1999.
- [28] V. Lakshmikantham and R. N. Mohapatra, "Basic properties of solutions of fuzzy differential equations," *Nonlinear Studies*, vol. 8, pp. 113–124, 2000.
- [29] J. Y. Park and H. K. Han, "Existence and uniqueness theorem for a solution of Fuzzy differential equations," *International Journal of Mathematics and Mathematical Sciences*, vol. 22, no. 2, pp. 271–279, 1999.
- [30] M. S. Hashemi, J. Malekinagad, and H. R. Marasi, "Series solution of the system of fuzzy differential equations," *Adv. in Fuzzy Syst*, vol. 16, 2012.
- [31] M. Mosleh, "Fuzzy neural network for solving a system of fuzzy differential equations," *Applied Soft Computing*, vol. 13, no. 8, pp. 3597–3607, 2013.
- [32] N. Gasilov, S. E. Amrahov, and A. G. Fatullayev, "A geometric approach to solve fuzzy linear systems of differential equations," *Appl. Math. Inf. Sci.* vol. 5, no. 3, pp. 484–499, 2011.
- [33] A. Khastan and J. J. Nieto, "A boundary value problem for second order fuzzy differential equations," *Nonlinear Analysis: Theory, Methods & Applications*, vol. 72, no. 9-10, pp. 3583–3593, 2010.
- [34] S. P. Mondal and T. K. Roy, "First order linear homogeneous ordinary differential equation in fuzzy environment based on laplace transform," *J. of Fuzzy Set Valued Anal*, vol. 1-18, 2013.
- [35] H. Zarei, A. V. Kamyad, and A. A. Heydari, "Fuzzy modeling and control of hiv infection," *Compu. Math. Meth. Medi.* vol. 2017, Article ID 893474, 2012.
- [36] S. P. Mondal, S. Banerjee, and T. K. Roy, "First order linear homogeneous ordinary differential equation in fuzzy environment," *Int. J. Pure Appl. Sci. Tech*, vol. 14, no. 1, pp. 16–26, 2013.
- [37] M. Guo, X. Xue, and R. Li, "Impulsive functional differential inclusions and fuzzy population models," *Fuzzy Sets and Systems*, vol. 138, no. 3, pp. 601–615, 2003.
- [38] L. C. Barros, R. C. Bassanezi, and P. A. Tonelli, "Fuzzy modelling in population dynamics," *Ecological Modelling*, vol. 128, no. 1, pp. 27–33, 2000.
- [39] M. Z. Ahmad and B. De Baets, "A Predator-Prey Model with Fuzzy Initial Populations," in *Proceedings of the Joint 2009 International Fuzzy Systems Association World Congress and 2009 European Society of Fuzzy Logic and Technology Conference*, IFSA-EUSFLAT, Lisbon, Portugal, July 2009.
- [40] J. Casasnovas and F. Rosselló, "Averaging fuzzy biopolymers," *Fuzzy Sets and Systems*, vol. 152, no. 1, pp. 139–158, 2005.
- [41] G. L. Diniz, J. F. R. Fernandes, J. F. C. A. Meyer, and L. C. Barros, "A fuzzy cauchy problem modeling the decay of the biochemical oxygen demand in water," vol. 1, pp. 512–516, in *Proceedings Joint 9th IFSA World Congress and 20th NAFIPS International Conference*, vol. 1, IEEE, Vancouver, BC, Canada, July 2001.
- [42] A. Bencsik, B. Bede, J. Tar, and J. Fodor, "Fuzzy differential equations in modeling hydraulic differential servo cylinders," in *In: Proceedings of the Third Romanian-Hungarian joint symposium on applied computational intelligence (SACI)*, Timisoara, Romania, 2006.
- [43] B. Bede, I. J. Rudas, and J. Fodor, "Friction model by fuzzy differential equations," vol. 4529, pp. 23–32, in *Proceedings of the Foundations of Fuzzy Logic and Soft Computing, 12th International Fuzzy Systems Association World Congress, IFSA 2007*, vol. 4529, pp. 23–32, Springer-Verlag, Cancun, Mexico, June 2007.
- [44] M. S. El Naschie, "From experimental quantum optics to quantum gravity via a fuzzy Kähler manifold," *Chaos, Solitons & Fractals*, vol. 25, no. 5, pp. 969–977, 2005.
- [45] T. Allahviranloo and S. Salahshour, "Applications of fuzzy Laplace transforms," *Soft Computing*, vol. 17, no. 1, pp. 145–158, 2013.
- [46] M. Oberguggenberger and S. Pittschmann, "Differential equations with fuzzy parameters," *Math. Mod. Syst*, vol. 5, pp. 181–202, 1999.
- [47] S. Hajighasemi, T. Allahviranloo, M. Khezerloo, M. Khorasany, and S. Salahshour, "Existence and uniqueness of solutions of fuzzy Volterra integro-differential equations," *Communications in Computer and Information Science*, vol. 81, pp. 491–500, 2010.
- [48] U. Biswal, S. Chakraverty, and B. K. Ojha, "Natural convection of nanofluid flow between two vertical flat plates with imprecise parameter," *Coupled Systems Mechanics*, vol. 9, no. 3, pp. 219–235, 2020.
- [49] G. Borah, P. Dutta, and G. C. Hazarika, "Numerical study on second-grade fluid flow problems using analysis of fractional derivatives under fuzzy environment," *Soft Computing Techniques and Applications. Advances in Intelligent Systems and Computing*, vol. 1248, 2021.
- [50] M. Nadeem, I. Siddique, F. Jarad, and R. N. Jamil, "Numerical study of mhd third-grade fluid flow through an inclined channel with ohmic heating under fuzzy environment," *Mathematical Problems in Engineering*, vol. 2021, Article ID 9137479, 17 pages, 2021.
- [51] U. Biswal, S. Chakraverty, B. K. Ojha, and A. K. Hussein, "Study of Jeffery-Hamel flow problem for nanofluid with fuzzy volume fraction using double parametric based Adomian decomposition method," *International Communications in Heat and Mass Transfer*, vol. 126, Article ID 105435, 2021.
- [52] E. I. Allaoui, S. Melliani, and L. S. Chadli, "A mathematical fuzzy model to giving up smoking," in *Proceedings of the IEEE 6th Inter. Conference on Optimization and Application*, pp. 1–6, ICOA, Beni Mellal, Morocco, April 2020.
- [53] R. M. Zulqarnain, X. L. Xin, I. Siddique, W. Asghar Khan, and M. A. Yousif, "TOPSIS method based on correlation coefficient under pythagorean fuzzy soft environment and its application towards green supply chain management," *Sustainability*, vol. 13, no. 4, 1642 pages, 2021.
- [54] R. M. Zulqarnain, I. Siddique, R. Ali, F. Jarad, A. Samad, and T. Abdeljawad, "Neutrosophic hypersoft matrices with application to solve multiattributive decision-making problems," *Complexity*, vol. 2021, Article ID 5589874, 17 pages, 2021.
- [55] R. M. Zulqarnain, I. Siddique, R. Ali, D. Pamucar, D. Marinkovic, and D. Bozanic, "Robust aggregation operators for intuitionistic fuzzy hypersoft set with their application to solve MCDM problem," *Entropy*, vol. 23, no. 6, 688 pages, 2021.
- [56] R. M. Zulqarnain, I. Siddique, F. Jarad, R. Ali, and T. Abdeljawad, "Development of TOPSIS technique under pythagorean fuzzy hypersoft environment based on correlation coefficient and its application towards the selection of antiviral mask in COVID-19 pandemic," *Complexity*, vol. 2021, Article ID 6634991, 27 pages, 2021.
- [57] I. Siddique, R. M. Zulqarnain, R. Ali, F. Jarad, and A. Iampan, "Multicriteria decision-making approach for aggregation operators of pythagorean fuzzy hypersoft sets," *Computational Intelligence and Neuroscience*, vol. 2021, pp. 1687–5265, Article ID 2036506, 2021.

- [58] M. Nadeem, A. Elmoasry, I. Siddique et al., "Study of triangular fuzzy hybrid nanofluids on the natural convection flow and heat transfer between two vertical plates," *Computational Intelligence and Neuroscience*, vol. 2021, Article ID 3678335, 15 pages, 2021.
- [59] I. Siddique, R. M. Zulqarnain, M. Nadeem, and F. Jarad, "Numerical simulation of mhd couette flow of a fuzzy nanofluid through an inclined channel with thermal radiation effect," *Computational Intelligence and Neuroscience*, vol. 2021, Article ID 6608684, 16 pages, 2021.

## Research Article

# Decision-Making Approach Based on Generalized Aggregation Operators with Complex Single-Valued Neutrosophic Hesitant Fuzzy Set Information

Harish Garg <sup>1</sup>, Zeeshan Ali,<sup>2</sup> Ibrahim M. Hezam <sup>3</sup>, and Jeonghwan Gwak <sup>4,5,6,7</sup>

<sup>1</sup>School of Mathematics, Thapar Institute of Engineering & Technology, Deemed University, Patiala 147004, Punjab, India

<sup>2</sup>Department of Mathematics and Statistics, International Islamic University Islamabad, Islamabad, Pakistan

<sup>3</sup>Department of Statistics & Operations Research, College of Sciences, King Saud University, Riyadh, Saudi Arabia

<sup>4</sup>Department of Software, Korea National University of Transportation, Chungju 27469, Republic of Korea

<sup>5</sup>Department of Biomedical Engineering, Korea National University of Transportation, Chungju 27469, Republic of Korea

<sup>6</sup>Department of AI Robotics Engineering, Korea National University of Transportation, Chungju 27469, Republic of Korea

<sup>7</sup>Department of IT & Energy Convergence (BK21 FOUR), Korea National University of Transportation, Chungju 27469, Republic of Korea

Correspondence should be addressed to Harish Garg; [harishg58iitr@gmail.com](mailto:harishg58iitr@gmail.com)

Received 25 September 2021; Accepted 13 December 2021; Published 10 January 2022

Academic Editor: Dragan Pamučar

Copyright © 2022 Harish Garg et al. This is an open access article distributed under the Creative Commons Attribution License, which permits unrestricted use, distribution, and reproduction in any medium, provided the original work is properly cited.

A strategic decision-making technique can help the decision maker to accomplish and analyze the information in an efficient manner. However, in our real life, an uncertainty will play a dominant role during the information collection phase. To handle such uncertainties in the data, we present a decision-making algorithm under the single-valued neutrosophic (SVN) environment. The SVN is a powerful way to deal the information in terms of three degrees, namely, “truth,” “falsity,” and “indeterminacy,” which all are considered independent. The main objective of this study is divided into three folds. In the first fold, we state the novel concept of complex SVN hesitant fuzzy (CSVNHF) set by incorporating the features of the SVN, complex numbers, and the hesitant element. The various fundamental and algebraic laws of the proposed CSVNHF set are described in details. The second fold is to state the various aggregation operators to obtain the aggregated values of the considered CSVNHF information. For this, we stated several generalized averaging operators, namely, CSVNHF generalized weighted averaging, ordered weighted average, and hybrid average. The various properties of these operators are also stated. Finally, we discuss a multiattribute decision-making (MADM) algorithm based on the proposed operators to address the problems under the CSVNHF environment. A numerical example is given to illustrate the work and compare the results with the existing studies’ results. Also, the sensitivity analysis and advantages of the stated algorithm are given in the work to verify and strengthen the study.

## 1. Introduction

The multiattribute decision-making (MADM) method is one of the efficient methods to solve the decision-making problems by considering the different experts, their preferences, and alternatives. The chief objective of this problem is to address the best alternatives, when the information related to them is accessed under the vague and imprecise information. In other words, the decision-making strategy aims to grow the chance of the benefits and reduce the

chance of the cost during the decision-making procedure for simplifying genuine life dilemmas. Since its appearance, a huge number of people have worked on decision-making strategies under the presence of a crisp set. However, in several situations, it is very complicated to provide the information related to the objects in terms of precise number, due to the involvement of the uncertainties in the data. To reduce the loss of data during the process, in 1965, Zadeh [1] firstly put forward the theory of fuzzy set (FS), by extending the range of the crisp set (which is  $\{0, 1\}$ ) to the unit interval.

Due to this beneficial work, a lot of space was created for a decision maker to make a beneficial decision from the family of alternatives. After the successful presentation of the FS theory, a huge number of individuals have described it in the circumstance of different places [2]. As ambiguity and complexity are involved in every region of life, in the presence of these dilemmas, it is very complicated for FS to survive with the old mathematical structure (covered only truth grade (TG)). In several cases, several experts have faced a lot of data in the arrangement of “yes” or “no,” which is very complex for FS to resolve. To reduce the level of the deficiencies and worries, Atanassov [3] changed the shape of FS and put forward the well-known shape, called intuitionistic FS (IFS). IFS is the modified technique of FS, which includes two different terms, called TG  $\overline{F}(u)$  and falsity grade (FG)  $F(u)$  with a satiable and strong character in the shape of  $0 \leq \overline{F}(u) + F(u) \leq 1$ . IFS is a different structure from the mathematical structure of FS to switch uncertain data. By taking advantage of the IFSs, several studies have been conducted by various scholars such as interval-valued IFSs [4], distance measures [5], circular IFS [6], and so on.

In the IFSs, each element is characterized with two degrees, truth and falsity, to access the information. However, in several real-life situations, very complex ambiguity is encountered during processing the information, and hence under the consideration of these dilemmas, it is very complicated for IFS to survive with the old mathematical structure (in terms of TG and FG only). In other words, sometimes several experts have faced a lot of data in the arrangement of “yes,” “abstinence,” and “no,” which is very complex for IFS to resolve. To reduce the level of such deficiencies, the fundamental mathematical structure of the neutrosophic set (NS) was put forward by Smarandache [7]. NS is one of the massive dominant and reliable techniques which can easily determine the solution to every complicated problem that occurs in genuine life dilemmas. The concept of NS is extended to the single-valued NS (SVNS) and its corresponding operators [8] by the researchers. Since its appearance, scholars have studied it under different environments. For instance, in [9], the authors have defined the Dombi weighted aggregation operators for the collections of SVNSs. In [10], the scholars put forward the Bonferroni mean operators for SVNS. In [11], the authors put forward the COPRAS method for SVNS. For more details about the study on NSs, we refer the readers to [12–17] and their corresponding references.

In all the studies listed above, almost all the studies were conducted by considering only the real component of the grades of the element. However, the periodic nature of the rating of the expert is not considered in the decision-making process. To address it completely, there is a need to express the rating of the expert from real interval  $[0, 1]$  to the unit disc in the complex plane. This idea was highlighted by Ramot et al. [18] in 2002 who presented the concept of complex FS (CFS). In CFS, each object is identified with two degrees TG and FG under complex domain such as  $t' e^{i2\pi\theta_{t'}}$  where  $t', \theta_{t'} \in [0, 1]$  represent the real and amplitude terms of the expert rating. It is clearly seen that CFS can handle the vague information with one or two sorts of data in the shape

of singleton terms. Some application of the CFS towards the decision-making process is summarized in [19]. Again, the scope of the CFS is limited as it considers only the truth degree and fails to consider the falsity degree at the time of the execution. For instance, if some expert diagnosed data like “yes” or “no” and each has two possibilities, then CFS is very complicated for diagnosing the solution of the above scenario. To reduce the above complications, Alkouri and Salleh [20] proposed the complex IFS (CIFIS), which includes the two different terms, called TG ( $t' e^{i2\pi\theta_{t'}}$ ) and FG ( $f' e^{i2\pi\theta_{f'}}$ ) in the shape of complex numbers with proficient and well-known characteristics  $0 \leq t' + f' \leq 1$  and  $0 \leq \theta_{t'} + \theta_{f'} \leq 1$ . To handle problematic and unseen situations, a huge number of people have employed the above theory in different regions, for illustration, the study in [21] includes the distance measures constructed under the CIFISs, while the study in [22] includes the information measures constructed under the CIFIS. Further, CIFIS theory has been widely applied in different categories such as aggregation operators [23], group theory [24], and generalized geometric operators [25].

Since CIFIS theory is able to deal only with “yes” or “no” decision in the form of degrees TG and FG, it is unable to deal with the term “abstinence.” For this, a structure of complex NS (CNS) was proposed by Ali and Smarandache [26] by considering the independent membership grades of “yes,” “abstinence,” and “no” over the unit disc of complex plane. The structure of CNS is easily implemented in every region of life which includes ambiguity and awkward sort of data. In order to flexibly share preferences, Torra [27] came up with the idea of hesitant fuzzy set (HFS), which allowed agents to provide multiple membership grades for a specific alternative-criterion pair. By this, the issue of hesitation was handled effectively. Related to MADM problems, several researchers have addressed the problem by using HFS features. For instance, Rodriguez et al. [28] investigated an interesting review on HFS models and its usage in MADM models. Xu and Zhou [29] identified a problem with HFS and designed a consensus building model by considering multiple experts for a specific alternative-criterion pair. In [30], the authors defined the similarity measures based on complex HFS and stated their application to pattern recognition.

From the above listed literature, we noted that the several researchers have utilized the advantages of CIFIS, HFS, NS, and CNS to address the problems related to the MADM. However, it is noted that all these theories are unable to handle some uncertain cases which occur during accessing the decision-making problems. For instance, if a person made committee, for laptop enterprise, which consists of ten members, the head of this committee would like to choose the suitable laptop according to the feasibility and suitability. To get the best one, each committee member provides their opinions about different laptops in terms of their prices and name of the model. As the model and price of the laptop change frequently over time, there exist a lot of uncertainties during the execution. Under such circumstances, it is difficult to access the information using several existing sets. To address it completely, in this article, we have presented an

extension of the NSs by keeping the features of hesitant set and complex membership degree and defined the novel set named as complex single-valued neutrosophic hesitant fuzzy set (CSVNHFS). The idea behind this set is to address the ambiguity in the data when it is arranged in the form of “yes,” “abstinence,” and “no” under the complex domain. In the presented set, each element is characterized with three independent hesitant degrees, namely, TG ( $t' e^{i\theta_{t'}}$ ), abstinence ( $a' e^{i\theta_{a'}}$ ), and FG ( $f' e^{i\theta_{f'}}$ ), over the unit disc of complex plane with the conditions  $0 \leq t' + a' + f' \leq 3$  and  $+$  where  $0 \leq t', a', f' \leq 1$  and  $0 \leq \theta_{t'}, \theta_{a'}, \theta_{f'} \leq 2$ . After managing the information under such features and to state more information about it, we define various operational laws and study their characteristics. To explore about the laws, we stated several weighted averaging operators to aggregate the collective information into a single one. Additionally, we state a MADM algorithm to explain the working of the proposed work and demonstrate it with the help of numerical examples. The major advantages of the proposed set are that several existing theories are considered as a special case of the proposed one. For instance, by removing the components  $\theta_{t'}, \theta_{a'}, \theta_{f'}$  during the information phase, the proposed set reduces to SVNS. On the other hand, when we set  $\theta_{a'} = \theta_{f'} = 0$ , then the set reduces to CHFS. Similarly, when we set  $\theta_{a'} = 0$  and all other degrees as a single number, then it reduces to CIFS. Finally, when we consider all the degrees in the form of singleton set, then the proposed CSVNHFS reduces to CSVNS, while when we set  $\theta_{t'} = \theta_{a'} = \theta_{f'} = 0$ , then the set reduces to SVN hesitant fuzzy set.

In this paper, the main contribution of the present work is summarized as follows:

- (1) To present a new concept named as CSVNHFS to address the uncertainties in the data and hence describe their algebraic and operational laws.
- (2) To initiate several generalized averaging operators, namely, CSVNHG generalized weighted averaging, ordered weighted average, and hybrid average, denoted by CSVNHFGWA, CSVNHFGOWA, and CSVNHFGHWA, respectively
- (3) To discuss the MADM technique under the presence of stated work. Also, to show the flexibility of the stated operators, several important results and their properties are also elaborated.
- (4) A numerical example is given to illustrate the work and compare the results with the existing studies' results. Also, the sensitivity analysis and advantages of the stated algorithm are given in the work to verify and strengthen the study.

The rest of the work is organized as follows. In Section 2, we revise various prevailing concepts like FSs, CFSs, NSs, SVNSs, CNSs, HFSS, generalized weighted averaging (GWA), generalized ordered weighted averaging (GOWA), generalized hybrid averaging (GHA) operators, and their operational laws. In Section 3, we analyze the fundamental theory of the CSVNHFS setting and described its algebraic

laws. In Section 4, we define the various generalized operators, namely, CSVNHFGWA, CSVNHFGOWA, and CSVNHFGHWA. To show the flexibility of the diagnosed operators, several important results and their properties are also elaborated. In Section 5, a MADM algorithm is stated and illustrated with numerical example. Sensitivity analysis and advantages of the work are also presented to verify and feasibility of the theory. Section 6 draws the conclusion of our study.

## 2. Preliminaries

In this section, some prevailing concepts are revised. Let  $X$ ,  $\mathbb{F}(u)$ ,  $\mathbb{A}(u)$ , and  $F(u)$ , be fixed set, TG, abstinence, and FG, respectively.

*Definition 1* (see [1]). The FS is initiated by

$$F = \left\{ \frac{(u, \mathbb{F}(u))}{u \in X} \right\}, \quad (1)$$

where  $0 \leq \mathbb{F}(u) \leq 1$ .

*Definition 2* (see [18]). The CFS is initiated by

$$N = \left\{ \frac{(u, \mathbb{F}(u))}{u \in X} \right\}, \quad (2)$$

where  $\mathbb{F}(u) = t' e^{i\theta_{t'}}$  with the conditions  $0 \leq t' \leq 1$  and  $0 \leq \theta_{t'} \leq 2$ .

*Definition 3* (see [7]). The NS is initiated by

$$N = \left\{ \frac{(u, \mathbb{F}(u), \mathbb{A}(u), F(u))}{u \in X} \right\}, \quad (3)$$

with the conditions  $0^- E\mathbb{F}(u) + \mathbb{A}(u) + F(u)E3^+$  and  $0^- E\mathbb{F}(u), \mathbb{A}(u), F(u)E1^+$ . Further,  $n = \{\mathbb{F}(u), \mathbb{A}(u), F(u)\}$  represents the NN (neutrosophic number).

*Definition 4* (see [8]). The SVNS is initiated by

$$N = \left\{ \frac{(u, \mathbb{F}(u), \mathbb{A}(u), F(u))}{u \in X} \right\}, \quad (4)$$

with the conditions  $0 \leq \mathbb{F}(u) + \mathbb{A}(u) + F(u) \leq 3$  and  $0 \leq \mathbb{F}(u), \mathbb{A}(u), F(u) \leq 1$ . Further,  $n = \{\mathbb{F}(u), \mathbb{A}(u), F(u)\}$  represents the single-valued neutrosophic number (SVNN); simply, we write  $n = (\mathbb{F}, \mathbb{A}, F)$ .

*Definition 5* (see [26]). The CNS is initiated by

$$N = \left\{ \frac{(u, \mathbb{F}(u), \mathbb{A}(u), F(u))}{u \in X} \right\}, \quad (5)$$

where  $\mathbb{F}(u) = t' e^{i\theta_{t'}}$ ,  $\mathbb{A}(u) = a' e^{i\theta_{a'}}$ , and  $F(u) = f' e^{i\theta_{f'}}$  with the conditions  $0^- \leq t' + a' + f' \leq 3^+$  and  $0^- \leq \theta_{t'} + \theta_{a'} + \theta_{f'} \leq 6^+$ , where  $0^- \leq t', a', f' \leq 1^+$  and  $0^- \leq \theta_{t'}, \theta_{a'}, \theta_{f'} \leq 2^+$ . Further,  $n = \{\mathbb{F}(u), \mathbb{A}(u), F(u)\}$  represents the complex neutrosophic number (CNN); simply, we write  $n = (\mathbb{F}, \mathbb{A}, F) = (t' e^{i\theta_{t'}}, a' e^{i\theta_{a'}}, f' e^{i\theta_{f'}})$ .

*Definition 6.* (see [27]). A HFS is initiated by

$$E = \{(u, h_E(u)) : \text{where } h_E(u) \text{ is a finite subset of } [0, 1]\}, \quad (6)$$

is called HFS, where  $h = h_E(u)$  is called hesitant fuzzy element (HFE).

*Definition 7* (see [27]). Let  $h, h_1$ , and  $h_2$  be three HFEs with  $\gamma > 0$ . Then,

- (1)  $h_1 \oplus h_2 = \coprod_{t_1 \in h_1, t_2 \in h_2} \{t_1 + t_2 - t_1 t_2\}$ .
- (2)  $h_1 \otimes h_2 = \coprod_{t_1 \in h_1, t_2 \in h_2} \{t_1 t_2\}$ .
- (3)  $h^\gamma = \prod_{t \in h} \{t^\gamma\}$ .
- (4)  $\gamma h = \coprod_{t \in h} \{1 - (1 - t)^\gamma\}$ .

*Definition 8* (see [8]). The generalized weighted average (GWA) operator is given by GWA:  $\Omega^n \rightarrow \Omega$ :

$$\text{GWA}(n_1, n_2, \dots, n_n) = \left( \sum_{i=1}^n \omega_i n_i^\gamma \right)^{1/\gamma}, \quad (7)$$

where  $\Omega$  represents the family of all positive integers with  $\gamma > 0$ . Further, the weighted vector is denoted and defined by  $\omega = (\omega_1, \omega_2, \dots, \omega_n)^\top$ ,  $\omega_i \in [0, 1]$ , where  $\sum_{i=1}^n \omega_i = 1$ .

*Definition 9* (see [8]). The generalized ordered weighted average (GOWA) operator is given by GOWA:  $\Omega^n \rightarrow \Omega$ :

$$\text{GOWA}(n_1, n_2, \dots, n_n) = \left( \sum_{i=1}^n \omega_i n_{o(i)}^\gamma \right)^{1/\gamma}, \quad (8)$$

where  $\Omega$  represents the family of all positive integers with  $\gamma > 0$  and  $n_{o(i)}$  is the  $i$ th largest term of  $n_i$ , i.e.,  $n_{o(i)} \leq n_{o(i-1)}$ . Further, the weighted vector is denoted and defined by  $\omega = (\omega_1, \omega_2, \dots, \omega_n)^\top$ ,  $\omega_i \in [0, 1]$ , where  $\sum_{i=1}^n \omega_i = 1$ .

*Definition 10* (see [8]). The generalized hybrid weighted average (GHWA) operator is given by GHWA:  $\Omega^n \rightarrow \Omega$ :

$$\text{GHWA}(n_1, n_2, \dots, n_n) = \left( \sum_{i=1}^n \omega_i n_{o(i)}^\gamma \right)^{1/\gamma}, \quad (9)$$

where  $\Omega$  represents the family of all positive integers with  $\gamma > 0$  and  $n_{o(i)}$  is the  $i$ th largest term of  $n_i$ , i.e.,  $n_{o(i)} \leq n_{o(i-1)}$ , where  $n'_i = n \omega_i n_i$ . Further, the weighted vector is denoted and defined by  $\omega = (\omega_1, \omega_2, \dots, \omega_n)^\top$ ,  $\omega_i \in [0, 1]$ , where  $\sum_{i=1}^n \omega_i = 1$ , and  $\omega = (\omega_1, \omega_2, \dots, \omega_n)^\top$ ,  $\omega_i \in [0, 1]$ , where  $\sum_{i=1}^n \omega_i = 1$ .

### 3. Proposed CSVNHFS

In this study, we explored two sets named as CSVNSs and CSVNHFSs and their algebraic laws.

#### 3.1. Complex Single-Valued Neutrosophic Fuzzy Set (CSVNFS)

*Definition 11.* The CSVNFS is initiated by

$$N = \left\{ \frac{(u, \overline{F}(u), \underline{A}(u), F(u))}{u \in X} \right\}, \quad (10)$$

where  $\overline{F}(u) = t' e^{i\theta_{t'}}$ ,  $\underline{A}(u) = a' e^{i\theta_{a'}}$ , and  $F(u) = f' e^{i\theta_{f'}}$  with the conditions  $0 \leq t' + a' + f' \leq 3$  and  $0 \leq \theta_{t'} + \theta_{a'} + \theta_{f'} \leq 6$ , where  $0 \leq t', a', f' \leq 1$  and  $0 \leq \theta_{t'}, \theta_{a'}, \theta_{f'} \leq 2$ . Further,  $u = \{\overline{F}(u), \underline{A}(u), F(u)\}$  represents the complex single-valued neutrosophic fuzzy number (CSVNFN). Symbolically,  $n = (\overline{F}, \underline{A}, F) = (t' e^{i\theta_{t'}}, a' e^{i\theta_{a'}}, f' e^{i\theta_{f'}})$ .

*Definition 12.* Let  $n_1 = (\overline{F}_1, \underline{A}_1, F_1) = (t'_1 e^{i\theta_{t'_1}}, a'_1 e^{i\theta_{a'_1}}, f'_1 e^{i\theta_{f'_1}})$  and  $n_2 = (\overline{F}_2, \underline{A}_2, F_2) = (t'_2 e^{i\theta_{t'_2}}, a'_2 e^{i\theta_{a'_2}}, f'_2 e^{i\theta_{f'_2}})$  be two CSVNFNs with  $\gamma > 0$ . Then,

- (1)  $n_1 \oplus n_2 = \left( (t'_1 + t'_2 - t'_1 t'_2) e^{i(\theta_{t'_1} + \theta_{t'_2} - \theta_{t'_1} \theta_{t'_2} / 2\pi)}, (a'_1 a'_2) e^{i(\theta_{a'_1} + \theta_{a'_2} - \theta_{a'_1} \theta_{a'_2} / 2\pi)}, (f'_1 f'_2) e^{i(\theta_{f'_1} + \theta_{f'_2} - \theta_{f'_1} \theta_{f'_2} / 2\pi)} \right)$ .
- (2)  $n_1 \otimes n_2 = \left( (t'_1 t'_2) e^{i(\theta_{t'_1} \theta_{t'_2} / 2\pi)}, (a'_1 + a'_2 - a'_1 a'_2) e^{i(\theta_{a'_1} + \theta_{a'_2} - \theta_{a'_1} \theta_{a'_2} / 2\pi)}, (f'_1 + f'_2 - f'_1 f'_2) e^{i(\theta_{f'_1} + \theta_{f'_2} - \theta_{f'_1} \theta_{f'_2} / 2\pi)} \right)$ .
- (3)  $\gamma n_1 = \left( (1 - (1 - t'_1)^\gamma) e^{i2\pi(1 - (1 - \theta_{t'_1} / 2\pi)^\gamma)}, a'_1 e^{i\theta_{a'_1}}, f'_1 e^{i\theta_{f'_1}} \right)$ .
- (4)  $n_1^\gamma = \left( t'_1 e^{i\theta_{t'_1}^\gamma}, (1 - (1 - a'_1)^\gamma) e^{i2\pi(1 - (1 - \theta_{a'_1} / 2\pi)^\gamma)}, (1 - (1 - f'_1)^\gamma) e^{i2\pi(1 - (1 - \theta_{f'_1} / 2\pi)^\gamma)} \right)$ .

**Theorem 1.** Let  $n_1 = (\overline{F}_1, \underline{A}_1, F_1) = (t'_1 e^{i\theta_{t'_1}}, a'_1 e^{i\theta_{a'_1}}, f'_1 e^{i\theta_{f'_1}})$  and  $n_2 = (\overline{F}_2, \underline{A}_2, F_2) = (t'_2 e^{i\theta_{t'_2}}, a'_2 e^{i\theta_{a'_2}}, f'_2 e^{i\theta_{f'_2}})$  be two CSVNFNs with  $\gamma, \gamma_1, \gamma_2 > 0$ . Then,

- (1)  $n_1 \oplus n_2 = n_2 \oplus n_1$ .
- (2)  $n_1 \otimes n_2 = n_2 \otimes n_1$ .
- (3)  $\gamma(n_1 \oplus n_2) = \gamma n_2 \oplus \gamma n_1$ .
- (4)  $\gamma_1 n_1 \oplus \gamma_2 n_1 = (\gamma_1 + \gamma_2) n_1$ .
- (5)  $n_1^\gamma \otimes n_2^\gamma = (n_1 \otimes n_2)^\gamma$ .
- (6)  $n_1^{\gamma_1} \otimes n_1^{\gamma_2} = n_1^{\gamma_1 + \gamma_2}$ .

*Proof.* It can be easily derived, so we omit it here. □

*Definition 13.* Let  $n = (t' e^{i\theta_{t'}}, a' e^{i\theta_{a'}}, f' e^{i\theta_{f'}})$  be CSVNFN. Then,

$$\begin{aligned} \S(n) = \frac{1}{6} & \left\{ (t' + (1 - a') + (1 - f')) + \frac{1}{2} (\theta_{t'} + (1 - \theta_{a'})) \right. \\ & \left. + (1 - \theta_{f'}) \right\} \end{aligned} \quad (11)$$

is called the score function (SF), and the accuracy function (AF) is defined as

$$H(n) = \frac{1}{6} \left\{ ((1 - t') + a' + f') + \frac{1}{2} ((1 - \theta_{t'}) + \theta_{a'} + \theta_{f'}) \right\}. \quad (12)$$

If we considered the two CSVNFNs  $n_1 = (\overline{F}_1, \underline{A}_1, F_1) = (t'_1 e^{i\theta_{t'_1}}, a'_1 e^{i\theta_{a'_1}}, f'_1 e^{i\theta_{f'_1}})$  and  $n_2 = (\overline{F}_2, \underline{A}_2, F_2) = (t'_2 e^{i\theta_{t'_2}}, a'_2 e^{i\theta_{a'_2}}, f'_2 e^{i\theta_{f'_2}})$ , then

- (1) If  $\S(n_1) > \S(n_2)$ , then  $n_1 > n_2$ .

- (2) If  $\zeta(n_1) < \zeta(n_2)$ , then  $n_1 < n_2$ .
- (3) If  $\zeta(n_1) = \zeta(n_2)$ , then  $n_1 = n_2$ .
  - (1) If  $H(n_1) > H(n_2)$ , then  $n_1 > n_2$ .
  - (2) If  $H(n_1) < H(n_2)$ , then  $n_1 < n_2$ .
  - (3) If  $H(n_1) = H(n_2)$ , then  $n_1 = n_2$ .

3.2. Complex Single-Valued Neutrosophic Hesitant Fuzzy Set (CSVNHFS)

Definition 14. The CSVNHFS is denoted and defined by

$$N = \left\{ \frac{(u, \overline{F}(u), \underline{A}(u), F(u))}{u \in X} \right\}, \quad (13)$$

where  $\overline{F}(u) = \{t = t' e^{i\theta_{t'}} / t \in \overline{F}(u)\}$ ,  $\underline{A}(u) = \{a = a' e^{i\theta_{a'}} / a \in \underline{A}(u)\}$ , and  $F(u) = \{f = f' e^{i\theta_{f'}} / f \in F(u)\}$  with the conditions  $0 \leq \max(t') + \max(a') + \max(f') \leq 3$  and  $0 \leq \max(\theta_{t'}) + \max(\theta_{a'}) + \max(\theta_{f'}) \leq 6$ , where  $0 \leq t', a', f' \leq 1$  and  $0 \leq \theta_{t'}, \theta_{a'}, \theta_{f'} \leq 2$ . Further,  $n = \{\overline{F}(u), \underline{A}(u), F(u)\}$  represents the CSVNHFN; simply, we write  $n = (\overline{F}, \underline{A}, F) = (t' e^{i\theta_{t'}}, a' e^{i\theta_{a'}}, f' e^{i\theta_{f'}})$ .

Definition 15. Let  $n_1 = (\overline{F}_1, \underline{A}_1, F_1) = (t'_1 e^{i\theta_{t'_1}}, a'_1 e^{i\theta_{a'_1}}, f'_1 e^{i\theta_{f'_1}})$  and  $n_2 = (\overline{F}_2, \underline{A}_2, F_2) = (t'_2 e^{i\theta_{t'_2}}, a'_2 e^{i\theta_{a'_2}}, f'_2 e^{i\theta_{f'_2}})$  be two CSVNHFNs. Then,

- (1)  $n_1 \cup n_2 = (\overline{F}_1 \cup \overline{F}_2, \underline{A}_1 \cap \underline{A}_2, F_1 \cap F_2) = \left( (t'_1 \vee t'_2) e^{i(\theta_{t'_1} \vee \theta_{t'_2})}, (a'_1 \wedge a'_2) e^{i(\theta_{a'_1} \wedge \theta_{a'_2})}, (f'_1 \wedge f'_2) e^{i(\theta_{f'_1} \wedge \theta_{f'_2})} \right)$ .
- (2)  $n_1 \cap n_2 = (\overline{F}_1 \cap \overline{F}_2, \underline{A}_1 \cup \underline{A}_2, F_1 \cup F_2) = \left( (t'_1 \wedge t'_2) e^{i(\theta_{t'_1} \wedge \theta_{t'_2})}, (a'_1 \vee a'_2) e^{i(\theta_{a'_1} \vee \theta_{a'_2})}, (f'_1 \vee f'_2) e^{i(\theta_{f'_1} \vee \theta_{f'_2})} \right)$ .

Definition 16. Let  $n_1 = (\overline{F}_1, \underline{A}_1, F_1) = (t'_1 e^{i\theta_{t'_1}}, a'_1 e^{i\theta_{a'_1}}, f'_1 e^{i\theta_{f'_1}})$  and  $n_2 = (\overline{F}_2, \underline{A}_2, F_2) = (t'_2 e^{i\theta_{t'_2}}, a'_2 e^{i\theta_{a'_2}}, f'_2 e^{i\theta_{f'_2}})$  be two CSVNHFNs with  $\gamma > 0$ . Then,

- (1)  $n_1 \oplus n_2 = (\overline{F}_1 \oplus \overline{F}_2, \underline{A}_1 \oplus \underline{A}_2, F_1 \oplus F_2) = \prod_{\substack{t'_1 \in \overline{F}_1, a'_1 \in \underline{A}_1, f'_1 \in F_1, \\ t'_2 \in \overline{F}_2, a'_2 \in \underline{A}_2, f'_2 \in F_2}} \left( \left( t'_1 + t'_2 \right) e^{i \left( \frac{\theta_{t'_1} + \theta_{t'_2}}{\theta_{t'_1} \theta_{t'_2} / 2\pi} \right)}, (a'_1 a'_2) e^{i(\theta_{a'_1} \theta_{a'_2} / 2\pi)}, (f'_1 f'_2) e^{i(\theta_{f'_1} \theta_{f'_2} / 2\pi)} \right)$ .

- (2)  $n_1 \otimes n_2 = (\overline{F}_1 \otimes \overline{F}_2, \underline{A}_1 \otimes \underline{A}_2, F_1 \otimes F_2) = \prod_{\substack{t'_1 \in \overline{F}_1, a'_1 \in \underline{A}_1, f'_1 \in F_1, \\ t'_2 \in \overline{F}_2, a'_2 \in \underline{A}_2, f'_2 \in F_2}} \left( (t'_1 t'_2) e^{i(\theta_{t'_1} \theta_{t'_2} / 2\pi)}, \left( \frac{a'_1 + a'_2}{a'_1 a'_2} \right) e^{i \left( \frac{\theta_{a'_1} + \theta_{a'_2}}{\theta_{a'_1} \theta_{a'_2} / 2\pi} \right)}, \left( \frac{f'_1 + f'_2}{f'_1 f'_2} \right) e^{i \left( \frac{\theta_{f'_1} + \theta_{f'_2}}{\theta_{f'_1} \theta_{f'_2} / 2\pi} \right)} \right)$ .
- (3)  $\gamma n_1 = \prod_{t'_1 \in \overline{F}_1, a'_1 \in \underline{A}_1, f'_1 \in F_1} \left( (1 - (1 - t'_1)^\gamma) e^{i2\pi(1 - (1 - \theta_{t'_1} / 2\pi)^\gamma)}, a_1^\gamma e^{i\theta_{a_1}^\gamma}, f_1^\gamma e^{i\theta_{f_1}^\gamma} \right)$ .
- (4)  $n_1^\gamma = \prod_{t'_1 \in \overline{F}_1, a'_1 \in \underline{A}_1, f'_1 \in F_1} \left( t_1^\gamma e^{i\theta_{t_1}^\gamma}, (1 - (1 - a_1')^\gamma) e^{i2\pi(1 - (1 - \theta_{a_1'} / 2\pi)^\gamma)} (1 - (1 - f_1')^\gamma) e^{i2\pi(1 - (1 - \theta_{f_1'} / 2\pi)^\gamma)} \right)$ .

Theorem 2. Let  $n_1 = (\overline{F}_1, \underline{A}_1, F_1) = (t'_1 e^{i\theta_{t'_1}}, a'_1 e^{i\theta_{a'_1}}, f'_1 e^{i\theta_{f'_1}})$  and  $n_2 = (\overline{F}_2, \underline{A}_2, F_2) = (t'_2 e^{i\theta_{t'_2}}, a'_2 e^{i\theta_{a'_2}}, f'_2 e^{i\theta_{f'_2}})$  be two CSVNHFNs with a positive real number  $\gamma, \gamma_1, \gamma_2 > 0$ . Then,

- (1)  $n_1 \oplus n_2 = n_2 \oplus n_1$ .
- (2)  $n_1 \otimes n_2 = n_2 \otimes n_1$ .
- (3)  $\gamma(n_1 \oplus n_2) = \gamma n_2 \oplus \gamma n_1 / 2$ .
- (4)  $\gamma_1 n_1 \oplus \gamma_2 n_2 = (\gamma_1 + \gamma_2) n_1$ .
- (5)  $n_1^\gamma \otimes n_2^\gamma = (n_1 \otimes n_2)^\gamma$ .
- (6)  $n_1^{\gamma_1} \otimes n_1^{\gamma_2} = n_1^{\gamma_1 + \gamma_2}$ .

Definition 17. Let  $n = (t'_i e^{i\theta_{t'_i}}, a'_i e^{i\theta_{a'_i}}, f'_i e^{i\theta_{f'_i}})$  be CSVNHFN. Then,

$$\zeta(n) = \frac{1}{6} \left\{ \left( \frac{1}{\alpha} \sum_{i=1}^{\alpha} t'_i + \frac{1}{\beta} \sum_{i=1}^{\beta} (1 - a'_i) + \frac{1}{\gamma} \sum_{i=1}^{\gamma} (1 - f'_i) \right) + \frac{1}{2} \left( \frac{1}{\alpha} \sum_{i=1}^{\alpha} \theta_{t'_i} + \frac{1}{\beta} \sum_{i=1}^{\beta} (2 - \theta_{a'_i}) + \frac{1}{\gamma} \sum_{i=1}^{\gamma} (2 - \theta_{f'_i}) \right) \right\} \quad (14)$$

Is called the SF, and the AF is denoted and defined by

$$H(n) = \frac{1}{6} \left\{ \left( \frac{1}{\alpha} \sum_{i=1}^{\alpha} (1 - t'_i) + \frac{1}{\beta} \sum_{i=1}^{\beta} a'_i + \frac{1}{\gamma} \sum_{i=1}^{\gamma} f'_i \right) + \frac{1}{2} \left( \frac{1}{\alpha} \sum_{i=1}^{\alpha} (1 - \theta_{t'_i}) + \frac{1}{\beta} \sum_{i=1}^{\beta} \theta_{a'_i} + \frac{1}{\gamma} \sum_{i=1}^{\gamma} \theta_{f'_i} \right) \right\}. \quad (15)$$

If we considered the two CSVNHFNs  $n_1 = (\overline{F}_1, \underline{A}_1, F_1) = (t'_1 e^{i\theta_{t'_1}}, a'_1 e^{i\theta_{a'_1}}, f'_1 e^{i\theta_{f'_1}})$  and  $n_2 = (\overline{F}_2, \underline{A}_2, F_2) = (t'_2 e^{i\theta_{t'_2}}, a'_2 e^{i\theta_{a'_2}}, f'_2 e^{i\theta_{f'_2}})$ , then



- (1) If  $\zeta(n_1) > \zeta(n_2)$ , then  $n_1 > n_2$ .
- (2) If  $\zeta(n_1) < \zeta(n_2)$ , then  $n_1 < n_2$ .
- (3) If  $\zeta(n_1) = \zeta(n_2)$ , then  $n_1 = n_2$ .
  - (1) If  $H(n_1) > H(n_2)$ , then  $n_1 > n_2$ .
  - (2) If  $H(n_1) < H(n_2)$ , then  $n_1 < n_2$ .
  - (3) If  $H(n_1) = H(n_2)$ , then  $n_1 = n_2$ .

#### 4. Some Aggregation Operators Based on CSVNHFSS

In this section, we propose new aggregation operators called CSVNHFPGA operator, CSVNHFPGWA operator, and CSVNHFPGHWA operator to aggregate the CSVNHFNS effectively. Throughout the paper,  $X$  represents the fixed set and the weighted vector is denoted and defined by  $\omega = (\omega_1, \omega_2, \dots, \omega_n)^T$ ,  $\omega_i \in [0, 1]$ , where  $\sum_{i=1}^n \omega_i = 1$ .

*Definition 18.* The CSVNHFPGA operator is given by CSVNHFPGA:  $\Omega^n \rightarrow \Omega$ :

$$\text{CSVNHFPGA}(n_1, n_2, \dots, n_n) = \left( \sum_{i=1}^n \omega_i n_i^\gamma \right)^{1/\gamma}, \quad (16)$$

where  $\Omega$  represents the family of all CSVNHFNS with  $\gamma > 0$ . The CSVNHFNS is of the form  $n_i = (t_i e^{i\theta_i}, a_i e^{i\theta_{a_i}}, f_i e^{i\theta_{f_i}})$  ( $i = 1, 2, \dots, n$ ).

**Theorem 3.** Let  $n_i = (t_i e^{i\theta_i}, a_i e^{i\theta_{a_i}}, f_i e^{i\theta_{f_i}})$  ( $i = 1, 2, \dots, n$ ) be the family of CSVNHFNS with  $\gamma > 0$ . Then, consider the concept of CSVNHFPGA operator, and we get CSVNHFPGA( $n_1, n_2, \dots, n_n$ ).

$$\left( \begin{array}{c} \left( 1 - \prod_{i=1}^n \prod_{t_i \in T_i} (1 - (t_i)^\gamma)^{\omega_i} \right) e^{i2\pi \left( 1 - \prod_{i=1}^n \prod_{t_i \in T_i} (1 - (\theta_i/2\pi)^\gamma)^{\omega_i} \right)^{1/\gamma}} \\ \left( 1 - \left( 1 - \prod_{i=1}^n \prod_{a_i \in A_i} (1 - (1 - a_i)^\gamma)^{\omega_i} \right)^{1/\gamma} \right) e^{i2\pi \left( 1 - \left( 1 - \prod_{i=1}^n \prod_{a_i \in A_i} (1 - (1 - \theta_{a_i}/2\pi)^\gamma)^{\omega_i} \right)^{1/\gamma}} \right) \\ \left( 1 - \left( 1 - \prod_{i=1}^n \prod_{f_i \in F_i} (1 - (1 - f_i)^\gamma)^{\omega_i} \right)^{1/\gamma} \right) \end{array} \right). \quad (17)$$

*Proof.* (1) First, we have proven that

$$\sum_{i=1}^n \omega_i n_i^\gamma = \left( \begin{array}{c} \left( 1 - \prod_{i=1}^n \prod_{t_i \in T_i} (1 - (t_i)^\gamma)^{\omega_i} \right) e^{i2\pi \left( 1 - \prod_{i=1}^n \prod_{t_i \in T_i} (1 - (\theta_{f_i}'/2\pi)^\gamma)^{\omega_i} \right)} \\ \left( \prod_{i=1}^n \prod_{a_i \in A_i} (1 - (1 - a_i)^\gamma)^{\omega_i} \right) e^{i2\pi \left( \prod_{i=1}^n \prod_{a_i \in A_i} (1 - (1 - \theta_{a_i}'/2\pi)^\gamma)^{\omega_i} \right)} \\ \left( \prod_{i=1}^n \prod_{f_i \in F_i} (1 - (1 - f_i)^\gamma)^{\omega_i} \right) e^{i2\pi \left( \prod_{i=1}^n \prod_{f_i \in F_i} (1 - (1 - \theta_{f_i}'/2\pi)^\gamma)^{\omega_i} \right)} \end{array} \right). \quad (18)$$

We utilize the mathematical induction on  $n$  to proof equation (18). Case 1. If we considered  $n = 1$ ,

□

$$\begin{aligned}
 n_1^\gamma &= \prod_{t'_1 \in T_1, a'_1 \in A_1, f'_1 \in f_1} \left( \begin{array}{l} (t'_1)^\gamma e^{i(\theta_{t'_1})^\gamma}, (1 - (1 - a'_1)^\gamma) e^{i2\pi(1 - (1 - \theta_{a'_1}/2\pi))} \\ (1 - (1 - f'_1)^\gamma) e^{i2\pi(1 - (1 - \theta_{f'_1}/2\pi))} \end{array} \right), \\
 \omega_1 n_1^\gamma &= \prod_{t'_1 \in T_1, a'_1 \in A_1, f'_1 \in f_1} \left( \begin{array}{l} (1 - (1 - (t'_1)^\gamma)^{\omega_1}) e^{i2\pi(1 - (1 - (\theta_{t'_1})^\gamma)^{\omega_1})} \\ (1 - (1 - (a'_1)^\gamma)^{\omega_1}) e^{i2\pi(1 - (1 - \theta_{a'_1}/2\pi))^\gamma} \\ (1 - (1 - (f'_1)^\gamma)^{\omega_1}) e^{i2\pi(1 - (1 - \theta_{f'_1}/2\pi))^\gamma} \end{array} \right).
 \end{aligned} \tag{19}$$

It is true for  $n = 1$ .

Case 2. If  $n = k$  is right, then

$$\sum_{i=1}^k \omega_{in_i}^\gamma = \left( \begin{array}{l} \left( 1 - \prod_{i=1}^k \prod_{t'_i \in T_i} (1 - (t'_i)^\gamma)^{\omega_i} \right) e^{i2\pi \left( 1 - \prod_{i=1}^k \prod_{t'_i \in T_i} (1 - (\theta_{t'_i}/2\pi)^\gamma)^{\omega_i} \right)} \\ \left( \prod_{i=1}^k \prod_{a'_i \in A_i} (1 - (1 - a'_i)^\gamma)^{\omega_i} \right) e^{i2\pi \left( \prod_{i=1}^k \prod_{a'_i \in A_i} (1 - (1 - \theta_{a'_i}/2\pi)^\gamma)^{\omega_i} \right)} \\ \left( \prod_{i=1}^k \prod_{f'_i \in f_i} (1 - (1 - f'_i)^\gamma)^{\omega_i} \right) e^{i2\pi \left( \prod_{i=1}^k \prod_{f'_i \in f_i} (1 - (1 - \theta_{f'_i}/2\pi)^\gamma)^{\omega_i} \right)} \end{array} \right). \tag{20}$$

Then, we checked for  $n = k + 1$ , and we get

$$\omega_{k+1} n_{k+1}^\gamma = \prod_{\substack{t_{k+1} \in T_{k+1}, t'_{k+1} \in T_{k+1}, a_{k+1} \in A_{k+1}, a'_{k+1} \in A_{k+1}, f_{k+1} \in F_{k+1}, f'_{k+1} \in F_{k+1}}} \left( \begin{array}{l} (1 - (1 - (t_{k+1})^\gamma)^{\omega_{k+1}}) e^{i2\pi(1 - (1 - (\theta_{t_{k+1}})^\gamma)^{\omega_{k+1}})} \\ (1 - (1 - a_{k+1})^\gamma)^{\omega_{k+1}} e^{i2\pi(1 - (1 - \theta_{a_{k+1}}/2\pi)^\gamma)^{\omega_{k+1}}} \\ (1 - (1 - f_{k+1})^\gamma)^{\omega_{k+1}} e^{i2\pi(1 - (1 - \theta_{f_{k+1}}/2\pi)^\gamma)^{\omega_{k+1}}} \end{array} \right), \tag{21}$$

and

$$\sum_{i=1}^{k+1} \omega_i n_i^\gamma = \left( \begin{array}{l} \left( \prod_{i=1}^k \prod_{a'_i \in \mathbb{A}_i} (1 - (1 - a'_i)^\gamma)^{\omega_i} \right) e^{i2\pi \left( \prod_{i=1}^k \prod_{a'_i \in \mathbb{A}_i} (1 - (1 - a'_i/2\pi)^\gamma)^{\omega_i} \right)}, \\ \left( \prod_{i=1}^k \prod_{f'_i \in F_i} (1 - (1 - f'_i)^\gamma)^{\omega_i} \right) e^{i2\pi \left( \prod_{i=1}^k \prod_{f'_i \in F_i} (1 - (1 - f'_i/2\pi)^\gamma)^{\omega_i} \right)}, \\ \left( 1 - \prod_{i=1}^k \prod_{t'_i \in T_i} (1 - (t'_i)^\gamma)^{\omega_i} \right) e^{i2\pi \left( 1 - \prod_{i=1}^k \prod_{t'_i \in T_i} (1 - (t'_i/2\pi)^\gamma)^{\omega_i} \right)} \\ \prod_{\substack{t_{k+1}' \in T_{k+1}, a_{k+1}' \in \mathbb{A}_{k+1}, f_{k+1}' \in F_{k+1}}} \left( \begin{array}{l} (1 - (1 - (a'_{k+1})^\gamma)^{\omega_{k+1}}) e^{i(1 - (1 - (a'_{k+1}/2\pi)^\gamma)^{\omega_{k+1}})}, \\ (1 - (1 - (f'_{k+1})^\gamma)^{\omega_{k+1}}) e^{i(1 - (1 - (f'_{k+1}/2\pi)^\gamma)^{\omega_{k+1}})}, \\ (1 - (1 - (t'_{k+1})^\gamma)^{\omega_{k+1}}) e^{i(1 - (1 - (t'_{k+1}/2\pi)^\gamma)^{\omega_{k+1}})}, \end{array} \right) \end{array} \right) \quad (22)$$

$$= \left( \begin{array}{l} \left( 1 - \prod_{i=1}^{k+1} \prod_{a'_i \in T_i} (1 - (1 - a'_i)^\gamma)^{\omega_i} \right) e^{i2\pi \left( 1 - \prod_{i=1}^{k+1} \prod_{a'_i \in \mathbb{A}_i} (1 - (a'_i/2\pi)^\gamma)^{\omega_i} \right)} \\ \left( 1 - \prod_{i=1}^{k+1} \prod_{t'_i \in T_i} (1 - (f'_i)^\gamma)^{\omega_i} \right) e^{i2\pi \left( 1 - \prod_{i=1}^{k+1} \prod_{f'_i \in F_i} (1 - (f'_i/2\pi)^\gamma)^{\omega_i} \right)} \\ \left( 1 - \prod_{i=1}^{k+1} \prod_{t'_i \in T_i} (1 - (t'_i)^\gamma)^{\omega_i} \right) e^{i2\pi \left( 1 - \prod_{i=1}^{k+1} \prod_{t'_i \in T_i} (1 - (t'_i/2\pi)^\gamma)^{\omega_i} \right)} \end{array} \right).$$

It is true also for  $n = k + 1$ , so it is true for all  $n$ .

Now, we have

$$\text{CSVNHFHFGWA}(n_1, n_2, \dots, n_n) = \left( \sum_{i=0}^n \omega_i n_i \right) = \left( \begin{array}{l} \left( 1 - \prod_{i=1}^n \prod_{t'_i \notin T_i} (1 - t'_i)^{\omega_i} \right) e^{i2\pi \left( 1 - \prod_{i=1}^n \prod_{t'_i \notin T_i} (1 - (t'_i/2\pi)^\gamma)^{\omega_i} \right)}, \\ \left( 1 - \prod_{i=1}^n \prod_{a'_i \notin \mathbb{A}_i} (a'_i)^{\omega_i} \right) e^{i2\pi \left( 1 - \prod_{i=1}^n \prod_{a'_i \notin \mathbb{A}_i} (a'_i/2\pi)^\gamma)^{\omega_i}}, \\ \left( 1 - \prod_{i=1}^n \prod_{f'_i \notin F} (f'_i)^{\omega_i} \right) e^{i2\pi \left( 1 - \prod_{i=1}^n \prod_{f'_i \notin F} (f'_i/2\pi)^\gamma)^{\omega_i}}, \end{array} \right) \quad (23)$$

Hence, the result is completed.

Next, we state some properties for CSVNHFHFGWA operator.

**Theorem 4.** Let  $n = n_i$  ( $i = 1, 2, \dots, n$ ) be the family of CSVNHFHFNs with  $\gamma > 0$ . Then,  $\text{CSVNHFHFGWA}(n_1, n_2, \dots, n_n) = n$ .

*Proof.* If  $n = n_i$ , then

$$\begin{aligned} \text{CSVNHFGWA}(n_1, n_2, \dots, n_n) &= \left( \sum_{i=1}^n \omega_i n_i^\gamma \right)^{1/\gamma} \\ &= \left( \sum_{i=1}^n \omega_i n^\gamma \right)^{1/\gamma} \quad (24) \\ &= \left( n^\gamma \sum_{i=1}^n \gamma \omega_i \right)^{1/\gamma} \\ &= n. \end{aligned}$$

Hence, the result is completed.  $\square$

**Theorem 5.** Let  $n_i = (t'_i e^{i\theta_{t'_i}}, a'_i e^{i\theta_{a'_i}}, f'_i e^{i\theta_{f'_i}}) (i = 1, 2, \dots, n)$  be the family of CSVNHFNs with  $\gamma > 0$ . If  $n_i \geq n'_i$ , then

$$\begin{aligned} \text{CSVNHFGWA}(n_1, n_2, \dots, n_n) \\ \geq \text{CSVNHFGWA}(n'_1, n'_2, \dots, n'_n). \end{aligned} \quad (25)$$

*Proof.* We considered  $n_i \geq n'_i$ , that is,  $t'_i \geq t''_i, a'_i \leq a''_i, f'_i \leq f''_i$  and  $\theta_{t'_i} \geq \theta_{t''_i}, \theta_{a'_i} \leq \theta_{a''_i}, \theta_{f'_i} \leq \theta_{f''_i}$  for all  $i$ ; then, firstly we prove for membership grades such that

---


$$\begin{aligned} &(1 - (t'_i)^\gamma)^{\omega_i} e^{i2\pi(1 - (\theta_{t'_i}/2\pi)^\gamma)^{\omega_i}} \\ &\leq (1 - (t''_i)^\gamma)^{\omega_i} e^{i2\pi(1 - (\theta_{t''_i}/2\pi)^\gamma)^{\omega_i}} \prod_{i=1}^n \prod_{t'_i \in \mathbb{F}_i} (1 - (t'_i)^\gamma)^{\omega_i} e^{i2\pi \left( \prod_{i=1}^n \prod_{t'_i \in \mathbb{F}_i} (1 - (\theta_{t'_i}/2\pi)^\gamma)^{\omega_i} \right)} \\ &\leq \prod_{i=1}^n \prod_{t'_i \in \mathbb{F}_i} (1 - (t''_i)^\gamma)^{\omega_i} e^{i2\pi \left( \prod_{i=1}^n \prod_{t'_i \in \mathbb{F}_i} (1 - (\theta_{t'_i}/2\pi)^\gamma)^{\omega_i} \right)} \left( 1 - \prod_{i=1}^n \prod_{t'_i \in \mathbb{F}_i} (1 - (t'_i)^\gamma)^{\omega_i} \right)^{1/\gamma} e^{i2\pi \left( 1 - \prod_{i=1}^n \prod_{t'_i \in \mathbb{F}_i} (1 - (\theta_{t'_i}/2\pi)^\gamma)^{\omega_i} \right)^{1/\gamma}} \\ &\geq \left( 1 - \prod_{i=1}^n \prod_{t'_i \in \mathbb{F}_i} (1 - (t''_i)^\gamma)^{\omega_i} \right)^{1/\gamma} e^{i2\pi \left( 1 - \prod_{i=1}^n \prod_{t'_i \in \mathbb{F}_i} (1 - (\theta_{t'_i}/2\pi)^\gamma)^{\omega_i} \right)^{1/\gamma}}. \end{aligned} \quad (26)$$

Similarly, for falsity and non-membership grades, we get

---


$$\begin{aligned} &\left( 1 - \left( 1 - \prod_{i=1}^n \prod_{a'_i \in \mathbb{A}_i} (1 - (1 - a'_i)^\gamma)^{\omega_i} \right)^{1/\gamma} \right) e^{i2\pi \left( 1 - \left( 1 - \prod_{i=1}^n \prod_{a'_i \in \mathbb{A}_i} (1 - (1 - \theta_{a'_i}/2\pi)^\gamma)^{\omega_i} \right)^{1/\gamma} \right)} \\ &\leq \left( 1 - \left( 1 - \prod_{i=1}^n \prod_{a'_i \in \mathbb{A}_i} (1 - (1 - a''_i)^\gamma)^{\omega_i} \right)^{1/\gamma} \right) e^{i2\pi \left( 1 - \left( 1 - \prod_{i=1}^n \prod_{a'_i \in \mathbb{A}_i} (1 - (1 - \theta_{a'_i}/2\pi)^\gamma)^{\omega_i} \right)^{1/\gamma} \right)}, \end{aligned} \quad (27)$$

and

---


$$\begin{aligned} &\left( 1 - \left( 1 - \prod_{i=1}^n \prod_{f'_i \in \mathbb{F}_i} (1 - (1 - f'_i)^\gamma)^{\omega_i} \right)^{1/\gamma} \right) e^{i2\pi \left( 1 - \left( 1 - \prod_{i=1}^n \prod_{f'_i \in \mathbb{F}_i} (1 - (1 - \theta_{f'_i}/2\pi)^\gamma)^{\omega_i} \right)^{1/\gamma} \right)} \\ &\leq \left( 1 - \left( 1 - \prod_{i=1}^n \prod_{f'_i \in \mathbb{F}_i} (1 - (1 - f''_i)^\gamma)^{\omega_i} \right)^{1/\gamma} \right) e^{i2\pi \left( 1 - \left( 1 - \prod_{i=1}^n \prod_{f'_i \in \mathbb{F}_i} (1 - (1 - \theta_{f'_i}/2\pi)^\gamma)^{\omega_i} \right)^{1/\gamma} \right)}. \end{aligned} \quad (28)$$

Hence, we combine the above equations such that

$$\left( \begin{array}{l} \left( 1 - \prod_{i=1}^n \prod_{t_i \notin T_i} (1 - (t_i)^\gamma)^{\omega_i} \right)^{1/\gamma} e^{i2\pi \left( 1 - \prod_{i=1}^n \prod_{t_i \notin T_i} (1 - (\theta t_i/2\pi)^\gamma)^{\omega_i} \right)^{1/\gamma}}, \\ \left( 1 - \left( 1 - \prod_{i=1}^n \prod_{a_i \notin A_i} (1 - (a_i)^\gamma)^{\omega_i} \right)^{1/\gamma} \right) e^{i2\pi \left( 1 - \prod_{i=1}^n \prod_{a_i \notin A_i} (1 - (\theta a_i/2\pi)^\gamma)^{\omega_i} \right)^{1/\gamma}}, \\ \left( 1 - \left( 1 - \prod_{i=1}^n \prod_{f_i \notin F_i} (1 - (f_i)^\gamma)^{\omega_i} \right)^{1/\gamma} \right) e^{i2\pi \left( 1 - \prod_{i=1}^n \prod_{f_i \notin F_i} (1 - (\theta f_i/2\pi)^\gamma)^{\omega_i} \right)^{1/\gamma}}, \end{array} \right) \tag{29}$$

$$\geq \left( \begin{array}{l} \left( 1 - \prod_{i=1}^n \prod_{t_i \notin T_i} (1 - (t_i')^\gamma)^{\omega_i} \right)^{1/\gamma} e^{i2\pi \left( 1 - \prod_{i=1}^n \prod_{t_i \notin T_i} (1 - (\theta' t_i'/2\pi)^\gamma)^{\omega_i} \right)^{1/\gamma}}, \\ \left( 1 - \left( 1 - \prod_{i=1}^n \prod_{a_i \notin A_i} (1 - (a_i')^\gamma)^{\omega_i} \right)^{1/\gamma} \right) e^{i2\pi \left( 1 - \prod_{i=1}^n \prod_{a_i \notin A_i} (1 - (\theta' a_i'/2\pi)^\gamma)^{\omega_i} \right)^{1/\gamma}}, \\ \left( 1 - \left( 1 - \prod_{i=1}^n \prod_{f_i \notin F_i} (1 - (f_i')^\gamma)^{\omega_i} \right)^{1/\gamma} \right) e^{i2\pi \left( 1 - \prod_{i=1}^n \prod_{f_i \notin F_i} (1 - (\theta' f_i'/2\pi)^\gamma)^{\omega_i} \right)^{1/\gamma}}, \end{array} \right)$$

So,

$$\begin{aligned} & \text{CSVNHFGWA}(n_1, n_2, \dots, n_n) \\ & \geq \text{CSVNHFGWA}(n'_1, n'_2, \dots, n'_n). \end{aligned} \tag{30}$$

Hence, the result is completed.  $\square$

**Theorem 6.** Let  $n_i = (t_i e^{i\theta_i}, a_i e^{i\theta_i}, f_i e^{i\theta_i}) (i = 1, 2, \dots, n)$  be the family of CSVNHFNs which lies between max and min operators with  $\gamma > 0$ . Then,

$$\begin{aligned} \min(n_1, n_2, \dots, n_n) & \leq \text{CSVNHFGWA}(n_1, n_2, \dots, n_n) \\ & \leq \max(n_1, n_2, \dots, n_n). \end{aligned} \tag{31}$$

*Proof.* We know that  $\alpha = \min(n_1, n_2, \dots, n_n)$  and  $\beta = \max(n_1, n_2, \dots, n_n)$ ; then,

$$\alpha \leq \text{CSVNHFGWA}(n_1, n_2, \dots, n_n) \leq \beta. \tag{32}$$

Then, we get

$$\left( \sum_{i=1}^n \omega_i \alpha^\gamma \right)^{1/\gamma} \leq \left( \sum_{i=1}^n \omega_i n_i^\gamma \right)^{1/\gamma} \leq \left( \sum_{i=1}^n \omega_i \beta^\gamma \right)^{1/\gamma}. \tag{33}$$

This implies that

$$\alpha \leq \left( \sum_{i=1}^n \omega_i n_i^\gamma \right)^{1/\gamma} \leq \beta, \tag{34}$$

i.e.,

$$\begin{aligned} \min(n_1, n_2, \dots, n_n) & \leq \text{CSVNHFGWA}(n_1, n_2, \dots, n_n) \\ & \leq \max(n_1, n_2, \dots, n_n). \end{aligned} \tag{35}$$

Hence, the result is completed.  $\square$

*Remark 1.* The aim of this study is to discover the particular cases of the presented approach.

- (1) If  $\gamma \rightarrow 0$ , our proposed work will be reduced to CSVNHFG weighted geometric operator:

$$\text{CSVNHFWG}(n_1, n_2, \dots, n_n) = \prod_{i=1}^n (n_i)^{\omega_i} = \left( \begin{array}{c} \left( \prod_{i=1}^n \prod_{t'_i \in \mathbb{T}_i} (t'_i)^{\omega_i} \right) e^{i2\pi \left( \prod_{i=1}^n \prod_{t'_i \in \mathbb{T}_i} (\theta t'_i / 2\pi)^{\omega_i} \right)} \\ \left( 1 - \prod_{i=1}^n \prod_{a'_i \in \mathbb{A}_i} (1 - a'_i)^{\omega_i} \right) e^{i2\pi \left( 1 - \prod_{i=1}^n \prod_{a'_i \in \mathbb{A}_i} (1 - \theta a'_i / 2\pi)^{\omega_i} \right)} \\ \left( 1 - \prod_{i=1}^n \prod_{f'_i \in \mathbb{F}_i} (1 - f'_i)^{\omega_i} \right) e^{i2\pi \left( 1 - \prod_{i=1}^n \prod_{f'_i \in \mathbb{F}_i} (1 - \theta f'_i / 2\pi)^{\omega_i} \right)} \end{array} \right). \quad (36)$$

(2) If  $\gamma = 1$ , our proposed work will be reduced to CSVNHF weighted averaging operator:

$$\text{CSVNHFGWA}(n_1, n_2, \dots, n_n) = \left( \sum_{i=0}^n \omega_i n_i \right) = \left( \begin{array}{c} \left( 1 - \prod_{i=1}^n \prod_{t'_i \notin \mathbb{T}_i} (1 - t'_i)^{\omega_i} \right) e^{i2\pi \left( 1 - \prod_{i=1}^n \prod_{t'_i \notin \mathbb{T}_i} (1 - (\theta t'_i / 2\pi))^{\omega_i} \right)}, \\ \left( 1 - \prod_{i=1}^n \prod_{a'_i \notin \mathbb{A}_i} (a'_i)^{\omega_i} \right) e^{i2\pi \left( 1 - \prod_{i=1}^n \prod_{a'_i \notin \mathbb{A}_i} (\theta a'_i / 2\pi)^{\omega_i} \right)}, \\ \left( 1 - \prod_{i=1}^n \prod_{f'_i \notin \mathbb{F}_i} (f'_i)^{\omega_i} \right) e^{i2\pi \left( 1 - \prod_{i=1}^n \prod_{f'_i \notin \mathbb{F}_i} (\theta f'_i / 2\pi)^{\omega_i} \right)}, \end{array} \right). \quad (37)$$

If  $\gamma = 2$ , our proposed work will be reduced to CSVNHF weighted quadratic averaging operator:

$$\text{CSVNHFGWQA}(n_1, n_2, \dots, n_n) = \left( \sum_{i=0}^n \omega_i n_i \right)^{1/2} = \left( \begin{array}{c} \left( 1 - \prod_{i=1}^n \prod_{t'_i \notin \mathbb{T}_i} (1 - (t'_i)^2)^{\omega_i} \right)^{1/2} e^{i2\pi \left( 1 - \prod_{i=1}^n \prod_{t'_i \notin \mathbb{T}_i} (1 - (\theta t'_i / 2\pi)^2)^{\omega_i} \right)^{1/2}}, \\ \left( 1 - \left( 1 - \prod_{i=1}^n \prod_{a'_i \notin \mathbb{A}_i} (1 - (1 - a'_i)^2)^{\omega_i} \right)^{1/2} \right) e^{i2\pi \left( 1 - \left( 1 - \prod_{i=1}^n \prod_{a'_i \notin \mathbb{A}_i} (1 - (\theta a'_i / 2\pi)^2)^{\omega_i} \right)^{1/2} \right)}, \\ \left( 1 - \left( 1 - \prod_{i=1}^n \prod_{f'_i \notin \mathbb{F}_i} (1 - (1 - f'_i)^2)^{\omega_i} \right)^{1/2} \right) e^{i2\pi \left( 1 - \left( 1 - \prod_{i=1}^n \prod_{f'_i \notin \mathbb{F}_i} (1 - (\theta f'_i / 2\pi)^2)^{\omega_i} \right)^{1/2} \right)}, \end{array} \right). \quad (38)$$

**Definition 19.** The CSVNHFGOWA operator is given by CSVNHFGOWA:  $\Omega^n \rightarrow \Omega$ :

$$\text{CSVNHFGOWA}(n_1, n_2, \dots, n_n) = \left( \sum_{i=1}^n \omega_i n_{o(i)}^\gamma \right)^{1/\gamma}, \quad (39)$$

where  $\Omega$  represents the family of all CSVNHFNs with  $\gamma > 0$  and  $n_{o(i)}$  is the ordered CSVNHFNs which is an ascending ordered (AO) or descending ordered (DO) i.e.,  $n_{o(i)} \leq n_{o(i-1)}$ . The CSVNHFN is of the form  $n_i = (t_i e^{i\theta_i}, a_i e^{i\theta_i}, f_i e^{i\theta_i}) (i = 1, 2, \dots, n)$ .

**Theorem 7.** Let  $n_i = (t_i e^{i\theta_i}, a_i e^{i\theta_i}, f_i e^{i\theta_i}) (i = 1, 2, \dots, n)$  be the family of CNHFNs with  $\gamma > 0$ . Then, considering the concept of CSVNHFOWA, we get

$$\text{CSVNHFOWA}(n_1, n_2, \dots, n_n) = \left( \begin{array}{l} \left( 1 - \prod_{i=1}^n \prod_{t_i \in T_i} (1 - (t_i)^\gamma)^{\omega_i} \right)^{1/\gamma} e^{i2\pi \left( 1 - \prod_{i=1}^n \prod_{t_i \in T_i} (1 - (\theta_{t_i}/2\pi)^\gamma)^{\omega_i} \right)^{1/\gamma}}, \\ \left( 1 - \prod_{i=1}^n \prod_{a_i \in A_i} (1 - (a_i)^\gamma)^{\omega_i} \right)^{1/\gamma} e^{i2\pi \left( 1 - \prod_{i=1}^n \prod_{a_i \in A_i} (1 - (\theta_{a_i}/2\pi)^\gamma)^{\omega_i} \right)^{1/\gamma}}, \\ \left( 1 - \prod_{i=1}^n \prod_{f_i \in F_i} (1 - (f_i)^\gamma)^{\omega_i} \right)^{1/\gamma} e^{i2\pi \left( 1 - \prod_{i=1}^n \prod_{f_i \in F_i} (1 - (\theta_{f_i}/2\pi)^\gamma)^{\omega_i} \right)^{1/\gamma}}, \end{array} \right). \quad (40)$$

*Proof.* Straightforward. □

**Theorem 8.** Let  $n_i = (t_i e^{i\theta_i}, a_i e^{i\theta_i}, f_i e^{i\theta_i}) (i = 1, 2, \dots, n)$  be the family of CSVNHFNs with  $\gamma > 0$ . Then,

$$\text{CSVNHFOWA}(n_1, n_2, \dots, n_n) = n. \quad (41)$$

*Proof.* Straightforward. □

**Theorem 9.** Let  $n_i = (t_i e^{i\theta_i}, a_i e^{i\theta_i}, f_i e^{i\theta_i}) (i = 1, 2, \dots, n)$  be the family of CSVNHFNs with  $\gamma > 0$ . If  $n_i \geq n_j$ , then

$$\text{CSVNHFOWA}(n_1, n_2, \dots, n_n) \geq \text{CSVNHFOWA}(n'_1, n'_2, \dots, n'_n). \quad (42)$$

*Proof.* Straightforward. □

**Theorem 10.** Let  $n_i = (t_i e^{i\theta_i}, a_i e^{i\theta_i}, f_i e^{i\theta_i}) (i = 1, 2, \dots, n)$  be the family of CSVNHFNs which lies between max and min operators with  $\gamma > 0$ . Then,

$$\min(n_1, n_2, \dots, n_n) \leq \text{CSVNHFOWA}(n_1, n_2, \dots, n_n) \leq \max(n_1, n_2, \dots, n_n). \quad (43)$$

*Proof.* We know that  $\alpha = \min(n_1, n_2, \dots, n_n)$  and  $\beta = \max(n_1, n_2, \dots, n_n)$ ; then,

$$\alpha \leq \text{CSVNHFOWA}(n_1, n_2, \dots, n_n) \leq \beta. \quad (44)$$

Then, we get

$$\left( \sum_{i=1}^n \omega_i \alpha^\gamma \right)^{1/\gamma} \leq \left( \sum_{i=1}^n \omega_i n_{o(i)}^\gamma \right)^{1/\gamma} \leq \left( \sum_{i=1}^n \omega_i \beta^\gamma \right)^{1/\gamma}. \quad (45)$$

This implies that

$$\alpha \leq \left( \sum_{i=1}^n \omega_i n_{o(i)}^\gamma \right)^{1/\gamma} \leq \beta. \quad (46)$$

That is,

$$\min(n_1, n_2, \dots, n_n) \leq \text{CSVNHFOWA}(n_1, n_2, \dots, n_n) \leq \max(n_1, n_2, \dots, n_n). \quad (47)$$

Hence, the result is completed. □

**Remark 2.** The aim of this study is to discover the particular cases of the presented approach.

- (1) If  $\gamma \rightarrow 0$ , our proposed work will be reduced to CSVNHF ordered weighted geometric operator:

$$\text{CSVNHFGOWA}(n_1, n_2, \dots, n_n) = \prod_{i=1}^n (n_{0(i)})^{\omega_i} = \left( \begin{array}{l} \left( \prod_{i=1}^n \prod_{t' \in T_i} (t'_{o(i)})^{\omega_i} \right) e^{i2\pi \left( \prod_{i=1}^n \prod_{t' \in T_i} (\theta t_{o(i)}/2\pi)^{\omega_i} \right)} \\ \left( \prod_{i=1}^n \prod_{a' \in A_i} (a'_{o(i)})^{\omega_i} \right) e^{i2\pi \left( \prod_{i=1}^n \prod_{a' \in A_i} (\theta a_{o(i)}/2\pi)^{\omega_i} \right)} \\ \left( \prod_{i=1}^n \prod_{f' \in F_i} (f'_{o(i)})^{\omega_i} \right) e^{i2\pi \left( \prod_{i=1}^n \prod_{f' \in F_i} (\theta f_{o(i)}/2\pi)^{\omega_i} \right)} \end{array} \right). \quad (48)$$

(2) If  $\gamma = 1$ , our proposed work will be reduced to CSVNHF ordered weighted averaging operator:

$$\text{CSVNHFGOWA}(n_1, n_2, \dots, n_n) = \prod_{i=1}^n (n_{0(i)})^{\omega_i} = \left( \begin{array}{l} \left( \prod_{i=1}^n \prod_{t' \in T_i} (t_{o(i)'})^{\omega_i} \right) e^{i2\pi \left( \prod_{i=1}^n \prod_{t' \in T_i} (\theta t_{o(i)}/2\pi)^{\omega_i} \right)} \\ \left( \prod_{i=1}^n \prod_{a' \in A_i} (a_{o(i)'})^{\omega_i} \right) e^{i2\pi \left( \prod_{i=1}^n \prod_{a' \in A_i} (\theta a_{o(i)}/2\pi)^{\omega_i} \right)} \\ \left( \prod_{i=1}^n \prod_{f' \in F_i} (f_{o(i)'})^{\omega_i} \right) e^{i2\pi \left( \prod_{i=1}^n \prod_{f' \in F_i} (\theta f_{o(i)}/2\pi)^{\omega_i} \right)} \end{array} \right). \quad (49)$$

(3) If  $\gamma = 2$ , the proposed work will be reduced to CSVNHF ordered weighted quadratic averaging operator:

$$\text{CSVNHFGOWA}(n_1, n_2, \dots, n_n) = \left( \sum_{i=1}^n \omega_i n_{o(i)} \right) = \left( \begin{array}{l} 1 - \left( \prod_{i=1}^n \prod_{t' \in T_i} (t_{o(i)'})^{\omega_i} \right) e^{i2\pi \left( \prod_{i=1}^n \prod_{t' \in T_i} (\theta t_{o(i)}/2\pi)^{\omega_i} \right)} \\ 1 - \left( \prod_{i=1}^n \prod_{a' \in A_i} (a_{o(i)'})^{\omega_i} \right) e^{i2\pi \left( \prod_{i=1}^n \prod_{a' \in A_i} (\theta a_{o(i)}/2\pi)^{\omega_i} \right)} \\ 1 - \left( \prod_{i=1}^n \prod_{f' \in F_i} (f_{o(i)'})^{\omega_i} \right) e^{i2\pi \left( \prod_{i=1}^n \prod_{f' \in F_i} (\theta f_{o(i)}/2\pi)^{\omega_i} \right)} \end{array} \right). \quad (50)$$

*Definition 20.* The CSVNHFGHWA operator is given by  $\text{CSVNHFGHWA}(n_1, n_2, \dots, n_n) = \left( \sum_{i=1}^n \omega_i n_{o(i)}^\gamma \right)^{1/\gamma}$ , (51)  
 CSVNHFGHWA:  $\Omega^n \rightarrow \Omega$ :



where  $\Omega$  represents the family of all CSVNHFNs with  $\gamma > 0$  and  $\dot{n}_{o(i)} = n\dot{\omega}_i n_i$  i.e.  $n_{o(i)} \leq n_{o(i-1)}$ . The CSVNHFN is of the form  $n_i = (t_i e^{i\theta_i}, a_i e^{i\theta_i}, f_i e^{i\theta_i}) (i = 1, 2, \dots, n)$ . Where  $\sum_{i=1}^n \dot{\omega}_i = 1$ .

**Theorem 11.** Let  $n_i = (t_i e^{i\theta_i}, a_i e^{i\theta_i}, f_i e^{i\theta_i}) (i = 1, 2, \dots, n)$  be the family of CSVNHFNs with  $\gamma > 0$ . Then, considering the concept of CSVNHFHWA, we get

$$\text{CSVNHFHWA}(n_1, n_2, \dots, n_n) = \left( \begin{array}{c} \left( 1 - \prod_{i=1}^n \prod_{t_i \in T_i} (1 - (t'_{o(i)})^\gamma)^{w_i} \right)^{1/\gamma} e^{i2\pi \left( 1 - \prod_{i=1}^n \prod_{t_i \in T_i} (1 - (\theta'_{t'_{o(i)}}/2\pi)^\gamma)^{w_i} \right)^{1/\gamma}}, \\ \left( 1 - \left( 1 - \prod_{i=1}^n \prod_{a_i \in A_i} (1 - (1 - \dot{a}'_{o(i)})^\gamma)^{w_i} \right)^{1/\gamma} \right) e^{i2\pi \left( 1 - \left( 1 - \prod_{i=1}^n \prod_{a_i \in A_i} (1 - (1 - \theta_{\dot{a}'_{o(i)}}/2\pi)^\gamma)^{w_i} \right)^{1/\gamma} \right)}, \\ \left( 1 - \left( 1 - \prod_{i=1}^n \prod_{f_i \in F_i} (1 - (1 - \dot{f}'_{o(i)})^\gamma)^{w_i} \right)^{1/\gamma} \right) e^{i2\pi \left( 1 - \left( 1 - \prod_{i=1}^n \prod_{f_i \in F_i} (1 - (1 - \theta_{\dot{f}'_{o(i)}}/2\pi)^\gamma)^{w_i} \right)^{1/\gamma} \right)} \end{array} \right). \tag{52}$$

*Proof.* Straightforward. □

**Theorem 12.** Let  $n_i = (t_i e^{i\theta_i}, a_i e^{i\theta_i}, f_i e^{i\theta_i}) (i = 1, 2, \dots, n)$  be the family of CSVNHFNs with  $\gamma > 0$ . If  $n_i \geq n_j$ , then

$$\begin{aligned} &\text{CSVNHFHWA}(n_1, n_2, \dots, n_n) \\ &\geq \text{CSVNHFHWA}(n'_1, n'_2, \dots, n'_n). \end{aligned} \tag{53}$$

*Proof.* Straightforward. □

**Theorem 13.** Let  $n_i = (t_i e^{i\theta_i}, a_i e^{i\theta_i}, f_i e^{i\theta_i}) (i = 1, 2, \dots, n)$  be the family of CSVNHFNs which lies between max and min operators with  $\gamma > 0$ . Then,

$$\begin{aligned} \min(n_1, n_2, \dots, n_n) &\leq \text{CSVNHFHWA}(n_1, n_2, \dots, n_n) \\ &\leq \max(n_1, n_2, \dots, n_n). \end{aligned} \tag{54}$$

*Proof.* We know that  $\alpha = \min(n_1, n_2, \dots, n_n)$  and  $\beta = \max(n_1, n_2, \dots, n_n)$ ; then,

$$\alpha \leq \text{CSVNHFHWA}(n_1, n_2, \dots, n_n) \leq \beta. \tag{55}$$

Then, we get

$$\left( \sum_{i=1}^n \omega_i \alpha^\gamma \right)^{1/\gamma} \leq \left( \sum_{i=1}^n \omega_i \dot{n}_{o(i)}^\gamma \right)^{1/\gamma} \leq \left( \sum_{i=1}^n \omega_i \beta^\gamma \right)^{1/\gamma}. \tag{56}$$

This implies that

$$\alpha \leq \left( \sum_{i=1}^n \omega_i \dot{n}_{o(i)}^\gamma \right)^{1/\gamma} \leq \beta. \tag{57}$$

That is,

$$\begin{aligned} \min(n_1, n_2, \dots, n_n) &\leq \text{CSVNHFHWA}(n_1, n_2, \dots, n_n) \\ &\leq \max(n_1, n_2, \dots, n_n). \end{aligned} \tag{58}$$

Hence, the result is completed. □

*Remark 3.* The aim of this study is to discover the cases of the presented approach.

- (1) If  $\gamma \rightarrow 0$ , our proposed work will be reduced to CSVNHF hybrid weighted geometric (CSVNHFHWG) operator:

$$\text{CSVNHFHWA}(n_1, n_2, \dots, n_n) = \prod_{i=1}^n (\dot{n}_{o(i)})^{w_i} = \left( \begin{array}{l} \left( \prod_{i=1}^n \prod_{t'_i \in T_i} (t'_{o(i)})^{w_i} \right) e^{i2\pi \left( 1 - \prod_{i=1}^n \prod_{t'_i \in T_i} (\theta_{t'_{o(i)}}/2\pi)^{w_i} \right)}, \\ \left( 1 - \prod_{i=1}^n \prod_{a'_i \in A_i} (1 - a'_{o(i)})^{w_i} \right) e^{i2\pi \left( 1 - \prod_{i=1}^n \prod_{a'_i \in A_i} (1 - \theta_{a'_{o(i)}}/2\pi)^{w_i} \right)}, \\ \left( 1 - \prod_{i=1}^n \prod_{f'_i \in F_i} (1 - f'_{o(i)})^{w_i} \right) e^{i2\pi \left( 1 - \prod_{i=1}^n \prod_{f'_i \in F_i} (1 - \theta_{f'_{o(i)}}/2\pi)^{w_i} \right)} \end{array} \right). \tag{59}$$

(2) If  $\gamma = 1$ , our proposed work will be reduced to CSVNHF hybrid weighted averaging (CSVNHFHWA) operator:

$$\text{CSVNHFHWA}(n_1, n_2, \dots, n_n) = \left( \sum_{i=1}^n W_i \dot{n}_{o(i)} \right) = \left( \begin{array}{l} \left( 1 - \prod_{i=1}^n \prod_{t'_i \in T_i} (1 - t'_{o(i)})^{w_i} \right) e^{i2\pi \left( 1 - \prod_{i=1}^n \prod_{t'_i \in T_i} (1 - \theta_{t'_{o(i)}}/2\pi)^{w_i} \right)}, \\ \left( \prod_{i=1}^n \prod_{a'_i \in A_i} (1 - a'_{o(i)})^{w_i} \right) e^{i2\pi \left( \prod_{i=1}^n \prod_{a'_i \in A_i} (\theta_{a'_{o(i)}}/2\pi)^{w_i} \right)}, \\ \left( \prod_{i=1}^n \prod_{f'_i \in F} (f'_{o(i)})^{w_i} \right) e^{i2\pi \left( \prod_{i=1}^n \prod_{f'_i \in F_i} (\theta_{f'_{o(i)}}/2\pi)^{w_i} \right)} \end{array} \right). \tag{60}$$

(3) If  $\gamma = 2$ , our proposed work will be reduced to CSVNHF hybrid weighted quadratic averaging (CSVNHFHWQA) operator:

$$\text{CSVNHFHWQA}(n_1, n_2, \dots, n_n) = \left( \sum_{i=1}^n W_i \dot{n}_{o(i)}^2 \right)^{1/2} = \left( \begin{array}{l} \left( 1 - \prod_{i=1}^n \prod_{t'_i \in T_i} (1 - (t'_{o(i)})^2)^{w_i} \right)^{1/2} e^{i2\pi \left( 1 - \prod_{i=1}^n \prod_{t'_i \in T_i} (1 - (\theta_{t'_{o(i)}}/2\pi)^2)^{w_i} \right)^{1/2}}, \\ \left( 1 - \left( 1 - \prod_{i=1}^n \prod_{a'_i \in A_i} (1 - (1 - a'_{o(i)})^2)^{w_i} \right)^{1/2} \right) e^{i2\pi \left( 1 - \left( 1 - \prod_{i=1}^n \prod_{a'_i \in A_i} (1 - (1 - \theta_{a'_{o(i)}}/2\pi)^2)^{w_i} \right)^{1/2} \right)}, \\ \left( 1 - \left( 1 - \prod_{i=1}^n \prod_{f'_i \in F} (1 - (1 - f'_{o(i)})^2)^{w_i} \right)^{1/2} \right) e^{i2\pi \left( 1 - \left( 1 - \prod_{i=1}^n \prod_{f'_i \in F_i} (1 - (1 - \theta_{f'_{o(i)}}/2\pi)^2)^{w_i} \right)^{1/2} \right)} \end{array} \right). \tag{61}$$

### 5. Proposed MADM Method

The decision-making strategy aims to grow the chance of the benefits and reduce the chance of the cost during the decision-making procedure for simplifying genuine life dilemmas. Several people have worked on decision-making strategies under the presence of a crisp set. In several situations, it is very complicated to study the decision-making strategy considering fuzzy sets because they have covered a lot of possibilities. Inspired by the MADM technique, we will employ it here in the presence of the proposed works.

*5.1. Decision-Making Algorithm.* During the decision-making process, ambiguity and complexity always occur in our day-to-day life. This study aims to employ the decision-making strategy in the presence of proposed works. For this, consider a finite number of alternatives  $X = \{u_1, u_2, \dots, u_m\}$  and attributes  $C = \{c_1, c_2, \dots, c_n\}$ . To evaluate each alternative under each attribute, we assign a weight vector for attribute as  $\omega = (\omega_1, \omega_2, \dots, \omega_n)^T, \sum_{i=1}^n \omega_i = 1$ . Experts are invited to evaluate each alternative  $A_i$  and give their preferences in terms of the CSVNHF information  $n_{ij} = (t_{ij}, a_{ij}, f_{ij}) (i, j = 1, 2, \dots, n)$  for criteria  $C_j$  where  $\left\{ t_{ij} = t'_{ij} e^{i\theta_{t_{ij}}} / t_{ij} \in \mathbb{F}(u) \right\}, \left\{ a_{ij} = a'_{ij} e^{i\theta_{a_{ij}}} / a_{ij} \in \mathbb{A}(u) \right\}$  and  $\left\{ f_{ij} = f'_{ij} e^{i\theta_{f_{ij}}} / f_{ij} \in F(u) \right\}$ , gives the TG, abstinence grade, and FG. Then, the following are the steps summarized to find the best alternative(s).

Step 1: collect the data in the shape of the CSVNHF setting and summarize them in the form of the matrix called as decision matrix.

Step 2: normalize the collective information, if needed by using the following equation.

$$D(r_{ij}) = \begin{cases} (t_{ij}, a_{ij}, f_{ij}), & \text{for benefit criteria,} \\ (f_{ij}, a_{ij}, t_{ij}), & \text{for cost criteria.} \end{cases} \quad (62)$$

Step 3: aggregate the collective information by using stated operators. For instance, utilize equation (7) to aggregate the information  $r_{ij}$  into  $r_i = (t'_i e^{i\theta_{t'_i}}, a'_i e^{i\theta_{a'_i}}, f'_i e^{i\theta_{f'_i}})$ .

Step 4: compute the crisp value for each number  $r_i = (t'_i e^{i\theta_{t'_i}}, a'_i e^{i\theta_{a'_i}}, f'_i e^{i\theta_{f'_i}})$  by using the following equation:

$$\begin{aligned} \zeta(r_i) = \frac{1}{6} & \left\{ \left( \frac{1}{\alpha} \sum_{i=1}^{\alpha} t'_i + \frac{1}{\beta} \sum_{i=1}^{\beta} (1 - a'_i) + \frac{1}{\gamma} \sum_{i=1}^{\gamma} (1 - f'_i) \right) \right. \\ & \left. + \frac{1}{2} \left( \frac{1}{\alpha} \sum_{i=1}^{\alpha} \theta_{t'_i} + \frac{1}{\beta} \sum_{i=1}^{\beta} (2 - \theta_{a'_i}) + \frac{1}{\gamma} \sum_{i=1}^{\gamma} (2 - \theta_{f'_i}) \right) \right\}. \end{aligned} \quad (63)$$

If for any two indices,  $\zeta(r_i)$  values are equal, then compute accuracy degree as

$$H(r_i) = \frac{1}{6} \left\{ \left( \frac{1}{\alpha} \sum_{i=1}^{\alpha} (1 - t'_i) + \frac{1}{\beta} \sum_{i=1}^{\beta} a'_i + \frac{1}{\gamma} \sum_{i=1}^{\gamma} f'_i \right) + \frac{1}{2} \left( \frac{1}{\alpha} \sum_{i=1}^{\alpha} (1 - \theta_{t'_i}) + \frac{1}{\beta} \sum_{i=1}^{\beta} \theta_{a'_i} + \frac{1}{\gamma} \sum_{i=1}^{\gamma} \theta_{f'_i} \right) \right\}. \quad (64)$$

Step 5: rank the alternatives based on the crisp values and get the beneficial optimal.

*5.2. Illustrated Example.* To illustrate the working of the above stated algorithm to the decision-making process, we consider a numerical example which can be read as follows.

Consider a decision-making process related to the selection of the best enterprise for the investment. Since the market always shows an up and down phases at a regular interval of time, the decision maker will always look for the desired option for the investment. After deep analysis of the market scenario, an investor selects the following four potential options, considered as an alternative, which are characterized as

- (i)  $A_1$ : invest in the local market.
- (ii)  $A_2$ : invest in the southern Asian market.
- (iii)  $A_3$ : invest in the northeastern market.
- (iv)  $A_4$ : invest in the European market.

To access all these alternatives deeply, we have taken the following three attributes with attribute weights taken as  $\omega = (0.5, 0.4, 0.1)^T$ :

- (i)  $C_1$ : economic growth.
- (ii)  $C_2$ : profit in the long term.
- (iii)  $C_3$ : social political impact analysis.

Then, the following steps of the stated algorithms are implemented to find the best alternative as follows.

Step 1: a senior expert from the market sector is hired for accessing the given alternatives under each attribute. Their corresponding rating is summarized in Table 1

Step 2: as all the criteria are of benefit types, there is no need for normalization.

Step 3: with attribute weights taken as  $\omega = (0.5, 0.4, 0.1)^T$ , utilize CSVNHF operator as stated in equation. (52) to aggregate the information for  $\gamma = 1$ .

Step 4: the score values of all the aggregated numbers (as obtained from Step 3) are calculated, and their results are summarized in Table 2 along with the ranking order.

TABLE 1: CSVNHF generalized aggregation operator decision matrix.

Data representations	$C_1$	$C_2$	$C_3$
$A_1$	$\begin{pmatrix} \left( \begin{matrix} (0.7)e^{i.2(0.9)} \\ (0.5)e^{i.2(0.4)} \\ (0.7)e^{i.2(0.7)} \end{matrix} \right) \\ \left( \begin{matrix} (0.6)e^{i.2(0.87)} \\ (0.56)e^{i.2(0.45)} \\ (0.76)e^{i.2(0.66)} \end{matrix} \right) \\ \left( \begin{matrix} (0.67)e^{i.2(0.98)} \\ (0.65)e^{i.2(0.67)} \\ (0.14)e^{i.2(0.56)} \end{matrix} \right) \end{pmatrix}$	$\begin{pmatrix} \left( \begin{matrix} (0.77)e^{i.2(0.8)} \\ (0.78)e^{i.2(0.81)} \\ (0.79)e^{i.2(0.82)} \end{matrix} \right) \\ \left( \begin{matrix} (0.83)e^{i.2(0.67)} \\ (0.84)e^{i.2(0.45)} \\ (0.85)e^{i.2(0.67)} \end{matrix} \right) \\ \left( \begin{matrix} (0.56)e^{i.2(0.78)} \\ (0.56)e^{i.2(0.79)} \\ (0.67)e^{i.2(0.69)} \end{matrix} \right) \end{pmatrix}$	$\begin{pmatrix} \left( \begin{matrix} (0.13)e^{i.2(0.46)} \\ (0.23)e^{i.2(0.64)} \\ (0.45)e^{i.2(0.66)} \end{matrix} \right) \\ \left( \begin{matrix} (0.45)e^{i.2(0.56)} \\ (0.54)e^{i.2(0.65)} \\ (0.55)e^{i.2(0.87)} \end{matrix} \right) \\ \left( \begin{matrix} (0.89)e^{i.2(0.89)} \\ (0.67)e^{i.2(0.66)} \\ (0.47)e^{i.2(0.88)} \end{matrix} \right) \end{pmatrix}$
$A_2$	$\begin{pmatrix} \left( \begin{matrix} (0.45)e^{i.2(0.93)} \\ (0.56)e^{i.2(0.45)} \\ (0.78)e^{i.2(0.76)} \end{matrix} \right), \\ \left( \begin{matrix} (0.67)e^{i.2(0.88)} \\ (0.6)e^{i.2(0.5)} \\ (0.7)e^{i.2(0.7)} \end{matrix} \right), \\ \left( \begin{matrix} (0.8)e^{i.2(0.3)} \\ (0.6)e^{i.2(0.67)} \\ (0.6)e^{i.2(0.56)} \end{matrix} \right) \end{pmatrix}$	$\begin{pmatrix} \left( \begin{matrix} (0.77)e^{i.2(0.56)} \\ (0.34)e^{i.2(0.89)} \\ (0.56)e^{i.2(0.78)} \end{matrix} \right), \\ \left( \begin{matrix} (0.67)e^{i.2(0.77)} \\ (0.92)e^{i.2(0.66)} \\ (0.57)e^{i.2(0.45)} \end{matrix} \right), \\ \left( \begin{matrix} (0.67)e^{i.2(0.45)} \\ (0.56)e^{i.2(0.79)} \\ (0.45)e^{i.2(0.57)} \end{matrix} \right) \end{pmatrix}$	$\begin{pmatrix} \left( \begin{matrix} (0.58)e^{i.2(0.69)} \\ (0.67)e^{i.2(0.49)} \\ (0.68)e^{i.2(0.59)} \end{matrix} \right), \\ \left( \begin{matrix} (0.59)e^{i.2(0.58)} \\ (0.39)e^{i.2(0.67)} \\ (0.49)e^{i.2(0.34)} \end{matrix} \right), \\ \left( \begin{matrix} (0.33)e^{i.2(0.55)} \\ (0.44)e^{i.2(0.65)} \\ (0.45)e^{i.2(0.77)} \end{matrix} \right) \end{pmatrix}$
$A_3$	$\begin{pmatrix} \left( \begin{matrix} (0.7)e^{i.2(0.45)} \\ (0.45)e^{i.2(0.45)} \\ (0.45)e^{i.2(0.45)} \end{matrix} \right) \\ \left( \begin{matrix} (0.76)e^{i.2(0.23)} \\ (0.5)e^{i.2(0.43)} \\ (0.7)e^{i.2(0.45)} \end{matrix} \right) \\ \left( \begin{matrix} (0.54)e^{i.2(0.64)} \\ (0.65)e^{i.2(0.57)} \\ (0.46)e^{i.2(0.74)} \end{matrix} \right) \end{pmatrix}$	$\begin{pmatrix} \left( \begin{matrix} (0.68)e^{i.2(0.85)} \\ (0.86)e^{i.2(0.48)} \\ (0.58)e^{i.2(0.84)} \end{matrix} \right) \\ \left( \begin{matrix} (0.66)e^{i.2(0.45)} \\ (0.9)e^{i.2(0.67)} \\ (0.57)e^{i.2(0.36)} \end{matrix} \right) \\ \left( \begin{matrix} (0.67)e^{i.2(0.56)} \\ (0.45)e^{i.2(0.67)} \\ (0.33)e^{i.2(0.34)} \end{matrix} \right) \end{pmatrix}$	$\begin{pmatrix} \left( \begin{matrix} (0.45)e^{i.2(0.68)} \\ (0.46)e^{i.2(0.48)} \\ (0.67)e^{i.2(0.46)} \end{matrix} \right) \\ \left( \begin{matrix} (0.5)e^{i.2(0.45)} \\ (0.39)e^{i.2(0.67)} \\ (0.49)e^{i.2(0.67)} \end{matrix} \right) \\ \left( \begin{matrix} (0.56)e^{i.2(0.57)} \\ (0.45)e^{i.2(0.45)} \\ (0.67)e^{i.2(0.34)} \end{matrix} \right) \end{pmatrix}$
$A_4$	$\begin{pmatrix} \left( \begin{matrix} (0.4)e^{i.2(0.45)} \\ (0.56)e^{i.2(0.78)} \\ (0.46)e^{i.2(0.46)} \end{matrix} \right) \\ \left( \begin{matrix} (0.6)e^{i.2(0.9)} \\ (0.7)e^{i.2(0.2)} \\ (0.8)e^{i.2(0.3)} \end{matrix} \right) \\ \left( \begin{matrix} (0.4)e^{i.2(0.47)} \\ (0.5)e^{i.2(0.49)} \\ (0.45)e^{i.2(0.59)} \end{matrix} \right) \end{pmatrix}$	$\begin{pmatrix} \left( \begin{matrix} (0.8)e^{i.2(0.67)} \\ (0.8)e^{i.2(0.54)} \\ (0.9)e^{i.2(0.63)} \end{matrix} \right) \\ \left( \begin{matrix} (0.66)e^{i.2(0.9)} \\ (0.78)e^{i.2(0.88)} \\ (0.89)e^{i.2(0.45)} \end{matrix} \right) \\ \left( \begin{matrix} (0.56)e^{i.2(0.69)} \\ (0.57)e^{i.2(0.67)} \\ (0.68)e^{i.2(0.7)} \end{matrix} \right) \end{pmatrix}$	$\begin{pmatrix} \left( \begin{matrix} (0.35)e^{i.2(0.48)} \\ (0.67)e^{i.2(0.49)} \\ (0.38)e^{i.2(0.51)} \end{matrix} \right) \\ \left( \begin{matrix} (0.52)e^{i.2(0.65)} \\ (0.53)e^{i.2(0.75)} \\ (0.54)e^{i.2(0.85)} \end{matrix} \right) \\ \left( \begin{matrix} (0.86)e^{i.2(0.75)} \\ (0.87)e^{i.2(0.73)} \\ (0.74)e^{i.2(0.71)} \end{matrix} \right) \end{pmatrix}$

TABLE 2: Ranking results of the CSVNHFSS.

Alternatives	Score function	Rank
$A_1$	$\zeta(A_1) = 0.467$	4
$A_2$	$\zeta(A_2) = 0.515$	2
$A_3$	$\zeta(A_3) = 0.524$	1
$A_4$	$\zeta(A_4) = 0.478$	3

Step 5: based on the score values, we rank the given alternatives as

$$A_3 \geq A_2 \geq A_4 \geq A_1, \tag{65}$$

and found that  $A_3$  is the best one for this suitable job.

5.3. Comparative Analysis. To compare the study with the several existing studies, we compare the performance of the existing algorithms in [20, 21, 26, 31–34] under different environments. The result corresponding to each method is listed in Table 3. It is clear that from Table 3 that  $A_3$  is the best alternative identified by all existing methods and the proposed method. Although the ranking result is same by all the methods, the proposed MADM algorithm has several advantages over such existing studies.

To highlight such things, we summarize the characteristics of the stated method over the existing ones in Table 4. It is seen from this table that proposed method in this paper is more generalized than the existing methods. Also, it is clear that the proposed concept is more general and reliable than IFS [3], CIFS [20], CNS [26], and NS [7], and all are

TABLE 3: Comparative study with the existing methods.

Method	Score values	Ranking results	Best alternatives
Ali and Smarandache [26]	Cannot be calculated	No	No
Alkouri and Salleh [20]	Cannot be calculated	No	No
Garg and Rani [31, 32]	Cannot be calculated	No	No
Rani and Garg [21, 33]	Cannot be calculated	No	No
Beg and Rashid [35]	$\zeta(A_1) = 0.66, \zeta(A_2) = 0.71, \zeta(3) = 0.72, \zeta(A_4) = 0.67$	$A_3 \geq A_2 \geq A_4 \geq A_1$	$A_3$
Torra [27]	$\zeta(A_1) = 0.573, \zeta(A_2) = 0.601, \zeta(3) = 0.603, \zeta(A_4) = 0.579$	$A_3 \geq A_2 \geq A_4 \geq A_1$	$A_3$
Beg and Rashid [35]	$\zeta(A_1) = 0.47, \zeta(A_2) = 0.52, \zeta(3) = 0.53, \zeta(A_4) = 0.49$	$A_3 \geq A_2 \geq A_4 \geq A_1$	$A_3$
Proposed method	$\zeta(A_1) = 0.467, \zeta(A_2) = 0.515, \zeta(3) = 0.524, \zeta(A_4) = 0.478$	$A_3 \geq A_2 \geq A_4 \geq A_1$	$A_3$

TABLE 4: Characteristic comparison between proposed work and existing methods.

Methods	Ability to integrate information	Ability to capture information using complex numbers	Ability to handle two-dimensional information	Flexible according to decision makers' preferences	Superior characteristic of the ideas	Dealing hesitant kind of information
Atanassov [3]	Yes	No	No	No	No	No
Alkouri and Salleh [20]	Yes	Yes	Yes	No	No	No
Garg and Rani [31, 32]	Yes	Yes	Yes	No	No	No
Rani and Garg [21, 33]	Yes	Yes	Yes	No	No	No
Smarandache [7]	Yes	No	No	Yes	Yes	No
Ali and Smarandache [26]	Yes	Yes	Yes	Yes	Yes	No
Proposed work	Yes	Yes	Yes	Yes	Yes	Yes

TABLE 5: Impact of the parameter  $\gamma$  on the ratings.

Parameter $\gamma$	Score values	Ranking
$\gamma = 1$	$\zeta(A_1) = 0.467, \zeta(A_2) = 0.515, \zeta(A_3) = 0.524, \zeta(A_4) = 0.478$	$A_3 \geq A_2 \geq A_4 \geq A_1$
$\gamma = 4$	$\zeta(A_1) = 0.496, \zeta(A_2) = 0.539, \zeta(A_3) = 0.545, \zeta(A_4) = 0.518$	$A_3 \geq A_2 \geq A_4 \geq A_1$
$\gamma = 10$	$\zeta(A_1) = 0.522, \zeta(A_2) = 0.566, \zeta(A_3) = 0.571, \zeta(A_4) = 0.553$	$A_3 \geq A_2 \geq A_4 \geq A_1$
$\gamma = 15$	$\zeta(A_1) = 0.531, \zeta(A_2) = 0.57, \zeta(A_3) = 0.58, \zeta(A_4) = 0.56$	$A_3 \geq A_2 \geq A_4 \geq A_1$
$\gamma = 20$	$\zeta(A_1) = 0.536, \zeta(A_2) = 0.584, \zeta(A_3) = 0.588, \zeta(A_4) = 0.57$	$A_3 \geq A_2 \geq A_4 \geq A_1$

considered as special cases of CSVNHFS. For instance, by taking  $\gamma = 1$  in the proposed work, the stated method reduces to CSVNHFWA operators, and if  $\gamma = 2$ , then our proposed work is reduced to CSVNHFVG.

5.4. Sensitivity Analysis of the Parameter  $\gamma$ . In this section, we examined the influence of parameter  $\gamma$  on to the decision-making process. For this, we vary the value of the parameter  $\gamma$  from 1 to 20 (by taking arbitrary values) and implement the steps of the proposed algorithm on it. The final score values and the ranking order for each value of  $\gamma$  are recorded and listed in Table 5. Also, we have listed some special cases of the proposed operators with  $\gamma$  in Remarks 1–3. From this investigation, we noted that as we increase the value of  $\gamma$ , the score value corresponding to each alternative increases which shows the optimistic nature. Decision makers can select the suitable value as per their choice by seeing the

overall score value of each alternative. From the above analysis, we conclude that the proposed strategies are more unrivaled and more broad than existing work.

### 6. Conclusion

The main contribution of this paper is discussed below.

- (1) A novel concept of CSVNHFS is defined in the paper by incorporating the features of SVN, hesitant, and complex sets. The idea behind this set is to address the ambiguity in the data when it is arranged in the form of “yes,” “abstinence,” and “no” under the complex domain. In the presented set, each element is characterized with three independent hesitant degrees, namely, TG ( $t' e^{i\theta_{t'}}$ ), abstinence ( $a' e^{i\theta_{a'}}$ ), and FG ( $f' e^{i\theta_{f'}}$ ), over the unit disc of complex plane with the conditions  $0 \leq t' + a' + f' \leq 3$  and  $0 \leq \theta_{t'} + \theta_{a'} + \theta_{f'} \leq 6$  where  $0 \leq t', a', f' \leq 1$  and  $0 \leq \theta_{t'}, \theta_{a'}, \theta_{f'} \leq 2$ .

- (2) The fundamental properties and the operations of the stated set are investigated. Also, it is analyzed that the proposed CSVNHFS is the generalization of the existing sets such as IFS [3], CIFS [20], CNS [26], and NS [7].
- (3) By taking the features of the CSVNHFS, we defined generalized weighted average (CSVNHFGWA), ordered weighted (CSVNHFGOWA), and hybrid weighted averaging (CSVNHFGHWA) operators to aggregate different pairs of the given information. Some of their basic properties are also discussed.
- (4) A MADM algorithm based on the stated operators is presented by using the features of CSVNHFS and illustrated with the numerical examples.
- (5) To determine the supremacy and efficiency of investigated operators, we utilized the advantages, sensitive analysis, and geometrical expressions of the proposed work to discover the dominance of the elaborated approaches.

In the future, we will try to implement the application of the stated algorithm and extend it to different fuzzy environments [35–42].

## Data Availability

No data were used to support this study.

## Conflicts of Interest

The authors declare that they have no conflicts of interest.

## Acknowledgments

This study was supported by the Research Supporting Project King Saud University, Riyadh, Saudi Arabia. (RSP-2021/389).

## References

- [1] L. A. Zadeh, "Fuzzy sets," *Information and Control*, vol. 8, no. 3, pp. 338–353, 1965.
- [2] J. A. Goguen, "L-fuzzy sets," *Journal of Mathematical Analysis and Applications*, vol. 18, no. 1, pp. 145–174, 1967.
- [3] K. T. Atanassov, "Intuitionistic fuzzy sets," *Fuzzy Sets and Systems*, vol. 20, no. 1, pp. 87–96, 1986.
- [4] S. Liu, W. Yu, F. T. S. Chan, and B. Niu, "A variable weight-based hybrid approach for multi-attribute group decision making under interval-valued intuitionistic fuzzy sets," *International Journal of Intelligent Systems*, vol. 36, no. 2, pp. 1015–1052, 2021.
- [5] H. Garg and D. Rani, "Novel similarity measure based on the transformed right-angled triangles between intuitionistic fuzzy sets and its applications," *Cognitive Computation*, vol. 13, no. 2, pp. 447–465, 2021.
- [6] K. Atanassov and E. Marinov, "Four distances for circular intuitionistic fuzzy sets," *Mathematics*, vol. 9, no. 10, 2021.
- [7] F. Smarandache, *A Unifying Field in logics. Neutrosophy: Neutrosophic Probability, Set and Logic*, American Research Press, Champaign, IL, USA, 1999.
- [8] P. Liu, "The aggregation operators based on Archimedean t-conorm and t-norm for single-valued neutrosophic numbers and their application to decision making," *International Journal of Fuzzy Systems*, vol. 18, no. 5, pp. 849–863, 2016.
- [9] J. Chen and J. Ye, "Some single-valued neutrosophic Dombi weighted aggregation operators for multiple attribute decision-making," *Symmetry*, vol. 9, no. 6, 2017.
- [10] G. Wei and Z. Zhang, "Some single-valued neutrosophic Bonferroni power aggregation operators in multiple attribute decision making," *Journal of Ambient Intelligence and Humanized Computing*, vol. 10, no. 3, pp. 863–882, 2019.
- [11] H. Garg and Nancy, "Algorithms for possibility linguistic single-valued neutrosophic decision-making based on COPRAS and aggregation operators with new information measures," *Measurement*, vol. 138, pp. 278–290, 2019.
- [12] H. Garg and Nancy, "New Logarithmic operational laws and their applications to multiattribute decision making for single-valued neutrosophic numbers," *Cognitive Systems Research*, vol. 52, pp. 931–946, 2018.
- [13] P. Liu and L. Zhang, "Multiple criteria decision making method based on neutrosophic hesitant fuzzy Heronian mean aggregation operators," *Journal of Intelligent & Fuzzy Systems*, vol. 32, no. 1, pp. 303–319, 2017.
- [14] L. Q. Dat, N. T. Thong, L. H. Son et al., "Linguistic approaches to interval complex neutrosophic sets in decision making," *IEEE Access*, vol. 7, Article ID 38917, 2019.
- [15] S. Iryna, Y. Zhong, W. Jiang, X. Deng, and J. Geng, "Single-valued neutrosophic set correlation coefficient and its application in fault diagnosis," *Symmetry*, vol. 12, no. 8, 2020.
- [16] J. Wang, X. Tang, and G. Wei, "Models for multiple attribute decision-making with dual generalized single-valued neutrosophic Bonferroni mean operators," *Algorithms*, vol. 11, no. 1, 2018.
- [17] H. Wang, F. Smarandache, Y. Zhang, and R. Sunderraman, "Single valued neutrosophic sets," *Review of the Air Force Academy*, vol. 10, 2010.
- [18] D. Ramot, R. Milo, M. Friedman, and A. Kandel, "Complex fuzzy sets," *IEEE Transactions on Fuzzy Systems*, vol. 10, no. 2, pp. 171–186, 2002.
- [19] P. Liu, Z. Ali, and T. Mahmood, "The distance measures and cross-entropy based on complex fuzzy sets and their application in decision making," *Journal of Intelligent & Fuzzy Systems*, vol. 39, no. 3, pp. 1–24, 2020.
- [20] A. M. D. J. S. Alkouri and A. R. Salleh, "Complex intuitionistic fuzzy sets," *AIP Conference Proceedings*, vol. 1482, no. 1, pp. 464–470, 2012.
- [21] D. Rani and H. Garg, "Distance measures between the complex intuitionistic fuzzy sets and their applications to the decision-making process," *International Journal for Uncertainty Quantification*, vol. 7, no. 5, pp. 423–439, 2017.
- [22] H. Garg and D. Rani, "Some results on information measures for complex intuitionistic fuzzy sets," *International Journal of Intelligent Systems*, vol. 34, no. 10, pp. 2319–2363, 2019.
- [23] H. Garg and D. Rani, "Novel aggregation operators and ranking method for complex intuitionistic fuzzy sets and their applications to decision-making process," *Artificial Intelligence Review*, vol. 53, no. 5, pp. 3595–3620, 2020.
- [24] M. Gulzar, M. H. Mateen, D. Alghazzawi, and N. Kausar, "A novel applications of complex intuitionistic fuzzy sets in group theory," *IEEE Access*, vol. 8, Article ID 196085, 2020.
- [25] H. Garg and D. Rani, "Generalized geometric aggregation operators based on t-norm operations for complex intuitionistic fuzzy sets and their application to decision-making," *Cognitive Computation*, vol. 12, no. 3, pp. 679–698, 2020.

- [26] M. Ali and F. Smarandache, "Complex neutrosophic set," *Neural Computing and Applications*, vol. 28, no. 7, pp. 1817–1834, 2017.
- [27] V. Torra, "Hesitant fuzzy sets," *International Journal of Intelligent Systems*, vol. 25, no. 6, pp. 529–539, 2010.
- [28] R. M. Rodríguez, L. Martínez, V. Torra, Z. S. Xu, and F. Herrera, "Hesitant fuzzy sets: state of the art and future directions," *International Journal of Intelligent Systems*, vol. 29, no. 2, pp. 495–524, 2014.
- [29] Z. S. Xu and W. Zhou, "Consensus building with a group of decision makers under the hesitant probabilistic fuzzy environment," *Fuzzy Optimization and Decision Making*, vol. 16, no. 4, pp. 1–23, 2016.
- [30] T. Mahmood, U. Rehman, Z. Ali, and T. Mahmood, "Hybrid vector similarity measures based on complex hesitant fuzzy sets and their applications to pattern recognition and medical diagnosis," *Journal of Intelligent & Fuzzy Systems*, vol. 40, no. 1, pp. 625–646, 2021.
- [31] H. Garg and D. Rani, "A robust correlation coefficient measure of complex intuitionistic fuzzy sets and their applications in decision-making," *Applied Intelligence*, vol. 49, no. 2, pp. 496–512, 2019.
- [32] H. Garg and D. Rani, "Novel aggregation operators and ranking method for complex intuitionistic fuzzy sets and their applications to decision-making process," *Artificial Intelligence Review*, pp. 1–26, 2019.
- [33] D. Rani and H. Garg, "Complex intuitionistic fuzzy power aggregation operators and their applications in multicriteria decision-making," *Expert Systems*, vol. 35, no. 6, Article ID e12325, 2018.
- [34] S. Broumi, A. Bakali, M. Talea et al., "Bipolar complex neutrosophic sets and its application in decision making problem," in *Fuzzy Multi-criteria Decision-Making Using Neutrosophic Sets*, pp. 677–710, Springer, Berlin, Germany., 2019.
- [35] I. Beg and T. Rashid, "Group decision making using intuitionistic hesitant fuzzy sets," *International Journal of Fuzzy Logic and Intelligent Systems*, vol. 14, no. 3, pp. 181–187, 2014.
- [36] F. Smarandache, "Introduction to the complex refined neutrosophic set, critical review," pp. 5–9, 2017, <http://fs.unm.edu/CR/ComplexRefinedNeutrosophicSet.pdf>.
- [37] J. S. Chai, G. Selvachandran, F. Smarandache et al., "New similarity measures for single-valued neutrosophic sets with applications in pattern recognition and medical diagnosis problems," *Complex & Intelligent Systems*, vol. 7, no. 2, pp. 703–723, 2021.
- [38] R. Tan and W. Zhang, "Decision-making method based on new entropy and refined single-valued neutrosophic sets and its application in typhoon disaster assessment," *Applied Intelligence*, vol. 51, no. 1, pp. 283–307, 2021.
- [39] C. Karamaşa, D. Karabasevic, D. Stanujkic, A. Kookhdan, A. Mishra, and M. Ertürk, "An extended single-valued neutrosophic AHP and MULTIMOORA method to evaluate the optimal training aircraft for flight training organizations," *Facta Universitatis, Series: Mechanical Engineering*, vol. 19, no. 3, pp. 555–578, 2021.
- [40] Z. Ali, T. Mahmood, T. Mahmood, K. Ullah, and Q. Khan, "Einstein geometric aggregation operators using a novel complex interval-valued pythagorean fuzzy setting with application in green supplier chain management," *Reports in Mechanical Engineering*, vol. 2, no. 1, pp. 105–134, 2021.
- [41] R. T. Ngan, L. H. Son, M. Ali, D. E. Tamir, N. D. Rishe, and A. Kandel, "Representing complex intuitionistic fuzzy set by quaternion numbers and applications to decision making," *Applied Soft Computing*, vol. 87, Article ID 105961, 2020.
- [42] Y. A. Qudah, M. Hassan, and N. Hassan, "Fuzzy parameterized complex multi-fuzzy soft expert set theory and its application in decision-making," *Symmetry*, vol. 11, no. 3, 2019.

## Research Article

# Inertia Theory Frequency Dynamic Analysis and Control of Power System with High Proportion of Renewable Source

Badar ul Islam <sup>1</sup>, Zuhairi Baharudin,<sup>1</sup> and Parameshwari Kattel <sup>2</sup>

<sup>1</sup>Department of Electrical Engineering, University Technology Petronas, Seri Iskandar, Malaysia

<sup>2</sup>Department of Mathematics, Tri-Chandra Multiple Campus, Tribhuvan University, Kathmandu, Nepal

Correspondence should be addressed to Parameshwari Kattel; parameshwari.kattel@trc.tu.edu.np

Received 12 November 2021; Revised 13 December 2021; Accepted 14 December 2021; Published 31 December 2021

Academic Editor: Dragan Pamučar

Copyright © 2021 Badar ul Islam et al. This is an open access article distributed under the Creative Commons Attribution License, which permits unrestricted use, distribution, and reproduction in any medium, provided the original work is properly cited.

Power plant emissions are a major cause of pollution in the environment. This necessitates the progressive replacement of conventional power plants with renewable energy sources. Changes in the quotas for conventional generating and renewable energy sources present new issues for modern power networks for example photovoltaic and wind turbines are replacing conventional power plants, which do not add to system inertia and due to the earth's diurnal cycle and weather conditions. Solar radiations are not consistent all through the day, and photovoltaic (PV) generation is sometimes insufficient to meet the power requirement of the shifting local load. The amount of inertia in the power system, as well as the action of adjustable frequency reserves and the amount of power imbalance, all have an impact on frequency stability. As a result, estimating power system inertia and assessing frequency response are required so that necessary actions can be taken to assure frequency stability. In this way, the system frequency, power, and voltage stability are the major issues when high proportion of renewables are added. In this paper, we explained estimating power system inertia-related frequency problems. The approach account for the frequency and voltage fluctuations that occur after a disturbance and estimate the system's total inertia constant as well as its overall power imbalance. The anticipated technique based on computational intelligence is used to analyze frequency responses from simulations of a test system under various circumstances on SIMULINK and focuses on the standalone PV system is critical for controlling it. As a result, the modelling of a PV system, battery, and generator using analogous circuits is discussed. As a matter of fact, maximum power should be harvested from a PV array to increase its efficiency that is depicted from the result outcomes of this research.

## 1. Introduction

This section of the article provides background information on the microgrid in the context of renewable energy penetration including inertia and frequency. The introduction and significance of microgrids and renewable energy sources are discussed and the awareness of the renewable connected to microgrid problems is also focused. A brief overview of the research background of inertia and frequency stability of grid with penetration on renewable sources and explanation of the research motivation and project's problem statements are highlighted. The previous researches done to cope these issues are explained along with the objectives.

Malaysia has abundant solar energy resources and is one of the world's sunniest countries. At the moment, Malaysia's

wind, light, and other renewable energy generation accounts for a relatively small proportion of total energy generation. To promote energy transformation, the government has issued a series of reform plans, with the goal of achieving more than 30 percent renewable energy generation by 2030 [1]. Renewable energy sources have emerged as a viable option for meeting rising energy demand, mitigating climate change and contributing to sustainable growth [2, 3]. The introduction of such systems is primarily accomplished through the use of well-organized microgrid systems; this provides a collection of technical explanations that allow the sharing of knowledge between customers and distributed generation centers, implying that they must be handled optimally [4].

Exponential energy demand has contributed to the reduction of fossil fuels such as oil, coal, and biomass. This in



turn raises the emissions from the greenhouse effect. Power systems have integrated small and large-scale renewable energy sources, such as wind, solar, tidal energy, and biomass to alleviate the above difficulties on a worldwide platform. The rise in energy demand and the reconsidering of energy systems have led to the generation of power near the depletion sites. This power comes from renewable sources, which are becoming extremely important fall in costs, particularly in the situation of solar photovoltaics and wind power.

The inertia problem can be divided into three parts: inertia theory, inertia identification, and virtual inertia control. The power electronic equipment are constantly replacing the synchronous generators because of the physical structure of power electronic equipment that differs from the traditional synchronous generator. This results in gradual change in power system inertia [2]. The research in this domain has emphasized that high-energetic power penetration system is increasing energy efficiency. A large number of wind turbines and photovoltaic systems have taken the place of many synchronous generators. But the rotating inertia of the synchronous machines itself was lacking, which resulted in a reduction in constant, poor inertia equivalent system steadiness.

The high proportion of renewable energy power systems in operation faces a slew of dynamic security issues. According to [3], renewable energy generation is highly volatile and random. When the system's inertia is insufficient, and renewable energy output fluctuates widely, the system may produce new regional power grid security and stability problems due to a lack of effective resistance to this energy fluctuation, which not only severely limits access and utilization of renewable energy but also causes systematic security risks. As a result, further investigation into the inertia principle of renewable energy power systems is required.

There are, however, few studies on the inertia principle of high proportion new energy power systems at the moment. More research is being done on virtual inertia (VI) control and the effect of decreasing system rotation inertia on system frequency stability after increasing renewable energy permeability. Reference [4] examines the relationship between the frequency change rate, the lowest point of frequency, and the inertia of system to reveal the effect of system inertia reduction on frequency stability. Instead of synchronous generators, system reserve capacity and battery energy storage are used to provide inertia energy for smoothing renewable energy generation fluctuations [5]. A wind turbine is used to add virtual inertial control to the system's inertial support capacity, allowing wind power inertial capacity to match traditional grid inertial capacity [6].

Electric power frequency is a metric for power system balance. Frequency stability is defined as the capacity to refurbish system generation and load demand balance with minimal load loss as shown in Figure 1.

The influential aspects of frequency control are frequency response phase, control object, control number, and control algorithm. According to the different frequency response phases, the control participants can be divided into

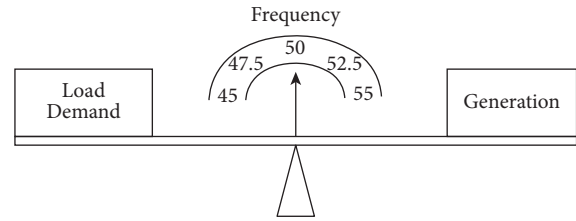


FIGURE 1: Relationship between frequency and variations in load demand and generation.

inertial controls, primary frequency regulation, and secondary frequency regulation. Depending on the number of controllers, to control the various frequency reaction stages of a given object and coordinate several objects during the same frequency reaction stage. According to the various control algorithms, the frequency response stages of the same object can be divided into coordination control, and multiple object coordinating control in the same frequency reply stage is devised. Examples include linear quadratic control [7], adaptive control [8], sliding mode control [9], and fluid control [10]. For a particular stage of frequency response, the control strategy used with a specific control object must be proposed.

In the last decade, solar PV energy has gotten a lot of attention. It was one of the fastest increasing sources in 2018, with 181 GW installed globally [11]. This is due to the fact that the cost of PV modules has steadily decreased over the last decade. It is also widely accepted by many industries due to its ease of installation, scalability, and low maintenance requirements and owing to the lack of moving parts in its operation. PV charge controllers are extensively used in unconnected systems such as street lighting, rural electrification, and other applications [12]. Maximum power point tracking (MPPT) tracker and a battery charge controller are both included in a Solar PV MPPT charge controller. The MPPT observers and distributes as much power as possible from the solar panel to the charge controller. The charge controller creates a hybrid charging strategy to ensure that the battery is charged efficiently while avoiding overcharging and excessive heat, which can cause battery damage. Many research papers mentioned the modelling of solar PV charge controllers [13], but there was little modelling detail and no efficiency analysis, as well as no model validation reference point with commercial charge controllers. To summarize, the models presented in the preceding literatures were incomplete, lacking MPPT and whole charge controller efficiency performance examination, as well as validation of the model with commercial charge controllers [14]. Combined power plants use synchronous generators with inertial response to abrupt frequency variation. Furthermore, if there are sufficient rotating reservoirs, their droop characteristics contribute to load-frequency regulation. Renewable energy system-based plants, unlike conventional power plants (CPP), are grid connected via power electronic converters [15]. In wind power plants, such power electronic interfaces decouple grid frequency from CPP. Static dc generators are also used in PV plant. As a result, RES-based plants cannot provide inertial response or load-frequency regulation on

their own and their large-scale integration. This problem may cause the loss of inertia and primary frequency reserve.

However, because an increment in power output is characterized by a decrease in the speed of rotor, resulting in a shift in the operating point, the increase in output power is only temporary. The duration of this assistance is usually around 10 seconds. Furthermore, while the rotor speed recovers, a second frequency dip may occur. Grid stability could be jeopardized as a result of such an occurrence [16]. The authors of [17] looked into how HVDC technology by differing the DC voltage, inertial response can be provided. In addition, the demand-side management (DSM) method is appropriate for delivering primary frequency response through the use of temperature controlled loads [18]. DSM, on the other hand, would necessitate the deployment of new infrastructure, such as smart devices and communication networks. Electric vehicles (EVs) will be used as a source of frequency support in future concepts, such as vehicle connected to the grid and grid connected to the vehicle [19]. However, the infrastructure is not yet in place, and the current fleet of electric vehicles is not enough to keep the grid running. Furthermore, energy storage system (ESS), which provide a variety of storage devices, are available [20], which offer both IR and primary frequency response (PFR) as viable options [20, 21]. As an outcome of environmental regulations and hard work to improve energy conservation, the number of renewable energy sources for electricity production has increased [22]. The increase in electricity generation from PE converter RES has no inertia without a proper control technique. A high inertia and rate of change of frequency (ROCOF), which can cause protective relays to trip, is the first challenge identified by Irish grid operators [23]. Load shedding and cascading failure can be caused by large frequency deviations [24, 25].

In [26], various imitated inertia control methods for PE converters were anticipated to mimic the synchronous generator inertia characteristics. These methods are primarily concerned with control design, with only a few addressing practical application. Emulated inertia control (EIC) is discussed as a developing concept to implement regulating the frequency in this paper. The EIC approach is a good fit for a system with low inertia. In [27, 28], a small-signal investigation of EIC implemented at an ideal grid-connected inverter was evaluated. However, previous EIC research has primarily focused on controller design, with only a few researchers discussing EIC functional implementation [29]. The concept of deloading control method for PV systems in addition to the EIC for controlling frequency and providing an inertial response is also proposed [30]. On the other hand, PV modules are forced to operate at a lower power level.

Rising energy costs, power system losses, and the dangers of nuclear power generation are all encouraging people to find new ways to generate electricity. Everyone in the globe wants to rely increasingly on renewable energy resources (RERs) for electricity generation [31, 32]. RERs provide economic benefits while increasing greenhouse gas emissions. By integration of more renewable resources, the stability issues take places in the system so we motivated to

study the stability issues and to provide the solution for unstable states as follows:

- (i) Inertial constraints: because solar technologies are static generation technologies, they have no inertia. When combined with conventional energy resources, it causes an inertia problem.
- (ii) Fluctuations in frequency: PV systems have low inertia and pose a hazard to the mechanical inertia balance of the power system. It poses a significant challenge to the power system's frequency stability.
- (iii) Voltage fluctuation: the intermittent nature of the PV system causes voltage fluctuation in the power system's generation profile. Falls, tripping, and blinding of protection devices can occur as a result of islanding events.
- (iv) Issues of stability: PV systems can put a strain on traditional system operations if their penetration increases the grid's hosting capacity.

Solar and wind are the two widely used and capable renewable sources for producing electrical energy among the various RERs. They are linked by converters that disconnect them from the electric grid, despite their intermittent nature. As a result, when traditional generators are replaced with RER, the electrical grid's effective inertia is reduced [33]. Frequency reliability and dynamic response are harmed when a huge amount of renewable sources are integrated into the grid [34]. In fact, over a short time period, a system having less inertia is linked to a faster ROCOF and larger frequency deviations [35]. Total system inertia is expected to decrease as renewable energy generation increases and conventional steam generation decreases [36]. This could be especially important in a scenario where the grid has a high renewable penetration but little demand. In these circumstances, the frequency drop may be severe enough to require additional safeguards like load shedding [37]. When the frequency goes below to 49 Hz, 10–20% load shedding is required [36]. At 48.7 and 48.4 Hz, additional shedding of 10–15 percent of the load is required. The generators must be disengaged from the grid to avoid blackout if the above procedures does not stop the frequency descent at 47.5 Hz. Fast frequency response's main aim is to decrease frequency dip and the degree at which they occur in the system to safe from blackouts. The use of conventional generators is one traditional solution. Consider synthetic inertia, such as the SVC PLUS Frequency stabilizer, or batteries. Full power availability is one of their advantages.

This paper's goal is to give a broad overview of system inertia and how it affects the grid stability. The research looks at a variety of frequency response solutions. Both conventional and alternative solutions, as well as their experimental specifications, are explained. In conventional generators, the amount of energy and highest available power for the initial inertia response have been indicated to be restricted. These solutions explain that the active power is exchanged when the value of frequency deviates with the power grid. For instance, the energy needed before a less frequency event can be kept during a successive event. In this section, the

lithium-ion battery storages and the SVC frequency stabilizer have been thoroughly examined. Battery storage systems are becoming more popular in developed countries as a result of the growing trend of highly volatile renewable energy in the grid. A variety of battery storage systems in various capacities are available. High load management, power quality, power storage, voltage regulation, auxiliary grid services, and renewable stabilizing are just a few of the applications that have been discussed with such solutions. On the other hand, the high permeation of renewable energies into the power grid creates difficult reliability and security issues. Frequency instability caused by synchronous generator replacement is a significant challenge [38].

The moment of inertia of a synchronous generator can be haul out to backing frequency deviancy because the speed of rotor is tightly fixed with the grid frequency. Renewable energy sources, on the other hand, lack inertia in most cases. A doubly fed induction generator, for example, has a restricted inertial reaction [39]. A permanent magnet synchronous generator's rotor speed is completely detached from grid-related frequency, and it has no inertial response, unlike solar PV. PV usually run in MPPT mode, which explains that the active power interaction with the grid fluctuates, resulting in an absence of inertia energy when it is needed. A second major trial is the complication of power system dynamics [40]. In the past years, some power instability events have been noted in delayed fed induction generator (DFIG) wind plants [41]. As a result, power grids with high renewable energy penetration will require improved damping capability. To increase stability, a control scheme called virtual inertia or virtual synchronous generator is proposed to make renewable energies act like synchronous generators [42]. To achieve sufficient power interaction with the grid in the case of PV, an ancillary energy storage unit is used. Auxiliary damping controllers for wind turbines are also designed to improve damping [43]. However, performing well in practice is never easy for them.

A converter's surplus load and transitory voltage support abilities are inferior to those of a synchronous generator because it cannot support high amount of short circuit current when sudden and huge disturbance occur. To achieve sufficient power interaction with the grid in the case of PV, an ancillary energy storage unit is used. Auxiliary damping controllers for wind turbines are also designed to improve damping [43]. However, performing well in practice is never easy for them. A converter's surplus load and transitory voltage support abilities are inferior to those of a synchronous generator because it cannot support high amount of short circuit current when sudden and huge disturbance occur. There is a substantial body of research papers that supports the use of the additional services market to bridge the gap between grid and DG resources. The concept of "unbundled or ancillary services" is discussed in reference [44]. Voltage regulation, frequency control, load following, spinning reserve, additional reserve, standby supply, and maximum shaving are all examples of ancillary services that active, nonactive power regulation support can provide.

The value derived from ancillary services is determined by technical and economic factors, as well as dependability. These services can also be classified according to the maximum advantage they would deliver to the grid, the DG owner, or both. The availability of high-energy density storage devices and advancements in semiconductor technology have given these services a new edge [44, 45]. They emphasize the importance of developing new standards of grid and developed new mathematical models for forecasting system behavior in the existence of high insertion intermittent energy resources.

Renewable energy source's stochastic nature has also been investigated. For forecasting ancillary services, Bevrani et al. used an ANN-based approach. This method aids in the prediction of spinning and nonspinning reserves, as well as up and downregulation requirements [45]. Raugei and Frankl [46] also pointed out that by using the twofold increase in PV generation would reduce cost by 1/5th. Liu and Bebic have connected the increase in PV inverter insertion to the level to which voltage regulation equipment on a line can be replaced. So even though a 5% increase does not have any effect during high load demands, an increase of 30% to 50% can completely displace the voltage-regulating capacitors. Tapanlis and Wollny proposed using AC coupling to control the frequency and voltages of microgrids powered by solar, wind system, and batteries. Borlea et al. [47] projected an ideal solution for ancillary service facility at the substations. In this study, they considered using FC (fuel cells) as a standby reserve for system support.

To further investigate the problem of inertia, frequency, and voltage fluctuation in high proportion renewable energy power systems, we attempted to redefine system inertia from the standpoint of system energy and angular momentum, and we investigate a new method of carrying out this research. To begin, the power system's inertia principle and the mechanism of new energy injecting energy and angular momentum into power grid nodes to affect the inertial behavior of the power system are investigated. Second, the inertia transfer and frequency dynamic process are investigated. We investigated the voltage fluctuation and the improved method in the standalone conditions. Finally, the agent group control of source load coordination improves system frequency stability based on the inertia theory as major objective.

To regulate active and reactive power from solar and an ESS, Babu et al. [48] projected a power management structure with consecutive multilevel inverters combined into the grid. For reactive power control between PV panels and batteries, a two-stage DFT and PLL strategy founded on active and reactive power management was utilized. Sun et al. used DC to DC converters for solar arrays, DC to AC converters for the grid linking, and a DC to DC converter for the battery to join the PV generation system and battery to the grid. Switching between constant voltage and MPPT operations is prompted by the DC bus signals.

Wu et al. have explained an end-user power controlling strategy that includes a PV system and battery storage. They were able to achieve multimode operation of the system by using inverters to connect the individual sources on the AC side. It becomes more expensive to perform frequency

control using only conventional generation. The combination of demand-side manageable devices to adjust frequency is a novel technique for meeting the growing demand in nonrenewable power generators [49]. DERs are getting increasingly more appealing for supplying loads together with traditional generators. EV, BESS, and water heaters are a challenge. As a result, DER allocation is critical for improving power system frequency and enhancing the integration of these power sources [50]. A review of bottleneck management approaches for the distribution network with excessive DER perception was also presented in [51].

The procedures for power regulation [52] presented load regulator with the addition of electric vehicles and DG. As per technicality and market situations, the load-shifting optimization problem was solved. This method can be used for a variety of DERs, including smart charging for electric vehicles. The market and direct control methods were discussed. Furthermore, under the smart grid scenario, an analysis of PE-based DER and their stability issues was proposed. Power electronics-based DERs were cited as examples of renewable energy resources and modern loads. In today's power systems, IEDs are the typical protection and control apparatus. These smart devices are used for a variety of purposes, including system regulator and protection, and as a result, power system modelling and analysis can get off to a good start [53]. In [54], demand-side frequency control and battery energy storage system were considered in the power system of the United Kingdom. They are DER's most significant components in today's power system. In previous work, BESSs were considered for the use of frequency regulation in the power system. It had a quick dynamic reaction and recompensed for load fluctuations on the electric grid. As a result, the combined BESSs can influence the frequency of both low- and high-frequency reserve services.

In an electric power system, frequency is a constantly varying variable that represents the equilibrium between generation and demand. The National Grid is operator in the United Kingdom, and it is responsible for keeping the power system's frequency response within acceptable limits. The working limit, which is equivalent to 0.2 Hz, and the statutory limit, which is equivalent to 0.5 Hz, are the two key levels that describe these limits. An interruption by frequency protection relays is provided to regulate frequency of both the generation side and demand side when the major frequency drops happen. The facilities cover both supply and utilize side. FFR, MFR, and EFR are examples of frequency response services [55]. The National Grid recently negotiated 201 MW of EFR facilities from ESS from a variety of providers. By the end of 2021, the majority of these providers should be able to offer their services [56, 57]. Timescale of the frequency response in accordance with load response in the system can be seen in Figure 2.

Large-sized synchronous generators, such as those used in the United Kingdom's power system, account for roughly 70% of the system's inertia. Small-sized synchronous generators deliver regulated power in the moderate power grids [56]. Challenges of inertia reduction due to their power electronics, some RES, such as wind and solar, do not have through connection between the machine and the system,

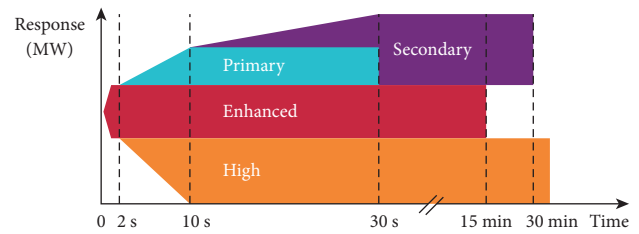


FIGURE 2: Timescale of frequency response.

preventing their spinning mass from backing to system inertia [57, 58]. As a result, RES decreases total system inertia, resulting in decrement in system steadiness and increasing the difficulty of power system process and regulator. Due to variations in wind speed and solar irradiance, RESs experience power fluctuations, which have an important impact on the frequency deviancy's stability.

## 2. Materials and Methods

This paper focuses on a microgrid test that uses a renewable energy-based power generation system that includes a PV array, batteries as ESS, diesel generator, power converters, filters, controllers, loads, and electric grid. A comprehensive simulation has been conducted of a grid-connected PV, battery and diesel generation system. A converter is used to optimize PV output and an inverter to convert the solar panel DC voltages into an AC system connected to the PV array and a utility grid. Meanwhile, a charge controller connects the battery to the common DC bus to deliver regulated PV voltage. The projected model of all components and the control method of system is replicated using the MATLAB/SIMPOWERSYSTEM program. The results validated the strength of the models and the efficiency of control mechanism.

A prototype of the model is also designed and developed to show the stability of the system. We integrated the PV, battery, and diesel generator in isolated system. We developed the inverter successfully and converted the DC supply to AC supply. We used DC bus bar, and all the sources are connected to it. We controlled the battery PV with the microcontroller to make coordination between them and controlled the load through IoT to turn it on and off.

*2.1. Modelling of Energy Resources and Storage System.* The important hurdles of using most renewable energy resources as distributed generators, such as wind farms and PV systems, are that their output powers are changeable and uncontrollable. Indeed, these key characteristics increase extra worries about the use of DG in a power system. An ESS is one of the most suitable approaches in this field. Due to which the Engineers can now achieve the power system more excellently. Furthermore, the fluctuation of RES and the corresponding decrease in system inertia requires innovative, flexible controllers and energy storage for optimal integration. Exact models for the diesel generator, PV array, and battery stacks must be developed in order to test our control techniques.

**2.2. Diesel Generator Model.** Due to the DG's complexity and high nonlinearity, investigations of diesel generators are now limited to the existing mechanical or electrical dynamics of the process. This study reviews many models that can be used to represent the complete dynamic process of a diesel generator. A model is then used to study the interplay between mechanical and electric aspects of a DG. The conventional model of the diesel generator and governor for speed management is depicted in the form of block diagram in Figure 3. This model is broadly employed because the active behavior of small generator sets is precisely reflected. The power delivered and inertia provided by the DG can only be controlled if the impact and proportion of the renewable sources are determined with a careful parametric analysis. This is the main reason behind the simulation analysis and design of DG model.

**2.3. Photovoltaic Array Model.** The PV cell is one of the most fundamental generating component in an electrical system. To replicate silicon photovoltaic cells, a single-diode mathematical model with a PV current source  $I_{ph}$ , nonlinear diode, and inner resistances  $R_s$  &  $R_{sh}$  can be used as depicted in Figure 4.

In the diode equivalent circuit, the mathematical relationship between current and voltage is as follows:

$$I + I_{ph} - I_s \left( e^{q(V - IR_s / AKT)} - 1 \right) - \frac{V + IR_s}{R_{sh}}, \quad (1)$$

where  $I_{ph}$  is the photoelectric current,  $I$  is the current of diode saturation current, and  $q$  is the constant coulomb equals to  $1.602e^{-19}$  Columbs,  $k$  is known as the Boltzmann constant equals to  $1.38e^{-23}$  Joule/Kelvin,  $t$  is the PV cell temperature in Kelvin,  $A$  is the ideal of the P-N connection, and  $R_s$  and  $R_{sh}$  are parallel to the inherent series. A solar radiation and cells temperature function of photocurrent is explained. The simulation design of solar inverter is depicted in Figure 5.

$$I_{ph} = \left( \frac{S}{S_{ref}} \right) \left[ I_{ph} - ref + C_t (T - T_{ref}) \right], \quad (2)$$

where  $S$  is the true PV solar rays ( $W/m^2$ ); the solar radiation, the absolute cell temperature and  $I_{ph} - ref$  are  $S_{ref}$ ,  $T_{ref}$  and  $I_{ph} - ref$  respectively; in conventional test conditions  $C_t$  is the temperature coefficient ( $A/K$ ). The saturation current of a diode changes with cell temperature. The simulation design and analysis of the inverter system as shown in Figure 5 is required because all the renewable sources' output depends on the attributes and parameters of this device.

**2.4. Energy Storage Model.** The energy storage itself and the operator of devices such as electronic, electrical, and mechanical that allow the storage and rescue methods to take place are both included in a simulation of the storage subsystem. The driver subsystem is a generic wrapper for a complex system that uses a number of different technologies. For active simulation, the batteries corresponding circuit model are most suitable. Based on the battery model, a general battery model for simulation is proposed, supposing that the battery model is assembled with a controllable

voltage source and resistances as shown in Figure 6. The simulation design of all the abovementioned components of the system is given in Figure 7.

**2.5. Prototype Design.** The design of hardware prototype is on the integration of PV system with battery to stabilize the system and to increase its working time. The reason to integrate RES is that traditional power is highly expensive; we use RES since it is less expensive, and the energy produced by RES does not pollute the environment.

For the project, we used 18 volt dc and 150 watt solar panel, and we used AC generator and connected all the sources with the common DC bus bar. The DC supply is converted into AC supply using an inverter. A battery with PV panel in parallel position is used. We controlled the PV and battery coordination with Arduino microcontroller. After the conversion in the AC supply, we supplied the AC to loads to run them. Finally, we used IoT technology for the load management system and display all the parameters of the system on mobiles. The block diagram of the hardware design is shown in Figure 8.

**2.6. Power Sources.** We used three power sources as also mentioned in the block diagram and their pictorial view is shown in Figure 9. These power sources include PV panel, battery, and AC generator.

**2.7. Inverter and Rectifier.** An inverter is a device that is used to alter direct current (DC) power into alternating (AC). H-bridge Inverter circuit is designed to alter DC supply from the PV panels to AC for loads. Arduino-based microcontroller is used to provide voltage signals of 5 V to input terminal. It has the total capacity of 1 kW. We connected all sources from DC bus bar to inverter, as shown in Figure 10. A rectifier is a modest dc current convertor with a voltage output vary from 0 V to 12 V. We used a complete wave rectifier with a voltage regulator to yield a consistent output. To connect all sources on the DC bus bar, we used a rectifier to convert 220 AC voltages from the generator 12 V DC.

**2.8. IoT Control of Prototype.** Distributes power usage to appliances under its supervision by connecting with load controllers. Using Bluetooth (BLE), connect to a smartphone provides all of the information required to be displayed on display screen. It performs multiple useful functions including, data collection from sensors, data collection from appliances, and scheduling of switching of electrical loads. Flowchart of the prototype design and IoT system is shown in Figure 11, highlighting the explanation of the flow process of the whole IoT system. This flowchart gives each step from the configuration of the mobile with the Bluetooth device including the operation of the relay and ends at showing the status of the loads on the LCD display.

Figure 12 gives a pictorial view of all the components that are assembled and connected. This also depicts all the loads connected.

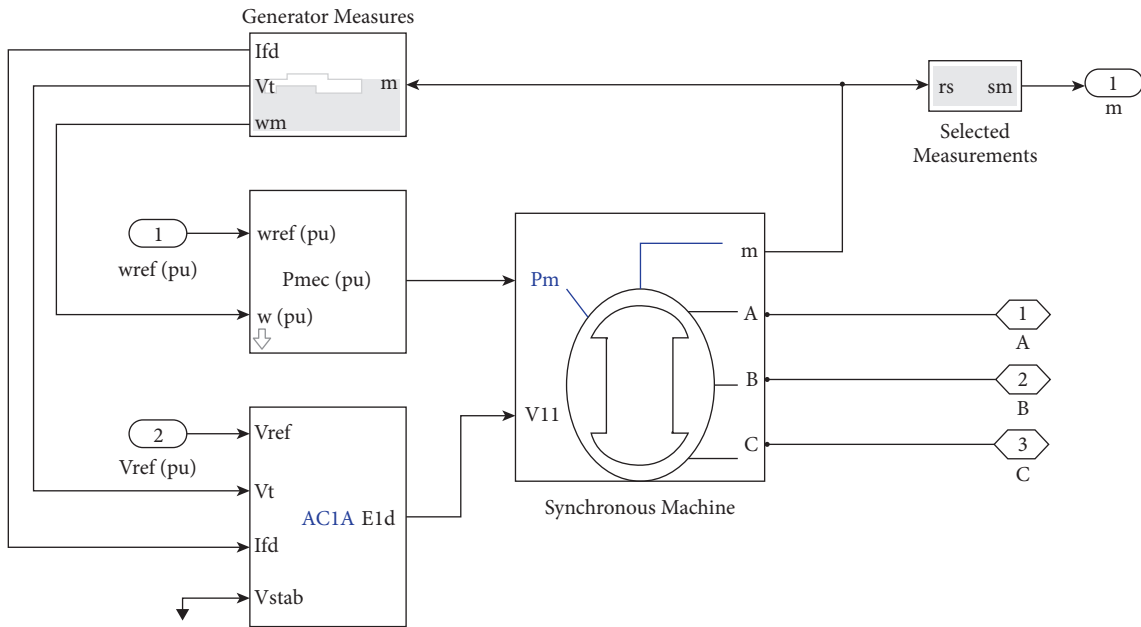


FIGURE 3: Diesel generator Simulink model.

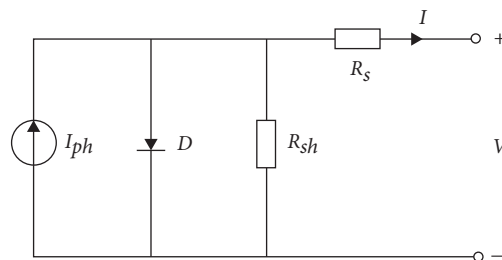


FIGURE 4: Simple model of single PV cell.

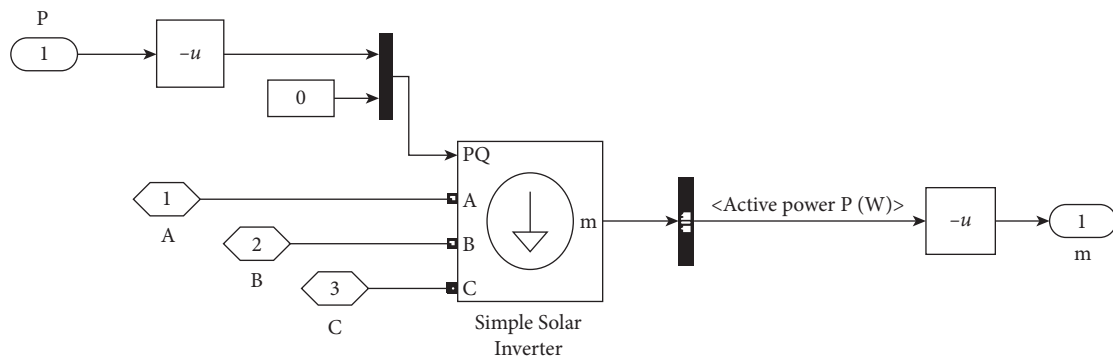


FIGURE 5: Simple solar inverter system in Simulink.

### 3. Results and Discussion

Taking into account the frequency instability and inertia in the renewable fed microgrid systems, multiple experiments are conducted. The results of these experiments along with the problem factors, as well as the technical methods and techniques for addressing them for the system, are described in this section. Figure 13 depicts the frequency of grid starting at the 50 Hz then at the moment of 15 sec the

microgrid is islanded from the utility that is the reason why the frequency is dropping and the other event happens when load increases from 200 kW to 500 kW at that point the frequency deviation take place.

Figure 14 depicts that the power of the distributed power resources that is shown in yellow with solar power curve. The line in red is diesel generator starting with relatively low power, but when the microgrid is disconnected, it increases power immediately and will deliver

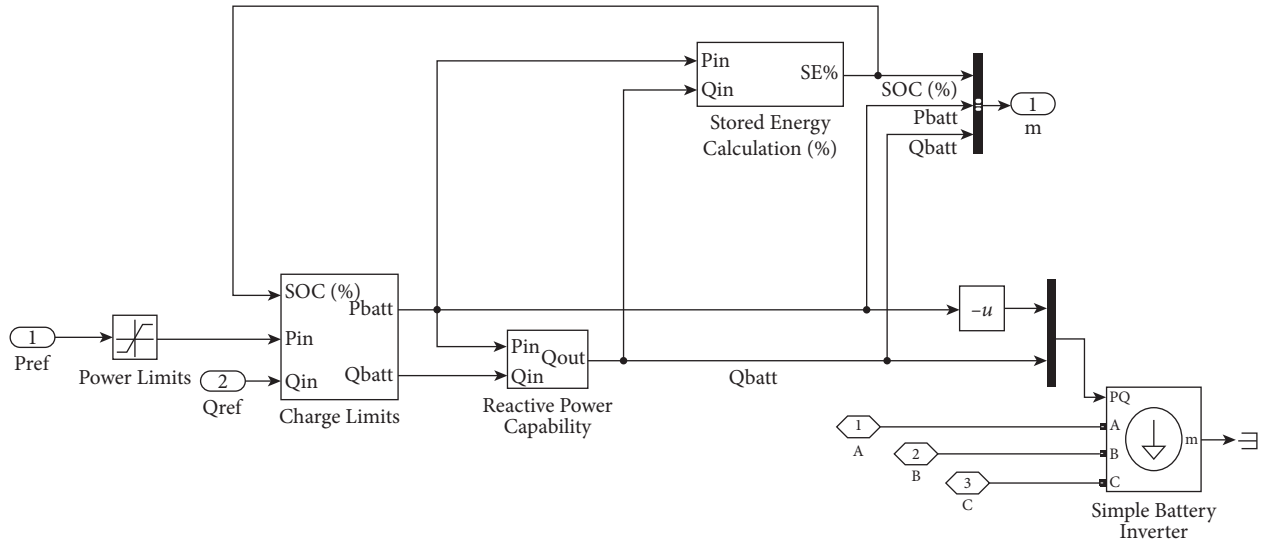


FIGURE 6: Battery block connection Simulink model.

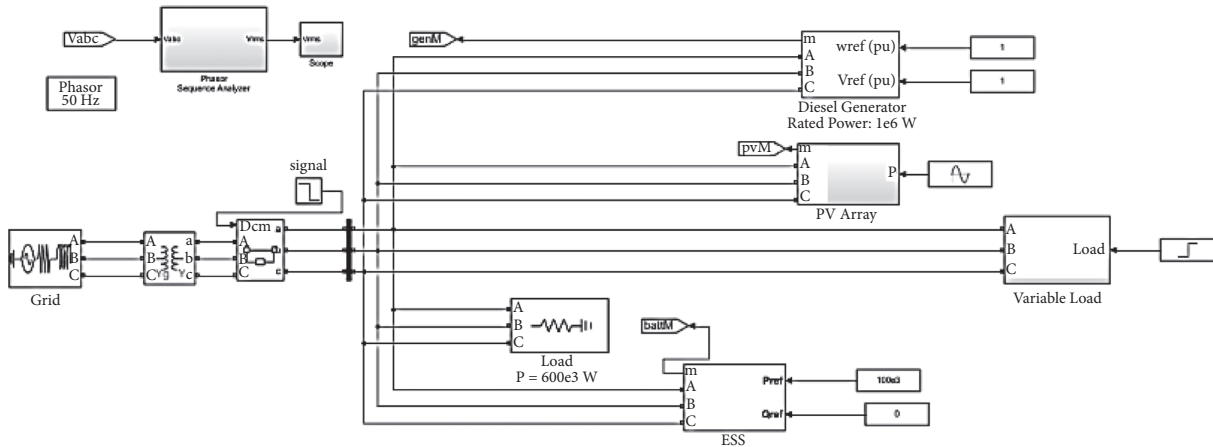


FIGURE 7: Complete grid-connected system simulation.

power that sums up with the solar power to the required power level from the loads similarly we get another step when load is increased.

Figure 15 shows the battery is operated in which it is just giving power to the grid so that is the main reason that SOC is decreasing. We used battery as an ESS so that when our primary backup system generator also gets off, then ESS can supply power to stable the whole system.

Figure 16 shows microgrid voltages level, and it depicts the voltage disturbances happening at the point when frequency deviates at the time of islanding and addition of the loads and shows the recovery of voltages as well.

**3.1. Prototype Results.** The voltage, as we know, is load dependent, and the voltages in PV panel are determined by the amount of energy received from the sun and the amount of current drawn. Many solar panels are watt-rated. Because the generated power is affected by lighting conditions, either the current or voltage is variable.

The type of PV material used, the amount of irradiation received, the PV cell temperature, resistances, clouding and other shading effects, inverter efficiency, dust, module alignment, weather conditions, topographical location, cable width, and so on are some of these factors that affect the efficiency of panel. All the critical parameters of the system including PV voltage, battery voltage, generator voltage, time, frequency, power, and motor RPM are summarized in Table 1.

As can be seen from Table 1, the variation in the PV voltage has a direct impact on RPM and hence the frequency. However, the system power and battery voltage can be maintained due to their negligible impact on the system load. The last column shows the relevance of the frequency and RPM. It has been noticed that the PV voltages varies with the time as irradiances changes. We recorded the change in voltages and recorded in the table. It is important to check the voltage of PV continuously because it has the direct effect on power of the systems. If desired PV voltages are not obtained, it can damage the load connected and whole system can get off, as shown in Figure 17.

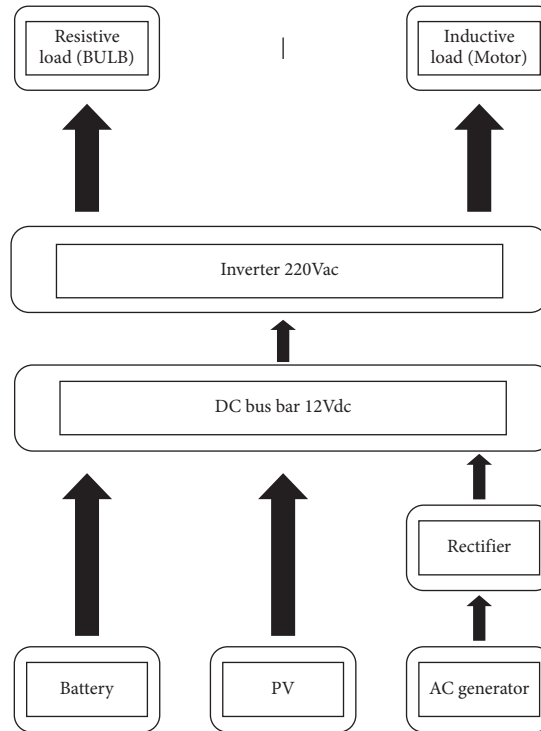


FIGURE 8: Block diagram of hardware prototype.



FIGURE 9: Integrated power sources solar panel, battery, and AC generator.

An inverter is a device that consists of different components to alter a direct current (DC) supply to an alternating current (AC) supply. It is important that the inverter should provide constant voltages and the frequency designed for the load. As the frequency fluctuates more than the allowed limit, it can cause the damage to the whole system, if the frequency increases the limit, the loads can be damaged, and if it decreases the limit, then the system can get trip.

So during our testing of the hardware, we operated our system with different loads and different sources to check our inverter output frequency, we notes down all the readings in table and depicted the variation in the form of graph shown in Figure 18. We noticed that our frequency remained constant at 50 Hz, but it fluctuates once and frequency drops.

A motor of 450 W is used in the project as an inductor load. We operated the motor at different RPM. We decreased RPM to check the effect on the system stability and

effect on resources. Initially, the motor is operated at its maximum RPM and later on the RPM are decreased gradually with the help of regulator. The impact of decreasing of RPM is represented in graph shown in Figure 19.

The change of the rpm of the motor is to check the effect on generator voltages. Initially, we operated the motor at maximum RPM of 2200 and recorded the voltages of generator at that time which was 220 V utilizing the maximum voltages gradually the RPM are reduced with the help of regulator to 2070 and voltages at that time was recorded as 200 V. This show that when we reduces RPM of motor the voltages also decreases. We recorded all the RPM and voltages in Table 1 and depicted the voltage decreasing trend in the graph shown in Figure 20.

Figure 21 shows the power stability of the system. As PV source voltages change with time, it effects on the power of the system. The purpose of integrating different resources



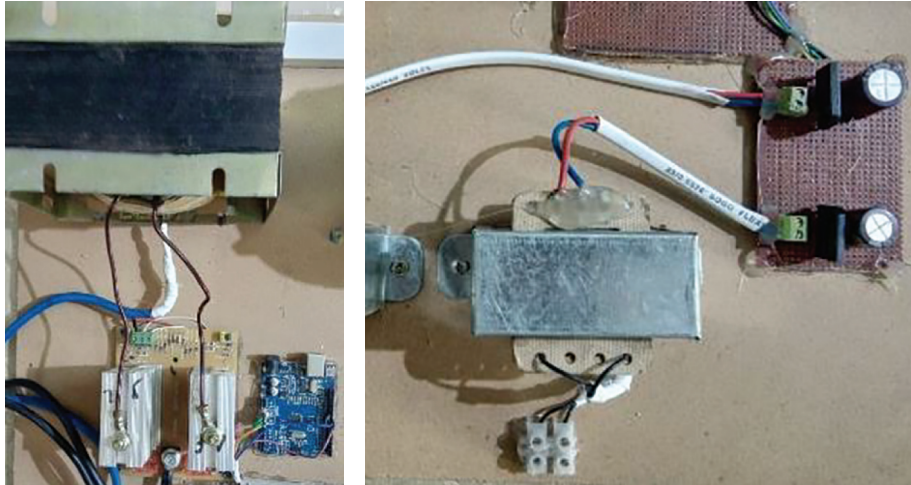


FIGURE 10: Hardware design of inverter and rectified.

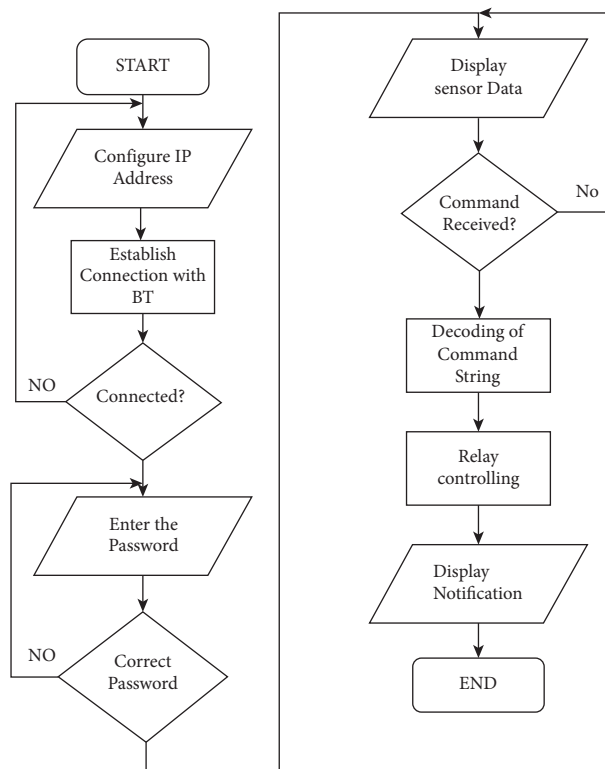


FIGURE 11: Flowchart for IoT control of prototype.

plays its role to keep the whole system balanced, which includes the battery and AC generator to fill the differences and to make the whole desired power constant. In this way, the system provides the accurate amount of the power to keep proper functioning of the loads.

In Figure 22, relationship between the motor RPM and generator voltages is shown. It makes clear that whenever the RPM decrease the voltages at the generator side also decrease as shown in the graph. In contrary, when RPM decrease from 2200 to 2070, the voltage

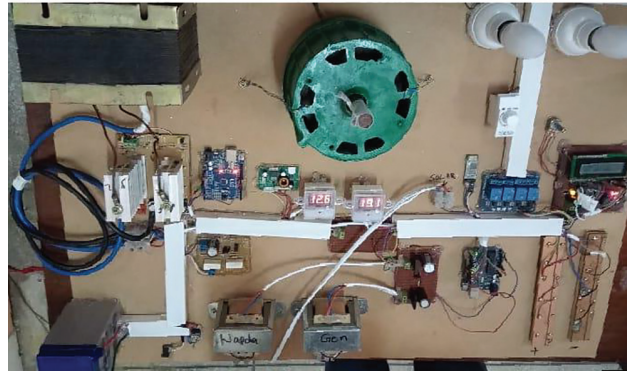


FIGURE 12: Pictorial view of complete hardware prototype.

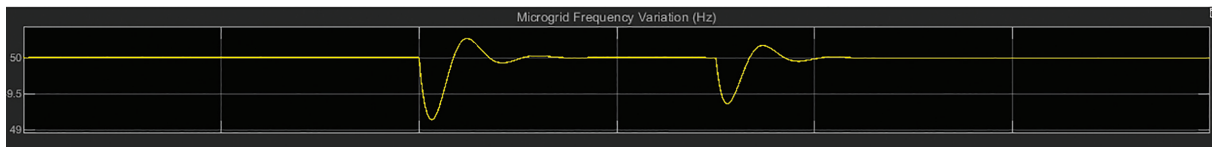


FIGURE 13: Grid frequency regulation.



FIGURE 14: Distributed resources response.

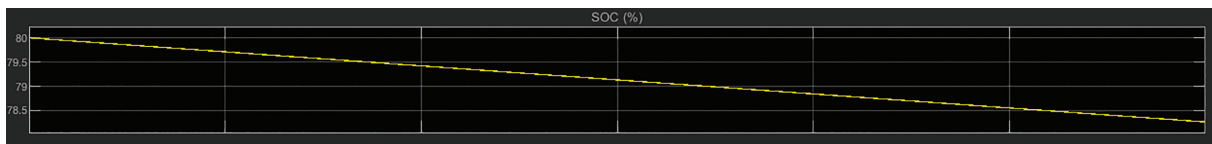


FIGURE 15: Battery SOC.

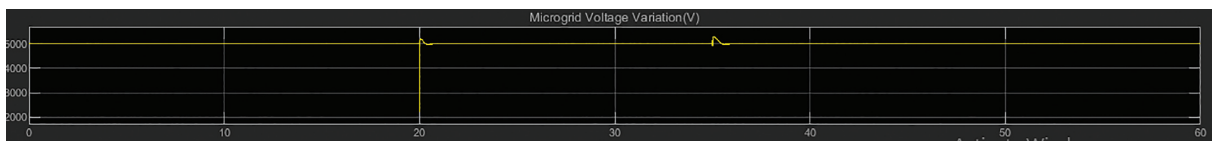


FIGURE 16: Grid voltage regulation.

TABLE 1: Hardware prototype readings (1 RPM = 0.01667 Hz).

PV (V)	Battery (V)	Time	Inverter frequency (Hz)	Power (W)	Motor RPM	Generator (V)	RPM to Hz
18.1	12.6	1	50	480	2200	220	$2200 * 0.01667 = 36.667$
15.3							
19.1	12	7	50	480	2070	200	34.50
14	12	18	49.5	480	1937	180	32.28
20	12	23	50	480	1795	150	29.92
17	12	30	50	480	1645	140	27.417

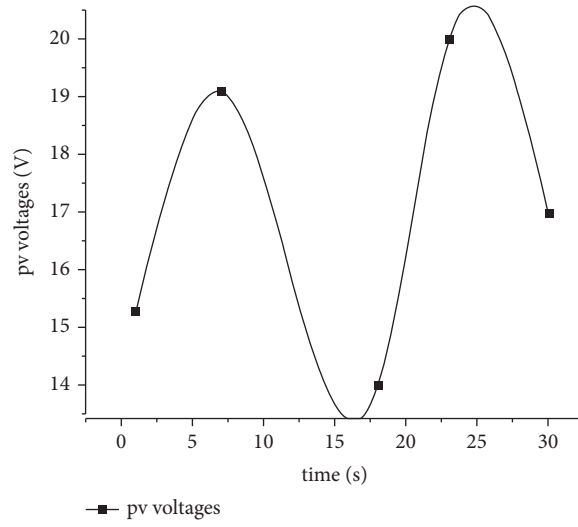


FIGURE 17: PV voltage variation graph.

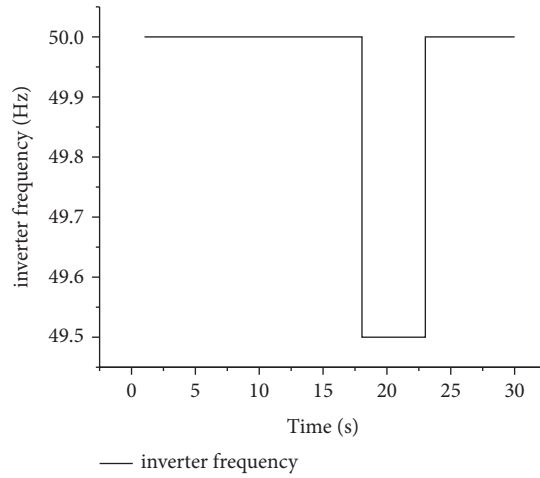


FIGURE 18: Inverter frequency variation graph.

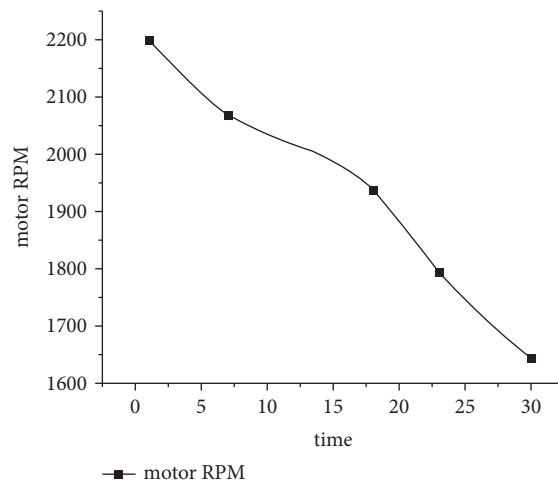


FIGURE 19: Motor RPM variation graph.

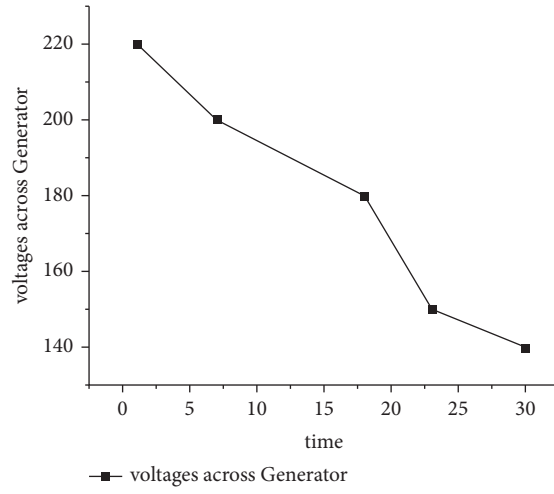


FIGURE 20: Generator voltage variation graph.

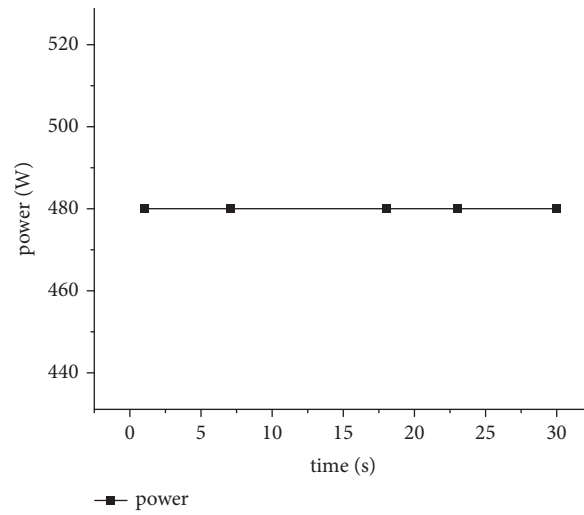


FIGURE 21: Power graph of the system.

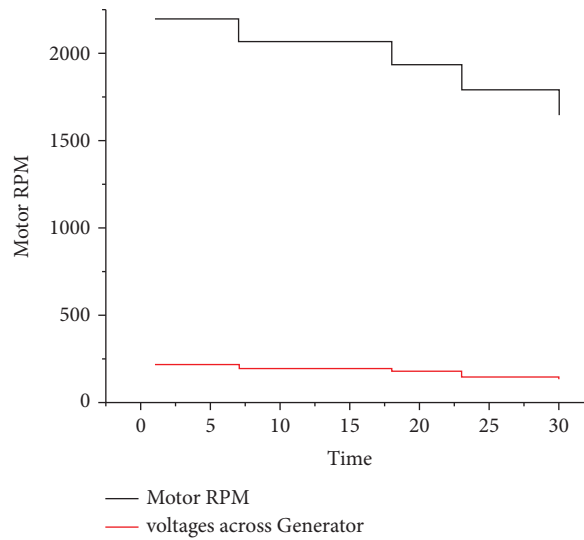


FIGURE 22: Graph between motor RPM and generator voltages.

across the generator drops from 220 V to 200 V. Since the load changing effects the voltages of the generator.

#### 4. Conclusions

Due to the depletion of natural resources, the world is currently experiencing an energy crisis. Pollution of the environment is caused by natural resources such as fossil fuels. They emit CO<sub>2</sub> that contributes to the greenhouse effect and global warming. Price fluctuations affect countries whose economies are reliant on fossil fuels because the majority of sectors rely on gas and oil. As a result, renewable energy production is becoming increasingly significant. In this research, the focus is on power system inertia-related frequency problems. The approach account for the frequency and voltage fluctuations that occur after a disturbance and estimate the system's total inertia constant as well as its overall power imbalance. This was achieved by including a function that approximates the frequencies and voltages that show reliance of loads. The proposed method used was the PV, battery, and diesel generator integration in grid-connected system to analyses frequency responses from simulations of a test system under disturbance. Furthermore, it also focuses on the standalone PV system when they are integrated with the microgrid systems for controlling the critical parameters. As a result, the modelling of a PV system and a battery using analogous circuits are discussed. As the maximum power should be harvested from a PV array to increase its efficiency. A buck converter has a capability of shifting power in both directions with acceptable voltage level, which is used for the purpose of charging and discharging the accumulators in the system. The inverter alters the direct current dc bus voltage to a single-phase alternating current voltage with the suitable amplitude and frequency to power any load or appliance. A control loop is used for optimal power extraction from the PV module, as well as a battery control loop is implemented for bidirectional power flow between batteries. Computational intelligence based IoT technique is used to control the loads with the ease. This system's prototype is designed and tested to validate the simulation results in real time systems.

#### Data Availability

No data were used in the study.

#### Disclosure

The statements made and views expressed are solely the responsibility of the authors.

#### Conflicts of Interest

The authors declare that there are no conflicts of interest.

#### Authors' Contributions

All authors contributed equally to this article.

#### References

- [1] L. Huang, H. Xin, W. Huang, H. Yang, and Z. Wang, "Quantitative analysis method of frequency response characteristics of power system with virtual inertia," *Power System Automation*, vol. 42, no. 8, pp. 31–38, 2018.
- [2] S. Eftekharijad, V. Vittal, Heydt, B. Keel, and J. Loehr, "Impact of increased penetration of photovoltaic generation on power systems," *IEEE Transactions on Power Systems*, vol. 28, no. 2, pp. 893–901, 2013.
- [3] P. N. Papadopoulos and J. V. Milanovic, "Probabilistic framework for transient stability assessment of power systems with high penetration of renewable generation," *IEEE Transactions on Power Systems*, vol. 32, no. 4, pp. 3078–3088, 2017.
- [4] A. Adrees, P. N. Papadopoulos, and J. V. Milanović, "A framework to assess the effect of reduction in inertia on system frequency response," in *Proceedings of the IEEE PES General Meeting*, July 2016.
- [5] V. Knap, S. K. Chaudhary, D.-I. Stroe, M. Swierczynski, B.-I. Craciun, and R. Teodorescu, "Sizing of an energy storage system for grid inertial response and primary frequency reserve," *IEEE Transactions on Power Systems*, vol. 31, no. 5, pp. 3447–3456, 2016.
- [6] M. E. M. Arani and E. F. El-Saadany, "Implementing virtual inertia in dfig-based wind power generation," *IEEE Transactions on Power Systems*, vol. 28, no. 2, pp. 1373–1384, 2013.
- [7] U. Markovic, Z. Chu, P. Aristidou, and G. Hug, "Lqr-based adaptive virtual synchronous machine for power systems with high inverter penetration," *IEEE Transactions on Sustainable Energy*, vol. 10, p. 1, 2018.
- [8] L. M. A. Torres, L. A. C. Lopes, T. L. A. Moran, and C. R. Espinoza, "Self-tuning virtual synchronous machine: a control strategy for energy storage systems to support dynamic frequency control," *IEEE Transactions on Energy Conversion*, vol. 29, no. 4, pp. 833–840, 2014.
- [9] C. Wang, Y. Mi, Y. Fu, and P. Wang, "Frequency control of an isolated micro-grid using double sliding mode controllers and disturbance observer," *IEEE Transactions on Smart Grid*, vol. 9, no. 2, pp. 923–930, 2018.
- [10] A. Karimi, Y. Khayat, M. Naderi et al., "Inertia response improvement in ac microgrids: a fuzzy-based virtual synchronous generator control," *IEEE Transactions on Power Electronics*, vol. 35, no. 4, pp. 4321–4331, 2020.
- [11] Renewables 2019 Global Status Report, *Renewables Now*, p. 40, REN21, Paris, France, 2019.
- [12] B. N. Mohaparta, A. Dash, and B. P. Jarika, "Power saving solar street lights," *International Journal of Emerging Trends in Engineering Research*, vol. 5, pp. 105–109, 2017.
- [13] S. Salman, A. I. Xin, and W. U. Zhouyang, "Design of a p-&o algorithm based mppt charge controller for a stand-alone 200 w pv system," *Protection and Control of Modern Power Systems*, vol. 3, no. 1, pp. 1–8, 2018.
- [14] Scenario Outlook And Adequacy Forecast 2014–2030, "European network of transmission system operators for electricity (ENTSO-E)," Tech. Rep., entso-e, Brussels, Belgium, 2014.
- [15] P. Tielens and D. V. Hertem, "Grid inertia and frequency control in power systems with high penetration of renewables," in *Proceedings of the Young Researchers Symposium*, vol. 6, Elect. Power Eng., Delft, Netherlands, April 2012.
- [16] J. Van de Vyver, J. D. M. De Kooning, B. Meersman, L. Vandeveld, and T. L. Vandoorn, "Droop control as an alternative inertial response strategy for the synthetic inertia

- on wind turbines," *IEEE Transactions on Power Systems*, vol. 31, no. 2, pp. 1129–1138, 2016.
- [17] J. Zhu, C. D. Booth, G. P. Adam, A. J. Roscoe, and C. G. Bright, "Inertia emulation control strategy for VSC-HVDC transmission systems," *IEEE Transactions on Power Systems*, vol. 28, no. 2, pp. 1277–1287, 2013.
- [18] P. J. Douglass, R. Garcia-Valle, P. Nyeng, J. Ostergaard, and M. Togeby, "Smart demand for frequency regulation: experimental results," *IEEE Transactions on Smart Grid*, vol. 4, no. 3, pp. 1713–1720, 2013.
- [19] Y. Mu, J. Wu, J. Ekanayake, N. Jenkins, and H. Jia, "Primary frequency response from electric vehicles in the great britain power system," *IEEE Transactions on Smart Grid*, vol. 4, no. 2, pp. 1142–1150, 2013.
- [20] U. Cali and V. Sharma, "Short-term wind power forecasting using long-short term memory based recurrent neural network model and variable selection," *International Journal of Smart Grid and Clean Energy*, vol. 8, no. 2, pp. 103–110, 2019.
- [21] V. Knap, R. Sinha, M. Swierczynski, D.-I. Stroe, and S. Chaudhary, "Grid inertial response with lithium-ion battery energy storage systems," in *Proceedings of the 2014 IEEE International Symposium Industrial Electronics (ISIE)*, pp. 1813–1818, Istanbul, Turkey, June 2014.
- [22] S. Dwyer and S. Teske, *Renewables 2018 Global Status Report*, 2018, <https://www.ren21.net/status-of-renewables/global-statusreport/>.
- [23] P. Energy, "Rate of change of frequency (ROCOF)-review of TSO and generator submissions final report," *Commission for Energy Regulation (CER)*, 2013.
- [24] P. Kundur, N. J. Balu, M. G. Lauby, and P. S. Kundur, *Power System Stability and Control*, McGraw-Hill, New York, NY, USA, 1994.
- [25] L. Bird, L. Debra, M. Michael et al., "Wind and solar energy curtailment: a review of international experience," *Renewable and Sustainable Energy Reviews*, vol. 65, pp. 577–586, 2016.
- [26] Q. C. Zhong, P.-L. Nguyen, Z. Wanxing Sheng, and W. Sheng, "Self-synchronized synchronverters: inverters without a dedicated synchronization unit," *IEEE Transactions on Power Electronics*, vol. 29, no. 2, pp. 617–630, 2014.
- [27] R. K. Sarojini and P. Kaliannan, "Small signal modelling and determination of critical value of inertia for virtual synchronous generator," in *Proceedings of the 2019 Innovations in Power and Advanced Computing Technologies (i-PACT)*, pp. 1–6, IEEE, Piscataway, NJ, USA, March 2019.
- [28] A. F. Hoke, M. Shirazi, S. Chakraborty, E. Muljadi, and D. Maksimovic, "Rapid active power control of photovoltaic systems for grid frequency support," *IEEE Journal of Emerging and Selected Topics in Power Electronics*, vol. 5, no. 3, pp. 1154–1163, 2017.
- [29] R. Kamala Sarojini and K. Palanisamy, "Emulated inertia control for the stand-alone microgrid with high penetration of renewable energy sources," *International Journal of Renewable Energy Resources*, vol. 10, pp. 831–842, 2020.
- [30] R. K. Sarojini and P. Kaliannan, "Inertia emulation through supercapacitor for a weak grid," *IEEE Access*, vol. 9, pp. 30793–30802, 2021.
- [31] S. K. Kollimalla, M. K. Mishra, and N. L. Narasamma, "Design and analysis of novel control strategy for battery and supercapacitor storage system," *IEEE Transactions on Sustainable Energy*, vol. 5, no. 4, pp. 1137–1144, 2014.
- [32] J. Fang, Y. Tang, H. Li, and X. Li, "A battery/ultracapacitor hybrid energy storage system for implementing the power management of virtual synchronous generators," *IEEE Transactions on Power Electronics*, vol. 33, no. 4, pp. 2820–2824, 2018.
- [33] D. Gautam, L. Goel, R. Ayyanar, V. Vittal, and T. Harbour, "Control strategy to mitigate the impact of reduced inertia due to doubly fed induction generators on large power systems," *IEEE Transactions on Power Systems*, vol. 26, no. 1, pp. 214–224, 2011.
- [34] P. Du and J. Matevosyan, "Forecast system inertia condition and its impact to integrate more renewables," *IEEE Transactions on Smart Grid*, vol. 9, no. 2, pp. 1531–1533, 2018.
- [35] P. Daly, D. Flynn, and N. Cuniffe, "Inertia considerations within unit commitment and economic dispatch for systems with high non-synchronous penetrations," in *Proceedings of the 2015 IEEE Eindhoven PowerTech*, pp. 1–6, IEEE, Eindhoven, Netherlands, June 2015.
- [36] P. Tielens and D. Van Hertem, "The relevance of inertia in power systems," *Renewable and Sustainable Energy Reviews*, vol. 55, pp. 999–1009, 2016.
- [37] G. Delille, B. Francois, and G. Malarange, "Dynamic frequency control support by energy storage to reduce the impact of wind and solar generation on isolated power system's inertia," *IEEE Transactions on Sustainable Energy*, vol. 3, no. 4, pp. 931–939, 2012.
- [38] H. Golpira, H. Seifi, A. R. Messina, and M.-R. Haghifam, "Maximum penetration level of micro-grids in large-scale power systems: frequency stability viewpoint," *IEEE Transactions on Power Systems*, vol. 31, no. 6, pp. 5163–5171, 2016.
- [39] L. Holdsworth, J. Ekanayake, and N. Jenkins, "Power system frequency response from fixed speed and doubly fed induction generator-based wind turbines," *Wind Energy*, vol. 7, no. 1, pp. 21–35.
- [40] J. Ma, S. Wang, Z. Wang, Y. Qiu, and J. S. Thorp, "Power system energy stability region based on dynamic damping theory," *IET Generation, Transmission & Distribution*, vol. 10, no. 12, pp. 2907–2914, 2016.
- [41] L. C. Gross, "Sub-synchronous grid conditions: new event new problem and new solutions," in *Proceedings of the Western Protective Relay Conference*, pp. 1–19, College Station, TX, USA, October 2010.
- [42] J. Ma, Y. Qiu, Y. Li, W. Zhang, Z. Song, and J. S. Thorp, "Research on the impact of dfig virtual inertia control on power system small-signal stability considering the phase-locked loop," *IEEE Transactions on Power Systems*, vol. 32, no. 3, pp. 2094–2105, 2017.
- [43] N. Mithulananthan, R. Shah, and K. Y. Lee, "Small-disturbance angle stability control with high penetration of renewable generations," *IEEE Transactions on Power Systems*, vol. 29, no. 3, pp. 1463–1472, 2014.
- [44] X. Yu and L. M. Tolbert, "Ancillary services provided from DER with power electronics interface," in *Proceedings of the 2006 IEEE Power Engineering Society General Meeting*, p. 8, IEEE, Montreal, Canada, June 2006.
- [45] H. Bevrani, A. Ghosh, and G. Ledwich, "Renewable energy sources and frequency regulation: survey and new perspectives," *IET Renewable Power Generation*, vol. 4, no. 5, p. 438, 2010.
- [46] M. Raugei and P. Frankl, "Life cycle impacts and costs of photovoltaic systems: current state of the art and future outlooks," *Energy*, vol. 34, no. 3, pp. 392–399, 2009.
- [47] I. Borlea, C. Barbulescu, and D. Cristian, "Substation ancillary services fuel cell power supply. Part 1. Solution overview," in *Proceedings of the 2010 International Joint Conference on Computational Cybernetics and Technical Informatics*, pp. 585–588, IEEE, Timisora, Romania, May 2010.

- [48] N. R. Babu, K. V. Narayana, and C. Hari Babu, "Active & reactive power control of large scale grid connected pv system by cascaded modular multi-level inverters with fuzzy logic control approach," *International Journal of Modern Trends in Engineering & Research*, vol. 4, no. 4, pp. 115–124, 2017.
- [49] D. Wu, T. Yang, A. A. Stoorvogel, and J. Stoustrup, "Distributed optimal coordination for distributed energy resources in power systems," *IEEE Transactions on Automation Science and Engineering*, vol. 14, no. 2, pp. 414–424, 2016.
- [50] A. C. Chapman and G. Verbic, "Dynamic distributed energy resource allocation for load-side emergency reserve provision," in *Proceedings of the 2016 IEEE Innovative Smart Grid Technologies-Asia (ISGT-Asia)*, pp. 1189–1194, IEEE, Melbourne, Australia, November 2016.
- [51] M. Georgiev, R. Stanev, and A. Krusteva, "Flexible load control in electric power systems with distributed energy resources and electric vehicle charging," in *Proceedings of the 2016 IEEE International Power Electronics and Motion Control Conference (PEMC)*, pp. 1034–1040, IEEE, Varna, Bulgaria, September 2016.
- [52] S. Huang, Q. Wu, Z. Liu, and A. H. Nielsen, "Review of congestion management methods for distribution networks with high penetration of distributed energy resources," in *Proceedings of the IEEE PES Innovative Smart Grid Technologies*, pp. 1–6, IEEE, Europe, October 2014.
- [53] A. P. Apostolov, "Modeling of legacy intelligent electronic devices for UCA based substation integration systems," in *Proceedings of the LESCOPE 01. 2001 Large Engineering Systems Conference on Power Engineering. Conference Proceedings. Theme: Powering Beyond 2001*, pp. 38–43, IEEE, Halifax, Canada, July 2001.
- [54] Z. A. Obaid, L. M. Cipcigan, S. Sami, and M. Muhssin, "Control of a population of battery energy storage systems for dynamic frequency control institute of energy," Dissertation, Cardiff University, Cardiff, Wales, 2017.
- [55] Z. A. Obaid, L. M. Cipcigan, L. Abraham, and M. T. Muhssin, "Frequency control of future power systems: reviewing and evaluating challenges and new control methods," *Journal of Modern Power Systems and Clean Energy*, vol. 7, no. 1, pp. 9–25, 2019.
- [56] B. C. Feijó, A. Pavlovic, L. A. O. Rocha, L. A. Isoldi, S. Lorente, and E. D. dos Santos, "Geometrical investigation of micro-channel with two trapezoidal blocks subjected to laminar convective flows with and without boiling," *Reports in Mechanical Engineering*, vol. 3, no. 1, pp. 20–36, 2022.
- [57] F. M. Gonzalez-Longatt and S. M. Alhejaj, "Enabling inertial response in utility-scale battery energy storage system," in *Proceedings of the 2016 IEEE Innovative Smart Grid Technologies-Asia (ISGT-Asia)*, pp. 605–610, IEEE, Melbourne, Australia, November 2016.
- [58] V. V. Sinyavski, M. Shatrov, M. G. Shatrov, V. V. Kremnev, and P. Grigori, "Forecasting of a boosted locomotive gas diesel engine parameters with one- and two-stage charging systems," *Reports in Mechanical Engineering*, vol. 1, no. 1, pp. 192–198, 2020.

## Research Article

# Analysis and Implementation of Thermal Heat Exchanger Tube Performance with Helically Pierced Twisted Tape Inserts Using ANFIS Model

Faisal Altarazi,<sup>1</sup> Sunil Kumar ,<sup>2</sup> Gaurav Gupta ,<sup>2</sup> Muhammad Gulzar ,<sup>3</sup>  
Yaé Ulrich Gaba ,<sup>4</sup> Anil Kumar,<sup>5</sup> and Rajesh Maithani <sup>5</sup>

<sup>1</sup>Applied College, University of Jeddah, Jeddah, Saudi Arabia

<sup>2</sup>Yogananda School of Artificial Intelligence Computers and Data Science, Shoolini University, Solan, India

<sup>3</sup>Department of Mathematics, Government College University Faisalabad, Faisalabad 38000, Pakistan

<sup>4</sup>Quantum Leap Africa (QLA) AIMS Rwanda Centre, Remera Sector KN 3, Kigali, Rwanda

<sup>5</sup>School of Engineering, University of Petroleum and Energy Studies, Dehradun, India

Correspondence should be addressed to Sunil Kumar; reachtome.sunil@gmail.com and Yaé Ulrich Gaba; yaeulrich.gaba@gmail.com

Received 13 August 2021; Accepted 17 November 2021; Published 20 December 2021

Academic Editor: Debiao Meng

Copyright © 2021 Faisal Altarazi et al. This is an open access article distributed under the Creative Commons Attribution License, which permits unrestricted use, distribution, and reproduction in any medium, provided the original work is properly cited.

The present work used ANFIS, an adaptive neuro-fuzzy inference system modeling to analyze the effect of the variable parameters of helically pierced twisted tape inserts on the Nusselt number, friction factor, and thermo-hydraulic heat exchanger tube performance. The experimental data utilized for ANFIS modeling considered a diameter ratio ranging from 0.57 to 0.80, a relative pitch ratio ranging from 0.046 to 0.107, a perforation index ranging from 5% to 20% as variable twisted tape parameters and flow parameters. The Reynolds number varies from 4000 to 30000. The analysis showed that the maximum thermo-hydraulic performance was obtained at a diameter ratio of 0.65, a relative pitch ratio of 0.085, and a perforation index equal to 10%. The result predicts that the ANFIS model and experimental results are in good agreement as they have only  $\pm 0.53\%$  deviations.

## 1. Introduction

Heat exchangers are broadly utilized in designing applications, for example, refrigeration and cooling systems, automobiles, thermal power plants, textile and chemical handling industries, and so forth. The efficiency of the heat exchanger is decided on the basis of the effective heat transfer between two working fluids [1, 2]. Numerous methods and approaches were instigated for the augmentation of heat transfer to improve thermal efficiency. The ultimate aim of these approaches is to increase the heat transfer and provide the stability of the heat exchanger [3–6].

Rounded tubes are prominently used in most engineering industries because of their compact structure for a given available space [7, 8]. Nakhchi and Esfahani [9] studied experimentally the thermal performance of a heat exchanger tube fortified with cross-cut twisted tape using

$Cu - H_2O$  nanofluid. The outcomes showed that the thermal performance of  $Cu - H_2O$  nanofluid flow in the plain tube is lesser than the tubes equipped with the cross-cut twisted tapes. Xiaowen et al. [10] performed experimental studies on a domestic water-cooled air conditioner (WAC) and reported that the COP of WAC increases to 12.3% with the insertion of the heat recovery option. Ishak et al. [11] evaluated the Nusselts number ( $Nu$ ) for the bundles of the flat tube and found that  $Nu$  increases, whereas the friction factor decreases, with an escalation in the mean air velocity. Fullerton and Anand [12] and Jang and Yang [13–16] analyzed the heat transfer enhancement techniques on the heat exchangers.

Modern investigations are more focused on soft computing fields and computational intelligence. Computational intelligence includes computational fluid dynamic (CFD), artificial neural networks (ANN), fuzzy inference system



(FIS), genetic algorithm (GA), particle swarm optimization (PSO), and fuzzy logic [17]. The fuzzy sets play important role in artificial neural network [18] and inference system [19]. The fuzzy models can be pooled with ANN to produce ANFIS. The modeling of a nonlinear system is now quite easier with ANFIS as ANFIS has the benefits of neural and fuzzy logic systems [20, 21]. Kiran and Rajput [22] determined that soft computing tools, such as FIS, ANN, and ANFIS, provide a modest but influential technique for predicting the performance of a heat exchanger.

Suparta and Samah [23] predicted rainfall by exploring the application of the ANFIS model with various input structures and membership functions. The analyses of six-year rainfall data on a monthly basis in South Tangerang city, Indonesia found that the rainfall prediction based on the ANFIS time series is promising, where 80% of the data testing is well-predicted. Elijah Onu et al. [24] carried the comparative analysis of RSM, ANN, ANFIS, and mechanistic modeling in the Eriochrome black-T (EBT) dye adsorption using modified clay. They found that ANFIS is the best predictive model, whereas RSM is the least in the adsorption of EBT dye. Mehrabi et al. [25] and Esen et al. [26] used ANFIS, whereas Beigzadeh and Rahimi [27, 28] used ANFIS and GA for modeling the influence of the essential parameters of the heat exchangers. Esen and Inalli [29], Hayati et al. [30], and Esen et al. [31] predicted  $Nu$  using novel geometry in a heat exchanger using ANFIS.

Chen et al. [32] and Mohammad [33] studied experimentally the  $Nu$  and  $f$  in a double tube heat exchanger using ANN. The 99.76% and 99.54% of data regression coefficients for  $Nu$  and  $f$ , respectively, illustrated the accurateness of the method applied. Gill and Singh [34], Zarei et al. [35], and Abadi et al. [36] adopted the ANFIS approach for predicting the energetic performance analysis and found that the ANFIS predictions agreed well with the experimental results with an absolute fraction of variance in the range of 0.994–0.998, a root mean square error in the range of 0.0018–0.1907, and a mean absolute percentage error in the range of 0.103–0.897%. Onyelowe et al. [37] implemented ANFIS and its evolutionary hybrid techniques, ANFIS-PSO and ANFIS-GA, to forecast the coefficients of curvature and the uniformity of unsaturated lateritic soil and concluded that ANFIS and its evolutionary hybrids techniques showed great accuracy. Marjani et al. [38] used the application of ANFIS to obtain the results of CFD modeling to facilitate the prediction of the pressure of the nanofluid convective flow. The ANFIS predictions show a good agreement with the CFD results. Saeed et al. [39], Beiki [40], Bahiraei et al. [41], Yashawantha and Vinod [42], Bahl et al. [43], Safarzadeh et al. [44], and Safarzadeh et al. [44] used the ANFIS model for different heat transfer enhancement applications, and their major findings are listed in Table 1.

From the literature review, it can be concluded that ANFIS is a better modeling system as it is an amalgamation of ANN combined with FIS to improve the speed, adaptiveness, and fault tolerance. It can assimilate the linguistic variables that are a part of human language, reasoning, and understanding [46–48]. The use of modern and advanced

techniques leads to the saving of time, energy, and material by analyzing them on the basis of the performance dominance parameter [49]. Furthermore, the literature review shows so many studies on predicting the performance of the heat exchanger. However, very limited research has been found on the passive methods with helically pierced twisted tape inserts using ANFIS. In the present study, ANFIS modeling is used to predict  $Nu_{TT}$  and  $f_{TT}$  of the heat exchanger tube. It is also used to determine the geometrical parameter values by finding out their dominance and involvement in the performance assessment. The novelty of the present work is the prediction of the geometric parameter that delivers the maximum heat transfer inside a heat exchanger tube. The ANFIS method determines the dominating parameter on the basis of thermal performance to lower the experimental runs and saves time and money. The determined best-suited parameters can be used in a heat exchanger tube to enhance the heat transfer with the lowest possible pressure drop penalty.

## 2. Range of Parameters

The variable geometrical parameters of the helical pierced twisted-tape inserts and the corresponding range taken for the investigations [50] are as follows: diameter ratio ( $d_R/D_I$ ) ranging from 0.57 to 0.80, relative pitch ratio ( $P_{PT}/L_T$ ) ranging from 0.046 to 0.107, perforation Index ( $P_A/T_A$ ) ranging from 5% to 20%, and Reynolds number ( $Re_{num}$ ) ranging from 4000 to 30000. For the graphic representation of the helical pierced twisted tape inserts, see Figure 1.

## 3. Experimental Setup Details

The heat exchanger tube is made of galvanized iron with outer and inner diameters of 68 mm and 65 mm, respectively. The heat exchanger tube has three sections, viz., the inlet, outlet, and test section, which are of 2.5 m, 1.5 m, and 1.4 m, respectively, as shown in Figure 2 [50]. The fluid flow across the tube is carried by a centrifugal blower. A tailored Nicrome wire heater is employed to maintain a  $1000\text{ W/m}^2$  constant heat flux in the test section. The pressure drop across the test section is determined by a digital micromanometer (TESTO-510) with a least count of 1 Pa. The temperature is determined by 12 thermocouples attached on the test section, 3 thermocouples at the outlet, and 1 thermocouple at the inlet section [50]. The thermocouples have been calibrated in laboratory conditions against a dry block temperature calibrated instant (Presys Instruments T-25N, 2004), having the least count of  $0.01^\circ\text{C}$ . The thermocouple to be calibrated was placed in the calibration bath where a constant temperature was maintained. The response of the thermocouple and the standard probe were noted with the help of a digital temperature indicator for various preset values of the standard probe, and the error between the reading of the standard probe and the thermocouple were calculated.

TABLE 1: Previous investigations on ANFIS modeling.

S. No.	Authors	Major findings
1.	Saeed et al. [39]	ANFIS model is an easy-to-use tool to estimate nucleate pool boiling heat transfer properties of refrigerant-oil mixtures with nanoparticles.
2.	Beiki [40]	FIS and ANFIS are a most powerful weapon to attack mass transfer in nanofluids. Also these models could predict convective mass transfer in nanofluids very effectively. Nanoparticles size and type could play an important role in mass transfer.
3.	Bahiraee et al. [41]	PSO-ANFIS acts as most capable predictive model, followed by PSO-ANN, ANFIS, and ANN. ANFIS and ANN can be optimized by PSO approach.
4.	Yashawantha and Vinod [42]	Correlation and ANFIS model were developed for effective thermal conductivity. ANFIS model showed better performance compared to correlation.
5.	Bahl et al. [43]	The predictions obtained by using the ANFIS model are found to be very close to the experimental findings which prove that the model proposed is capable to accurately predict the behavior of heat transfer system.
6.	Safarzadeh et al. [44]	The ANFIS model predicted the results with relative and average relative errors of 1.76% and 0.67% for nusselt number, 11.34% and 4.48% for friction factor, and 8.56% and 2.83% for entropy generation. ANN and ANFIS models can be used confidently to estimate the exergy efficiency.
7.	Kaveh et al. [45]	The ANFIS model had more capability to predict the energy and exergy items as compared to ANN method.

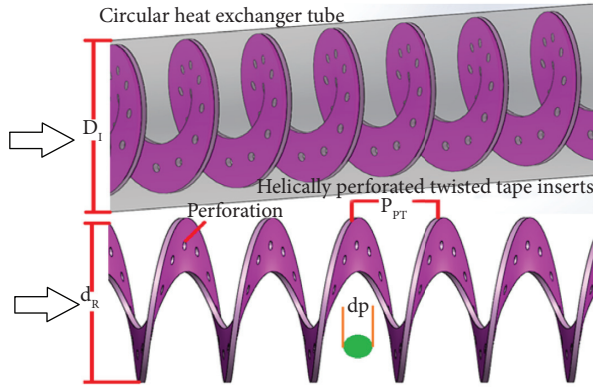


FIGURE 1: Twisted tape insert parameters [50].

#### 4. ANFIS Model

ANFIS is an adaptive network that utilizes the features of ANN and fuzzy logic. ANFIS implicitly executes these two approaches. In this study, Takagi-Sugeno fuzzy inference system with a five-layered structure is employed. The structure of the proposed model (ANFIS) is represented in Figure 3 [42], whereas the plotted membership function of the input and output parameters are demonstrated by Figure 4. To regulate the output parameters in the model, the structured rules are given in Table 2.

For effortlessness, we use two inputs  $X$  and  $Y$  and corresponding one output  $FF$ . Two criteria were used in the approach of "if-Then" for Takagi-Sugeno model, as follows:

Criteria 1 = If  $X$  is  $A_1$  and  $Y$  is  $B_1$ ,

$$f_1 = P_1X + Q_1Y + R_1, \quad (1)$$

Criteria 2 = If  $X$  is  $A_2$  and  $Y$  is  $B_2$ ,

$$f_2 = P_2X + Q_2Y + R_2, \quad (2)$$

where  $A_1$  and  $A_2$  are the membership functions for input  $X$ . Similarly,  $B_1$  and  $B_2$  are the membership functions for input  $Y$ .  $P_1$ ,  $Q_1$ ,  $R_1$ ,  $P_2$ ,  $Q_2$ , and  $R_2$  are the linear parameters of Takagi-Sugeno fuzzy inference model.

ANFIS model comprises of five layers, and the brief narrative of all these is as follows [21]:

Layer 1: Each node of this layer acclimates with a parameter function and output of each node is a degree of membership, which is given by the input of the membership functions.

$$Z_{Ai}(X) = \frac{1}{1 + |(X - c_i/a_i)|^{2b}}, \quad (3)$$

$$L_{1i} = Z_{Ai}(X), \quad i = 1, 2,$$

$$L_{1i} = Z_{Bi}(Y), \quad i = 1, 2,$$

where  $Z_{Ai}(X)$  and  $Z_{Bi}(Y)$  are the degree of the membership functions of fuzzy sets  $A_i$  and  $B_i$ , respectively, whereas  $a_i$ ,  $b_i$ ,  $c_i$  are the parameters of the membership function.

Layer 2: In this layer, each node is nonadaptive and categorized as  $E$ . The output node is the outcome of the multiplication of signal coming into the node and carried out to the next node. The outputs of these nodes are given as follows:

$$L_{2i} = W_i = Z_{Ai}(X) * Z_{Bi}(Y), \quad i = 1, 2, \quad (4)$$

where output  $W_i$  represents the firing strength of each rule.

Layer 3: Each node in the third layer is categorized as  $N$ . Every node is a calculation of the ratio between the  $i^{\text{th}}$  rule and the sum of all rules.

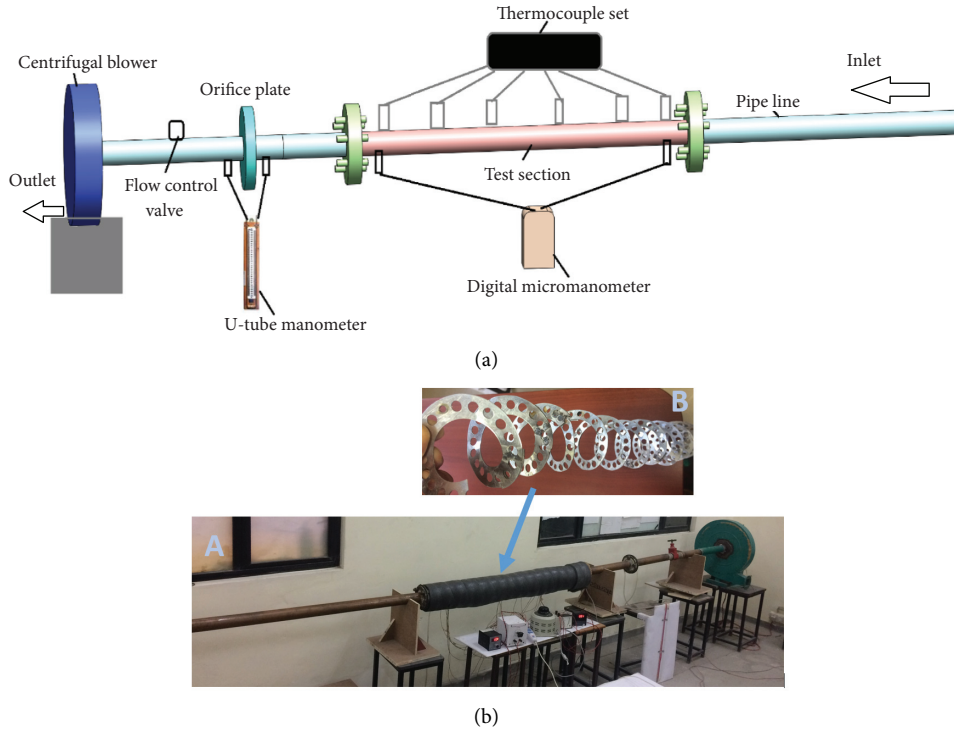


FIGURE 2: (a) Schematic of experimental setup. (b) Photographic view of experimental setup and insert.

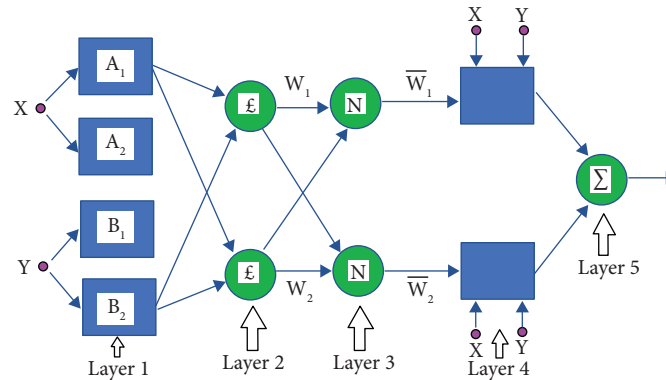


FIGURE 3: Schematic ANFIS model [17].

$$L_{3i} = \underline{W}_i = \frac{W_i}{W_1 + W_2}, \quad i = 1, 2. \quad (5)$$

Layer 4: Every node in layer four is an adaptive node to an output that is defined as [21] follows:

$$L_{4i} = \underline{W}_i f_i = \underline{W}_i (P_i X + Q_i Y + R_i), \quad i = 1, 2. \quad (6)$$

Layer 5: The single node of layer five is labeled as  $\Sigma$ , which calculates the whole output of all received signals of the earlier nodes.

$$L_{5i} = \sum_{i=1}^2 \underline{W}_i f_i = \frac{\sum_{i=1}^2 W_i f_i}{W_1 + W_2}. \quad (7)$$

## 5. Data Reduction

From the experimental data recorded for the heat exchanger under the steady state conditions,  $Nu_{TT}$ ,  $Nu_{UT}$ ,  $f_{TT}$ , and  $\eta_{per}$  were computed as follows [50, 51]:

$f_{TT}$  across the test section is calculated using the Darcy equation as follows [50, 51]:

$$f_{TT} = \frac{2(\Delta P)_d \cdot D}{4 \cdot \rho \cdot L \cdot V^2}, \quad (8)$$

where  $(\Delta P)_d = 9.81 \times (\Delta h)_d \times \rho_m$ .

$Nu_{TT}$  is determined from the following equation:

$$Nu_{TT} = \frac{h \cdot D}{k}, \quad (9)$$

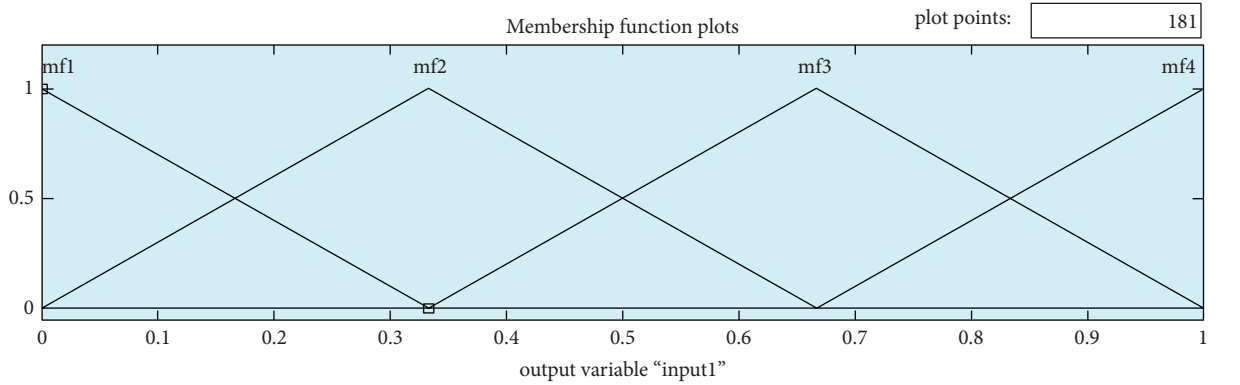
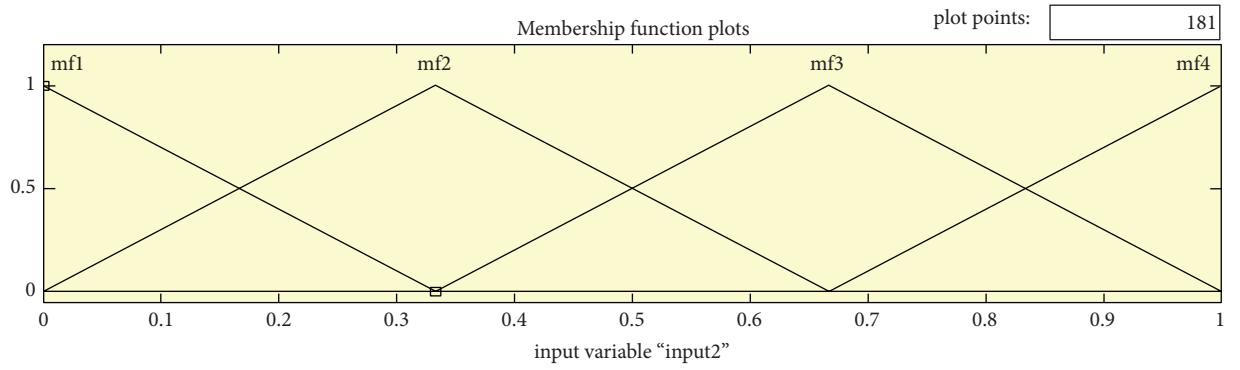
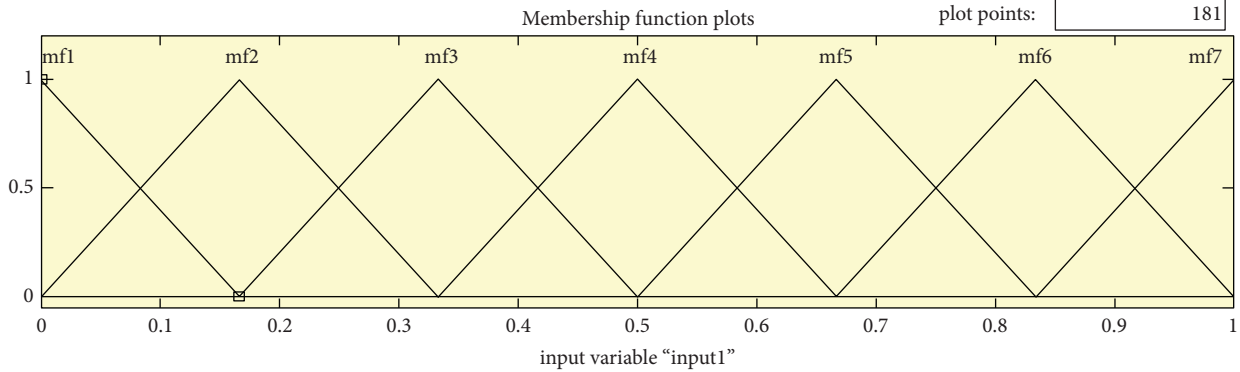
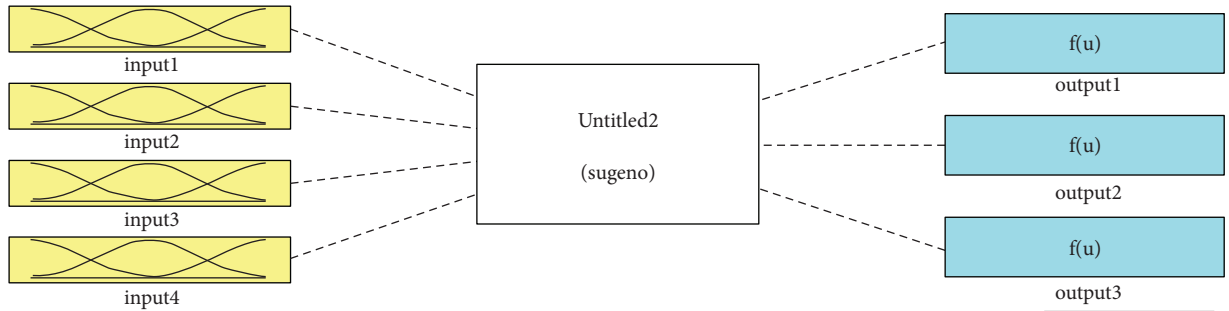


FIGURE 4: Membership function plot for input and output variables.

where,

$$h = \frac{Q_u}{A_T \cdot (T_{tm} - T_{fm})} \quad (10)$$

The useful heat transfer rate  $Q_u$  of the fluid is given by,

$$Q_u = \dot{m} \times C_{p,nf} (T_0 - T_i) \quad (11)$$

The heat exchanger with the pierced twisted tape inserts thermal performance compared to a smooth tube is obtained as follows [50, 51]:

$$\eta_{per} = \frac{[(Nu_{TT}/Nu_{smooth})]}{[(f_{TT}/f_{smooth})]^{(1/3)}} \quad (12)$$

TABLE 2: ANFIS input and output rule for modeling pierced twisted tape inserts heat exchanger.

S. no.	Rules
1	If (input1 is in 1mf1) and (input2 is in 2mf1) then (output is 1mf1) (1)
2	If (input1 is in 1mf1) and (input2 is in 2mf2) then (output is 1mf2) (1)
3	If (input1 is in 1mf1) and (input2 is in 2mf3) then (output is 1mf3) (1)
4	If (input1 is in 1mf1) and (input2 is in 2mf4) then (output is 1mf4) (1)
5	If (input1 is in 1mf2) and (input2 is in 2mf1) then (output is 1mf5) (1)
6	If (input1 is in 1mf2) and (input2 is in 2mf2) then (output is 1mf6) (1)
7	If (input1 is in 1mf2) and (input2 is in 2mf3) then (output is 1mf7) (1)
8	If (input1 is in 1mf2) and (input2 is in 2mf4) then (output is 1mf8) (1)
9	If (input1 is in 1mf3) and (input2 is in 2mf1) then (output is 1mf9) (1)
10	If (input1 is in 1mf3) and (input2 is in 2mf2) then (output is 1mf10) (1)
11	If (input1 is in 1mf3) and (input2 is in 2mf3) then (output is 1mf11) (1)
12	If (input1 is in 1mf3) and (input2 is in 2mf4) then (output is 1mf12) (1)
13	If (input1 is in 1mf4) and (input2 is in 2mf1) then (output is 1mf13) (1)
14	If (input1 is in 1mf4) and (input2 is in 2mf2) then (output is 1mf14) (1)
15	If (input1 is in 1mf4) and (input2 is in 2mf3) then (output is 1mf15) (1)
16	If (input1 is in 1mf4) and (input2 is in 2mf4) then (output is 1mf16) (1)
17	If (input1 is in 1mf5) and (input2 is in 2mf1) then (output is 1mf17) (1)
18	If (input1 is in 1mf5) and (input2 is in 2mf2) then (output is 1mf18) (1)
19	If (input1 is in 1mf5) and (input2 is in 2mf3) then (output is 1mf19) (1)
20	If (input1 is in 1mf5) and (input2 is in 2mf4) then (output is 1mf20) (1)
21	If (input1 is in 1mf6) and (input2 is in 2mf1) then (output is 1mf21) (1)
22	If (input1 is in 1mf6) and (input2 is in 2mf2) then (output is 1mf22) (1)
23	If (input1 is in 1mf6) and (input2 is in 2mf3) then (output is 1mf23) (1)
24	If (input1 is in 1mf6) and (input2 is in 2mf4) then (output is 1mf24) (1)
25	If (input1 is in 1mf7) and (input2 is in 2mf1) then (output is 1mf25) (1)
26	If (input1 is in 1mf7) and (input2 is in 2mf2) then (output is 1mf26) (1)
27	If (input1 is in 1mf7) and (input2 is in 2mf3) then (output is 1mf27) (1)
28	If (input1 is in 1mf7) and (input2 is in 2mf4) then (output is 1mf28) (1)

## 6. Uncertainties Analysis

The uncertainty calculation majorly relies on the errors linked to the measuring instruments [50]. The uncertainty evaluation is performed on a single test run with a single set of geometric parameters. The uncertainty results are presented in Table 3 [50].

## 7. Validation of Experimental Results

The smooth tube experimental data for  $Nu_{\text{smooth}}$  was validated with the Dittus-Boelter equation (13), and  $f_{\text{smooth}}$  by the Blasius equation (14) [25, 35, 47, 50, 51].

$$Nu_{\text{smooth}} = 0.023Re_{\text{num}}^{0.8}Pr^{0.4}, \quad (13)$$

$$f_{\text{smooth}} = 0.085Re_{\text{num}}^{-0.25}. \quad (14)$$

The comparative data of the experimental and standard correlations for  $Nu_{\text{smooth}}$  and  $f_{\text{smooth}}$  are displayed in Figure 5, respectively. An equitably validation data is seen that ensures the accuracy of the data collected in the experimentation [50].

## 8. Results and Discussion

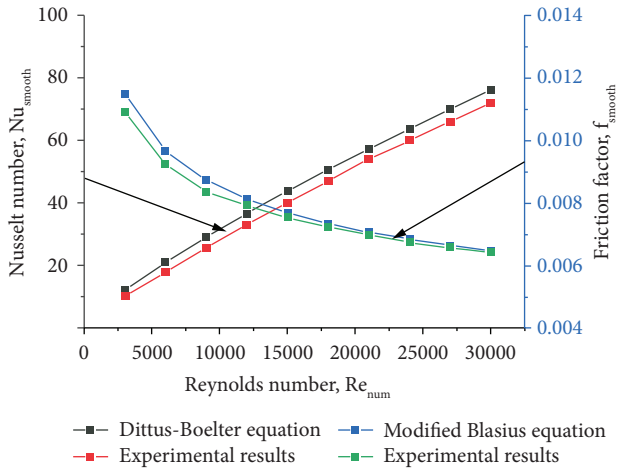
The experimental [50] and ANFIS values of the Nusselt number ( $Nu_{TT}$ ) with the Reynolds number ( $Re_{\text{num}}$ ) for a selected diameter ratio ( $d_R/D_I$ ) range with other parameter values, such as  $(P_{PT}/L_T) = 0.086$  and

$(P_A/T_A) = 10\%$ , being fixed are represented in Figure 6(a). A continuous increase in  $Nu_{TT}$  is observed by for incremental  $Re_{\text{num}}$  range. Both experimental and ANFIS results showed that  $Nu_{TT}$  increases with an increase in  $(d_R/D_I)$  from 0.57 to 0.65. However, with a further increase in the value of  $(d_R/D_I)$ ,  $Nu_{TT}$  starts to decrease. The maximum and minimum values of  $Nu_{TT}$  are achieved for the diameter ratio of 0.65 and 0.80, respectively.  $Nu_{TT}$  with the diameter ratio of 0.65 helically pierced twisted tape is higher by approximately 27.11% than the diameter ratio of 0.80 helically pierced twisted tape that provides a low heat transfer rate. The helical ring diameter is the reason for the heat transfer increment. The turbulence is enhanced by an increase in the diameter that breaks the boundary layer leading to heat transfer enhancement. Any further increase in the diameter beyond a certain limit tends to decrease the rate of heat transfer because of less attachment and detachment locations on the heated tube.

Figure 6(b) displays the experimental and ANFIS results of variation in  $f_{TT}$  with  $Re_{\text{num}}$  at selected  $(d_R/D_I)$  values, and the other parameters  $(P_{PT}/L_T) = 0.086$  and  $(P_A/T_A) = 10\%$  are kept constant. It is noticed that  $f_{TT}$  is enhanced by increasing the diameter ratio. The maximum  $f_{TT}$  is achieved at  $(d_R/D_I)$  of 0.80. The minimum and maximum values of  $f_{TT}$  are found for the diameter ratio of 0.57 and 0.80, respectively. The friction factor with the diameter ratio of 0.80 helically pierced twisted tape is higher by approximately 10.69% than the diameter ratio of 0.57 helically pierced twisted tape that provides a low pressure drop. The increase

TABLE 3: Uncertainty range of parameter.

Sr. no.	Parameter	Range of error (%)
1	Reynolds number	0.78–1.56
2	Nusselt number	1.09–3.32
3	Friction factor	0.78–1.67


 FIGURE 5: Comparison of experimental data with standard correlations  $Nu_{smooth}$  and  $f_{smooth}$ .

in the diameter leads to a higher resistance in the path of the fluid flow. This development is detected because an increase in the diameter resists the flow, and higher turbulence is achieved. However, the pressure drop increases, which enhances  $f_{TT}$ . The main cause behind this disparity is the diameter of the helical ring.

Figure 7(a) illustrates the experimental and ANFIS results on the effect of  $(P_{PT}/L_T)$  on  $Nu_{TT}$  with varying  $Re_{num}$ , keeping other geometrical parameters constant, such as  $(P_A/T_A) = 10\%$  and  $(d_R/D_I) = 0.65$ . It is seen that  $Nu_{TT}$  is boosted by an increase in  $(P_{PT}/L_T)$ , and the maximum  $Nu_{TT}$  is at  $(P_{PT}/L_T)$  of 0.086. A further increase in  $(P_{PT}/L_T)$  decreases  $Nu_{TT}$ , and the trend observed is because of a smaller number of attachment and detachment points. The maximum and minimum values of  $Nu_{TT}$  are found for the pitch ratio of 0.086 and 0.046, respectively.  $Nu_{TT}$  with  $(d_R/D_I) = 0.65$  of 0.086 helically pierced twisted tape is higher by approximately 10.57% than  $(d_R/D_I) = 0.65$  of 0.046 helically pierced twisted tape that provides a low heat transfer rate. The increases in the twist ratio provides less twists on the test length that generates a lower secondary flow inside the tube. This low number of twists on the tube decreases the heat transferring spots, and hence, the heat transfer rate is reduced.

The experimental and ANFIS values of  $f_{TT}$  with  $Re_{num}$  for a varying range of  $(P_{PT}/L_T)$  with other parameter values, such as  $(P_A/T_A) = 10\%$  and  $(d_R/D_I) = 0.65$  are represented in Figure 7(b). It is seen that as  $(P_{PT}/L_T)$  increases,  $f_{TT}$  decreases continuously because of a lower interference offered by a smaller number of helices on the tape. The highest and lowest values of the friction factor are found for the pitch ratio of 0.046 and 0.107, respectively.

The friction factor with the pitch ratio of 0.046 helically pierced twisted tape is higher by approximately 24.48% than the pitch ratio of 0.107 helically pierced twisted tape that provides a low pressure drop. It is because a decrease in  $f_{TT}$  in the test section occurs as the  $(P_{PT}/L_T)$  value increases, which is because the surface of the tape tends to become parallel to the flow direction.

The experimental and ANFIS results on the effect of  $(P_A/T_A)$  on  $Nu_{TT}$  for varying flow  $Re_{num}$  are represented in Figure 8(a). The plot displays an increased  $Nu_{TT}$  with an increase in  $(P_A/T_A)$  and produces the maximum  $Nu_{TT}$  for  $(P_A/T_A)$  of 10%. The maximum and minimum values of  $Nu_{TT}$  are found for the perforation index of 10% and 20%, respectively.  $Nu_{TT}$  with the perforation index of 10% helically pierced twisted tape is higher by approximately 9.33% than the perforation index of 20% helically pierced twisted tape that provides a low heat transfer. A reduction in  $Nu_{TT}$  is seen for increasing the value of  $(P_A/T_A)$  beyond 10%. A reduction in the turbulence intensity inside the tube is observed because of a larger perforation area. At lower perforation, the small dimension diameter delivers in the form of jet, thus producing a high turbulence. A further increase in the  $(P_A/T_A)$  value beyond 10% allows the fluid to flow through the larger perforation, and thus, a low-intensity turbulence is produced.

Figure 8(b) illustrates the experimental and ANFIS results on the variation of  $(P_A/T_A)$  on  $f_{TT}$  against the  $Re_{num}$ . A decreasing trend of  $f_{TT}$  is observed by boosting up the  $(P_A/T_A)$  percentage. The higher and the lower values of the hostility factor are found for the perforation index of 5% and 20%, respectively. The friction factor with the perforation index of 5% helically pierced twisted tape is higher by approximately 16.17% than the perforation index of 20% helically pierced twisted tape that provides a low pressure drop. As  $(P_A/T_A)$  is leveled up from 5% to 20%,  $f_{TT}$  goes down, and this consequence occurs because of a large open area available for fluid flow with a lower flow resistance.

The thermal hydraulic performance ( $\eta_{per}$ ) of the heat exchanger incorporated with the helical pierced twisted tape comprises of the simultaneous assessment of  $Nu_{TT}$  and  $f_{TT}$  as related to the smooth tube. Figure 9(a) illustrates the effect of  $(d_R/D_I)$  on  $\eta_{per}$ . It is seen that  $\eta_{per}$  is observed to elevate the value of  $(d_R/D_I)$  up to 0.65, and thereafter, any increase in  $(d_R/D_I)$  reduces  $\eta_{per}$ . The higher value of  $\eta_{per}$  is 2.13.

Figure 9(b) illustrates the effect of  $(P_{PT}/L_T)$  on  $\eta_{per}$ , the maximum  $\eta_{per}$  is attained corresponding to  $(P_{PT}/L_T)$ , and the value is found to be 2.08.  $\eta_{per}$  for  $P_A/T_A$  is represented in Figure 9(c), which illustrated the effect of  $P_A/T_A$  in the range of 5% to 20%. The maximum  $\eta_{per}$  is found at  $P_A/T_A$  of 10%, and the maximum  $\eta_{per}$  is found to be 2.09. Thus, the inference is that the optimum value of  $\eta_{per}$  takes place at the values of  $(d_R/D_I)$ ,  $(P_{PT}/L_T)$ , and  $P_A/T_A$  of 0.65, 0.8, and 5%, respectively.

Figures 10(a)–10(c) illustrates the comparison between the experimental and ANFIS-predicted results for  $Nu_{TT}$ ,  $f_{TT}$ , and  $\eta_{per}$ . It may be seen that the ANFIS-predicted results and experimental results are in good consideration with each other, which assures the correctness of the information generated.

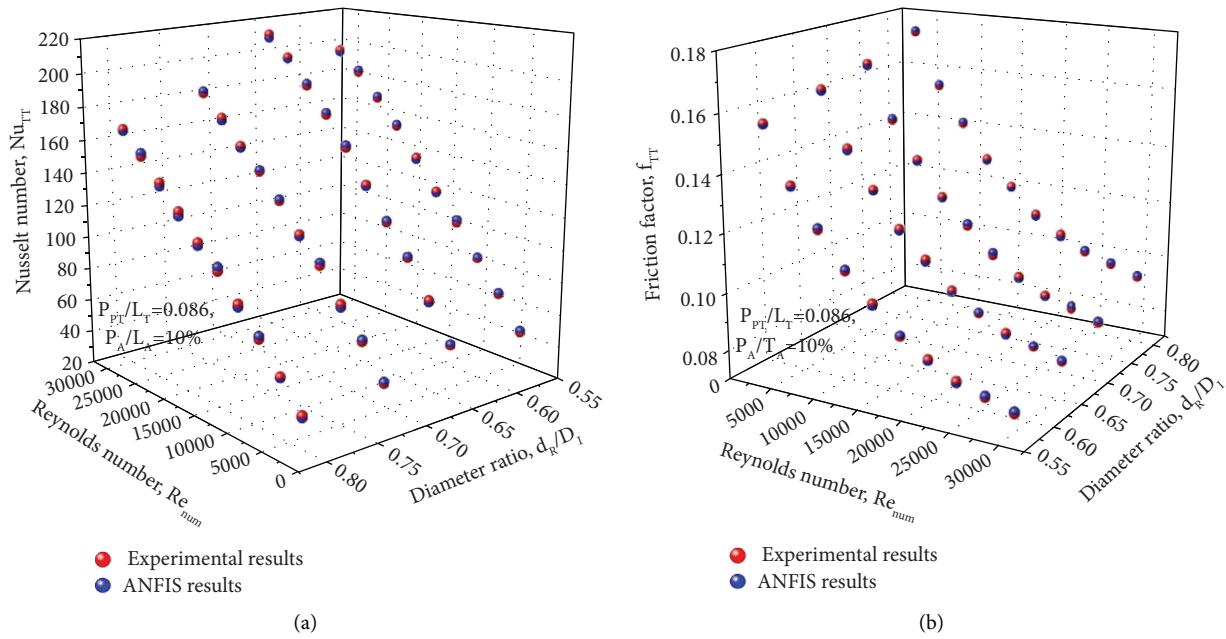


FIGURE 6: Experimental and ANFIS results of the variation of (a)  $Nu_{TT}$  and (b)  $f_{TT}$  for various values of  $(d_R/D_I) = 0.65$  at different  $Re_{num}$ .

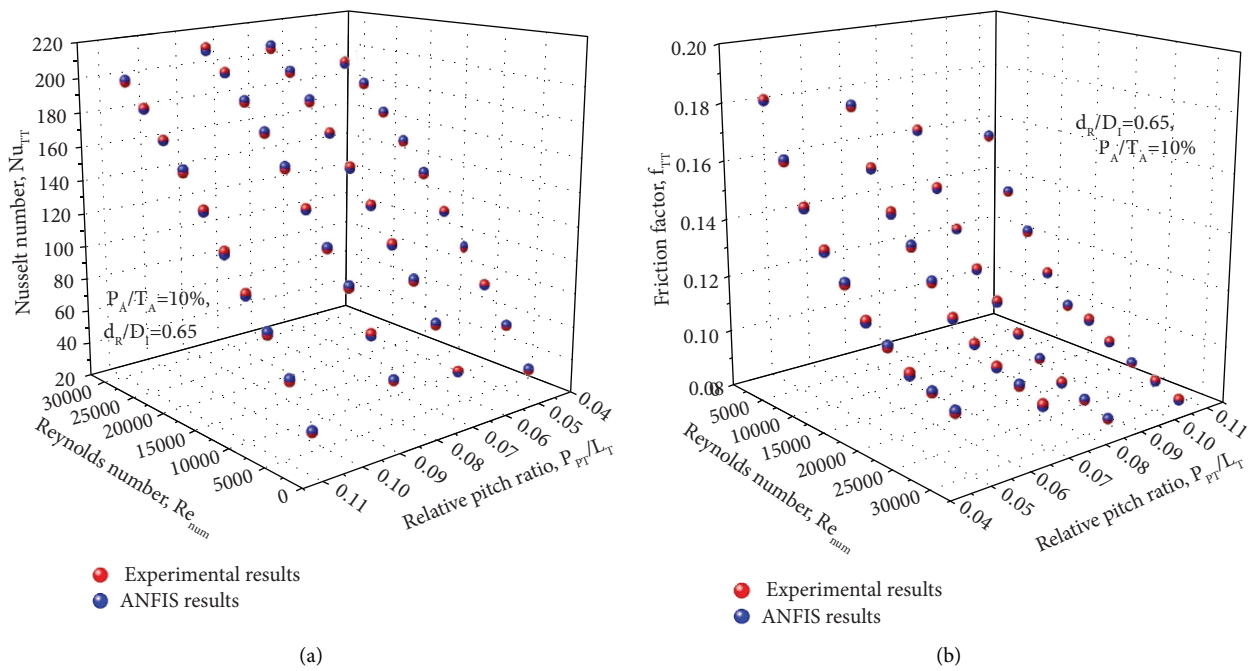


FIGURE 7: Experimental and ANFIS results of variation of (a)  $Nu_{TT}$  and (b)  $f_{TT}$  for various values of  $(P_{PT}/L_T)$  at different  $Re_{num}$ .

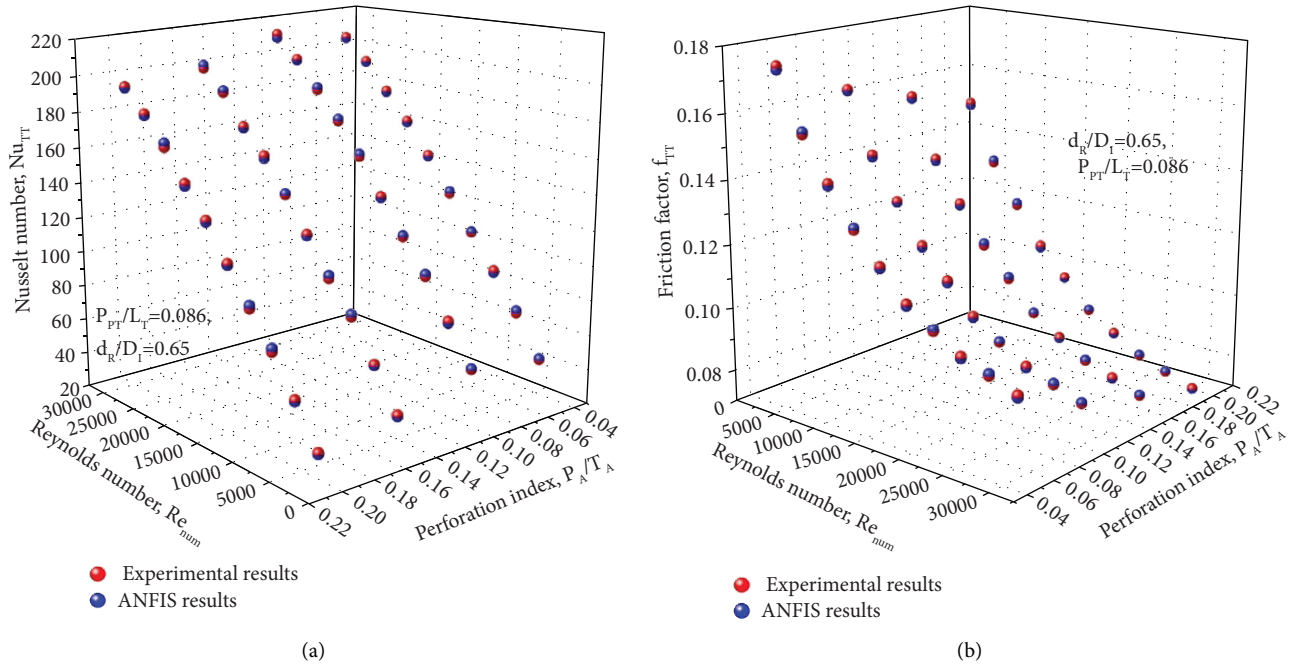


FIGURE 8: Experimental and ANFIS results of variation of (a)  $Nu_{TT}$  and (b)  $f_{TT}$  for various values of  $(P_A/T_A)$  at different  $Re_{num}$ .

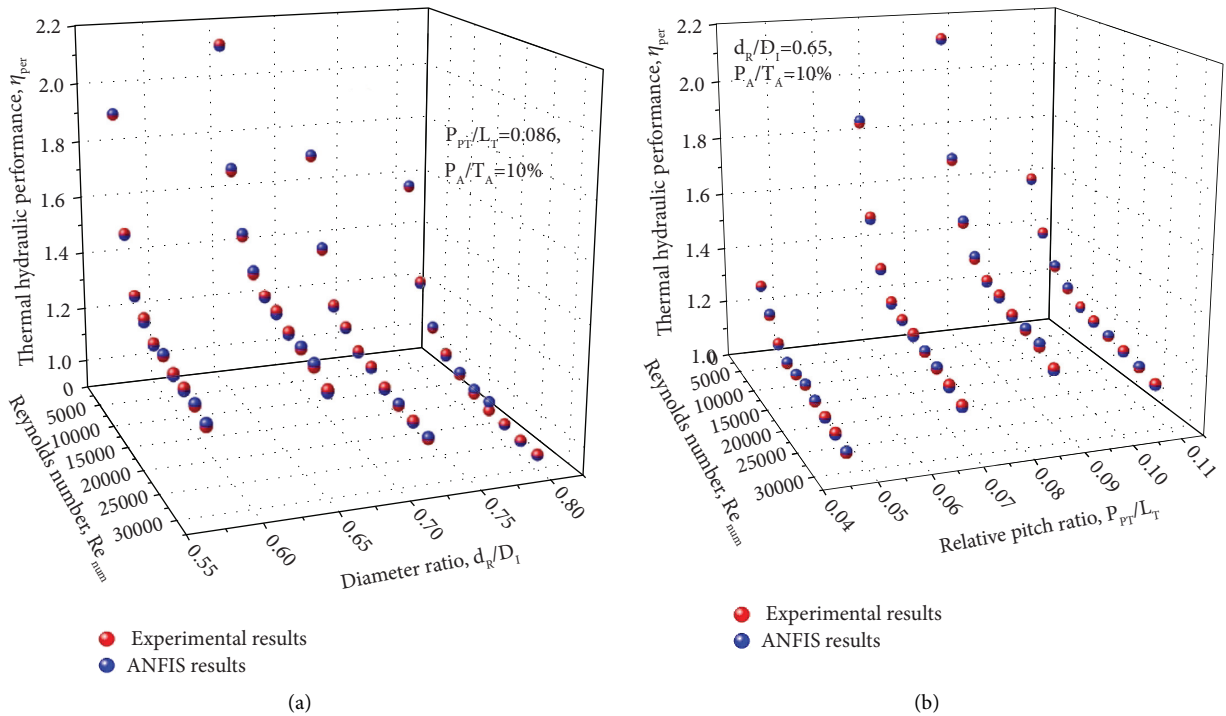
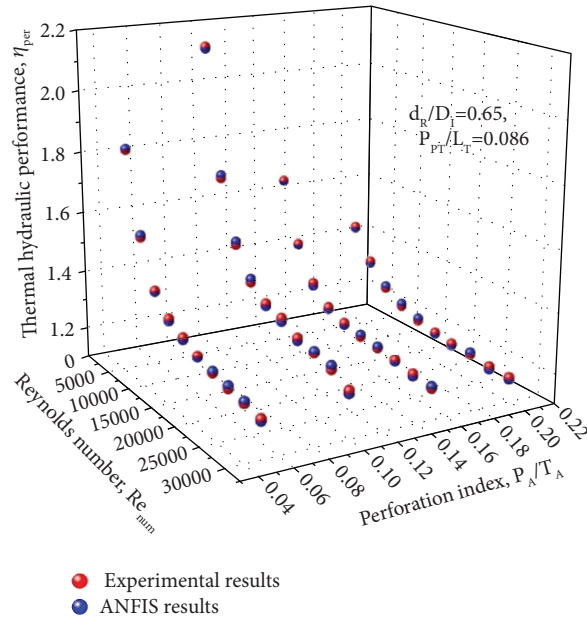


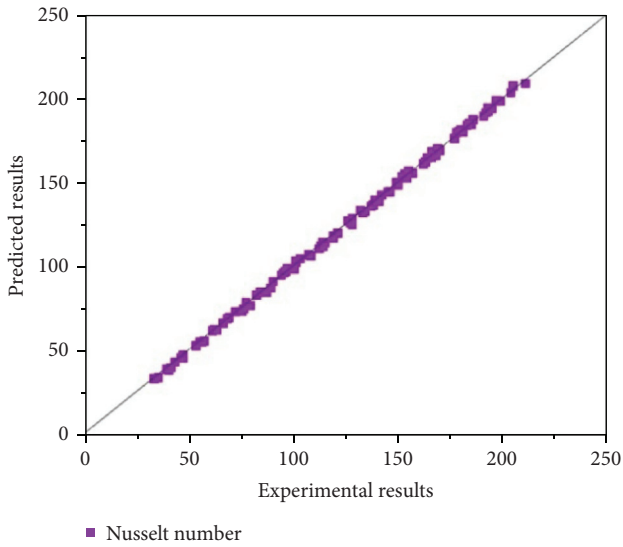
FIGURE 9: Continued.



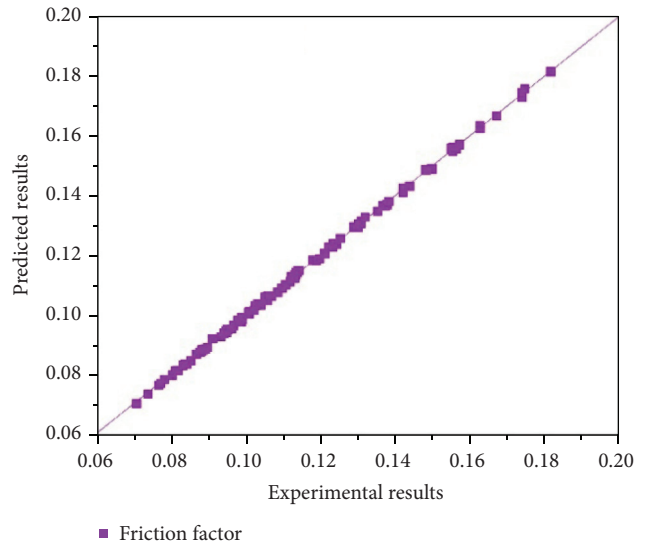


(c)

FIGURE 9: Experimental and ANFIS results of variation of  $\eta_{per}$  for various values of  $(d_R/D_I)$ ,  $(P_{PT}/L_T)$ , and  $(P_A/T_A)$  at different  $Re_{num}$ .



(a)



(b)

FIGURE 10: Continued.

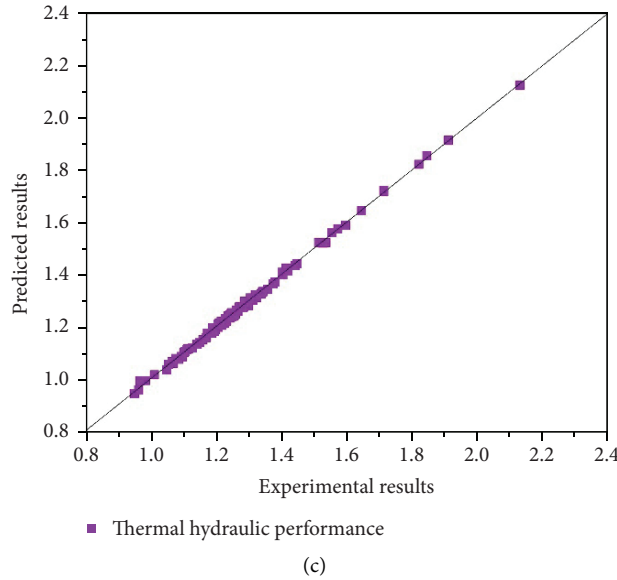


FIGURE 10: Comparison of experimental vs predicted ANFIS results for (a)  $Nu_{TT}$ , (b)  $f_{TT}$ , and (c)  $\eta_{per}$ .

## 9. Conclusions

This article deals with the analysis of the effect of flow and geometric parameters on the thermal performance of the heat exchanger tube fitted with a pierced twisted tape using the experimental and ANFIS models. The experimental and ANFIS models used four input parameters ( $d_R/D_I$ ),  $(P_{PT}/L_T)$ ,  $(P_A/T_A)$ , and  $Re_{num}$ , and three output parameters  $Nu_{TT}$ ,  $f_{TT}$ , and  $\eta_{per}$ . The inferences drawn are as follows:

- (1) The experimental and ANFIS results observed that the value of  $Nu_{TT}$  increases with an increase in  $(d_R/D_I)$ , and it attains the highest value at the  $(d_R/D_I)$  value equal to 0.65. Then, it starts decreasing with a further increase in the value of  $(d_R/D_I)$ . However,  $f_{TT}$  continuously increases with an increase in the value of  $(d_R/D_I)$ .
- (2) The experimental and ANFIS results showed that the value of  $Nu_{TT}$  increases with an increase in  $(P_{PT}/L_T)$  and reaches to a higher value at the  $(P_{PT}/L_T)$  value of 0.086. With more rise in the value of  $(P_{PT}/L_T)$ ,  $Nu_{TT}$  decreases. However,  $f_{TT}$  increases with a decrease in the value of  $(P_{PT}/L_T)$  and attains a higher value in relation to a  $(P_{PT}/L_T)$  value of 0.046.
- (3) The experimental and ANFIS results showed that the value of  $Nu_{TT}$  increased with an increase in  $(P_A/T_A)$  and attained the highest value corresponding to the  $(P_A/T_A)$  value of 10%. With a further increase in the value of  $(P_A/T_A)$ ,  $Nu_{TT}$  decreases. However,  $f_{TT}$  increases with a decrease in the value of  $(P_A/T_A)$  and reaches to an extreme value corresponding to the  $(P_A/T_A)$  value of 5%.
- (4) The maximum thermal hydraulic performance was obtained with the  $(d_R/D_I)$  value of 0.65, the  $(P_{PT}/L_T)$  value of 0.085, and the  $(P_A/T_A)$

value of 10%. The prediction of the  $Nu_{TT}$ ,  $f_{TT}$ , and  $\eta_{per}$  with the ANFIS model agrees with the experimental investigation with a higher error of less than 0.53.

- (5) It is evident from the ANFIS and experimental results that the enhancement of heat transfer mainly depends on the type of geometrical parameters and the nature of fluid. Hence, in future, the ANFIS model can be used to predict the heat transfer and pressure drop of a nanofluid flow through twisted tape heat exchangers. Also, the Particle Swarm Optimization (PSO) algorithm can be employed to improve the ANFIS model for prediction.

## Nomenclature

$A_T$ :	Area of test section, $m^2$
$D_i$ :	Diameter of tube, m
$d_R$ :	Diameter of helical tape, m
$(d_R/D_I)$ :	Diameter ratio
$h$ :	Heat transfer coefficient, $W/m^2 \cdot K$
$E$ :	Energy, J
$f_{TT}$ :	Friction factor for twisted tape inserts
$f_{smooth}$ :	Friction factor for smooth surface
$L_t$ :	Length of test section, m
$\dot{m}$ :	Mass flow rate, kg/s
$P_{PT}$ :	Pitch of helical pierced tape, m
$(P_{PT}/L_T)$ :	Relative pitch ratio
$(P_A/T_A)$ :	Perforation Index
$T_A$ :	Total area of helical tape, $m^2$
$Nu_{TT}$ :	Nusselt number for twisted tape inserts
$Nu_{smooth}$ :	Nusselt number for smooth surface
$p$ :	Pressure, Pa
$\Delta p_{ave}$ :	Average pressure drops, Pa
$Q_u$ :	Heat transfer rate, W
$Re_{num}$ :	Reynolds number

$V$ : Mean velocity of fluid, m/s  
 $\eta_{\text{per}}$ : Thermohydraulic performance parameter.

## Data Availability

The data used to support the findings of the study are included within the article.

## Conflicts of Interest

The authors declare that there are no conflicts of interest regarding the publication of this article.

## Acknowledgments

This study was funded by the University of Jeddah, Jeddah, Saudi Arabia.

## References

- [1] M. Mohanraj, S. Jayaraj, and C. Muraleedharan, "Applications of artificial neural networks for thermal analysis of heat exchangers—a review," *International Journal of Thermal Sciences*, vol. 90, pp. 150–172, 2015.
- [2] A. Sivakumar, N. Alagumurthi, and T. Senthilvelan, "Experimental investigation of forced convective heat transfer performance in nanofluids of Al<sub>2</sub>O<sub>3</sub>/water and CuO/water in a serpentine shaped micro channel heat sink," *Heat and Mass Transfer*, vol. 52, no. 7, pp. 1265–1274, 2015.
- [3] S. Kumar, M. Shandilya, A. Chauhan, R. Maithani, and A. Kumar, "Experimental analysis of zinc oxide/water/ethylene glycol-based nanofluid in a square duct roughened with inclined ribs," *Journal of Enhanced Heat Transfer*, vol. 27, no. 8, pp. 687–709, 2020.
- [4] M. H. Hamzah, N. A. C. Sidik, T. L. Ken, R. Mamat, and G. Najafi, "Factors affecting the performance of hybrid nanofluids: a comprehensive review," *International Journal of Heat and Mass Transfer*, vol. 115, pp. 630–646, 2017.
- [5] A. Al-Rashed, "Optimization of heat transfer and pressure drop of nano-antifreeze using statistical method of response surface methodology," *Physica A: Statistical Mechanics and its Applications*, vol. 521, 2019.
- [6] S. Kumar and A. Kumar, "A comprehensive review on the heat transfer and nanofluid flow characteristics in different shaped channels," *International Journal of Ambient Energy*, vol. 42, no. 3, pp. 345–361, 2021.
- [7] S. Kumar, R. Maithani, and A. Kumar, "Optimal design parameter selection for performance of alumina nano-material particles and turbulence promoters in heat exchanger: an AHP-TOPSIS technique," *Materials Today: Proceedings*, vol. 43, pp. 3152–3155, 2021.
- [8] G. Huminic and A. Huminic, "Heat transfer and flow characteristics of conventional fluids and nanofluids in curved tubes: a review," *Renewable and Sustainable Energy Reviews*, vol. 58, pp. 1327–1347, 2016.
- [9] M. E. Nakhchi and J. A. Esfahani, "Cu-water nanofluid flow and heat transfer in a heat exchanger tube equipped with cross-cut twisted tape," *Powder Technology*, vol. 339, pp. 985–994, 2018.
- [10] Y. Xiaowen and W. L. Lee, "The use of helical heat exchanger for heat recovery domestic water-cooled air-conditioners," *Energy Conversion and Management*, vol. 50, no. 2, pp. 240–246, 2009.
- [11] M. Ishak, T. A. Tahseen, and M. M. Rahman, "Experimental investigation on heat transfer and pressure drop characteristics of air flow over a staggered flat tube bank in crossflow," *International Journal of Automotive and Mechanical Engineering*, vol. 7, pp. 900–911, 2013.
- [12] T. L. Fullerton and N. K. Anand, "Periodically fully-developed flow and heat transfer over flat and oval tubes using a control volume finite-element method," *Numerical Heat Transfer, Part A: Applications*, vol. 57, no. 9, pp. 642–665, 2010.
- [13] J. Y. Jang and J. Y. Yang, "Experimental and 3-D numerical analysis of the thermal-hydraulic characteristics of elliptic finned-tube heat exchangers," *Heat Transfer Engineering*, vol. 19, no. 4, pp. 55–67, 1998.
- [14] M. Zeeshan, S. Nath, and D. Bhanja, "Numerical study to predict optimal configuration of fin and tube compact heat exchanger with various tube shapes and spatial arrangements," *Energy Conversion and Management*, vol. 148, pp. 737–752, 2017.
- [15] N. Benarji, C. Balaji, and S. P. Venkateshan, "Unsteady fluid flow and heat transfer over a bank of flat tubes," *Heat and Mass Transfer*, vol. 44, no. 4, pp. 445–461, 2007.
- [16] T. A. Tahseen, M. Ishak, and M. M. Rahman, "An overview on thermal and fluid flow characteristics in a plain plate finned and un-finned tube banks heat exchanger," *Renewable and Sustainable Energy Reviews*, vol. 43, pp. 363–380, 2015.
- [17] A. M. Hussein, "Adaptive neuro-fuzzy inference system of friction factor and heat transfer nanofluid turbulent flow in a heated tube," *Case Studies in Thermal Engineering*, vol. 8, pp. 94–104, 2016.
- [18] H. Esen, M. Inalli, A. Sengur, and M. Esen, "Artificial neural networks and adaptive neuro-fuzzy assessments for ground-coupled heat pump system," *Energy and Buildings*, vol. 40, no. 6, pp. 1074–1083, 2008.
- [19] T. A. Tahseen, M. Ishak, and M. M. Rahman, "Performance predictions of laminar heat transfer and pressure drop in an in-line flat tube bundle using an adaptive neuro-fuzzy inference system (ANFIS) model," *International Communications in Heat and Mass Transfer*, vol. 50, pp. 85–97, 2014.
- [20] C. N. Huang and C. C. Yu, "Integration of taguchi's method and multiple-input, multiple-output ANFIS inverse model for the optimal design of a water-cooled condenser," *Applied Thermal Engineering*, vol. 98, pp. 605–609, 2016.
- [21] F. Selimefendigil and H. F. Öztop, "Numerical analysis and ANFIS modeling for mixed convection of CNT-water nanofluid filled branching channel with an annulus and a rotating inner surface at the junction," *International Journal of Heat and Mass Transfer*, vol. 127, pp. 583–599, 2018.
- [22] T. R. Kiran and S. P. S. Rajput, "An effectiveness model for an indirect evaporative cooling (IEC) system: comparison of artificial neural networks (ANN), adaptive neuro-fuzzy inference system (ANFIS) and fuzzy inference system (FIS) approach," *Applied Soft Computing*, vol. 11, no. 4, pp. 3525–3533, 2011.
- [23] W. Suparta and A. A. Samah, "Rainfall prediction by using ANFIS times series technique in south tangerang, Indonesia," *Geodesy and Geodynamics*, vol. 11, no. 6, pp. 411–417, 2020.
- [24] C. E. Onu, J. T. Nwabanne, P. E. Ohale, and C. O. Asadu, "Comparative analysis of RSM, ANN and ANFIS and the mechanistic modeling in rioschrome black-T dye adsorption using modified clay," *South African Journal of Chemical Engineering*, vol. 36, pp. 24–42, 2021.
- [25] M. Mehrabi, S. M. Pesteei, and T. Pashae, "Modeling of heat transfer and fluid flow characteristics of helicoidal double-pipe heat exchangers using adaptive neuro-fuzzy inference

- system (ANFIS),” *International Communications in Heat and Mass Transfer*, vol. 38, no. 4, pp. 525–532, 2011.
- [26] H. Esen, M. Inalli, A. Sengur, and M. Esen, “Modelling a ground-coupled heat pump system using adaptive neuro-fuzzy inference systems,” *International Journal of Refrigeration*, vol. 31, no. 1, pp. 65–74, 2008.
- [27] R. Beigzadeh and M. Rahimi, “Prediction of thermal and fluid flow characteristics in helically coiled tubes using ANFIS and GA based correlations,” *International Communications in Heat and Mass Transfer*, vol. 39, no. 10, pp. 1647–1653, 2012.
- [28] R. Beigzadeh and M. Rahimi, “Prediction of heat transfer and flow characteristics in helically coiled tubes using artificial neural networks,” *International Communications in Heat and Mass Transfer*, vol. 39, no. 8, pp. 1279–1285, 2012.
- [29] H. Esen and M. Inalli, “ANN and ANFIS models for performance evaluation of a vertical ground source heat pump system,” *Expert Systems with Applications*, vol. 37, no. 12, pp. 8134–8147, 2010.
- [30] M. Hayati, A. Rezaei, and M. Seifi, “Prediction of the heat transfer rate of a single layer wire-on-tube type heat exchanger using ANFIS,” *International Journal of Refrigeration*, vol. 32, no. 8, pp. 1914–1917, 2009.
- [31] H. Esen, M. Inalli, A. Sengur, and M. Esen, “Predicting performance of a ground-source heat pump system using fuzzy weighted pre-processing-based ANFIS,” *Building and Environment*, vol. 43, no. 12, pp. 2178–2187, 2008.
- [32] S. Chen, J. Mao, F. Chen, P. Hou, and Y. Li, “Development of ANN model for depth prediction of vertical ground heat exchanger,” *International Journal of Heat and Mass Transfer*, vol. 117, pp. 617–626, 2018.
- [33] M. Hemmat Esfe, “Designing a neural network for predicting the heat transfer and pressure drop characteristics of Ag/water nanofluids in a heat exchanger,” *Applied Thermal Engineering*, vol. 126, pp. 559–565, 2017.
- [34] J. Gill and J. Singh, “Energetic and exergetic performance analysis of the vapor compression refrigeration system using adaptive neuro-fuzzy inference system approach,” *Experimental Thermal and Fluid Science*, vol. 88, pp. 246–260, 2017.
- [35] M. J. Zarei, F. Gholizadeh, S. Sabbaghi, and P. Keshavarz, “Estimation of CO<sub>2</sub> mass transfer rate into various types of nanofluids in hollow fiber membrane and packed bed column using adaptive neuro-fuzzy inference system,” *International Communications in Heat and Mass Transfer*, vol. 96, pp. 90–97, 2018.
- [36] S. M. A. N. R. Abadi, M. Mehrabi, and J. P. Meyer, “Prediction and optimization of condensation heat transfer coefficients and pressure drops of R134a inside an inclined smooth tube,” *International Journal of Heat and Mass Transfer*, vol. 124, pp. 953–966, 2018.
- [37] K. C. Onyelowe, J. Shakeri, H. Salahudeen, A. B. Salahudeene, E. E. Arinze, and H. U. Ugwu, “Application of ANFIS hybrids to predict coefficients of curvature and uniformity of treated unsaturated lateritic soil for sustainable earthworks,” *Cleaner Materials*, vol. 1, Article ID 100005, 2021.
- [38] A. Marjani, M. Babanezhad, and S. Shirazian, “Application of adaptive network-based fuzzy inference system (ANFIS) in the numerical investigation of Cu/water nanofluid convective flow,” *Case Studies in Thermal Engineering*, vol. 22, Article ID 100793, 2020.
- [39] A. D. Saeed, A. Baghban, F. Zarei, Z. Zhang, and S. Habibzadeh, “ANFIS based evolutionary concept for estimating nucleate pool boiling heat transfer of refrigerant-ester oil containing nanoparticles,” *International Journal of Refrigeration*, vol. 96, pp. 38–49, 2018.
- [40] H. Beiki, “Developing convective mass transfer of nanofluids in fully developed flow regimes in a circular tube: modeling using fuzzy inference system and ANFIS,” *International Journal of Heat and Mass Transfer*, vol. 173, Article ID 121285, 2021.
- [41] M. Bahiraei, S. Nazari, and H. Safarzadeh, “Modeling of energy efficiency for a solar still fitted with thermoelectric modules by ANFIS and PSO-enhanced neural network: a nanofluid application,” *Powder Technology*, vol. 385, pp. 185–198, 2021.
- [42] K. M. Yashawantha and A. V. Vinod, “ANFIS modelling of effective thermal conductivity of ethylene glycol and water nanofluids for low temperature heat transfer application,” *Thermal Science and Engineering Progress*, vol. 24, Article ID 100936, 2021.
- [43] S. Bahl, S. Singh, P. Goyal, and A. K. Bagha, “Experimental investigations on brass material and pin-fin based heat transfer system and its modeling by using adaptive neuro-fuzzy inference system,” *Materials Today: Proceedings*, vol. 45, no. 6, pp. 5323–5327, 2021.
- [44] S. Safarzadeh, M. Niknam-Azodi, A. Aldaghi, A. Taheri, M. Passandideh-Fard, and M. Mohammadi, “Energy and entropy generation analyses of a nanofluid-based helically coiled pipe under a constant magnetic field using smooth and micro-fin pipes: experimental study and prediction via ANFIS model,” *International Communications in Heat and Mass Transfer*, vol. 126, Article ID 105405, 2021.
- [45] M. Kaveh, R. A. Chayjan, I. Golpour, S. Poncet, F. Seirafi, and B. Khezri, “Evaluation of exergy performance and onion drying properties in a multi-stage semi-industrial continuous dryer: artificial neural networks (ANNs) and ANFIS models,” *Food and Bioprocess Processing*, vol. 127, pp. 58–76, 2021.
- [46] M. Vilela, G. Oluyemi, G. Oluyemi, and A. Petrovski, “A fuzzy inference system applied to value of information assessment for oil and gas industry,” *Decision Making: Applications in Management and Engineering*, vol. 2, no. 2, pp. 1–18, 2019.
- [47] H. Alolaiyan, H. A. Alshehri, M. H. Mateen, D. Pamucar, and M. Gulzar, “A novel algebraic structure of  $(\alpha, \beta)$ -complex fuzzy subgroups,” *Entropy*, vol. 23, no. 8, p. 992, 2021.
- [48] R. E. Precup, S. Preitl, E. Petriu et al., “Model-based fuzzy control results for networked control systems,” *Reports in Mechanical Engineering*, vol. 1, no. 1, pp. 10–25, 2020.
- [49] S. Thapa, S. Samir, K. Kumar, and S. Singh, “A review study on the active methods of heat transfer enhancement in heat exchangers using electroactive and magnetic materials,” *Materials Today: Proceedings*, vol. 45, no. 6, pp. 4942–4947, 2021.
- [50] R. Maithani and A. Kumar, “Effect of helical perforated twisted tape parameters on thermal and hydrodynamic performance in heat exchanger circular tube,” *Heat and Mass Transfer*, vol. 56, no. 2, pp. 507–519, 2020.
- [51] A. R. S. Suri, A. Kumar, and R. Maithani, “Heat transfer enhancement of heat exchanger tube with multiple square perforated twisted tape inserts: experimental investigation and correlation development,” *Chemical Engineering and Processing: Process Intensification*, vol. 116, pp. 76–96, 2017.

## Research Article

# Measuring the Return on Investment of Training Modules of Electrical Protection and Uninterruptible Power Supply (UPS) Using the Corrective and AHP Approaches

Farhad Salimian 

Department of Entrepreneurship Development, Faculty of Entrepreneurship, University of Tehran, Tehran, Iran

Correspondence should be addressed to Farhad Salimian; [salimian.farhad@ut.ac.ir](mailto:salimian.farhad@ut.ac.ir)

Received 14 September 2021; Revised 7 November 2021; Accepted 29 November 2021; Published 18 December 2021

Academic Editor: Dragan Pamučar

Copyright © 2021 Farhad Salimian. This is an open access article distributed under the Creative Commons Attribution License, which permits unrestricted use, distribution, and reproduction in any medium, provided the original work is properly cited.

The main purpose of this study is to calculate the return on investment of two training modules of electrical protection and uninterruptible power supply (UPS) using the corrective approaches applied to the basic model presented in previous research. In this study, first, the effect points of the training were identified using open questionnaires completed by experts. Then, its content validity is ensured by Lawshe, Waltz, and Basel approaches. Data on training costs were extracted through financial documentation and estimates. Details of measures, savings, internal supply, and so on were identified and cited to convert the observed effects into financial equivalents. Using the analytic hierarchy process (AHP) approach, the role of training in comparison with other initiatives in each of the effects and achievements was determined, and the net financial achievements of the training were determined. The training return on investment for the electrical protection module was 243% and for the UPS module was 1637%.

## 1. Introduction

According to studies conducted so far, if employees are actively involved in training and development programs and increase their skills and knowledge to better use their responsibilities and authorities in line with the mission of the organization, they will show more effort in their work and show better performance outcomes [1]. In this context, there is ample evidence that managers are concerned with the significance of improving productivity and performance due to the training programs [2]. On the other hand, employees also consider training and development programs as part of performance improvement mechanisms. Such programs reduce the costs associated with dismissal and, as a result, attract and recruit a new replacement and trained staff. Not only does obtaining feedback on the effects of training help managers identify areas for improvement, but it also provides employees with the necessary knowledge about how to progress and develop their careers [3]. Therefore, in a new competitive business, having competent and flexible human resources is necessary. Part of the investment in human

resources is allocated to the planning and implementation of training and development programs [4]. However, according to DeCenzo et al. [5], training and development are costly, and there are many pros and cons to the consequences [5]. Some of these actions have had financial consequences such as revenue, cost reduction, savings, and profitability, and some other reports have referred to nonfinancial aspects such as justice, customer satisfaction, reduced layoffs, and replacement of staff [6]. The return on investment (ROI) of training based on financial consequences is obvious, and its calculation is possible and practical. ROI is defined and understood in different ways by different stakeholders. However, many costs and benefits can be measured in terms of money and simply quantified [6]. The model presented in [7] pointed to the weakness of Kirkpatrick's model of not considering the costs and benefits of training and proposed this category as the fifth level of the Kirkpatrick model in evaluating the effectiveness of training. Rotem et al. [8] emphasized that the benefits of training should be inferred from the fourth level of the Kirkpatrick model and compared with the costs of training [8]. If the

evaluation at the fourth level of the Kirkpatrick model is erroneous, the calculation of the ROI from training will also be erroneous.

The gas industry is one of the strategic industries in Iran and has a wide range of technical and economic activities. Iran ranks second in the world in terms of gas resources. The gas industry, as a core business, extracts, refines, and supplies gas, gas condensate, liquefied petroleum gas, and other products for domestic and external consumers, including ordinary people, industries, and export. The gas industry is one of the most important pillars of energy saving and food supply for other important industries such as petrochemicals. The main purpose of this study is to calculate the return on investment of two training modules of electrical protection and uninterruptible power supply (UPS) using the corrective approaches applied to the basic model presented in previous research. In this study, first, the effect points of the training were identified using open questionnaires completed by experts. Then, its content validity is ensured by Lawshe, Waltz, and Basel approaches. According to the explanations provided, it can be said that this study seeks to answer the following questions:

- (i) What are the most important impact points of the practiced training and development programs?
- (ii) What is the role of training in the outcomes and results observed in the organization and executive processes?
- (iii) What is the rate of return on investment from training?

## 2. Literature Review

South Pars Gas Complex Company is one of the subsidiaries of the National Iranian Gas Company (NIGC), which was established in 1998 and is responsible for operating the onshore facilities of the multiple phases of the South Pars gas field. The South Pars refineries are located at sites 1 and 2 in Assaluyeh and Kangan counties, which contain 24 gas phases. Phases 1 to 10 and 15 to 21 are located at site 1 (Assaluyeh), and phases 11 to 14, phase 19, and phases 22 to 24 are located at site 2 (Kangan). The South Pars gas field is located in the territorial waters of Iran and Qatar and is shared between the two countries with an area of 6027 square miles and a depth of 1.9 miles below the seafloor. As the largest gas field in the world, it is 105 km away from the coast of Assaluyeh port. According to NIGC, the Iranian part covers an area of 2299 square miles, and its reserves are equivalent to 8% of the world's gas reserves and 50% of Iran's gas reserves. In terms of material resources, this field is the most important and valuable economic source and wealth and a huge and unique national treasure in Iran. In the field of training, the company pursues the mission of providing the necessary scientific and educational background for promoting organizational culture, transformation, and organizational growth and development by promoting the capabilities and competencies of managers and employees at the global level. The company's competitive vision requires that training programs be planned and implemented in the

best possible way and that, as a company responsible for national investments, it could achieve the best possible ROI. Furthermore, by calculating the return on investment from training, it is possible to identify programs related to the real needs of the company and increase the variety of training programs in terms of title, content, and implementation methods. Also, in this way, the support of senior and middle managers in the field of staff training and development can be obtained.

Increasing competition requires that organizations continuously improve their processes and gain a competitive advantage in the new business [9]. Competitive advantage is the factor with which an organization can create a defensive position against competitors and includes capabilities that allow an organization to differentiate itself from competitors [10]. Competitive advantage is achieved by creating value for customers, and value is manifested by providing goods and services that are different from competitors at a lower price. Human resources have the potential to create a competitive advantage for the organization. In general, employee performance depends on several factors such as motivation, performance appraisal, job satisfaction, training, and development [11].

Researchers have introduced some prioritizing methods such as a combination of analytical hierarchy process (AHP) and Ranking of Alternatives through Functional mapping of criterion subintervals into a Single Interval (RAFSI) [12], Fuzzy Measurement Alternatives and Ranking according to Compromise Solution (F-MARCOS) [13], third-party logistics [14], and Data-Envelopment-Analysis-based approach [15]. Moreover, the sensitivity analysis methods are also provided in the literature, including Full Consistency Method (FUCOM) [16], hybrid fuzzy MCDM [17], fuzzy Pivot Pairwise Relative Criteria Importance Assessment and fuzzy Measurement Alternatives and Ranking according to the Compromise Solution [18], Level Based Weight Assessment and fuzzy Multiattributive Border Approximation Area Comparison [19], and Best Worst Method and Multiattributive Ideal-Real Comparative Analysis [20].

Training and development are basically about creating perception, technical knowledge, techniques, and methods [21–23]. In fact, training and development are two of the necessities of human resource management. Because they can improve performance at the individual, administrative, and organizational levels, this is how today's organizations strive for inclusive and comprehensive training and development [24, 25]. Training and development are not only an opportunity for growth but also an investment that has significant benefits for the organization and employees [26–28]. For the organization, training and development lead to improved profitability while at the same time creating more positive attitudes toward profit orientation. For employees, training and development of job knowledge improve and at the same time help them to understand the goals of the organization. Human capital distinguishes a great organization from a good one. Organizations that invest in effective training and development for their human resources tend to gain benefits in the short and long term.

In 1975, Kirkpatrick designed his famous quadratic evaluation model, including reaction, learning, behavior, and results, for training programs. Phillips [29] noted the growing tendency for accountability in the form of higher levels of training evaluation that is relevant to business outcomes [29]. Based on the Kirkpatrick model, he concluded that there was a more prominent level of evaluation or the fifth level and called it an ROI. At this level of evaluation, the monetary value of the results is compared to the cost of the program and is usually expressed as a percentage. Despite the prominence of this evaluation, evaluators use it less than other evaluations because it is more difficult to manage and analyze. Phillips went on to show in a framework how monetary or financial amounts should be included in the value of training and the ROI of a training program, which is shown in Figure 1. Rooz [30] examined the rate of ROI from the leadership training program at the University of Georgia [31]. He considered two groups of managers as control and experimental and used the Phillips model. Data analysis showed that the dismissal and replacement rates for the trained group were significantly lower than the control group. The rate of ROI also showed that, for every dollar spent in the mentioned training program, a profit of \$ 3.86 was obtained, which in fact means 286% of the net return on investment in this investment. Sachdefa [32] addresses the challenges associated with measuring ROI and suggests how to address them in order to institutionalize the training ROI in organizations. The author categorized the challenges as the inability of human resource experts to collect data, lack of support and motivation of top managers, underestimation of achievable results, separation of the impact of training from other development programs, differences in the value of ROI outcome for managers at different levels and the need for them to agree on this, intangible benefits, and the risk of simplistic estimates to prove the constructive impact of training. There are several ways to detect faults in some studies in electrical systems, such as diagnosis based on P systems [33], microbially fault diagnostics depending on an initial set [34]; defect detection in energy systems based on fuzzy logic spiking neural P system [35], a failure analysis technique for three-phase motor drives [36], and H load frequency monitoring using event triggering [37].

Teixeira and Pereira [38] in their study confirmed that estimating and measuring the financial impact of human resource initiatives, including training and development programs, are not very common [38]. However, due to the high focus on training as a way to achieve business goals, it is important to ensure the proper implementation of these programs and determine the extent of their impact on the benefits. Thus, despite the difficulty of calculating the ROI and its high error rate, they have emphasized that if organizations do not use the necessary information and as a result make wrong decisions, they will not only waste financial resources, time, and human capital but may run the risk of losing talented employees and being deprived of business results.

### 3. Methods and Materials

**3.1. Proposed Method.** The present study is descriptive in terms of purpose and applied in terms of the type of use because it is an attempt to understand a specific situation in the

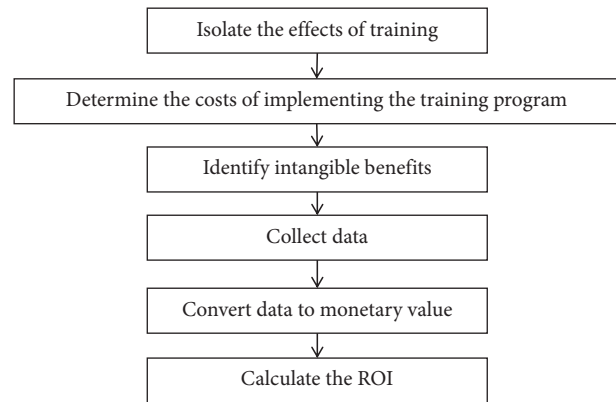


FIGURE 1: The framework of Phillips for calculating training return on investment.

real world in order to apply the findings to provide development solutions. Therefore, in terms of purpose, it is considered practical. This research is descriptive-case and is conducted in the field. Given that it follows the effects of training programs and the researcher has no role in those events, it is also considered postevent. It is a cross-sectional study in terms of time. Also, in terms of data type, it is a combination of qualitative and quantitative. The present study was started based on a library study in the field of calculating the training ROI and the use of training documents and records related to the two modules of electrical protection and uninterruptible power supply (UPS) and then using the points of view received through open and closed questionnaires provided to experts as well as performance information of the company and various units were followed. Given that this study was conducted for the first time in the company, the necessary information was unavailable. Therefore, it was necessary to gradually identify blind spots and ambiguities through documents and reports and refer to experts and experienced managers for clarification. The experts and stakeholders of both training modules were almost the same and included a total of twelve individuals, all of whom worked closely with the research team from the beginning to the end of the study. To identify the tangible effects and benefits of the modules, Lawshe, Waltz, and Basel approaches were used to ensure content validity.

The questionnaires used varied. The initial questionnaires were open-ended questionnaires for understanding technical events in the workplace, while the pairwise comparison questionnaire based on the analytic hierarchy process approach (AHP) was used to identify the role of the training program implemented in the updated functions. Expert choice software was used for its analysis. All data were collected and analyzed in coordination with experts and stakeholders through interviews and open and closed questionnaires, and the researchers had no involvement other than using the research mechanism. Therefore, the formal validity of the data is guaranteed. The research model is shown in Figure 2.

**3.2. Analytical Hierarchy Process.** The basis of this approach is to choose one option from several options, according to several specific criteria. This multicriteria evaluation method

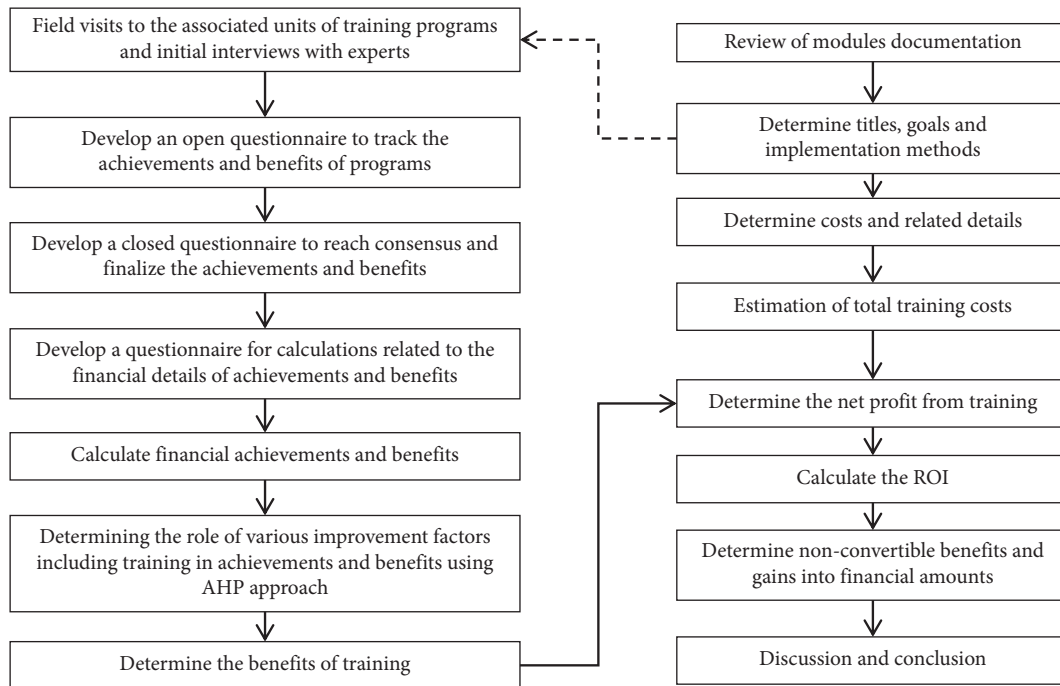


FIGURE 2: The research model used to calculate the ROI from training programs.

was first proposed in 1980 by Thomas L. Saati. Using the analytical hierarchy process (AHP) model, difficult and complex problems can be transformed into simple forms. This method has found many applications in economic and social issues and has found a special place in management.

The proposed criteria can be quantitative and qualitative. The basis of this decision-making method is based on pairwise comparisons. Decision-making begins with providing the decision hierarchy. The decision hierarchy tree shows the factors being compared and the competing options being evaluated in the decision. Then, a series of pairwise comparisons are made. These comparisons determine the weight of each factor in terms of competing options. Finally, matrices from pairwise comparisons are combined to make the optimal decision.

The first step based on this method is to determine the hierarchical diagram of the indicators and their pairwise comparisons with each other. This comparison is such that if element  $i$  is compared with element  $j$ , the degree of importance of one over the other will be one of the states of “completely more important,” “very strong importance,” “strong importance,” “less important,” “importance is the same” which represent the values of 9, 7, 5, 3, and 1,

respectively. The importance between the distances is also indicated by the values 2, 4, 6, and 8. Weighing operations are performed in three ways: referring to the knowledge of experts and specialists, using data and documents, and also combining them. In order to calculate the weight of each of the criteria and options, the methods of ordinary least squares, logarithmic least squares, eigenvectors, and arithmetic mean can be used. In this research, Expert Choice software has been used to extract the weights.

**3.3. Content Validity.** The content validity ratio (CVR) is calculated based on equation (1). In order to calculate this ratio, experts’ opinions on the content of the questionnaire are used, and by explaining the objectives of the questionnaire to them and providing them with operational definitions related to the content of the questions, they are asked to score each item based on the 3-point scale of “*not necessary, useful but not essential, essential.*”<sup>6</sup> Questions for which the calculated CVR is less than the numeric value determined by the Lawshe table should be excluded from the questionnaire. The acceptable ratio for 10 respondents is 0.6 that has been applied.

$$\text{CVR} = \frac{\text{number of experts indicating } \{ \text{essential} \} - (\text{total number of experts}/2)}{(\text{total number of experts}/2)} \quad (1)$$

Waltz and Basel’s method was used to examine the content validity index. Experts define each item as “relevant,” “clear,” and “simple” based on a four-part Likert scale. Experts rate each item as relevant from 1 to 4: 1 “not

relevant,” 2 “relatively relevant,” 3 “relevant,” and 4 “completely relevant.” The clarity of a statement is determined from 1 to 4: 1 “not clear,” 2 “relatively clear,” 3 “clear,” and 4 “clearly relevant,” respectively. The minimum



acceptable value for the CVI is 0.79, and if the CVI is less than 0.79, that item should be removed. The content validity index (CVI) was obtained from the following equation:

$$CVI = \frac{\text{number of experts rating item 3 or 4}}{\text{total number of experts}}. \quad (2)$$

## 4. Findings

**4.1. Training Modules.** The two major modules studied in this study were electrical protection and UPS with 23 and 17 participants, respectively. Both of them were conducted in 2017, and the duration of the modules was 48 hours.

**4.2. Calculating Training Costs.** A special form was used to calculate the costs of the studied modules, and it reflected the costs as much as possible. For cases where there was no documentation, subindices were used to estimate the costs. For example, items such as the salaries of the teaching staff were considered according to the time spent in different stages of training planning, from needs assessment to evaluation. Subindicators and standards were set to convert the activities performed into financial amounts. A detailed description of the training costs is provided in Table 1.

All real and estimated data were entered in Excel software and extracted financially related to each training module. The result related to training costs is shown in Table 2.

**4.3. Impacts and Benefits Observed.** During numerous observations, interviews, and careful examination of the details of the events reflected in the performance documentation and reports, the effects were clearly identified, and, separately, the financial benefits arising from them were determined. In the open questionnaires submitted to the experts, significant financial implications were included. Using the content validity approach, finally, five items were agreed upon, which are mentioned in Table 3.

The report of the effects related to the two training modules is shown in Tables 4–8. Given the importance of confidentiality and preventing possible abuse, some cases are not intentionally presented here.

Summarizing and calculating the total effects and achievement of the two training modules implemented show that the 5-year financial achievement of the electrical protection module is equal to \$202,138, and the 10-year financial achievement of the UPS module is \$1,797,099.

**4.4. The Role of Various Factors in the Benefits Obtained.** Based on the agreement reached with the training officials as well as the beneficiaries of the implemented training, in general, seven important factors affecting the improvement of performance and gaining benefits were identified. Using the AHP approach and the defined pairwise comparison questionnaire, the weight of each of the mentioned factors in each of the observed or estimated effects was determined.

A total of twelve experts (six experts for each module) completed the questionnaires, and the geometric mean of their opinions was considered as the final number of pairwise comparisons. The results of the mentioned analysis are shown in Table 9.

**4.5. Calculating the ROI of Training.** According to the weight of training in the benefits and achievements, the share of training was calculated as the net profit from training, which is shown in Tables 10 and 11. By dividing the net profit by the cost of education, the ROI is obtained.

**4.6. Determining the Nonconvertible Effects on Financial Values.** By conducting surveys through dialogue with experts and obtaining their agreement, nonconvertible achievements into financial values were also considered as described in Table 12 for the modules held.

## 5. Discussion

Based on the quantitative data alone, 2.43 times the cost of 5 years for the electrical protection training module and 16.37 times the cost of 10 years for the UPS training module will be returned to the company. In this set of training programs, learners gained new knowledge about electrical protection and UPS and learned about the types of parts and materials suitable for use in work processes and the possibility of designing, manufacturing, and developing significant electronic components and circuits domestically.

- (i) The learners gained new knowledge about electrical protection and UPS, learned about the types of parts and materials.
- (ii) There was a kind of resistance to the ineffectiveness of training and an emphasis on the effectiveness of other actions and initiatives among the beneficiaries of training programs.
- (iii) The research team played the role of facilitator in the form of justifying how to obtain, summarize, and apply data in the designed model.
- (iv) It was emphasized by the training officials that the designed approach should be institutionalized in the company and used from time to time.
- (v) Items such as the salaries of the teaching staff were considered according to the time spent in different stages of training planning from needs assessment to evaluation.
- (vi) Subindicators and standards were set to convert the activities performed into financial amounts.
- (vii) Using the AHP approach and the defined pairwise comparison questionnaire, the weight of each of the mentioned factors in each of the observed or estimated effects was determined.
- (viii) The experts in the field of training explained how to advance the activities, and the necessary training was provided to them.

TABLE 1: Details of training costs.

Cost title	Description
Instructors and lecturers	Tuition, transportation, catering, etc.
Training management and learning	Salary of educational staff in various processes of training, communication, etc.
Missed opportunity	Time spent training employees at different levels and not being active in the workplace
Educational space and facilities	Educational space, educational materials, teaching aids, etc.
Other costs	Reception of learners, transportation of learners, etc.

TABLE 2: Estimated amounts for training costs.

Cost title	Electrical protection (\$)	UPS (\$)
Instructors and lecturers	3823	2347
Training management and learning	434	230
Missed opportunity	4793	2758
Educational space and facilities	232	216
Other costs	81	73
Total	9364	5624

TABLE 3: Achievements from training agreed upon by experts.

Module	Convertible achievements	CVR	Relevancy CVI	Clarity CVI
Electrical protection	Eliminate the bus bar trip	0.83	0.92	0.83
	Reduce time delay relay	0.67	0.92	0.83
UPS	Reduce device and equipment failure	0.83	0.92	0.92
	Reduce special consumable parts	1.00	0.92	0.83
	Buy from domestic suppliers	0.67	1.00	0.92

TABLE 4: Elimination of bus bar trip as a result of electrical protection module implementation.

Number of breakdowns	Rate of gas loss (million m <sup>3</sup> )	Condensate drop-out	Sulfur drop (tons)	Total savings for two years (\$)
***	*** (Sale per cubic meter *** dollars)	*** (Sale per barrel *** dollars)	*** (Sale per ton *** dollars)	66261
	*** (Sale per cubic meter *** dollars)	*** (Sale per barrel *** dollars)	*** (Sale per ton *** dollars)	13062
		Total		79323

TABLE 5: Reduction of time delay relay as a result of electrical protection module implementation.

Number of relay types	Total number	Annual test title	Test time of each type (person-hour)		Total annual savings (\$)
			Before	After	
12	127	Relay performance test	10	5	766

It should be noted that the holding of these training programs was not predetermined with a specific strategy and program and was voluntary and spontaneous and based on the attractions created during the series of training programs. Therefore, in the future, it is necessary

to focus on educational needs assessment and appropriate goal setting. In addition, the goals should be pursued step by step with continuous monitoring and evaluation and to address shortcomings and improvements during implementation.

TABLE 6: Reduction of device and equipment failure as a result of UPS module implementation.

Device/module	Code	Number of failures in 10 years		Estimated savings in 10 years (\$)
		Before	After	
* - L2 - E - * - *	***	2	1	351
* - L4 - E - * - *	***	2	1	294
* - C3 - E - * - *	***	1	0.5	50
* - C1 - E - * - *	***	1	0.5	73
* - C2 - E - * - *	***	1	0.5	99
* - L5 - E - * - *	***	2	1	2094
* - UP *	***	2	1	4852
Total				78129

TABLE 7: Reduction of special consumable parts as a result of UPS module implementation.

Part name	Code	Consumption in ten years		Unit price (\$)	Estimated savings in 10 years (\$)
		Before	After		
IGBT	MODULE IGBT	2	1	8938	894
Thyristor	SEMICRON-IXYS-SKKT-INFINEON	16	4	1404	1685
PCB card	ALIP-CDIM-IGBT TRIG-THY TRIG-STABILIZER-MAIN BOARD-CCOT	20	5	5618	8427
Battery	ALCAD-SAFT	400	100	55414	1662411
Total					1673417

TABLE 8: Expected achievement of purchasing from domestic manufacturers as a result of UPS module implementation.

Part name	Code	Number of purchases in ten years		Unit price (\$)		Estimated savings in 10 years (\$)
		Before	After	Domestic	Foreign	
***	***	0	5	766	1277	2555
***	***	0	6	2043	4341	13788
***	***	0	10	511	1277	7660
***	***	0	5	511	2298	9040
***	***	0	10	281	1532	12510
Total						45553

TABLE 9: The weight of different factors in the indicators related to the observed effects.

Factor	Electrical protection			UPS	
	Eliminate the bus bar trip	Reduce time delay relay	Reduce device and equipment failure	Reduce special consumable parts	Buy from domestic suppliers
Attendance of people in the training program	16	9	15	5	5
Learn from other sources and methods (self-study, counseling, etc.)	3	4	10	25	15
Change in the process or method of doing task	14	16	15	15	15
Improve the hardware and software equipment	4	2	5	10	10
Improve workplace conditions (physical facilities, light, and noise)	3	21	5	5	5
Motivation of people to do the job well	30	25	25	25	30
How to employ people in the assigned job or task	30	23	25	15	20

TABLE 10: Application of training-related weight to the electrical protection module financial achievement of the.

Achievement	Coefficient of effect of participation in the program	Financial achievement in 5 years	Financial achievement from training
Eliminate the bus bar trip	16	198308	31729
Reduce time delay relay	9	3830	345
Total achievement of training		32074	
Training cost		9364	
Net profit		22710	
ROI		243%	

TABLE 11: Application of training-related weight to the UPS financial achievement.

Achievement	Coefficient of effect of people's attendance	Financial achievement	Financial achievement from training
Reduce device and equipment failure	15	78129	11719
Reduce special consumable parts	5	1673417	83671
Buy from domestic suppliers	5	45553	2278
Total achievement of training		97668	
Training cost		5624	
Net profit		92044	
ROI		1637%	

TABLE 12: Irreversible effects on financial amounts due to educational modules.

Module	Impact section	Achievement
Electrical protection	Training of expert human resources	No need for outside forces Less need for ongoing monitoring of the maintenance employees
	Adjusting the sting of protection relays	Reducing the number of errors
UPS	Manufacturing new parts	Manufacturing new parts within the company
	Internal purchase	Entrepreneurship in the production of new parts by domestic manufacturers and purchase from them

## 6. Conclusion

In this study, using the general Phillips model and the AHP approach, the ROI for the training module related to UPS and electrical protection was calculated. These two fields are costly for the company, and the consequences of negligence or lack of sufficient competence in that regard are catastrophic. The financial impact of these important issues was not calculated and was not reflected in the rate of ROI. In calculating the ROI for the two training modules for electrical protection and UPS, which was carried out as a pilot project at the South Pars refinery, the researchers initially had the least relevant information. In fact, the calculation of ROI or basically any indicators related to cost and income or profit in the mentioned training programs has never been considered and, therefore, there was no necessary preparation to do so. However, with the follow-up of the researchers, the cooperation of the managers, and the efforts and perseverance of the experts, the necessary data were gradually collected, and step by step, the researchers reached a better common understanding. There was a kind of resistance to the ineffectiveness of training and an emphasis on the effectiveness of other actions and initiatives among the beneficiaries of training programs, which, of course, was

recognized and not denied. However, top managers were surprised to see the achievement of training given its low cost. Therefore, the research team only played the role of facilitator in the form of justifying how to obtain, summarize, and apply data in the designed model and avoid any interference in the data and information. It was emphasized by the training officials that the designed approach should be institutionalized in the company and used from time to time. Therefore, the data extraction form related to design training costs and the necessary standards for extracting all costs were also determined. Finally, the report of the research activity was seen by the managers and experts of the company. The experts in the field of training also explained how to advance the activities, and the necessary training was provided to them to implement similar projects in the future.

## Data Availability

Data are available and can be provided over the emails querying directly to the author (salimian.farhad@ut.ac.ir).

## Conflicts of Interest

The author declares there are no conflicts of interest.

## References

- [1] E. Ari, O. M. Karatepe, H. Rezapourghdam, and T. Avci, "A conceptual model for green human resource management: indicators, differential pathways, and multiple pro-environmental outcomes," *Sustainability*, vol. 12, no. 17, Article ID 7089, 2020.
- [2] G. K. Gosnell, J. A. List, and R. D. Metcalfe, "The impact of management practices on employee productivity: a field experiment with airline captains," *Journal of Political Economy*, vol. 128, no. 4, pp. 1195–1233, 2020.
- [3] M. M. Karim, M. M. Choudhury, and W. B. Latif, "The impact of training and development on employees' performance: an analysis of quantitative data," *Noble International Journal of Business and Management Research*, vol. 3, no. 2, pp. 25–33, 2019.
- [4] T. G. Deladem, Z. Xiao, S. Doku, T. T. Siueia, and K. Gyader, "The effectiveness of training and its impact on employee performance and productivity in the tourism sector of Ghana," *European Journal of Economic and Financial Research*, vol. 3, no. 5, 2019.
- [5] D. A. DeCenzo, S. P. Robbins, and S. L. Verhulst, *Fundamentals of Human Resource Management*, John Wiley & Sons, Hoboken, NJ, USA, 2016.
- [6] C. C. Jasson and C. M. Govender, "Measuring return on investment and risk in training-A business training evaluation model for managers and leaders," *Acta Commercii*, vol. 17, no. 1, pp. 1–9, 2017.
- [7] P. P. Phillips, *The Bottomline on ROI: Basics, Benefits, & Barriers to Measuring Training & Performance Improvement*, CEP Press, Moscow, Russia, 2002.
- [8] A. Rotem, M. A. Zinovieff, and A. Goubarev, "A framework for evaluating the impact of the United Nations fellowship programmes," *Human Resources for Health*, vol. 8, no. 1, pp. 1–8, 2010.
- [9] M. R. Sadeghi Moghadam, A. Mohaghar, and A. Sheikhabir, "Simulation of pallet management system under risk pooling approach (case study of Saipa corporation supply chain)," *Modern Research in Decision Making*, vol. 1, no. 2, pp. 77–116, 2016.
- [10] S. Li, B. Ragu-Nathan, T. Ragu-Nathan, and S. S. Rao, "The impact of supply chain management practices on competitive advantage and organizational performance," *Omega*, vol. 34, no. 2, pp. 107–124, 2006.
- [11] O.-I. Dobre, "Employee motivation and organizational performance," *Review of Applied Socio-Economic Research*, vol. 5, no. 1, 2013.
- [12] A. Alosta, O. Elmansuri, and I. Badi, "Resolving a location selection problem by means of an integrated AHP-RAFSI approach," *Reports in Mechanical Engineering*, vol. 2, no. 1, pp. 135–142, 2021.
- [13] M. Bakır and Ö. Atalık, "Application of fuzzy AHP and fuzzy MARCOS approach for the evaluation of e-service quality in the airline industry," *Decision Making: Applications in Management and Engineering*, vol. 4, no. 1, pp. 127–152, 2021.
- [14] Ç. Karamaşa, E. Demir, S. Memiş, and S. Korucuk, "Weighting the factors affecting logistics outsourcing," *Decision Making Applications in Management and Engineering*, vol. 4, no. 1, 2020.
- [15] A. Blagojević, S. Vesković, S. Kasalica, A. Gojić, and A. Allamani, "The application of the fuzzy AHP and DEA for measuring the efficiency of freight transport railway undertakings," *Operational Research in Engineering Sciences: Theory and Applications*, vol. 3, no. 2, pp. 1–23, 2020.
- [16] E. Durmić, Ž. Stević, P. Chatterjee, M. Vasiljević, and M. Tomašević, "Sustainable supplier selection using combined FUCOM–Rough SAW model," *Reports in mechanical engineering*, vol. 1, no. 1, pp. 34–43, 2020.
- [17] O. F. Gorcun, S. Senthil, and H. Küçükönder, "Evaluation of tanker vehicle selection using a novel hybrid fuzzy MCDM technique," *Decision Making: Applications in Management and Engineering*, vol. 4, no. 2, pp. 140–162, 2021.
- [18] M. Bakır, Ş. Akan, and E. Özdemir, "Regional aircraft selection with fuzzy piprecia and fuzzy marcos: a case study of the Turkish airline industry," *Facta Universitatis – Series: Mechanical Engineering*, vol. 19, no. 3, pp. 423–445, 2021.
- [19] Ž. Jokić, D. Božanić, and D. Pamučar, "Selection of fire position of mortar units using LBWA and Fuzzy MABAC model," *Operational Research in Engineering Sciences: Theory and Applications*, vol. 4, no. 1, pp. 115–135, 2021.
- [20] D. S. Pamučar and L. M. Savin, "Multiple-criteria model for optimal off-road vehicle selection for passenger transportation: BWM-COPRAS model," *Vojnotehnički glasnik*, vol. 68, no. 1, pp. 28–64, 2020.
- [21] Y. Ma and D. Bennett, "The relationship between higher education students' perceived employability, academic engagement and stress among students in China," *Education+ Training*, 2021.
- [22] L. Zhang, X. Wang, Z. Zhang, Y. Cui, L. Ling, and G. Cai, "An adaptive control strategy for interfacing converter of hybrid microgrid based on improved virtual synchronous generator," *IET Renewable Power Generation*, 2021.
- [23] N. Ghorbani and A. Korzeniowski, "Adaptive risk hedging for call options under cox-ingersoll-ross interest rates," *Journal of Mathematical Finance*, vol. 10, no. 4, pp. 697–704, 2020.
- [24] X. Peng, Z. Liu, and D. Jiang, "A review of multiphase energy conversion in wind power generation," *Renewable and Sustainable Energy Reviews*, vol. 147, Article ID 111172, 2021.
- [25] B. Li, G. Xiao, R. Lu, R. Deng, and H. Bao, "On feasibility and limitations of detecting false data injection attacks on power grid state estimation using D-FACTS devices," *IEEE Transactions on Industrial Informatics*, vol. 16, no. 2, pp. 854–864, 2019.
- [26] X. Xu, D. Niu, B. Xiao, X. Guo, L. Zhang, and K. Wang, "Policy analysis for grid parity of wind power generation in China," *Energy Policy*, vol. 138, Article ID 111225, 2020.
- [27] A. Korzeniowski and N. Ghorbani, "Put options with linear investment for Hull-White interest rates," *Journal of Mathematical Finance*, vol. 11, no. 1, pp. 152–162, 2021.
- [28] N. Ghorbani and A. Korzeniowski, "Call and put option pricing with discrete linear investment strategy," 2021, <https://arxiv.org/abs/2110.04676>.
- [29] J. J. Phillips, "The return-on-investment (ROI) process: issues and trends," *Educational Technology*, vol. 38, no. 4, pp. 7–14, 1998.
- [30] F. R. Rohs, "Return on Investment (ROI)," *Journal of Leadership Education*, vol. 3, no. 1, pp. 27–38, 2004.
- [31] F. R. Rohs, "Return on investment (ROI): calculating the monetary return of a leadership development program," *Journal of Leadership Education*, vol. 3, no. 1, pp. 27–39, 2004.
- [32] S. Sachdeva, "ROI of training and development programmes: challenges and developments," *The SIJ Transactions on Industrial, Financial & Business Management (IFBM)*, vol. 2, no. 6, pp. 284–289, 2014.
- [33] X. Chen, T. Wang, R. Ying, and Z. Cao, "A fault diagnosis method considering meteorological factors for transmission networks based on P systems," *Entropy*, vol. 23, no. 8, p. 1008, 2021.

- [34] T. Wang, W. Liu, J. Zhao, X. Guo, and V. Terzija, "A rough set-based bio-inspired fault diagnosis method for electrical substations," *International Journal of Electrical Power & Energy Systems*, vol. 119, Article ID 105961, 2020.
- [35] W. Tao, X. Wei, J. Wang et al., "A weighted corrective fuzzy reasoning spiking neural P system for fault diagnosis in power systems with variable topologies," *Engineering Applications of Artificial Intelligence*, vol. 92, Article ID 103680, 2020.
- [36] H. Zhu, T. Wang, W. Liu, L. Valencia-Cabrera, M. J. Pérez-Jiménez, and P. Li, "A fault analysis method for three-phase induction motors based on spiking neural P systems," *Complexity*, vol. 2021, Article ID 2087027, 19 pages, 2021.
- [37] Q. Zhong, J. Yang, K. Shi, S. Zhong, Z. Li, and M. A. Sotelo, "Event-triggered  $H_\infty$  load frequency control for multi-area nonlinear power systems based on non-fragile proportional integral control strategy," *IEEE Transactions on Intelligent Transportation Systems*, 2021.
- [38] C. Teixeira and L. Pereira, "ROI in Training: how do HR Executives make investment decisions?" *International Journal of Scientific and Research Publications*, vol. 5, no. 7, pp. 1–6, 2015.

## Research Article

# A New TOPSIS Approach Using Cosine Similarity Measures and Cubic Bipolar Fuzzy Information for Sustainable Plastic Recycling Process

Muhammad Riaz <sup>1</sup>, Dragan Pamucar <sup>2</sup>, Anam Habib,<sup>1</sup> and Mishal Riaz<sup>1</sup>

<sup>1</sup>Department of Mathematics, University of the Punjab, Lahore, Pakistan

<sup>2</sup>Department of Logistics, Military Academy, University of Defence in Belgrade, Belgrade 11000, Serbia

Correspondence should be addressed to Dragan Pamucar; [dragan.pamucar@va.mod.gov.rs](mailto:dragan.pamucar@va.mod.gov.rs)

Received 9 September 2021; Accepted 30 October 2021; Published 15 December 2021

Academic Editor: Ali Ahmadian

Copyright © 2021 Muhammad Riaz et al. This is an open access article distributed under the Creative Commons Attribution License, which permits unrestricted use, distribution, and reproduction in any medium, provided the original work is properly cited.

A cubic bipolar fuzzy set (CBFS) is a robust paradigm to express bipolarity and vagueness in terms of bipolar fuzzy numbers and interval-valued bipolar fuzzy numbers. The abstraction of similarity measures (SMs) has a large number of applications in various fields. Therefore, in this study, taking the advantage of CBFSs, three cosine similarity measures for CBFSs are proposed successively by using cosine of the angle between two vectors, new distance measures, and cosine function. Some key properties of these similarity measures (SMs) are explored. Based on suggested SMs, the problem of bacteria recognition is analyzed and an important application is provided to exhibit the efficiency of proposed SMs for CBF information. Moreover, the TOPSIS approach based on cosine SMs is developed for multicriteria group decision-making (MCGDM) problems. An illustrative example about the selection of sustainable plastic recycling process is presented to discuss the efficiency of the suggested MCGDM technique.

## 1. Introduction

Fuzzy set (FS) theory [1] by using the concept of membership function (MF) is a robust approach for modeling uncertainty. A membership function is the generalization of characteristic function in the crisp set theory. An interval-valued fuzzy set (IVFS) [2] is the generalization of FS that assigns an interval of membership grades to the elements in the universe. The idea of orthopair has been extended to the ordered pair of membership grade (MG) and nonmembership grade (NMG) in the studies of intuitionistic fuzzy sets (IFSs) [3], Pythagorean fuzzy sets (PFSS) [4, 5], and  $q$ -rung orthopair fuzzy sets ( $q$ -ROPFSs) [6]. The values of MG and NMG are the elements of  $[0, 1]$ , i.e., any real number between 0 and 1. A number  $(\mu, \nu)$  is called an intuitionistic fuzzy number (IFN) if  $0 \leq \mu + \nu \leq 1$ , a Pythagorean fuzzy number (PFN) if  $0 \leq \mu^2 + \nu^2 \leq 1$ , and a

$q$ -rung orthopair fuzzy number ( $q$ -ROFN) if  $0 \leq \mu^q + \nu^q \leq 1$ , ( $q \geq 1$ ).

In many real-life problems, the indeterminacy is an essential factor to express expert opinion of the decision makers (DMs). To express such information, the idea of ordered triples with three components (MG, indeterminacy, and NMG) of neutrosophic set (NS) [7] and single-valued neutrosophic set (SVNS) [8] has been focused by many researchers. The concepts of spherical fuzzy sets [9–11] and picture fuzzy sets [12, 13] are strong models to deal with uncertain real-life problems with three components.

Zhang [14, 15] proposed the notion of bipolar fuzzy set (BFS) and bipolar (crisp) set to deal with bipolarity and fuzziness. Lee [16] proposed some results for bipolar-valued fuzzy sets. Deli et al. [17] studied bipolar neutrosophic set (BNS) and proposed novel features of BNSs with application towards MCDM. Wei et al. [18] studied interval-valued

bipolar fuzzy set (IVBFS) for uncertainty and bipolarity and positive and negative intervals based MCDM approach.

A hybrid concept of cubic set (CS) has been studied by Jun et al. [19]. He proposed novel concepts of internal (external) cubic sets of  $P$ -intersection,  $P$ -union,  $R$ -intersection, and  $R$ -union. The degree of similarity between two objects can be determined by the notion of similarity measure (SM). Ye [20] introduced cosine similarity measures for IFSSs. Wei and Wei [21] defined 10 different kinds of similarity measures for medical science and pattern recognition using PFS information using hesitation, MG and NMG, cosine function, and distance measures. Uluçay et al. [22] proposed new SMs for bipolar neutrosophic sets (BNSs) like hybrid vector SMs, Dice SMs, weighted Dice SMs, and weighted hybrid vector SMs. A comparative analysis for different values of the operational parameter is developed to express the validity of suggested SMs. Abdel-Basset et al. [23] investigated medical diagnosis of bipolar disorders by using BNSs-based SMs. They developed new MADM methods based on SMs and their weighted versions and illustrated them with some numerical examples. Tu et al. [24] suggested Dice SMs and Jaccard and cotangent SMs for neutrosophic cubic sets (NCSs) and applied them in MCDM. Lu and Ye [25] defined cosine SMs for NCSs by using cosine functions, distance, and cosine angle of two vectors. They investigated certain properties and propositions of proposed SMs. Peng et al. [26, 27] studied information measures for PFSs and q-ROFSs with corresponding applications in MCDM. Naem et al. [28] investigated new SMs for PFS information for the analysis of psychological disorder under uncertainty. Hussian and Yang [29] introduced Pythagorean fuzzy Hausdorff metric-based new distance and similarity measures and TOPSIS approach for MCDM.

TOPSIS is a well-known MCDM approach which was first introduced by Hwang and Yoon [30]. Zhang and Xu [31] initiated the Pythagorean fuzzy TOPSIS technique by defining a distance measure. Rani et al. [32] established the TOPIS method based on SMs for the PF environment and applied it for project delivery system selection. Akram et al. [33] developed bipolar fuzzy TOPSIS and utilized it in medical diagnosis. Garg and Arora [34] introduced the IFSS-TOPSIS method by using the correlation coefficient for solving MCDM problems. Garg and Kaur [35] developed TOPSIS based on cubic intuitionistic fuzzy (CIFS) information. They proposed a nonlinear-programming-based MCDM approach to deal with cubic intuitionistic fuzzy (CIFS) uncertain information. Riaz and Tehrim [36–38] initiated the novel hybrid model, namely, cubic bipolar fuzzy set (CBFS), by incorporating the features of BFS and IVBFS. They suggested some AOs named as CBF weighted averaging (geometric) AOs with R (P) orders for external (internal) CBF information.

Ali et al. [39] proposed Einstein geometric aggregation operators using novel complex interval-valued Pythagorean fuzzy sets. Alost et al. [40] developed a new AHP-RAFSI approach for resolving a location selection problem. Hashemkhani Zolfani et al. [41] introduced a VIKOR- and TOPSIS-focused reanalysis of the MADM methods based on logarithmic normalization. Ramakrishnan and Chakraborty

[42] proposed a cloud TOPSIS model for green supplier selection. Dobrosavljevic and Urosevic [43] suggested analysis of business process management defining and structuring activities. Yorulmaz et al. [44] proposed a robust Mahalanobis distance-based TOPSIS to evaluate the economic development of provinces. Petrovic and Kankaras [45] developed a hybridized IT2FS-DEMATEL-AHP-TOPSIS multicriteria decision-making approach as a case study of selection and evaluation of criteria for determination of air traffic control radar position. Badi and Pamucar [46] introduced a supplier selection method for steel-making companies by using combined Grey-MARCOS. Riaz et al. [47] proposed essential characteristics for soft multiset topology and robust MCDM applications.

The advantages and objectives of this manuscript are as follows: (1) To deal with vagueness and bipolarity with cubic bipolar fuzzy sets (CBFSs) which are a superior model to existing bipolar fuzzy models. (2) To define cosine SMs between CBFSs based on cosine of the angle between two vectors, new distance measures, and cosine function. Moreover, their weighted extensions are also introduced. (3) To apply these similarity measures to bacteria recognition problem. (4) To propose the TOPSIS approach based on cosine SMs to deal with the plastic recycling method selection problem.

The arrangement of this manuscript is planned as follows: In Section 2, we discuss some rudimentary concepts of bipolarity and fuzziness. In Section 3, we define cosine SMs, weighted cosine SMs, and related propositions. In Section 4, we establish an algorithm to handle pattern recognition problems under the CBF environment and a complex pattern recognition problem is presented to exhibit the efficiency of proposed algorithm. In Section 5, we introduce TOPSIS approach based on cosine SMs and an application concerning the selection of most sustainable plastic recycling process is discussed. Finally, we assess the validity and usefulness of our suggested technique by comparing it with some existing methodologies. Section 6 is designed for concluding remarks to express advantages and objectives of this manuscript.

## 2. Preliminaries

Some rudimentary concepts can be reviewed to understand the necessary fundamentals related to this manuscript (see [1, 2, 14, 18, 19, 36–38]).

*Definition 1* (see [37]). A cubic bipolar fuzzy set (CBFS)  $\mathcal{U}$  on the universe of discourse  $\mathfrak{R}$  can be defined as

$$\mathcal{U} = \{ \langle \tilde{q}, \mathfrak{T}(\tilde{q}), \mathfrak{S}(\tilde{q}) \rangle : \tilde{q} \in \mathfrak{R} \}, \quad (1)$$

where  $\mathfrak{T}$  is an IVBFS and  $\mathfrak{S}$  is a BFS on  $\mathfrak{R}$ . Thus, CBFS can also be written as

$$\mathcal{U} = \{ \langle \tilde{q}, [\rho_{\ell\mathcal{U}}^+(\tilde{q}), \rho_{u\mathcal{U}}^+(\tilde{q})], [\rho_{\ell\mathcal{U}}^-(\tilde{q}), \rho_{u\mathcal{U}}^-(\tilde{q})], (\rho_{\mathcal{U}}^+(\tilde{q}), \rho_{\mathcal{U}}^-(\tilde{q})) \rangle : \tilde{q} \in \mathfrak{R} \}, \quad (2)$$

where  $[\rho_{\ell\mathcal{U}}^+(\tilde{q}), \rho_{u\mathcal{U}}^+(\tilde{q})] \in I([0, 1])$  and  $[\rho_{\ell\mathcal{U}}^-(\tilde{q}), \rho_{u\mathcal{U}}^-(\tilde{q})] \in I^*([-1, 0])$  represent the interval-valued positive and



negative MGs, respectively, and  $\rho_{\mathcal{U}}^+(\bar{q}) \in [0, 1]$  and  $\rho_{\mathcal{U}}^-(\bar{q}) \in [-1, 0]$  represent the single-valued positive and negative MGs, respectively, of an object  $\bar{q} \in \mathfrak{R}$ .

2.1. Operations on CBFSS

**Definition 2** (see [37]). Let  $\mathcal{U} = \{\langle \bar{q}, [\rho_{\mathcal{U}}^+(\bar{q}), \rho_{\mathcal{U}}^-(\bar{q})], [\rho_{\mathcal{U}}^+(\bar{q}), \rho_{\mathcal{U}}^-(\bar{q})] \rangle : \bar{q} \in \mathfrak{R}\}$  and  $\mathcal{Q} = \{\langle \bar{q}, [\rho_{\mathcal{Q}}^+(\bar{q}), \rho_{\mathcal{Q}}^-(\bar{q})], [\rho_{\mathcal{Q}}^+(\bar{q}), \rho_{\mathcal{Q}}^-(\bar{q})] \rangle : \bar{q} \in \mathfrak{R}\}$  be two CBFSSs on  $\mathfrak{R}$  and  $\lambda > 0$ . Then, the operations on these CBFSSs under  $P$ -order are given as follows:

- (i)  $\mathcal{U} \cup_P \mathcal{Q} = \{\langle \bar{q}, [\max\{\rho_{\mathcal{U}}^+(\bar{q}), \rho_{\mathcal{Q}}^+(\bar{q})\}, \max\{\rho_{\mathcal{U}}^-(\bar{q}), \rho_{\mathcal{Q}}^-(\bar{q})\}], [\min\{\rho_{\mathcal{U}}^+(\bar{q}), \rho_{\mathcal{Q}}^+(\bar{q})\}, \min\{\rho_{\mathcal{U}}^-(\bar{q}), \rho_{\mathcal{Q}}^-(\bar{q})\}], (\max\{\rho_{\mathcal{U}}^+(\bar{q}), \rho_{\mathcal{Q}}^+(\bar{q})\}, \min\{\rho_{\mathcal{U}}^-(\bar{q}), \rho_{\mathcal{Q}}^-(\bar{q})\}) \rangle : \bar{q} \in \mathfrak{R}\}$
- (ii)  $\mathcal{U} \cap_P \mathcal{Q} = \{\langle \bar{q}, [\min\{\rho_{\mathcal{U}}^+(\bar{q}), \rho_{\mathcal{Q}}^+(\bar{q})\}, \min\{\rho_{\mathcal{U}}^-(\bar{q}), \rho_{\mathcal{Q}}^-(\bar{q})\}], [\max\{\rho_{\mathcal{U}}^+(\bar{q}), \rho_{\mathcal{Q}}^+(\bar{q})\}, \max\{\rho_{\mathcal{U}}^-(\bar{q}), \rho_{\mathcal{Q}}^-(\bar{q})\}], (\min\{\rho_{\mathcal{U}}^+(\bar{q}), \rho_{\mathcal{Q}}^+(\bar{q})\}, \max\{\rho_{\mathcal{U}}^-(\bar{q}), \rho_{\mathcal{Q}}^-(\bar{q})\}) \rangle : \bar{q} \in \mathfrak{R}\}$
- (iii)  $\mathcal{U} \oplus_P \mathcal{Q} = \{\langle \bar{q}, [\rho_{\mathcal{U}}^+(\bar{q}) + \rho_{\mathcal{Q}}^+(\bar{q}) - \rho_{\mathcal{U}}^-(\bar{q})\rho_{\mathcal{Q}}^+(\bar{q}), \rho_{\mathcal{U}}^-(\bar{q}) + \rho_{\mathcal{Q}}^-(\bar{q}) - \rho_{\mathcal{U}}^+(\bar{q})\rho_{\mathcal{Q}}^-(\bar{q})], [-(\rho_{\mathcal{U}}^+(\bar{q}) - \rho_{\mathcal{U}}^-(\bar{q}))\rho_{\mathcal{Q}}^+(\bar{q}) - (\rho_{\mathcal{U}}^-(\bar{q}) - \rho_{\mathcal{U}}^+(\bar{q}))\rho_{\mathcal{Q}}^-(\bar{q})], (\rho_{\mathcal{U}}^+(\bar{q}) + \rho_{\mathcal{Q}}^+(\bar{q}) - \rho_{\mathcal{U}}^-(\bar{q})\rho_{\mathcal{Q}}^+(\bar{q}), -(\rho_{\mathcal{U}}^-(\bar{q}) - \rho_{\mathcal{U}}^+(\bar{q})\rho_{\mathcal{Q}}^-(\bar{q})) \rangle : \bar{q} \in \mathfrak{R}\}$
- (iv)  $\mathcal{U} \otimes_P \mathcal{Q} = \{\langle \bar{q}, [\rho_{\mathcal{U}}^+(\bar{q})\rho_{\mathcal{Q}}^+(\bar{q}), \rho_{\mathcal{U}}^-(\bar{q})\rho_{\mathcal{Q}}^-(\bar{q})], [-(\rho_{\mathcal{U}}^+(\bar{q}) - \rho_{\mathcal{U}}^-(\bar{q}))\rho_{\mathcal{Q}}^+(\bar{q}) - (\rho_{\mathcal{U}}^-(\bar{q}) - \rho_{\mathcal{U}}^+(\bar{q}))\rho_{\mathcal{Q}}^-(\bar{q})], -(\rho_{\mathcal{U}}^+(\bar{q}) - \rho_{\mathcal{U}}^-(\bar{q}))\rho_{\mathcal{Q}}^+(\bar{q}) - (\rho_{\mathcal{U}}^-(\bar{q}) - \rho_{\mathcal{U}}^+(\bar{q}))\rho_{\mathcal{Q}}^-(\bar{q})], (\rho_{\mathcal{U}}^+(\bar{q})\rho_{\mathcal{Q}}^+(\bar{q}), -(\rho_{\mathcal{U}}^-(\bar{q}) - \rho_{\mathcal{U}}^+(\bar{q})\rho_{\mathcal{Q}}^-(\bar{q})) \rangle : \bar{q} \in \mathfrak{R}\}$
- (v)  $\mathcal{U}^\lambda = \{\langle r, [(\rho_{\mathcal{U}}^+(\bar{q}))^\lambda, (\rho_{\mathcal{U}}^-(\bar{q}))^\lambda], [-(1 - (\rho_{\mathcal{U}}^+(\bar{q}))^\lambda), -(1 - (\rho_{\mathcal{U}}^-(\bar{q}))^\lambda)], ((\rho_{\mathcal{U}}^+(\bar{q}))^\lambda, - (1 - (\rho_{\mathcal{U}}^-(\bar{q}))^\lambda)) \rangle : \bar{q} \in \mathfrak{R}\}$
- (vi)  $\lambda\mathcal{U} = \{\langle \bar{q}, [1 - (1 - \rho_{\mathcal{U}}^+(\bar{q}))^\lambda, 1 - (1 - \rho_{\mathcal{U}}^-(\bar{q}))^\lambda], [-(\rho_{\mathcal{U}}^+(\bar{q}))^\lambda, -(\rho_{\mathcal{U}}^-(\bar{q}))^\lambda], (1 - (1 - \rho_{\mathcal{U}}^+(\bar{q}))^\lambda, -(\rho_{\mathcal{U}}^-(\bar{q}))^\lambda) \rangle : \bar{q} \in \mathfrak{R}\}$
- (vii)  $\mathcal{U} \subseteq_P \mathcal{Q}$  if  $[\rho_{\mathcal{U}}^+(\bar{q}), \rho_{\mathcal{U}}^-(\bar{q})] \leq [\rho_{\mathcal{Q}}^+(\bar{q}), \rho_{\mathcal{Q}}^-(\bar{q})]$  and  $[\rho_{\mathcal{U}}^+(\bar{q}), \rho_{\mathcal{U}}^-(\bar{q})] \geq [\rho_{\mathcal{Q}}^+(\bar{q}), \rho_{\mathcal{Q}}^-(\bar{q})]$ ,  $\rho_{\mathcal{U}}^+(\bar{q}) \leq \rho_{\mathcal{Q}}^+(\bar{q})$  and  $\rho_{\mathcal{U}}^-(\bar{q}) \geq \rho_{\mathcal{Q}}^-(\bar{q})$ ,  $\forall \bar{q} \in \mathfrak{R}$

**Definition 3** (see [37]). Let  $\mathcal{U} = \{\langle \bar{q}, [\rho_{\mathcal{U}}^+(\bar{q}), \rho_{\mathcal{U}}^-(\bar{q})], [\rho_{\mathcal{U}}^+(\bar{q}), \rho_{\mathcal{U}}^-(\bar{q})] \rangle : \bar{q} \in \mathfrak{R}\}$  and  $\mathcal{Q} = \{\langle \bar{q}, [\rho_{\mathcal{Q}}^+(\bar{q}), \rho_{\mathcal{Q}}^-(\bar{q})], [\rho_{\mathcal{Q}}^+(\bar{q}), \rho_{\mathcal{Q}}^-(\bar{q})] \rangle : \bar{q} \in \mathfrak{R}\}$

$\bar{q} \in \mathfrak{R}$  be two CBFSSs on  $\mathfrak{R}$  and  $\lambda > 0$ . Then, we have the following:

- (i)  $\mathcal{R} \cup_R \mathcal{Q} = \{\langle \bar{q}, [\max\{\rho_{\mathcal{U}}^+(\bar{q}), \rho_{\mathcal{Q}}^+(\bar{q})\}, \max\{\rho_{\mathcal{U}}^-(\bar{q}), \rho_{\mathcal{Q}}^-(\bar{q})\}], [\min\{\rho_{\mathcal{U}}^+(\bar{q}), \rho_{\mathcal{Q}}^+(\bar{q})\}, \min\{\rho_{\mathcal{U}}^-(\bar{q}), \rho_{\mathcal{Q}}^-(\bar{q})\}], (\min\{\rho_{\mathcal{U}}^+(\bar{q}), \rho_{\mathcal{Q}}^+(\bar{q})\}, \max\{\rho_{\mathcal{U}}^-(\bar{q}), \rho_{\mathcal{Q}}^-(\bar{q})\}) \rangle : \bar{q} \in \mathfrak{R}\}$
- (ii)  $\mathcal{R} \cap_R \mathcal{Q} = \{\langle \bar{q}, [\min\{\rho_{\mathcal{U}}^+(\bar{q}), \rho_{\mathcal{Q}}^+(\bar{q})\}, \min\{\rho_{\mathcal{U}}^-(\bar{q}), \rho_{\mathcal{Q}}^-(\bar{q})\}], [\max\{\rho_{\mathcal{U}}^+(\bar{q}), \rho_{\mathcal{Q}}^+(\bar{q})\}, \max\{\rho_{\mathcal{U}}^-(\bar{q}), \rho_{\mathcal{Q}}^-(\bar{q})\}], (\max\{\rho_{\mathcal{U}}^+(\bar{q}), \rho_{\mathcal{Q}}^+(\bar{q})\}, \min\{\rho_{\mathcal{U}}^-(\bar{q}), \rho_{\mathcal{Q}}^-(\bar{q})\}) \rangle : \bar{q} \in \mathfrak{R}\}$
- (iii)  $\mathcal{R} \oplus_R \mathcal{Q} = \{\langle \bar{q}, [\rho_{\mathcal{U}}^+(\bar{q}) + \rho_{\mathcal{Q}}^+(\bar{q}) - \rho_{\mathcal{U}}^-(\bar{q})\rho_{\mathcal{Q}}^+(\bar{q}), \rho_{\mathcal{U}}^-(\bar{q}) + \rho_{\mathcal{Q}}^-(\bar{q}) - \rho_{\mathcal{U}}^+(\bar{q})\rho_{\mathcal{Q}}^-(\bar{q})], [-(\rho_{\mathcal{U}}^+(\bar{q}) - \rho_{\mathcal{U}}^-(\bar{q}))\rho_{\mathcal{Q}}^+(\bar{q}) - (\rho_{\mathcal{U}}^-(\bar{q}) - \rho_{\mathcal{U}}^+(\bar{q}))\rho_{\mathcal{Q}}^-(\bar{q})], (\rho_{\mathcal{U}}^+(\bar{q}) + \rho_{\mathcal{Q}}^+(\bar{q}) - \rho_{\mathcal{U}}^-(\bar{q})\rho_{\mathcal{Q}}^+(\bar{q}), -(\rho_{\mathcal{U}}^-(\bar{q}) - \rho_{\mathcal{U}}^+(\bar{q})\rho_{\mathcal{Q}}^-(\bar{q})) \rangle : \bar{q} \in \mathfrak{R}\}$
- (iv)  $\mathcal{R} \otimes_R \mathcal{Q} = \{\langle \bar{q}, [\rho_{\mathcal{U}}^+(\bar{q})\rho_{\mathcal{Q}}^+(\bar{q}), \rho_{\mathcal{U}}^-(\bar{q})\rho_{\mathcal{Q}}^-(\bar{q})], [-(\rho_{\mathcal{U}}^+(\bar{q}) - \rho_{\mathcal{U}}^-(\bar{q}))\rho_{\mathcal{Q}}^+(\bar{q}) - (\rho_{\mathcal{U}}^-(\bar{q}) - \rho_{\mathcal{U}}^+(\bar{q}))\rho_{\mathcal{Q}}^-(\bar{q})], -(\rho_{\mathcal{U}}^+(\bar{q}) - \rho_{\mathcal{U}}^-(\bar{q}))\rho_{\mathcal{Q}}^+(\bar{q}) - (\rho_{\mathcal{U}}^-(\bar{q}) - \rho_{\mathcal{U}}^+(\bar{q}))\rho_{\mathcal{Q}}^-(\bar{q})], (\rho_{\mathcal{U}}^+(\bar{q})\rho_{\mathcal{Q}}^+(\bar{q}), -(\rho_{\mathcal{U}}^-(\bar{q}) - \rho_{\mathcal{U}}^+(\bar{q})\rho_{\mathcal{Q}}^-(\bar{q})) \rangle : \bar{q} \in \mathfrak{R}\}$
- (v)  $\mathcal{U}^\lambda = \{\langle r, [(\rho_{\mathcal{U}}^+(\bar{q}))^\lambda, (\rho_{\mathcal{U}}^-(\bar{q}))^\lambda], [-(1 - (\rho_{\mathcal{U}}^+(\bar{q}))^\lambda), -(1 - (\rho_{\mathcal{U}}^-(\bar{q}))^\lambda)], (1 - (1 - \rho_{\mathcal{U}}^+(\bar{q}))^\lambda, -(\rho_{\mathcal{U}}^-(\bar{q}))^\lambda) \rangle : \bar{q} \in \mathfrak{R}\}$
- (vi)  $\lambda\mathcal{U} = \{\langle \bar{q}, [1 - (1 - \rho_{\mathcal{U}}^+(\bar{q}))^\lambda, 1 - (1 - \rho_{\mathcal{U}}^-(\bar{q}))^\lambda], [-(\rho_{\mathcal{U}}^+(\bar{q}))^\lambda, -(\rho_{\mathcal{U}}^-(\bar{q}))^\lambda], ((\rho_{\mathcal{U}}^+(\bar{q}))^\lambda, - (1 - (1 - \rho_{\mathcal{U}}^-(\bar{q}))^\lambda)) \rangle : \bar{q} \in \mathfrak{R}\}$
- (vii)  $\mathcal{U} \subseteq_R \mathcal{Q}$  if  $[\rho_{\mathcal{U}}^+(\bar{q}), \rho_{\mathcal{U}}^-(\bar{q})] \leq [\rho_{\mathcal{Q}}^+(\bar{q}), \rho_{\mathcal{Q}}^-(\bar{q})]$  and  $[\rho_{\mathcal{U}}^+(\bar{q}), \rho_{\mathcal{U}}^-(\bar{q})] \geq [\rho_{\mathcal{Q}}^+(\bar{q}), \rho_{\mathcal{Q}}^-(\bar{q})]$ ,  $\rho_{\mathcal{U}}^+(\bar{q}) \geq \rho_{\mathcal{Q}}^+(\bar{q})$  and  $\rho_{\mathcal{U}}^-(\bar{q}) \leq \rho_{\mathcal{Q}}^-(\bar{q})$ ,  $\forall \bar{q} \in \mathfrak{R}$

3. Cosine Similarity Measures for CBFSS

In this section, we define three cosine SMs for CBFSSs. We examine their properties and give examples for better understanding. Later on, the weighted versions of these similarity measures will also be presented.

**Definition 4.** Let  $\mathfrak{R} = \{\bar{q}_1, \bar{q}_2, \dots, \bar{q}_n\}$  be a finite universe of discourse.

Let  $\mathcal{U} = \{\langle \bar{q}_i, [\rho_{\mathcal{U}}^+(\bar{q}_i), \rho_{\mathcal{U}}^-(\bar{q}_i)], [\rho_{\mathcal{U}}^+(\bar{q}_i), \rho_{\mathcal{U}}^-(\bar{q}_i)] \rangle : \bar{q}_i \in \mathfrak{R}\}$  and  $\mathcal{Q} = \{\langle \bar{q}_i, [\rho_{\mathcal{Q}}^+(\bar{q}_i), \rho_{\mathcal{Q}}^-(\bar{q}_i)], [\rho_{\mathcal{Q}}^+(\bar{q}_i), \rho_{\mathcal{Q}}^-(\bar{q}_i)] \rangle : \bar{q}_i \in \mathfrak{R}\}$  be two CBFSSs on  $\mathfrak{R}$ ; then, cosine SM based on the cosine of the angle between two vectors is given by

$$S_1(\mathcal{U}, \mathcal{Q}) = \frac{1}{n} \sum_{i=1}^n \left\{ \frac{\rho_{\mathcal{U}}^+(\bar{q}_i)\rho_{\mathcal{Q}}^+(\bar{q}_i) + \rho_{\mathcal{U}}^-(\bar{q}_i)\rho_{\mathcal{Q}}^-(\bar{q}_i) + \rho_{\mathcal{U}}^+(\bar{q}_i)\rho_{\mathcal{Q}}^-(\bar{q}_i) + \rho_{\mathcal{U}}^-(\bar{q}_i)\rho_{\mathcal{Q}}^+(\bar{q}_i) + \rho_{\mathcal{U}}^+(\bar{q}_i)\rho_{\mathcal{Q}}^+(\bar{q}_i) + \rho_{\mathcal{U}}^-(\bar{q}_i)\rho_{\mathcal{Q}}^-(\bar{q}_i)}{\left\{ \sqrt{(\rho_{\mathcal{U}}^+(\bar{q}_i))^2 + (\rho_{\mathcal{U}}^-(\bar{q}_i))^2 + (\rho_{\mathcal{U}}^+(\bar{q}_i))^2 + (\rho_{\mathcal{U}}^-(\bar{q}_i))^2 + (\rho_{\mathcal{U}}^+(\bar{q}_i))^2 + (\rho_{\mathcal{U}}^-(\bar{q}_i))^2} \right\} \times \left\{ \sqrt{(\rho_{\mathcal{Q}}^+(\bar{q}_i))^2 + (\rho_{\mathcal{Q}}^-(\bar{q}_i))^2 + (\rho_{\mathcal{Q}}^+(\bar{q}_i))^2 + (\rho_{\mathcal{Q}}^-(\bar{q}_i))^2 + (\rho_{\mathcal{Q}}^+(\bar{q}_i))^2 + (\rho_{\mathcal{Q}}^-(\bar{q}_i))^2} \right\}} \right\} \tag{3}$$

**Theorem 1.** For two CBFSs  $\mathbf{U}$  and  $\mathfrak{S}$ , the cosine SM proposed in equation (3) possesses the following properties:

- (i)  $0 \leq \mathcal{S}_1(\mathbf{U}, \mathfrak{S}) \leq 1$
- (ii)  $\mathcal{S}_1(\mathbf{U}, \mathfrak{S}) = \mathcal{S}_1(\mathfrak{S}, \mathbf{U})$
- (iii)  $\mathcal{S}_1(\mathbf{U}, \mathfrak{S}) = 1$  if  $\mathbf{U} = \mathfrak{S}$

*Proof.*

(i) It is obvious that  $\mathcal{S}_1(\mathbf{U}, \mathfrak{S}) \geq 0$ . We only have to show that  $\mathcal{S}_1(\mathbf{U}, \mathfrak{S}) \leq 1$ . The Cauchy-Schwarz inequality further implies that

$$(a_1 b_1 + a_2 b_2 + \dots + a_n b_n) \leq \sqrt{(a_1^2 + a_2^2 + \dots + a_n^2)} \times \sqrt{(b_1^2 + b_2^2 + \dots + b_n^2)}. \tag{4}$$

Utilizing the above inequality, we have

$$\begin{aligned} & \rho_{eU}^+(\bar{Q}_i)\rho_{e\mathfrak{S}}^+(\bar{Q}_i) + \rho_{uU}^+(\bar{Q}_i)\rho_{u\mathfrak{S}}^+(\bar{Q}_i) + \rho_{eU}^-(\bar{Q}_i)\rho_{e\mathfrak{S}}^-(\bar{Q}_i) + \rho_{uU}^-(\bar{Q}_i)\rho_{u\mathfrak{S}}^-(\bar{Q}_i) + \rho_{U}^+(\bar{Q}_i)\rho_{\mathfrak{S}}^+(\bar{Q}_i) + \rho_{U}^-(\bar{Q}_i)\rho_{\mathfrak{S}}^-(\bar{Q}_i) \\ & \leq \left\{ \begin{aligned} & \sqrt{(\rho_{eU}^+(\bar{Q}_i))^2 + (\rho_{uU}^+(\bar{Q}_i))^2 + (\rho_{eU}^-(\bar{Q}_i))^2 + (\rho_{uU}^-(\bar{Q}_i))^2 + (\rho_{U}^+(\bar{Q}_i))^2 + (\rho_{U}^-(\bar{Q}_i))^2} \\ & \times \sqrt{(\rho_{e\mathfrak{S}}^+(\bar{Q}_i))^2 + (\rho_{u\mathfrak{S}}^+(\bar{Q}_i))^2 + (\rho_{e\mathfrak{S}}^-(\bar{Q}_i))^2 + (\rho_{u\mathfrak{S}}^-(\bar{Q}_i))^2 + (\rho_{\mathfrak{S}}^+(\bar{Q}_i))^2 + (\rho_{\mathfrak{S}}^-(\bar{Q}_i))^2} \end{aligned} \right\} \\ & \Rightarrow \frac{\rho_{eU}^+(\bar{Q}_i)\rho_{e\mathfrak{S}}^+(\bar{Q}_i) + \rho_{uU}^+(\bar{Q}_i)\rho_{u\mathfrak{S}}^+(\bar{Q}_i) + \rho_{eU}^-(\bar{Q}_i)\rho_{e\mathfrak{S}}^-(\bar{Q}_i) + \rho_{uU}^-(\bar{Q}_i)\rho_{u\mathfrak{S}}^-(\bar{Q}_i) + \rho_{U}^+(\bar{Q}_i)\rho_{\mathfrak{S}}^+(\bar{Q}_i) + \rho_{U}^-(\bar{Q}_i)\rho_{\mathfrak{S}}^-(\bar{Q}_i)}{\left\{ \begin{aligned} & \sqrt{(\rho_{eU}^+(\bar{Q}_i))^2 + (\rho_{uU}^+(\bar{Q}_i))^2 + (\rho_{eU}^-(\bar{Q}_i))^2 + (\rho_{uU}^-(\bar{Q}_i))^2 + (\rho_{U}^+(\bar{Q}_i))^2 + (\rho_{U}^-(\bar{Q}_i))^2} \\ & \times \sqrt{(\rho_{e\mathfrak{S}}^+(\bar{Q}_i))^2 + (\rho_{u\mathfrak{S}}^+(\bar{Q}_i))^2 + (\rho_{e\mathfrak{S}}^-(\bar{Q}_i))^2 + (\rho_{u\mathfrak{S}}^-(\bar{Q}_i))^2 + (\rho_{\mathfrak{S}}^+(\bar{Q}_i))^2 + (\rho_{\mathfrak{S}}^-(\bar{Q}_i))^2} \end{aligned} \right\}} \leq 1 \\ & \Rightarrow \frac{1}{n} \sum_{i=1}^n \left[ \frac{\rho_{eU}^+(\bar{Q}_i)\rho_{e\mathfrak{S}}^+(\bar{Q}_i) + \rho_{uU}^+(\bar{Q}_i)\rho_{u\mathfrak{S}}^+(\bar{Q}_i) + \rho_{eU}^-(\bar{Q}_i)\rho_{e\mathfrak{S}}^-(\bar{Q}_i) + \rho_{uU}^-(\bar{Q}_i)\rho_{u\mathfrak{S}}^-(\bar{Q}_i) + \rho_{U}^+(\bar{Q}_i)\rho_{\mathfrak{S}}^+(\bar{Q}_i) + \rho_{U}^-(\bar{Q}_i)\rho_{\mathfrak{S}}^-(\bar{Q}_i)}{\left\{ \begin{aligned} & \sqrt{(\rho_{eU}^+(\bar{Q}_i))^2 + (\rho_{uU}^+(\bar{Q}_i))^2 + (\rho_{eU}^-(\bar{Q}_i))^2 + (\rho_{uU}^-(\bar{Q}_i))^2 + (\rho_{U}^+(\bar{Q}_i))^2 + (\rho_{U}^-(\bar{Q}_i))^2} \\ & \times \sqrt{(\rho_{e\mathfrak{S}}^+(\bar{Q}_i))^2 + (\rho_{u\mathfrak{S}}^+(\bar{Q}_i))^2 + (\rho_{e\mathfrak{S}}^-(\bar{Q}_i))^2 + (\rho_{u\mathfrak{S}}^-(\bar{Q}_i))^2 + (\rho_{\mathfrak{S}}^+(\bar{Q}_i))^2 + (\rho_{\mathfrak{S}}^-(\bar{Q}_i))^2} \end{aligned} \right\}} \right] \leq 1. \tag{5} \end{aligned}$$

Hence,  $0 \leq \mathcal{S}_1(\mathbf{U}, \mathfrak{S}) \leq 1$ .

(ii) It is obvious.

(iii) If  $\mathbf{U} = \mathfrak{S}$ , then  $[\rho_{eU}^+(\bar{Q}_i), \rho_{uU}^+(\bar{Q}_i)] = [\rho_{e\mathfrak{S}}^+(\bar{Q}_i), \rho_{u\mathfrak{S}}^+(\bar{Q}_i)]$ ,  $[\rho_{eU}^-(\bar{Q}_i), \rho_{uU}^-(\bar{Q}_i)] = [\rho_{e\mathfrak{S}}^-(\bar{Q}_i), \rho_{u\mathfrak{S}}^-(\bar{Q}_i)]$ ,  $\rho_{U}^+(\bar{Q}_i) = \rho_{\mathfrak{S}}^+(\bar{Q}_i)$ , and  $\rho_{U}^-(\bar{Q}_i) = \rho_{\mathfrak{S}}^-(\bar{Q}_i)$ , for all  $\bar{Q}_i \in \mathfrak{R}$ . Thus,  $\mathcal{S}_1(\mathbf{U}, \mathfrak{S}) = 1$ .  $\square$

*Example 1.* Let  $\mathbf{U} = \{\langle \bar{Q}_1, [0.11, 0.26], [-0.38, -0.23], (0.12, -0.31) \rangle, \langle \bar{Q}_2, [0.22, 0.37], [-0.44, -0.29], (0.23, -0.42) \rangle\}$  and  $\mathfrak{S} = \{\langle \bar{Q}_1, [0.61, 0.76], [-0.59, -0.44], (0.73, -0.41) \rangle, \langle \bar{Q}_2, [0.59, 0.74], [-0.29, -0.14], (0.72, -0.11) \rangle\}$  be two CBFSs on  $\mathfrak{R} = \{\bar{Q}_1, \bar{Q}_2\}$ . Then, by utilizing equation (3), we calculate the cosine similarity measure between  $\mathbf{U}$  and  $\mathfrak{S}$  as

$$\begin{aligned}
 \mathcal{S}_1(\mathcal{U}, \mathfrak{H}) &= \frac{1}{2} \sum_{i=1}^2 \left\{ \frac{\rho_{\ell\mathcal{U}}^+(\bar{q}_i)\rho_{\ell\mathfrak{H}}^+(\bar{q}_i) + \rho_{u\mathcal{U}}^+(\bar{q}_i)\rho_{u\mathfrak{H}}^+(\bar{q}_i) + \rho_{\ell\mathcal{U}}^-(\bar{q}_i)\rho_{\ell\mathfrak{H}}^-(\bar{q}_i) + \rho_{u\mathcal{U}}^-(\bar{q}_i)\rho_{u\mathfrak{H}}^-(\bar{q}_i) + \rho_{\ell\mathcal{U}}^+(\bar{q}_i)\rho_{\mathfrak{H}}^+(\bar{q}_i) + \rho_{\mathcal{U}}^-(\bar{q}_i)\rho_{\mathfrak{H}}^-(\bar{q}_i)}{\left\{ \sqrt{(\rho_{\ell\mathcal{U}}^+(\bar{q}_i))^2 + (\rho_{u\mathcal{U}}^+(\bar{q}_i))^2 + (\rho_{\ell\mathcal{U}}^-(\bar{q}_i))^2 + (\rho_{u\mathcal{U}}^-(\bar{q}_i))^2 + (\rho_{\mathcal{U}}^+(\bar{q}_i))^2 + (\rho_{\mathcal{U}}^-(\bar{q}_i))^2} \right.} \\
 &\quad \left. \times \sqrt{(\rho_{\ell\mathfrak{H}}^+(\bar{q}_i))^2 + (\rho_{u\mathfrak{H}}^+(\bar{q}_i))^2 + (\rho_{\ell\mathfrak{H}}^-(\bar{q}_i))^2 + (\rho_{u\mathfrak{H}}^-(\bar{q}_i))^2 + (\rho_{\mathfrak{H}}^+(\bar{q}_i))^2 + (\rho_{\mathfrak{H}}^-(\bar{q}_i))^2} \right\}} \\
 &= \frac{1}{2} \left\{ \left( \frac{(0.11 \times 0.61) + (0.26 \times 0.76) + (-0.38 \times -0.59) + (-0.23 \times -0.44) + (0.12 \times 0.73) + (-0.31 \times -0.41)}{\sqrt{(0.11)^2 + (0.26)^2 + (-0.38)^2 + (-0.23)^2 + (0.12)^2 + (-0.31)^2} \times \sqrt{(0.61)^2 + (0.76)^2 + (-0.59)^2 + (-0.44)^2 + (0.73)^2 + (-0.41)^2}} \right) \right. \\
 &\quad \left. + \left( \frac{(0.22 \times 0.59) + (0.37 \times 0.74) + (-0.44 \times -0.29) + (-0.29 \times -0.14) + (0.23 \times 0.72) + (-0.42 \times -0.11)}{\sqrt{(0.22)^2 + (0.37)^2 + (-0.44)^2 + (-0.29)^2 + (0.23)^2 + (-0.42)^2} \times \sqrt{(0.59)^2 + (0.74)^2 + (-0.29)^2 + (-0.14)^2 + (0.72)^2 + (-0.11)^2}} \right) \right\} \\
 &= 0.8173.
 \end{aligned} \tag{6}$$

*Definition 5.* Let  $\mathfrak{R} = \{\bar{q}_1, \bar{q}_2, \dots, \bar{q}_n\}$  be a finite universe of discourse, and let  $\mathcal{U} = \{\langle \bar{q}_i, [\rho_{\ell\mathcal{U}}^+(\bar{q}_i), \rho_{u\mathcal{U}}^+(\bar{q}_i)], [\rho_{\ell\mathcal{U}}^-(\bar{q}_i), \rho_{u\mathcal{U}}^-(\bar{q}_i)] \rangle, \langle \bar{q}_i, [\rho_{\mathcal{U}}^+(\bar{q}_i), \rho_{\mathcal{U}}^-(\bar{q}_i)] \rangle : \bar{q}_i \in \mathfrak{R}\}$  and  $\mathfrak{H} = \{\langle \bar{q}_i, [\rho_{\ell\mathfrak{H}}^+(\bar{q}_i), \rho_{u\mathfrak{H}}^+(\bar{q}_i)], [\rho_{\ell\mathfrak{H}}^-(\bar{q}_i), \rho_{u\mathfrak{H}}^-(\bar{q}_i)] \rangle, \langle \bar{q}_i, [\rho_{\mathfrak{H}}^+(\bar{q}_i), \rho_{\mathfrak{H}}^-(\bar{q}_i)] \rangle : \bar{q}_i \in \mathfrak{R}\}$  be

two CBFs on  $\mathfrak{R}$ ; then, cosine SM based on distance is given by

$$\mathcal{S}_2(\mathcal{U}, \mathfrak{H}) = \frac{1}{n} \sum_{i=1}^n \cos \left\{ \begin{aligned} & \left( \left| \rho_{\ell\mathcal{U}}^+(\bar{q}_i) - \rho_{\ell\mathfrak{H}}^+(\bar{q}_i) \right| + \left| \rho_{u\mathcal{U}}^+(\bar{q}_i) - \rho_{u\mathfrak{H}}^+(\bar{q}_i) \right| + \left| \rho_{\ell\mathcal{U}}^-(\bar{q}_i) - \rho_{\ell\mathfrak{H}}^-(\bar{q}_i) \right| \right) \\ & \left. + \left| \rho_{u\mathcal{U}}^-(\bar{q}_i) - \rho_{u\mathfrak{H}}^-(\bar{q}_i) \right| + \left| \rho_{\mathcal{U}}^+(\bar{q}_i) - \rho_{\mathfrak{H}}^+(\bar{q}_i) \right| + \left| \rho_{\mathcal{U}}^-(\bar{q}_i) - \rho_{\mathfrak{H}}^-(\bar{q}_i) \right| \right) \frac{\pi}{12} \end{aligned} \right\}. \tag{7}$$

**Theorem 2.** For two CBFs  $\mathcal{U}$  and  $\mathfrak{H}$ , the cosine similarity measure proposed in equation (7) possesses the following properties:

*Proof*

- (i)  $0 \leq \mathcal{S}_2(\mathcal{U}, \mathfrak{H}) \leq 1$
- (ii)  $\mathcal{S}_2(\mathcal{U}, \mathfrak{H}) = \mathcal{S}_2(\mathfrak{H}, \mathcal{U})$
- (iii)  $\mathcal{S}_2(\mathcal{U}, \mathfrak{H}) = 1$  iff  $\mathcal{U} = \mathfrak{H}$

- (i) We know that  $0 \leq |\rho_{\ell\mathcal{U}}^+(\bar{q}_i) - \rho_{\ell\mathfrak{H}}^+(\bar{q}_i)| \leq 1$ ,  $0 \leq |\rho_{u\mathcal{U}}^+(\bar{q}_i) - \rho_{u\mathfrak{H}}^+(\bar{q}_i)| \leq 1$ ,  $0 \leq |\rho_{\ell\mathcal{U}}^-(\bar{q}_i) - \rho_{\ell\mathfrak{H}}^-(\bar{q}_i)| \leq 1$ ,  $0 \leq |\rho_{u\mathcal{U}}^-(\bar{q}_i) - \rho_{u\mathfrak{H}}^-(\bar{q}_i)| \leq 1$ ,  $0 \leq |\rho_{\mathcal{U}}^+(\bar{q}_i) - \rho_{\mathfrak{H}}^+(\bar{q}_i)| \leq 1$ , and  $0 \leq |\rho_{\mathcal{U}}^-(\bar{q}_i) - \rho_{\mathfrak{H}}^-(\bar{q}_i)| \leq 1$ , for all  $\bar{q}_i \in \mathfrak{R}$ .

By combining all these inequalities, we get

$$\begin{aligned}
 & 0 \leq \left| \rho_{\ell\mathcal{U}}^+(\bar{q}_i) - \rho_{\ell\mathfrak{H}}^+(\bar{q}_i) \right| + \left| \rho_{u\mathcal{U}}^+(\bar{q}_i) - \rho_{u\mathfrak{H}}^+(\bar{q}_i) \right| + \left| \rho_{\ell\mathcal{U}}^-(\bar{q}_i) - \rho_{\ell\mathfrak{H}}^-(\bar{q}_i) \right| + \left| \rho_{u\mathcal{U}}^-(\bar{q}_i) - \rho_{u\mathfrak{H}}^-(\bar{q}_i) \right| \\
 & \quad + \left| \rho_{\mathcal{U}}^+(\bar{q}_i) - \rho_{\mathfrak{H}}^+(\bar{q}_i) \right| + \left| \rho_{\mathcal{U}}^-(\bar{q}_i) - \rho_{\mathfrak{H}}^-(\bar{q}_i) \right| \leq 6 \\
 & \Rightarrow 0 \leq \frac{1}{6} \left( \left| \rho_{\ell\mathcal{U}}^+(\bar{q}_i) - \rho_{\ell\mathfrak{H}}^+(\bar{q}_i) \right| + \left| \rho_{u\mathcal{U}}^+(\bar{q}_i) - \rho_{u\mathfrak{H}}^+(\bar{q}_i) \right| + \left| \rho_{\ell\mathcal{U}}^-(\bar{q}_i) - \rho_{\ell\mathfrak{H}}^-(\bar{q}_i) \right| + \left| \rho_{u\mathcal{U}}^-(\bar{q}_i) - \rho_{u\mathfrak{H}}^-(\bar{q}_i) \right| \right. \\
 & \quad \left. + \left| \rho_{\mathcal{U}}^+(\bar{q}_i) - \rho_{\mathfrak{H}}^+(\bar{q}_i) \right| + \left| \rho_{\mathcal{U}}^-(\bar{q}_i) - \rho_{\mathfrak{H}}^-(\bar{q}_i) \right| \right) \leq 1 \\
 & \Rightarrow 0 \leq \cos \left\{ \frac{\pi}{2} \left( \frac{1}{6} \left( \left| \rho_{\ell\mathcal{U}}^+(\bar{q}_i) - \rho_{\ell\mathfrak{H}}^+(\bar{q}_i) \right| + \left| \rho_{u\mathcal{U}}^+(\bar{q}_i) - \rho_{u\mathfrak{H}}^+(\bar{q}_i) \right| + \left| \rho_{\ell\mathcal{U}}^-(\bar{q}_i) - \rho_{\ell\mathfrak{H}}^-(\bar{q}_i) \right| + \left| \rho_{u\mathcal{U}}^-(\bar{q}_i) - \rho_{u\mathfrak{H}}^-(\bar{q}_i) \right| \right. \right. \right. \\
 & \quad \left. \left. \left. + \left| \rho_{\mathcal{U}}^+(\bar{q}_i) - \rho_{\mathfrak{H}}^+(\bar{q}_i) \right| + \left| \rho_{\mathcal{U}}^-(\bar{q}_i) - \rho_{\mathfrak{H}}^-(\bar{q}_i) \right| \right) \right) \right\} \leq 1 \\
 & \Rightarrow 0 \leq \frac{1}{n} \sum_{i=1}^n \cos \left\{ \left( \left| \rho_{\ell\mathcal{U}}^+(\bar{q}_i) - \rho_{\ell\mathfrak{H}}^+(\bar{q}_i) \right| + \left| \rho_{u\mathcal{U}}^+(\bar{q}_i) - \rho_{u\mathfrak{H}}^+(\bar{q}_i) \right| + \left| \rho_{\ell\mathcal{U}}^-(\bar{q}_i) - \rho_{\ell\mathfrak{H}}^-(\bar{q}_i) \right| + \left| \rho_{u\mathcal{U}}^-(\bar{q}_i) - \rho_{u\mathfrak{H}}^-(\bar{q}_i) \right| \right. \right. \\
 & \quad \left. \left. + \left| \rho_{\mathcal{U}}^+(\bar{q}_i) - \rho_{\mathfrak{H}}^+(\bar{q}_i) \right| + \left| \rho_{\mathcal{U}}^-(\bar{q}_i) - \rho_{\mathfrak{H}}^-(\bar{q}_i) \right| \right) \frac{\pi}{12} \right\} \leq 1.
 \end{aligned} \tag{8}$$

Hence,  $0 \leq \mathcal{S}_2(\mathbf{U}, \mathfrak{H}) \leq 1$ .

(ii) It is obvious.

(iii) If  $\mathbf{U} = \mathfrak{H}$ , then  $[\rho_{\ell\mathbf{U}}^+(\tilde{Q}_i), \rho_{u\mathbf{U}}^+(\tilde{Q}_i)] = [\rho_{\ell\mathfrak{H}}^+(\tilde{Q}_i), \rho_{u\mathfrak{H}}^+(\tilde{Q}_i)]$ ,  $[\rho_{\ell\mathbf{U}}^-(\tilde{Q}_i), \rho_{u\mathbf{U}}^-(\tilde{Q}_i)] = [\rho_{\ell\mathfrak{H}}^-(\tilde{Q}_i), \rho_{u\mathfrak{H}}^-(\tilde{Q}_i)]$ ,  $\rho_{\mathbf{U}}^+(\tilde{Q}_i) = \rho_{\mathfrak{H}}^+(\tilde{Q}_i)$ , and  $\rho_{\mathbf{U}}^-(\tilde{Q}_i) = \rho_{\mathfrak{H}}^-(\tilde{Q}_i)$ , for all  $\tilde{Q}_i \in \mathfrak{R}$ . Therefore,

$$\begin{aligned} |\rho_{\ell\mathbf{U}}^+(\tilde{Q}_i) - \rho_{\ell\mathfrak{H}}^+(\tilde{Q}_i)| &= 0, \\ |\rho_{u\mathbf{U}}^+(\tilde{Q}_i) - \rho_{u\mathfrak{H}}^+(\tilde{Q}_i)| &= 0, \\ |\rho_{\ell\mathbf{U}}^-(\tilde{Q}_i) - \rho_{\ell\mathfrak{H}}^-(\tilde{Q}_i)| &= 0, \\ |\rho_{u\mathbf{U}}^-(\tilde{Q}_i) - \rho_{u\mathfrak{H}}^-(\tilde{Q}_i)| &= 0, \\ |\rho_{\mathbf{U}}^+(\tilde{Q}_i) - \rho_{\mathfrak{H}}^+(\tilde{Q}_i)| &= 0, \\ |\rho_{\mathbf{U}}^-(\tilde{Q}_i) - \rho_{\mathfrak{H}}^-(\tilde{Q}_i)| &= 0, \quad \text{for all } \tilde{Q}_i \in \mathfrak{R}. \end{aligned} \quad (9)$$

So,  $\mathcal{S}_2(\mathbf{U}, \mathfrak{H}) = 1$ .

Conversely, consider  $\mathcal{S}_2(\mathbf{U}, \mathfrak{H}) = 1$ . Since  $\cos(0) = 1$ , we infer that

$$\begin{aligned} |\rho_{\ell\mathbf{U}}^+(\tilde{Q}_i) - \rho_{\ell\mathfrak{H}}^+(\tilde{Q}_i)| &= 0, \\ |\rho_{u\mathbf{U}}^+(\tilde{Q}_i) - \rho_{u\mathfrak{H}}^+(\tilde{Q}_i)| &= 0, \\ |\rho_{\ell\mathbf{U}}^-(\tilde{Q}_i) - \rho_{\ell\mathfrak{H}}^-(\tilde{Q}_i)| &= 0, \\ |\rho_{u\mathbf{U}}^-(\tilde{Q}_i) - \rho_{u\mathfrak{H}}^-(\tilde{Q}_i)| &= 0, \\ |\rho_{\mathbf{U}}^+(\tilde{Q}_i) - \rho_{\mathfrak{H}}^+(\tilde{Q}_i)| &= 0, \\ |\rho_{\mathbf{U}}^-(\tilde{Q}_i) - \rho_{\mathfrak{H}}^-(\tilde{Q}_i)| &= 0, \quad \text{for all } \tilde{Q}_i \in \mathfrak{R}. \end{aligned} \quad (10)$$

This gives  $[\rho_{\ell\mathbf{U}}^+(\tilde{Q}_i), \rho_{u\mathbf{U}}^+(\tilde{Q}_i)] = [\rho_{\ell\mathfrak{H}}^+(\tilde{Q}_i), \rho_{u\mathfrak{H}}^+(\tilde{Q}_i)]$ ,  $[\rho_{\ell\mathbf{U}}^-(\tilde{Q}_i), \rho_{u\mathbf{U}}^-(\tilde{Q}_i)] = [\rho_{\ell\mathfrak{H}}^-(\tilde{Q}_i), \rho_{u\mathfrak{H}}^-(\tilde{Q}_i)]$ ,  $\rho_{\mathbf{U}}^+(\tilde{Q}_i) = \rho_{\mathfrak{H}}^+(\tilde{Q}_i)$ , and  $\rho_{\mathbf{U}}^-(\tilde{Q}_i) = \rho_{\mathfrak{H}}^-(\tilde{Q}_i)$ , for all  $\tilde{Q}_i \in \mathfrak{R}$ . Hence,  $\mathbf{U} = \mathfrak{H}$ .  $\square$

*Example 2.* Consider the CBFSS  $\mathbf{U}$  and  $\mathfrak{H}$  from the previous example. By utilizing equation (7), another cosine similarity measure between  $\mathbf{U}$  and  $\mathfrak{H}$  can be computed as

$$\begin{aligned} \mathcal{S}_2(\mathbf{U}, \mathfrak{H}) &= \frac{1}{2} \sum_{i=1}^2 \cos \left\{ \left( |\rho_{\ell\mathbf{U}}^+(\tilde{Q}_i) - \rho_{\ell\mathfrak{H}}^+(\tilde{Q}_i)| + |\rho_{u\mathbf{U}}^+(\tilde{Q}_i) - \rho_{u\mathfrak{H}}^+(\tilde{Q}_i)| + |\rho_{\ell\mathbf{U}}^-(\tilde{Q}_i) - \rho_{\ell\mathfrak{H}}^-(\tilde{Q}_i)| \right. \right. \\ &\quad \left. \left. + |\rho_{u\mathbf{U}}^-(\tilde{Q}_i) - \rho_{u\mathfrak{H}}^-(\tilde{Q}_i)| + |\rho_{\mathbf{U}}^+(\tilde{Q}_i) - \rho_{\mathfrak{H}}^+(\tilde{Q}_i)| + |\rho_{\mathbf{U}}^-(\tilde{Q}_i) - \rho_{\mathfrak{H}}^-(\tilde{Q}_i)| \right) \frac{\pi}{12} \right\} \\ &= \frac{1}{2} \left\{ \cos \left\{ (|0.11 - 0.61| + |0.26 - 0.76| + | -0.38 + 0.59| + | -0.23 + 0.44| + |0.12 - 0.73| + | -0.31 + 0.41|) \frac{\pi}{12} \right\} \right. \\ &\quad \left. + \cos \left\{ (|0.22 - 0.59| + |0.37 - 0.74| + | -0.44 + 0.29| + | -0.29 + 0.14| + |0.23 - 0.72| + | -0.42 + 0.11|) \frac{\pi}{12} \right\} \right\} = 0.8674. \end{aligned} \quad (11)$$

*Definition 6.* Let  $\{\langle \tilde{Q}_i, [\rho_{\ell\mathbf{U}}^+(\tilde{Q}_i), \rho_{u\mathbf{U}}^+(\tilde{Q}_i)], [\rho_{\ell\mathbf{U}}^-(\tilde{Q}_i), \rho_{u\mathbf{U}}^-(\tilde{Q}_i)], (\rho_{\mathbf{U}}^+(\tilde{Q}_i), \rho_{\mathbf{U}}^-(\tilde{Q}_i)) \rangle : \tilde{Q}_i \in \mathfrak{R}\}$  and  $\mathfrak{H} = \{\langle \tilde{Q}_i, [\rho_{\ell\mathfrak{H}}^+(\tilde{Q}_i), \rho_{u\mathfrak{H}}^+(\tilde{Q}_i)], [\rho_{\ell\mathfrak{H}}^-(\tilde{Q}_i), \rho_{u\mathfrak{H}}^-(\tilde{Q}_i)], (\rho_{\mathfrak{H}}^+(\tilde{Q}_i), \rho_{\mathfrak{H}}^-(\tilde{Q}_i)) \rangle : \tilde{Q}_i \in \mathfrak{R}\}$  be

two CBFSS on  $\mathfrak{R} = \{\tilde{Q}_1, \tilde{Q}_2, \dots, \tilde{Q}_n\}$ ; then, cosine similarity measure based on cosine function is defined as

$$\mathcal{S}_3(\mathbf{U}, \mathfrak{H}) = \frac{1}{4n(\sqrt{2} - 1)} \sum_{i=1}^n \left\{ \begin{aligned} & \left[ \sqrt{2} \cos \left( \frac{\pi}{8} (\rho_{\ell\mathbf{U}}^+(\tilde{Q}_i) - \rho_{\ell\mathfrak{H}}^+(\tilde{Q}_i) + \rho_{u\mathbf{U}}^+(\tilde{Q}_i) - \rho_{u\mathfrak{H}}^+(\tilde{Q}_i)) \right) - 1 \right] \\ & + \left[ \sqrt{2} \cos \left( \frac{\pi}{8} (\rho_{\ell\mathbf{U}}^-(\tilde{Q}_i) - \rho_{\ell\mathfrak{H}}^-(\tilde{Q}_i) + \rho_{u\mathbf{U}}^-(\tilde{Q}_i) - \rho_{u\mathfrak{H}}^-(\tilde{Q}_i)) \right) - 1 \right] \\ & + \left[ \sqrt{2} \cos \left( \frac{\pi}{4} (\rho_{\mathbf{U}}^+(\tilde{Q}_i) - \rho_{\mathfrak{H}}^+(\tilde{Q}_i)) \right) - 1 \right] \\ & + \left[ \sqrt{2} \cos \left( \frac{\pi}{4} (\rho_{\mathbf{U}}^-(\tilde{Q}_i) - \rho_{\mathfrak{H}}^-(\tilde{Q}_i)) \right) - 1 \right] \end{aligned} \right\}. \quad (12)$$

**Theorem 3.** For two CBFSS  $\mathbf{U}$  and  $\mathfrak{H}$ , the cosine similarity measure proposed in equation (12) satisfies the following conditions:

- (i)  $0 \leq \mathcal{S}_3(\mathbf{U}, \mathfrak{H}) \leq 1$
- (ii)  $\mathcal{S}_3(\mathbf{U}, \mathfrak{H}) = \mathcal{S}_3(\mathfrak{H}, \mathbf{U})$
- (iii)  $\mathcal{S}_3(\mathbf{U}, \mathfrak{H}) = 1$  if  $\mathbf{U} = \mathfrak{H}$

*Proof*

$$(i) \text{ Let } k_1 = (\rho_{\ell\mathbf{U}}^+(\bar{Q}_i) - \rho_{\ell\mathfrak{S}}^+(\bar{Q}_i) + \rho_{u\mathbf{U}}^+(\bar{Q}_i) - \rho_{u\mathfrak{S}}^+(\bar{Q}_i))/2, \\ k_2 = (\rho_{\ell\mathbf{U}}^-(\bar{Q}_i) - \rho_{\ell\mathfrak{S}}^-(\bar{Q}_i) + \rho_{u\mathbf{U}}^-(\bar{Q}_i) - \rho_{u\mathfrak{S}}^-(\bar{Q}_i))/2,$$

$k_3 = \rho_{\mathbf{U}}^+(\bar{Q}_i) - \rho_{\mathfrak{S}}^+(\bar{Q}_i)$ , and  $k_4 = \rho_{\mathbf{U}}^-(\bar{Q}_i) - \rho_{\mathfrak{S}}^-(\bar{Q}_i)$ . We see that  $-1 \leq k_\ell \leq 1$ ,  $\ell = 1, 2, 3, 4$ .

$$\Rightarrow \frac{1}{\sqrt{2}} \leq \cos\left(\frac{\pi}{4}k_\ell\right) \leq 1$$

$$\Rightarrow 1 \leq \sqrt{2} \cos\left(\frac{\pi}{4}k_\ell\right) \leq \sqrt{2}$$

$$\Rightarrow 0 \leq \sqrt{2} \cos\left(\frac{\pi}{4}k_\ell\right) - 1 \leq \sqrt{2} - 1$$

$$\Rightarrow 0 \leq \left(\sqrt{2} \cos\left(\frac{\pi}{4}k_1\right) - 1\right) + \left(\sqrt{2} \cos\left(\frac{\pi}{4}k_2\right) - 1\right) + \left(\sqrt{2} \cos\left(\frac{\pi}{4}k_3\right) - 1\right) + \left(\sqrt{2} \cos\left(\frac{\pi}{4}k_4\right) - 1\right) \leq 4(\sqrt{2} - 1)$$

$$\Rightarrow 0 \leq \frac{1}{4(\sqrt{2} - 1)} \left[ \left(\sqrt{2} \cos\left(\frac{\pi}{4}k_1\right) - 1\right) + \left(\sqrt{2} \cos\left(\frac{\pi}{4}k_2\right) - 1\right) + \left(\sqrt{2} \cos\left(\frac{\pi}{4}k_3\right) - 1\right) + \left(\sqrt{2} \cos\left(\frac{\pi}{4}k_4\right) - 1\right) \right] \leq 1$$

$$\Rightarrow 0 \leq \frac{1}{4n(\sqrt{2} - 1)} \sum_{i=1}^n \left[ \left(\sqrt{2} \cos\left(\frac{\pi}{4}k_1\right) - 1\right) + \left(\sqrt{2} \cos\left(\frac{\pi}{4}k_2\right) - 1\right) + \left(\sqrt{2} \cos\left(\frac{\pi}{4}k_3\right) - 1\right) + \left(\sqrt{2} \cos\left(\frac{\pi}{4}k_4\right) - 1\right) \right] \leq 1.$$

(13)

On substituting the values of  $k_1, k_2, k_3$ , and  $k_4$ , we get  $0 \leq \mathcal{S}_3(\mathbf{U}, \mathfrak{S}) \leq 1$ .

(ii) Since cosine is an even function,  $\mathcal{S}_3(\mathbf{U}, \mathfrak{S}) = \mathcal{S}_3(\mathfrak{S}, \mathbf{U})$ .

(iii) If  $\mathbf{U} = \mathfrak{S}$ , then  $[\rho_{\ell\mathbf{U}}^+(\bar{Q}_i), \rho_{u\mathbf{U}}^+(\bar{Q}_i)] = [\rho_{\ell\mathfrak{S}}^+(\bar{Q}_i), \rho_{u\mathfrak{S}}^+(\bar{Q}_i)]$ ,  $[\rho_{\ell\mathbf{U}}^-(\bar{Q}_i), \rho_{u\mathbf{U}}^-(\bar{Q}_i)] = [\rho_{\ell\mathfrak{S}}^-(\bar{Q}_i), \rho_{u\mathfrak{S}}^-(\bar{Q}_i)]$ ,  $\rho_{\mathbf{U}}^+(\bar{Q}_i) = \rho_{\mathfrak{S}}^+(\bar{Q}_i)$ , and  $\rho_{\mathbf{U}}^-(\bar{Q}_i) = \rho_{\mathfrak{S}}^-(\bar{Q}_i)$ , for all

$\bar{Q}_i \in \mathfrak{R}$ . Hence, one can easily infer that  $\mathcal{S}_3(\mathbf{U}, \mathfrak{S}) = 1$ .  $\square$

*Example 3.* Consider the CBFs  $\mathbf{U}$  and  $\mathfrak{S}$  from Example 1. Then, by utilizing equation (12), we calculate cosine SM between  $\mathbf{U}$  and  $\mathfrak{S}$  given by

$$\mathcal{S}_3(\mathbf{U}, \mathfrak{S}) = \frac{1}{4(2)(\sqrt{2} - 1)} \sum_{i=1}^2 \left\{ \begin{array}{l} \left[ \sqrt{2} \cos\left(\frac{\pi}{8}(\rho_{\ell\mathbf{U}}^+(\bar{Q}_i) - \rho_{\ell\mathfrak{S}}^+(\bar{Q}_i) + \rho_{u\mathbf{U}}^+(\bar{Q}_i) - \rho_{u\mathfrak{S}}^+(\bar{Q}_i))\right) - 1 \right] \\ + \left[ \sqrt{2} \cos\left(\frac{\pi}{8}(\rho_{\ell\mathbf{U}}^-(\bar{Q}_i) - \rho_{\ell\mathfrak{S}}^-(\bar{Q}_i) + \rho_{u\mathbf{U}}^-(\bar{Q}_i) - \rho_{u\mathfrak{S}}^-(\bar{Q}_i))\right) - 1 \right] \\ + \left[ \sqrt{2} \cos\left(\frac{\pi}{4}(\rho_{\mathbf{U}}^+(\bar{Q}_i) - \rho_{\mathfrak{S}}^+(\bar{Q}_i))\right) - 1 \right] \\ + \left[ \sqrt{2} \cos\left(\frac{\pi}{4}(\rho_{\mathbf{U}}^-(\bar{Q}_i) - \rho_{\mathfrak{S}}^-(\bar{Q}_i))\right) - 1 \right] \end{array} \right\} \\ = \frac{1}{8(\sqrt{2} - 1)} \left\{ \left[ \sqrt{2} \cos\left(\frac{\pi}{8}(0.11 - 0.61 + 0.26 - 0.76)\right) - 1 \right] + \left[ \sqrt{2} \cos\left(\frac{\pi}{8}(-0.38 + 0.59 - 0.23 + 0.44)\right) - 1 \right] \right. \\ + \left[ \sqrt{2} \cos\left(\frac{\pi}{4}(0.12 - 0.73)\right) - 1 \right] + \left[ \sqrt{2} \cos\left(\frac{\pi}{8}(-0.31 + 0.41)\right) - 1 \right] + \left[ \sqrt{2} \cos\left(\frac{\pi}{8}(0.22 - 0.59 + 0.37 - 0.74)\right) - 1 \right] \\ + \left[ \sqrt{2} \cos\left(\frac{\pi}{8}(-0.44 + 0.29 - 0.29 + 0.14)\right) - 1 \right] + \left[ \sqrt{2} \cos\left(\frac{\pi}{4}(0.23 - 0.72)\right) - 1 \right] \\ \left. + \left[ \sqrt{2} \cos\left(\frac{\pi}{8}(-0.42 + 0.11)\right) - 1 \right] \right\} \\ = 0.8477.$$

(14)

If the weights of the elements  $\bar{q}_i \in \mathfrak{R}$ , ( $i = 1, 2, \dots, n$ ) are taken into consideration, then we must use weighted versions of the above-defined cosine similarity measures as follows.

*Definition 7.* Let  $\mathfrak{R} = \{\bar{q}_1, \bar{q}_2, \dots, \bar{q}_n\}$  be the universe of discourse, and let  $\psi = \{\psi_1, \psi_2, \dots, \psi_n\}$  be the weight vector of  $\bar{q}_i$  ( $i = 1, 2, \dots, n$ ) such that  $\psi_i \geq 0$  and  $\sum_{i=1}^n \psi_i = 1$ . Then, for CBFSS  $\mathbf{U}$  and  $\mathfrak{S}$  on  $\mathfrak{R}$ , the weighted versions of the proposed cosine similarity measures can be defined as

$$\mathcal{S}_{\psi_1}(\mathbf{U}, \mathfrak{S}) = \sum_{i=1}^n \psi_i \left\{ \frac{\rho_{\ell\mathbf{U}}^+(\bar{q}_i)\rho_{\ell\mathfrak{S}}^+(\bar{q}_i) + \rho_{u\mathbf{U}}^+(\bar{q}_i)\rho_{u\mathfrak{S}}^+(\bar{q}_i) + \rho_{\ell\mathbf{U}}^-(\bar{q}_i)\rho_{\ell\mathfrak{S}}^-(\bar{q}_i) + \rho_{u\mathbf{U}}^-(\bar{q}_i)\rho_{u\mathfrak{S}}^-(\bar{q}_i) + \rho_{\mathbf{U}}^+(\bar{q}_i)\rho_{\mathfrak{S}}^+(\bar{q}_i) + \rho_{\mathbf{U}}^-(\bar{q}_i)\rho_{\mathfrak{S}}^-(\bar{q}_i)}{\left\{ \begin{array}{l} \sqrt{(\rho_{\ell\mathbf{U}}^+(\bar{q}_i))^2 + (\rho_{u\mathbf{U}}^+(\bar{q}_i))^2 + (\rho_{\ell\mathbf{U}}^-(\bar{q}_i))^2 + (\rho_{u\mathbf{U}}^-(\bar{q}_i))^2 + (\rho_{\mathbf{U}}^+(\bar{q}_i))^2 + (\rho_{\mathbf{U}}^-(\bar{q}_i))^2} \\ \times \sqrt{(\rho_{\ell\mathfrak{S}}^+(\bar{q}_i))^2 + (\rho_{u\mathfrak{S}}^+(\bar{q}_i))^2 + (\rho_{\ell\mathfrak{S}}^-(\bar{q}_i))^2 + (\rho_{u\mathfrak{S}}^-(\bar{q}_i))^2 + (\rho_{\mathfrak{S}}^+(\bar{q}_i))^2 + (\rho_{\mathfrak{S}}^-(\bar{q}_i))^2} \end{array} \right\}} \right\}, \quad (15)$$

$$\mathcal{S}_{\psi_2}(\mathbf{U}, \mathfrak{S}) = \sum_{i=1}^n \psi_i \cos \left\{ \begin{array}{l} \left( \left| \rho_{\ell\mathbf{U}}^+(\bar{q}_i) - \rho_{\ell\mathfrak{S}}^+(\bar{q}_i) \right| + \left| \rho_{u\mathbf{U}}^+(\bar{q}_i) - \rho_{u\mathfrak{S}}^+(\bar{q}_i) \right| + \left| \rho_{\ell\mathbf{U}}^-(\bar{q}_i) - \rho_{\ell\mathfrak{S}}^-(\bar{q}_i) \right| \right) \\ + \left| \rho_{u\mathbf{U}}^-(\bar{q}_i) - \rho_{u\mathfrak{S}}^-(\bar{q}_i) \right| + \left| \rho_{\mathbf{U}}^+(\bar{q}_i) - \rho_{\mathfrak{S}}^+(\bar{q}_i) \right| + \left| \rho_{\mathbf{U}}^-(\bar{q}_i) - \rho_{\mathfrak{S}}^-(\bar{q}_i) \right| \end{array} \right\} \frac{\pi}{12}, \quad (16)$$

$$\mathcal{S}_{\psi_3}(\mathbf{U}, \mathfrak{S}) = \frac{1}{4(\sqrt{2} - 1)} \sum_{i=1}^n \psi_i \left\{ \begin{array}{l} \left[ \sqrt{2} \cos\left(\frac{\pi}{8}(\rho_{\ell\mathbf{U}}^+(\bar{q}_i) - \rho_{\ell\mathfrak{S}}^+(\bar{q}_i) + \rho_{u\mathbf{U}}^+(\bar{q}_i) - \rho_{u\mathfrak{S}}^+(\bar{q}_i))\right) - 1 \right] \\ + \left[ \sqrt{2} \cos\left(\frac{\pi}{8}(\rho_{\ell\mathbf{U}}^-(\bar{q}_i) - \rho_{\ell\mathfrak{S}}^-(\bar{q}_i) + \rho_{u\mathbf{U}}^-(\bar{q}_i) - \rho_{u\mathfrak{S}}^-(\bar{q}_i))\right) - 1 \right] \\ + \left[ \sqrt{2} \cos\left(\frac{\pi}{4}(\rho_{\mathbf{U}}^+(\bar{q}_i) - \rho_{\mathfrak{S}}^+(\bar{q}_i))\right) - 1 \right] \\ + \left[ \sqrt{2} \cos\left(\frac{\pi}{4}(\rho_{\mathbf{U}}^-(\bar{q}_i) - \rho_{\mathfrak{S}}^-(\bar{q}_i))\right) - 1 \right] \end{array} \right\}. \quad (17)$$

**Theorem 4.** The weighted cosine similarity measures  $\mathcal{S}_{\psi_x}(\mathbf{U}, \mathfrak{S})$  ( $x = 1, 2, 3$ ) satisfy the following axioms:

- (i)  $0 \leq \mathcal{S}_{\psi_x}(\mathbf{U}, \mathfrak{S}) \leq 1$
- (ii)  $\mathcal{S}_{\psi_x}(\mathbf{U}, \mathfrak{S}) = \mathcal{S}_{\psi_x}(\mathfrak{S}, \mathbf{U})$
- (iii)  $\mathcal{S}_{\psi_x}(\mathbf{U}, \mathfrak{S}) = 1$  if  $\mathbf{U} = \mathfrak{S}$  (converse also holds in case of  $\mathcal{S}_{\psi_2}(\mathbf{U}, \mathfrak{S})$ )

*Proof.* The proof follows by using Theorems 1–3, respectively. Therefore, we exclude them here.  $\square$

*Remark 1.* If  $\psi = \{(1/n), (1/n), \dots, (1/n)\}$ , then weighted cosine similarity measures given in equations (15)–(17) reduce to unweighted cosine similarity measures given in equations (3)–(12), respectively.

#### 4. Application of Cosine Similarity Measures

Pattern recognition approaches employ machine learning and computational intelligence algorithms to identify regularities in existing patterns and to discover a pattern that is compatible with uncertain and partial data. In this section, the proposed cosine SMs are applied for the analysis of pattern recognition problem. In order to identify an

unknown pattern into one of the known patterns under CBFSS, we adopt the following steps in Algorithm 1.

**4.1. Illustrative Example.** Bacteria recognition is an important task in microbiology. Bacteria are mainly divided into three categories on the basis of their shapes (round shape, spiral shape, and cylindrical shape). Round-shaped bacteria are called cocci, spiral-shaped bacteria are called spirilla, and cylindrical-shaped bacteria are called bacilli (<https://microbiologyinfo.com>). Figure 1 demonstrates three types of bacteria.

Another way to classify bacteria is to investigate their behavior towards Gram staining test. A Gram stain is purple in color. When the stain homogenizes with bacteria in the sample, the bacteria will be pink or purple. If they remain purple, they are Gram-positive. If they are pink, they are Gram-negative (<https://medlineplus.gov>). Now, consider a bacterial collection consisting of *Salmonella*, *Escherichia coli*, and *Shigella*. All these intestinal bacteria belong to bacilli, and they are Gram-negative. The main features of these bacteria are described by

$$\mathfrak{R} = \{\bar{q}_1 (\text{size}), \bar{q}_2 (\text{flagellum}), \bar{q}_3 (\text{colony size})\}. \quad (18)$$

**Step 1.** Let  $\mathfrak{C}_1, \mathfrak{C}_2, \dots, \mathfrak{C}_m$  be the finite number of known patterns in terms of CBFS information in a finite universe of discourse  $\mathfrak{R}$ .  
**Step 2.** Consider unknown pattern  $\mathfrak{D}$  in the form of CBFS in  $\mathfrak{R}$ ; this pattern is to be recognized.  
**Step 3.** Compute the proposed cosine similarity measure between  $\mathfrak{D}$  and  $\mathfrak{C}_j$  ( $j = 1, 2, \dots, m$ ) by using equations (3)–(12). If the elements of the universe of discourse  $\mathfrak{R}$  carry some weights, then weighted similarity measures given in equations (15)–(17) can be utilized.  
**Step 4.** The pattern  $\mathfrak{D}$  having maximum similarity measure with finite pattern  $\mathfrak{C}_j$  is the required pattern.

ALGORITHM 1: Pattern recognition based on CBF information.

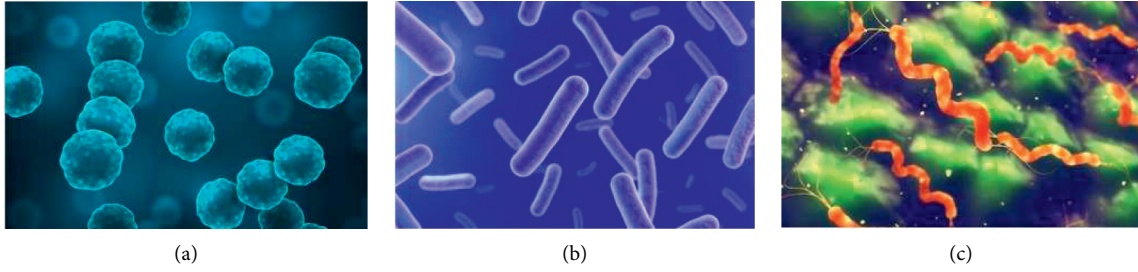


FIGURE 1: Three types of bacteria. (a) Cocci. (b) Bacilli. (c) Spirilla.

Suppose that a team of microbiologists assesses the presence of above features in the three bacteria and give their evaluation in the form of CBFSSs.

$$\begin{aligned}
 \mathfrak{C}_1 (\text{Salmonella}) &= \left\{ \begin{array}{l} \langle \tilde{q}_1, [0.61, 0.72], [-0.46, -0.31], (0.52, -0.42) \rangle, \\ \langle \tilde{q}_2, [0.82, 0.93], [-0.23, -0.17], (0.73, -0.33) \rangle, \\ \langle \tilde{q}_3, [0.47, 0.58], [-0.53, -0.48], (0.36, -0.28) \rangle, \end{array} \right\} \\
 \mathfrak{C}_2 (E. coli) &= \left\{ \begin{array}{l} \langle \tilde{q}_1, [0.34, 0.49], [-0.64, -0.51], (0.29, -0.67) \rangle, \\ \langle \tilde{q}_2, [0.79, 0.88], [-0.25, -0.18], (0.76, -0.27) \rangle, \\ \langle \tilde{q}_3, [0.62, 0.77], [-0.37, -0.28], (0.49, -0.57) \rangle, \end{array} \right\} \\
 \mathfrak{C}_3 (\text{Shigella}) &= \left\{ \begin{array}{l} \langle \tilde{q}_1, [0.57, 0.69], [-0.32, -0.27], (0.47, -0.36) \rangle, \\ \langle \tilde{q}_2, [0.19, 0.28], [-0.67, -0.42], (0.22, -0.57) \rangle, \\ \langle \tilde{q}_3, [0.53, 0.68], [-0.44, -0.31], (0.51, -0.46) \rangle. \end{array} \right\}
 \end{aligned} \tag{19}$$

Here, positive and negative MGs for each feature indicate the degree of existence and nonexistence of that feature in a certain bacterium. The aim of the team of microbiologists is to identify the unknown bacteria which is given as follows:

$$\mathfrak{D} = \left\{ \begin{array}{l} \langle \tilde{q}_1, [0.48, 0.61], [-0.36, -0.27], (0.39, -0.27) \rangle, \\ \langle \tilde{q}_2, [0.36, 0.48], [-0.59, -0.42], (0.41, -0.57) \rangle, \\ \langle \tilde{q}_3, [0.73, 0.87], [-0.29, -0.11], (0.65, -0.32) \rangle. \end{array} \right\} \tag{20}$$

The team wants to know to which bacteria does  $\mathfrak{D}$  belong. For such objective, we compute cosine similarity measures by utilizing equations (3)–(12). The results are summarized in Table 1.

It is obvious that the unknown bacteria belong to *Shigella*  $\mathfrak{C}_3$ . It is noteworthy that the computations obtained from all three cosine similarity measures are compatible with one another. Now, suppose that a weight vector  $\psi = \{0.39, 0.37, 0.24\}$  is assigned to the elements of  $\mathfrak{R}$ ; then, we calculate weighted cosine similarity measures by using equations (15)–(17). The computations are expressed in Table 2.

The unknown bacteria are again classified into *Shigella*  $\mathfrak{C}_3$ .

## 5. Extended TOPSIS Method Based on Cosine Similarity Measures

In this section, we propose the TOPSIS method based on cosine similarity measures to deal with MCGDM problems under cubic bipolar fuzzy information. Linguistic variables and terms are expressed in Table 3.

TABLE 1: Cosine similarity measures between unknown and known patterns.

	$\mathcal{S}(\mathcal{C}_1, \mathcal{D})$	$\mathcal{S}(\mathcal{C}_2, \mathcal{D})$	$\mathcal{S}(\mathcal{C}_3, \mathcal{D})$
$\mathcal{S}_1$	0.8976	0.8868	0.9701
$\mathcal{S}_2$	0.9218	0.9256	0.9819
$\mathcal{S}_3$	0.9326	0.9268	0.9823

TABLE 2: Weighted cosine similarity measures between unknown and known patterns.

	$\mathcal{S}_\psi(\mathcal{C}_1, \mathcal{D})$	$\mathcal{S}_\psi(\mathcal{C}_2, \mathcal{D})$	$\mathcal{S}_\psi(\mathcal{C}_3, \mathcal{D})$
$\mathcal{S}_{\psi 1}$	0.9015	0.8772	0.9726
$\mathcal{S}_{\psi 2}$	0.9227	0.9196	0.9844
$\mathcal{S}_{\psi 3}$	0.9335	0.9214	0.9839

TABLE 3: Linguistic terms for the assessment of criteria.

Linguistic terms	Fuzzy weights
Very important (VI)	0.95
Important (I)	0.80
Medium (M)	0.50
Less important (LI)	0.40

Figure 2 displays the flowchart diagram of Algorithm 2.

**5.1. Case Study.** Plastics are one of the most widely used materials in the world. The term “plastic” is derived from a Greek word “plastikos” which means fit for being shaped or molded. Plastic can embrace any shape or form. This is the reason it is utilized for a wide assortment of uses, from ordinary single-use items like bottles, boxes, and packaging to items like electronics, furniture, building materials, clothes, and food. Plastics have supplanted a broader scope of conventional materials including glass, wood, steel, and surprisingly concrete. Plastic is flexible, lightweight, moisture-resistant, and cost-friendly. These are the alluring attributes which lead to huge consumption of plastic worldwide. Due to this reason, the global plastic production has drastically increased from some 1.5 million metric tons in 1950 to 368 million metric tons in 2019. China is the world’s largest manufacturer of plastic, accounting for 31 percent of global plastic production (<https://www.statista.com/statistics/282732/global-production-of-plastics-since-1950/>). Figure 3 shows the expansion in global plastic production from 1950 to 2019.

However, owing to the durability and very slow degradation of plastics, the problem arises in the life management of the goods made from them. Plastics account for more than 12 percent of all solid wastes discharged (<https://datatopics.worldbank.org>). Figure 4 shows how much time different plastic items take to degrade. Most of the plastic waste has been dumped in the landfills or in the wild. Since plastics take too much time to decay, so throwing them into landfills just clogs up the valuable landfill space. About 8 million metric tons of plastic garbage is washed into the oceans by rivers around the world [49] every year. This has severe environmental consequences on marine life and human health.

Plastic recycling is the best way to manage plastic waste. Recycling of plastics can be defined as a process which

involves collection, separation, and processing of plastic wastes to form useful products. Plastic recycling has several advantages. Recycling one ton amount of plastics can conserve 7.4 cubic yards of landfill space (<https://www.online-sciences.com>). It also helps to reduce water pollution. Since plastics are made up of fossil fuels (crude oil, natural gas, etc.) or renewables (sugar cane, starch, etc.), recycling of plastics reduces the consumption of these natural resources resulting in their conservation.

There are three methods of plastic recycling.

**5.1.1. Mechanical Recycling.** The physical method of material reprocessing of plastic wastes into plastic products is known as mechanical recycling. First of all, the plastics are categorized by their resin type. Then, plastic recyclables are shredded. Impurities such as paper labels are subsequently removed from the shredded particles. This substance is melted and frequently extruded into pellets which are then utilized to manufacture other products.

**5.1.2. Chemical Recycling.** Chemical recycling is based on the principle of breaking down a polymeric product into its individual components (monomers for plastics), which can then be used as input raw material to recreate the original product or others.

**5.1.3. Energy Recovery.** Waste-to-energy technology is known as energy recovery. Although the process of combustion and gasification is similar on a fundamental level, cremation provides the vitality of high-temperature heat. Waste materials are incinerated, which produces ash, flue gas, and heat. The heat created by incineration can be used to create electricity in some instances.

Plastics life cycle is demonstrated in Figure 5.

Now-a-days, the industries which manufacture plastic products are keen to recycle their waste materials. The key issue is determining which recycling method to use. Selecting the best plastic recycling method is a MCGDM problem. To select the best plastic recycling method, the criteria under consideration are given in Table 4.

**5.2. Numerical Illustration.** Plastic materials are widely used during the manufacturing of electronic devices. Therefore, it is necessary for the electronics manufacturing companies to manage plastic waste:

*Step 1.* Suppose that a well-known electronic devices manufacturing company wants to manage plastic waste from end-of-life electronics. Let  $\mathcal{A} = \{\mathcal{A}_1, \mathcal{A}_2, \mathcal{A}_3\}$  be the set of alternatives, where  $\mathcal{A}_1$  = mechanical recycling,  $\mathcal{A}_2$  = chemical recycling, and  $\mathcal{A}_3$  = energy recovery. To choose the best alternative, the set of criteria is given in Table 4 and let the set of decision makers be  $\mathcal{E} = \{\mathcal{E}_1, \mathcal{E}_2, \mathcal{E}_3, \mathcal{E}_4\}$ .

*Step 2.* The weighted criterion matrix  $\mathcal{L}$  is constructed on the basis of linguistic variables given in Table 3 as follows:



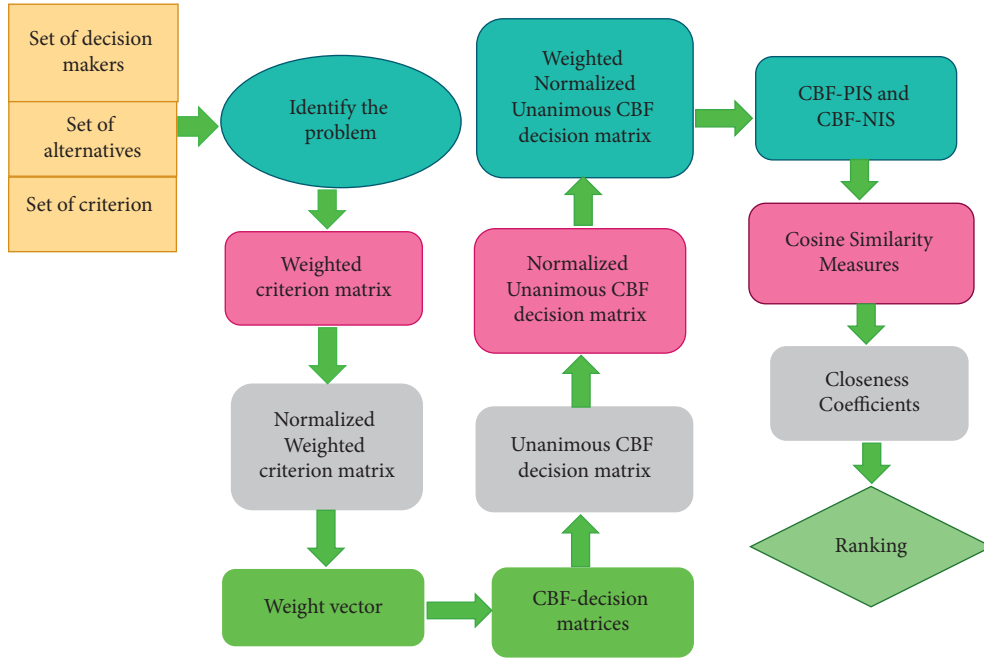


FIGURE 2: Flowchart diagram of Algorithm 2.

$$\mathcal{L} = [q_{ik}]_{4 \times 4} = \begin{pmatrix} VI & I & I & M \\ I & M & VI & I \\ VI & I & M & LI \\ M & VI & I & M \end{pmatrix}, \quad (21)$$

$$\mathcal{L} = [q_{ik}]_{4 \times 4} = \begin{pmatrix} 0.95 & 0.80 & 0.80 & 0.50 \\ 0.80 & 0.50 & 0.95 & 0.80 \\ 0.95 & 0.80 & 0.50 & 0.40 \\ 0.50 & 0.95 & .80 & 0.50 \end{pmatrix}.$$

Step 3. The normalized weighted criterion matrix  $\mathcal{M}$  is obtained by using Algorithm 2 as follows:

$$\mathcal{M} = [\psi_{ik}]_{4 \times 4} = \begin{pmatrix} 0.5787 & 0.5129 & 0.5129 & 0.4385 \\ 0.4873 & 0.3206 & 0.6091 & 0.7016 \\ 0.5787 & 0.5129 & 0.3206 & 0.3508 \\ 0.3046 & 0.6091 & 0.5129 & 0.4385 \end{pmatrix}. \quad (22)$$

Step 4. By using Algorithm 2, the weight vector is given by  $\mathcal{W} = \{0.2502, 0.2510, 0.2510, 0.2477\}$ .

Step 5. The CBF decision matrices  $\mathcal{Q}_i$  are provided by the decision makers in which each row represents an alternative and each column represents a criterion. The unanimous CBF decision matrix  $T$  is obtained by using Algorithm 2.

Step 6. Since cost, CO<sub>2</sub> emissions, and energy consumption are cost-type criteria, we construct normalized unanimous CBF decision matrix  $\hat{T}$  by utilizing Algorithm 2.

Step 7. By using Algorithm 2, the weighted normalized CBF decision matrix  $Y$  is obtained.

Step 8. The CBF-PIS and CBF-NIS are obtained by using Algorithm 2:

$$\begin{aligned} \text{CBF - PIS} &= \left\{ \begin{aligned} &\langle [0.2150, 0.2663], [-0.9573, -0.9243], (0.1904, -0.9113) \rangle, \\ &\langle [0.2735, 0.3590], [-0.8760, -0.8138], (0.2869, -0.9077) \rangle, \\ &\langle [0.2429, 0.3409], [-0.9044, -0.8486], (0.1957, -0.9077) \rangle, \\ &\langle [0.2080, 0.3051], [-0.9661, -0.9250], (0.2236, -0.9715) \rangle, \end{aligned} \right\} \\ \text{CBF - NIS} &= \left\{ \begin{aligned} &\langle [0.0102, 0.0514], [-0.9113, -0.8763], (0.0573, -0.8365) \rangle, \\ &\langle [0.0344, 0.0666], [-0.8361, -0.7791], (0.0791, -0.8138) \rangle, \\ &\langle [0.0515, 0.0791], [-0.7791, -0.7131], (0.0760, -0.7453) \rangle, \\ &\langle [0.0480, 0.0813], [-0.9218, -0.8953], (0.1081, -0.8918) \rangle. \end{aligned} \right\} \end{aligned} \quad (23)$$

**Step 1.** Identify MCGDM problem:

Suppose that  $\mathcal{E} = \{\mathcal{E}_i: i = 1, 2, \dots, n\}$  is the set of DMs,  $\mathcal{A} = \{\mathcal{A}_j: j = 1, 2, \dots, \ell\}$  is the set of alternatives, and  $\mathcal{C} = \{\mathcal{C}_k: k = 1, 2, \dots, m\}$  is the set of criterion.

**Step 2.** Construct the weighted criterion matrix with the help of linguistic variables that are given in Table 3.  $\mathcal{L} = [\mathcal{Q}_{ik}]_{n \times m} =$

$$\begin{pmatrix} \mathcal{Q}_{11} & \mathcal{Q}_{12} & \dots & \mathcal{Q}_{1m} \\ \mathcal{Q}_{21} & \mathcal{Q}_{22} & \dots & \mathcal{Q}_{2m} \\ \vdots & \vdots & \ddots & \vdots \\ \mathcal{Q}_{i1} & \mathcal{Q}_{i2} & \dots & \mathcal{Q}_{im} \\ \vdots & \vdots & \ddots & \vdots \\ \mathcal{Q}_{n1} & \mathcal{Q}_{n2} & \dots & \mathcal{Q}_{nm} \end{pmatrix},$$

where  $\mathcal{Q}_{ik}$  is the fuzzy weight assigned by the decision maker  $\mathcal{E}_i$  to the criterion  $\mathcal{C}_k$  by considering the values of linguistic variables.

**Step 3.** Obtain normalized weighted criterion matrix  $\mathcal{M} = [\psi_{ik}]_{n \times m} =$

$$\begin{pmatrix} \psi_{11} & \psi_{12} & \dots & \psi_{1m} \\ \psi_{21} & \psi_{22} & \dots & \psi_{2m} \\ \vdots & \vdots & \ddots & \vdots \\ \psi_{i1} & \psi_{i2} & \dots & \psi_{im} \\ \vdots & \vdots & \ddots & \vdots \\ \psi_{n1} & \psi_{n2} & \dots & \psi_{nm} \end{pmatrix},$$

where  $\psi_{ik} = \mathcal{Q}_{ik} / \sqrt{\sum_{i=1}^n \mathcal{Q}_{ik}^2}$ .

**Step 4.** Construct weight vector  $\mathcal{W} = \{w_1, w_2, \dots, w_m\}$  as follows:  $w_k = (w_k / \sum_{k=1}^m w_k)$ , where  $w_k = (1/n) \sum_{i=1}^n \psi_{ik}$ .

**Step 5.** Construct CBF-decision matrices  $Q_i = [q_{jk}^i]_{l \times m} =$

$$\begin{pmatrix} q_{11}^i & q_{12}^i & \dots & q_{1m}^i \\ q_{21}^i & q_{22}^i & \dots & q_{2m}^i \\ \vdots & \vdots & \ddots & \vdots \\ q_{j1}^i & q_{j2}^i & \dots & q_{jm}^i \\ \vdots & \vdots & \ddots & \vdots \\ q_{l1}^i & q_{l2}^i & \dots & q_{lm}^i \end{pmatrix},$$

where  $q_{jk}^i$  is a CBFS element which is assigned by the decision maker  $\mathcal{E}_i$ . The unanimous CBF decision matrix can be obtained as

follows  $T = [t_{jk}]_{l \times m} =$

$$\begin{pmatrix} t_{11} & t_{12} & \dots & t_{1m} \\ t_{21} & t_{22} & \dots & t_{2m} \\ \vdots & \vdots & \ddots & \vdots \\ t_{j1} & t_{j2} & \dots & t_{jm} \\ \vdots & \vdots & \ddots & \vdots \\ t_{l1} & t_{l2} & \dots & t_{lm} \end{pmatrix},$$

where  $t_{jk} = \cup_{i=1}^n q_{jk}^i = \langle \max_{1 \leq i \leq n} [\rho_{\mathcal{E}_i}^+, \rho_{u_{\mathcal{E}_i}^+}], \min_{1 \leq i \leq n} [\rho_{\mathcal{E}_i}^-, \rho_{u_{\mathcal{E}_i}^-}], (\max_{1 \leq i \leq n} \rho_{\mathcal{E}_i}^+, \min_{1 \leq i \leq n} \rho_{\mathcal{E}_i}^-) \rangle$ .

**Step 6.** In many decision-making problems, the criteria under consideration are of two types, i.e., cost and benefit. Therefore, we need

to normalize our unanimous CBF decision matrix  $\hat{T} = [\hat{t}_{jk}]_{l \times m} =$

$$\begin{pmatrix} \hat{t}_{11} & \hat{t}_{12} & \dots & \hat{t}_{1m} \\ \hat{t}_{21} & \hat{t}_{22} & \dots & \hat{t}_{2m} \\ \vdots & \vdots & \ddots & \vdots \\ \hat{t}_{j1} & \hat{t}_{j2} & \dots & \hat{t}_{jm} \\ \vdots & \vdots & \ddots & \vdots \\ \hat{t}_{l1} & \hat{t}_{l2} & \dots & \hat{t}_{lm} \end{pmatrix},$$

The complement can be computed by using Definition 2.9.

**Step 7.** Construct weighted normalized CBF decision matrix as follows:  $Y = [y_{jk}]_{l \times m} =$

$$\begin{pmatrix} y_{11} & y_{12} & \dots & y_{1m} \\ y_{21} & y_{22} & \dots & y_{2m} \\ \vdots & \vdots & \ddots & \vdots \\ y_{j1} & y_{j2} & \dots & y_{jm} \\ \vdots & \vdots & \ddots & \vdots \\ y_{l1} & y_{l2} & \dots & y_{lm} \end{pmatrix},$$

where  $y_{jk} = w_k \otimes_p \hat{t}_{jk}$ .

**Step 8.** Obtain the CBF-PIS and CBF-NIS given by the following formulas: CBF – PIS =  $\{y_k^p: k = 1, 2, \dots, m\} = \{ \cup_{j=1}^l y_{jk}: k = 1, 2, \dots, m \} = \{ \langle \max_{1 \leq j \leq l} [\rho_{\mathcal{E}_j}^+, \rho_{u_{\mathcal{E}_j}^+}], \min_{1 \leq j \leq l} [\rho_{\mathcal{E}_j}^-, \rho_{u_{\mathcal{E}_j}^-}], (\max_{1 \leq j \leq l} \rho_{\mathcal{E}_j}^+, \min_{1 \leq j \leq l} \rho_{\mathcal{E}_j}^-) \rangle: k = 1, 2, \dots, m \}$ ,

CBF – NIS =  $\{y_k^n: k = 1, 2, \dots, m\} = \{ \cap_{j=1}^l y_{jk}: k = 1, 2, \dots, m \} = \{ \langle \min_{1 \leq j \leq l} [\rho_{\mathcal{E}_j}^+, \rho_{u_{\mathcal{E}_j}^+}], \max_{1 \leq j \leq l} [\rho_{\mathcal{E}_j}^-, \rho_{u_{\mathcal{E}_j}^-}], (\min_{1 \leq j \leq l} \rho_{\mathcal{E}_j}^+, \max_{1 \leq j \leq l} \rho_{\mathcal{E}_j}^-) \rangle: k = 1, 2, \dots, m \}$ .

**Step 9.** Compute the cosine similarity measure between each alternative and PIS and the cosine similarity measure between each alternative and NIS by utilizing equations (3)–(12).

If we use equation (3), then  $\mathcal{S}_1(\mathcal{A}_j, \text{CBF – PIS}) = (1/m) \sum_{k=1}^m \left\{ (\rho_{\mathcal{E}_j}^+ \rho_{\mathcal{E}_k^p}^+ + \rho_{u_{\mathcal{E}_j}^+} \rho_{u_{\mathcal{E}_k^p}^+} + \rho_{\mathcal{E}_j}^- \rho_{\mathcal{E}_k^p}^- + \rho_{u_{\mathcal{E}_j}^-} \rho_{u_{\mathcal{E}_k^p}^-} + \rho_{\mathcal{E}_j}^+ \rho_{\mathcal{E}_k^p}^+ + \rho_{u_{\mathcal{E}_j}^+} \rho_{\mathcal{E}_k^p}^+) / \left[ \sqrt{(\rho_{\mathcal{E}_j}^+)^2 + (\rho_{u_{\mathcal{E}_j}^+}^+)^2 + (\rho_{\mathcal{E}_j}^-)^2 + (\rho_{u_{\mathcal{E}_j}^-}^-)^2 + (\rho_{\mathcal{E}_k^p}^+)^2 + (\rho_{u_{\mathcal{E}_k^p}^p}^+)^2} \right] \right\} \left\{ \times \sqrt{(\rho_{\mathcal{E}_j}^+)^2 + (\rho_{u_{\mathcal{E}_j}^+}^+)^2 + (\rho_{\mathcal{E}_k^p}^-)^2 + (\rho_{u_{\mathcal{E}_k^p}^-}^-)^2 + (\rho_{\mathcal{E}_k^p}^+)^2 + (\rho_{u_{\mathcal{E}_k^p}^p}^+)^2} \right\}$ ,

$$\mathcal{S}_1(\mathcal{A}_j, \text{CBF} - \text{NIS}) = (1/m) \sum_{k=1}^m \left\{ \frac{(\rho_{\ell y_{jk}}^+ \rho_{\ell y_k^n}^+ + \rho_{u y_{jk}}^+ \rho_{u y_k^n}^+ + \rho_{\ell y_{jk}}^- \rho_{\ell y_k^n}^- + \rho_{u y_{jk}}^- \rho_{u y_k^n}^- + \rho_{y_{jk}}^+ \rho_{y_k^n}^+ + \rho_{y_{jk}}^- \rho_{y_k^n}^-) / \sqrt{(\rho_{\ell y_{jk}}^+)^2 + (\rho_{u y_{jk}}^+)^2 + (\rho_{\ell y_{jk}}^-)^2 + (\rho_{u y_{jk}}^-)^2 + (\rho_{y_{jk}}^+)^2 + (\rho_{y_{jk}}^-)^2}}{\sqrt{(\rho_{\ell y_k^n}^+)^2 + (\rho_{u y_k^n}^+)^2 + (\rho_{\ell y_k^n}^-)^2 + (\rho_{u y_k^n}^-)^2 + (\rho_{y_k^n}^+)^2 + (\rho_{y_k^n}^-)^2}} \right\} \cdot \left\{ (\rho_{\ell y_{jk}}^+ \rho_{\ell y_k^n}^+ + \rho_{u y_{jk}}^+ \rho_{u y_k^n}^+ + \rho_{\ell y_{jk}}^- \rho_{\ell y_k^n}^- + \rho_{u y_{jk}}^- \rho_{u y_k^n}^- + \rho_{y_{jk}}^+ \rho_{y_k^n}^+ + \rho_{y_{jk}}^- \rho_{y_k^n}^-) / \sqrt{(\rho_{\ell y_{jk}}^+)^2 + (\rho_{u y_{jk}}^+)^2 + (\rho_{\ell y_{jk}}^-)^2 + (\rho_{u y_{jk}}^-)^2 + (\rho_{y_{jk}}^+)^2 + (\rho_{y_{jk}}^-)^2} \right\}$$

If we use equation (7), then  $\mathcal{S}_2(\mathcal{A}_j, \text{CBF} - \text{PIS}) = (1/m) \sum_{k=1}^m \cos \left\{ \frac{(|\rho_{\ell y_{jk}}^+ - \rho_{\ell y_k^n}^+| + |\rho_{u y_{jk}}^+ - \rho_{u y_k^n}^+| + |\rho_{\ell y_{jk}}^- - \rho_{\ell y_k^n}^-| + |\rho_{u y_{jk}}^- - \rho_{u y_k^n}^-| + |\rho_{y_{jk}}^+ - \rho_{y_k^n}^+| + |\rho_{y_{jk}}^- - \rho_{y_k^n}^-|) (\pi/12)}{\dots} \right\}$

$$\mathcal{S}_2(\mathcal{A}_j, \text{CBF} - \text{NIS}) = (1/m) \sum_{k=1}^m \cos \left\{ \frac{(|\rho_{\ell y_{jk}}^+ - \rho_{\ell y_k^n}^+| + |\rho_{u y_{jk}}^+ - \rho_{u y_k^n}^+| + |\rho_{\ell y_{jk}}^- - \rho_{\ell y_k^n}^-| + |\rho_{u y_{jk}}^- - \rho_{u y_k^n}^-| + |\rho_{y_{jk}}^+ - \rho_{y_k^n}^+| + |\rho_{y_{jk}}^- - \rho_{y_k^n}^-|) (\pi/12)}{\dots} \right\}$$

If we use equation (12), then  $\mathcal{S}_3(\mathcal{A}_j, \text{CBF} - \text{PIS}) = (1/4m(\sqrt{2} - 1)) \sum_{k=1}^m \{ [\sqrt{2} \cos((\pi/8)(\rho_{\ell y_{jk}}^+ - \rho_{\ell y_k^n}^+ + \rho_{u y_{jk}}^+ - \rho_{u y_k^n}^+)) - 1] + [\sqrt{2} \cos((\pi/8)(\rho_{\ell y_{jk}}^- - \rho_{\ell y_k^n}^- + \rho_{u y_{jk}}^- - \rho_{u y_k^n}^-)) - 1] + [\sqrt{2} \cos((\pi/4)(\rho_{y_{jk}}^+ - \rho_{y_k^n}^+)) - 1] + [\sqrt{2} \cos((\pi/4)(\rho_{y_{jk}}^- - \rho_{y_k^n}^-)) - 1] \}$

$$\mathcal{S}_3(\mathcal{A}_j, \text{CBF} - \text{NIS}) = (1/4m(\sqrt{2} - 1)) \sum_{k=1}^m \{ [\sqrt{2} \cos((\pi/8)(\rho_{\ell y_{jk}}^+ - \rho_{\ell y_k^n}^+ + \rho_{u y_{jk}}^+ - \rho_{u y_k^n}^+)) - 1] + [\sqrt{2} \cos((\pi/8)(\rho_{\ell y_{jk}}^- - \rho_{\ell y_k^n}^- + \rho_{u y_{jk}}^- - \rho_{u y_k^n}^-)) - 1] + [\sqrt{2} \cos((\pi/4)(\rho_{y_{jk}}^+ - \rho_{y_k^n}^+)) - 1] + [\sqrt{2} \cos((\pi/4)(\rho_{y_{jk}}^- - \rho_{y_k^n}^-)) - 1] \}$$

**Step 10.** Calculate the value of closeness coefficient of each alternative to ideal solution by using the following:  
 If we use  $\mathcal{S}_1$ , then  $\alpha_j = \mathcal{S}_1(\mathcal{A}_j, \text{CBF} - \text{PIS}) / (\mathcal{S}_1(\mathcal{A}_j, \text{CBF} - \text{PIS}) + \mathcal{S}_1(\mathcal{A}_j, \text{CBF} - \text{NIS}))$   
 If we use  $\mathcal{S}_2$ , then  $\beta_j = \mathcal{S}_2(\mathcal{A}_j, \text{CBF} - \text{PIS}) / (\mathcal{S}_2(\mathcal{A}_j, \text{CBF} - \text{PIS}) + \mathcal{S}_2(\mathcal{A}_j, \text{CBF} - \text{NIS}))$   
 If we use  $\mathcal{S}_3$ , then  $\gamma_j = \mathcal{S}_3(\mathcal{A}_j, \text{CBF} - \text{PIS}) / (\mathcal{S}_3(\mathcal{A}_j, \text{CBF} - \text{PIS}) + \mathcal{S}_3(\mathcal{A}_j, \text{CBF} - \text{NIS}))$

**Step 11.** Rank the alternatives by arranging the values of closeness coefficients in the descending order. The best alternative has the maximum value of closeness coefficient.

ALGORITHM 2: Extension of TOPSIS towards CBF information.

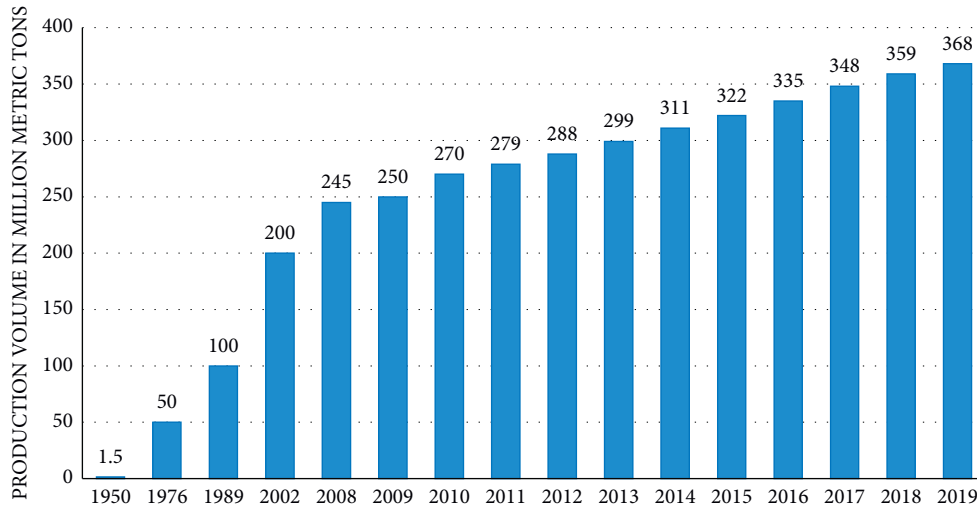


FIGURE 3: Global plastic production from 1950 to 2019.

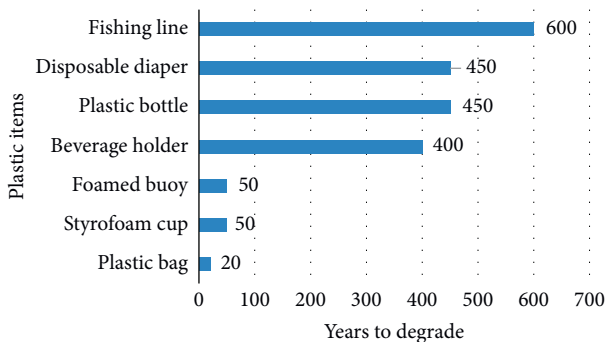


FIGURE 4: Degradation of different plastic items [48].

Step 9. Now, we compute the SMs between each alternative  $\mathcal{A}_j$  and PIS and the similarity measure between  $\mathcal{A}_j$  and NIS. By using equation (3), we get

$$\begin{aligned} \mathcal{S}_1(\mathcal{A}_1, \text{CBF} - \text{PIS}) &= 0.9948, \\ \mathcal{S}_1(\mathcal{A}_2, \text{CBF} - \text{PIS}) &= 0.9807, \\ \mathcal{S}_1(\mathcal{A}_3, \text{CBF} - \text{PIS}) &= 0.9818, \\ \mathcal{S}_1(\mathcal{A}_1, \text{CBF} - \text{NIS}) &= 0.9787, \\ \mathcal{S}_1(\mathcal{A}_2, \text{CBF} - \text{NIS}) &= 0.9994, \\ \mathcal{S}_1(\mathcal{A}_3, \text{CBF} - \text{NIS}) &= 0.9941. \end{aligned} \tag{24}$$

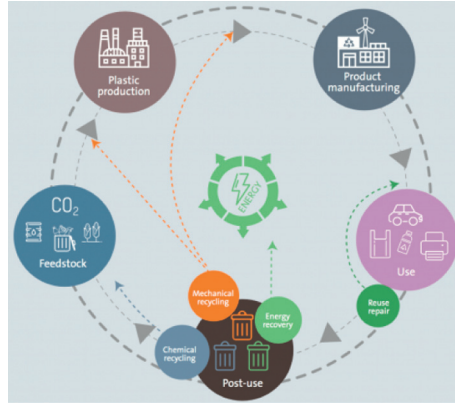


FIGURE 5: Plastics life cycle.

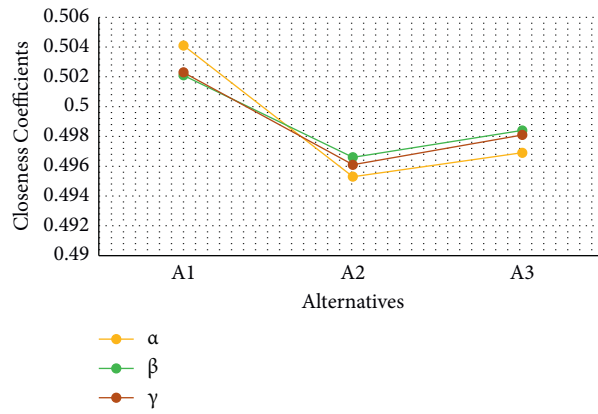


FIGURE 6: Ranking of alternatives.

TABLE 4: Criteria for the selection of best plastic recycling method.

Criteria	Description
(i) Cost ( $\mathcal{C}_1$ )	This includes transportation cost of plastic waste, cost of plastic separation, worker's salary, chemical costs
(ii) CO <sub>2</sub> emissions ( $\mathcal{C}_2$ )	This is related to the CO <sub>2</sub> emissions during recycling process
(iii) Technical capability ( $\mathcal{C}_3$ )	This includes operating capability of instruments, ingredients, and configuration plan during recycling
(iv) Energy consumption ( $\mathcal{C}_4$ )	This includes the total energy required to carry out a recycling process

By using equation (7), we have

$$\begin{aligned}
 \mathcal{S}_2(\mathcal{A}_1, \text{CBF} - \text{PIS}) &= 0.9956, \\
 \mathcal{S}_2(\mathcal{A}_2, \text{CBF} - \text{PIS}) &= 0.9850, \\
 \mathcal{S}_2(\mathcal{A}_3, \text{CBF} - \text{PIS}) &= 0.9892, \\
 \mathcal{S}_2(\mathcal{A}_1, \text{CBF} - \text{NIS}) &= 0.9872, \\
 \mathcal{S}_2(\mathcal{A}_2, \text{CBF} - \text{NIS}) &= 0.9985, \\
 \mathcal{S}_2(\mathcal{A}_3, \text{CBF} - \text{NIS}) &= 0.9956.
 \end{aligned} \tag{25}$$

By using equation (7), we get

$$\begin{aligned}
 \mathcal{S}_3(\mathcal{A}_1, \text{CBF} - \text{PIS}) &= 0.9931, \\
 \mathcal{S}_3(\mathcal{A}_2, \text{CBF} - \text{PIS}) &= 0.9829, \\
 \mathcal{S}_3(\mathcal{A}_3, \text{CBF} - \text{PIS}) &= 0.9849, \\
 \mathcal{S}_3(\mathcal{A}_1, \text{CBF} - \text{NIS}) &= 0.9840, \\
 \mathcal{S}_3(\mathcal{A}_2, \text{CBF} - \text{NIS}) &= 0.9982, \\
 \mathcal{S}_3(\mathcal{A}_3, \text{CBF} - \text{NIS}) &= 0.9923.
 \end{aligned} \tag{26}$$

Step 10. The values of closeness coefficient for three different cosine similarity measures are calculated by using Algorithm 2:

$$\begin{aligned}
 \alpha_1 &= 0.5041, \\
 \alpha_2 &= 0.4953, \\
 \alpha_3 &= 0.4969, \\
 \beta_1 &= 0.5021, \\
 \beta_2 &= 0.4966, \\
 \beta_3 &= 0.4984, \\
 \gamma_1 &= 0.5023, \\
 \gamma_2 &= 0.4961, \\
 \gamma_3 &= 0.4981.
 \end{aligned} \tag{27}$$

TABLE 5: Weighted normalized CBF decision matrix.

$Y$	$\mathcal{C}_1$	$\mathcal{C}_2$	$\mathcal{C}_3$	$\mathcal{C}_4$
$\mathcal{A}_1$	$\langle [0.102, 0.0514], [-0.9573, -0.9243], [0.0694, -0.8763] \rangle$	$\langle [0.2735, 0.3590], [-0.8760, -0.8138], [0.2869, -0.8684] \rangle$	$\langle [0.2429, 0.3409], [-0.7791, -0.7131], [0.1957, -0.7453] \rangle$	$\langle [0.2080, 0.3051], [-0.9218, -0.9122], [0.2236, -0.9715] \rangle$
$\mathcal{A}_2$	$\langle [0.0287, 0.0603], [-0.9427, -0.8908], [0.0573, -0.9113] \rangle$	$\langle [0.0635, 0.0889], [-0.8527, -0.7995], [0.0791, -0.8138] \rangle$	$\langle [0.0760, 0.1131], [-0.8722, -0.7995], [0.1433, -0.8091] \rangle$	$\langle [0.0480, 0.0813], [-0.9250, -0.8953], [0.1536, -0.8918] \rangle$
$\mathcal{A}_3$	$\langle [0.2150, 0.2663], [-0.9113, -0.8763], [0.1904, -0.8365] \rangle$	$\langle [0.0344, 0.0666], [-0.8361, -0.7791], [0.0990, -0.9077] \rangle$	$\langle [0.0515, 0.0791], [-0.9044, -0.8486], [0.0760, -0.9077] \rangle$	$\langle [0.0567, 0.0944], [-0.9661, -0.9250], [0.1081, -0.9187] \rangle$

TABLE 6: Comparison of proposed Algorithm 2 with existing methods.

Methods	Ranking	Optimal alternative
Algorithm (Eraslan and Karaaslan [50])	$\mathcal{A}_1 > \mathcal{A}_3 > \mathcal{A}_2$	$\mathcal{A}_1$
Algorithm (Mahmood et al. [10])	$\mathcal{A}_1 > \mathcal{A}_3 > \mathcal{A}_2$	$\mathcal{A}_1$
Algorithm (Gundogdu and Kahraman [11])	$\mathcal{A}_1 > \mathcal{A}_3 > \mathcal{A}_2$	$\mathcal{A}_1$
Algorithm (Zhang and Xu [31])	$\mathcal{A}_1 > \mathcal{A}_2 > \mathcal{A}_3$	$\mathcal{A}_1$
Algorithm (Garg and Kaur [35])	$\mathcal{A}_1 > \mathcal{A}_3 > \mathcal{A}_2$	$\mathcal{A}_1$
Algorithm (Tehrim and Riaz [36–38])	$\mathcal{A}_1 > \mathcal{A}_2 > \mathcal{A}_3$	$\mathcal{A}_1$
Algorithm (proposed)	$\mathcal{A}_1 > \mathcal{A}_3 > \mathcal{A}_2$	$\mathcal{A}_1$

Step 11. The ranking order of alternatives w.r.t.  $\alpha_j$  is  $\mathcal{A}_1 > \mathcal{A}_3 > \mathcal{A}_2$ . The ranking order of alternatives w.r.t.  $\beta_j$  is  $\mathcal{A}_1 > \mathcal{A}_3 > \mathcal{A}_2$ . The ranking order of alternatives w.r.t.  $\gamma_j$  is  $\mathcal{A}_1 > \mathcal{A}_3 > \mathcal{A}_2$ .

All three ranking orders show that  $\mathcal{A}_1$ , i.e., mechanical recycling, is the best alternative. It is important to note

that the ranking orders obtained by employing three different cosine similarity measures are the same which shows the effectiveness and compatibility of these cosine similarity measures. The three ranking orders are shown in Figure 6:

$$\begin{aligned}
 \hat{a}_1 &= \left( \begin{array}{cccc} \langle [0.72, 0.80], [-0.27, -0.16], (0.67, -0.38) \rangle & \langle [0.17, 0.26], [-0.51, -0.38], (0.21, -0.37) \rangle & \langle [0.51, 0.71], [-0.36, -0.25], (0.49, -0.21) \rangle & \langle [0.15, 0.31], [-0.31, -0.28], (0.27, -0.11) \rangle \\ \langle [0.72, 0.80], [-0.27, -0.16], (0.67, -0.38) \rangle & \langle [0.17, 0.26], [-0.51, -0.38], (0.21, -0.37) \rangle & \langle [0.51, 0.71], [-0.36, -0.25], (0.49, -0.21) \rangle & \langle [0.15, 0.31], [-0.31, -0.28], (0.27, -0.11) \rangle \\ \langle [0.72, 0.80], [-0.27, -0.16], (0.67, -0.38) \rangle & \langle [0.17, 0.26], [-0.51, -0.38], (0.21, -0.37) \rangle & \langle [0.51, 0.71], [-0.36, -0.25], (0.49, -0.21) \rangle & \langle [0.15, 0.31], [-0.31, -0.28], (0.27, -0.11) \rangle \end{array} \right) \\
 \hat{a}_2 &= \left( \begin{array}{cccc} \langle [0.61, 0.74], [-0.26, -0.13], (0.75, -0.41) \rangle & \langle [0.15, 0.28], [-0.46, -0.36], (0.18, -0.43) \rangle & \langle [0.65, 0.81], [-0.35, -0.26], (0.46, -0.26) \rangle & \langle [0.23, 0.33], [-0.30, -0.17], (0.36, -0.09) \rangle \\ \langle [0.78, 0.89], [-0.31, -0.18], (0.57, -0.29) \rangle & \langle [0.62, 0.72], [-0.57, -0.47], (0.57, -0.56) \rangle & \langle [0.19, 0.26], [-0.54, -0.39], (0.40, -0.33) \rangle & \langle [0.71, 0.82], [-0.29, -0.16], (0.39, -0.37) \rangle \\ \langle [0.29, 0.38], [-0.41, -0.26], (0.26, -0.41) \rangle & \langle [0.57, 0.66], [-0.63, -0.49], (0.49, -0.15) \rangle & \langle [0.16, 0.28], [-0.67, -0.52], (0.22, -0.41) \rangle & \langle [0.67, 0.71], [-0.27, -0.13], (0.63, -0.21) \rangle \end{array} \right) \\
 \hat{a}_3 &= \left( \begin{array}{cccc} \langle [0.81, 0.96], [-0.24, -0.14], (0.54, -0.33) \rangle & \langle [0.14, 0.25], [-0.56, -0.41], (0.10, -0.27) \rangle & \langle [0.67, 0.79], [-0.32, -0.22], (0.52, -0.31) \rangle & \langle [0.28, 0.39], [-0.29, -0.18], (0.27, -0.07) \rangle \\ \langle [0.67, 0.76], [-0.37, -0.20], (0.79, -0.31) \rangle & \langle [0.51, 0.67], [-0.59, -0.39], (0.72, -0.49) \rangle & \langle [0.11, 0.26], [-0.48, -0.31], (0.36, -0.31) \rangle & \langle [0.61, 0.72], [-0.36, -0.27], (0.51, -0.33) \rangle \\ \langle [0.26, 0.33], [-0.40, -0.31], (0.43, -0.32) \rangle & \langle [0.67, 0.73], [-0.59, -0.41], (0.56, -0.32) \rangle & \langle [0.18, 0.26], [-0.55, -0.41], (0.27, -0.53) \rangle & \langle [0.65, 0.79], [-0.24, -0.12], (0.47, -0.26) \rangle \end{array} \right) \\
 \hat{a}_4 &= \left( \begin{array}{cccc} \langle [0.57, 0.69], [-0.21, -0.11], (0.46, -0.39) \rangle & \langle [0.11, 0.21], [-0.55, -0.37], (0.26, -0.31) \rangle & \langle [0.57, 0.71], [-0.37, -0.24], (0.58, -0.21) \rangle & \langle [0.21, 0.37], [-0.28, -0.16], (0.33, -0.05) \rangle \\ \langle [0.71, 0.86], [-0.36, -0.21], (0.68, -0.25) \rangle & \langle [0.69, 0.77], [-0.42, -0.33], (0.66, -0.41) \rangle & \langle [0.27, 0.38], [-0.58, -0.41], (0.43, -0.43) \rangle & \langle [0.65, 0.71], [-0.34, -0.21], (0.46, -0.29) \rangle \\ \langle [0.25, 0.36], [-0.39, -0.29], (0.26, -0.49) \rangle & \langle [0.44, 0.53], [-0.57, -0.51], (0.66, -0.19) \rangle & \langle [0.11, 0.26], [-0.54, -0.42], (0.17, -0.68) \rangle & \langle [0.56, 0.72], [-0.21, -0.10], (0.57, -0.29) \rangle \end{array} \right) \\
 T &= \left( \begin{array}{cccc} \langle [0.81, 0.96], [-0.27, -0.16], (0.75, -0.41) \rangle & \langle [0.17, 0.28], [-0.56, -0.41], (0.26, -0.43) \rangle & \langle [0.67, 0.81], [-0.37, -0.26], (0.58, -0.31) \rangle & \langle [0.23, 0.39], [-0.31, -0.28], (0.36, -0.11) \rangle \\ \langle [0.78, 0.89], [-0.37, -0.21], (0.79, -0.31) \rangle & \langle [0.69, 0.77], [-0.59, -0.47], (0.72, -0.56) \rangle & \langle [0.27, 0.38], [-0.58, -0.41], (0.46, -0.43) \rangle & \langle [0.71, 0.82], [-0.36, -0.27], (0.51, -0.37) \rangle \\ \langle [0.29, 0.38], [-0.41, -0.31], (0.43, -0.51) \rangle & \langle [0.76, 0.87], [-0.63, -0.51], (0.66, -0.32) \rangle & \langle [0.19, 0.28], [-0.67, -0.52], (0.27, -0.68) \rangle & \langle [0.67, 0.79], [-0.27, -0.13], (0.63, -0.29) \rangle \end{array} \right) \\
 \hat{T} &= \left( \begin{array}{cccc} \langle [0.04, 0.19], [-0.84, -0.73], (0.25, -0.59) \rangle & \langle [0.72, 0.83], [-0.59, -0.44], (0.74, -0.57) \rangle & \langle [0.67, 0.81], [-0.37, -0.26], (0.58, -0.31) \rangle & \langle [0.61, 0.77], [-0.72, -0.69], (0.64, -0.89) \rangle \\ \langle [0.11, 0.22], [-0.79, -0.63], (0.21, -0.69) \rangle & \langle [0.23, 0.31], [-0.53, -0.41], (0.28, -0.44) \rangle & \langle [0.27, 0.38], [-0.58, -0.41], (0.46, -0.43) \rangle & \langle [0.18, 0.29], [-0.73, -0.64], (0.49, -0.63) \rangle \\ \langle [0.62, 0.71], [-0.69, -0.59], (0.57, -0.49) \rangle & \langle [0.13, 0.24], [-0.49, -0.37], (0.34, -0.68) \rangle & \langle [0.19, 0.28], [-0.67, -0.52], (0.27, -0.68) \rangle & \langle [0.21, 0.33], [-0.87, -0.73], (0.37, -0.71) \rangle \end{array} \right)
 \end{aligned}
 \tag{28}$$

Table 5 shows the proposed CBF-TOPSIS method based on cosine SMs compared with some existing methods, and the ranking is summarized in Table 6. As shown in Table 6, the best alternative provided by any other technique acknowledges the validity and efficacy of the suggested MCGDM approach.

The existing MCGDM methods are designed to deal with vague information under some limitations imposed on membership grades. These methods cannot deal with cubic bipolar fuzzy information. The proposed mathematical models are more efficient and reliable to address bipolarity, vagueness, and fuzziness with cubic bipolar fuzzy sets. The computations provide a robust analysis for ranking of alternatives and the selection of feasible alternatives.

## 6. Conclusion

The researchers have developed different approaches, methods, models, and techniques to address vagueness and uncertainties in real-life problems. Bipolarity is a key factor in humanized computing that defines both positive and negative aspects in the objects. Bipolar fuzzy information with ordered pairs of positive and negatives grades and interval-valued bipolar fuzzy information with intervals of positive and negative grades are strong models to address bipolarity, respectively. A cubic bipolar fuzzy set (CBFS) is a new hybrid approach for dealing with vagueness, fuzziness, and bipolarity with BFS and IVBFS information simultaneously. The main objectives of the manuscript are itemized as follows:

- (1) Three different cosine SMs are developed for cubic bipolar fuzzy sets (CBFSs) based on the cosine of the angle between two vectors, new distance measures, and cosine function, respectively
- (2) The problem of bacteria recognition is analyzed by using similarity measures for cubic bipolar fuzzy information
- (3) An extended TOPSIS approach is developed with the help of similarity measures for MCGDM
- (4) A practical application of the suggested MCDGM approach is presented towards sustainable plastic recycling process

A comparison analysis of the suggested technique with some existing techniques is also presented to depict the efficacy, validity, and superiority of the suggested technique [51].

### Data Availability

Data sharing is not applicable to this article as no datasets were generated or analyzed during the current study.

### Conflicts of Interest

The authors declare that they have no conflicts of interest.

### References

- [1] L. A. Zadeh, "Fuzzy sets," *Information and Control*, vol. 8, no. 3, pp. 338–353, 1965.
- [2] L. A. Zadeh, "The concept of a linguistic variable and its application to approximate reasoning-I," *Information Sciences*, vol. 8, no. 3, pp. 199–249, 1975.
- [3] K. T. Atanassov, "Intuitionistic fuzzy sets," *Fuzzy Sets and Systems*, vol. 20, no. 1, pp. 87–96, 1986.
- [4] R. R. Yager, "Pythagorean fuzzy subsets," in *Proceedings of the Joint IFSA World Congress and NAFIPS Annual Meeting*, pp. 57–61, Edmonton, Canada, 2013.
- [5] R. R. Yager, "Pythagorean membership grades in multicriteria decision making," *IEEE Transactions on Fuzzy Systems*, vol. 22, no. 4, pp. 958–965, 2014.
- [6] R. R. Yager, "Generalized orthopair fuzzy sets," *IEEE Transactions on Fuzzy Systems*, vol. 25, no. 5, pp. 1220–1230, 2017.
- [7] F. Smarandache, "A unifying field in logics: neutrosophic logic," *Neutrosophy, Neutrosophic Set, Neutrosophic Probability and Statistics*, Vol. 155, American Research Press, Washington D. C., USA, 4th edition, 2005.
- [8] H. Wang, F. Smarandache, Y. Q. Zhang, and R. Sunderraman, "Single valued neutrosophic sets," *Multispace and Multistructure*, vol. 4, pp. 410–413, 2010.
- [9] S. Ashraf and S. Abdullah, "Spherical aggregation operators and their application in multiattribute group decision-making," *International Journal of Intelligent Systems*, vol. 34, no. 3, pp. 493–523, 2019.
- [10] T. Mahmood, K. Ullah, Q. Khan, and N. Jan, "An approach toward decision-making and medical diagnosis problems using the concept of spherical fuzzy sets," *Neural Computing & Applications*, vol. 31, no. 11, pp. 7041–7053, 2019.
- [11] F. K. Gundogdu and C. Kahraman, "Spherical fuzzy sets and spherical fuzzy TOPSIS method," *Journal of Intelligent and Fuzzy Systems*, vol. 36, no. 9–12, pp. 1–16, 2018.
- [12] B. C. Cuong and V. Kreinovich, "Picture fuzzy sets—a new concept for computational intelligence problems," in *Proceedings of the 2013 Third World Congress on Information and Communication Technologies (WICT 2013)*, pp. 1–6, Hanoi, Vietnam, December 2013.
- [13] B. C. Cuong, "Picture fuzzy sets," *Journal of Computer Science and Cybernetics*, vol. 30, no. 4, pp. 409–420, 2014.
- [14] W. R. Zhang, "Bipolar fuzzy sets and relations, a computational framework for cognitive modeling and multiagent decision analysis," in *Proceedings of the 1994 IEEE Conference Fuzzy Information Processing Society Biannual Conference*, pp. 305–309, San Antonio, TX, USA, December 1994.
- [15] W. R. Zhang, "Bipolar fuzzy sets," in *Proceedings of the IEEE International Conference on Fuzzy Systems*, pp. 835–840, Anchorage, AK, USA, May 1998.
- [16] K. M. Lee, "Bipolar-valued fuzzy sets and their basic operations," in *Proceedings of the International Conference*, pp. 307–317, Bangkok, Thailand, 2000.
- [17] I. Deli, M. Ali, and F. Smarandache, "Bipolar neutrosophic sets and their application based on multi-criteria decision making problems," in *Proceedings of the 2015 International Conference on Advanced Mechatronic Systems*, Beijing, China, 2015.
- [18] G. Wei, C. Wei, and H. Gao, "Multiple attribute decision making with interval-valued bipolar fuzzy information and their application to emerging technology commercialization evaluation," *IEEE Access*, vol. 6, pp. 60930–60955, 2018.
- [19] Y. B. Jun, C. S. Kim, and K. O. Yang, "Cubic sets," *Annals of Fuzzy Mathematics and Informatics*, vol. 4, no. 1, pp. 83–98, 2012.
- [20] J. Ye, "Cosine similarity measures for intuitionistic fuzzy sets and their applications," *Mathematical and Computer Modelling*, vol. 53, no. 1–2, pp. 91–97, 2011.
- [21] G. Wei and Y. Wei, "Similarity measures of Pythagorean fuzzy sets based on the cosine function and their applications," *International Journal of Intelligent Systems*, vol. 33, no. 3, pp. 634–652, 2018.
- [22] V. Uluçay, I. Deli, and M. Şahin, "Similarity measures of bipolar neutrosophic sets and their application to multiple criteria decision making," *Neural Computing & Applications*, vol. 29, no. 3, pp. 739–748, 2018.
- [23] M. Abdel-Basset, M. Mohamed, M. Elhoseny, L. H. Son, F. Chiclana, and A. E.-N. H. Zaied, "Cosine similarity measures of bipolar neutrosophic set for diagnosis of bipolar disorder diseases," *Artificial Intelligence in Medicine*, vol. 101, Article ID 101735, 2019.
- [24] A. Tu, J. Ye, and B. Wang, "Multiple attribute decision-making method using similarity measures of neutrosophic cubic sets," *Symmetry*, vol. 10, no. 6, pp. 1–11, 2018.
- [25] Z. Lu and J. Ye, "Cosine measures of neutrosophic cubic sets for multiple attribute decision-making," *Symmetry*, vol. 9, no. 7, p. 121, 2017.
- [26] X. Peng, H. Yuan, and Y. Yang, "Pythagorean fuzzy information measures and their applications," *International Journal of Intelligent Systems*, vol. 32, no. 10, pp. 991–1029, 2017.
- [27] X. Peng and L. Liu, "Information measures for  $q$ -rung orthopair fuzzy sets," *International Journal of Intelligent Systems*, vol. 34, no. 8, pp. 1795–1834, 2019.
- [28] M. Riaz, K. Naeem, and D. Afzal, "A similarity measure under Pythagorean fuzzy soft environment with applications,"

- Computational and Applied Mathematics*, vol. 39, pp. 1–17, 2020.
- [29] Z. Hussian and M. S. Yang, “Distance and similarity measures of Pythagorean fuzzy sets based on the Hausdorff metric with application to fuzzy TOPSIS,” *International Journal of Intelligent Systems*, vol. 34, no. 10, pp. 2633–2654, 2019.
- [30] C.-L. Hwang and K. Yoon, “Methods for multiple attribute decision making,” in *Multiple Attribute Decision Making*, G. Fandel and W. Trockel, Eds., Springer, Berlin, Germany, pp. 58–191, 1981.
- [31] X. Zhang and Z. Xu, “Extension of TOPSIS to multiple criteria decision making with Pythagorean fuzzy sets,” *International Journal of Intelligent Systems*, vol. 29, no. 12, pp. 1061–1078, 2014.
- [32] P. Rani, A. R. Mishra, G. Rezaei, H. Liao, and A. Mardani, “Extended Pythagorean fuzzy topsis method based on similarity measure for sustainable recycling partner selection,” *International Journal of Fuzzy Systems*, vol. 22, no. 2, pp. 735–747, 2020.
- [33] M. Akram, Shumaiza, and M. Arshad, “Bipolar fuzzy topsis and bipolar fuzzy electre-I methods to diagnosis,” *Journal of Computational and Applied Mathematics*, vol. 39, pp. 1–21, 2019.
- [34] H. Garg and R. Arora, “Topsis method based on correlation coefficient for solving decision-making problems with intuitionistic fuzzy soft set information,” *AIMS Mathematics*, vol. 5, no. 4, pp. 2944–2966, 2020.
- [35] H. Garg and G. Kaur, “Topsis based on nonlinear-programming methodology for solving decision-making problems under cubic intuitionistic fuzzy set environment,” *Computational and Applied Mathematics*, vol. 38, pp. 1–19, 2019.
- [36] M. Riaz and S. T. Tehrim, “Multi-attribute group decision making based on cubic bipolar fuzzy information using averaging aggregation operators,” *Journal of Intelligent & Fuzzy Systems*, vol. 37, no. 2, pp. 2473–2494, 2019.
- [37] M. Riaz and S. T. Tehrim, “Cubic bipolar fuzzy ordered weighted geometric aggregation operators and their application using internal and external cubic bipolar fuzzy data,” *Computational and Applied Mathematics*, vol. 38, no. 2, p. 87, 2019.
- [38] M. Riaz and S. T. Tehrim, “Cubic bipolar fuzzy set with application to multi-criteria group decision making using geometric aggregation operators,” *Soft Computing*, vol. 24, no. 16, pp. 16111–16133, 2020.
- [39] Z. Ali, T. Mahmood, T. Mahmood, K. Ullah, and Q. Khan, “Einstein geometric aggregation operators using a novel complex interval-valued pythagorean fuzzy setting with application in green supplier chain management,” *Reports in Mechanical Engineering*, vol. 2, no. 1, pp. 105–134, 2021.
- [40] A. Alost, O. Elmansuri, and I. Badi, “Resolving a location selection problem by means of an integrated AHP-RAFSI approach,” *Reports in Mechanical Engineering*, vol. 2, no. 1, pp. 135–142, 2021.
- [41] S. Hashemkhani Zolfani, M. Yazdani, D. Pamucar, and P. Zarate, “A VIKOR and TOPSIS focused reanalysis of the MADM methods based on logarithmic normalization,” *Facta Universitatis, Series: Mechanical Engineering*, vol. 18, no. 3, pp. 341–355, 2020.
- [42] K. R. Ramakrishnan and S. Chakraborty, “A cloud TOPSIS model for green supplier selection,” *Facta Universitatis-Series: Mechanical Engineering*, vol. 18, no. 3, pp. 375–397, 2020.
- [43] A. Dobrosavljevic and S. Urosevic, “Analysis of business process management defining and structuring activities in micro, small and medium sized enterprises,” *Operational Research in Engineering Sciences: Theory and Applications*, vol. 2, no. 3, pp. 40–54, 2019.
- [44] O. Yorulmaz, S. K. Yildirim, and B. F. Yildirim, “Robust Mahalanobis distance based TOPSIS to evaluate the economic development of provinces,” *Operational Research in Engineering Sciences: Theory and Applications*, vol. 4, no. 2, pp. 102–123, 2021.
- [45] I. Petrovic and M. Kankaras, “A hybridized IT2FS-DEMATEL-AHP-TOPSIS multicriteria decision making approach: case study of selection and evaluation of criteria for determination of air traffic control radar position,” *Decision Making: Applications in Management and Engineering*, vol. 3, no. 1, pp. 146–164, 2020.
- [46] I. Badi and D. Pamucar, “Supplier selection for steelmaking company by using combined grey-MARCOS methods,” *Decision Making: Applications in Management and Engineering*, vol. 3, no. 2, pp. 37–48, 2020.
- [47] M. Riaz, N. Cagman, N. Wali, and A. Mushtaq, “Certain Properties of Soft multi-set topology with applications in multi-criteria decision making,” *Decision Making: Applications in Management and Engineering*, vol. 3, no. 2, pp. 70–96, 2020.
- [48] Z. S. Mazhandu, E. Muzenda, T. A. Mamvura, M. Belaid, and T. Nhubu, “Integrated and consolidated review of plastic waste management and bio-based biodegradable plastics: challenges and opportunities,” *Sustainability*, vol. 12, no. 20, p. 8360, 2020.
- [49] W. d’ Ambrieres, “Plastics recycling worldwide: current overview and desirable changes,” *Field Actions Science Reports*, vol. 19, pp. 12–21, 2019.
- [50] S. Eraslan and F. Karaaslan, “A group decision making method based on TOPSIS under fuzzy soft environment,” *Journal of New Theory*, vol. 3, pp. 30–40, 2015.
- [51] S. Geetha, S. Narayanamoorthy, J. V. Kureethara, D. Baleanu, and D. Kang, “The hesitant Pythagorean fuzzy ELECTRE III: an adaptable recycling method for plastic materials,” *Journal of Cleaner Production*, vol. 291, no. 1, Article ID 125281, 2021.



## Research Article

# Pythagorean Fuzzy Soft Einstein Ordered Weighted Average Operator in Sustainable Supplier Selection Problem

Rana Muhammad Zulqarnain <sup>1</sup>, Imran Siddique <sup>2</sup>, Shahzad Ahmad,<sup>1</sup>  
Aiyared Iampan <sup>3</sup>, Goran Jovanov <sup>4</sup>, Đorđe Vranješ <sup>5</sup> and Jovica Vasiljević<sup>6</sup>

<sup>1</sup>Department of Mathematics, School of Science, University of Management and Technology, Sialkot Campus, Lahore, Pakistan

<sup>2</sup>Department of Mathematics, School of Science, University of Management and Technology, Lahore 54770, Pakistan

<sup>3</sup>Department of Mathematics, School of Science, University of Phayao, Mae Ka, Mueang, Phayao 56000, Thailand

<sup>4</sup>University of Criminal Investigation and Police Studies, Department of Forensics, Cara Dušana 196, 11080 Belgrade, Serbia

<sup>5</sup>Environ, D.O.O, Čukarička 9, Belgrade, Serbia

<sup>6</sup>City Secretary, City Administration of Belgrade, Secretariat for Public Transport, 43-45 27 Marta Street, 11000 Belgrade, Serbia

Correspondence should be addressed to Imran Siddique; [imransiddique@umt.edu.pk](mailto:imransiddique@umt.edu.pk) and Đorđe Vranješ; [djordjevranches@yahoo.com](mailto:djordjevranches@yahoo.com)

Received 5 October 2021; Revised 30 October 2021; Accepted 2 November 2021; Published 30 November 2021

Academic Editor: Muhammet Deveci

Copyright © 2021 Rana Muhammad Zulqarnain et al. This is an open access article distributed under the Creative Commons Attribution License, which permits unrestricted use, distribution, and reproduction in any medium, provided the original work is properly cited.

Pythagorean fuzzy soft set (PFSS) is the most influential and operative extension of the Pythagorean fuzzy set (PFS), which contracts with the parametrized standards of the substitutes. It is also a generalized form of the intuitionistic fuzzy soft set (IFSS) and delivers a well and accurate estimation in the decision-making (DM) procedure. The primary purpose is to prolong and propose ideas related to Einstein's ordered weighted aggregation operator from fuzzy to PFSS, comforting the condition that the sum of the degrees of membership function and nonmembership function is less than one and the sum of the squares of the degree of membership function and nonmembership function is less than one. We present a novel Pythagorean fuzzy soft Einstein ordered weighted averaging (PFSEOWA) operator based on operational laws for Pythagorean fuzzy soft numbers. Furthermore, some essential properties such as idempotency, boundedness, and homogeneity for the proposed operator have been presented in detail. The choice of a sustainable supplier is also examined as an essential part of sustainable supply chain management (SSCM) and is considered a crucial multiattribute group decision-making (MAGDM) issue. In some MAGDM problems, the relationship between alternatives and uncertain environments will be the main reason for deficient consequences. We have presented a novel aggregation operator for PFSS information to choose sustainable suppliers to cope with those complex issues. The Pythagorean fuzzy soft number (PFSN) helps to represent the obscure information in such real-world perspectives. The priority relationship of PFSS details is beneficial in coping with SSCM. The proposed method's effectiveness is proved by comparing advantages, effectiveness, and flexibility among the existing studies.

## 1. Introduction

Decision-making is a preconceived strategy of picking a logical choice between many objects. Decision-making (DM) plays a crucial part in real-life scenarios. Better decision-making will change the process to determine the limits, benefits, and characteristics of the decision-maker. To cope with the designated scenario, Zaheh [1] launched the fuzzy set (FS) paradigm that puts advancement in several fields of science and technology, nominating the

membership grade for each object real values among 0 and 1. In conventional set theory, elements of a set can be either 0 or 1, but in FS, the degree of membership ranges from 0 to 1. Atanassov [2] extended the concept of FS and introduced an intuitionistic fuzzy set (IFS) which considered both membership and nonmembership grades. Zeshui Xu [3] presented some novel aggregation operators (AOs) for IFS and utilized their developed operators for DM. Wang and Liu [4] offered intuitionistic fuzzy Einstein weighted geometric and intuitionistic fuzzy Einstein ordered weighted geometric

operators with desirable properties. They also constructed multiple attribute decision-making (MADM) techniques based on their developed operators. Atanassov and Gargov [5] prolonged the notion of IFS and established the concept of the interval-valued intuitionistic fuzzy set with some novel operations and their characteristics.

IFS is a powerful concept, which various researchers have studied since its development. However, the dominant concept of IFS has some shortcomings, such as degree of membership and nonmembership taken so that their sum exceeds 1. To cope with these limitations, IFS fails to overcome the scenarios mentioned above. Yager [6] extended the notion of IFS and developed the Pythagorean fuzzy set (PFS) by amending the condition  $MG + NMG \leq 1$  to  $MG^2 + NMG^2 \leq 1$ . Rehman et al. [7] developed the Pythagorean fuzzy weighted averaging aggregation operator with fundamental properties and offered a DM method based on their developed operator. Pamučar and Savin [8] established the best worst method and the compressed proportional assessment models for the assortment of the optimum off-road vehicle. Rehman et al. [9] presented a Pythagorean fuzzy ordered weighted averaging aggregation operator with desirable properties and constructed a MADM approach for the developed operator. Wang and Li [10] planned Bonferroni mean AOs for PFS and built the MADM method utilizing their settled operators. Devenci et al. [11] presented a comprehensive survey to justify the operations and properties for PFS. Garg [12] developed Pythagorean fuzzy geometric interactive AOs based on Einstein operations with their essential properties. Ali et al. [13] proposed the Einstein operational laws utilizing  $t$ -norm and  $t$ -conorm for complex interval-valued PFS. Alostta et al. [14] utilized the multicriteria decision-making technique to enhance emergency medical service centers' finest sites. Milosevic et al. [15] constructed a novel model operating fuzzy logic systems to select a route for the transportation of harmful ingredients.

Above mentioned theories and their corresponding DM approaches are acknowledged and utilized by experts in several fields. Still, due to the lack of parametrized values, these approaches cannot solve parametrization problems. Molodtsov [16] presented the solution of vagueness and uncertainty, introduced a soft set (SS), and discussed some basic operations with their properties. Maji et al. [17] extended the concept of SS and defined numerous basic operations with their essential features and operated to solve DM [18] complications. Maji et al. [19] protracted the notion of FSS and introduced the IFSS with some fundamental operations. Zulqarnain et al. [20] established the correlation coefficient (CC) for interval-valued IFSS and operated their settled CC for the structure of the TOPSIS method. Zulqarnain and Dayan [21] employed the intuitionistic fuzzy TOPSIS for the assortment of an autocorporation. Muhammad Zulqarnain et al. [22] protracted the idea of the IFSS to an intuitionistic fuzzy hypersoft set and presented the TOPSIS method based on the CC. Garg and Arora [23] planned the generalized AOs for the IFSS.

Several investigators prolonged the SS concept utilizing the fundamental definition of FSS. Peng et al. [24] proposed

the impression of IFSS to PFSS by modifying the condition  $MG + NMG \leq 1$  to  $MG^2 + NMG^2 \leq 1$  with some desirable operations. Athira et al. [25] utilized the Hamming distance and Euclidean distance to propose the entropy measure for PFSS. Athira et al. [26] established a DM technique using distance-based entropy measures to resolve DM complications for PFSS. Naeem et al. [27] considered the linguistic PFSS and introduced some basic operations with their properties for PFSS. They also proposed the TOPSIS and VIKOR methods under considered environment to solve DM issues. Riaz et al. [28] prolonged the notion of  $m$ -polar PFSS and offered the TOPSIS technique for  $m$  polar PFSS to resolve multicriteria group decision-making (MCGDM) problems. Riaz et al. [29] anticipated the similarity measures for PFSS and constructed a DM method for PFSS using their developed similarity measures. Zulqarnain et al. [30] settled the AOs for PFSS and projected a DM procedure based on their developed operators. Zulqarnain et al. [31] prolonged the TOPSIS method for PFSS based on CC and employed their progressive approach for MADM problems. Zulqarnain et al. [32] introduced some novel operational laws considering the interaction and proposed interactive AOs for PFSS. They also developed the MCDM approach utilizing their established interactive AOs. Siddique et al. [33] acquired some algebraic operations for PFSS and built a DM technique for PFSS based on a score matrix. It has been observed that fuzzy numbers can only measure uncertainty, and intuitionistic fuzzy numbers can measure true and false membership values. The sum of true and false membership values must be less than 1. However, in our developed methodology, we can measure the values of truth and false membership by modifying the intuitionistic fuzzy numbers condition, such as the sum of the square of true and false values must be less or equal to 1.

Selection and evaluation of suppliers are essential features in professional activities. The fluctuations of the current government strategy use supplier classification as measured by multiple theories with environmental and social needs. Therefore, in the literature, the issue is called sustainable supplier selection, a reference issue of MCGDM. At the same time, multiple credentials [34–37] point to the need for further study through the MCDM approach in supplier selection, focusing on appropriate glossary considerations on environmental realities and expert predictions. To solve such shortcomings, we have implemented a method of choosing sustainable suppliers with Pythagorean fuzzy soft information. The stimulation reassessment is considered by utilizing Pythagorean fuzzy soft numbers. The PFSN is helpful to comply with imprecise information in everyday life complications. In the prevailing literature [38, 39], numerous Einstein AOs have been familiarized, such as Pythagorean fuzzy Einstein weighted average, Einstein weighted geometric, Einstein ordered weighted average, and Einstein ordered weighted geometric operators, to solve the complex problems of DM. The Einstein weighted AOs only weight the Pythagorean fuzzy argument. At the same time, the Einstein weighted ordered AOs only weight the orderly position of the Pythagorean fuzzy argument not the Pythagorean fuzzy argument itself. These Einstein

ordered operators for PFS are unable to accommodate the parametrization values of the alternatives. To overcome the drawbacks mentioned above, we focus on developing some novel Einstein AOs for PFSS.

Thus, the current work intends to offer a novel PFSEOWA operator. It is expected to follow the proposed operator's algorithm rules to solve the DM problem and numerical examples used to prove the effectiveness of the introduced DM method. The proposed operators' key benefit is that the proposed operator can reduce IFSS and FSS operators under specific confident limitations. The rest of the research is organized as follows: some fundamental concepts like FS, IFS, PFS, SS, FSS, IFSS, and PFSS are discussed in Section 2. In Section 3, we developed the PFSEOWA operator. Some desired properties of proposed operators also have been discussed in Section 3. Section 4 developed the MAGDM approach based on proposed operators and presented a numerical example of SSCM. In Section 5, a comparison with some existing methodologies has been provided.

## 2. Preliminaries

This section comprises some basic definitions such as SS, IFS, PFS, IFSS, and PFSS, which will provide a foundation to form the structure of the following manuscript.

*Definition 1* (see [16]). Let  $X$  be a universal set and  $\mathbb{N} = \{t_1, t_2, t_3, \dots, t_m\}$  be the set of attributes, then a pair  $(\Omega, \mathbb{N})$  is called a soft set (SS) over  $X$  where  $\Omega: \mathbb{N} \rightarrow K^X$  is a mapping and  $K^X$  is known as a collection of all subsets of universal set  $X$ .

*Definition 2* (see [6]). Let  $X$  be a collection of objects, then a PFS  $A$  over  $X$  is defined as

$$A = \{(t, \mathbf{a}_A(t), \mathbf{b}_A(t)) \mid t \in X\}, \quad (1)$$

where  $\mathbf{a}_A(t), \mathbf{b}_A(t): X \rightarrow [0, 1]$  represent the membership and nonmembership grade functions, respectively. Furthermore,  $0 \leq \mathbf{a}_A(t)^2 + \mathbf{b}_A(t)^2 \leq 1$  and  $I = 1 - \mathbf{a}_A(t)^2 - \mathbf{b}_A(t)^2$  is called degree of indeterminacy.

We can see from the above definitions that the only difference is in the conditions, i.e., in IFS, we deal with the state  $0 \leq \mathbf{a}_A(t) + \mathbf{b}_A(t) \leq 1$  and  $I = 1 - \mathbf{a}_A(t) - \mathbf{b}_A(t)$  whereas in PFS, we have condition  $0 \leq \mathbf{a}_A(t)^2 + \mathbf{b}_A(t)^2 \leq 1$  and  $I = 1 - \mathbf{a}_A(t)^2 - \mathbf{b}_A(t)^2$ . We can say that a PFS is the general case of IFS.

*Definition 3* (see [24]). Let  $X$  be a universal set and  $\mathbb{N}$  be set of attributes, then a pair  $(\Omega, \mathbb{N})$  is called an IFSS over  $X$  where  $\Omega: \mathbb{N} \rightarrow IK^X$  is a mapping and  $IK^X$  is known as a collection of all IFS subsets of universal set  $X$ .

$$(\Omega, A) = \{t, (\mathbf{a}_A(t), \mathbf{b}_A(t)) \mid t \in A\}, \quad (2)$$

where  $\mathbf{a}_A(t), \mathbf{b}_A(t): A \rightarrow [0, 1]$  are membership grade and nonmembership functions, respectively, with  $0 \leq \mathbf{a}_A(t) + \mathbf{b}_A(t) \leq 1$  and  $A \subset \mathbb{N}$ .

*Definition 4* (see [24]). Let  $(\Omega, A)$  and  $(\Omega, B)$  be two IFSS. Then, some basic operations for IFSS are defined as follows:

- (1)  $(\Omega, A)$  is said to be an intuitionistic fuzzy soft subset of  $(\Omega, B)$ . If and  $A \subset B$  and  $\mathbf{a}_A(t) \leq \mathbf{a}_B(t)$ ,  $\mathbf{b}_A(t) \geq \mathbf{b}_B(t)$  for all  $t \in A$ .
- (2) Complement of  $(\Omega, A)$  is denoted by  $(\Omega, A^c)$  and is defined as

$$(\Omega, A^c) = \{t, (\mathbf{b}_A(t), \mathbf{a}_A(t)) \mid t \in A\}. \quad (3)$$

- (3) Union of two IFSSs is defined as follows:

$$(\Omega, A) \cup (\Omega, B) = \{t, \max(\mathbf{a}_A(t), \mathbf{a}_B(t)) \mid \forall t \in A\}. \quad (4)$$

- (4) The intersection of  $(\Omega, A)$  and  $(\Omega, B)$  can be defined as follows:

$$(\Omega, A) \cap (\Omega, B) = \{t, \min(\mathbf{a}_A(t), \mathbf{a}_B(t)) \mid \forall t \in A\}. \quad (5)$$

*Definition 5* (see [24]). Let  $X$  be a universal set and  $\mathbb{N}$  be set of attributes, then a pair  $(\Omega, \mathbb{N})$  is called a PFSS over  $X$  where  $\Omega: \mathbb{N} \rightarrow \wp K^X$  is a mapping and  $\wp K^X$  is known as the collection of all PFS subsets of universal set  $X$ .

$$(\Omega, A) = \{t, (\mathbf{a}_A(t), \mathbf{b}_A(t)) \mid t \in A\}, \quad (6)$$

where  $\mathbf{a}_A(t), \mathbf{b}_A(t): A \rightarrow [0, 1]$  represent the membership grade and nonmembership functions, respectively, with  $0 \leq \mathbf{a}_A(t)^2 + \mathbf{b}_A(t)^2 \leq 1$ , degree of independency  $\mathfrak{I} = 1 - \mathbf{a}_A(t)^2 - \mathbf{b}_A(t)^2$ , and  $A \subset \mathbb{N}$ .

For the sake of readers convenience, we express the PFSN as  $\mathcal{H}_{ij} = \langle \mathbf{a}_{ij}, \mathbf{b}_{ij} \rangle$ . For calculating the ranking of alternatives, Zulqarnain et al. [30] introduced the score and accuracy functions for  $\mathcal{H}_{ij}$  as follows:

$$S(\mathcal{H}_{ij}) = \mathbf{a}_{ij}^2 - \mathbf{b}_{ij}^2, \quad (7)$$

where  $S(\mathcal{H}_{ij}) \in [-1, 1]$ . It is informed that the score function is unable to differentiate the PFSNs in some cases. For example, let  $H_{11} = \langle 0.3162, 0.4472 \rangle$  and  $H_{12} = \langle 0.5477, 0.6324 \rangle$ , then according to the definition of score function, we have  $S(H_{11}) = -0.1$  and  $S(H_{12}) = -0.1$ . So, it is impossible to find the most acceptable alternative utilizing the score function in this case. To handle this drawback, an accuracy function has been developed.

$$A(\mathcal{H}_{ij}) = \mathbf{a}_{ij}^2 + \mathbf{b}_{ij}^2, \quad (8)$$

where  $A(\mathcal{H}_{ij}) \in [-1, 1]$ .

Thus, to compare two PFSNs  $\mathcal{H}_{ij}$  and  $\mathcal{R}_{ij}$ , following comparison laws are defined:

- (1) If  $S(\mathcal{H}_{ij}) > S(\mathcal{R}_{ij})$ , then  $\mathcal{H}_{ij} > \mathcal{R}_{ij}$
- (2) If  $S(\mathcal{H}_{ij}) = S(\mathcal{R}_{ij})$ , then

- (a) If  $A(H_{ij}) > A(R_{ij})$ , then  $H_{ij} > R_{ij}$
- (b) If  $A(H_{ij}) = A(R_{ij})$ , then  $H_{ij} = R_{ij}$

### 3. Pythagorean Fuzzy Soft Einstein Ordered Weighted Average Operator

The following section will develop the Einstein ordered weighted average operator for PFSS with some fundamental properties.

*Definition 6.* Let  $H_{ij} = (a_{ij}, b_{ij})$  be a collection of PFSNs, where  $(i = 1, 2, \dots, n)$  and  $(j = 1, 2, \dots, m)$ , then the Pythagorean fuzzy soft Einstein ordered weighted averaging (PFSEOWA) operator is defined as follows:

$$PFSEOWA(H_{11}, H_{12}, \dots, H_{nm}) = \bigoplus_{j=1}^m \mathcal{F}_j \left( \bigoplus_{i=1}^n \mathcal{O}_i H_{\mathbf{r}(i)\mathfrak{s}(j)} \right), \tag{9}$$

where  $\mathcal{O}_i$  and  $\mathcal{F}_j$  represent the weight vectors such that  $\mathcal{O}_i > 0$ ,  $\sum_{i=1}^n \mathcal{O}_i = 1$ , and  $\mathcal{F}_j > 0$ ,  $\sum_{j=1}^m \mathcal{F}_j = 1$ , and  $\mathbf{r}$  and  $\mathfrak{s}$  are permutations of  $(i = 1, 2, \dots, n)$  and  $(j = 1, 2, \dots, m)$  such that  $H_{\mathbf{r}(i-1)j} \geq H_{\mathbf{r}(i)j}$  and  $H_{i\mathfrak{s}(j-1)} \geq H_{i\mathfrak{s}(j)} \forall i, j$ .

**Theorem 1.** Let  $H_{ij} = (a_{ij}, b_{ij})$  be a collection of PFSNs, where  $(i = 1, 2, \dots, n)$  and  $(j = 1, 2, \dots, m)$ , then the aggregated value obtained by equation (9) is given as

$$PFSEOWA(H_{11}, H_{12}, \dots, H_{nm}) = \bigoplus_{j=1}^m \mathcal{F}_j \left( \bigoplus_{i=1}^n \mathcal{O}_i H_{\mathbf{r}(i)\mathfrak{s}(j)} \right) = \left\langle \frac{\sqrt{\prod_{j=1}^m \left( \prod_{i=1}^n (1 + a_{\mathbf{r}(i)\mathfrak{s}(j)}^2)^{\mathcal{O}_i} \right)^{\mathcal{F}_j} - \prod_{j=1}^m \left( \prod_{i=1}^n (1 - a_{\mathbf{r}(i)\mathfrak{s}(j)}^2)^{\mathcal{O}_i} \right)^{\mathcal{F}_j}}}{\sqrt{\prod_{j=1}^m \left( \prod_{i=1}^n (1 + a_{\mathbf{r}(i)\mathfrak{s}(j)}^2)^{\mathcal{O}_i} \right)^{\mathcal{F}_j} + \prod_{j=1}^m \left( \prod_{i=1}^n (1 - a_{\mathbf{r}(i)\mathfrak{s}(j)}^2)^{\mathcal{O}_i} \right)^{\mathcal{F}_j}}}, \frac{\sqrt{2 \prod_{j=1}^m \left( \prod_{i=1}^n (b_{\mathbf{r}(i)\mathfrak{s}(j)}^2)^{\mathcal{O}_i} \right)^{\mathcal{F}_j}}}{\sqrt{\prod_{j=1}^m \left( \prod_{i=1}^n (2 - b_{\mathbf{r}(i)\mathfrak{s}(j)}^2)^{\mathcal{O}_i} \right)^{\mathcal{F}_j} + \prod_{j=1}^m \left( \prod_{i=1}^n (b_{\mathbf{r}(i)\mathfrak{s}(j)}^2)^{\mathcal{O}_i} \right)^{\mathcal{F}_j}}} \right\rangle, \tag{10}$$

where  $\mathcal{O}_i$  and  $\mathcal{F}_j$  represent the weight vectors such that  $\mathcal{O}_i > 0$ ,  $\sum_{i=1}^n \mathcal{O}_i = 1$ , and  $\mathcal{F}_j > 0$ ,  $\sum_{j=1}^m \mathcal{F}_j = 1$ , and  $\mathbf{r}$  and  $\mathfrak{s}$  are permutations of  $(i = 1, 2, \dots, n)$  and  $(j = 1, 2, \dots, m)$  such that  $H_{\mathbf{r}(i-1)j} \geq H_{\mathbf{r}(i)j}$  and  $H_{i\mathfrak{s}(j-1)} \geq H_{i\mathfrak{s}(j)} \forall i, j$ .

*Proof.* We will prove it by using mathematical induction.

For  $n = 1$ , we get  $\mathcal{O}_i = 1$ .

$$PFSEOWA(H_{11}, H_{12}, \dots, H_{nm}) = \bigoplus_{j=1}^m \mathcal{F}_j H_{\mathbf{r}(1)\mathfrak{s}(j)} = \left\langle \frac{\sqrt{\prod_{j=1}^m (1 + a_{\mathbf{r}(1)\mathfrak{s}(j)}^2)^{\mathcal{F}_j} - \prod_{j=1}^m (1 - a_{\mathbf{r}(1)\mathfrak{s}(j)}^2)^{\mathcal{F}_j}}}{\sqrt{\prod_{j=1}^m (1 + a_{\mathbf{r}(1)\mathfrak{s}(j)}^2)^{\mathcal{F}_j} + \prod_{j=1}^m (1 - a_{\mathbf{r}(1)\mathfrak{s}(j)}^2)^{\mathcal{F}_j}}}, \frac{\sqrt{2 \prod_{j=1}^m (b_{\mathbf{r}(1)\mathfrak{s}(j)}^2)^{\mathcal{F}_j}}}{\sqrt{\prod_{j=1}^m (2 - b_{\mathbf{r}(1)\mathfrak{s}(j)}^2)^{\mathcal{F}_j} + \prod_{j=1}^m (b_{\mathbf{r}(1)\mathfrak{s}(j)}^2)^{\mathcal{F}_j}}} \right\rangle = \left\langle \frac{\sqrt{\prod_{j=1}^m \left( \prod_{i=1}^1 (1 + a_{\mathbf{r}(i)\mathfrak{s}(j)}^2)^{\mathcal{O}_i} \right)^{\mathcal{F}_j} - \prod_{j=1}^m \left( \prod_{i=1}^1 (1 - a_{\mathbf{r}(i)\mathfrak{s}(j)}^2)^{\mathcal{O}_i} \right)^{\mathcal{F}_j}}}{\sqrt{\prod_{j=1}^m \left( \prod_{i=1}^1 (1 + a_{\mathbf{r}(i)\mathfrak{s}(j)}^2)^{\mathcal{O}_i} \right)^{\mathcal{F}_j} + \prod_{j=1}^m \left( \prod_{i=1}^1 (1 - a_{\mathbf{r}(i)\mathfrak{s}(j)}^2)^{\mathcal{O}_i} \right)^{\mathcal{F}_j}}}, \frac{\sqrt{2 \prod_{j=1}^m \left( \prod_{i=1}^1 (b_{\mathbf{r}(i)\mathfrak{s}(j)}^2)^{\mathcal{O}_i} \right)^{\mathcal{F}_j}}}{\sqrt{\prod_{j=1}^m \left( \prod_{i=1}^1 (2 - b_{\mathbf{r}(i)\mathfrak{s}(j)}^2)^{\mathcal{O}_i} \right)^{\mathcal{F}_j} + \prod_{j=1}^m \left( \prod_{i=1}^1 (b_{\mathbf{r}(i)\mathfrak{s}(j)}^2)^{\mathcal{O}_i} \right)^{\mathcal{F}_j}}} \right\rangle. \tag{11}$$

For  $m = 1$ , we get  $\mathcal{F}_j = 1$ .

$$\begin{aligned}
 \text{PFSEOWA}(H_{11}, H_{12}, \dots, H_{nm}) &= \bigoplus_{i=1}^n \mathcal{O}_i H_{\mathbf{r}(i)\mathfrak{s}(1)} \\
 &= \left\langle \frac{\sqrt{\prod_{i=1}^n (1 + \mathbf{a}_{\mathbf{r}(i)\mathfrak{s}(1)}^2)^{\mathcal{O}_i}} - \prod_{i=1}^n (1 - \mathbf{a}_{\mathbf{r}(i)\mathfrak{s}(1)}^2)^{\mathcal{O}_i}}{\sqrt{\prod_{i=1}^n (1 + \mathbf{a}_{\mathbf{r}(i)\mathfrak{s}(1)}^2)^{\mathcal{O}_i}} + \prod_{i=1}^n (1 - \mathbf{a}_{\mathbf{r}(i)\mathfrak{s}(1)}^2)^{\mathcal{O}_i}}, \right. \\
 &\quad \left. \frac{\sqrt{2 \prod_{i=1}^n (\mathbf{b}_{\mathbf{r}(i)\mathfrak{s}(1)}^2)^{\mathcal{O}_i}}}{\sqrt{\prod_{i=1}^n (2 - \mathbf{b}_{\mathbf{r}(i)\mathfrak{s}(1)}^2)^{\mathcal{O}_i}} + \prod_{i=1}^n (\mathbf{b}_{\mathbf{r}(i)\mathfrak{s}(1)}^2)^{\mathcal{O}_i}} \right\rangle \\
 &= \left\langle \frac{\sqrt{\prod_{j=1}^1 \left( \prod_{i=1}^n (1 + \mathbf{a}_{\mathbf{r}(i)\mathfrak{s}(j)}^2)^{\mathcal{O}_i} \right)^{\mathcal{F}_j}} - \prod_{j=1}^1 \left( \prod_{i=1}^n (1 - \mathbf{a}_{\mathbf{r}(i)\mathfrak{s}(j)}^2)^{\mathcal{O}_i} \right)^{\mathcal{F}_j}}{\sqrt{\prod_{j=1}^1 \left( \prod_{i=1}^n (1 + \mathbf{a}_{\mathbf{r}(i)\mathfrak{s}(j)}^2)^{\mathcal{O}_i} \right)^{\mathcal{F}_j}} + \prod_{j=1}^1 \left( \prod_{i=1}^n (1 - \mathbf{a}_{\mathbf{r}(i)\mathfrak{s}(j)}^2)^{\mathcal{O}_i} \right)^{\mathcal{F}_j}}, \right. \\
 &\quad \left. \frac{\sqrt{2 \prod_{j=1}^1 \left( \prod_{i=1}^n (\mathbf{b}_{\mathbf{r}(i)\mathfrak{s}(j)}^2)^{\mathcal{O}_i} \right)^{\mathcal{F}_j}}}{\sqrt{\prod_{j=1}^1 \left( \prod_{i=1}^n (2 - \mathbf{b}_{\mathbf{r}(i)\mathfrak{s}(j)}^2)^{\mathcal{O}_i} \right)^{\mathcal{F}_j}} + \prod_{j=1}^1 \left( \prod_{i=1}^n (\mathbf{b}_{\mathbf{r}(i)\mathfrak{s}(j)}^2)^{\mathcal{O}_i} \right)^{\mathcal{F}_j}} \right\rangle.
 \end{aligned} \tag{12}$$

So, equation (9) is true for  $n = 1$  and  $m = 1$ .

Suppose that equation holds for  $n = \delta_2$ ,  $m = \delta_1 + 1$ , and for  $n = \delta_2 + 1$ ,  $m = \delta_1$ .

$$\begin{aligned}
 &\bigoplus_{j=1}^{\delta_1+1} \mathcal{F}_j \left( \bigoplus_{i=1}^{\delta_2} \mathcal{O}_i H_{\mathbf{r}(i)\mathfrak{s}(j)} \right) \\
 &= \left\langle \frac{\sqrt{\prod_{j=1}^{\delta_1+1} \left( \prod_{i=1}^{\delta_2} (1 + \mathbf{a}_{\mathbf{r}(i)\mathfrak{s}(j)}^2)^{\mathcal{O}_i} \right)^{\mathcal{F}_j}} - \prod_{j=1}^{\delta_1+1} \left( \prod_{i=1}^{\delta_2} (1 - \mathbf{a}_{\mathbf{r}(i)\mathfrak{s}(j)}^2)^{\mathcal{O}_i} \right)^{\mathcal{F}_j}}{\sqrt{\prod_{j=1}^{\delta_1+1} \left( \prod_{i=1}^{\delta_2} (1 + \mathbf{a}_{\mathbf{r}(i)\mathfrak{s}(j)}^2)^{\mathcal{O}_i} \right)^{\mathcal{F}_j}} + \prod_{j=1}^{\delta_1+1} \left( \prod_{i=1}^{\delta_2} (1 - \mathbf{a}_{\mathbf{r}(i)\mathfrak{s}(j)}^2)^{\mathcal{O}_i} \right)^{\mathcal{F}_j}}, \right. \\
 &\quad \left. \frac{\sqrt{2 \prod_{j=1}^{\delta_1+1} \left( \prod_{i=1}^{\delta_2} (\mathbf{b}_{\mathbf{r}(i)\mathfrak{s}(j)}^2)^{\mathcal{O}_i} \right)^{\mathcal{F}_j}}}{\sqrt{\prod_{j=1}^{\delta_1+1} \left( \prod_{i=1}^{\delta_2} (2 - \mathbf{b}_{\mathbf{r}(i)\mathfrak{s}(j)}^2)^{\mathcal{O}_i} \right)^{\mathcal{F}_j}} + \prod_{j=1}^{\delta_1+1} \left( \prod_{i=1}^{\delta_2} (\mathbf{b}_{\mathbf{r}(i)\mathfrak{s}(j)}^2)^{\mathcal{O}_i} \right)^{\mathcal{F}_j}} \right\rangle, \\
 &\bigoplus_{j=1}^{\delta_1} \mathcal{F}_j \left( \bigoplus_{i=1}^{\delta_2+1} \mathcal{O}_i H_{\mathbf{r}(i)\mathfrak{s}(j)} \right) \\
 &= \left\langle \frac{\sqrt{\prod_{j=1}^{\delta_1} \left( \prod_{i=1}^{\delta_2+1} (1 + \mathbf{a}_{\mathbf{r}(i)\mathfrak{s}(j)}^2)^{\mathcal{O}_i} \right)^{\mathcal{F}_j}} - \prod_{j=1}^{\delta_1} \left( \prod_{i=1}^{\delta_2+1} (1 - \mathbf{a}_{\mathbf{r}(i)\mathfrak{s}(j)}^2)^{\mathcal{O}_i} \right)^{\mathcal{F}_j}}{\sqrt{\prod_{j=1}^{\delta_1} \left( \prod_{i=1}^{\delta_2+1} (1 + \mathbf{a}_{\mathbf{r}(i)\mathfrak{s}(j)}^2)^{\mathcal{O}_i} \right)^{\mathcal{F}_j}} + \prod_{j=1}^{\delta_1} \left( \prod_{i=1}^{\delta_2+1} (1 - \mathbf{a}_{\mathbf{r}(i)\mathfrak{s}(j)}^2)^{\mathcal{O}_i} \right)^{\mathcal{F}_j}}, \right. \\
 &\quad \left. \frac{\sqrt{2 \prod_{j=1}^{\delta_1} \left( \prod_{i=1}^{\delta_2+1} (\mathbf{b}_{\mathbf{r}(i)\mathfrak{s}(j)}^2)^{\mathcal{O}_i} \right)^{\mathcal{F}_j}}}{\sqrt{\prod_{j=1}^{\delta_1} \left( \prod_{i=1}^{\delta_2+1} (2 - \mathbf{b}_{\mathbf{r}(i)\mathfrak{s}(j)}^2)^{\mathcal{O}_i} \right)^{\mathcal{F}_j}} + \prod_{j=1}^{\delta_1} \left( \prod_{i=1}^{\delta_2+1} (\mathbf{b}_{\mathbf{r}(i)\mathfrak{s}(j)}^2)^{\mathcal{O}_i} \right)^{\mathcal{F}_j}} \right\rangle.
 \end{aligned} \tag{13}$$

Now, we prove the equation for  $m = \delta_1 + 1$  and  $n = \delta_2 + 1$ :

$$\begin{aligned}
 \bigoplus_{j=1}^{\delta_1+1} \mathcal{F}_j \left( \bigoplus_{i=1}^{\delta_2+1} \mathcal{O}_i H_{\mathbf{r}(i)\mathfrak{s}(j)} \right) &= \bigoplus_{j=1}^{\delta_1+1} H_{\mathfrak{s}(j)} \left( \bigoplus_{i=1}^{\delta_2} \mathcal{O}_i H_{\mathbf{r}(i)\mathfrak{s}(j)} \oplus \mathcal{O}_{i+1} H_{\mathbf{r}(\delta_2+1)\mathfrak{s}(j)} \right) \\
 &= \left( \bigoplus_{j=1}^{\delta_1+1} \bigoplus_{i=1}^{\delta_2} \mathcal{O}_i \mathcal{F}_j H_{\mathbf{r}(i)\mathfrak{s}(j)} \right) \left( \bigoplus_{j=1}^{\delta_1+1} \mathcal{F}_j \mathcal{O}_{i+1} H_{\mathbf{r}(\delta_2+1)\mathfrak{s}(j)} \right) \\
 &= \left\langle \frac{\sqrt{2 \prod_{j=1}^{\delta_1+1} \left( \prod_{i=1}^{\delta_2} (\mathbf{b}_{\mathbf{r}(i)\mathfrak{s}(j)}^2)^{\mathcal{O}_i} \right)^{\mathcal{F}_j}}}{\sqrt{\prod_{j=1}^{\delta_1+1} \left( \prod_{i=1}^{\delta_2} (2 - \mathbf{b}_{\mathbf{r}(i)\mathfrak{s}(j)}^2)^{\mathcal{O}_i} \right)^{\mathcal{F}_j} + \prod_{j=1}^{\delta_1+1} \left( \prod_{i=1}^{\delta_2} (\mathbf{b}_{\mathbf{r}(i)\mathfrak{s}(j)}^2)^{\mathcal{O}_i} \right)^{\mathcal{F}_j}}} \right. \\
 &\quad \oplus \left. \frac{\sqrt{2 \prod_{j=1}^{\delta_1+1} \left( (\mathbf{b}_{\mathbf{r}(\delta_2+1)\mathfrak{s}(j)}^2)^{\mathcal{O}_{\delta_2+1}} \right)^{\mathcal{F}_j}}}{\sqrt{\prod_{j=1}^{\delta_1+1} \left( (2 - \mathbf{b}_{\mathbf{r}(\delta_2+1)\mathfrak{s}(j)}^2)^{\mathcal{O}_{\delta_2+1}} \right)^{\mathcal{F}_j} + \prod_{j=1}^{\delta_1+1} \left( (\mathbf{b}_{\mathbf{r}(\delta_2+1)\mathfrak{s}(j)}^2)^{\mathcal{O}_{\delta_2+1}} \right)^{\mathcal{F}_j}}} \right\rangle \tag{14} \\
 &= \left\langle \frac{\sqrt{\prod_{j=1}^{\delta_1+1} \left( \prod_{i=1}^{\delta_2+1} (1 + \mathbf{a}_{\mathbf{r}(i)\mathfrak{s}(j)}^2)^{\mathcal{O}_i} \right)^{\mathcal{F}_j} - \prod_{j=1}^{\delta_1+1} \left( \prod_{i=1}^{\delta_2+1} (1 - \mathbf{a}_{\mathbf{r}(i)\mathfrak{s}(j)}^2)^{\mathcal{O}_i} \right)^{\mathcal{F}_j}}}{\sqrt{\prod_{j=1}^{\delta_1+1} \left( \prod_{i=1}^{\delta_2+1} (1 + \mathbf{a}_{\mathbf{r}(i)\mathfrak{s}(j)}^2)^{\mathcal{O}_i} \right)^{\mathcal{F}_j} + \prod_{j=1}^{\delta_1+1} \left( \prod_{i=1}^{\delta_2+1} (1 - \mathbf{a}_{\mathbf{r}(i)\mathfrak{s}(j)}^2)^{\mathcal{O}_i} \right)^{\mathcal{F}_j}}} \right. \\
 &\quad \left. \frac{\sqrt{2 \prod_{j=1}^{\delta_1+1} \left( \prod_{i=1}^{\delta_2+1} (\mathbf{b}_{\mathbf{r}(i)\mathfrak{s}(j)}^2)^{\mathcal{O}_i} \right)^{\mathcal{F}_j}}}{\sqrt{\prod_{j=1}^{\delta_1+1} \left( \prod_{i=1}^{\delta_2+1} (2 - \mathbf{b}_{\mathbf{r}(i)\mathfrak{s}(j)}^2)^{\mathcal{O}_i} \right)^{\mathcal{F}_j} + \prod_{j=1}^{\delta_1+1} \left( \prod_{i=1}^{\delta_2+1} (\mathbf{b}_{\mathbf{r}(i)\mathfrak{s}(j)}^2)^{\mathcal{O}_i} \right)^{\mathcal{F}_j}}} \right\rangle \\
 &= \bigoplus_{j=1}^{\delta_1+1} \mathcal{F}_j \left( \bigoplus_{i=1}^{\delta_2+1} \mathcal{O}_i H_{\mathbf{r}(i)\mathfrak{s}(j)} \right).
 \end{aligned}$$

So, it is valid for  $m = \delta_1 + 1$  and  $n = \delta_2 + 1$ . □

*Example 1.* Let  $R = \{R_1, R_2, R_3\}$  be a set of decision-makers with weight vector  $\mathcal{O}_i = (0.1, 0.3, 0.3, 0.3)^T$ , who want to decide a bike under the set of attributes  $A = \{A_1 = \text{fuel milage}, A_2 = \text{speed per hour}, A_3 = \text{price}, A_4 =$

comfort level,  $A_5 = \text{design}\}$  with weight vector  $\mathcal{F}_j = (0.2, 0.2, 0.2, 0.4)^T$ . The assumed rating values for each attribute in the form of PFSNs  $(H_{4 \times 4}, A) = (\mathbf{a}_{ij}, \mathbf{b}_{ij})_{4 \times 4}$  are given as follows:

$$(H_{4 \times 4}, A) = \begin{bmatrix} (0.5, 0.8) & (0.7, 0.5) & (0.4, 0.6) & (0.7, 0.4) \\ (0.5, 0.6) & (0.9, 0.1) & (0.3, 0.7) & (0.4, 0.5) \\ (0.4, 0.8) & (0.7, 0.5) & (0.4, 0.6) & (0.3, 0.5) \\ (0.3, 0.7) & (0.6, 0.5) & (0.5, 0.4) & (0.5, 0.7) \end{bmatrix}. \tag{15}$$

First, we find the associated ordered position matrix by using the score function, which is as follows:

$$(H_{4 \times 4}, A) = \begin{bmatrix} (0.7, 0.4) & (0.7, 0.5) & (0.4, 0.6) & (0.5, 0.8) \\ (0.9, 0.1) & (0.4, 0.5) & (0.3, 0.7) & (0.5, 0.6) \\ (0.7, 0.5) & (0.4, 0.6) & (0.3, 0.5) & (0.4, 0.8) \\ (0.6, 0.5) & (0.5, 0.4) & (0.3, 0.7) & (0.5, 0.7) \end{bmatrix}. \tag{16}$$

As we know,

$$\begin{aligned} \text{PFSEOWA}(H_{11}, H_{12}, \dots, H_{mm}) &= \left\langle \frac{\sqrt{\prod_{j=1}^m \left( \prod_{i=1}^m (1 + a_{\tau(i)\otimes(j)}^2)^{\theta_i} \right)^{\mathcal{F}_j} - \prod_{j=1}^m \left( \prod_{i=1}^m (1 - a_{\tau(i)\otimes(j)}^2)^{\theta_i} \right)^{\mathcal{F}_j}}}{\sqrt{\prod_{j=1}^m \left( \prod_{i=1}^m (1 + a_{\tau(i)\otimes(j)}^2)^{\theta_i} \right)^{\mathcal{F}_j} + \prod_{j=1}^m \left( \prod_{i=1}^m (1 - a_{\tau(i)\otimes(j)}^2)^{\theta_i} \right)^{\mathcal{F}_j}}}, \frac{\sqrt{2 \prod_{j=1}^m \left( \prod_{i=1}^m (b_{\tau(i)\otimes(j)}^2)^{\theta_i} \right)^{\mathcal{F}_j}}}{\sqrt{\prod_{j=1}^m \left( \prod_{i=1}^m (2 - b_{\tau(i)\otimes(j)}^2)^{\theta_i} \right)^{\mathcal{F}_j} + \prod_{j=1}^m \left( \prod_{i=1}^m (b_{\tau(i)\otimes(j)}^2)^{\theta_i} \right)^{\mathcal{F}_j}}} \right\rangle \\ \text{PFSEOWA}(H_{11}, H_{12}, \dots, H_{44}) &= \left\langle \frac{\sqrt{\prod_{j=1}^4 \left( \prod_{i=1}^4 (1 + a_{\tau(i)\otimes(j)}^2)^{\theta_i} \right)^{\mathcal{F}_j} - \prod_{j=1}^4 \left( \prod_{i=1}^4 (1 - a_{\tau(i)\otimes(j)}^2)^{\theta_i} \right)^{\mathcal{F}_j}}}{\sqrt{\prod_{j=1}^4 \left( \prod_{i=1}^4 (1 + a_{\tau(i)\otimes(j)}^2)^{\theta_i} \right)^{\mathcal{F}_j} + \prod_{j=1}^4 \left( \prod_{i=1}^4 (1 - a_{\tau(i)\otimes(j)}^2)^{\theta_i} \right)^{\mathcal{F}_j}}}, \frac{\sqrt{2 \prod_{j=1}^4 \left( \prod_{i=1}^4 (b_{\tau(i)\otimes(j)}^2)^{\theta_i} \right)^{\mathcal{F}_j}}}{\sqrt{\prod_{j=1}^4 \left( \prod_{i=1}^4 (2 - b_{\tau(i)\otimes(j)}^2)^{\theta_i} \right)^{\mathcal{F}_j} + \prod_{j=1}^4 \left( \prod_{i=1}^4 (b_{\tau(i)\otimes(j)}^2)^{\theta_i} \right)^{\mathcal{F}_j}}} \right\rangle \\ &= \left\langle \frac{\sqrt{2 \left[ \left\{ (0.16)^{0.1} (0.01)^{0.3} (0.25)^{0.3} (0.25)^{0.3} \right\}^{0.2} \left\{ (0.25)^{0.1} (0.25)^{0.3} (0.36)^{0.3} (0.16)^{0.3} \right\}^{0.2} \left\{ (0.36)^{0.1} (0.49)^{0.3} (0.25)^{0.3} (0.49)^{0.3} \right\}^{0.2} \left\{ (0.64)^{0.1} (0.36)^{0.3} (0.64)^{0.3} (0.49)^{0.3} \right\}^{0.4} \right]}{\sqrt{\left\{ (1.84)^{0.1} (1.99)^{0.3} (1.75)^{0.3} (1.75)^{0.3} \right\}^{0.2} \left\{ (1.75)^{0.1} (1.75)^{0.3} (1.64)^{0.3} (1.84)^{0.3} \right\}^{0.2} \left\{ (1.64)^{0.1} (1.51)^{0.3} (1.36)^{0.3} (1.51)^{0.3} \right\}^{0.2} \left\{ (1.36)^{0.1} (1.64)^{0.3} (1.36)^{0.3} (1.51)^{0.3} \right\}^{0.4} +}} \right\rangle \\ &= \langle 0.5283, 0.5242 \rangle. \tag{17} \end{aligned}$$

$$\text{PFSEOWA}(H_{11}, H_{12}, \dots, H_{mm}) = H, \tag{18}$$

where  $\theta_i$  and  $\mathcal{F}_j$  represent the weight vectors such that  $\theta_i > 0$ ,  $\sum_{i=1}^n \theta_i = 1$ , and  $\mathcal{F}_j > 0$ ,  $\sum_{j=1}^m \mathcal{F}_j = 1$ .

*Proof.* As we know,

### 3.1. Properties of PFSEOWA Operator

3.1.1. *Idempotency.* Let  $H_{ij} = (a_{ij}, b_{ij})$  be a collection of PFNSNs, where  $(i = 1, 2, \dots, n)$  and  $(j = 1, 2, \dots, m)$ .

If  $H_{\tau(i)\otimes(j)} = H_{11}$  are mathematically identical, then

PFSEOWA( $H_{11}, H_{12}, \dots, H_{nm}$ )

$$= \left\langle \frac{\sqrt{\prod_{j=1}^m \left( \prod_{i=1}^n (1 + \mathbf{a}_{\mathbf{r}(i)\mathfrak{s}(j)}^2)^{\mathcal{O}_i} \right)^{\mathcal{F}_j} - \prod_{j=1}^m \left( \prod_{i=1}^n (1 - \mathbf{a}_{\mathbf{r}(i)\mathfrak{s}(j)}^2)^{\mathcal{O}_i} \right)^{\mathcal{F}_j}}}{\sqrt{\prod_{j=1}^m \left( \prod_{i=1}^n (1 + \mathbf{a}_{\mathbf{r}(i)\mathfrak{s}(j)}^2)^{\mathcal{O}_i} \right)^{\mathcal{F}_j} + \prod_{j=1}^m \left( \prod_{i=1}^n (1 - \mathbf{a}_{\mathbf{r}(i)\mathfrak{s}(j)}^2)^{\mathcal{O}_i} \right)^{\mathcal{F}_j}}, \frac{\sqrt{2 \prod_{j=1}^m \left( \prod_{i=1}^n (\mathbf{b}_{\mathbf{r}(i)\mathfrak{s}(j)}^2)^{\mathcal{O}_i} \right)^{\mathcal{F}_j}}}{\sqrt{\prod_{j=1}^m \left( \prod_{i=1}^n (2 - \mathbf{b}_{\mathbf{r}(i)\mathfrak{s}(j)}^2)^{\mathcal{O}_i} \right)^{\mathcal{F}_j} + \prod_{j=1}^m \left( \prod_{i=1}^n (\mathbf{b}_{\mathbf{r}(i)\mathfrak{s}(j)}^2)^{\mathcal{O}_i} \right)^{\mathcal{F}_j}}} \right\rangle$$

As  $H_{\mathbf{r}(i)\mathfrak{s}(j)} = H_{ij}$ , So

$$= \left\langle \frac{\sqrt{\left( (1 + \mathbf{a}_{ij}^2)^{\sum_{i=1}^n \mathcal{O}_i} \right)^{\sum_{j=1}^m \mathcal{F}_j} - \left( (1 - \mathbf{a}_{ij}^2)^{\sum_{i=1}^n \mathcal{O}_i} \right)^{\sum_{j=1}^m \mathcal{F}_j}}}{\sqrt{\left( (1 + \mathbf{a}_{ij}^2)^{\sum_{i=1}^n \mathcal{O}_i} \right)^{\sum_{j=1}^m \mathcal{F}_j} + \left( (1 - \mathbf{a}_{ij}^2)^{\sum_{i=1}^n \mathcal{O}_i} \right)^{\sum_{j=1}^m \mathcal{F}_j}}, \frac{\sqrt{2 \left( (\mathbf{b}_{ij}^2)^{\sum_{i=1}^n \mathcal{O}_i} \right)^{\sum_{j=1}^m \mathcal{F}_j}}}{\sqrt{\left( (2 - \mathbf{b}_{ij}^2)^{\sum_{i=1}^n \mathcal{O}_i} \right)^{\sum_{j=1}^m \mathcal{F}_j} + \left( (\mathbf{b}_{ij}^2)^{\sum_{i=1}^n \mathcal{O}_i} \right)^{\sum_{j=1}^m \mathcal{F}_j}}} \right\rangle$$

$$= \left\langle \frac{\sqrt{(1 + \mathbf{a}_{ij}^2) - (1 - \mathbf{a}_{ij}^2)}}{\sqrt{(1 + \mathbf{a}_{ij}^2) + (1 - \mathbf{a}_{ij}^2)}}, \frac{\sqrt{2\mathbf{b}_{ij}^2}}{\sqrt{(2 - \mathbf{b}_{ij}^2) + (\mathbf{b}_{ij}^2)}} \right\rangle$$

$$= \langle \mathbf{a}_{ij}, \mathbf{b}_{ij} \rangle = H.$$

(19)

3.1.2. *Boundedness.* Let  $H_{ij} = (\mathbf{a}_{ij}, \mathbf{b}_{ij})$  be a collection of PFSNs, where  $(i = 1, 2, \dots, n)$  and  $(j = 1, 2, \dots, m)$ .

If  $H_{\min} = \min(H_{\mathbf{r}(i)\mathfrak{s}(j)})$  and  $H_{\max} = \max(H_{\mathbf{r}(i)\mathfrak{s}(j)})$ , then

$$H_{\min} \leq \text{PFSEOWA}(H_{11}, H_{12}, \dots, H_{nm}) \leq H_{\max}, \quad (20)$$

where  $\mathcal{O}_i$  and  $\mathcal{F}_j$  represent the weight vectors such that  $\mathcal{O}_i > 0$ ,  $\sum_{i=1}^n \mathcal{O}_i = 1$ , and  $\mathcal{F}_j > 0$ ,  $\sum_{j=1}^m \mathcal{F}_j = 1$ .

*Proof.* Let  $g(y) = \sqrt{(1 - y^2)/(1 + y^2)}$ ,  $y \in ]0, 1]$ , then  $(d/dy)(g(y)) = -2y/(1 + y^2)^2 \sqrt{(1 + y^2)/(1 - y^2)} < 0$ ,

which shows that  $g(y)$  is decreasing function on  $]0, 1]$ . So,

$$\mathbf{a}_{\min} \leq \mathbf{a}_{\mathbf{r}(i)\mathfrak{s}(j)} \leq \mathbf{a}_{\max}.$$

Hence,  $g(\mathbf{a}_{\max}) \leq g(\mathbf{a}_{\mathbf{r}(i)\mathfrak{s}(j)}) \leq g(\mathbf{a}_{\min})$ :

$$\Rightarrow \sqrt{\frac{1 - \mathbf{a}_{\max}^2}{1 + \mathbf{a}_{\max}^2}} \leq \sqrt{\frac{1 - \mathbf{a}_{\mathbf{r}(i)\mathfrak{s}(j)}^2}{1 + \mathbf{a}_{\mathbf{r}(i)\mathfrak{s}(j)}^2}} \leq \sqrt{\frac{1 - \mathbf{a}_{\min}^2}{1 + \mathbf{a}_{\min}^2}}. \quad (21)$$

Let  $\mathcal{O}_i$  and  $\mathcal{F}_j$  represent the weight vectors such that  $\mathcal{O}_i > 0$ ,  $\sum_{i=1}^n \mathcal{O}_i = 1$ , and  $\mathcal{F}_j > 0$ ,  $\sum_{j=1}^m \mathcal{F}_j = 1$ . Then, we have

$$\Leftrightarrow \sqrt{\prod_{j=1}^m \left( \prod_{i=1}^n \left( \frac{1 - \mathbf{a}_{\max}^2}{1 + \mathbf{a}_{\max}^2} \right)^{\mathcal{O}_i} \right)^{\mathcal{F}_j}} \leq \sqrt{\prod_{j=1}^m \left( \prod_{i=1}^n \left( \frac{1 - \mathbf{a}_{\mathbf{r}(i)\mathfrak{s}(j)}^2}{1 + \mathbf{a}_{\mathbf{r}(i)\mathfrak{s}(j)}^2} \right)^{\mathcal{O}_i} \right)^{\mathcal{F}_j}} \leq \sqrt{\prod_{j=1}^m \left( \prod_{i=1}^n \left( \frac{1 - \mathbf{a}_{\min}^2}{1 + \mathbf{a}_{\min}^2} \right)^{\mathcal{O}_i} \right)^{\mathcal{F}_j}}$$

$$\Leftrightarrow \sqrt{\left( \left( \frac{1 - \mathbf{a}_{\max}^2}{1 + \mathbf{a}_{\max}^2} \right)^{\sum_{i=1}^n \mathcal{O}_i} \right)^{\sum_{j=1}^m \mathcal{F}_j}} \leq \sqrt{\prod_{j=1}^m \left( \prod_{i=1}^n \left( \frac{1 - \mathbf{a}_{\mathbf{r}(i)\mathfrak{s}(j)}^2}{1 + \mathbf{a}_{\mathbf{r}(i)\mathfrak{s}(j)}^2} \right)^{\mathcal{O}_i} \right)^{\mathcal{F}_j}} \leq \sqrt{\left( \left( \frac{1 - \mathbf{a}_{\min}^2}{1 + \mathbf{a}_{\min}^2} \right)^{\sum_{i=1}^n \mathcal{O}_i} \right)^{\sum_{j=1}^m \mathcal{F}_j}}$$



$$\begin{aligned}
 &\Leftrightarrow \sqrt{1 + \left(\frac{1 - \mathbf{a}_{\max}^2}{1 + \mathbf{a}_{\max}^2}\right)} \leq \sqrt{1 + \prod_{j=1}^m \left(\prod_{i=1}^n \left(\frac{1 - \mathbf{a}_{\mathbf{r}(i)\mathfrak{s}(j)}^2}{1 + \mathbf{a}_{\mathbf{r}(i)\mathfrak{s}(j)}^2}\right)^{\mathcal{O}_i}\right)^{\mathcal{F}_j}} \leq \sqrt{1 + \left(\frac{1 - \mathbf{a}_{\min}^2}{1 + \mathbf{a}_{\min}^2}\right)} \\
 &\Leftrightarrow \sqrt{\frac{2}{1 + \mathbf{a}_{\max}^2}} \leq \sqrt{1 + \prod_{j=1}^m \left(\prod_{i=1}^n \left(\frac{1 - \mathbf{a}_{\mathbf{r}(i)\mathfrak{s}(j)}^2}{1 + \mathbf{a}_{\mathbf{r}(i)\mathfrak{s}(j)}^2}\right)^{\mathcal{O}_i}\right)^{\mathcal{F}_j}} \leq \sqrt{\frac{2}{1 + \mathbf{a}_{\min}^2}} \\
 &\Leftrightarrow \sqrt{\frac{1 + \mathbf{a}_{\min}^2}{2}} \leq \frac{1}{\sqrt{1 + \prod_{j=1}^m \left(\prod_{i=1}^n \left(\frac{(1 - \mathbf{a}_{\mathbf{r}(i)\mathfrak{s}(j)}^2)}{(1 + \mathbf{a}_{\mathbf{r}(i)\mathfrak{s}(j)}^2)}\right)^{\mathcal{O}_i}\right)^{\mathcal{F}_j}}} \leq \sqrt{\frac{1 + \mathbf{a}_{\max}^2}{2}} \\
 &\Leftrightarrow \sqrt{1 + \mathbf{a}_{\min}^2} \leq \sqrt{\frac{2}{1 + \prod_{j=1}^m \left(\prod_{i=1}^n \left(\frac{(1 - \mathbf{a}_{\mathbf{r}(i)\mathfrak{s}(j)}^2)}{(1 + \mathbf{a}_{\mathbf{r}(i)\mathfrak{s}(j)}^2)}\right)^{\mathcal{O}_i}\right)^{\mathcal{F}_j}}} \leq \sqrt{1 + \mathbf{a}_{\max}^2} \\
 &\Leftrightarrow \sqrt{1 + \mathbf{a}_{\min}^2} - 1 \leq \sqrt{\frac{2}{1 + \prod_{j=1}^m \left(\prod_{i=1}^n \left(\frac{(1 - \mathbf{a}_{\mathbf{r}(i)\mathfrak{s}(j)}^2)}{(1 + \mathbf{a}_{\mathbf{r}(i)\mathfrak{s}(j)}^2)}\right)^{\mathcal{O}_i}\right)^{\mathcal{F}_j}}} - 1 \leq \sqrt{1 + \mathbf{a}_{\max}^2} - 1 \\
 &\Leftrightarrow \sqrt{\mathbf{a}_{\min}^2} \leq \sqrt{\frac{2}{1 + \prod_{j=1}^m \left(\prod_{i=1}^n \left(\frac{(1 - \mathbf{a}_{\mathbf{r}(i)\mathfrak{s}(j)}^2)}{(1 + \mathbf{a}_{\mathbf{r}(i)\mathfrak{s}(j)}^2)}\right)^{\mathcal{O}_i}\right)^{\mathcal{F}_j}}} - 1 \leq \sqrt{\mathbf{a}_{\max}^2} \\
 &\Leftrightarrow \mathbf{a}_{\min} \leq \sqrt{\frac{2}{1 + \prod_{j=1}^m \left(\prod_{i=1}^n \left(\frac{(1 - \mathbf{a}_{\mathbf{r}(i)\mathfrak{s}(j)}^2)}{(1 + \mathbf{a}_{\mathbf{r}(i)\mathfrak{s}(j)}^2)}\right)^{\mathcal{O}_i}\right)^{\mathcal{F}_j}}} - 1 \leq \mathbf{a}_{\max} \\
 &\mathbf{a}_{\min} \leq \frac{\sqrt{\prod_{j=1}^m \left(\prod_{i=1}^n (1 + \mathbf{a}_{\mathbf{r}(i)\mathfrak{s}(j)}^2)^{\mathcal{O}_i}\right)^{\mathcal{F}_j}} - \prod_{j=1}^m \left(\prod_{i=1}^n (1 - \mathbf{a}_{\mathbf{r}(i)\mathfrak{s}(j)}^2)^{\mathcal{O}_i}\right)^{\mathcal{F}_j}}{\sqrt{\prod_{j=1}^m \left(\prod_{i=1}^n (1 + \mathbf{a}_{\mathbf{r}(i)\mathfrak{s}(j)}^2)^{\mathcal{O}_i}\right)^{\mathcal{F}_j}} + \prod_{j=1}^m \left(\prod_{i=1}^n (1 - \mathbf{a}_{\mathbf{r}(i)\mathfrak{s}(j)}^2)^{\mathcal{O}_i}\right)^{\mathcal{F}_j}} \leq \mathbf{a}_{\max}.
 \end{aligned} \tag{22}$$

Let  $f(x) = \sqrt{(2 - x^2)/x^2}$ ,  $x \in ]0, 1]$ , then  $(d/dx)(f(x)) = (-2/x^3)\sqrt{x^2/(2 - x^2)} < 0$ . So,  $f(x)$  is decreasing function on  $]0, 1]$ .

As  $\mathbf{b}_{\min} \leq \mathbf{b}_{\mathbf{r}(i)\mathfrak{s}(j)} \leq \mathbf{b}_{\max}$ ,  $\forall i, j$ , so  $f(\mathbf{b}_{\max}) \leq f(\mathbf{b}_{\mathbf{r}(i)\mathfrak{s}(j)}) \leq f(\mathbf{b}_{\min})$  and  $\sqrt{(2 - \mathbf{b}_{\max}^2)/\mathbf{b}_{\max}^2} \leq \sqrt{(2 - \mathbf{b}_{\mathbf{r}(i)\mathfrak{s}(j)}^2)/\mathbf{b}_{\mathbf{r}(i)\mathfrak{s}(j)}^2} \leq \sqrt{(2 - \mathbf{b}_{\min}^2)/\mathbf{b}_{\min}^2}$ .

Let  $\mathcal{O}_i$  and  $\mathcal{F}_j$  represent the weight vectors such that  $\mathcal{O}_i > 0$ ,  $\sum_{i=1}^n \mathcal{O}_i = 1$ , and  $\mathcal{F}_j > 0$ ,  $\sum_{j=1}^m \mathcal{F}_j = 1$ , then we have

$$\begin{aligned}
 &\Leftrightarrow \sqrt{\prod_{j=1}^m \left(\prod_{i=1}^n \left(\frac{2 - \mathbf{b}_{\max}^2}{\mathbf{b}_{\max}^2}\right)^{\mathcal{O}_i}\right)^{\mathcal{F}_j}} \leq \sqrt{\prod_{j=1}^m \left(\prod_{i=1}^n \left(\frac{2 - \mathbf{b}_{\mathbf{r}(i)\mathfrak{s}(j)}^2}{\mathbf{b}_{\mathbf{r}(i)\mathfrak{s}(j)}^2}\right)^{\mathcal{O}_i}\right)^{\mathcal{F}_j}} \leq \sqrt{\prod_{j=1}^m \left(\prod_{i=1}^n \left(\frac{2 - \mathbf{b}_{\min}^2}{\mathbf{b}_{\min}^2}\right)^{\mathcal{O}_i}\right)^{\mathcal{F}_j}} \\
 &\Leftrightarrow \sqrt{\left(\left(\frac{2 - \mathbf{b}_{\max}^2}{\mathbf{b}_{\max}^2}\right)^{\sum_{i=1}^n \mathcal{O}_i}\right)^{\sum_{j=1}^m \mathcal{F}_j}} \leq \sqrt{\prod_{j=1}^m \left(\prod_{i=1}^n \left(\frac{2 - \mathbf{b}_{\mathbf{r}(i)\mathfrak{s}(j)}^2}{\mathbf{b}_{\mathbf{r}(i)\mathfrak{s}(j)}^2}\right)^{\mathcal{O}_i}\right)^{\mathcal{F}_j}} \leq \sqrt{\left(\left(\frac{2 - \mathbf{b}_{\min}^2}{\mathbf{b}_{\min}^2}\right)^{\sum_{i=1}^n \mathcal{O}_i}\right)^{\sum_{j=1}^m \mathcal{F}_j}}
 \end{aligned}$$

$$\begin{aligned}
 &\Leftrightarrow \sqrt{1 + \left(\frac{2 - \mathfrak{b}_{\max}^2}{\mathfrak{b}_{\max}^2}\right)} \leq \sqrt{1 + \prod_{j=1}^m \left(\prod_{i=1}^n \left(\frac{2 - \mathfrak{b}_{\mathfrak{r}(i)\mathfrak{s}(j)}^2}{\mathfrak{b}_{\mathfrak{r}(i)\mathfrak{s}(j)}^2}\right)^{\mathcal{O}_i}\right)^{\mathcal{F}_j}} \leq \sqrt{1 + \left(\frac{2 - \mathfrak{b}_{\min}^2}{\mathfrak{b}_{\min}^2}\right)} \\
 &\Leftrightarrow \sqrt{\frac{2}{\mathfrak{b}_{\max}^2}} \leq \sqrt{1 + \prod_{j=1}^m \left(\prod_{i=1}^n \left(\frac{2 - \mathfrak{b}_{\mathfrak{r}(i)\mathfrak{s}(j)}^2}{\mathfrak{b}_{\mathfrak{r}(i)\mathfrak{s}(j)}^2}\right)^{\mathcal{O}_i}\right)^{\mathcal{F}_j}} \leq \sqrt{\frac{2}{\mathfrak{b}_{\min}^2}} \\
 &\Leftrightarrow \sqrt{\frac{\mathfrak{b}_{\min}^2}{2}} \leq \frac{1}{\sqrt{1 + \prod_{j=1}^m \left(\prod_{i=1}^n \left(\frac{2 - \mathfrak{b}_{\mathfrak{r}(i)\mathfrak{s}(j)}^2}{\mathfrak{b}_{\mathfrak{r}(i)\mathfrak{s}(j)}^2}\right)^{\mathcal{O}_i}\right)^{\mathcal{F}_j}}} \leq \sqrt{\frac{\mathfrak{b}_{\max}^2}{2}} \tag{23} \\
 &\Leftrightarrow \mathfrak{b}_{\min} \leq \sqrt{\frac{2}{1 + \prod_{j=1}^m \left(\prod_{i=1}^n \left(\frac{2 - \mathfrak{b}_{\mathfrak{r}(i)\mathfrak{s}(j)}^2}{\mathfrak{b}_{\mathfrak{r}(i)\mathfrak{s}(j)}^2}\right)^{\mathcal{O}_i}\right)^{\mathcal{F}_j}}} \leq \mathfrak{b}_{\max} \\
 &\mathfrak{b}_{\min} \leq \frac{\sqrt{2 \prod_{j=1}^m \left(\prod_{i=1}^n \left(\mathfrak{b}_{\mathfrak{r}(i)\mathfrak{s}(j)}^2\right)^{\mathcal{O}_i}\right)^{\mathcal{F}_j}}}{\sqrt{\prod_{j=1}^m \left(\prod_{i=1}^n \left(2 - \mathfrak{b}_{\mathfrak{r}(i)\mathfrak{s}(j)}^2\right)^{\mathcal{O}_i}\right)^{\mathcal{F}_j} + \prod_{j=1}^m \left(\prod_{i=1}^n \left(\mathfrak{b}_{\mathfrak{r}(i)\mathfrak{s}(j)}^2\right)^{\mathcal{O}_i}\right)^{\mathcal{F}_j}}} \leq \mathfrak{b}_{\max}.
 \end{aligned}$$

Let

$$\text{PFSEOWA}(H_{11}, H_{12}, \dots, H_{nm}) = \mathcal{H}. \tag{24}$$

Then, equations (22) and (23) can be written as

$\mathfrak{a}_{\min} \leq \mathfrak{a} \leq \mathfrak{a}_{\max}$  and  $\mathfrak{b}_{\min} \leq \mathfrak{b} \leq \mathfrak{b}_{\max}$ . Thus,  $S(H) = \mathfrak{a}^2 - \mathfrak{b}^2 \leq \mathfrak{a}_{\max}^2 - \mathfrak{b}_{\min}^2 = S(H_{\max})$  and

$$S(H) = \mathfrak{a}^2 - \mathfrak{b}^2 \geq \mathfrak{a}_{\min}^2 - \mathfrak{b}_{\max}^2 = S(H_{\min}). \tag{25}$$

If  $S(H) < S(H_{\max})$  and  $S(H) > S(H_{\min})$ , then we have

$$H_{\min} < \text{PFSEOWA}(H_{11}, H_{12}, \dots, H_m) < H_{\max}. \tag{26}$$

If  $S(H) = S(H_{\max})$ , then we have  $\mathfrak{a}^2 = \mathfrak{a}_{\max}^2$  and  $\mathfrak{b}^2 = \mathfrak{b}_{\max}^2$ . Thus,  $A(H) = \mathfrak{a}^2 + \mathfrak{b}^2 = A(H_{\max})$ . Therefore,

$$\text{PFSEOWA}(H_{11}, H_{12}, \dots, H_{nm}) = H_{\max}. \tag{27}$$

If  $S(H) = S(H_{\min})$ , then we have  $\mathfrak{a}^2 - \mathfrak{b}^2 = \mathfrak{a}_{\min}^2 - \mathfrak{b}_{\min}^2$ .  $\mathfrak{a}^2 = \mathfrak{a}_{\min}^2$  and  $\mathfrak{b}^2 = \mathfrak{b}_{\min}^2$ .

Thus,  $A(H)\mathfrak{a}^2 + \mathfrak{b}^2 = \mathfrak{a}_{\min}^2 + \mathfrak{b}_{\min}^2 = A(H_{\min})$ . Therefore,

$$\text{PFSEOWA}(H_{11}, H_{12}, \dots, H_{nm}) = H_{\min}. \tag{28}$$

So, using (26)–(28), we get

$$H_{\min} \leq \text{PFSEOWA}(H_{11}, H_{12}, \dots, H_{nm}) \leq H_{\max}. \tag{29} \quad \square$$

**3.1.3. Homogeneity.** Prove that  $\text{PFSEOWA}(H_{11}, H_{12}, \dots, H_{nm}) = \partial$ ,  $\text{PFSEOWA}(H_{11}, H_{12}, \dots, H_{nm})$  for any positive real number  $\partial$ .

*Proof.* Let  $H_{ij}$  be a PFSN and  $\partial > 0$ . Then, we know that

$$\partial H_{ij} = \left\langle \frac{\sqrt{(1 + \mathfrak{a}^2)^\partial - (1 - \mathfrak{a}^2)^\partial}}{\sqrt{(1 + \mathfrak{a}^2)^\partial + (1 - \mathfrak{a}^2)^\partial}}, \frac{\sqrt{2(\mathfrak{b}^2)^\partial}}{\sqrt{(2 - \mathfrak{b}^2)^\partial + (\mathfrak{b}^2)^\partial}} \right\rangle. \tag{30}$$

So,

$$\text{PFSEOWA}(H_{11}, H_{12}, \dots, H_{nm})$$

$$\begin{aligned}
 &= \left\langle \frac{\sqrt{\prod_{j=1}^m \left(\prod_{i=1}^n \left(1 + \mathfrak{a}_{\mathfrak{r}(i)\mathfrak{s}(j)}^2\right)^{\mathcal{O}_i}\right)^{\mathcal{F}_j} - \prod_{j=1}^m \left(\prod_{i=1}^n \left(1 - \mathfrak{a}_{\mathfrak{r}(i)\mathfrak{s}(j)}^2\right)^{\mathcal{O}_i}\right)^{\mathcal{F}_j}}}{\sqrt{\prod_{j=1}^m \left(\prod_{i=1}^n \left(1 + \mathfrak{a}_{\mathfrak{r}(i)\mathfrak{s}(j)}^2\right)^{\mathcal{O}_i}\right)^{\mathcal{F}_j} + \prod_{j=1}^m \left(\prod_{i=1}^n \left(1 - \mathfrak{a}_{\mathfrak{r}(i)\mathfrak{s}(j)}^2\right)^{\mathcal{O}_i}\right)^{\mathcal{F}_j}}}, \right. \\
 &\quad \left. \frac{\sqrt{2 \prod_{j=1}^m \left(\prod_{i=1}^n \left(\mathfrak{b}_{\mathfrak{r}(i)\mathfrak{s}(j)}^2\right)^{\mathcal{O}_i}\right)^{\mathcal{F}_j}}}{\sqrt{\prod_{j=1}^m \left(\prod_{i=1}^n \left(2 - \mathfrak{b}_{\mathfrak{r}(i)\mathfrak{s}(j)}^2\right)^{\mathcal{O}_i}\right)^{\mathcal{F}_j} + \prod_{j=1}^m \left(\prod_{i=1}^n \left(\mathfrak{b}_{\mathfrak{r}(i)\mathfrak{s}(j)}^2\right)^{\mathcal{O}_i}\right)^{\mathcal{F}_j}}}\right\rangle
 \end{aligned}$$

$$\begin{aligned}
 &= \left\langle \frac{\sqrt{\left(\prod_{j=1}^m \left(\prod_{i=1}^n (1 + \alpha_{\mathbf{r}(i)\mathfrak{s}(j)}^2)^{\mathcal{O}_i}\right)^{\mathcal{F}_j}\right)^{\bar{\delta}}} - \left(\prod_{j=1}^m \left(\prod_{i=1}^n (1 - \alpha_{\mathbf{r}(i)\mathfrak{s}(j)}^2)^{\mathcal{O}_i}\right)^{\mathcal{F}_j}\right)^{\bar{\delta}}}{\sqrt{\left(\prod_{j=1}^m \left(\prod_{i=1}^n (1 + \alpha_{\mathbf{r}(i)\mathfrak{s}(j)}^2)^{\mathcal{O}_i}\right)^{\mathcal{F}_j}\right)^{\bar{\delta}} + \left(\prod_{j=1}^m \left(\prod_{i=1}^n (1 - \alpha_{\mathbf{r}(i)\mathfrak{s}(j)}^2)^{\mathcal{O}_i}\right)^{\mathcal{F}_j}\right)^{\bar{\delta}}}} \right. \\
 &\quad \left. \frac{\sqrt{\left(2 \prod_{j=1}^m \left(\prod_{i=1}^n (\mathfrak{b}_{\mathbf{r}(i)\mathfrak{s}(j)}^2)^{\mathcal{O}_i}\right)^{\mathcal{F}_j}\right)^{\bar{\delta}}}}{\sqrt{\left(\prod_{j=1}^m \left(\prod_{i=1}^n (2 - \mathfrak{b}_{\mathbf{r}(i)\mathfrak{s}(j)}^2)^{\mathcal{O}_i}\right)^{\mathcal{F}_j}\right)^{\bar{\delta}} + \left(\prod_{j=1}^m \left(\prod_{i=1}^n (\mathfrak{b}_{\mathbf{r}(i)\mathfrak{s}(j)}^2)^{\mathcal{O}_i}\right)^{\mathcal{F}_j}\right)^{\bar{\delta}}}} \right\rangle \\
 &= \partial \text{PFSEOWA } (H_{11}, H_{12}, \dots, H_{mm}).
 \end{aligned} \tag{31}$$

### 4. Proposed Multiattribute Group Decision-Making Approach

This section has developed a DM approach for solving MAGDM problems based on the proposed PFSEOWA operator and its application.

**4.1. Proposed Approach.** Let  $S = \{S^1, S^2, S^3, \dots, S^s\}$  be the set of  $s$  alternatives,  $W = \{W_1, W_2, W_3, \dots, W_r\}$  be the set of  $r$  experts (decision-makers), and  $\mathbb{N} = \{t_1, t_2, t_3, \dots, t_m\}$  be the set of  $m$  attributes. Let weighted vector of experts  $W (i = 1, 2, 3, \dots, r)$  be  $O = (\mathcal{O}_1, \mathcal{O}_2, \mathcal{O}_3, \dots, \mathcal{O}_n)^T$  such that  $\mathcal{O}_i > 0$ ,  $\sum_{i=1}^n \mathcal{O}_i = 1$ . Let weight vector of attributes  $t_i (i = 1, 2, 3, \dots, m)$  be  $\mathcal{F} = (\mathcal{F}_1, \mathcal{F}_2, \mathcal{F}_3, \dots, \mathcal{F}_n)^T$  such that  $\mathcal{F}_j > 0$ ,  $\sum_{j=1}^n \mathcal{F}_j = 1$ . Team of experts  $O_i (i = 1, 2, 3, \dots, r)$  consider the alternatives  $S^i (i = 1, 2, 3, \dots, s)$  for attributes in the form of PFSNs such as  $F = (\mathcal{H}_{ij})_{n \times m} = (\alpha_{ij}, \mathfrak{b}_{ij})_{n \times m}$  where  $0 \leq \alpha_{ij}, \mathfrak{b}_{ij} \leq 1$  and  $0 \leq \alpha_{ij}^2, \mathfrak{b}_{ij}^2 \leq 1 \ \forall i, j$  are given in Tables 1–5.

We will apply the proposed PFSEOWA operator to solve the MAGDM problem, which has the following steps:

*Step 1.* Obtain decision matrices  $F = (H_{ij})_{n \times m}$  in the form of PFSNs for alternatives relative to attributes.

*Step 2.* Find the associated ordered position matrix by using the score function.

*Step 3.* By using the normalization formula, normalize the decision matrix to convert the rating value of cost type parameters into benefit type parameters.

$$M_{ij} = \begin{cases} \mathcal{H}_{ij}^c = (b_{ij}, \alpha_{ij}) \text{ cost type parameter,} \\ \mathcal{H}_{ij} = (\alpha_{ij}, b) \text{ benefit type parameter.} \end{cases} \tag{32}$$

*Step 4.* Use the developed PFSEOWA operator to aggregate the PFSNs  $H_{ij}$  for each alternative  $S = \{S^1, S^2, S^3, \dots, S^s\}$  into the decision matrix  $H_{ij}$ .

*Step 5.* Calculate the score values of  $H$  for all alternatives by using equation (7).

*Step 6.* Select the alternative which has the maximum score value and examine the ranking.

**4.2. Case Study.** The problem of supplier selection is both logically and practically imperative. The best quality supplier is the foundation of supply chain operation management, realizing low-cost efficiency, and an important issue for enterprises. Including eco-friendly elements and other sustainable and progressive features in the supplier selection process makes accurate supplier selection complex and multidimensional. According to the selection of activities that are beneficial to the environment or the society, supplier selection is often referred to as “sustainable supplier selection” in the literature. This is a multifaceted and multidimensional problem with inconsistent standards, and the evaluation process needs to pay attention to multiple perceptions. From these points of view, the issue of supplier selection is often reserved as a “reference” problem in the literature, in which multistandard decision support methods have been widely used. The problem of selecting and evaluating sustainable suppliers has been solved in various tasks. Srivastava [40] proposed intensive stipulations on SSCM, which explains environmental intelligence activity in SSCM, which included construction and material procurement, selection, manufacturing process, packaging, and sanitation items supplied to consumers.

The parable that greening will cause sales to decrease and sophisticated operational expenses has vanished as numerous corporations have now grasped that they will not be able to gratify the customer’s craving to combine ecological safety strategies into their desires SSCM and turn it into advanced revenues. There is a connection among a healthier atmosphere where various corporations grow sustainability and economic inducements. Business grown perceptions obsessed by SSCM and determining zones can change how to work to raise revenue. Green logistics can support many diminishing productions such as carbon dioxide and CO. Consumption comprising nonfossil causes of energy alleviates haze that affects our environs irritating to breathe. Quite a lot of measures of fossil fuels have been damaging the atmosphere because of prosperity. For example, for marine life, air travel will also affect adulteration because of diesel engine consumption. In the literature, we explored the aspects for indicating sustainable suppliers consistent with different scientists. In this article, the assortment values for

□

TABLE 1: Standards for the selection of the appropriate supplier in SSCM.

	Criteria	Definition
$t_1$	Quality of service	Rejection ratio, upgrading practice, assurance exposure, and human rights, and advantage guarantee
$t_2$	Pollution control	Reducing the waste created and unconstrained in the atmosphere
$t_3$	Price	Supplier's market, buyers' market, supply, demand
$t_4$	Environmental efficiency	Eco-design stipulations, compounds containing ozone-depleting

TABLE 2: PFS decision matrix for  $S^1$ .

	$t_1$	$t_2$	$t_3$	$t_4$
$O^1$	(0.8, 0.5)	(0.7, 0.5)	(0.6, 0.4)	(0.7, 0.4)
$O^2$	(0.6, 0.5)	(0.9, 0.1)	(0.7, 0.3)	(0.4, 0.5)
$O^3$	(0.8, 0.4)	(0.7, 0.5)	(0.6, 0.4)	(0.3, 0.5)
$O^4$	(0.7, 0.3)	(0.6, 0.5)	(0.4, 0.5)	(0.5, 0.7)

TABLE 4: PFS decision matrix for  $S^3$ .

	$t_1$	$t_2$	$t_3$	$t_4$
$O^1$	(0.7, 0.5)	(0.7, 0.4)	(0.6, 0.4)	(0.8, 0.4)
$O^2$	(0.6, 0.6)	(0.9, 0.1)	(0.6, 0.3)	(0.4, 0.5)
$O^3$	(0.8, 0.3)	(0.7, 0.2)	(0.6, 0.5)	(0.4, 0.5)
$O^4$	(0.7, 0.6)	(0.3, 0.5)	(0.4, 0.5)	(0.5, 0.6)

TABLE 3: PFS decision matrix for  $S^2$ .

	$t_1$	$t_2$	$t_3$	$t_4$
$O^1$	(0.7, 0.5)	(0.8, 0.5)	(0.6, 0.4)	(0.8, 0.4)
$O^2$	(0.6, 0.3)	(0.9, 0.2)	(0.8, 0.3)	(0.7, 0.5)
$O^3$	(0.5, 0.4)	(0.6, 0.5)	(0.6, 0.3)	(0.3, 0.6)
$O^4$	(0.7, 0.4)	(0.6, 0.4)	(0.7, 0.5)	(0.5, 0.7)

TABLE 5: PFS decision matrix for  $S^4$ .

	$t_1$	$t_2$	$t_3$	$t_4$
$O^1$	(0.8, 0.5)	(0.7, 0.5)	(0.7, 0.4)	(0.6, 0.4)
$O^2$	(0.6, 0.4)	(0.8, 0.1)	(0.7, 0.3)	(0.4, 0.7)
$O^3$	(0.7, 0.4)	(0.7, 0.5)	(0.6, 0.4)	(0.3, 0.5)
$O^4$	(0.6, 0.3)	(0.6, 0.3)	(0.8, 0.5)	(0.5, 0.6)

sustainable suppliers that have been considered are given in Table 1.

This example of sustainable supplier selection analyzes papers [41–43] and uses review papers [44–47]. We decided to extract the following four essential criteria. These are  $t_1$ : quality of service;  $t_2$ : pollution control;  $t_3$ : price;  $t_4$ : environmental efficiency.

Let  $\{S^1, S^2, S^3, S^4, S^5\}$  be a set of alternatives and  $\{t_1, t_2, t_3, t_4\}$  be a set of attributes with the weight vector  $\mathcal{F} = (0.2, 0.2, 0.2, 0.4)^T$ . Here,  $t_1$  and  $t_3$  are cost type parameters and  $t_2$  and  $t_4$  are benefit type parameters. A team of four experts  $O_r$  ( $r = 1, 2, 3, 4$ ) with weights  $\mathcal{O} = (0.1, 0.3, 0.3, 0.3)^T$  decided which supplier is most suitable.

*Step 1.* According to the expert's opinion, Pythagorean fuzzy soft decision matrices for all alternatives are given in Tables 2–6.

*Step 2.* Find ordered Pythagorean fuzzy soft decision matrices for all alternatives according to the expert's opinion which are given in Tables 7–11.

*Step 3.* Because  $t_1$  and  $t_3$  are cost type parameters, utilize the normalization formula to obtain normalized ordered Pythagorean fuzzy soft decision matrices which are given in Tables 12–16.

*Step 4.* Applying the proposed PFSEOWA operator on the acquired data (Tables 12–16), then we get the opinion of decision-makers for alternatives in the form of PFSN such as  $H_1 = \langle 0.5423, 0.5345 \rangle$ ,  $H_2 = \langle 0.5601, 0.6118 \rangle$ ,  $H_3 = \langle 0.4930, 0.5001 \rangle$ ,  $H_4 = \langle 0.5233, 0.6071 \rangle$ , and  $H_5 = \langle 0.5917, 0.5412 \rangle$ .

*Step 5.* Use equation (7),  $\mathfrak{S} = \alpha_{ij}^2 - b_{ij}^2$  to calculate the score values for all alternatives

TABLE 6: PFS decision matrix for  $S^5$ .

	$t_1$	$t_2$	$t_3$	$t_4$
$O^1$	(0.6, 0.5)	(0.6, 0.5)	(0.6, 0.4)	(0.5, 0.4)
$O^2$	(0.6, 0.4)	(0.8, 0.1)	(0.8, 0.3)	(0.7, 0.5)
$O^3$	(0.6, 0.4)	(0.7, 0.3)	(0.6, 0.4)	(0.6, 0.5)
$O^4$	(0.7, 0.4)	(0.7, 0.5)	(0.4, 0.5)	(0.5, 0.8)

$$\mathfrak{S}(H_1) = 0.0083, \mathfrak{S}(H_2) = -0.0605, \mathfrak{S}(H_3) = 0.0070$$

$$\text{and } \mathfrak{S}(H_4) = -0.0947, \mathfrak{S}(H_5) = 0.0572.$$

*Step 6.* After calculation, we get the ranking of alternatives  $\mathfrak{S}(H_5) > \mathfrak{S}(H_1) > \mathfrak{S}(H_3) > \mathfrak{S}(H_2) > \mathfrak{S}(H_4)$ . So,  $S^5 > S^1 > S^3 > S^2 > S^4$ .

Hence, the best alternative is  $S^5$ .

### 5. Comparative Studies

To show the effectiveness of the proposed methods, a comparison with some existing techniques offered approach is presented in the following section.

*5.1. Comparative Analysis.* To verify the effectiveness of the proposed method, a brief comparative analysis has been discussed with some approaches under the considered environment. A summary of all results is given in Table 17. In this work, aggregation operator such as PFSEOWA operators is proposed to fuse evaluation information, and then by using the score function, the ranking of alternatives is evaluated. Furthermore, if only one parameter is supposed rather than one parameter, the PFSS theory reduces to PFS. Thus, PFSS theory is the generalized form of Pythagorean fuzzy set (PFS) theory. Hence, admittedly, the proposed

TABLE 7: Ordered PFS decision matrix for  $S^1$ .

	$t_1$	$t_2$	$t_3$	$t_4$
$O^1$	(0.8, 0.5)	(0.7, 0.5)	(0.6, 0.4)	(0.7, 0.4)
$O^2$	(0.6, 0.5)	(0.9, 0.1)	(0.7, 0.3)	(0.4, 0.5)
$O^3$	(0.8, 0.4)	(0.7, 0.5)	(0.6, 0.4)	(0.3, 0.5)
$O^4$	(0.7, 0.3)	(0.6, 0.5)	(0.4, 0.5)	(0.5, 0.7)

TABLE 8: Ordered PFS decision matrix for  $S^2$ .

	$t_1$	$t_2$	$t_3$	$t_4$
$O^1$	(0.7, 0.5)	(0.8, 0.5)	(0.6, 0.4)	(0.8, 0.4)
$O^2$	(0.6, 0.3)	(0.9, 0.2)	(0.8, 0.3)	(0.7, 0.5)
$O^3$	(0.5, 0.4)	(0.6, 0.5)	(0.6, 0.3)	(0.3, 0.6)
$O^4$	(0.7, 0.4)	(0.6, 0.4)	(0.7, 0.5)	(0.5, 0.7)

TABLE 9: Ordered PFS decision matrix for  $S^3$ .

	$t_1$	$t_2$	$t_3$	$t_4$
$O^1$	(0.7, 0.5)	(0.7, 0.4)	(0.6, 0.4)	(0.8, 0.4)
$O^2$	(0.6, 0.6)	(0.9, 0.1)	(0.6, 0.3)	(0.4, 0.5)
$O^3$	(0.8, 0.3)	(0.7, 0.2)	(0.6, 0.5)	(0.4, 0.5)
$O^4$	(0.7, 0.6)	(0.3, 0.5)	(0.4, 0.5)	(0.5, 0.6)

TABLE 10: Ordered PFS decision matrix for  $S^4$ .

	$t_1$	$t_2$	$t_3$	$t_4$
$O^1$	(0.8, 0.5)	(0.7, 0.5)	(0.7, 0.4)	(0.6, 0.4)
$O^2$	(0.6, 0.4)	(0.8, 0.1)	(0.7, 0.3)	(0.4, 0.7)
$O^3$	(0.7, 0.4)	(0.7, 0.5)	(0.6, 0.4)	(0.3, 0.5)
$O^4$	(0.6, 0.3)	(0.6, 0.3)	(0.8, 0.5)	(0.5, 0.6)

TABLE 11: Ordered PFS decision matrix for  $S^5$ .

	$t_1$	$t_2$	$t_3$	$t_4$
$O^1$	(0.6, 0.5)	(0.6, 0.5)	(0.6, 0.4)	(0.5, 0.4)
$O^2$	(0.6, 0.4)	(0.8, 0.1)	(0.8, 0.3)	(0.7, 0.5)
$O^3$	(0.6, 0.4)	(0.7, 0.3)	(0.6, 0.4)	(0.6, 0.5)
$O^4$	(0.7, 0.4)	(0.7, 0.5)	(0.4, 0.5)	(0.5, 0.8)

TABLE 12: Normalized ordered PFS decision matrix for  $S^1$ .

	$t_1$	$t_2$	$t_3$	$t_4$
$O^1$	(0.5, 0.8)	(0.7, 0.5)	(0.4, 0.6)	(0.7, 0.4)
$O^2$	(0.5, 0.6)	(0.9, 0.1)	(0.3, 0.7)	(0.4, 0.5)
$O^3$	(0.4, 0.8)	(0.7, 0.5)	(0.4, 0.6)	(0.3, 0.5)
$O^4$	(0.3, 0.7)	(0.6, 0.5)	(0.5, 0.4)	(0.5, 0.7)

TABLE 13: Normalized ordered PFS decision matrix for  $S^2$ .

	$t_1$	$t_2$	$t_3$	$t_4$
$O^1$	(0.5, 0.7)	(0.8, 0.5)	(0.4, 0.6)	(0.8, 0.4)
$O^2$	(0.3, 0.6)	(0.9, 0.2)	(0.3, 0.8)	(0.7, 0.5)
$O^3$	(0.4, 0.5)	(0.6, 0.5)	(0.3, 0.6)	(0.3, 0.6)
$O^4$	(0.4, 0.7)	(0.6, 0.4)	(0.5, 0.7)	(0.5, 0.7)

TABLE 14: Normalized ordered PFS decision matrix for  $S^3$ .

	$t_1$	$t_2$	$t_3$	$t_4$
$O^1$	(0.5, 0.7)	(0.7, 0.4)	(0.4, 0.6)	(0.8, 0.4)
$O^2$	(0.6, 0.6)	(0.9, 0.1)	(0.3, 0.6)	(0.4, 0.5)
$O^3$	(0.3, 0.8)	(0.7, 0.2)	(0.5, 0.6)	(0.4, 0.5)
$O^4$	(0.6, 0.7)	(0.3, 0.5)	(0.5, 0.4)	(0.5, 0.6)

TABLE 15: Normalized ordered PFS decision matrix for  $S^4$ .

	$t_1$	$t_2$	$t_3$	$t_4$
$O^1$	(0.5, 0.8)	(0.7, 0.5)	(0.4, 0.7)	(0.6, 0.4)
$O^2$	(0.4, 0.6)	(0.8, 0.1)	(0.3, 0.7)	(0.4, 0.7)
$O^3$	(0.4, 0.7)	(0.7, 0.5)	(0.4, 0.6)	(0.3, 0.5)
$O^4$	(0.3, 0.6)	(0.6, 0.3)	(0.5, 0.8)	(0.5, 0.6)

TABLE 16: Normalized PFS ordered decision matrix for  $S^5$ .

	$t_1$	$t_2$	$t_3$	$t_4$
$O^1$	(0.5, 0.6)	(0.6, 0.5)	(0.4, 0.6)	(0.5, 0.4)
$O^2$	(0.4, 0.6)	(0.8, 0.1)	(0.3, 0.8)	(0.7, 0.5)
$O^3$	(0.4, 0.6)	(0.7, 0.3)	(0.4, 0.6)	(0.6, 0.5)
$O^4$	(0.4, 0.7)	(0.7, 0.5)	(0.5, 0.4)	(0.5, 0.8)

TABLE 17: Comparison of proposed operators with some existing operators.

Approach	$S^1$	$S^2$	$S^3$	$S^4$	$S^5$	Alternatives ranking
Proposed PFSEOWA operator	0.0083	-0.0605	0.0070	-0.0947	0.0572	$S^5 > S^1 > S^3 > S^2 > S^4$
PFSWA [30]	0.0293	0.0369	0.0783	-0.0938	0.0858	$S^5 > S^3 > S^1 > S^4 > S^2$
PFSWG [30]	-0.3306	-0.1383	-0.1092	-0.1661	-0.5957	$S^5 > S^3 > S^1 > S^4 > S^2$
PFSEWA [48]	0.0039	-0.0376	0.0433	-0.0179	0.0644	$S^5 > S^3 > S^1 > S^4 > S^2$
PFSEWG [49]	-0.4975	-0.1204	-0.1775	-0.0778	-0.1211	$S^5 > S^2 > S^4 > S^3 > S^1$

operator in this work is more powerful, reliable, and successful based on the facts mentioned above.

### 6. Conclusion

This manuscript recommends a novel technique for picking sustainable suppliers under PFSS. The deficiency of deliberation of the connection among attributes and ambiguous situations may disturb the inferences of some MAGDM difficulties. The core objective of this research is to develop a PFSEOWA operator to overcome these deficiencies. Moreover, some fundamental properties have been presented, such as idempotency, homogeneity, and boundedness for developed Einstein AO. Furthermore, a DM approach has been established to resolve MAGDM difficulties based on the presented operator. To ensure the strength of the established technique, a comprehensive numerical example has been given to select the sustainable supplier in SSCM. A comparative analysis with some existing approaches is presented. Finally, based on obtained results, it has been concluded that the proposed method in this research is the most feasible and successful method for the MAGDM problem. The future studies will essence on developing more decision-making methods utilizing other operators such as Einstein hybrid geometric and Einstein

hybrid averaging operators under the environment of PFSS. We have confidence that nearby these substantial growth and prospects will be helpful to consider world climate-centric organizational research fields.

### Data Availability

No data were used to support this study.

### Conflicts of Interest

The authors declare that they have no conflicts of interest.

### References

- [1] L. A. Zadeh, "Fuzzy sets," *Information and Control*, vol. 8, no. 3, pp. 338–353, 1965.
- [2] K. T. Atanassov, "Intuitionistic fuzzy sets," *Fuzzy Sets and Systems*, vol. 20, no. 1, pp. 87–96, 1986.
- [3] Z. Zeshui Xu, "Intuitionistic fuzzy aggregation operators," *IEEE Transactions on Fuzzy Systems*, vol. 15, no. 6, pp. 1179–1187, 2007.
- [4] W. Wang and X. Liu, "Intuitionistic fuzzy geometric aggregation operators based on Einstein operations," *International Journal of Intelligent Systems*, vol. 26, no. 11, pp. 1049–1075, 2011.



- [5] K. Atanassov and G. Gargov, "Interval valued intuitionistic fuzzy sets," *Fuzzy Sets and Systems*, vol. 31, no. 3, pp. 343–349, 1989.
- [6] R. R. Yager, "Pythagorean membership grades in multicriteria decision making," *IEEE Transactions on Fuzzy Systems*, vol. 22, no. 4, pp. 958–965, 2013.
- [7] K. Rahman, A. Ali, M. Shakeel, M. A. Khan, and M. Ullah, "Pythagorean fuzzy weighted averaging aggregation operator and its application to decision making theory," *The Nucleus*, vol. 54, no. 3, pp. 190–196, 2017.
- [8] D. S. Pamučar and L. M. Savin, "Multiple-criteria model for optimal off-road vehicle selection for passenger transportation: BWM-COPRAS model," *Vojnotehnički Glasnik*, vol. 68, no. 1, pp. 28–64, 2020.
- [9] K. Rahman, S. Abdullah, A. Ali, and F. Amin, "Pythagorean fuzzy ordered weighted averaging aggregation operator and their application to multiple attribute group decision-making," *EURO Journal on Decision Processes*, vol. 8, no. 1, pp. 61–77, 2020.
- [10] L. Wang and N. Li, "Pythagorean fuzzy interaction power Bonferroni mean aggregation operators in multiple attribute decision making," *International Journal of Intelligent Systems*, vol. 35, no. 1, pp. 150–183, 2020.
- [11] M. Deveci, L. Eriskin, and M. Karatas, "A survey on recent applications of pythagorean fuzzy sets: a state-of-the-art between 2013 and 2020," *Pythagorean Fuzzy Sets*, pp. 3–38, Springer, Berlin, Germany, 2021.
- [12] H. Garg, "Generalised Pythagorean fuzzy geometric interactive aggregation operators using Einstein operations and their application to decision making," *Journal of Experimental & Theoretical Artificial Intelligence*, vol. 30, no. 6, pp. 763–794, 2018.
- [13] Z. Ali, T. Mahmood, T. Mahmood, K. Ullah, and Q. Khan, "Einstein geometric aggregation operators using a novel complex interval-valued pythagorean fuzzy setting with application in green supplier chain management," *Reports in Mechanical Engineering*, vol. 2, no. 1, pp. 105–134, 2021.
- [14] A. Alosta, O. Elmansuri, and I. Badi, "Resolving a location selection problem by means of an integrated AHP-RAFSI approach," *Reports in Mechanical Engineering*, vol. 2, no. 1, pp. 135–142, 2021.
- [15] T. Milosevic, D. Pamucar, and P. Chatterjee, "Model for selecting a route for the transport of hazardous materials using a fuzzy logic system," *Military Technical Courier*, vol. 69, no. 2, pp. 355–390, 2021.
- [16] D. Molodtsov, "Soft set theory—first results," *Computers & Mathematics with Applications*, vol. 37, no. 4-5, pp. 19–31, 1999.
- [17] P. K. Maji, R. Biswas, and A. R. Roy, "Soft set theory," *Computers & Mathematics with Applications*, vol. 45, no. 4-5, pp. 555–562, 2003.
- [18] P. K. Maji, A. R. Roy, and R. Biswas, "An application of soft sets in a decision making problem," *Computers & Mathematics with Applications*, vol. 44, no. 8-9, pp. 1077–1083, 2002.
- [19] P. K. Maji, R. Biswas, and A. R. Roy, "Intuitionistic fuzzy soft sets," *Journal of Fuzzy Mathematics*, vol. 9, no. 3, pp. 677–692, 2001.
- [20] R. M. Zulqarnain, X. L. Xin, M. Saqlain, and W. A. Khan, "TOPSIS method based on the correlation coefficient of interval-valued intuitionistic fuzzy soft sets and aggregation operators with their application in decision-making," *Journal of Mathematics*, vol. 2021, Article ID 6656858, 16 pages, 2021.
- [21] M. Zulqarnain and F. Dayan, "Selection of best alternative for an automotive company by intuitionistic fuzzy TOPSIS method," *International Journal of Scientific & Technology Research*, vol. 6, no. 10, pp. 126–132, 2017.
- [22] R. Muhammad Zulqarnain, X. L. Xin, X. Long Xin, and M. Saeed, "Extension of TOPSIS method under intuitionistic fuzzy hypersoft environment based on correlation coefficient and aggregation operators to solve decision making problem," *AIMS Mathematics*, vol. 6, no. 3, pp. 2732–2755, 2021.
- [23] H. Garg and R. Arora, "Generalized intuitionistic fuzzy soft power aggregation operator based on t-norm and their application in multicriteria decision-making," *International Journal of Intelligent Systems*, vol. 34, no. 2, pp. 215–246, 2019.
- [24] X. Peng, Y. Yang, and J. Song, "Pythagoren fuzzy soft set and its application," *Computer Engineering*, vol. 41, no. 7, pp. 224–229, 2015.
- [25] T. M. Athira, S. J. John, S. Jacob John, and H. Garg, "A novel entropy measure of pythagorean fuzzy soft sets," *AIMS Mathematics*, vol. 5, no. 2, pp. 1050–1061, 2020.
- [26] T. M. Athira, S. J. John, and H. Garg, "Entropy and distance measures of pythagorean fuzzy soft sets and their applications," *Journal of Intelligent and Fuzzy Systems*, vol. 37, no. 3, pp. 4071–4084, 2019.
- [27] K. Naeem, M. Riaz, X. Peng, and D. Afzal, "Pythagorean fuzzy soft MCGDM methods based on TOPSIS, VIKOR and aggregation operators," *Journal of Intelligent and Fuzzy Systems*, vol. 37, no. 5, pp. 6937–6957, 2019.
- [28] M. Riaz, K. Naeem, and D. Afzal, "Pythagorean m-polar fuzzy soft sets with TOPSIS method for MCGDM," *Punjab University Journal of Mathematics*, vol. 52, no. 3, pp. 21–46, 2020.
- [29] M. Riaz, N. Khalid, and D. Afzal, "A similarity measure under pythagorean fuzzy soft environment with applications," *Computational and Applied Mathematics*, vol. 39, no. 4, pp. 1–17, 2020.
- [30] R. M. Zulqarnain, X. L. Xin, H. Garg, and W. A. Khan, "Aggregation operators of pythagorean fuzzy soft sets with their application for green supplier chain management," *Journal of Intelligent and Fuzzy Systems*, vol. 40, no. 3, pp. 5545–5563, 2021.
- [31] R. M. Zulqarnain, X. L. Xin, I. Siddique, W. Asghar Khan, and M. A. Yousif, "TOPSIS method based on correlation coefficient under pythagorean fuzzy soft environment and its application towards green supply chain management," *Sustainability*, vol. 13, Article ID 1642, 2021.
- [32] R. M. Zulqarnain, X. L. Xin, H. Garg, and R. Ali, "Interaction aggregation operators to solve multi criteria decision making problem under pythagorean fuzzy soft environment," *Journal of Intelligent and Fuzzy Systems*, vol. 41, no. 1, pp. 1151–1171, 2021.
- [33] I. Siddique, R. M. Zulqarnain, R. Ali, A. Alburaikan, A. Iampan, and A. Hamiden, "A decision-making approach based on score matrix for pythagorean fuzzy soft set," *Computational Intelligence and Neuroscience*, vol. 2021, Article ID 5447422, 16 pages, 2021.
- [34] K. Chatterjee, D. Pamucar, and E. K. Zavadskas, "Evaluating the performance of suppliers based on using the R'AMATEL-MAIRCA method for green supply chain implementation in electronics industry," *Journal of Cleaner Production*, vol. 184, pp. 101–129, 2018.
- [35] Z. Stevic, D. Pamucar, M. Vasiljevic, G. Stojic, and S. Korica, "Novel integrated multicriteria model for supplier selection: case study construction company," *Symmetry*, vol. 9, no. 11, Article ID 279, 2017.
- [36] G. Stojic, Z. Stevic, J. Antucheviciene, D. Pamucar, and M. Vasiljevic, "A novel rough WASPAS approach for supplier selection in a company manufacturing PVC carpentry products," *Information*, vol. 9, no. 5, Article ID 121, 2018.

- [37] Z. Stevic, D. Pamucar, A. Puska, and P. Chatterjee, "Sustainable supplier selection in healthcare industries using a new MCDM method: measurement of alternatives and ranking according to COMPROMISE solution (MARCOS)," *Computers & Industrial Engineering*, vol. 140, Article ID 106231, 2020.
- [38] H. Garg, "A new generalized Pythagorean fuzzy information aggregation using Einstein operations and its application to decision making," *International Journal of Intelligent Systems*, vol. 31, no. 9, pp. 886–920, 2016.
- [39] H. Garg, "Generalized pythagorean fuzzy geometric aggregation operators using einsteint-norm andt-conorm for multicriteria decision-making process," *International Journal of Intelligent Systems*, vol. 32, no. 6, pp. 597–630, 2017.
- [40] S. K. Srivastava, "Green supply-chain management: a state-of-the-art literature review," *International Journal of Management Reviews*, vol. 9, no. 1, pp. 53–80, 2007.
- [41] J. Watrobski, W. Sałabun, and G. Ladorucki, "The temporal supplier evaluation model based on multicriteria decision analysis methods," in *Proceedings of the Asian Conference on Intelligent Information and Database Systems*, pp. 432–442, Kanazawa, Japan, April 2017.
- [42] M. Vasiljevic, H. Fazlollahtabar, H. Fazlollahtabar, Ž. Stević, and S. Vesković, "A rough multicriteria approach for evaluation of the supplier criteria in automotive industry," *Decision Making: Applications in Management and Engineering*, vol. 1, no. 1, pp. 82–96, 2018.
- [43] J. Watrobski and W. Sałabun, "Green supplier selection framework based on multicriteria decision-analysis approach," in *Proceedings of the International Conference on Sustainable Design and Manufacturing*, pp. 361–371, Heraklion, Greece, April 2016.
- [44] L. De Boer, E. Labro, and P. Morlacchi, "A review of methods supporting supplier selection," *European Journal of Purchasing & Supply Management*, vol. 7, no. 2, pp. 75–89, 2001.
- [45] J. Chai, J. N. K. Liu, and E. W. T. Ngai, "Application of decision-making techniques in supplier selection: a systematic review of literature," *Expert Systems with Applications*, vol. 40, no. 10, pp. 3872–3885, 2013.
- [46] K. Govindan, S. Rajendran, J. Sarkis, and P. Murugesan, "Multi criteria decision making approaches for green supplier evaluation and selection: a literature review," *Journal of Cleaner Production*, vol. 98, pp. 66–83, 2015.
- [47] K. Zimmer, M. Fröhling, and F. Schultmann, "Sustainable supplier management-a review of models supporting sustainable supplier selection, monitoring and development," *International Journal of Production Research*, vol. 54, no. 5, pp. 1412–1442, 2016.
- [48] K. Rahman, S. Abdullah, A. Ali, and F. Amin, "Pythagorean fuzzy Einstein hybrid averaging aggregation operator and its application to multiple-attribute group decision making," *Journal of Intelligent Systems*, vol. 29, no. 1, pp. 736–752, 2020.
- [49] K. Rahman, S. Abdullah, S. Abdullah, R. Ahmed, and M. Ullah, "Pythagorean fuzzy Einstein weighted geometric aggregation operator and their application to multiple attribute group decision making," *Journal of Intelligent and Fuzzy Systems*, vol. 33, no. 1, pp. 635–647, 2017.



## Research Article

# Weak Hopf Algebra and Its Quiver Representation

Muhammad Naseer Khan,<sup>1</sup> Ahmed Munir,<sup>1</sup> Muhammad Arshad,<sup>1</sup> Ahmed Alsanad <sup>2</sup>,  
and Suheer Al-Hadhrami <sup>3</sup>

<sup>1</sup>Department of Mathematics and Statistics, FBAS, International Islamic University, Islamabad 44000, Pakistan

<sup>2</sup>STC's Artificial Intelligence Chair, Department of Information Systems, College of Computer and Information Sciences, King Saud University, Riyadh 11543, Saudi Arabia

<sup>3</sup>Computer Engineering Department, Engineering College, Hadhramout University, Hadhramout, Yemen

Correspondence should be addressed to Ahmed Alsanad; [aasanad@ksu.edu.sa](mailto:aasanad@ksu.edu.sa) and Suheer Al-Hadhrami; [s.alhadhrami@hu.edu.ye](mailto:s.alhadhrami@hu.edu.ye)

Received 8 August 2021; Accepted 15 October 2021; Published 3 November 2021

Academic Editor: Dragan Pamučar

Copyright © 2021 Muhammad Naseer Khan et al. This is an open access article distributed under the Creative Commons Attribution License, which permits unrestricted use, distribution, and reproduction in any medium, provided the original work is properly cited.

This study induced a weak Hopf algebra from the path coalgebra of a weak Hopf quiver. Moreover, it gave a quiver representation of the said algebra which gives rise to the various structures of the so-called weak Hopf algebra through the quiver. Furthermore, it also showed the canonical representation for each weak Hopf quiver. It was further observed that a Cayley digraph of a Clifford monoid can be embedded in its corresponding weak Hopf quiver of a Clifford monoid. This led to the development of the foundation structures of weak Hopf algebra. Such quiver representation is useful for the classification of its path coalgebra. Additionally, some structures of module theory of algebra were also given. Such algebras can also be applied for obtaining the solutions of “quantum Yang–Baxter equation” that has many applications in the dynamical systems for finding interesting results.

## 1. Introduction

A bialgebra  $H$  is equipped with the structures of algebra  $(H, m)$  and coalgebra. If  $H$  is a linear space over a field  $K$ , then  $H$  is called an algebra if  $H$  has a unit  $u: K \rightarrow H$  and a multiplication  $m: H \otimes H \rightarrow H$ , such that  $m(\text{Id} \otimes m) = m(m \otimes \text{Id})$  (associativity) and  $\text{Id} = m(u \otimes \text{Id}) = m(\text{Id} \otimes u)$  (unitary property), where  $\text{Id}$  is the identity map of  $H$ .  $H$  is called a coalgebra if  $H$  has a comultiplication  $\Delta: H \rightarrow H \otimes H$  and a counit  $\varepsilon: H \rightarrow K$ , such that  $(\Delta \otimes \text{Id})\Delta = (\text{Id} \otimes \Delta)\Delta$  (coassociativity of  $\Delta$ ) and  $\text{Id} = (\varepsilon \otimes \text{Id})\Delta = (\text{Id} \otimes \varepsilon)\Delta$  (counit property) [1]. Then, we have a unique element  $\rho \in \text{Hom}_k(H, H)$ , such that  $\text{id}_H * \rho = \rho * \text{id}_H = \mu\varepsilon$ , where “ $*$ ” is the convolution in  $\text{Hom}_k(H, H)$ . With this map  $\rho$ ,  $H$  becomes a Hopf algebra. Montgomery [2] described the action of Hopf algebra on rings, Me [3] wrote a series of mathematics lecture notes, Redford [4] deliberated the structure of Hopf algebras with a projection, Daele and Wang [5] discussed the source and target algebras for weak multiplier Hopf algebras, Yang and

Zhang [6] proposed the ore extensions for Sweedler’s Hopf algebra, Smith [7] formulated the quantum Yang–Baxter equation and quantum quasigroups, Nichita [8] introduced the Yang–Baxter equation with open problems, and Cibils and Rosso [9] introduced the Hopf quiver. According to them, a Hopf quiver is just a Cayley graph of a group. They discussed some matters regarding representations of Hopf algebra/quantum group and quiver. A quiver representation is a set  $\{V_i | i \in Q_0\}$  of  $k$ -vector spaces  $V_i$  having finite bases together with the set  $\{\varnothing_a: V_{t(a)} \rightarrow V_{h(a)} \in Q_1\}$  of  $k$ -linear maps. We denote a representation by  $R = (V_i, \varnothing_a)$  [10].

A bialgebra  $H$  over a field  $k$  is called a weak Hopf algebra if there is an element  $T$  in the convolution algebra  $\text{Hom}_k(H, H)$ , such that  $\text{id} * T * \text{id} = \rho * \text{id}$  and  $T * \text{id} * T = T$ , and  $T$  represents a weak antipode of  $H$ . Li obtained solutions for quantum Yang–Baxter equation using such weak Hopf algebra [1, 11, 12]. A weak Hopf algebra  $H$  with a weak antipode  $T$  is a semilattice graded weak Hopf algebra if  $H = \bigoplus_{\lambda \in Y} H_\lambda$ , where the graded sums  $H_\lambda$ ;  $\lambda \in Y$  are the subweak Hopf algebras (which are Hopf algebras) with

antipodes restrictions  $T|_{H_\lambda}$  for each  $\lambda \in Y$  [13]. Then, there exist a homomorphism  $\varphi_{\lambda,\mu}: H_\lambda \rightarrow H_\mu$  if  $\lambda\mu = \mu$ , such that  $a \in H_\lambda$  and  $b \in H_\mu$ , and the multiplication  $a \cdot b$  in  $H$  is given by

$$a \cdot b = \varphi_{\lambda,\mu}(a)\varphi_{\mu,\lambda}(b). \quad (1)$$

A Clifford monoid  $S$  is a regular semigroup  $S$ . Its center  $C(S)$  contains each of its idempotent. In other words, this is a semilattice of groups which is a collection of maximal subgroups  $\{G_\lambda: \lambda \in Y\}$  of a regular monoid  $S$ , such that  $S = \cup_{\lambda \in Y} G_\lambda$  and  $G_\lambda G_\mu \subseteq G_{\lambda\mu}$  for all  $\lambda, \mu \in Y$ , where  $Y$  is a semilattice. For any  $\lambda, \mu \in Y$  with  $\lambda\mu = \mu$ , there are group homomorphism  $\varphi_{\lambda,\mu}: G_\lambda \rightarrow G_\mu$  with  $\varphi_{\lambda,\lambda}$  as an identity homomorphism on  $G_\lambda$ , and if  $\lambda\mu = \mu$  and  $\mu\nu = \nu$ , then  $\varphi_{\mu,\nu}\varphi_{\lambda,\mu} = \varphi_{\lambda,\nu}$ . The multiplication in  $S$  for all  $a, b \in S$  is defined as above in  $H$ . The partial ordering " $\leq$ " in  $Y$  is given by " $\lambda \leq \mu$  if and only if  $\lambda\mu = \lambda$  for all  $\lambda, \mu \in Y$ ."

Cibils introduced the Hopf quiver and discussed the structures of the Hopf algebra obtained corresponding to the Hopf quiver [9]. By [14], the categories of Hopf algebra are discussed for the representation has tensor structures induced from the graded Hopf structures of  $k\Gamma$ . By [15], the path coalgebra  $k\Gamma$  of a quiver  $\Gamma$  admits a coquasitriangular Majid algebra structure if and only if  $\Gamma$  is a Hopf quiver of the form  $\Gamma(G, R)$  with  $G$  abelian. Here, the authors gave a classification of the set of graded coquasitriangular Majid structures on connected Hopf quiver. Huang and Tao gave a thorough list of coquasitriangular structures of the graded Hopf algebra over a connected Hopf quiver [16]. Ahmed and Li introduced the concept of the so-called weak Hopf quiver and discussed some structures of its corresponding weak Hopf algebras and weak Hopf modules [17]. Some literature that help for better understanding of these algebra is listed. Auslander et al. [18] gave the theory of representation of artin algebra, China and Montgomery [19] defined the basic coalgebras, Cibils [20] found the tensor product of Hopf bimodules on a group, Nakajima [21] initiated the quiver varieties for ring and representation theorists, Simson [22] discussed the coalgebras, comodules, pseudocompact algebras, and tame comodule type, and Woodcock [23] put some remarks on the theory of representation of coalgebras.

In this study, we introduce a notion of weak Hopf quiver representation that generalizes the Hopf quiver representation. We also prove that the Cayley digraph of a Clifford monoid  $S$  is embedded in the weak Hopf quiver of the algebra of the Clifford monoid which is also a weak Hopf algebra. Some calculations are made for obtaining the images of various mappings calculated by the tool of Mathematica.

## 2. Preliminaries

We include some necessary concepts of the related matter in this study to make the reader familiar with the matter of the work. First, we include the definition of weak Hopf quiver which is given as follows:

**Definition 1** (see [17]). Let  $S = \cup_{\lambda \in Y} G_\lambda$  be a Clifford monoid, where  $Y$  is a semilattice of  $G_\lambda; \lambda \in Y$ , the subgroups of  $S$ .

- (1) A ramification data  $r$  of  $S$  means a sum of  $r_\lambda = \sum_{c_\lambda \in C_\lambda} \sim r_{c_\lambda} C_\lambda$  of subgroups  $G_\lambda; \lambda \in Y$ , i.e.,  $r = \sum_{\lambda \in Y} r_\lambda = \sum_{\lambda \in Y} \sum_{c_\lambda \in C_\lambda} \sim r_{c_\lambda} C_\lambda$ .
- (2) Then,  $r$  could be viewed as a positive central element of the Clifford monoid ring of  $S$ , where  $\widetilde{C}_\lambda$  represents the collection of total conjugacy classes of subgroup  $G_\lambda$  for  $\lambda \in Y$ .

Let  $\Gamma$  be a quiver satisfying the following conditions:

- (a) The set of vertices of  $\Gamma$  just represents the set  $S$
- (b) Let  $x \in G_\mu, y \in G_\lambda; x, y \in S$  and  $\lambda, \mu \in Y$ ; if  $\mu \not\geq \lambda$ , then there does not exist an arrow from  $x$  to  $y$ , and if  $\mu \geq \lambda$ , then the number of arrows from  $x$  to  $y$  is equal to that from  $\varphi_{\mu,\lambda}(x)$  to  $y$  which is equal to  $r_{c_\lambda}$ , if there exist  $c_\lambda \in C_\lambda$ , such that  $y = c_\lambda \varphi_{\mu,\lambda}(x)$ .

Then,  $\Gamma$  is said to be the corresponding weak Hopf quiver of  $r$ .  $\Gamma_0$  is the set of vertices and  $\Gamma_1$  is the set of arrows of  $\Gamma$ .

**Definition 2** (see [17]). Let for a quiver  $\Gamma$  and  $k\Gamma$  be the  $k$ -space with basis the set of all paths in  $\Gamma$ , where  $k$  is a field. Define  $k\Gamma^a$  by the algebra with multiplication and underlying  $k$ -space  $k\Gamma$  as

$$qp = \begin{cases} b_m, \dots, b_1 a_n, \dots, a_1, & \text{if } t(a_n) = s(b_1), \\ 0, & \text{otherwise,} \end{cases} \quad (2)$$

for the paths  $p = a_n, \dots, a_1$  and  $q = b_n, \dots, b_1$ . Then,  $k\Gamma^a$  becomes an associative algebra, known as path algebra of  $\Gamma$  [3,16].

**Definition 3** (see [4]). Let  $\Gamma$  be a quiver (finite or infinite) and define  $k\Gamma^C$  to be a coalgebra with comultiplication  $\Delta$  of  $k\Gamma^C$  defined by

$$\Delta(p) = p \otimes s(p) + \sum_{i=1}^{n-1} a_n, \dots, a_{i+1} \otimes a_i, \dots, a_1 + t(p) \otimes p, \quad (3)$$

for any path  $p = a_n, \dots, a_1; a_i \in \Gamma_1; i = 1, \dots, n$ . For special case, a trivial path  $e_i$ , the comultiplication is  $\Delta$  and is described by  $\Delta(e_i) = e_i \otimes e_i$  for each vertex  $i \in \Gamma_0$  and the counit  $\varepsilon$  is defined by

$$\varepsilon(p) = \begin{cases} 0, & \text{if } n \geq 1, \\ 1, & \text{otherwise.} \end{cases} \quad (4)$$

We use  $k\Gamma$  the path coalgebra of the quiver  $\Gamma$ .

**Lemma 1** (see [4]). *If  $k\Gamma$  is the path coalgebra corresponding to the quiver  $\Gamma$ , then  $k\Gamma$  is pointed and  $G(k\Gamma) = \Gamma_0$ . There is a necessary and sufficient condition between the semilattice-graded weak Hopf algebra and the existence of a weak Hopf quiver corresponding to a Clifford monoid with some ramification data.*

**Theorem 1** (see [1]). *Let  $\Gamma$  represent a quiver; then, the following two statements are equivalent:*

- (i) The path coalgebra  $k\Gamma$  acknowledges a semilattice-graded weak Hopf algebra structure, such that all graded summands are themselves graded Hopf algebra
- (ii) With respect to some ramification data,  $\Gamma$  is the weak Hopf quiver of some Clifford monoid  $S$

The following proposition tells us that the collection of elements of group-like of path coalgebra  $k\Gamma$  of a weak Hopf quiver  $\Gamma$  is a Clifford monid.

**Proposition 1** (see [1]). *If  $\Gamma(S, r)$  is a weak Hopf quiver corresponding to a ramification data  $r$  of a Clifford monoid  $S$ , then  $\Gamma_0$  is the collection of elements of group-like of path coalgebra  $k\Gamma$ , and  $k\Gamma_0 \cong kS$ , the Clifford monoid algebra of  $S$  is a subweak Hopf algebra of  $k\Gamma$ .*

**Definition 4** (see [4]). Suppose  $u$  and  $v$  represent the vertices in  $\Gamma$ , and  $k$  represents a field. The  $(v, u)$ -isotypic component of a  $k\Gamma_0$ -bicomodule  $M$  is  ${}^vM^u = \{m \in M \mid \delta_L(m) = v \otimes m, \delta_R(m) = m \otimes u\}$ . In particular,  ${}^v(k\Gamma_n)^u$  is the vector space of  $n$ -paths from vertex  $u$  to vertex  $v$ .

### 3. Structures of Weak Hopf Quivers

Here, we discuss the structures of weak Hopf quiver and its algebra. We start by the following example.

**3.1. An Illustrative Example.** Let  $Y = \{\alpha, \beta, \gamma, \rho, \sigma, \delta\}$  be the semilattice with multiplication “ $\cdot$ ” as given in Table 1.

For a ring  $R$  with identity  $R^{2 \times 2}$  denotes the  $2 \times 2$  full matrix ring over  $R$ ,  $U(R)$  the group consisting of all units in  $R$ . Let  $Z$  be the integer numbers ring. For a prime  $p$ ,  $Z_p$  is a field, and  $U(Z^{2 \times 2})$  is just the  $2 \times 2$  general linear group  $GL_2(Z_p)$  over  $Z_p$ . Assume that  $G_\alpha = \{e_\alpha\}$  and  $G_\delta = \{e_\delta\}$  are the trivial groups,  $G_\beta = GL_2(Z_2)$ ,  $G_\gamma = U(Z_4^{2 \times 2})$ ,  $G_\rho = GL_2(Z_3)$ ,  $G_\sigma = U(Z_6^{2 \times 2})$ . Then,  $G_u \cap G_v = \emptyset$ , for any  $u, v \in Y, u \neq v$ , setting  $S = \cup_{u \in Y} G_u$ . The multiplication is defined as above on  $S$  makes  $S = \cup_{u \in Y} G_u$  a Clifford monoid with regards to the semilattice  $Y$  [11].

The following mappings exist between the subgroups of the Clifford monoid.

$$\varphi_{\delta, \delta}: G_\delta \longrightarrow G_\delta, \text{ defined by } \varphi_{\delta, \delta}(e_\delta) = e_\delta$$

$$\varphi_{\delta, \sigma}: G_\delta \longrightarrow G_\sigma, \text{ defined by } \varphi_{\delta, \sigma}(e_\delta) = e_\sigma$$

$$\varphi_{\delta, \gamma}: G_\delta \longrightarrow G_\gamma, \text{ defined by } \varphi_{\delta, \gamma}(e_\delta) = e_\gamma$$

$$\varphi_{\delta, \beta}: G_\delta \longrightarrow G_\beta, \text{ defined by } \varphi_{\delta, \beta}(e_\delta) = e_\beta$$

$$\varphi_{\delta, \rho}: G_\delta \longrightarrow G_\rho, \text{ defined by } \varphi_{\delta, \rho}(e_\delta) = e_\rho$$

$$\varphi_{\delta, \alpha}: G_\delta \longrightarrow G_\alpha, \text{ defined by } \varphi_{\delta, \alpha}(e_\delta) = e_\alpha$$

We denote  $C_\lambda$  as a conjugacy class of the group  $G_\lambda, \lambda \in Y$ . For each  $x \in G_\delta$  and  $y \in G_\delta$ , there exists  $c_\delta \in C_\delta$ , such that  $y = c_\delta \varphi_{\delta, \delta}(x)$ . Since there is only one arrow (the loop) from  $G_\delta$  to  $G_\delta$ , therefore,  $r_{C_\alpha} = 1$ .

$$\varphi_{\sigma, \sigma}: G_\sigma \longrightarrow G_\sigma, \text{ defined by } \varphi_{\sigma, \sigma}: Z_6 \longrightarrow Z_6, \\ U(Z_6) = \{\bar{1}, \bar{5}\}$$

TABLE 1: The semilattice ( $Y = \{\alpha, \beta, \gamma, \rho, \sigma, \delta\}, \cdot$ ).

	$\alpha$	$\beta$	$\gamma$	$\rho$	$\sigma$	$\delta$
$\alpha$	$\alpha$	$\alpha$	$\alpha$	$\alpha$	$\alpha$	$\alpha$
$\beta$	$\alpha$	$\beta$	$\beta$	$\alpha$	$\beta$	$\beta$
$\gamma$	$\alpha$	$\beta$	$\gamma$	$\alpha$	$\beta$	$\gamma$
$\rho$	$\alpha$	$\alpha$	$\alpha$	$\rho$	$\rho$	$\rho$
$\sigma$	$\alpha$	$\beta$	$\beta$	$\rho$	$\sigma$	$\sigma$
$\delta$	$\alpha$	$\beta$	$\gamma$	$\rho$	$\sigma$	$\delta$

$$\varphi_{\sigma, \sigma}(\bar{1}) = \bar{1}, \varphi_{\sigma, \sigma}(\bar{2}) = \bar{2}, \varphi_{\sigma, \sigma}(\bar{3}) = \bar{3}, \varphi_{\sigma, \sigma}(\bar{4}) = \bar{4}, \varphi_{\sigma, \sigma}(\bar{5}) \\ = \bar{5}, \varphi_{\sigma, \sigma}(\bar{6}) = \bar{0}, \quad (5)$$

$$\varphi_{\sigma, \gamma}: G_\sigma \longrightarrow G_\gamma, \text{ defined by } \varphi_{\sigma, \gamma}: Z_6 \longrightarrow Z_4, \\ U(Z_4) = \{\bar{1}, \bar{3}\} \\ \varphi_{\sigma, \gamma}(\bar{1}) = \bar{1}, \varphi_{\sigma, \gamma}(\bar{2}) = \bar{2}, \varphi_{\sigma, \gamma}(\bar{3}) = \bar{3}, \varphi_{\sigma, \gamma}(\bar{4}) = \bar{0}, \varphi_{\sigma, \gamma}(\bar{5}) \\ = \bar{1}, \varphi_{\sigma, \gamma}(\bar{6}) = \bar{2}, \quad (6)$$

$$\varphi_{\sigma, \beta}: G_\sigma \longrightarrow G_\beta, \text{ defined by } \varphi_{\sigma, \beta}: Z_6 \longrightarrow Z_2, U(Z_2) = \\ \{\bar{1}\} \\ \varphi_{\sigma, \beta}(\bar{1}) = \bar{1}, \varphi_{\sigma, \beta}(\bar{2}) = \bar{0}, \varphi_{\sigma, \beta}(\bar{3}) = \bar{1}, \varphi_{\sigma, \beta}(\bar{4}) = \bar{0}, \varphi_{\sigma, \beta}(\bar{5}) \\ = \bar{1}, \varphi_{\sigma, \beta}(\bar{6}) = \bar{0}, \quad (7)$$

$$\varphi_{\sigma, \rho}: G_\sigma \longrightarrow G_\rho, \text{ defined by } \varphi_{\sigma, \rho}: Z_6 \longrightarrow Z_3, \\ U(Z_3) = \{\bar{1}, \bar{2}\} \\ \varphi_{\sigma, \rho}(\bar{1}) = \bar{1}, \varphi_{\sigma, \rho}(\bar{2}) = \bar{2}, \varphi_{\sigma, \rho}(\bar{3}) = \bar{0}, \varphi_{\sigma, \rho}(\bar{4}) = \bar{1}, \varphi_{\sigma, \rho}(\bar{5}) \\ = \bar{2}, \varphi_{\sigma, \rho}(\bar{6}) = \bar{0}, \quad (8)$$

$$\varphi_{\sigma, \alpha}: G_\sigma \longrightarrow G_\alpha, \text{ defined by } \varphi_{\sigma, \alpha}(a_\sigma) = e_\alpha \forall a_\sigma \in G_\sigma \\ \varphi_{\gamma, \gamma}: G_\gamma \longrightarrow G_\gamma, \text{ defined by } \varphi_{\gamma, \gamma}: Z_4 \longrightarrow Z_4, \\ U(Z_4) = \{\bar{1}, \bar{3}\} \\ \varphi_{\gamma, \gamma}(\bar{1}) = \bar{1}, \varphi_{\gamma, \gamma}(\bar{2}) = \bar{2}, \varphi_{\gamma, \gamma}(\bar{3}) = \bar{3}, \varphi_{\gamma, \gamma}(\bar{4}) = \bar{0}, \quad (9)$$

$$\varphi_{\gamma, \beta}: G_\gamma \longrightarrow G_\beta, \text{ defined by } \varphi_{\gamma, \beta}: Z_4 \longrightarrow Z_2, \\ U(Z_2) = \{\bar{1}\} \\ \varphi_{\gamma, \beta}(\bar{1}) = \bar{1}, \varphi_{\gamma, \beta}(\bar{2}) = \bar{0}, \varphi_{\gamma, \beta}(\bar{3}) = \bar{1}, \varphi_{\gamma, \beta}(\bar{4}) = \bar{0}, \quad (10)$$

$$\varphi_{\gamma, \alpha}: G_\gamma \longrightarrow G_\alpha, \text{ defined by } \varphi_{\gamma, \alpha}(a_\gamma) = e_\alpha \forall a_\gamma \in G_\gamma \\ \varphi_{\beta, \beta}: G_\beta \longrightarrow G_\beta, \text{ defined by } \varphi_{\beta, \beta}: Z_2 \longrightarrow Z_2, \\ U(Z_2) = \{\bar{1}\} \\ \varphi_{\beta, \beta}(\bar{1}) = \bar{1}, \varphi_{\beta, \beta}(\bar{2}) = \bar{0}, \quad (11)$$

$$\varphi_{\beta, \rho}: G_\beta \longrightarrow G_\rho, \text{ defined by } \varphi_{\beta, \rho}: Z_2 \longrightarrow Z_3, \\ U(Z_3) = \{\bar{1}, \bar{2}\} \\ \varphi_{\beta, \rho}(\bar{1}) = \bar{1}, \varphi_{\beta, \rho}(\bar{2}) = \bar{2}, \varphi_{\beta, \rho}(\bar{3}) = \bar{0}, \quad (12)$$

$$\begin{aligned} \varphi_{\beta,\alpha}: G_\beta &\longrightarrow G_\alpha, \text{ defined by } \varphi_{\beta,\alpha}(a_\beta) = e_\alpha \forall a_\beta \in G_\beta \\ \varphi_{\rho,\rho}: G_\rho &\longrightarrow G_\rho, \text{ defined by } \varphi_{\rho,\rho}: Z_3 \longrightarrow Z_3, U(Z_3) = \\ &\{1, 2\} \\ \varphi_{\rho,\rho}(\bar{1}) &= \bar{1}, \varphi_{\rho,\rho}(\bar{2}) = \bar{2}, \varphi_{\rho,\rho}(\bar{3}) = \bar{0}, \end{aligned} \quad (13)$$

$$\begin{aligned} \varphi_{\rho,\alpha}: G_\rho &\longrightarrow G_\alpha, \text{ defined by } \varphi_{\rho,\alpha}(a_\rho) = e_\alpha, \forall a_\rho \in G_\rho \\ \varphi_{\alpha,\alpha}: G_\alpha &\longrightarrow G_\alpha, \text{ defined by } \varphi_{\alpha,\alpha}(e_\alpha) = e_\alpha \end{aligned}$$

For each given mapping  $\varphi_{\lambda,\mu}: G_\lambda \longrightarrow G_\mu$ , if it exists, and for any  $x \in G_\lambda$  and  $y \in G_\mu$ , there exists  $c_\mu \in C_\mu$ , such that  $y = c_\mu \varphi_{\lambda,\mu}(x)$  for all  $\lambda, \mu \in Y, \mu \geq \lambda$ . The semilattice of the subgroups of the Clifford monoid along with the mappings among them is shown in Figure 1.

In Figure 1, the arrows show the mappings  $\varphi_{\lambda,\mu}: G_\lambda \longrightarrow G_\mu \forall \lambda \geq \mu; \lambda, \mu \in Y$ .

$$H = kS = kG_\lambda. \quad (14)$$

The weak Hopf quiver for the weak Hopf algebra  $H = kS = \oplus_{\lambda \in Y} kG_\lambda = \oplus_{\lambda \in Y} H_\lambda$ , where each  $H_\lambda = kG_\lambda$  is a Hopf algebra.  $H$  is in fact a semilattice-graded weak Hopf algebra with  $H_\lambda H_\mu \subseteq H_\mu$ , if and only if  $\lambda \geq \mu; \lambda, \mu \in Y$ .

The vertices and arrows of the weak Hopf quiver  $\Gamma = (S, r)$  corresponding to  $H$  is described in the following table instead of drawing its huge digraph, since there is a large number of vertices and arrows in this quiver. The mappings of the type  $\varphi_{\lambda,\mu}: G_\lambda \longrightarrow G_\mu, \forall \lambda, \mu \in Y$  which exist are shown by the symbol " $\longrightarrow$ " in Table 2.

Particularly in the above quiver given in Section 3.1, the number of arrows originating in  $\Gamma(S, r)$  is given by

$$\begin{aligned} N &= 440 \times 1 + 439 \times 288 + 103 \times 96 + 55 \times 6 + 49 \\ &\times 48 + 1 \times 1 = 139443. \end{aligned} \quad (15)$$

The number of arrows ending in  $\Gamma(S, r)$  is given by

$$\begin{aligned} N &= 1 \times 1 + 289 \times 288 + 385 \times 96 + 391 \times 6 + 343 \\ &\times 48 + 440 \times 1 = 139443. \end{aligned} \quad (16)$$

We note that the originating number of arrows is equal to that ending in the quiver.

Let  $N$  denotes the amount of arrows of quiver  $\Gamma(S, r)$ ,  $N_\lambda$  denote the amount of arrows originating from the vertex represented by the element  $a_\lambda$  of subgroup  $G_\lambda$ , and  $N^\lambda$  denotes the amount of arrows ending at the vertex corresponding to the element of subgroup  $G_\lambda$ . Then, we have the following lemma:

### Lemma 2

- The number of arrows originating in  $\Gamma(S, r)$  is given by  $N = \sum_{\lambda \in Y} N_\lambda |G_\lambda|$
- The number of arrows ending in  $\Gamma(S, r)$  is given by  $N' = \sum_{\lambda \in Y} N^\lambda |G_\lambda|$
- $N = N' = \text{total numbers of arrows of the weak Hopf quiver } \Gamma(S, r)$ .

*Proof.* The proofs of (a), (b), and (c) are obvious from Table 2.

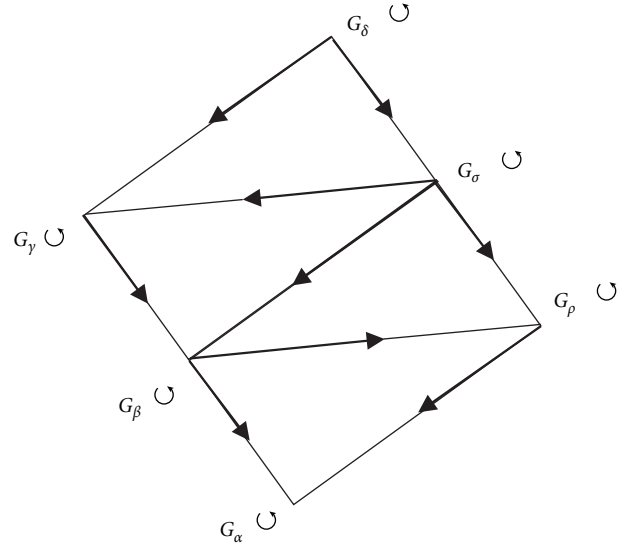


FIGURE 1: Diagram of the semilattice of the subgroups of the Clifford monoid.

In view of Section 3.1, the following results can immediately be identified and obtained in a weak Hopf quiver  $\Gamma(S, r)$ .  $\square$

3.2. *Results.* Let  $x \in G_\lambda, y \in G_\mu$ , and  $\varphi_{\lambda,\mu}: G_\lambda \longrightarrow G_\mu, \lambda \geq \mu; \lambda, \mu \in Y$ . Then, there exists a unique arrow from  $x$  to  $y$  (or  $\varphi_{\lambda,\mu}$  to  $y$ ) and satisfies  $y = c_\mu \varphi_{\lambda,\mu}(x), c_\mu \in C_\mu$ ; therefore,  $r_{C_\mu} = 1 \forall \mu \in Y$ .

(i) If  $r_\lambda$  is the ramification data of group  $G_\lambda$ , then  $r_\lambda = \sum_{C_\lambda \in \tilde{C}_\lambda} \tilde{r}_{C_\lambda} C_\lambda$  using (i)

(ii) The ramification data of the Clifford monoid  $S = \cup_{\lambda \in Y} G_\lambda$  is

$$r = \sum_{\lambda \in Y} r_\lambda = \sum_{\lambda \in Y} \sum_{C_\lambda \in \tilde{C}_\lambda} \tilde{r}_{C_\lambda} C_\lambda = \sum_{\substack{\lambda \in Y \\ c \in \tilde{C}_\lambda}} C_\lambda, \quad (17)$$

Where  $C_\lambda$  represents the collection of total conjugacy classes of a group  $G_\lambda$ .

- The number of arrows in  $\Gamma$  as obtained from Section 3.1 is 139443
- The number of vertices of the weak Hopf quiver  $\Gamma(S, r)$  from Section 3.1 is  $|S| = \sum_{\lambda \in Y} |G_\lambda| = 440$
- If there is an arrow from some element  $x \in G_\lambda$  to some element  $y \in G_\mu$ , then there are arrows from each  $x \in G_\lambda$  to  $y \in G_\mu$
- The dimension of weak Hopf algebra  $H$  corresponding to  $\Gamma$  is the number of vertices of the weak Hopf quiver
- The loops which exist are the arrows from each idempotent to itself. Thus, the number of loops is the order of the semilattice  $Y$ .
- For a finite Clifford monoid,  $\Gamma(S, r)$  corresponding to  $H = kS$  has no loop if and only if  $r = 0$ . Then, the

TABLE 2: The vertices and arrows of the weak Hopf quiver  $\Gamma = (S, r)$  corresponding to the weak Hopf algebra  $H$ .

Range → Domain ↓	$G_\delta,  G_\delta  = 01$	$G_\sigma,  G_\sigma  = 288$	$G_\gamma,  G_\gamma  = 96$	$G_\beta,  G_\beta  = 06$	$G_\rho,  G_\rho  = 48$	$G_a,  G_a  = 01$	Number of arrows originating at each element of group	Number of arrows originating from the whole of group
$G_\delta,  G_\delta  = 01$	→	→	→	→	→	→	440	$440 \times 1 = 440$
$G_\sigma,  G_\sigma  = 288$		→	→	→	→	→	439	$439 \times 288 = 12643$
$G_\gamma,  G_\gamma  = 96$			→	→	→	→	103	$103 \times 96 = 9888$
$G_\beta,  G_\beta  = 06$				→	→	→	55	$55 \times 6 = 330$
$G_\rho,  G_\rho  = 48$					→	→	49	$49 \times 48 = 2352$
$G_a,  G_a  = 01$						→	01	$01 \times 01 = 01$
Number of arrows ending at each element of group	01	289	385	391	343	440		Total number of originating arrows ↓
Number of arrows ending on the whole group	$01 \times 01 = 01$	$289 \times 288 = 83232$	$385 \times 96 = 36960$	$391 \times 06 = 2346$	$343 \times 48 = 16464$	$440 \times 01 = 440$	Total number of ending arrows →	139443

quiver is a set  $|S|$  of number of isolated vertices. Otherwise, the weak Hopf quiver is a connected digraph.

- (ix) Let  $S$  and  $S'$  be two finite Clifford monoids, and  $\Gamma(S, r)$  and  $\Gamma'(S', r')$  be the weak Hopf quivers corresponding to two weak Hopf algebras  $H = kS$  and  $H' = kS'$ , respectively. Then, the quivers  $\Gamma$  and  $\Gamma'$  are isomorphic if and only if there is a bijective mapping  $\varphi: \Gamma \rightarrow \Gamma'$  between their sets of vertices, such that the number of arrows from  $v_1$  to  $v_2$ ,  $v_1, v_2 \in \Gamma_0$ , is equal to that from  $\varphi(v_1)$  to  $\varphi(v_2)$ , where  $\varphi(v_1), \varphi(v_2) \in \Gamma_0$  [1].

$$\{\phi_{\lambda,\mu}^m: V_{t(m),\lambda} \longrightarrow V_{s(m),\mu} \mid m \in \Gamma_1, t(m), s(m) \in \Gamma_0, \mu \geq \lambda, \lambda, \mu \in Y\}. \quad (18)$$

We denote  $\{(V_{i,\lambda}, V_{j,\mu}); \phi_{\lambda,\mu}^m; i, j \in \Gamma_0\}$  by  $\mathcal{R}_{\lambda,\mu}$ . A representation  $\mathcal{R}$  of the weak Hopf quiver is given by  $\mathcal{R} = \{\mathcal{R}_{\lambda,\mu}; \mu \geq \lambda, \lambda, \mu \in Y\}$ .

Let  $\mathcal{R} = \{\mathcal{R}_{\lambda,\mu}; \mu \geq \lambda, \lambda, \mu \in Y\}$  and  $S = \{S_{\lambda,\mu}; \mu \geq \lambda, \lambda, \mu \in Y\}$  be two representations of weak Hopf quiver  $\Gamma(S, r)$ , where  $\mathcal{R}_{\lambda,\mu} = \{(V_{i,\lambda}, V_{j,\mu}); \phi_{\lambda,\mu}^m\}$  and  $S_{\lambda,\mu} = \{(W_{i,\lambda}, W_{j,\mu}); \psi_{\lambda,\mu}^m\}$ . The representation  $S_{\lambda,\mu}$  is a subrepresentation of  $\mathcal{R}_{\lambda,\mu}$  if

- (a) For all  $i, j \in \Gamma_0$ ,  $W_{i,\lambda}, W_{j,\mu}$  are the subspaces of  $V_{i,\lambda}$  and  $V_{j,\mu}$ , respectively, and
- (b) For every  $m \in \Gamma_1$ , the restriction of  $\phi_{\lambda,\mu}^m$  to  $W_{t(m),\lambda}$  is the mapping  $\phi_{\lambda,\mu}^m|_{W_{t(m),\lambda}}$  and is given by  $\phi_{\lambda,\mu}^m|_{W_{t(m),\lambda}}: W_{t(m),\lambda} \longrightarrow W_{s(m),\mu}$ .

Then,  $S = \{S_{\lambda,\mu}; \mu \geq \lambda; \lambda, \mu \in Y\}$  is called subrepresentation of  $\mathcal{R} = \{\mathcal{R}_{\lambda,\mu}; \mu \geq \lambda; \lambda, \mu \in Y\}$ .

A nonzero representation  $V$  is called simple if the only subrepresentation of  $V$  is the zero representation and the  $V$  itself.

Given that a representation  $\mathcal{R} = (V_{i,\lambda}, \phi_{\lambda,\lambda}^i)$  of the quiver  $\Gamma(S, r)$ , we can obtain a representation  $\varphi_{\lambda,\lambda}^i: k\Gamma \longrightarrow \text{End}\left(\bigoplus_{\substack{i \in \Gamma_0 \\ \lambda \in Y}} V_{i,\lambda}\right)$  of  $k\Gamma$ , see also the framed representation in [13].

It suffices to define the representation on  $e_i$ 's and  $f_j$ 's, and these generate the basis of a ring.

$$\varphi_{\lambda,\lambda}^i(e_i) := \text{Id}|_{V_i}, \varphi_{\lambda,\lambda}^j(f_j): V_{t(j),\lambda} \longrightarrow V_{h(j),\lambda}, x \mapsto \varphi_{\lambda,\lambda}^j(x). \quad (19)$$

This gives an extension to a representation on all elements of  $k\Gamma$ .

The direct sum of two weak Hopf quiver representations is given as follows:

**Definition 6** (see [21]). If  $\mathcal{R} = \{\mathcal{R}_{\lambda,\mu}; \mu \geq \lambda, \lambda, \mu \in Y\}$  and  $S = \{S_{\lambda,\mu}; \mu \geq \lambda, \lambda, \mu \in Y\}$  be two representations of weak Hopf quiver  $\Gamma(S, r)$ , where  $\mathcal{R}_{\lambda,\mu} = \{(V_{i,\lambda}, V_{j,\mu}); \phi_{\lambda,\mu}^m\}$  and

## 4. Representation of Weak Hopf Quiver

A Hopf quiver representation is defined in [15] and some structures are given in this regard. We generalize this notion as a weak Hopf quiver representation and discuss its structures. One can see also the quiver representation of a bialgebra [17].

**Definition 5.** (See [13]). A weak Hopf quiver representation is a class of vector spaces  $\{V_{i,\lambda} \mid i \in \Gamma_0, \lambda \in Y\}$  of finite-dimensional  $k$ -vector spaces  $V_{i,\lambda}, i \in \Gamma_0, \lambda \in Y$  together with a collection of mappings.

$S_{\lambda,\mu} = \{(W_{i,\lambda}, W_{j,\mu}); \psi_{\lambda,\mu}^m\}$ , then we define a direct-sum representation as follows:

$$\mathcal{R} \oplus S = \{(\mathcal{R}_{\lambda,\mu} \oplus S_{\lambda,\mu}); \mu \geq \lambda; \lambda, \mu \in Y\}, \quad (20)$$

with  $\chi_{\lambda,\mu}^m = \{\phi_{\lambda,\mu}^m \oplus \psi_{\lambda,\mu}^m; \mu \geq \lambda; \lambda, \mu \in Y\}$  by

$$(a) \ u_{i,\lambda} = V_{i,\lambda} \oplus W_{i,\lambda} \text{ for every } i \in \Gamma_0 \text{ and } \lambda \in Y$$

$$(b) \ \chi_{\lambda,\mu}^m: V_{t(m),\lambda} \oplus W_{t(m),\lambda} \longrightarrow V_{s(m),\mu} \oplus W_{s(m),\mu} \text{ is defined by the matrix}$$

$$\begin{pmatrix} V_{\lambda}^m & 0 \\ 0 & W_{\lambda}^m \end{pmatrix}, \quad (21)$$

for  $m \in \Gamma_1$  and  $\lambda \in Y$ .

Now, we define a morphism of a weak Hopf quiver representation to another weak Hopf quiver representation as follows.

**Definition 7** (see [15]). If  $\mathcal{R}$  and  $S$  be two representations of the weak Hopf quiver  $\Gamma(S, r)$ , then  $\Phi: \mathcal{R} \rightarrow S$  as a representation morphism is a collection of  $k$ -linear maps  $\{\varphi_{\lambda,\mu}^i: V_{i,\lambda} \rightarrow W_{i,\mu} \mid i \in \Gamma_0 \& \mu \geq \lambda; \lambda, \mu \in Y\}$ , where  $\mathcal{R} = \{\mathcal{R}_{\lambda,\mu}; \mu \geq \lambda; \lambda, \mu \in Y\}$ ,  $S = \{S_{\lambda,\mu}; \mu \geq \lambda; \lambda, \mu \in Y\}$ , such that the following Figure 2 is commutative for all  $m \in \Gamma_1$ .

Suppose  $\varphi_{\lambda,\mu}^i: V_{i,\lambda} \rightarrow W_{i,\mu}$  is invertible for each  $i \in \Gamma_0$  and all  $\mu \geq \lambda; \lambda, \mu \in Y$ , we have the morphism  $\Phi: \mathcal{R} \rightarrow S$ , which is called isomorphism from  $\mathcal{R}$  to  $S$ .

A representation  $\mathcal{R}$  of a weak Hopf quiver  $\Gamma$  is decomposable if there exist two nonzero representations  $S$  and  $T$ , such that  $\mathcal{R} \cong S \oplus T$ , and a nonzero representation is indecomposable if it is not decomposable [15].

We introduce the notion of canonical representation of  $\Gamma$  and observe that it is also a simple one.

**Definition 8** (see [15]). A canonical representation  $\mathcal{R} = \{\mathcal{R}_{\lambda,\mu}; \mu \geq \lambda; \lambda, \mu \in Y\}$  for weak Hopf quiver  $\Gamma(S, r)$  is a collection of representations  $\mathcal{R}_{\lambda,\mu}$ , such that

$$\begin{array}{ccc}
 V_{t(m),\lambda} & \xrightarrow{\varphi_{\lambda,\lambda}^m} & V_{s(m),\lambda} \\
 \downarrow \varphi_{\lambda,\mu}^{t(m)} & & \downarrow \varphi_{\lambda,\mu}^{s(m)} \\
 W_{t(m),\mu} & \xrightarrow{\psi_{\mu,\mu}^m} & W_{s(m),\mu}
 \end{array}$$

 FIGURE 2: Commutative representation, where  $\psi_{\lambda,\mu}^m: W_{t(m),\lambda} \longrightarrow W_{s(m),\mu}$ .

$$\mathcal{R}_{\lambda,\mu} = \left\{ V_{i,\lambda} = \begin{cases} k, & \text{for one } i \in \Gamma_0, \\ 0, & \text{otherwise} \end{cases}, \varphi_{\lambda,\mu}^m = 0, \text{ for all } m \in \Gamma_1, \mu \geq \lambda; \lambda, \mu \in Y \right\}. \quad (22)$$

A canonical representation  $\mathcal{R}_{\lambda,\mu}$  must be a simple for all  $\lambda, \mu, \mu \geq \lambda; \lambda, \mu \in Y$ , since the only a subspace of each one is  $V_{i,\lambda}$ , the null space at every vertex.

Let  $\Gamma$  be a weak Hopf quiver having no oriented cycles. A representation  $\mathcal{R}$  of  $\Gamma$  is simple if and only if it is canonical.

If  $\Gamma(S, r)$  is a weak Hopf quiver without any oriented cycle, then there exists some vertex  $e_1 \in \Gamma_0$ , which is not a tail of some arrows. This type of arrow is called a sink.

Let  $\Gamma$  be a weak Hopf quiver with no oriented cycle, and  $e_1 \in \Gamma_0$  be a vertex, such that  $t(m) \neq e_1$ , for all  $m \in \Gamma_1$ .

**Proposition 2.** Let  $\mathcal{R}$  be a canonical representation of a weak Hopf quiver  $\Gamma(S, r)$ . Then, the representation  $S = \{S_{\lambda,\mu}: \mu \geq \lambda; \lambda, \mu \in Y\}$ , where

$$S_{\lambda,\mu} = \left\{ W_{i,\lambda} = \begin{cases} k, & i = x, \\ 0, & i \neq x \end{cases}, \varphi_{\lambda,\mu}^m = 0, \text{ for all } m \in \Gamma_1, \mu \geq \lambda; \lambda, \mu \in Y \right\}, \quad (23)$$

for the weak Hopf quiver  $\Gamma(S, r)$  is a subrepresentation of  $\mathcal{R}$ .

*Proof.* Obviously, for each  $i \neq x$ ,  $\{0\} = W_{i,\lambda}$  is a subspace of  $V_{i,\lambda}$ . Since  $V_{x,\lambda}$  is a nonzero  $k$ -vector space,  $k = W_{x,\lambda} \subseteq V_{x,\lambda}$ . Define  $\{p = p_{i,\lambda}; \lambda \in Y: i \in \Gamma_0\}$  a representation morphism, such that  $p_{i,\lambda}: W_{i,\lambda} \longrightarrow V_{i,\lambda}$  is the inclusion mapping. To verify that all mappings commute,  $m \in \Gamma_1$ , such that  $t(m) \neq x$ ,  $W_{t(m),\lambda} = \{0\}$ . So,  $\psi_{\lambda,\mu}^m: W_{t(m),\lambda} \longrightarrow W_{h(m),\mu}$  has its domain as  $\{0\}$ , i.e.,  $\psi_{\lambda,\mu}^m = 0$ . Similarly,  $p_{t(m),\lambda}: W_{t(m),\lambda} \longrightarrow V_{t(m),\lambda}$  is the inclusion of  $\{0\}$  that implies  $p_{t(m),\lambda} = 0$ . Hence, for all  $m \in \Gamma_1$ , such that  $t(m) \neq x$ , we have  $p_{h(m),\lambda} \circ \psi_{\lambda,\mu}^m = p_{h(m),\lambda} \circ 0 = 0$  and  $\psi_{\lambda,\mu}^m \circ p_{t(m),\lambda} = \psi_{\lambda,\mu}^m \circ 0 = 0$ , so the diagram is commutative. For each  $m \in \Gamma_1$  with  $t(m) = x$ , we have that  $V_{h(m),\lambda} = \{0\}$ . Hence,  $\varphi_{\lambda,\mu}^m: V_{t(m),\lambda} \longrightarrow V_{h(m),\mu}$  is  $\varphi_{\lambda,\mu}^m: V_{x,\lambda} \longrightarrow V_{x,\mu} = \{0\}$ , i.e.,  $\varphi_{\lambda,\mu}^m = \{0\}$ . Similarly,  $\psi_{\lambda,\mu}^m = \{0\}$ , and  $p_{h(m),\lambda}: \{0\} \longrightarrow \{0\}$  is also the zero mapping. So, for all  $m \in \Gamma_1$ , such that  $t(m) = x$ , we have  $p_{h(m),\lambda} = \psi_{\lambda,\mu}^m = 0 \circ 0 = 0$ . Hence, the diagram is commutative. Thus,  $S$  becomes a subrepresentation of  $\mathcal{R}$ .  $\square$

## 5. Weak Hopf Quiver as Cayley Graph

Let  $S$  be a semigroup and  $C$  be a subset of  $S$ . Recall that the Cayley graph  $\text{Cay}(S, C)$  of  $S$  with the connection set  $C$  is defined as the digraph with a vertex set  $S$  and arc set  $E(\text{Cay}(S, C)) = \{(s, cs): s \in S, c \in C\}$ .

In the following result, we give an embedding of a Cayley graph of a Clifford monoid  $S$  into the weak Hopf quiver of the corresponding weak Hopf algebra  $kS$ .

**Theorem 2.** Every Cayley graph  $\text{Cay}(S, C)$  of a Clifford monoid  $S$  can be embedded into its corresponding weak Hopf quiver  $\Gamma(S, r)$  of the weak Hopf algebra  $H = kS = \bigoplus_{\lambda \in Y} kG_\lambda$ .

*Proof.* Define mapping  $\varphi: \text{Cay}(S, C) \longrightarrow \Gamma(S, r)$ , such that  $\varphi(x) = e_x \in \Gamma_0$ , for all  $x \in V(S)$ .

Let  $c^y u^x$  represents the edge of the Cayley graph from vertex  $x$  to vertex  $y$  in  $E(C)$ .

Then,  $\varphi(c^y u^x) = c^y v^x \in \Gamma_1, \forall c^y u^x \in E(C)$ , where  $y = cx$  for some  $c \in C, x, y \in S$ , and  $c^y v^x$  is the arrow in  $\Gamma_1$ , such that  $y = c_\lambda \varphi_{\lambda,\mu}(x)$  for some  $c_\lambda$  (if it exist) in  $C_\lambda$ , the conjugacy class of  $G_\lambda$  for all  $x \in G_\lambda, y \in G_\mu; \mu \geq \lambda; \lambda, \mu \in Y$ .

Clearly,  $\varphi$  is an injective mapping from  $\text{Cay}(S, C)$  to the weak Hopf quiver  $\Gamma(S, r)$ .

Thus, the Cayley graph of a Clifford monoid  $S$  can be embedded into its corresponding weak Hopf quiver  $\Gamma(S, r)$ .  $\square$

## 6. Conclusion

In this article, the formula that enumerates the arrows in the weak Hopf quiver  $\Gamma(S, r)$  is devised. In addition, the verification of the fact is that the number of arrows originating and ending is equal in such quiver. It is further observed that a weak Hopf quiver representation appears as a generalization of the Hopf quiver representation. For each canonical representation, there exists a subrepresentation as given in Proposition 2.

Furthermore, it is perceived that the Cayley digraph of a Clifford monoid is embedded in the corresponding weak Hopf quiver of its corresponding weak Hopf algebra.

## Data Availability

No data were used to support this study.

## Conflicts of Interest

The authors declare that there are no conflicts of interest.

## Acknowledgments

The authors are grateful to the Deanship of Scientific Research, King Saud University, for funding through Vice Deanship of Scientific Research Chairs.

## References

- [1] F. Li, "Weak Hopf algebras and some new solutions of the quantum yang-baxter equation," *Journal of Algebra*, vol. 208, no. 1, pp. 72–100, 1998.
- [2] S. Montgomery, "Hopf algebras and their actions on rings," *Journal of the American Mathematical Society*, vol. 82, 1993.
- [3] S. Me, *Hopf Algebras. Mathematics Lecture Notes Series*, Benjamin, New York, NY, USA, 1969.
- [4] D. E. Radford, "The structure of Hopf algebras with a projection," *Journal of Algebra*, vol. 92, no. 2, pp. 322–347, 1985.
- [5] A. V. Daele and S. Wang, "Weak multiplier Hopf algebras II: source and target algebras," *Symmetry*, vol. 12, no. 12, Article ID 1975, 2020.
- [6] S. Yang and Y. Zhang, "Ore extensions for the Sweedler's Hopf algebra  $H_4$ ," *Mathematics*, vol. 8, no. 8, Article ID 1293, 2020.
- [7] J. Smith, "Quantum quasigroups and the quantum Yang–Baxter equation," *Axioms*, vol. 5, no. 4, Article ID 25, 2016.
- [8] F. Nichita, "Introduction to the Yang-Baxter equation with open problems," *Axioms*, vol. 1, no. 1, pp. 33–37, 2012.
- [9] C. Cibils and M. Rosso, "Hopf quivers," *Journal of Algebra*, vol. 254, no. 2, pp. 241–251, 2002.
- [10] L. Virginia, Tiago, and Eloy, "Quivers," *Universidade Estadual de Campinas*, vol. 3, no. 1, pp. 1–17, 2006.
- [11] F. Li, "Weak Hopf algebras and regular monoids," *Journal of Mathematical Research and Exposition-Chinese Edition*, vol. 19, pp. 325–331, 1999.
- [12] F. Li and Y.-Z. Zhang, "Quantum doubles from a class of non cocommutative weak Hopf algebras," *Journal of Mathematical Physics*, vol. 45, no. 8, pp. 3266–3281, 2004.
- [13] F. Li and H. Cao, "Semilattice graded weak Hopf algebra and its related quantum G-double," *Journal of Mathematical Physics*, vol. 46, no. 8, pp. 1–17, Article ID 083519, 2005.
- [14] H.-L. Huang and Y. Yang, "The green ring of minimal Hopf quiver," *Proceedings of the Edinburgh Mathematical Society*, vol. 59, 2014.
- [15] H.-L. Huang and G. Liu, "On Coquasitriangular Pointed Majid algebra, communications in algebra," *Communications in Algebra*, vol. 40, 2010.
- [16] H.-L. Huang and W. Q. Tao, "Coquasitriangular structures on Hopf quivers," *Journal of Algebra and Its Applications*, vol. 14, no. 8, 2015.
- [17] M. Ahmed and F. Li, "Weak Hopf quivers, Clifford monoids and weak Hopf algebras," *Arabian Journal for Science and Engineering*, vol. 36, no. 3, pp. 375–392, 2011.
- [18] M. Auslander, I. Reiten, and S. O. Smalø, "Representation theory of artin algebra," *Cambridge Studies in Advanced Mathematics*, Cambridge University Press, Cambridge, UK, 1995.
- [19] W. Chin and S. Montgomery, "Basic coalgebras," *AMS/IP Studies in Advanced Mathematics*, vol. 4, pp. 41–47, 1997.
- [20] C. Cibils, "Tensor product of Hopf bimodules over a group," *Proceedings of the American Mathematical Society*, vol. 125, no. 5, pp. 1315–1321, 1997.
- [21] H. Nakajima, "Introduction to quiver varieties for ring and representation theorists," 2016, <https://arxiv.org/pdf/2006.09282>.
- [22] D. Simson, "Coalgebras, comodules, pseudocompact algebras and tame comodule type," *Colloquium Mathematicum*, vol. 90, no. 1, pp. 101–150, 2001.
- [23] D. Woodcock, "Some categorical remarks on the representation theory of coalgebras," *Communications in Algebra*, vol. 25, no. 9, pp. 2775–2794, 1997.



## Research Article

# Computer-Based Fuzzy Numerical Method for Solving Engineering and Real-World Applications

**Naila Rafiq** <sup>1</sup>, **Naveed Yaqoob** <sup>2</sup>, **Nasreen Kausar** <sup>3</sup>, **Mudassir Shams** <sup>2</sup>,  
**Nazir Ahmad Mir** <sup>1</sup>, **Yaé Ulrich Gaba** <sup>4,5,6</sup> and **Naveed Khan**<sup>2</sup>

<sup>1</sup>Department of Mathematics, NUML, Islamabad, Pakistan

<sup>2</sup>Department of Mathematics and Statistics, Riphah International University I-14, Islamabad 44000, Pakistan

<sup>3</sup>Department of Mathematics, Yildiz Technical University, Faculty of Arts and Science, Esenler, 34210 Istanbul, Turkey

<sup>4</sup>Quantum Leap Africa (QLA), AIMS Rwanda Centre, Remera Sector KN 3, Kigali, Rwanda

<sup>5</sup>Institut de Mathématiques et de Sciences Physiques (IMSP/UAC), Laboratoire de Topologie Fondamentale, Computationnelle et Leurs Applications (Lab-ToFoCApp), BP 613, Porto-Novo, Benin

<sup>6</sup>African Center for Advanced Studies, P.O. Box 4477, Yaounde, Cameroon

Correspondence should be addressed to Yaé Ulrich Gaba; [yaeulrich.gaba@gmail.com](mailto:yaeulrich.gaba@gmail.com)

Received 27 August 2021; Accepted 12 October 2021; Published 1 November 2021

Academic Editor: Hao Gao

Copyright © 2021 Naila Rafiq et al. This is an open access article distributed under the Creative Commons Attribution License, which permits unrestricted use, distribution, and reproduction in any medium, provided the original work is properly cited.

The nonlinear equation is a fundamentally important area of study in mathematics, and the numerical solutions of the nonlinear equations are also an important part of it. Fuzzy sets introduced by Zadeh are an extension of classical sets, which have several applications in engineering, medicine, economics, finance, artificial intelligence, decision-making, and so on. The most special types of fuzzy sets are fuzzy numbers. The important fuzzy numbers are trapezoidal fuzzy and triangular fuzzy numbers, which have several applications. In this research article, we propose an efficient numerical iterative method for estimating roots of fuzzy nonlinear equations, which are based on the special type of fuzzy number called triangular fuzzy number. Convergence analysis proves that the order of convergence of the numerical method is three. Some real-life applications are considered as numerical test problems from engineering, which contain fuzzy quantities in the parametric form. Engineering models include fractional conversion of nitrogen-hydrogen feed into ammonia and Van der Waal's equation for calculating the volume and pressure of a gas and motion of the object under constant force of gravity. Numerical illustrations are given to show the dominance efficiency of the newly constructed iterative schemes as compared to existing methods in the literature.

## 1. Introduction

One of the ancient problems of science and engineering in general and in mathematics in particular is to approximate roots of nonlinear equations. The nonlinear equations play a major role in the field of engineering, mathematics, physics, chemistry, economics, medicines, and finance. Many times the particular realization of such type of nonlinear problems involves imprecise and non-probabilistic uncertainties in the parameter, where the approximations are known due to expert knowledge or due to some experimental data. Due to these reasons, several real world applications contain vagueness and

uncertainties. Therefore, in most of real world problems, the parameters involved in the system or variables of the nonlinear equations are presented by a fuzzy number. The concepts of fuzzy numbers and arithmetic operation with fuzzy numbers were first introduced and investigated in [1–10]. Hence, it is necessary to approximate the root of fuzzy nonlinear equation:

$$F(x) = c. \quad (1)$$

The standard analytical technique like Buckley and Qu method [11–14] cannot be suitable for solving the nonlinear equations such as

$ax^6 + bx^4 - cx^3 + dx - e = f$ ,  $x + \cos(x) = g$ ,  $x \ln(x) + e^x - (1/(1+x^2)) + \tan(x) = h$ , where  $a, b, c, d, e, f, g$ , and  $h$  are fuzzy numbers and  $x$  is a fuzzy variable.

We therefore look towards numerical iterative schemes, which approximate the roots of fuzzy nonlinear equations. To approximate the roots of fuzzy nonlinear equations, Abbsbandy and Asady [15] used Newton Raphson method, Sulaiman et al. [16] give Levenberg-Marquest method, and Mosleh [17] used Adomian decomposition method; see also [16, 18–20]. Iterative methods presented by them have low convergence order to approximate the roots of fuzzy nonlinear equations. Iterative methods of lower convergence order have high computational time and cost according to Kung–Traub conjecture [21].

Engineers and mathematicians therefore look towards those numerical methods which are more efficient and with high convergence order and low computational cost, or time, to approximate the roots of highly nonlinear fuzzy equations. The main aim of this research article is to propose efficient higher order iterative method as compared to well-known classical methods [15]. Numerical test results, CPU time, and log of residual show the dominance efficiency of our newly constructed method over the existing methods in the literature.

This paper is organized as follows: after introduction in Section 2, we recall some fundamental results of fuzzy numbers. In Section 3, we propose numerical iterative schemes for approximating roots of fuzzy nonlinear equations and their convergence analysis. In Section 4, we illustrate some real world applications as numerical test examples to show the performance and efficiency of the constructed method and conclusions in the last section.

## 2. Preliminaries

*Definition 1.* A fuzzy number is a fuzzy set like  $x: \mathbb{R} \rightarrow I = [0, 1]$ , which satisfies the following [22, 23]:

- (1)  $x$  is upper semicontinuous
- (2)  $x(a) = 0$  outside some interval  $[a_1, a_2]$
- (3) The real numbers are  $b_1, b_2$  such that  $a_1 \leq b_1 \leq b_2 \leq a_2$  and

$$\begin{aligned} x(a) & \text{ is monotonic increasing on } [a_1, b_1] \\ x(a) & \text{ is monotonic decreasing on } [b_2, a_2] \\ x(a) & = 1, \text{ for } b_1 \leq a \leq b_2 \end{aligned}$$

We denote by  $E$  the set of all fuzzy numbers. An equivalent parametric form is also given in [24] as follows.

*Definition 2* (see [25]). A fuzzy number  $x$  in parametric form is a pair  $(x^L, x^U)$  of function  $x^L(\tau)$ ,  $x^U(\tau)$ ,  $0 \leq \tau \leq 1$ , which satisfies the following requirements:

- (1)  $x^L(\tau)$  is a bounded monotonic increasing left continuous function
- (2)  $x^U(\tau)$  is a bounded monotonic decreasing left continuous function
- (3)  $x^L(\tau) \leq x^U(\tau)$ ,  $0 \leq \tau \leq 1$

A popular fuzzy number is the triangular fuzzy number, which is formed by simply taking  $b_1 = b_2$  in Definition 1. Triangular fuzzy number is simply written as  $x = (a_1, a_2, a_3)$  and defined in the form of membership function as

$$x(a) = \begin{cases} \frac{x - a_1}{a_2 - a_1}, & \text{if } a_1 < x < a_2, \\ \frac{a_3 - x}{a_3 - a_2}, & \text{if } a_2 < x < a_3, \\ 0, & \text{otherwise.} \end{cases} \quad (2)$$

The parametric form is given as

$$\begin{aligned} x^L(\tau) & = a_1 + \tau(a_2 - a_1), \\ x^U(\tau) & = a_3 + \tau(a_2 - a_3). \end{aligned} \quad (3)$$

Let  $\text{TF}(\mathbb{R})$  be the set of all triangular fuzzy numbers. The addition and scalar multiplication of fuzzy numbers are defined by the extension principle and represented as follows.

For arbitrary  $x = (x^L, x^U)$ ,  $y = (y^L, y^U)$ , and  $k > 0$ , we define addition  $(x + y)$  and multiplication by scalar  $k$  as

$$\begin{cases} (x + y)^L(\tau) = x^L(\tau) + y^L(\tau), \\ (x + y)^U(\tau) = x^U(\tau) + y^U(\tau), \\ (kx)^L(\tau) = kx^L(\tau), \\ (kx)^U(\tau) = kx^U(\tau). \end{cases} \quad (4)$$

## 3. Construction of Iterative Schemes

Now, our aim is to obtain a solution for fuzzy nonlinear equation  $F(x) = c$ . The parametric form is as follows:

$$\begin{cases} F^L(x^L, x^U, \tau) = c^L(\tau), \\ F^U(x^L, x^U, \tau) = c^U(\tau), \end{cases} \quad \forall \tau \in [0, 1]. \quad (5)$$

Suppose that  $x = (\xi^L, \xi^U)$  is the solution to the system; that is,

$$\begin{cases} F^L(\xi^L, \xi^U, \tau) = c^L(\tau), \\ F^U(\xi^L, \xi^U, \tau) = c^U(\tau), \end{cases} \quad \forall \tau \in [0, 1]. \quad (6)$$

Therefore, if  $x_0 = (x_0^L, x_0^U)$  is an approximation solution for this system, then  $\forall \tau \in [0, 1]$  there exist  $h^L(\tau)$ ,  $h^U(\tau)$  such that

$$\begin{cases} \xi^L = x_0^L + h^L(\tau), \\ \xi^U = x_0^U + h^U(\tau). \end{cases} \quad (7)$$

Using Taylor series of  $F^L, F^U$  about  $(x_0^L, x_0^U)$ ,  $\forall \tau \in [0, 1]$ , we have

$$\begin{cases} F^L(\xi^L, \xi^U, \tau) = F^L(x_0^L, x_0^U, \tau) + h^L F_{x^L}^L(x_0^L, x_0^U, \tau) + h^U F_{x^U}^L(x_0^L, x_0^U, \tau) + \\ O\left((h^L)^2 + h^L h^U + (h^U)^2\right) = c^L, \\ F^U(\xi^L, \xi^U, \tau) = F^U(x_0^L, x_0^U, \tau) + h^L F_{x^L}^U(x_0^L, x_0^U, \tau) + h^U F_{x^U}^U(x_0^L, x_0^U, \tau) + \\ O\left((h^L)^2 + h^L h^U + (h^U)^2\right) = c^U. \end{cases} \quad (8)$$

If  $x_0^L$  and  $x_0^U$  are near to  $\xi^L$  and  $\xi^U$ , respectively, then  $h^L$  and  $h^U$  are small. We assume, of course, that all needed

partial derivatives exist and are bounded. Therefore, for enough small  $h^L$  and  $h^U$ , we have,  $\forall \tau \in [0, 1]$ ,

$$\begin{cases} F^L(x_0^L, x_0^U, \tau) + h^L F_{x^L}^L(x_0^L, x_0^U, \tau) + h^U F_{x^U}^L(x_0^L, x_0^U, \tau) = c^L(\tau), \\ F^U(x_0^L, x_0^U, \tau) + h^L F_{x^L}^U(x_0^L, x_0^U, \tau) + h^U F_{x^U}^U(x_0^L, x_0^U, \tau) = c^U(\tau), \end{cases} \quad (9)$$

and hence,  $h^L(\tau)$  and  $h^U(\tau)$  are unknown quantities that can be obtained by solving the following equations,  $\forall \tau \in [0, 1]$ ,

$$J(x_0^L, x_0^U, \tau) \begin{bmatrix} h_0^L(\tau) \\ h_0^U(\tau) \end{bmatrix} = \begin{bmatrix} c^L(\tau) - F^L(x_0^L, x_0^U, \tau) \\ c^U(\tau) - F^U(x_0^L, x_0^U, \tau) \end{bmatrix}, \quad (10)$$

where

$$J(x_0^L, x_0^U, \tau) = \begin{bmatrix} F_{x^L}^L(x_0^L, x_0^U, \tau) & F_{x^U}^L(x_0^L, x_0^U, \tau) \\ F_{x^L}^U(x_0^L, x_0^U, \tau) & F_{x^U}^U(x_0^L, x_0^U, \tau) \end{bmatrix}. \quad (11)$$

Thus, our method in component form becomes

$$\begin{aligned} \begin{bmatrix} x_1^L(\tau) \\ x_1^U(\tau) \end{bmatrix} &= \begin{bmatrix} x_0^L(\tau) \\ x_0^U(\tau) \end{bmatrix} + \begin{pmatrix} ((2-\beta)J(x_0^L, x_0^U, \tau) + \beta K(y_0^L, y_0^U, \tau))^{-1} \\ * ((3-\beta)J(x_0^L, x_0^U, \tau) + (\beta-1)K(y_0^L, y_0^U, \tau)) \end{pmatrix} \\ &\quad \cdot \begin{bmatrix} c^L(\tau) - F_{x^L}^L(x_0^L, x_0^U, \tau) \\ c^U(\tau) - F_{x^L}^U(x_0^L, x_0^U, \tau) \end{bmatrix}, \\ \begin{bmatrix} y_0^L(\tau) \\ y_0^U(\tau) \end{bmatrix} &= \begin{bmatrix} x_0^L(\tau) \\ x_0^L(\tau) \end{bmatrix} + \begin{bmatrix} h_0^L(\tau) \\ h_0^U(\tau) \end{bmatrix}, \\ K(y_0^L, y_0^U, \tau) &= \begin{bmatrix} F_{y^L}^L(y_0^L, y_0^U, \tau) & F_{y^U}^L(y_0^L, y_0^U, \tau) \\ F_{y^L}^U(y_0^L, y_0^U, \tau) & F_{y^U}^U(y_0^L, y_0^U, \tau) \end{bmatrix}. \end{aligned} \quad (12)$$

For approximate solutions of  $x^L$  and  $x^U$ , we use the following recursive relation:

$$\begin{aligned} \begin{bmatrix} x_{n+1}^L(\tau) \\ x_{n+1}^U(\tau) \end{bmatrix} &= \begin{bmatrix} x_n^L(\tau) \\ x_n^U(\tau) \end{bmatrix} + \begin{pmatrix} ((2-\beta)J(x_n^L, x_n^U, \tau) + \beta K(y_n^L, y_n^U, \tau))^{-1} \\ * ((3-\beta)J(x_n^L, x_n^U, \tau) + (\beta-1)K(y_n^L, y_n^U, \tau)) \end{pmatrix} \\ &\quad \cdot \begin{bmatrix} c^L(\tau) - F_{x^L}^L(x_n^L, x_n^U, \tau) \\ c^U(\tau) - F_{x^L}^U(x_n^L, x_n^U, \tau) \end{bmatrix}, \end{aligned} \quad (13)$$

where

$$\begin{aligned} \begin{bmatrix} y_n^L(\tau) \\ y_n^U(\tau) \end{bmatrix} &= \begin{bmatrix} x_n^L(\tau) \\ x_n^U(\tau) \end{bmatrix} + \begin{bmatrix} h_n^L(\tau) \\ h_n^U(\tau) \end{bmatrix}, \\ J(x_n^L, x_n^U, \tau) \begin{bmatrix} h_n^L(\tau) \\ h_n^U(\tau) \end{bmatrix} &= \begin{bmatrix} F_{x^L}^L(x_n^L, x_n^U, \tau) & F_{x^U}^L(x_n^L, x_n^U, \tau) \\ F_{x^L}^U(x_n^L, x_n^U, \tau) & F_{x^U}^U(x_n^L, x_n^U, \tau) \end{bmatrix}, \\ K(y_n^L, y_n^U, \tau) &= \begin{bmatrix} F_{y^L}^L(y_n^L, y_n^U, \tau) & F_{y^U}^L(y_n^L, y_n^U, \tau) \\ F_{y^L}^U(y_n^L, y_n^U, \tau) & F_{y^U}^U(y_n^L, y_n^U, \tau) \end{bmatrix}, \\ &\forall \tau \in [0, 1]. \end{aligned} \quad (14)$$

For initial guess, one can use the fuzzy number

$$x_0 = (x_0^L(1), x_0^U(1), x_1^L(1) - x_0^L(0), x_0^U(0) - x_0^U(1)), \quad (15)$$

and in the parametric form

$$\begin{aligned} x_0(\tau) &= x_0^L(1) + (x_0^L(1) - x_0^L(0))(\tau - 1), \\ x_0^U(\tau) &= x_0^U(1) + (x_0^U(0) - x_0^U(1))(1 - \tau). \end{aligned} \quad (16)$$

*Remark 1.* Sequence  $\{(x_n^L, x_n^U)\}_{n=0}^\infty$  converges to  $(\xi^L, \xi^U)$  iff  $\forall \tau \in [0, 1]$ ,  $\lim_{n \rightarrow \infty} x_n^L(\tau) = \xi^L(\tau)$  and  $\lim_{n \rightarrow \infty} x_n^U(\tau) = \xi^U(\tau)$ .

**Lemma 1.** Let  $F(\xi^L, \xi^U) = (c^L, c^U)$  and if the sequence of  $\{(x_n^L, x_n^U)\}_{n=0}^\infty$  converges to  $(\xi^L, \xi^U)$  to NM method, then

$$\lim_{n \rightarrow \infty} P_n = 0, \quad (17)$$

where

$$P_n = \sup_{0 \leq \tau \leq 1} \max\{h_n^L(\tau), h_n^U(\tau)\}. \quad (18)$$

*Proof.* It is obviously because  $\forall \tau \in [0, 1]$  in convergent case

$$\lim_{n \rightarrow \infty} h_n^L(\tau) = \lim_{n \rightarrow \infty} h_n^U(\tau) = 0. \quad (19) \quad \square$$

Under certain condition, finally it is shown that NM method is cubic convergence for fuzzy nonlinear equation  $F(x) = 0$ . Thus, in compact form, we write

$$\begin{cases} y_n = x_n - (F'(x_n))^{-1}F(x_n), \\ x_{n+1} = x_n - Z * (F'(x_n))^{-1}F(x_n), \end{cases} \quad \forall \tau \in [0, 1], \quad (20)$$

where  $Z = (((2 - \beta)F'(x_n^L, x_n^U, \tau) + \beta F'(y_n^L, y_n^U, \tau))^{-1} ((3 - \beta)F'(x_n^L, x_n^U, \tau) + (\beta - 1)F'(y_n^L, y_n^U, \tau)))$  and  $\beta \in \mathbb{R}$  (set of real numbers).

**Theorem 1.** Let,  $\forall \tau \in [0, 1]$ , the functions  $F^L$  and  $F^U$  be continuously differentiable with respect to  $x_n^L(\tau)$  and  $x_n^U(\tau)$ . Assume that there exist  $(\xi^L(\tau), \xi^U(\tau)) \in \mathbb{R}^2$  and  $\alpha_1, \alpha_2 > 0$  such that  $\|J^{-1}(\xi^L, \xi^U, \tau)\| \leq \alpha_1$ ,  $\|K^{-1}(\xi^L, \xi^U, \tau)^{-1}\| \leq \alpha_2$  and

$J, K$  will be Lipschitz continuous with respect to  $x_n^L$  and  $x_n^U$ ; then the NM method converges to  $(\xi^L, \xi^U)$  and satisfies the following error equation:

$$\mathbf{e}_{n+1} = \left(2(\mathbf{A}_2)^2 + \frac{1}{2}\mathbf{A}_3 - \beta(\mathbf{A}_2)^2\right)(\mathbf{e}_n)^3 + \|O(\mathbf{e}_n)^4\|, \quad (21)$$

where  $\mathbf{A}_j = (1/j!) * ((F^{(j)}(x_n, \tau))/F'(x_n, \tau))$ ,  $j = 2, 3, \dots$

*Proof.* Let  $\mathbf{e}_n = x_n - \xi$  and  $\mathbf{e}_{n+1} = x_{n+1} - \xi$  be the errors in  $x_n$  and  $x_{n+1}$ ; then, by Taylor series of  $F(x_n, \tau)$  in the neighborhood of  $\xi$ , if  $J^{-1}(x_n, \tau)$  exist, then

$$\begin{aligned} F(x, \tau) &= F(x_n, \tau) + F'(x_n, \tau)(x - x_n) \\ &\quad + \frac{1}{2!}F''(x_n, \tau)(x - x_n)^2 + \dots, \end{aligned} \quad (22)$$

and  $F(\xi, \tau) = 0$ ,

$$F(x_n, \tau) = F'(x, \xi)(\mathbf{e}_n + \mathbf{A}_2(\mathbf{e}_n)^2 + \mathbf{A}_3(\mathbf{e}_n)^3) + \|O(\mathbf{e}_n)^4\|. \quad (23)$$

This gives

$$\begin{aligned} (F'(x_n, \tau))^{-1}F(x_n, \tau) &= \mathbf{e}_n + \mathbf{A}_2(\mathbf{e}_n)^2 \\ &\quad + (2\mathbf{A}_2 + 2\mathbf{A}_3)(\mathbf{e}_n)^3 + \dots, \\ y_n - \xi &= \mathbf{A}_2(\mathbf{e}_n)^2 + (-2\mathbf{A}_2 \\ &\quad \cdot + 2\mathbf{A}_3)(\mathbf{e}_n)^3 + \dots. \end{aligned} \quad (24)$$

Expanding  $F'(y_n, \tau)$  about  $\xi$ , we have

$$\begin{aligned} F'(y_n, \tau) &= 1 + 2(\mathbf{A}_2)^2(\mathbf{e}_n)^2 + 2(-2(\mathbf{A}_2)^2 \\ &\quad + 2\mathbf{A}_3)(\mathbf{e}_n)^3 + \dots, \end{aligned}$$

$$Z(F'(x_n, \tau))^{-1}F(x_n, \tau) = (\mathbf{e}_n)^2 + \left(-2(\mathbf{A}_2)^2 - \frac{1}{2}\mathbf{A}_3\right.$$

$$\left. + \beta(\mathbf{A}_2)^2\right)(\mathbf{e}_n)^3 + \dots,$$

$$x_{n+1} - \xi = x_n - \xi - (\mathbf{e}_n)^2 + (-2(\mathbf{A}_2)^2$$

$$- \frac{1}{2}\mathbf{A}_3 + \beta(\mathbf{A}_2)^2)(\mathbf{e}_n)^3 + \dots,$$

$$\begin{aligned} \mathbf{e}_{n+1} &= \left(2(\mathbf{A}_2)^2 + \frac{1}{2}\mathbf{A}_3 - \beta(\mathbf{A}_2)^2\right)(\mathbf{e}_n)^3 \\ &\quad + \|O(\mathbf{e}_n)^4\|. \end{aligned} \quad (25)$$

Hence, the theorem is proved.  $\square$

There are some well-known existing methods in the literature for solving triangular fuzzy nonlinear equations.

Fuzzy version of well-known Newton method [15] (abbreviated as NR) for finding roots of triangular fuzzy equation is as follows:

$$\begin{bmatrix} x_{n+1}^L(\tau) \\ x_{n+1}^U(\tau) \end{bmatrix} = \begin{bmatrix} x_n^L(\tau) \\ x_n^U(\tau) \end{bmatrix} + \begin{bmatrix} h_n^L(\tau) \\ h_n^U(\tau) \end{bmatrix}, \quad (26)$$

where

$$\begin{bmatrix} h_n^L(\tau) \\ h_n^U(\tau) \end{bmatrix} = J^{-1}(x_n^L, x_n^U, \tau) \begin{bmatrix} c^L(\tau) - F^L(x_n^L, x_n^U, \tau) \\ c^U(\tau) - F^U(x_n^L, x_n^U, \tau) \end{bmatrix}. \quad (27)$$

Midpoint iterative schemes [26] (abbreviated as NP) for triangular fuzzy equation are as follows:

$$\begin{bmatrix} x_{n+1}^L(\tau) \\ x_{n+1}^U(\tau) \end{bmatrix} = \begin{bmatrix} y_n^L(\tau) \\ y_n^U(\tau) \end{bmatrix} + J^{-1}\left(\frac{x_n^L + y_n^L}{2}, \frac{y_n^U + x_n^U}{2}, \tau\right) \cdot \begin{bmatrix} c^L(\tau) - F^L(x_n^L, x_n^U, \tau) \\ c^U(\tau) - F^U(x_n^L, x_n^U, \tau) \end{bmatrix}, \quad (28)$$

where

$$\begin{bmatrix} y_n^L(\tau) \\ y_n^U(\tau) \end{bmatrix} = \begin{bmatrix} x_n^L(\tau) \\ x_n^U(\tau) \end{bmatrix} + \begin{bmatrix} h_n^L(\tau) \\ h_n^U(\tau) \end{bmatrix}. \quad (29)$$

### 4. Numerical Applications

Here, we present examples to illustrating Newton’s method for fuzzy nonlinear equations. Examples 1 and 2 are considered from Buckley and Qu [11, 27, 28]. All the

computations are performed using CAS Maple 18 with 64-digit floating point arithmetic with stopping criteria as follows:

$$\begin{aligned} (i) \mathbf{e}_n &= \|F(x, \tau)\| < \epsilon, \\ (ii) \mathbf{e}_n &= \|\mathbf{x}_{n+1}(\tau) - \mathbf{x}_n(\tau)\| < \epsilon, \end{aligned} \quad (30)$$

where  $\mathbf{e}_n$  represents the absolute error. We take  $\epsilon = 10^{-15}$ . In all numerical calculations, we used  $\beta = 0.000001$ .

Figure 1 shows computational time in seconds of iterative schemes NM, NR, and NP for nonlinear fuzzy equations in Examples 1–3 (Cases 1 and 2) and 4, respectively (Algorithm 1).

#### 4.1. Engineering Applications

*Example 1.* Fraction conversion of Nitrogen-Hydrogen feed to ammonia is known as fractional conversion. Here, we consider the value of temperature and pressure as triangular fuzzy number, which results in the following fuzzy nonlinear equation:

$$\nabla_1(x(\tau))^4 - \nabla_2(x(\tau))^3 + \nabla_3(x(\tau))^2 + \nabla_4x(\tau) = \nabla_5, \quad (31)$$

where  $\nabla_1 = (1, 2.5, 3.7)$ ,  $\nabla_2 = (7.7, 7.9, 8.1)$ ,  $\nabla_3 = (14.7, 14.8, 14.9)$ ,  $\nabla_4 = (2.5, 2.7, 2.9)$ , and  $\nabla_5 = (1.6, 1.7, 2.0)$  are triangular fuzzy numbers. Without any loss of generality, assume that  $x$  is positive; then the parametric form of this equation is as follows:

$$\begin{cases} (1 + 1.5\tau)(x^L(\tau))^4 - (7.7 + 0.2\tau)(x^L(\tau))^3 + (14.7 + 0.1\tau)(x^L(\tau))^2 + (2.5 + 0.2\tau)x^L(\tau) = (1.6 + 0.1\tau), \\ (3.7 - 1.2\tau)(x^U(\tau))^4 - (8.1 - 0.2\tau)(x^U(\tau))^3 + (14.9 - 0.1\tau)x^U(\tau) + (2.9 - 0.2\tau)x^U(\tau) = (2 - 0.3\tau). \end{cases} \quad (32)$$

Figure 2 shows analytical and numerical approximate solution of fuzzy nonlinear equation in Example 1.

Table 1 clearly shows the dominance behavior of NM over NR and NP in terms of absolute error on the same number of iterations  $n = 3$  for Example 1.

To obtain initial guess, we use the above system for  $\tau = 1$  and  $\tau = 0$ ; therefore,

$$\begin{cases} 2.5(x^L)^4(1) - 7.9(x^L)^2(1) + 14.8(x^L)^2(1) + 2.7(x^L)(1) = 1.7, \\ 2.5(x^U)^4(1) - 7.9(x^U)^2(1) + 14.8(x^U)^2(1) + 2.7(x^U)(1) = 1.7, \\ 1(x^L)^4(0) - 7.7(x^L)^3(0) + 14.7(x^L)^2(0) + 2.5(x^L)(0) = 1.6, \\ 3.7(x^U)^4(0) - 8.1(x^U)^2(0) + 14.9(x^U)(0) + 2.9(x^U)(0) = 2. \end{cases} \quad (33)$$

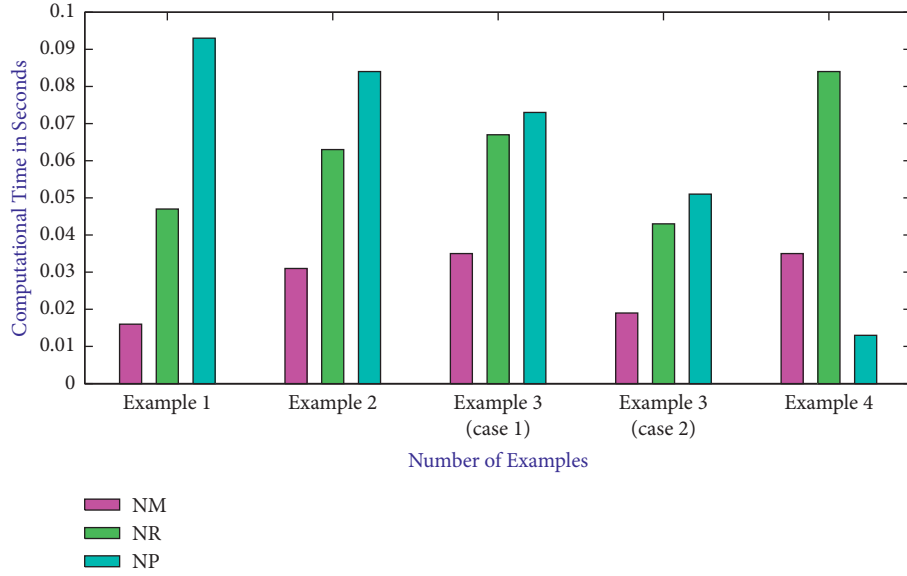


FIGURE 1: Computational time in seconds.

Step 1: transform  $F(x, \tau) = c$  into  $\begin{cases} F^L(x^L, x^U, \tau) = c^L(\tau), \\ F^U(x^L, x^U, \tau) = c^U(\tau), \end{cases} \forall \tau \in [0, 1].$   
 Step 2: solve  $\begin{cases} F^L(x^L, x^U, \tau) = c^L(\tau), \\ F^U(x^L, x^U, \tau) = c^U(\tau). \end{cases}$  for  $\tau = 0$  and  $\tau = 1$  to obtain  $x^L(0)$  and  $x^U(0)$ .  
 Step 3: evaluate  $F(x, \tau) = c$  at  $x^L(0)$  and  $x^U(0)$  and compute Jacobian matrix  $J(x^L, x^U, \tau)$ .  
 Step 4: use NM to compute next iterations.  
 Step 5: for given  $\epsilon > 0$ , (i)  $\mathbf{e}_n = \|F(x, \tau)\| < \epsilon$  (ii)  $\mathbf{e}_n = \|x_{n+1}(\tau) - x_n(\tau)\| < \epsilon$ , then stop.  
 Step 6: set  $k = k + 1$  and go to Step 1.

ALGORITHM 1: NM method.

Consequently  $x^L(0) = 0.2$ ,  $x^U(0) = 0.2$ , and  $x^L(1) = x^U(1) = 0.2737$ . Therefore, initial guess is  $x_0 = (0.26, 0.2737, 0.29)$ . After 3 iterations, we obtain the

solution which the maximum error would be less than  $10^{-3}$ . Now suppose  $x$  is negative; we have

$$\begin{cases} (1 + 1.5\tau)(x^L(\tau))^4 - (7.7 + 0.2\tau)(x^L(\tau))^3 + (14.7 + 0.1\tau)(x^L(\tau))^2 + (2.5 + 0.2\tau)x^L(\tau) = (1.6 + 0.1\tau), \\ (3.7 - 1.2\tau)(x^U(\tau))^4 - (8.1 - 0.2\tau)(x^U(\tau))^3 + (14.9 - 0.1\tau)x^U(\tau) + (2.9 - 0.2\tau)x^U(\tau) = (2 - 0.3\tau). \end{cases} \quad (34)$$

For  $\tau = 0$ , we have  $x^U(0) > x^L(0)$ , and therefore, negative root does not exist.

*Example 2.* A chemical engineering problem is finding the volume of van der Waal's equation. Van der Waal's equation interprets real and ideal gas behavior, which results in the following equation:

$$\left(P + \frac{A_1 n^2}{x^2}\right)(x - nA_2) = nRT. \quad (35)$$

By using the specific values of parameter, we have the following fuzzy nonlinear equation:

$$\Delta_1(x(\tau))^3 - \Delta_2(x(\tau))^2 + \Delta_3 x(\tau) = \Delta_4, \quad (36)$$

where  $\Delta_1 = (0.3, 0.4, 0.7)$ ,  $\Delta_2 = (1, 2.3, 3.4)$ ,  $\Delta_3 = (6.8, 7, 8.9)$ ,  $\Delta_4 = (4.1, 5.2, 6.7)$  are triangular fuzzy numbers and  $x$  represents the volume of the gas under observation,  $P$  for pressure,  $R$  for general gas constant,  $n$  for number of mole, and  $T$  for temperature, and  $A_1, A_2$  are used for general parameters. Without any loss of generality,

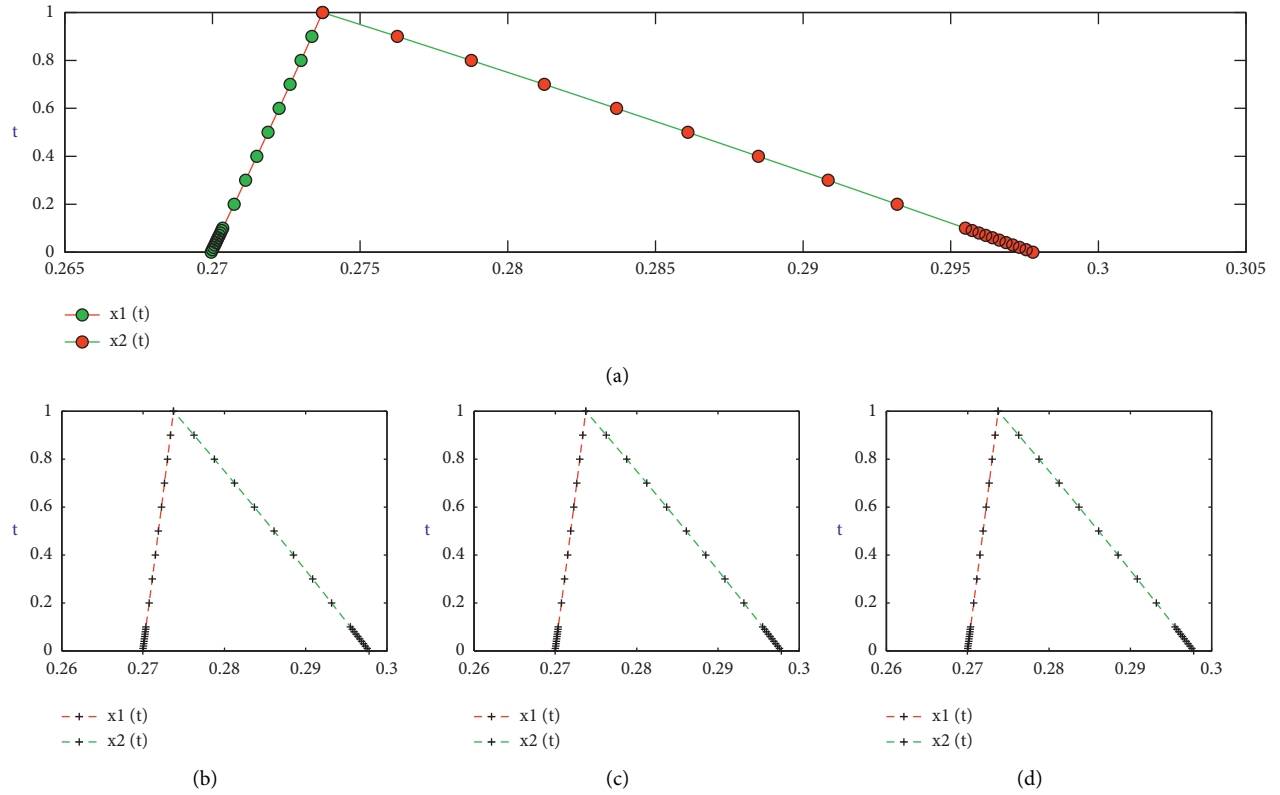


FIGURE 2: Analytical and numerical approximate solutions of Example 1. (a) Analytical solution for Example 1. (b) NM method for Example 1. (c) NR method for Example 1. (d) NP method for Example 1.

TABLE 1: Comparison of iterative schemes NM, NR, and NP on the same number of iterations  $n = 3$ .

$\tau$	$x^L$	$x^U$	NM		NR		NP	
			$\ x_{n+1} - x_n\ $	$\ f(x_n)\ $	$\ x_{n+1} - x_n\ $	$\ f(x_n)\ $	$\ x_{n+1} - x_n\ $	$\ f(x_n)\ $
0.0	0.2699	0.2977	$3.9e-19$	$6.9e-20$	$0.3e-5$	$2.7e-4$	$6.3e-8$	$7.3e-9$
0.1	0.2703	0.2954	$1.3e-19$	$1.3e-18$	$6.2e-5$	$5.2e-6$	$6.2e-9$	$5.9e-8$
0.2	0.2707	0.2931	$2.1e-17$	$7.1e-18$	$5.2e-5$	$7.4e-5$	$1.6e-9$	$6.4e-7$
0.3	0.2711	0.2908	$9.7e-15$	$1.8e-19$	$6.4e-6$	$4.6e-4$	$8.8e-9$	$4.3e-8$
0.4	0.2715	0.2884	$9.5e-16$	$8.5e-16$	$6.1e-5$	$5.3e-6$	$7.8e-9$	$1.4e-9$
0.5	0.2718	0.2860	$1.4e-15$	$1.9e-15$	$5.7e-7$	$8.3e-5$	$7.7e-9$	$0.5e-8$
0.6	0.2722	0.2836	$4.0e-16$	$6.9e-19$	$7.5e-5$	$3.4e-4$	$5.5e-8$	$3.8e-7$
0.7	0.2726	0.2812	$7.6e-17$	$3.9e-18$	$8.1e-6$	$4.8e-3$	$8.7e-9$	$1.2e-7$
0.8	0.2729	0.2787	$0.4e-18$	$8.2e-19$	$5.8e-7$	$0.4e-6$	$8.9e-8$	$2.6e-9$
0.9	0.2733	0.2762	$2.6e-17$	$6.1e-18$	$3.8e-5$	$1.3e-8$	$4.8e-9$	$2.3e-9$
1	0.2737	0.2737	$9.6e-19$	$1.2e-17$	$7.9e-5$	$7.8e-7$	$9.8e-8$	$1.8e-8$

assume that  $x(\tau)$  is positive; then the parametric form of this equation is as follows:

$$\begin{cases} (0.3 + 0.1\tau)(x^L(\tau))^3 - (1 + 1.3\tau)(x^L(\tau))^2 + (6.8 + 0.2\tau)x^L(\tau) = (4.1 + 1.1\tau), \\ (0.7 - 0.3\tau)(x^U(\tau))^3 - (3.4 - 1.1\tau)(x^U(\tau))^2 + (8.9 - 1.9\tau)x^U(\tau) = (6.7 - 1.5\tau). \end{cases} \quad (37)$$

Figure 3 shows analytical and numerical approximate solution of fuzzy nonlinear equation in Example 2.

Figure 3 shows analytical and numerical approximate solution of fuzzy nonlinear equation in Example 2.

Table 2 clearly shows the dominance behavior of NM over NR and NP in terms of absolute error on the same number of iterations  $n = 3$  for Example 2.

To obtain initial guess, we use the above system for  $\tau = 1$  and  $\tau = 0$ ; therefore

$$\begin{cases} 0.4(x^L)^3(1) - 2.3(x^L)^2(1) + 7.0(x^L)(1) = 5.2, \\ 0.4(x^U)^3(1) - 2.3(x^U)^2(1) + 7.0(x^U)(1) = 5.2, \\ 0.3(x^L)^3(0) - 1.0(x^L)^2(0) + 6.8(x^L)(0) = 4.1, \\ 0.7(x^U)^3(0) - 3.4(x^U)^2(0) + 8.9(x^U)(0) = 6.7. \end{cases} \quad (38)$$

$$\begin{cases} (0.3 + 0.1\tau)(x^L(\tau))^3 - (1 + 1.3\tau)(x^L(\tau))^2 + (6.8 + 0.2\tau)x^L(\tau) = (4.1 + 1.1\tau), \\ (0.7 - 0.3\tau)(x^U(\tau))^3 - (3.4 - 1.1\tau)(x^U(\tau))^2 + (8.9 - 1.9\tau)x^L(\tau) = (6.7 - 1.5\tau). \end{cases} \quad (39)$$

For  $\tau = 0$ , we have  $x^U(0) > x^L(0)$ , and therefore, negative root does not exist.

*Example 3.* In engineering, the problem concerns the motion of object under fuzzy environment, resulting in two cases.

*Case 1.* Vertical motion of object.

Here, we are concerned with the vertical motion of ball by neglecting air resistance and assume constant acceleration  $32 \text{ ft/sec}^2$ . Positive direction of the object  $y$  is upward from earth. Then, the resulting fuzzy nonlinear equation is written as

$$A_1 * x(\tau)^2 + V_1 * x(\tau) = Y_1, \quad (40)$$

where  $A_1 = (0.8, 1.0, 1.2)$ , free parameter,  $V_1 = (1.3, 1.75, 2.2)$ , velocity of the moving object under constant force of gravity, and  $Y_1 = (0.1, 0.15, 0.20)$ , initial position of the object. By substituting the value of  $A_1, V_1$ , and  $Y_1$  in the above equation of motion, we get

$$(0.8, 1.0, 1.2)(x(\tau)^2) + (1.3, 1.75, 2.2)x(\tau) = (0.1, 0.15, 0.20). \quad (41)$$

Then, we find the time  $x(\tau)$  of the ball to hit the ground which depends on fuzzy parameter  $\tau \in [0, 1]$ . Without any loss of generality, assume that  $x(\tau)$  is positive; then the parametric form of this equation is as follows:

$$\begin{cases} (0.8 + 0.2\tau)(x^L(\tau))^2 + (1.3 + 0.45\tau)x^L(\tau) = (0.1 + 0.05\tau), \\ (1.2 - 0.2\tau)(x^U(\tau))^2 + (2.2 - 0.45\tau)x^U(\tau) = (0.2 - 0.05\tau). \end{cases} \quad (42)$$

Figure 4 shows analytical and numerical approximate solution of fuzzy nonlinear equation in Example 3 (Case 1).

Figure 4 shows analytical and numerical approximate solution of fuzzy nonlinear equation in Example 3 (Case 1).

Consequently  $x^L(0) = 0.6$ ,  $x^U(0) = 1.1$ , and  $x^L(1) = x^U(1) = 1.028015150$ . Therefore, initial guess is  $x_0 = (0.6, 1.028015150, 1.1)$ . After 3 iterations, we obtain the solution which the maximum error would be less than  $10^{-3}$ . Now suppose  $x(\tau)$  is negative; we have

Table 3 clearly shows the dominance behavior of NM over NR and NP in terms of absolute error on the same number of iterations  $n = 3$  for Example 3 (Case 1).

To obtain initial guess, we use the above system for  $\tau = 0$  and  $\tau = 1$ ; therefore

$$\begin{cases} 1(x^L)^2(1) + 1.75(x^L)(1) = 0.6, \\ 1(x^U)^2(1) + 1.75(x^U)(1) = 0.15, \\ 0.8(x^L)^2(0) + 1.3(x^L)(0) = 0.1, \\ 1.2(x^U)^2(0) + 2.2(x^U)(0) = 0.2. \end{cases} \quad (43)$$

Consequently  $x^L(0) = 0.0735$ ,  $x^U(0) = 0.0867$ , and  $x^L(1) = x^U(1) = 0.0818$ . Therefore, initial guess is  $x_0 = (0.0735, 0.0818, 0.0867)$ . After 3 iterations, we obtain the solution which the maximum error would be less than  $10^{-3}$ . Now suppose  $x$  is negative; we have

$$\begin{cases} (0.8 + 0.2\tau)(x^L(\tau))^2 + (1.3 + 0.45\tau)x^L(\tau) = (0.1 + 0.05\tau), \\ (1.2 - 0.2\tau)(x^U(\tau))^2 + (2.2 - 0.45\tau)x^U(\tau) = (0.2 - 0.05\tau). \end{cases} \quad (44)$$

For  $\tau = 0$ , we have  $x^U(0) > x^L(0)$ , and therefore, negative root does not exist.

*Case 2.* Downward motion of object.

Here, we discuss the downward motion of object which results in the following fuzzy nonlinear equation:

$$(3, 4, 5)(x(\tau))^2 + (1, 2, 3)x(\tau) = (1, 2, 3). \quad (45)$$

Without any loss of generality, assume that  $x$  is positive; then the parametric form of this equation is as follows:

$$\begin{cases} (3 + \tau)(x^L(\tau))^2 + (1 + \tau)x^L(\tau) = (1 + \tau), \\ (5 - \tau)(x^U(\tau))^2 + (3 - \tau)x^U(\tau) = (3 - \tau). \end{cases} \quad (46)$$



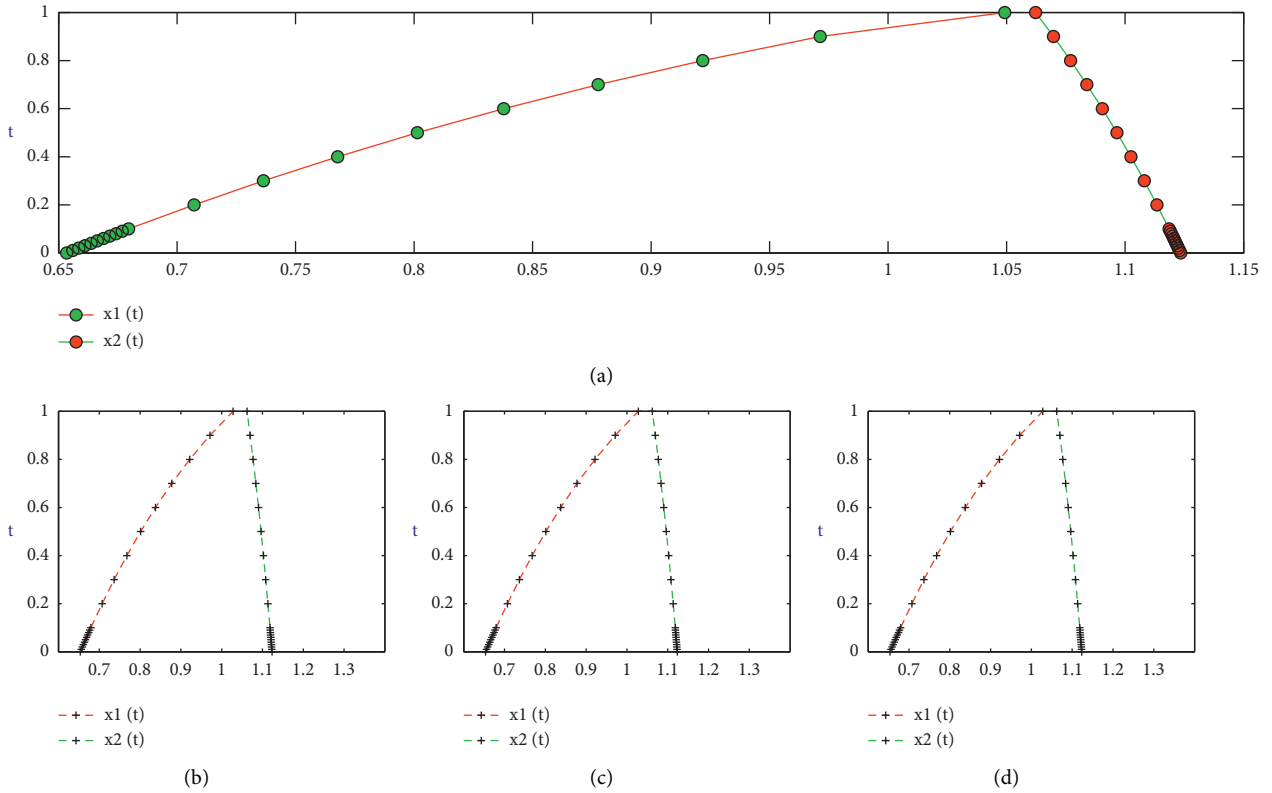


FIGURE 3: Analytical and numerical approximate solution of Example 2. (a) Analytical solution for Example 2. (b) NM method for Example 2. (c) NR method for Example 2. (d) NP method for Example 2.

TABLE 2: Comparison of iterative schemes NM, NR, and NP on the same number of iterations  $n = 3$ .

$\tau$	$x^L$	$x^U$	NM		NR		NP	
			$\ x_{n+1} - x_n\ $	$\ f(x_n)\ $	$\ x_{n+1} - x_n\ $	$\ f(x_n)\ $	$\ x_{n+1} - x_n\ $	$\ f(x_n)\ $
0.0	0.6534	1.1234	$3.9e-17$	$2.9e-16$	$7.3e-5$	$3.7e-3$	$5.3e-9$	$6.3e-8$
0.1	0.6795	1.1185	$1.3e-15$	$1.3e-16$	$1.2e-3$	$8.2e-6$	$4.2e-9$	$6.9e-8$
0.2	0.7071	1.1134	$3.1e-16$	$4.1e-16$	$1.2e-5$	$7.6e-6$	$5.6e-9$	$8.4e-9$
0.3	0.7364	1.1080	$2.7e-15$	$1.3e-17$	$4.4e-3$	$1.6e-4$	$8.8e-8$	$3.3e-8$
0.4	0.7677	1.1024	$3.5e-15$	$8.3e-13$	$6.0e-4$	$8.3e-4$	$7.2e-9$	$5.4e-9$
0.5	0.8013	1.0965	$1.4e-14$	$1.9e-15$	$6.7e-6$	$0.3e-5$	$7.7e-7$	$8.5e-9$
0.6	0.8378	1.0903	$4.0e-16$	$7.9e-17$	$7.5e-5$	$1.4e-6$	$5.2e-7$	$9.8e-8$
0.7	0.8776	1.0838	$7.6e-16$	$3.9e-18$	$8.6e-6$	$0.8e-6$	$8.7e-9$	$2.2e-8$
0.8	0.9218	1.0770	$8.4e-18$	$8.2e-16$	$6.8e-6$	$4.4e-6$	$3.9e-7$	$0.6e-9$
0.9	0.9713	1.0689	$9.6e-17$	$2.1e-17$	$4.8e-5$	$5.3e-7$	$4.1e-9$	$1.3e-9$
1	1.0280	1.0280	$9.0e-18$	$1.2e-17$	$7.9e-5$	$7.8e-7$	$9.6e-7$	$1.0e-7$

Figure 5 shows analytical and numerical approximate solution of fuzzy nonlinear equation in Example 3 (Case 2).

Figure 5 shows analytical and numerical approximate solution of fuzzy nonlinear equation in Example 3 (Case 2).

Table 4 clearly shows the dominance behavior of NM over NR and NP in terms of absolute error on the same number of iterations  $n = 3$  for Example 3 (Case 2).

To obtain initial guess, we use the above system for  $\tau = 0$  and  $\tau = 1$ ; therefore,

$$\begin{cases} 4(x^L)^2(1) + 2x^L(1) = 2, \\ 4(x^U)^2(1) + 2x^U(1) = 2, \\ 3(x^L)^2(0) + x^L(0) = 1, \\ 5(x^U)^2(0) + 3x^U(0) = 3. \end{cases} \quad (47)$$

Consequently  $x^L(0) = 0.4343$ ,  $x^U(0) = 0.5307$ , and  $x^L(1) = x^U(1) = 0.5$ . Therefore, initial guess is

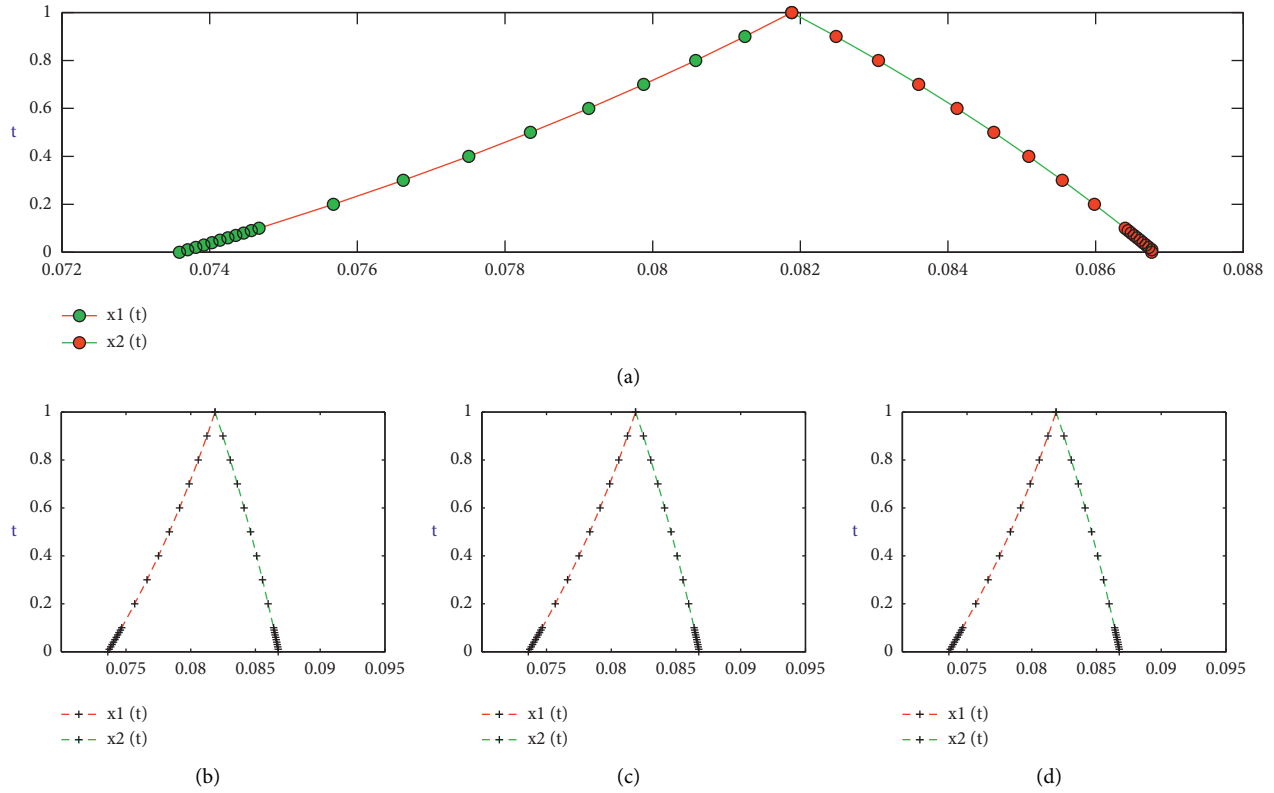


FIGURE 4: Analytical and numerical approximate solution of Example 3 (Case 1). (a) Analytical solution for Example 3 (Case 1). (b) NM method for Example 3 (Case 1). (c) NR method for Example 3 (Case 1). (d) NP method for Example 3 (Case 1).

TABLE 3: Comparison of iterative schemes NM, NR, and NP on the same number of iterations  $n = 3$ .

$\tau$	$x^L$	$x^U$	NM		NR		NP	
			$\ x_{n+1} - x_n\ $	$\ f(x_n)\ $	$\ x_{n+1} - x_n\ $	$\ f(x_n)\ $	$\ x_{n+1} - x_n\ $	$\ f(x_n)\ $
0.0	0.0735	0.0867	$4.9e-16$	$2.9e-16$	$7.3e-6$	$3.7e-6$	$1.4e-8$	$1.3e-8$
0.1	0.0746	0.0863	$2.3e-15$	$1.3e-15$	$1.2e-5$	$1.2e-5$	$3.2e-8$	$6.6e-8$
0.2	0.0756	0.0859	$3.1e-15$	$0.1e-16$	$1.2e-5$	$1.6e-5$	$5.6e-8$	$5.4e-8$
0.3	0.0766	0.0855	$1.7e-14$	$1.2e-15$	$2.4e-5$	$1.3e-5$	$8.8e-8$	$4.3e-8$
0.4	0.0775	0.0850	$3.5e-14$	$5.3e-14$	$3.0e-4$	$1.0e-4$	$1.2e-7$	$3.4e-8$
0.5	0.0783	0.0846	$6.4e-15$	$1.3e-15$	$3.7e-5$	$0.3e-5$	$1.7e-7$	$2.5e-8$
0.6	0.0791	0.0841	$1.0e-16$	$7.0e-16$	$4.5e-5$	$5.4e-5$	$2.2e-7$	$1.8e-8$
0.7	0.0798	0.0836	$1.6e-16$	$3.9e-16$	$5.6e-6$	$0.2e-6$	$2.7e-7$	$1.2e-8$
0.8	0.0805	0.0830	$2.4e-13$	$1.2e-16$	$4.8e-7$	$1.4e-7$	$3.3e-7$	$7.6e-9$
0.9	0.0812	0.0824	$3.6e-17$	$3.1e-17$	$3.8e-6$	$2.3e-6$	$4.0e-7$	$1.4e-9$
1	0.0818	0.0818	$7.0e-18$	$1.0e-18$	$7.0e-6$	$1.8e-6$	$4.6e-7$	$1.8e-9$

$x_0 = (0.4343, 0.5, 0.5307)$ . After 3 iterations, we obtain the solution which the maximum error would be less than  $10^{-3}$ . Now suppose  $x$  is negative; we have

$$\begin{cases} (3 + \tau)(x^L(\tau))^2 + (1 + \tau)x^L(\tau) = (1 + \tau), \\ (5 - \tau)(x^U(\tau))^2 + (3 - \tau)x^U(\tau) = (3 - \tau). \end{cases} \quad (48)$$

For  $\tau = 0$ , we have  $x^U(0) > x^L(0)$ , and therefore, negative root does not exist.

*Example 4.* Consider the fuzzy nonlinear equation:

$$(3, 4, 5)(x(\tau))^2 + (1, 2, 3)\sin(x(\tau)) = (1, 2, 3). \quad (49)$$

Without any loss of generality, assume that  $x$  is positive; then the parametric form of this equation is as follows:

$$\begin{cases} (3 + \tau)(x^L)^2 + (1 + \tau)\sin(x^L(\tau)) = (1 + \tau), \\ (5 - \tau)(x^U)^2 + (3 - \tau)\sin(x^U(\tau)) = (3 - \tau). \end{cases} \quad (50)$$

Figure 6 shows analytical and numerical approximate solution of fuzzy nonlinear equation in Example 4.

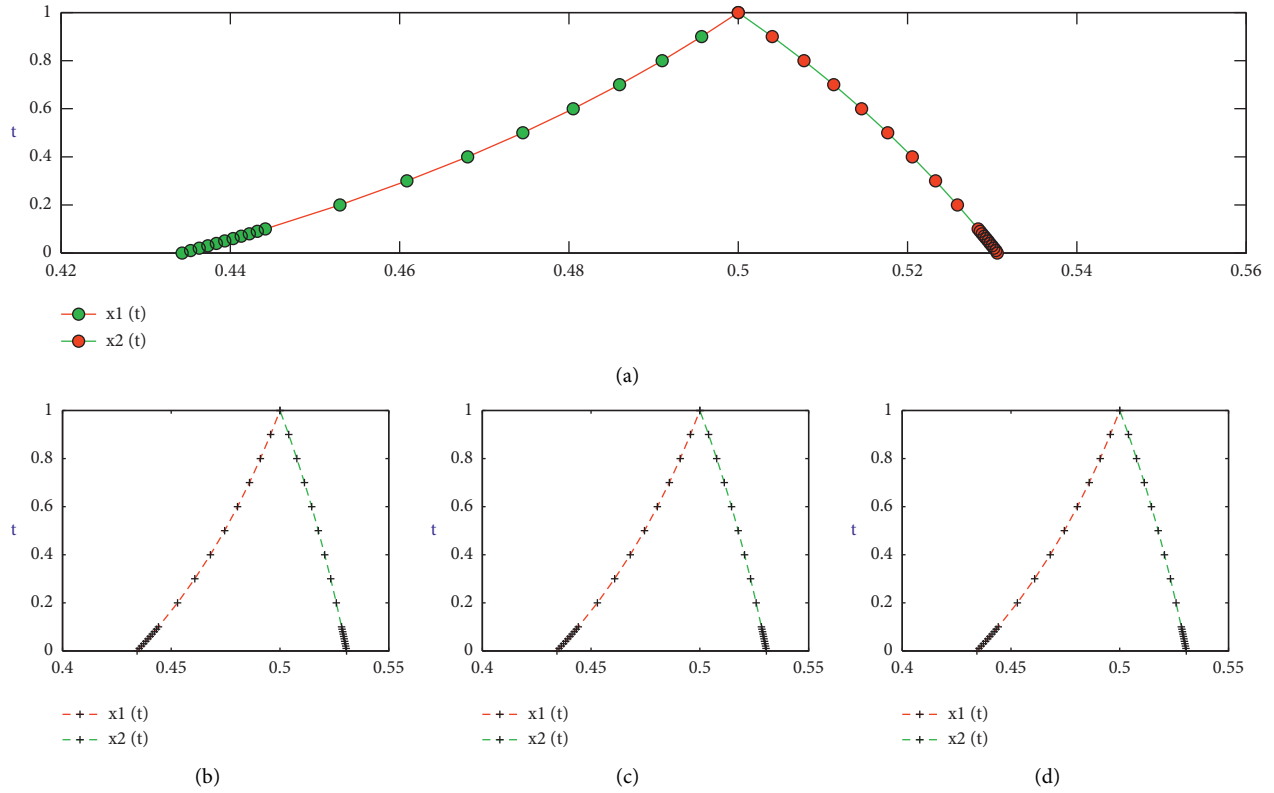


FIGURE 5: Analytical and numerical approximate solution of Example 3 (Case 2). (a) Analytical solution for Example 3 (Case 2). (b) NM method for Example 3 (Case 2). (c) NR method for Example 3 (Case 2). (d) NP method for Example 3 (Case 2).

TABLE 4: Comparison of iterative schemes NM, NR, and NP on the same number of iterations  $n = 3$ .

$\tau$	$x^L$	$x^U$	NM		NR		NP	
			$\ x_{n+1} - x_n\ $	$\ f(x_n)\ $	$\ x_{n+1} - x_n\ $	$\ f(x_n)\ $	$\ x_{n+1} - x_n\ $	$\ f(x_n)\ $
0.0	0.4343	0.5306	$1.4e-15$	$1.1e-29$	$3.0e-4$	$2.0e-7$	$4.4e-9$	$5.3e-16$
0.1	0.4441	0.5258	$6.9e-24$	$2.1e-29$	$2.0e-6$	$1.5e-7$	$1.5e-13$	$2.1e-16$
0.2	0.4529	0.5233	$1.3e-22$	$4.8e-30$	$4.4e-6$	$1.0e-7$	$6.5e-13$	$2.2e-16$
0.3	0.4608	0.5205	$1.1e-21$	$7.2e-31$	$7.2e-5$	$7.3e-8$	$1.9e-12$	$0.1e-20$
0.4	0.4680	0.5176	$6.1e-21$	$0.1e-32$	$1.0e-5$	$4.5e-8$	$4.5e-12$	$6.0e-17$
0.5	0.4745	0.5145	$2.6e-20$	$8.1e-35$	$1.4e-5$	$2.5e-8$	$9.0e-12$	$3.1e-17$
0.6	0.4805	0.5144	$8.3e-20$	$8.7e-33$	$1.9e-5$	$1.1e-8$	$1.5e-11$	$1.0e-16$
0.7	0.4859	0.5112	$2.1e-19$	$9.4e-33$	$2.3e-5$	$4.4e-9$	$2.5e-11$	$6.6e-17$
0.8	0.4910	0.5077	$4.9e-19$	$3.0e-33$	$2.8e-5$	$1.0e-9$	$3.8e-11$	$1.1e-15$
0.9	0.4956	0.5040	$9.9e-19$	$0.1e-36$	$3.3e-5$	$7.5e-11$	$5.3e-11$	$2.1e-16$
1	0.5	0.5	$1.8e-18$	$2.0e-36$	$3.9e-5$	$0.1e-15$	$7.2e-11$	$0.1e-18$

Figure 6 shows analytical and numerical approximate solution of fuzzy nonlinear equation in Example 4.

Table 5 clearly shows the dominance behavior of NM over NR and NP in terms of absolute error on the same number of iterations  $n = 3$  for Example 4.

To obtain initial guess, we use the above system for  $\tau = 0$  and  $\tau = 1$ ; therefore,

$$\begin{cases} 4(x^L)^2(1) + 2 \sin(x^L(1)) = 2, \\ 4(x^U)^2(1) + 2 \sin(x^U(1)) = 2, \\ 3(x^L)^2(0) + \sin(x^L(0)) = 1, \\ 5(x^U)^2(0) + 3 \sin(x^U(0)) = 3. \end{cases} \quad (51)$$

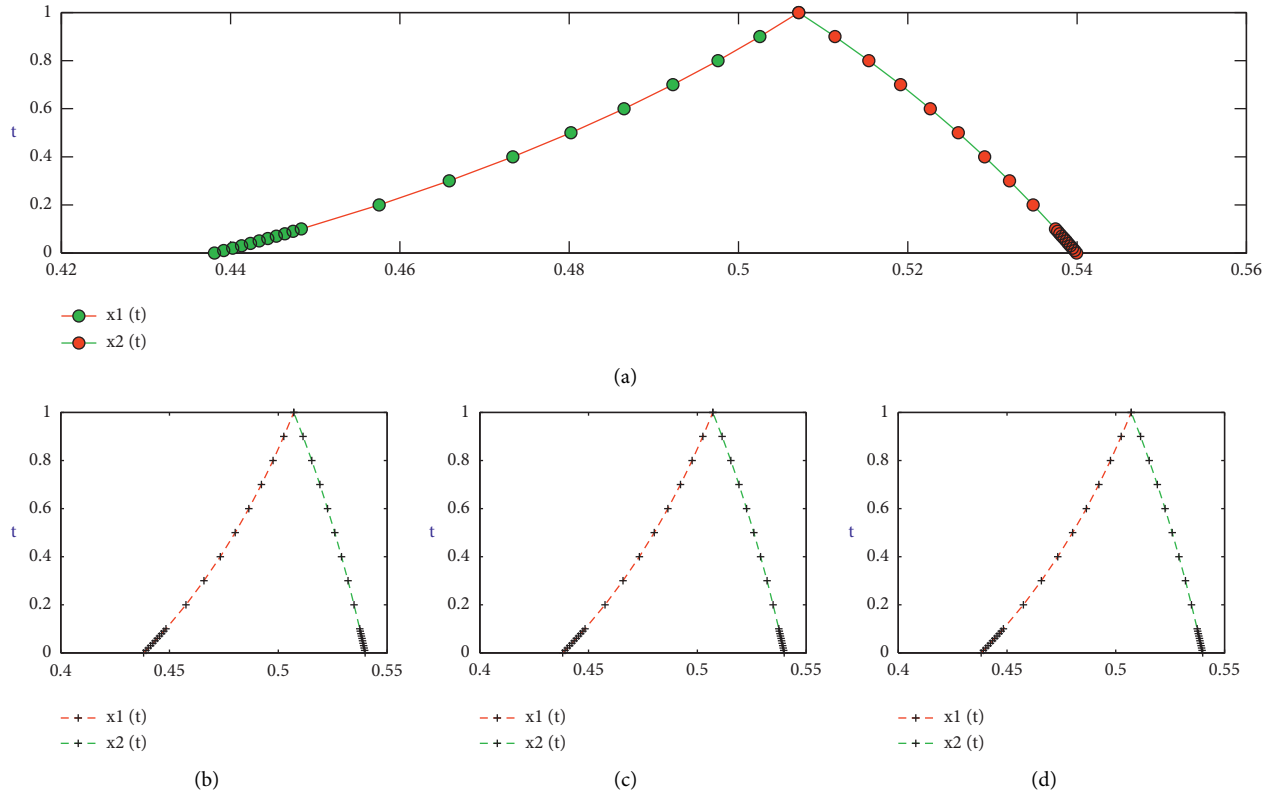


FIGURE 6: Analytical and numerical approximate solution of Example 4. (a) Analytical solution for Example 4. (b) NM method for Example 4. (c) NR method for Example 4. (d) NP method for Example 4.

TABLE 5: Comparison of iterative schemes NM, NR, and NP on the same number of iterations  $n = 3$ .

$\tau$	$x^L$	$x^U$	NM		NR		NP	
			$\ x_{n+1} - x_n\ $	$\ f(x_n)\ $	$\ x_{n+1} - x_n\ $	$\ f(x_n)\ $	$\ x_{n+1} - x_n\ $	$\ f(x_n)\ $
0.0	0.4380	0.5399	$2.7e-25$	$4.7e-28$	$3.6e-6$	$2.4e-7$	$1.1e-14$	$4.2e-15$
0.1	0.4483	0.5377	$1.2e-23$	$1.7e-28$	$2.4e-6$	$1.4e-7$	$2.8e-13$	$3.3e-15$
0.2	0.4575	0.5374	$1.8e-22$	$5.3e-29$	$9.5e-6$	$6.4e-7$	$5.2e-13$	$2.5e-16$
0.3	0.4658	0.5348	$1.4e-21$	$1.3e-29$	$2.6e-6$	$3.6e-7$	$8.2e-12$	$1.8e-16$
0.4	0.4733	0.5320	$6.8e-21$	$3.0e-30$	$5.8e-5$	$1.8e-7$	$1.1e-12$	$1.3e-16$
0.5	0.4801	0.5290	$2.4e-20$	$4.6e-31$	$1.1e-5$	$0.1e-8$	$1.7e-11$	$4.2e-17$
0.6	0.4864	0.5259	$6.8e-20$	$3.5e-32$	$4.5e-5$	$2.1e-8$	$2.0e-17$	$5.1e-18$
0.7	0.4922	0.5226	$1.6e-20$	$9.4e-33$	$2.8e-5$	$1.2e-8$	$2.5e-11$	$2.7e-18$
0.8	0.4975	0.5191	$3.3e-19$	$3.0e-34$	$4.1e-5$	$3.4e-8$	$2.4e-11$	$1.1e-19$
0.9	0.5025	0.5113	$6.2e-19$	$2.1e-35$	$5.7e-5$	$7.3e-9$	$3.4e-11$	$3.6e-19$
1	0.5071	0.5071	$1.0e-19$	$3.0e-36$	$7.6e-5$	$2.0e-10$	$3.9e-11$	$5.8e-19$

Consequently  $x^L(0) = 0.4380$ ,  $x^U(0) = 0.5399$ , and  $x^L(1) = x^U(1) = 0.5071$ . Therefore, initial guess is  $x_0 = (0.4380, 0.5071, 0.5399)$ . After 3 iterations, we obtain the solution which the maximum error would be less than  $10^{-3}$ . Now suppose  $x$  is negative; we have

$$\begin{cases} (3 + \tau)(x^L(\tau))^2 + (1 + \tau)x^L(\tau) = (1 + \tau), \\ (5 - \tau)(x^U(\tau))^2 + (3 - \tau)x^U(\tau) = (3 - \tau). \end{cases} \quad (52)$$

For  $\tau = 0$ , we have  $x^U(0) > x^L(0)$ , and therefore, negative root does not exist.

### 5. Conclusion

In this research paper, we construct highly efficient family of two-step numerical iterative method to approximate roots of triangular fuzzy nonlinear equations. A set of real life applications are considered as numerical test problems show the practical performance and dominance efficiency of NM over NP and NR. From Tables 1–5 and Figures 1–6, we observe that numerical results of test examples, CPU time, and residual errors corroborate theoretical analysis and illustrate the effectiveness and rapid convergence of our proposed family of iterative method NM as compared to the methods NP and NR.

## Data Availability

No data were used to support this study.

## Disclosure

The statements made and views expressed are solely the responsibility of the authors.

## Conflicts of Interest

The authors declare that there are no conflicts of interest regarding the publication of this article.

## Authors' Contributions

All authors contributed equally to the preparation of this manuscript.

## Acknowledgments

The author (YUG) would like to acknowledge that this publication was made possible by a grant from Carnegie Corporation of New York.

## References

- [1] M. Akram, G. Muhammad, and T. Allahviranloo, "Bipolar fuzzy linear system of equations," *Computational and Applied Mathematics*, vol. 38, no. 69, pp. 1–29, 2019.
- [2] M. Akram, G. Muhammad, A. N. A. Koam, and N. Hussain, "Iterative methods for solving a system of linear equation in bipolar fuzzy environment," *Mathematics*, vol. 7, no. 728, pp. 1–25, 2019.
- [3] S. S. L. Chang and L. A. Zadeh, "On fuzzy mapping and control," *IEEE Transactions on Systems, Man, and Cybernetics*, vol. SMC-2, no. 1, pp. 30–34, 1972.
- [4] D. Dubois and H. Prade, "Operations on fuzzy numbers," *International Journal of Systems Science*, vol. 9, no. 6, pp. 613–626, 1978.
- [5] A. N. A. Koam, M. Akram, G. Muhammad, and N. Hussain, "LU decomposition scheme for solving m-polar fuzzy system of linear equations," *Mathematical Problems in Engineering*, vol. 2020, Article ID 8384593, 19 pages, 2020.
- [6] M. Mizumoto, "Some properties of fuzzy numbers," in *Advances in Fuzzy Sets Theory and Applications*, M. M. Gupta, R. K. Ragarde, and R. R. Yager, Eds., pp. 156–164, North-Holland, Amsterdam, Netherlands, 1979.
- [7] M. Mizumoto and K. Tanaka, "The four operations of arithmetic on fuzzy numbers," *System—Computers—Controls*, vol. 7, no. 5, pp. 73–81, 1976.
- [8] S. Nahmias, "Fuzzy variables," *Fuzzy Sets and Systems*, vol. 1, no. 2, pp. 97–110, 1978.
- [9] M. Saqib, M. Akram, and B. Shahida, "Certain efficient iterative methods for bipolar fuzzy system of linear equations," *Journal of Intelligent and Fuzzy Systems*, vol. 39, no. 3, pp. 3971–3985, 2020.
- [10] L. A. Zadeh, "The concept of a linguistic variable and its application to approximate reasoning-I," *Information Sciences*, vol. 8, no. 3, pp. 199–249, 1975.
- [11] J. J. Buckley and Y. Qu, "Solving linear and quadratic fuzzy equations," *Fuzzy Sets and Systems*, vol. 38, no. 1, pp. 43–59, 1990.
- [12] J. J. Buckley and Y. Qu, "On using  $\alpha$ -cuts to evaluate fuzzy equations," *Fuzzy Sets and Systems*, vol. 38, no. 3, pp. 309–312, 1990.
- [13] J. J. Buckley and Y. Qu, "Solving fuzzy equations: a new solution concept," *Fuzzy Sets and Systems*, vol. 39, no. 3, pp. 291–301, 1991.
- [14] J. J. Buckley and Y. Qu, "Solving systems of linear fuzzy equations," *Fuzzy Sets and Systems*, vol. 43, no. 1, pp. 33–43, 1991.
- [15] S. Abbasbandy and B. Asady, "Newton's method for solving fuzzy nonlinear equations," *Applied Mathematics and Computation*, vol. 159, no. 2, pp. 349–356, 2004.
- [16] I. M. Sulaiman, M. Mamat, M. Y. Waziri, M. A. Mohamed, and F. S. Mohamad, "Solving fuzzy nonlinear equation via Levenberg-Marquardt method," *Far East Journal of Mathematical Sciences*, vol. 103, no. 10, pp. 1547–1558, 2018.
- [17] M. Mosleh, "Solution of dual fuzzy polynomial equations by modified Adomian decomposition method," *Fuzzy Information and Engineering*, vol. 5, no. 1, pp. 45–56, 2013.
- [18] Y. J. Cho, N. J. Huang, and S. M. Kang, "Nonlinear equations for fuzzy mappings in probabilistic normed spaces," *Fuzzy Sets and Systems*, vol. 110, no. 1, pp. 115–122, 2000.
- [19] J.-X. Fang, "On nonlinear equations for fuzzy mappings in probabilistic normed spaces," *Fuzzy Sets and Systems*, vol. 131, no. 3, pp. 357–364, 2002.
- [20] J. Ma and G. Feng, "An approach to  $H_\infty$  control of fuzzy dynamic systems," *Fuzzy Sets and Systems*, vol. 137, no. 3, pp. 367–386, 2003.
- [21] H. T. Kung and J. F. Traub, "Optimal order of one-point and multipoint iteration," *Journal of the ACM*, vol. 21, no. 4, pp. 643–651, 1974.
- [22] D. Dubois and H. Prade, *Fuzzy Sets and Systems: Theory and Application*, Academic Press, New York, NY, USA, 1980.
- [23] H. J. Zimmermann, *Fuzzy Sets Theory and its Application*, Kluwer Academic Press, Dordrecht, Netherlands, 1991.
- [24] R. Goetschel and W. Voxman, "Elementary fuzzy calculus," *Fuzzy Sets and Systems*, vol. 18, no. 1, pp. 31–43, 1986.
- [25] L. A. Zadeh, "Fuzzy sets," *Information and Control*, vol. 8, no. 3, pp. 338–353, 1965.
- [26] M. Keyanpour and T. Akbarian, "Solving intuitionistic fuzzy nonlinear equations," *Journal of Fuzzy Set Valued Analysis*, vol. 2014, pp. 1–6, 2014.
- [27] J. E. Dennis and R. B. Schnabel, *Numerical Methods for Unconstrained Optimization and Nonlinear Equations*, Prentice-Hall, Hoboken, NJ, USA, 1983.
- [28] M. A. Rehman, A. Naseem, and T. Abdeljawad, "Some novel sixth-order iteration schemes for computing zeros of non-linear scalar equations and their applications in engineering," *Journal of Function Spaces*, vol. 2021, Article ID 5566379, 11 pages, 2021.

## Research Article

# Novel Technique for Group Decision-Making under Fuzzy Parameterized $q$ -Rung Orthopair Fuzzy Soft Expert Framework

Ghous Ali <sup>1</sup> and Musavarah Sarwar <sup>2</sup>

<sup>1</sup>Department of Mathematics, Division of Science and Technology, University of Education, Lahore, Pakistan

<sup>2</sup>Department of Mathematics, Government College Women University, Sialkot, Pakistan

Correspondence should be addressed to Musavarah Sarwar; musavarah656@gmail.com

Received 8 August 2021; Revised 10 September 2021; Accepted 30 September 2021; Published 27 October 2021

Academic Editor: Yong Aaron Tan

Copyright © 2021 Ghous Ali and Musavarah Sarwar. This is an open access article distributed under the Creative Commons Attribution License, which permits unrestricted use, distribution, and reproduction in any medium, provided the original work is properly cited.

The  $q$ -rung orthopair fuzzy sets and their hybrid models are capable of dealing with uncertain situations very effectively than the theories of intuitionistic and Pythagorean fuzzy sets and thus have numerous decision-making applications in daily life, while the fuzzy parameterized soft set theory has its impact on different decision-making scenarios. Motivated by these facts, in this research article, these theories are combined to form a new structure named fuzzy parameterized  $q$ -rung orthopair fuzzy soft expert sets (FP <sup>$q$</sup>  ROFSESs) for dealing with more generalized information. The developed model is an efficient extension of fuzzy parameterized intuitionistic fuzzy soft expert sets. Some of its basic notions, including subset, complement, OR operation, AND operation, intersection, and union are studied and illustrated via examples. Moreover, to show the applicability and efficiency of the developed model, two real-life applications are solved under the FP <sup>$q$</sup>  ROFSES approach, which is supported by an algorithm, the first application is about selecting an appropriate site for a cafe outlet, and the second application is about selecting the Best News Channel for an award. At last, a comparison of the initiated model with some existing approaches is presented to verify its advantages over them.

## 1. Introduction

Nowadays, a lot of researchers and scientists across the globe keep on working to find the solutions to complexities and situations unsolvable by traditional mathematical tools; for example, crisp set theory is not capable of dealing with different real-world problems concerning uncertainties in various areas, including engineering, medicine, and artificial intelligence. A solution to these problems emerged as the notion of fuzzy sets initiated by Zadeh [1] in 1965. Instead of normally declaring a belongingness degree (i.e., 1) or a nonbelongingness degree (i.e., 0) of an element in the classical set theory, fuzzy sets allow partial belongingness degrees from the interval  $[0, 1]$  to be assigned to each element, thus claiming its vague boundary scenario by extending crisp set theory. This powerful concept fills the gaps in the previous traditional concepts allowing modeling of and solution to many vague situations. Inspection of the

last few decades leads us to an important fact that the fuzzy set model urged many scientists and experts to use and extend this model for solving numerous uncertain problems.

In a fuzzy set, the nonbelongingness degree is dependent on the belongingness degree and calculated as “1 minus belongingness degree.” However, there come situations where belongingness and nonbelongingness degrees may vary from this criterion. To tackle this difficulty, Atanassov [2] proposed intuitionistic fuzzy sets (IFSs) as an extension to fuzzy sets by providing two degrees, i.e., the belongingness degree  $\alpha_I$  and nonbelongingness degree  $\beta_I$  for an element with the constraint that  $0 \leq \alpha_I + \beta_I \leq 1$ . Thus, it allows dealing better with the uncertainties, e.g., a situation where  $\alpha_I = 0.3$  and  $\beta_I = 0.6$ . But this model fails to deal with situations where belongingness and nonbelongingness degrees sum up above unity. For this, Yager [3] initiated the concept of Pythagorean fuzzy sets (PFSs) as a generalization of IFSs, allowing higher applicability in two-dimensional

uncertainties. The belongingness degree  $\alpha_p$  and non-belongingness degree  $\beta_p$  are now conditioned with the constraint  $0 \leq (\alpha_p)^2 + (\beta_p)^2 \leq 1$ . Due to their higher ability to deal with uncertainties than IFSs, they have been utilized widely in many decision-making situations. Later on, Senapati and Yager [4] observed that in a particular situation where a belongingness degree of 0.65 and a non-belongingness degree of 0.85 are assigned to an element, then  $(0.65)^2 + (0.85)^2 = 1.145 \notin 1$ . Hence, PFSs fail to deal with it. To deal with such situations, Senapati and Yager [4] extended the PFSs to Fermatean fuzzy sets (FFSs) with the condition  $0 \leq (\alpha_F)^3 + (\beta_F)^3 \leq 1$ . Thus, this increased order of uncertainties allows handling of the problems as discussed above since  $(0.65)^3 + (0.85)^3 = 0.888 \leq 1$ . Afterward, Yager's [5] contribution came in the form of  $q$ -rung orthopair fuzzy sets ( $q$ -ROFSs) or generalized orthopair fuzzy sets with the characteristic of the sum of the  $q$ th power of belongingness and nonbelongingness values of elements not being more than one. The  $q$ -ROFSs are generally reduced to IFSs, PFSs, and FFSs for  $q = 1, 2$  and  $q = 3$ , respectively (see Figure 1). Later, Shaheen et al. [6] briefly investigated the reasons behind the construction of  $q$ -ROFSs. A number of decision-making problems have been solved by using the  $q$ -ROFS model [7–11].

All the models mentioned above have a common limitation in that they fail to deal with situations considering multiple parameters. To deal with this issue, Molodtsov [12] initiated the concept of soft set theory that provides parameterization tools for handling uncertainties. Actually, soft sets are modeled as parameterized families of sets, thus giving a parameterized methodology for multiattribute decision-making problems. Maji et al. [13] discussed some properties and operations of soft sets. The concepts of the soft set model were naturally extended and combined with other models by many experts to deal with uncertain situations. Some important models are fuzzy soft sets (FSSs) [14] and intuitionistic FSSs [15]. These models fail to deal with some practical situations. To overcome this difficulty, Hamid et al. [16] generalized intuitionistic FSSs and presented the idea of a novel hybrid model called  $q$ -ROF soft sets ( $q$ -ROFSSs). There is a deficiency in this model; that is, it cannot deal with bipolar information. In order to handle this issue, very recently, Ali et al. [17] presented a novel hybrid multi-criteria decision-making (MCDM) model, namely,  $q$ -ROF bipolar soft sets as a generalization of  $q$ -ROFSSs. In addition, Alkan and Kahraman [18] proposed a  $q$ -rung orthopair fuzzy TOPSIS method for the evaluation of government strategies against the COVID-19 pandemic.

In the soft set model, elements are categorized with respect to the parameters. However, it is seen that in most cases, some parameters have more preferences over others, and thus, higher degrees of less preferable parameter families may affect the decisions. For this, fuzzy parameterized soft sets were introduced by Aman and Enginoglu [19], where fuzzy memberships are assigned to the parameters which better demonstrate the weightage or the relative preferences of the parameters. In addition, the same authors extended it to fuzzy parameterized fuzzy soft sets (FPFSSs) [20]. This MCDM model fails to deal with data in an intuitionistic

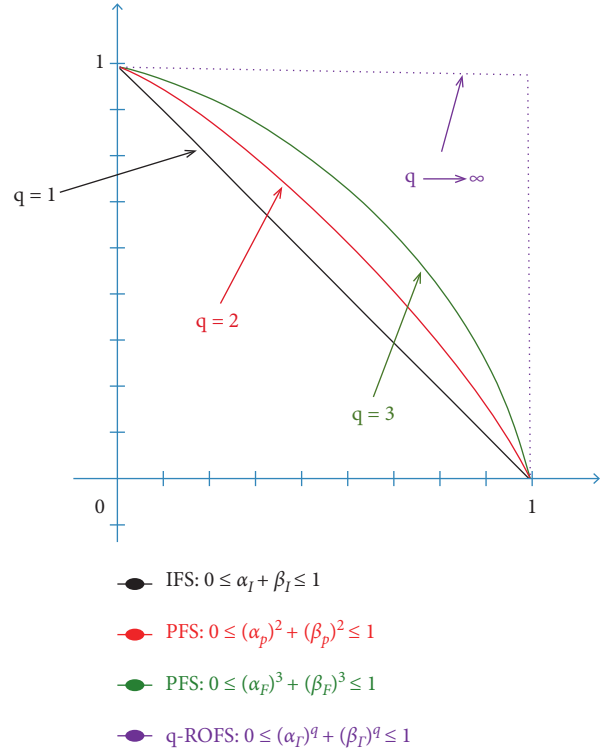


FIGURE 1: Comparison between the spaces of IFSs, PFSs, FFSs, and  $q$ -ROFSs.

fuzzy environment. That is why more improvements and extensions to this fruitful concept include intuitionistic fuzzy parameterized soft sets (IFPSSs) [21], intuitionistic fuzzy parameterized FSSs (IFPFSSs) [22], and intuitionistic fuzzy parameterized intuitionistic FSSs (IFPIFSSs) [23, 24]. All the mentioned above fuzzy parameterized soft models are not suitable in the case of interval-valued representation of data and information. To overcome this difficulty, recently, Aydın and Enginolu [25] presented a more generalized model called interval-valued intuitionistic fuzzy parameterized interval-valued intuitionistic FSSs (IVIFP-IVIFSSs) and solved a decision-making application.

Since the models and their hybridization discussed above have vital importance in handling uncertainties, one common restriction is that they deal with a single expert. However, many situations require multiple experts opinions or group decision-making. For instance, when dealing with the selection of an admin manager in a company, the committee of two or more people takes its judgments as scores on questionnaires and finally declares who will be the most suitable person. To deal with such scenarios, Alkhalzaleh and Salleh [26] introduced soft expert sets (SESs), which are capable of integrating the opinions of all experts in one place and hence are extremely efficient in multiattribute group decision-making (MAGDM) situations. Later, the same authors discussed the fuzziness of the SES model [27]. Due to group decision-making modeling capabilities of SESs, many hybrid models have been proposed till now as SESs are their major component, fuzzy  $N$ -SESs [28], fuzzy parameterized intuitionistic fuzzy SESs [29], fuzzy bipolar

soft expert sets [30], analysis of chat conversations of pedophiles based on bipolar fuzzy soft sets [31], risk assessment in automatic robots using rough ELECTRE-II approach [32], and decision support systems based on rough D-TOPSIS method [33]. Akram et al. [34] developed a new hybrid model called  $m$ -polar fuzzy SESs, which discusses the multipolarity of fuzzy SESs and solved some group decision-making problems. For more useful terms, the reader is referred to [35–44].

*1.1. Motivation and Contribution.* The motives of the current study are summarized as follows:

- (1) There is a considerably wider applicability scope of  $q$ -ROFSs as compared to IFSSs, PFSSs, and FFSSs in dealing with 2-dimensional uncertainties. To better understand this argument, consider a pair containing belongingness and nonbelongingness degrees as  $(0.80, 0.95)$ ; then, it is clear that  $0.80 + 0.95 \not\leq 1$ ,  $(0.80)^2 + (0.95)^2 \not\leq 1$ ,  $(0.80)^3 + (0.95)^3 \not\leq 1$ . But  $(0.80)^q + (0.95)^q < 1$  for all  $q \geq 6$ .
- (2) There are parameterization capabilities of fuzzy parameterized intuitionistic fuzzy SESs (FPIFSESS) for dealing with IFS information under multiple experts with weighted preferences.
- (3) The inability of FPIFSESS to deal with  $q$ -ROF information indicates the need for an extension of this model, which also preserves the existing abilities of the FPIFSES model.
- (4) The  $q$ -ROFS model was found to be more effective when extended to the range of parameterizations and used in different domains, that is,  $q$ -ROFSSs but the main drawback of this model is that it has no ability to tackle a situation where different weights are assigned to different parameters in  $q$ -ROF information. Actually, the fuzzy parameterized versions of  $q$ -ROFSSs and  $q$ -ROFSESSs are unattended to date.

Motivated by the above analysis, in this research article, the concept of FPIFSESS or  $q$ -ROFSSs is extended to  $FP^q$  ROFSESSs, thus allowing more uncertainties to be handled easily as the order of uncertainty is increased from 1 to  $q$ th power of belongingness and nonbelongingness degrees.

This research contributes the following:

- (1) A new and powerful extension of the FPIFSES model is provided, namely,  $FP^q$  ROFSES, which allows dealing with  $q$ -ROFS information efficiently
- (2) Basic operations, including subset, complement, OR operation, AND operation, intersection, and union of the newly developed model, are provided and supported with examples
- (3) Two real-life MAGDM problems, including the best site selection for a new cafe outlet and the selection of Best News Channel, are solved using a developed algorithm based on  $FP^q$  ROFSESS

- (4) A comparison of the developed group decision-making method under  $FP^q$  ROFSESSs with few existing approaches is also given

*1.2. Framework of the Paper.* Section 1 includes the introduction, related works, motivation, and contribution of the research article. Section 2 recalls some basic definitions and then introduces the main concept of  $FP^q$  ROFSESSs along with certain essential notions and basic operations for the  $FP^q$  ROFSESSs. Section 3 presents two real-life applications of the  $FP^q$  ROFSESSs with an algorithmic approach. Section 4 discusses a comparison of the developed method under  $FP^q$  ROFSESSs with few existing approaches. At last, Section 5 gives the concluding remarks and some future directions.

## 2. Fuzzy Parameterized $q$ -Rung Orthopair Fuzzy Soft Expert Sets

This section introduces the  $FP^q$  ROFSES model, its basic operations, and its properties. But before that, we need to review some essential definitions useful for its construction and further study throughout the article.

*Definition 1* (see [5]). Let  $\mathcal{Y}$  be a universal set. A pair  $\mathcal{E} = (\alpha_\Gamma, \beta_\Gamma)$  is called a  $q$ -rung orthopair fuzzy set or  $q$ -ROFS over  $\mathcal{Y}$  where  $\alpha_\Gamma$  is a membership function given by  $\alpha_\Gamma: \mathcal{Y} \rightarrow [0, 1]$  and  $\beta_\Gamma$  is a nonmembership function given by  $\beta_\Gamma: \mathcal{Y} \rightarrow [0, 1]$  with  $0 \leq (\alpha_\Gamma(\mathfrak{h}))^q + (\beta_\Gamma(\mathfrak{h}))^q \leq 1$  where  $q \geq 1$ ,  $\alpha_\Gamma(\mathfrak{h}), \beta_\Gamma(\mathfrak{h}) \in [0, 1]$  for all  $\mathfrak{h} \in \mathcal{Y}$ . In set form, a  $q$ -ROFS on  $\mathcal{Y}$  is given as

$$\mathcal{E} = \{ \langle \mathfrak{h}, (\alpha_\Gamma(\mathfrak{h}), \beta_\Gamma(\mathfrak{h})) \rangle \mid \mathfrak{h} \in \mathcal{Y} \}, \quad (1)$$

where  $\alpha_\Gamma(\mathfrak{h}), \beta_\Gamma(\mathfrak{h}) \in [0, 1]$  denotes the belongingness and nonbelongingness values, respectively, and satisfies  $0 \leq (\alpha_\Gamma(\mathfrak{h}))^q + (\beta_\Gamma(\mathfrak{h}))^q \leq 1$ . Moreover,  $(\alpha_\Gamma(\mathfrak{h}), \beta_\Gamma(\mathfrak{h}))$  is known as a  $q$ -rung orthopair fuzzy number ( $q$ -ROFN) and denoted by  $\mathcal{Q} = (\alpha_\Gamma(\mathfrak{h}), \beta_\Gamma(\mathfrak{h}))$ . The degree of hesitance for  $q$ -ROFN  $\mathcal{Q} = (\alpha_\Gamma(\mathfrak{h}), \beta_\Gamma(\mathfrak{h}))$  is defined by

$$\pi_{\mathcal{Q}} = \sqrt[q]{1 - ((\alpha_\Gamma(\mathfrak{h}))^q + (\beta_\Gamma(\mathfrak{h}))^q)}. \quad (2)$$

*Definition 2* (see [16]). Let  $\mathcal{Y}$  be a universe of discourse and let  $\mathcal{S}$  be a set of parameters. Let  $\mathcal{A} \subseteq \mathcal{S}$  and  $\mathfrak{Q}^{\mathcal{Y}}$  be a collection of all  $q$ -ROF subsets of  $\mathcal{S}$ . A pair  $(\Gamma, \mathcal{A})$  is said to be a  $q$ -rung orthopair fuzzy soft set ( $q$ -ROFSS) on  $\mathcal{Y}$ , if  $\Gamma$  is the function defined by  $\Gamma: \mathcal{A} \rightarrow \mathfrak{Q}^{\mathcal{Y}}$ .

For  $\mathfrak{h} \in \mathcal{Y}$  and  $\mathfrak{s} \in \mathcal{A}$ , a  $q$ -ROFS  $\Gamma(\mathfrak{s})$  is given as

$$\Gamma(\mathfrak{s}) = \{ \langle \mathfrak{h}, (\alpha_\Gamma(\mathfrak{s})(\mathfrak{h}), \beta_\Gamma(\mathfrak{s})(\mathfrak{h})) \rangle \mid \mathfrak{h} \in \mathcal{Y} \}, \quad (3)$$

such that the belongingness degree “ $\alpha_\Gamma$ ” and nonbelongingness degree “ $\beta_\Gamma$ ” are conditioned with the constraint  $0 \leq (\alpha_\Gamma(\mathfrak{s})(\mathfrak{h}))^q + (\beta_\Gamma(\mathfrak{s})(\mathfrak{h}))^q \leq 1$ , for all  $q \in (0, \infty)$ .

*Definition 3* (see [29]). Let  $\mathcal{Y}$  be a universe, let  $\mathcal{S}$  be a set of parameters, let  $\mathcal{E}$  be a set of experts, and let  $\mathcal{O} = \{0 = \text{disagree}, 1 = \text{agree}\}$  be their set of opinions. Let  $\mathcal{D}$  be the fuzzy subset of  $\mathcal{S}$ , and



$\mathcal{X} \subseteq \mathcal{D} \times \mathcal{E} \times \mathcal{O} = \{(\mathfrak{d}, \mathfrak{e}, \mathfrak{o}) \mid \mathfrak{d} \in \mathcal{D}, \mathfrak{e} \in \mathcal{E}, \mathfrak{o} \in \mathcal{O}\}$ . Consider a mapping  $\mathfrak{F}: \mathcal{X} \rightarrow \text{IF}^{\mathcal{Y}}$ , where  $\text{IF}^{\mathcal{Y}}$  is the collection of all IFSSs on  $\mathcal{Y}$ . A pair  $(\mathfrak{F}, \mathcal{X})_{\mathcal{D}}$  is called a fuzzy parameterized intuitionistic fuzzy soft expert set or FPIFSES, where

$$(\mathfrak{F}, \mathcal{X})_{\mathcal{D}} = \{(\mathfrak{z}, \mathfrak{F}(\mathfrak{z})): \mathfrak{z} \in \mathcal{X}\}, \quad (4)$$

such that  $\mathfrak{F}(\mathfrak{z}) = \{(\mathfrak{h}/(\alpha_{\mathfrak{F}}(\mathfrak{z})(\mathfrak{h}), \beta_{\mathfrak{F}}(\mathfrak{z})(\mathfrak{h}))) \mid \mathfrak{h} \in \mathcal{Y}\}$  with  $0 \leq (\alpha_{\mathfrak{F}}(\mathfrak{z})(\mathfrak{h}))^q + (\beta_{\mathfrak{F}}(\mathfrak{z})(\mathfrak{h}))^q \leq 1$ .

We are now ready to construct the notion of novel  $\text{FP}^q$  ROFSESs, which is given as follows.

*Definition 4.* Let  $\mathcal{Y}$  be a universe, let  $\mathcal{S}$  be a set of parameters, let  $\mathcal{E}$  be a set of experts, and let  $\mathcal{O} = \{0 = \text{disagree}, 1 = \text{agree}\}$  be their set of opinions. Let  $\mathcal{D}$  be the fuzzy subset of  $\mathcal{S}$ , and  $\mathcal{X} \subseteq \mathcal{D} \times \mathcal{E} \times \mathcal{O} = \{(\mathfrak{d}, \mathfrak{e}, \mathfrak{o}) \mid \mathfrak{d} \in \mathcal{D}, \mathfrak{e} \in \mathcal{E}, \mathfrak{o} \in \mathcal{O}\}$ . Consider a mapping  $\mathfrak{f}: \mathcal{X} \rightarrow \mathfrak{Q}^{\mathcal{Y}}$ , where  $\mathfrak{Q}^{\mathcal{Y}}$  is the collection of all  $q$ -ROFSSs on  $\mathcal{Y}$ . A pair  $(\mathfrak{f}, \mathcal{X})_{\mathcal{D}}$  is said to be a fuzzy parameterized  $q$ -rung orthopair fuzzy soft expert set or  $\text{FP}^q$  ROFSES, where

$$(\mathfrak{f}, \mathcal{X})_{\mathcal{D}} = \{(\mathfrak{z}, \mathfrak{f}(\mathfrak{z})): \mathfrak{z} \in \mathcal{X}\}, \quad (5)$$

such that  $\mathfrak{f}(\mathfrak{z}) = \{(\mathfrak{h}/(\alpha_{\mathfrak{f}}(\mathfrak{z})(\mathfrak{h}), \beta_{\mathfrak{f}}(\mathfrak{z})(\mathfrak{h}))) \mid \mathfrak{h} \in \mathcal{Y}\}$  with  $0 \leq (\alpha_{\mathfrak{f}}(\mathfrak{z})(\mathfrak{h}))^q + (\beta_{\mathfrak{f}}(\mathfrak{z})(\mathfrak{h}))^q \leq 1$ , for all  $q \in (0, \infty)$ .

This main concept is now explained by an example given as follows.

*Example 1.* Consider a person is interested in buying a house, but before spending on the house, he needs to be sure that the house meets all his needs. In such a condition, he decides to consider the opinions of experts in selecting a reasonable house. Consider there are four houses available in the desired area for purchase, constituting the universal set  $\mathcal{Y} = \{\mathfrak{h}_1, \mathfrak{h}_2, \mathfrak{h}_3, \mathfrak{h}_4\}$ . The person contacts two experts as in the set  $\mathcal{E} = \{e_1, e_2\}$ , for helping him in making the decision. These experts consider the following parameters  $\mathcal{S} = \{\mathfrak{s}_1, \mathfrak{s}_2, \mathfrak{s}_3, \mathfrak{s}_4\}$ , where  $\mathfrak{s}_1 = \text{cheap}$ ,  $\mathfrak{s}_2 = \text{beautiful}$ ,  $\mathfrak{s}_3 = \text{expensive}$ , and  $\mathfrak{s}_4 = \text{material}$ , for the selection of the house. Let  $\mathcal{D} = \{(0.6/\mathfrak{s}_1), (0.7/\mathfrak{s}_2), (0.9/\mathfrak{s}_3), (0.2/\mathfrak{s}_4)\}$  represents certain weights for the parameters according to the buyer's requirements and  $q = 4$ . Then, the  $\text{FP}^4$  ROFSES  $(\mathfrak{f}, \mathcal{X})_{\mathcal{D}}$  representing the opinions of experts about the houses regarding parameters is described as follows:

$$\begin{aligned} (\mathfrak{f}, \mathcal{X})_{\mathcal{D}} = & \left\langle \left\langle \left( \frac{0.6}{\mathfrak{s}_1}, e_1, 1 \right), \left\{ \frac{\mathfrak{h}_1}{(0.30, 0.60)}, \frac{\mathfrak{h}_2}{(0.80, 0.70)}, \frac{\mathfrak{h}_3}{(0.20, 0.10)}, \frac{\mathfrak{h}_4}{(0.50, 0.20)} \right\} \right\rangle, \right. \\ & \left\langle \left( \frac{0.7}{\mathfrak{s}_2}, e_1, 1 \right), \left\{ \frac{\mathfrak{h}_1}{(0.70, 0.90)}, \frac{\mathfrak{h}_2}{(0.60, 0.10)}, \frac{\mathfrak{h}_3}{(0.30, 0.20)}, \frac{\mathfrak{h}_4}{(0.10, 0.40)} \right\} \right\rangle, \\ & \left\langle \left( \frac{0.9}{\mathfrak{s}_3}, e_1, 1 \right), \left\{ \frac{\mathfrak{h}_1}{(0.10, 0.50)}, \frac{\mathfrak{h}_2}{(0.80, 0.10)}, \frac{\mathfrak{h}_3}{(0.80, 0.20)}, \frac{\mathfrak{h}_4}{(0.30, 0.80)} \right\} \right\rangle, \\ & \left\langle \left( \frac{0.2}{\mathfrak{s}_4}, e_1, 1 \right), \left\{ \frac{\mathfrak{h}_1}{(0.10, 0.20)}, \frac{\mathfrak{h}_2}{(0.70, 0.30)}, \frac{\mathfrak{h}_3}{(0.70, 0.40)}, \frac{\mathfrak{h}_4}{(0.90, 0.60)} \right\} \right\rangle, \\ & \left\langle \left( \frac{0.6}{\mathfrak{s}_1}, e_2, 1 \right), \left\{ \frac{\mathfrak{h}_1}{(0.80, 0.60)}, \frac{\mathfrak{h}_2}{(0.80, 0.70)}, \frac{\mathfrak{h}_3}{(0.80, 0.50)}, \frac{\mathfrak{h}_4}{(0.80, 0.60)} \right\} \right\rangle, \\ & \left\langle \left( \frac{0.7}{\mathfrak{s}_2}, e_2, 1 \right), \left\{ \frac{\mathfrak{h}_1}{(0.90, 0.16)}, \frac{\mathfrak{h}_2}{(0.50, 0.15)}, \frac{\mathfrak{h}_3}{(0.40, 0.14)}, \frac{\mathfrak{h}_4}{(0.30, 0.14)} \right\} \right\rangle, \\ & \left\langle \left( \frac{0.9}{\mathfrak{s}_3}, e_2, 1 \right), \left\{ \frac{\mathfrak{h}_1}{(0.66, 0.36)}, \frac{\mathfrak{h}_2}{(0.44, 0.72)}, \frac{\mathfrak{h}_3}{(0.48, 0.52)}, \frac{\mathfrak{h}_4}{(0.36, 0.44)} \right\} \right\rangle, \\ & \left\langle \left( \frac{0.2}{\mathfrak{s}_4}, e_2, 1 \right), \left\{ \frac{\mathfrak{h}_1}{(0.87, 0.45)}, \frac{\mathfrak{h}_2}{(0.45, 0.56)}, \frac{\mathfrak{h}_3}{(0.79, 0.36)}, \frac{\mathfrak{h}_4}{(0.62, 0.42)} \right\} \right\rangle, \\ & \left\langle \left( \frac{0.6}{\mathfrak{s}_1}, e_1, 0 \right), \left\{ \frac{\mathfrak{h}_1}{(0.70, 0.40)}, \frac{\mathfrak{h}_2}{(0.60, 0.30)}, \frac{\mathfrak{h}_3}{(0.70, 0.40)}, \frac{\mathfrak{h}_4}{(0.80, 0.20)} \right\} \right\rangle, \\ & \left\langle \left( \frac{0.7}{\mathfrak{s}_2}, e_1, 0 \right), \left\{ \frac{\mathfrak{h}_1}{(0.70, 0.10)}, \frac{\mathfrak{h}_2}{(0.80, 0.60)}, \frac{\mathfrak{h}_3}{(0.40, 0.14)}, \frac{\mathfrak{h}_4}{(0.56, 0.65)} \right\} \right\rangle, \end{aligned}$$

$$\begin{aligned}
 & \left\langle \left( \frac{0.9}{\mathfrak{s}_3}, e_1, 0 \right), \left\{ \frac{\eta_1}{(0.80, 0.70)}, \frac{\eta_2}{(0.90, 0.60)}, \frac{\eta_3}{(0.80, 0.20)}, \frac{\eta_4}{(0.80, 0.30)} \right\} \right\rangle, \\
 & \left\langle \left( \frac{0.2}{\mathfrak{s}_4}, e_1, 0 \right), \left\{ \frac{\eta_1}{(0.50, 0.15)}, \frac{\eta_2}{(0.77, 0.63)}, \frac{\eta_3}{(0.56, 0.56)}, \frac{\eta_4}{(0.27, 0.31)} \right\} \right\rangle, \\
 & \left\langle \left( \frac{0.6}{\mathfrak{s}_1}, e_2, 0 \right), \left\{ \frac{\eta_1}{(0.90, 0.60)}, \frac{\eta_2}{(0.62, 0.42)}, \frac{\eta_3}{(0.71, 0.81)}, \frac{\eta_4}{(0.72, 0.44)} \right\} \right\rangle, \\
 & \left\langle \left( \frac{0.7}{\mathfrak{s}_2}, e_2, 0 \right), \left\{ \frac{\eta_1}{(0.40, 0.14)}, \frac{\eta_2}{(0.53, 0.61)}, \frac{\eta_3}{(0.71, 0.81)}, \frac{\eta_4}{(0.90, 0.16)} \right\} \right\rangle, \\
 & \left\langle \left( \frac{0.9}{\mathfrak{s}_3}, e_2, 0 \right), \left\{ \frac{\eta_1}{(0.72, 0.42)}, \frac{\eta_2}{(0.77, 0.63)}, \frac{\eta_3}{(0.50, 0.80)}, \frac{\eta_4}{(0.30, 0.80)} \right\} \right\rangle, \\
 & \left\langle \left( \frac{0.2}{\mathfrak{s}_4}, e_2, 0 \right), \left\{ \frac{\eta_1}{(0.30, 0.80)}, \frac{\eta_2}{(0.79, 0.36)}, \frac{\eta_3}{(0.80, 0.70)}, \frac{\eta_4}{(0.50, 0.16)} \right\} \right\rangle.
 \end{aligned} \tag{6}$$

Now, we discuss some essential basic properties of  $FP^q$  ROFSEs together with illustrative numerical examples. We start with subset relation.

*Definition 5.* For any two  $FP^q$  ROFSEs  $(f, \mathcal{L})_{\mathcal{D}}$  and  $(g, \mathcal{W})_{\mathcal{K}}$  over  $\mathcal{Y}$ , the  $FP^q$  ROFSES  $(f, \mathcal{L})_{\mathcal{D}}$  is referred to as the fuzzy parameterized  $q$ -ROF soft expert subset of  $(g, \mathcal{W})_{\mathcal{K}}$  if

- (1)  $\mathcal{L} \subseteq \mathcal{W}$
- (2) For all  $z \in \mathcal{L}$ ,  $f_{\mathcal{D}}(z)$  is  $q$ -ROF subset of  $g_{\mathcal{K}}(z)$

This subset relation is shown as  $(f, \mathcal{L})_{\mathcal{D}} \subset (g, \mathcal{W})_{\mathcal{K}}$ , whereas  $(g, \mathcal{W})_{\mathcal{K}}$  is called a fuzzy parameterized  $q$ -ROF soft expert superset of  $(f, \mathcal{L})_{\mathcal{D}}$ .

*Definition 6.* Let  $(f, \mathcal{L})_{\mathcal{D}}$  and  $(g, \mathcal{W})_{\mathcal{K}}$  be  $FP^q$  ROFSEs over a universe  $\mathcal{Y}$ . Then,  $(f, \mathcal{L})_{\mathcal{D}}$  and  $(g, \mathcal{W})_{\mathcal{K}}$  are called equal if  $(f, \mathcal{L})_{\mathcal{D}}$  is a fuzzy parameterized  $q$ -ROF soft expert subset of  $(g, \mathcal{W})_{\mathcal{K}}$  and  $(g, \mathcal{W})_{\mathcal{K}}$  is a fuzzy parameterized  $q$ -ROF soft expert subset of  $(f, \mathcal{L})_{\mathcal{D}}$ .

*Example 2.* Considering Example 1, suppose that a second opinion of the experts is taken once again for buying the house as follows:

$$\begin{aligned}
 \mathcal{L} &= \left\{ \left( \frac{0.6}{\mathfrak{s}_1}, e_1, 1 \right), \left( \frac{0.7}{\mathfrak{s}_2}, e_1, 0 \right), \left( \frac{0.6}{\mathfrak{s}_1}, e_2, 1 \right), \left( \frac{0.7}{\mathfrak{s}_2}, e_2, 1 \right), \left( \frac{0.6}{\mathfrak{s}_1}, e_3, 0 \right), \left( \frac{0.7}{\mathfrak{s}_2}, e_3, 1 \right) \right\}, \\
 \mathcal{W} &= \left\{ \left( \frac{0.8}{\mathfrak{s}_1}, e_1, 1 \right), \left( \frac{0.9}{\mathfrak{s}_2}, e_1, 0 \right), \left( \frac{0.3}{\mathfrak{s}_3}, e_1, 1 \right), \left( \frac{0.8}{\mathfrak{s}_1}, e_2, 1 \right), \left( \frac{0.9}{\mathfrak{s}_2}, e_2, 1 \right), \left( \frac{0.8}{\mathfrak{s}_1}, e_3, 0 \right), \left( \frac{0.9}{\mathfrak{s}_2}, e_3, 1 \right), \left( \frac{0.3}{\mathfrak{s}_3}, e_3, 1 \right) \right\}.
 \end{aligned} \tag{7}$$

Clearly,  $\mathcal{L} \subseteq \mathcal{W}$ . Consider two  $FP^4$  ROFSEs  $(f, \mathcal{L})_{\mathcal{D}}$  and  $(g, \mathcal{W})_{\mathcal{K}}$  to be defined as follows:

$$\begin{aligned}
 (f, \mathcal{L})_{\mathcal{D}} &= \left\{ \left\langle \left( \frac{0.6}{\mathfrak{s}_1}, e_1, 1 \right), \left\{ \frac{\eta_1}{(0.80, 0.85)}, \frac{\eta_2}{(0.70, 0.65)}, \frac{\eta_3}{(0.90, 0.35)}, \frac{\eta_4}{(0.50, 0.80)} \right\} \right\rangle, \right. \\
 & \left\langle \left( \frac{0.7}{\mathfrak{s}_2}, e_1, 0 \right), \left\{ \frac{\eta_1}{(0.19, 0.40)}, \frac{\eta_2}{(0.60, 0.70)}, \frac{\eta_3}{(0.12, 0.55)}, \frac{\eta_4}{(0.22, 0.50)} \right\} \right\rangle, \\
 & \left. \left\langle \left( \frac{0.6}{\mathfrak{s}_1}, e_2, 1 \right), \left\{ \frac{\eta_1}{(0.23, 0.47)}, \frac{\eta_2}{(0.25, 0.80)}, \frac{\eta_3}{(0.12, 0.59)}, \frac{\eta_4}{(0.23, 0.85)} \right\} \right\rangle, \right.
 \end{aligned}$$

$$\begin{aligned}
& \left\langle \left\langle \left( \frac{0.7}{\mathfrak{s}_2}, e_2, 1 \right), \left\{ \frac{\eta_1}{(0.43, 0.40)}, \frac{\eta_2}{(0.44, 0.79)}, \frac{\eta_3}{(0.48, 0.50)}, \frac{\eta_4}{(0.50, 0.60)} \right\} \right\rangle, \right. \\
& \left\langle \left\langle \left( \frac{0.6}{\mathfrak{s}_1}, e_3, 0 \right), \left\{ \frac{\eta_1}{(0.35, 0.70)}, \frac{\eta_2}{(0.37, 0.80)}, \frac{\eta_3}{(0.38, 0.77)}, \frac{\eta_4}{(0.45, 0.30)} \right\} \right\rangle, \right. \\
& \left. \left\langle \left\langle \left( \frac{0.7}{\mathfrak{s}_2}, e_3, 1 \right), \left\{ \frac{\eta_1}{(0.54, 0.80)}, \frac{\eta_2}{(0.57, 0.93)}, \frac{\eta_3}{(0.61, 0.40)}, \frac{\eta_4}{(0.65, 0.85)} \right\} \right\rangle \right\}. \\
(\mathfrak{g}, \mathcal{W})_{\mathcal{X}} = & \left\langle \left\langle \left( \frac{0.8}{\mathfrak{s}_1}, e_1, 1 \right), \left\{ \frac{\eta_1}{(0.90, 0.60)}, \frac{\eta_2}{(0.80, 0.60)}, \frac{\eta_3}{(0.91, 0.32)}, \frac{\eta_4}{(0.60, 0.70)} \right\} \right\rangle, \right. \\
& \left\langle \left\langle \left( \frac{0.9}{\mathfrak{s}_2}, e_1, 0 \right), \left\{ \frac{\eta_1}{(0.29, 0.30)}, \frac{\eta_2}{(0.70, 0.60)}, \frac{\eta_3}{(0.20, 0.50)}, \frac{\eta_4}{(0.33, 0.40)} \right\} \right\rangle, \right. \\
& \left\langle \left\langle \left( \frac{0.3}{\mathfrak{s}_3}, e_1, 1 \right), \left\{ \frac{\eta_1}{(0.69, 0.21)}, \frac{\eta_2}{(0.71, 0.17)}, \frac{\eta_3}{(0.72, 0.32)}, \frac{\eta_4}{(0.73, 0.25)} \right\} \right\rangle, \right. \\
& \left\langle \left\langle \left( \frac{0.8}{\mathfrak{s}_1}, e_2, 1 \right), \left\{ \frac{\eta_1}{(0.29, 0.40)}, \frac{\eta_2}{(0.30, 0.70)}, \frac{\eta_3}{(0.16, 0.44)}, \frac{\eta_4}{(0.29, 0.70)} \right\} \right\rangle, \right. \\
& \left\langle \left\langle \left( \frac{0.9}{\mathfrak{s}_2}, e_2, 1 \right), \left\{ \frac{\eta_1}{(0.50, 0.30)}, \frac{\eta_2}{(0.55, 0.71)}, \frac{\eta_3}{(0.50, 0.40)}, \frac{\eta_4}{(0.60, 0.50)} \right\} \right\rangle, \right. \\
& \left\langle \left\langle \left( \frac{0.8}{\mathfrak{s}_1}, e_3, 0 \right), \left\{ \frac{\eta_1}{(0.40, 0.60)}, \frac{\eta_2}{(0.40, 0.70)}, \frac{\eta_3}{(0.42, 0.72)}, \frac{\eta_4}{(0.48, 0.20)} \right\} \right\rangle, \right. \\
& \left\langle \left\langle \left( \frac{0.9}{\mathfrak{s}_2}, e_3, 1 \right), \left\{ \frac{\eta_1}{(0.60, 0.72)}, \frac{\eta_2}{(0.59, 0.91)}, \frac{\eta_3}{(0.70, 0.30)}, \frac{\eta_4}{(0.66, 0.82)} \right\} \right\rangle, \right. \\
& \left. \left\langle \left\langle \left( \frac{0.3}{\mathfrak{s}_3}, e_3, 1 \right), \left\{ \frac{\eta_1}{(0.11, 0.29)}, \frac{\eta_2}{(0.31, 0.42)}, \frac{\eta_3}{(0.12, 0.24)}, \frac{\eta_4}{(0.11, 0.23)} \right\} \right\rangle \right\}.
\end{aligned} \tag{8}$$

Here,  $\forall \mathfrak{z} \in \mathcal{L}$ ,  $f_{\mathcal{D}}(\mathfrak{z})$  is a 4-ROF subset of  $g_{\mathcal{X}}(\mathfrak{z})$ . Hence  $(\mathfrak{f}, \mathcal{L})_{\mathcal{D}} \subset (\mathfrak{g}, \mathcal{W})_{\mathcal{X}}$ .

*Example 3.* Considering the  $\text{FP}^4$  ROFSES  $(\mathfrak{f}, \mathcal{L})_{\mathcal{D}}$  in Example 1, the associated agree- $\text{FP}^4$  ROFSES  $(\mathfrak{f}, \mathcal{L})_{\mathcal{D}}^1$  over  $\mathcal{Y}$  is

*Definition 7.* An agree- $\text{FP}^q$  ROFSES of  $(\mathfrak{f}, \mathcal{L})_{\mathcal{D}}$  over  $\mathcal{Y}$  denoted by  $(\mathfrak{f}, \mathcal{L})_{\mathcal{D}}^1$  is the  $\text{FP}^q$  ROFSES defined as  $(\mathfrak{f}, \mathcal{L})_{\mathcal{D}}^1 = \{\mathfrak{f}_{\mathcal{D}}(\mathfrak{z}) : \mathfrak{z} \in \mathcal{D} \times \mathcal{E} \times \{1\}\}$ .

$$\begin{aligned}
(\mathfrak{f}, \mathcal{L})_{\mathcal{D}}^1 = & \left\langle \left\langle \left( \frac{0.6}{\mathfrak{s}_1}, e_1, 1 \right), \left\{ \frac{\eta_1}{(0.30, 0.60)}, \frac{\eta_2}{(0.80, 0.70)}, \frac{\eta_3}{(0.20, 0.10)}, \frac{\eta_4}{(0.50, 0.20)} \right\} \right\rangle, \right. \\
& \left\langle \left\langle \left( \frac{0.7}{\mathfrak{s}_2}, e_1, 1 \right), \left\{ \frac{\eta_1}{(0.70, 0.90)}, \frac{\eta_2}{(0.60, 0.10)}, \frac{\eta_3}{(0.30, 0.20)}, \frac{\eta_4}{(0.10, 0.40)} \right\} \right\rangle, \right. \\
& \left\langle \left\langle \left( \frac{0.9}{\mathfrak{s}_3}, e_1, 1 \right), \left\{ \frac{\eta_1}{(0.10, 0.50)}, \frac{\eta_2}{(0.80, 0.10)}, \frac{\eta_3}{(0.80, 0.20)}, \frac{\eta_4}{(0.30, 0.80)} \right\} \right\rangle, \right. \\
& \left. \left\langle \left\langle \left( \frac{0.2}{\mathfrak{s}_4}, e_1, 1 \right), \left\{ \frac{\eta_1}{(0.10, 0.20)}, \frac{\eta_2}{(0.70, 0.30)}, \frac{\eta_3}{(0.70, 0.40)}, \frac{\eta_4}{(0.90, 0.60)} \right\} \right\rangle \right\}.
\end{aligned}$$

$$\begin{aligned} & \left\langle \left( \frac{0.6}{s_1}, e_2, 1 \right), \left\{ \frac{\eta_1}{(0.80, 0.60)}, \frac{\eta_2}{(0.80, 0.70)}, \frac{\eta_3}{(0.80, 0.50)}, \frac{\eta_4}{(0.80, 0.60)} \right\} \right\rangle, \\ & \left\langle \left( \frac{0.7}{s_2}, e_2, 1 \right), \left\{ \frac{\eta_1}{(0.90, 0.16)}, \frac{\eta_2}{(0.50, 0.15)}, \frac{\eta_3}{(0.40, 0.14)}, \frac{\eta_4}{(0.30, 0.14)} \right\} \right\rangle, \\ & \left\langle \left( \frac{0.9}{s_3}, e_2, 1 \right), \left\{ \frac{\eta_1}{(0.66, 0.36)}, \frac{\eta_2}{(0.44, 0.72)}, \frac{\eta_3}{(0.48, 0.52)}, \frac{\eta_4}{(0.36, 0.44)} \right\} \right\rangle, \\ & \left\langle \left( \frac{0.2}{s_4}, e_2, 1 \right), \left\{ \frac{\eta_1}{(0.87, 0.45)}, \frac{\eta_2}{(0.45, 0.56)}, \frac{\eta_3}{(0.79, 0.36)}, \frac{\eta_4}{(0.62, 0.42)} \right\} \right\rangle. \end{aligned} \tag{9}$$

*Definition 8.* A disagree- $FP^q$  ROFSES of  $(f, \mathcal{L})_{\mathcal{D}}$  over  $\mathcal{Y}$  denoted by  $(f, \mathcal{L})_{\mathcal{D}}^0$  is the  $FP^q$  ROFSES defined as  $(f, \mathcal{L})_{\mathcal{D}}^0 = \{f_{\mathcal{D}}(z) : z \in \mathcal{D} \times \mathcal{E} \times \{0\}\}$ .

*Example 4.* Considering the  $FP^4$  ROFSES  $(f, \mathcal{L})_{\mathcal{D}}$  in Example 1, then the related disagree  $FP^4$  ROFSES  $(f, \mathcal{L})_{\mathcal{D}}^0$  over  $\mathcal{Y}$  is

$$\begin{aligned} (f, \mathcal{L})_{\mathcal{D}}^0 = & \left\langle \left( \frac{0.6}{s_1}, e_1, 0 \right), \left\{ \frac{\eta_1}{(0.70, 0.40)}, \frac{\eta_2}{(0.60, 0.30)}, \frac{\eta_3}{(0.70, 0.40)}, \frac{\eta_4}{(0.80, 0.20)} \right\} \right\rangle, \\ & \left\langle \left( \frac{0.7}{s_2}, e_1, 0 \right), \left\{ \frac{\eta_1}{(0.70, 0.10)}, \frac{\eta_2}{(0.80, 0.60)}, \frac{\eta_3}{(0.40, 0.14)}, \frac{\eta_4}{(0.56, 0.65)} \right\} \right\rangle, \\ & \left\langle \left( \frac{0.9}{s_3}, e_1, 0 \right), \left\{ \frac{\eta_1}{(0.80, 0.70)}, \frac{\eta_2}{(0.90, 0.60)}, \frac{\eta_3}{(0.80, 0.20)}, \frac{\eta_4}{(0.80, 0.30)} \right\} \right\rangle, \\ & \left\langle \left( \frac{0.2}{s_4}, e_1, 0 \right), \left\{ \frac{\eta_1}{(0.50, 0.15)}, \frac{\eta_2}{(0.77, 0.63)}, \frac{\eta_3}{(0.56, 0.56)}, \frac{\eta_4}{(0.27, 0.31)} \right\} \right\rangle, \\ & \left\langle \left( \frac{0.6}{s_1}, e_2, 0 \right), \left\{ \frac{\eta_1}{(0.90, 0.60)}, \frac{\eta_2}{(0.62, 0.42)}, \frac{\eta_3}{(0.71, 0.81)}, \frac{\eta_4}{(0.72, 0.44)} \right\} \right\rangle, \\ & \left\langle \left( \frac{0.7}{s_2}, e_2, 0 \right), \left\{ \frac{\eta_1}{(0.40, 0.14)}, \frac{\eta_2}{(0.53, 0.61)}, \frac{\eta_3}{(0.71, 0.81)}, \frac{\eta_4}{(0.90, 0.16)} \right\} \right\rangle, \\ & \left\langle \left( \frac{0.9}{s_3}, e_2, 0 \right), \left\{ \frac{\eta_1}{(0.72, 0.42)}, \frac{\eta_2}{(0.77, 0.63)}, \frac{\eta_3}{(0.50, 0.80)}, \frac{\eta_4}{(0.30, 0.80)} \right\} \right\rangle, \\ & \left\langle \left( \frac{0.2}{s_4}, e_2, 0 \right), \left\{ \frac{\eta_1}{(0.30, 0.80)}, \frac{\eta_2}{(0.79, 0.36)}, \frac{\eta_3}{(0.80, 0.70)}, \frac{\eta_4}{(0.50, 0.16)} \right\} \right\rangle. \end{aligned} \tag{10}$$

*Definition 9.* Let  $(f, \mathcal{L})_{\mathcal{D}}$  be a  $FP^q$  ROFSES over  $\mathcal{Y}$ . Then, the complement of  $FP^q$  ROFSES  $(f, \mathcal{L})_{\mathcal{D}}$  represented as  $(f, \mathcal{L})_{\mathcal{D}}^c$  is defined by  $(f, \mathcal{L})_{\mathcal{D}}^c = (f^c, \mathcal{L})_{\mathcal{D}}$  where  $\mathcal{L} \subseteq \mathcal{D}^c \times \mathcal{E} \times \mathcal{O}$  and  $f_{\mathcal{D}}^c$  is given as  $f_{\mathcal{D}}^c(z) = c(f_{\mathcal{D}}(z)) \forall z \in \mathcal{L}$  such that

$$f_{\mathcal{D}}^c(z) = \left\{ \frac{\eta}{(\beta_f(z)(\eta), \alpha_f(z)(\eta))} \mid \eta \in \mathcal{Y} \right\}, \tag{11}$$

with  $0 \leq (\alpha_f(z)(\eta))^q + (\beta_f(z)(\eta))^q \leq 1$ , for all  $q \in (0, \infty)$ .

*Example 5.* Let  $(\mathfrak{f}, \mathcal{L})_{\mathcal{D}}$  be the  $\text{FP}^4$  ROFSES as discussed in Example 1. Then, by the definition of complement for  $\text{FP}^4$  ROFSES,

$$\begin{aligned}
 (\mathfrak{f}, \mathcal{L})_{\mathcal{D}}^c = & \left\langle \left\langle \left( \frac{0.6}{\mathfrak{s}_1}, e_1, 1 \right), \left\{ \frac{\mathfrak{h}_1}{(0.60, 0.30)}, \frac{\mathfrak{h}_2}{(0.70, 0.80)}, \frac{\mathfrak{h}_3}{(0.10, 0.20)}, \frac{\mathfrak{h}_4}{(0.20, 0.50)} \right\} \right\rangle, \right. \\
 & \left\langle \left( \frac{0.7}{\mathfrak{s}_2}, e_1, 1 \right), \left\{ \frac{\mathfrak{h}_1}{(0.90, 0.70)}, \frac{\mathfrak{h}_2}{(0.10, 0.60)}, \frac{\mathfrak{h}_3}{(0.20, 0.30)}, \frac{\mathfrak{h}_4}{(0.40, 0.10)} \right\} \right\rangle, \\
 & \left\langle \left( \frac{0.9}{\mathfrak{s}_3}, e_1, 1 \right), \left\{ \frac{\mathfrak{h}_1}{(0.50, 0.10)}, \frac{\mathfrak{h}_2}{(0.10, 0.80)}, \frac{\mathfrak{h}_3}{(0.20, 0.80)}, \frac{\mathfrak{h}_4}{(0.80, 0.30)} \right\} \right\rangle, \\
 & \left\langle \left( \frac{0.2}{\mathfrak{s}_4}, e_1, 1 \right), \left\{ \frac{\mathfrak{h}_1}{(0.20, 0.10)}, \frac{\mathfrak{h}_2}{(0.30, 0.70)}, \frac{\mathfrak{h}_3}{(0.40, 0.70)}, \frac{\mathfrak{h}_4}{(0.60, 0.90)} \right\} \right\rangle, \\
 & \left\langle \left( \frac{0.6}{\mathfrak{s}_1}, e_2, 1 \right), \left\{ \frac{\mathfrak{h}_1}{(0.60, 0.80)}, \frac{\mathfrak{h}_2}{(0.70, 0.80)}, \frac{\mathfrak{h}_3}{(0.50, 0.80)}, \frac{\mathfrak{h}_4}{(0.60, 0.80)} \right\} \right\rangle, \\
 & \left\langle \left( \frac{0.7}{\mathfrak{s}_2}, e_2, 1 \right), \left\{ \frac{\mathfrak{h}_1}{(0.16, 0.90)}, \frac{\mathfrak{h}_2}{(0.15, 0.50)}, \frac{\mathfrak{h}_3}{(0.14, 0.40)}, \frac{\mathfrak{h}_4}{(0.14, 0.30)} \right\} \right\rangle, \\
 & \left\langle \left( \frac{0.9}{\mathfrak{s}_3}, e_2, 1 \right), \left\{ \frac{\mathfrak{h}_1}{(0.36, 0.66)}, \frac{\mathfrak{h}_2}{(0.72, 0.44)}, \frac{\mathfrak{h}_3}{(0.52, 0.48)}, \frac{\mathfrak{h}_4}{(0.44, 0.36)} \right\} \right\rangle, \\
 & \left\langle \left( \frac{0.2}{\mathfrak{s}_4}, e_2, 1 \right), \left\{ \frac{\mathfrak{h}_1}{(0.45, 0.87)}, \frac{\mathfrak{h}_2}{(0.56, 0.45)}, \frac{\mathfrak{h}_3}{(0.36, 0.79)}, \frac{\mathfrak{h}_4}{(0.42, 0.62)} \right\} \right\rangle, \\
 & \left\langle \left( \frac{0.6}{\mathfrak{s}_1}, e_1, 0 \right), \left\{ \frac{\mathfrak{h}_1}{(0.40, 0.70)}, \frac{\mathfrak{h}_2}{(0.30, 0.60)}, \frac{\mathfrak{h}_3}{(0.40, 0.70)}, \frac{\mathfrak{h}_4}{(0.20, 0.80)} \right\} \right\rangle, \\
 & \left\langle \left( \frac{0.7}{\mathfrak{s}_2}, e_1, 0 \right), \left\{ \frac{\mathfrak{h}_1}{(0.10, 0.70)}, \frac{\mathfrak{h}_2}{(0.60, 0.80)}, \frac{\mathfrak{h}_3}{(0.14, 0.40)}, \frac{\mathfrak{h}_4}{(0.65, 0.56)} \right\} \right\rangle, \\
 & \left\langle \left( \frac{0.9}{\mathfrak{s}_3}, e_1, 0 \right), \left\{ \frac{\mathfrak{h}_1}{(0.70, 0.80)}, \frac{\mathfrak{h}_2}{(0.60, 0.90)}, \frac{\mathfrak{h}_3}{(0.20, 0.80)}, \frac{\mathfrak{h}_4}{(0.30, 0.80)} \right\} \right\rangle, \\
 & \left\langle \left( \frac{0.2}{\mathfrak{s}_4}, e_1, 0 \right), \left\{ \frac{\mathfrak{h}_1}{(0.15, 0.50)}, \frac{\mathfrak{h}_2}{(0.63, 0.77)}, \frac{\mathfrak{h}_3}{(0.56, 0.56)}, \frac{\mathfrak{h}_4}{(0.31, 0.27)} \right\} \right\rangle, \\
 & \left\langle \left( \frac{0.6}{\mathfrak{s}_1}, e_2, 0 \right), \left\{ \frac{\mathfrak{h}_1}{(0.60, 0.90)}, \frac{\mathfrak{h}_2}{(0.42, 0.62)}, \frac{\mathfrak{h}_3}{(0.81, 0.71)}, \frac{\mathfrak{h}_4}{(0.44, 0.72)} \right\} \right\rangle, \\
 & \left\langle \left( \frac{0.7}{\mathfrak{s}_2}, e_2, 0 \right), \left\{ \frac{\mathfrak{h}_1}{(0.14, 0.40)}, \frac{\mathfrak{h}_2}{(0.61, 0.53)}, \frac{\mathfrak{h}_3}{(0.81, 0.71)}, \frac{\mathfrak{h}_4}{(0.16, 0.90)} \right\} \right\rangle, \\
 & \left\langle \left( \frac{0.9}{\mathfrak{s}_3}, e_2, 0 \right), \left\{ \frac{\mathfrak{h}_1}{(0.42, 0.72)}, \frac{\mathfrak{h}_2}{(0.63, 0.77)}, \frac{\mathfrak{h}_3}{(0.80, 0.50)}, \frac{\mathfrak{h}_4}{(0.80, 0.30)} \right\} \right\rangle, \\
 & \left. \left\langle \left( \frac{0.2}{\mathfrak{s}_4}, e_2, 0 \right), \left\{ \frac{\mathfrak{h}_1}{(0.30, 0.80)}, \frac{\mathfrak{h}_2}{(0.79, 0.36)}, \frac{\mathfrak{h}_3}{(0.80, 0.70)}, \frac{\mathfrak{h}_4}{(0.50, 0.16)} \right\} \right\rangle \right\}.
 \end{aligned} \tag{12}$$

**Proposition 1.** Let  $(\mathfrak{f}, \mathcal{L})_{\mathcal{D}}$  be a  $FP^q$  ROFSES over  $\mathcal{Y}$ ; then,  $((\mathfrak{f}, \mathcal{L})_{\mathcal{D}})^c = (\mathfrak{f}, \mathcal{L})_{\mathcal{D}}$ .

*Proof.* Let  $(\mathfrak{f}, \mathcal{L})_{\mathcal{D}}$  be a  $FP^q$  ROFSES over  $\mathcal{Y}$ . Then, by Definition 9, a mapping  $(f_{\mathcal{D}}^c)^c: \mathcal{L} \rightarrow \mathfrak{Q}^{\mathcal{Y}}$  is defined as follows:

$$(f_{\mathcal{D}}^c)^c(\mathfrak{z}) = (f_{\mathcal{D}}^c(\mathfrak{z}))^c = f_{\mathcal{D}}(\mathfrak{z}), \quad (13)$$

for all  $\mathfrak{z} \in \mathcal{L}$ , where  $\mathcal{L} = D \times \mathcal{E} \times \mathcal{O}$ . Thus, it is proved that  $((\mathfrak{f}, \mathcal{L})_{\mathcal{D}})^c = (\mathfrak{f}, \mathcal{L})_{\mathcal{D}}$ .  $\square$

**Definition 10.** The union of two  $FP^q$  ROFSESs  $(\mathfrak{f}, \mathcal{L})_{\mathcal{D}}$  and  $(\mathfrak{g}, \mathcal{W})_{\mathcal{K}}$  over  $\mathcal{Y}$  denoted as  $(\mathfrak{f}, \mathcal{L})_{\mathcal{D}} \cup (\mathfrak{g}, \mathcal{W})_{\mathcal{K}}$  is the  $FP^q$

ROFSES  $(\mathcal{P}, \mathcal{Q})_{\mathcal{R}}$ , such that  $\mathcal{Q} = (\mathcal{R} \times \mathcal{E} \times \mathcal{O})$ , where  $\mathcal{R} = \mathcal{D} \cup \mathcal{K}$ ; then, for all  $\mathfrak{z} \in \mathcal{Q}$ ,  $\mathcal{P}_{\mathcal{R}}(\mathfrak{z})$  is given by

$$\mathcal{P}_{\mathcal{R}}(\mathfrak{z}) = \mathfrak{f}_{\mathcal{D}}(\mathfrak{z}) \cup \mathfrak{g}_{\mathcal{K}}(\mathfrak{z}), \quad (14)$$

where  $\cup$  is simply  $q$ -ROF union between  $q$ -ROFSs  $\mathfrak{f}_{\mathcal{D}}(\mathfrak{z})$  and  $\mathfrak{g}_{\mathcal{K}}(\mathfrak{z})$ .

*Example 6.* Let  $\mathcal{Y} = \{\mathfrak{u}_1, \mathfrak{u}_2, \mathfrak{u}_3\}$  be the universe, and let  $\mathcal{E} = \{e_1, e_2\}$  be the set of experts such that  $\mathcal{S}_{\mathcal{L}} = \{\mathfrak{s}_1, \mathfrak{s}_2\}$  and  $\mathcal{S}_{\mathcal{W}} = \{\mathfrak{s}_1\}$  represent the sets of parameters, and  $\mathcal{D} = \{(0.8/\mathfrak{s}_1), (0.6/\mathfrak{s}_2)\}$ , and  $\mathcal{K} = \{0.8/\mathfrak{s}_1\}$  represent the weights for the parameters. Suppose that  $(\mathfrak{f}, \mathcal{L})_{\mathcal{D}}$  and  $(\mathfrak{g}, \mathcal{W})_{\mathcal{K}}$  are  $FP^4$  ROFSESs over  $\mathcal{Y}$  such that

$$\begin{aligned} (\mathfrak{f}, \mathcal{L})_{\mathcal{D}} = & \left\{ \left\langle \left( \left( \frac{0.8}{\mathfrak{s}_1}, e_1, 1 \right), \left\{ \frac{\mathfrak{u}_1}{(0.80, 0.60)}, \frac{\mathfrak{u}_2}{(0.30, 0.14)}, \frac{\mathfrak{u}_3}{(0.45, 0.56)} \right\} \right) \right\rangle, \right. \\ & \left\langle \left( \left( \frac{0.6}{\mathfrak{s}_2}, e_1, 1 \right), \left\{ \frac{\mathfrak{u}_1}{(0.40, 0.50)}, \frac{\mathfrak{u}_2}{(0.52, 0.62)}, \frac{\mathfrak{u}_3}{(0.60, 0.42)} \right\} \right) \right\rangle, \\ & \left\langle \left( \left( \frac{0.8}{\mathfrak{s}_1}, e_2, 1 \right), \left\{ \frac{\mathfrak{u}_1}{(0.70, 0.40)}, \frac{\mathfrak{u}_2}{(0.43, 0.52)}, \frac{\mathfrak{u}_3}{(0.60, 0.75)} \right\} \right) \right\rangle, \\ & \left\langle \left( \left( \frac{0.6}{\mathfrak{s}_2}, e_2, 1 \right), \left\{ \frac{\mathfrak{u}_1}{(0.36, 0.25)}, \frac{\mathfrak{u}_2}{(0.30, 0.80)}, \frac{\mathfrak{u}_3}{(0.45, 0.51)} \right\} \right) \right\rangle, \\ & \left\langle \left( \left( \frac{0.8}{\mathfrak{s}_1}, e_1, 0 \right), \left\{ \frac{\mathfrak{u}_1}{(0.80, 0.10)}, \frac{\mathfrak{u}_2}{(0.90, 0.60)}, \frac{\mathfrak{u}_3}{(0.60, 0.60)} \right\} \right) \right\rangle, \\ & \left\langle \left( \left( \frac{0.6}{\mathfrak{s}_2}, e_1, 0 \right), \left\{ \frac{\mathfrak{u}_1}{(0.50, 0.36)}, \frac{\mathfrak{u}_2}{(0.48, 0.66)}, \frac{\mathfrak{u}_3}{(0.55, 0.22)} \right\} \right) \right\rangle, \\ & \left\langle \left( \left( \frac{0.8}{\mathfrak{s}_1}, e_2, 0 \right), \left\{ \frac{\mathfrak{u}_1}{(0.44, 0.75)}, \frac{\mathfrak{u}_2}{(0.71, 0.16)}, \frac{\mathfrak{u}_3}{(0.22, 0.51)} \right\} \right) \right\rangle, \\ & \left. \left\langle \left( \left( \frac{0.6}{\mathfrak{s}_2}, e_2, 0 \right), \left\{ \frac{\mathfrak{u}_1}{(0.66, 0.16)}, \frac{\mathfrak{u}_2}{(0.60, 0.50)}, \frac{\mathfrak{u}_3}{(0.28, 0.19)} \right\} \right) \right\rangle \right\}, \\ (\mathfrak{g}, \mathcal{W})_{\mathcal{K}} = & \left\{ \left\langle \left( \left( \frac{0.8}{\mathfrak{s}_1}, e_1, 1 \right), \left\{ \frac{\mathfrak{u}_1}{(0.70, 0.50)}, \frac{\mathfrak{u}_2}{(0.47, 0.55)}, \frac{\mathfrak{u}_3}{(0.74, 0.45)} \right\} \right) \right\rangle, \right. \\ & \left\langle \left( \left( \frac{0.5}{\mathfrak{s}_1}, e_2, 1 \right), \left\{ \frac{\mathfrak{u}_1}{(0.80, 0.40)}, \frac{\mathfrak{u}_2}{(0.50, 0.35)}, \frac{\mathfrak{u}_3}{(0.46, 0.78)} \right\} \right) \right\rangle, \\ & \left\langle \left( \left( \frac{0.5}{\mathfrak{s}_1}, e_1, 0 \right), \left\{ \frac{\mathfrak{u}_1}{(0.28, 0.51)}, \frac{\mathfrak{u}_2}{(0.75, 0.32)}, \frac{\mathfrak{u}_3}{(0.72, 0.56)} \right\} \right) \right\rangle, \\ & \left. \left\langle \left( \left( \frac{0.5}{\mathfrak{s}_1}, e_2, 0 \right), \left\{ \frac{\mathfrak{u}_1}{(0.81, 0.33)}, \frac{\mathfrak{u}_2}{(0.40, 0.25)}, \frac{\mathfrak{u}_3}{(0.62, 0.44)} \right\} \right) \right\rangle \right\}. \end{aligned} \quad (15)$$

Using Definition 10, we obtain  $(\mathfrak{f}, \mathcal{L})_{\mathcal{D}} \cup (\mathfrak{g}, \mathcal{W})_{\mathcal{K}} = (\mathcal{P}, \mathcal{Q})_{\mathcal{R}}$  as follows:

$$\begin{aligned}
 (\mathcal{P}, \mathcal{Q})_{\mathcal{R}} = & \left\langle \left\langle \left( \frac{0.8}{\mathfrak{s}_1}, e_1, 1 \right), \left\{ \frac{\eta_1}{(0.80, 0.50)}, \frac{\eta_2}{(0.47, 0.14)}, \frac{\eta_3}{(0.74, 0.45)} \right\} \right\rangle, \right. \\
 & \left\langle \left( \frac{0.6}{\mathfrak{s}_2}, e_1, 1 \right), \left\{ \frac{\eta_1}{(0.40, 0.50)}, \frac{\eta_2}{(0.52, 0.62)}, \frac{\eta_3}{(0.60, 0.42)} \right\} \right\rangle, \\
 & \left\langle \left( \frac{0.8}{\mathfrak{s}_1}, e_2, 1 \right), \left\{ \frac{\eta_1}{(0.80, 0.40)}, \frac{\eta_2}{(0.50, 0.35)}, \frac{\eta_3}{(0.60, 0.75)} \right\} \right\rangle, \\
 & \left\langle \left( \frac{0.6}{\mathfrak{s}_2}, e_2, 1 \right), \left\{ \frac{\eta_1}{(0.36, 0.25)}, \frac{\eta_2}{(0.30, 0.80)}, \frac{\eta_3}{(0.45, 0.51)} \right\} \right\rangle, \\
 & \left\langle \left( \frac{0.8}{\mathfrak{s}_1}, e_1, 0 \right), \left\{ \frac{\eta_1}{(0.80, 0.10)}, \frac{\eta_2}{(0.90, 0.32)}, \frac{\eta_3}{(0.72, 0.56)} \right\} \right\rangle, \\
 & \left\langle \left( \frac{0.6}{\mathfrak{s}_2}, e_1, 0 \right), \left\{ \frac{\eta_1}{(0.50, 0.36)}, \frac{\eta_2}{(0.48, 0.66)}, \frac{\eta_3}{(0.55, 0.22)} \right\} \right\rangle, \\
 & \left\langle \left( \frac{0.8}{\mathfrak{s}_1}, e_2, 0 \right), \left\{ \frac{\eta_1}{(0.81, 0.33)}, \frac{\eta_2}{(0.71, 0.16)}, \frac{\eta_3}{(0.62, 0.44)} \right\} \right\rangle, \\
 & \left. \left\langle \left( \frac{0.6}{\mathfrak{s}_2}, e_2, 0 \right), \left\{ \frac{\eta_1}{(0.66, 0.16)}, \frac{\eta_2}{(0.60, 0.50)}, \frac{\eta_3}{(0.28, 0.19)} \right\} \right\rangle \right\}.
 \end{aligned} \tag{16}$$

**Proposition 2.** Let  $(f, \mathcal{L})_{\mathcal{D}}$ ,  $(g, \mathcal{W})_{\mathcal{K}}$ , and  $(h, \mathcal{T})_{\mathcal{F}}$  are  $FP^q$  ROFSEs over the universe  $\mathcal{Y}$ ; then, the following conditions hold:

- (1)  $(f, \mathcal{L})_{\mathcal{D}} \cup (g, \mathcal{W})_{\mathcal{K}} = (g, \mathcal{W})_{\mathcal{K}} \cup (f, \mathcal{L})_{\mathcal{D}}$
- (2)  $((f, \mathcal{L})_{\mathcal{D}} \cup (g, \mathcal{W})_{\mathcal{K}}) \cup (h, \mathcal{T})_{\mathcal{F}} = (f, \mathcal{L})_{\mathcal{D}} \cup ((g, \mathcal{W})_{\mathcal{K}} \cup (h, \mathcal{T})_{\mathcal{F}})$
- (3)  $(f, \mathcal{L})_{\mathcal{D}} \cup (f, \mathcal{L})_{\mathcal{D}} = (f, \mathcal{L})_{\mathcal{D}}$

*Proof.* (1) Let  $(f, \mathcal{L})_{\mathcal{D}} \cup (g, \mathcal{W})_{\mathcal{K}} = (\mathcal{P}, \mathcal{Q})_{\mathcal{R}}$ ; then,  $\forall z \in \mathcal{Q}$ , we have

$$\begin{aligned}
 \mathcal{R} &= \mathcal{D} \cup \mathcal{K} = \mathcal{K} \cup \mathcal{D}, \\
 \mathcal{P}_{\mathcal{R}}(z) &= \mathfrak{f}_{\mathcal{D}}(z) \cup \mathfrak{g}_{\mathcal{K}}(z) = \mathfrak{g}_{\mathcal{K}}(z) \cup \mathfrak{f}_{\mathcal{D}}(z).
 \end{aligned} \tag{17}$$

This implies  $(\mathcal{P}, \mathcal{Q})_{\mathcal{R}} = (g, \mathcal{W})_{\mathcal{K}} \cup (f, \mathcal{L})_{\mathcal{D}}$ . Hence,  $(f, \mathcal{L})_{\mathcal{D}} \cup (g, \mathcal{W})_{\mathcal{K}} = (g, \mathcal{W})_{\mathcal{K}} \cup (f, \mathcal{L})_{\mathcal{D}}$ .

The proof of the remaining parts is similar. □

*Definition 11.* The intersection of two  $FP^q$  ROFSEs  $(f, \mathcal{L})_{\mathcal{D}}$  and  $(g, \mathcal{W})_{\mathcal{K}}$  over  $\mathcal{Y}$ , represented as  $(f, \mathcal{L})_{\mathcal{D}} \bar{\cap} (g, \mathcal{W})_{\mathcal{K}}$ , is the  $FP^q$  ROFSEs  $(\mathcal{F}, \mathcal{Q})$  such that  $\mathcal{Q} = (\mathcal{R} \times \mathcal{E} \times \mathcal{O})$  where  $\mathcal{R} = \mathcal{D} \cap \mathcal{K}$ . Then, for all  $z \in \mathcal{Q}$ ,  $\mathcal{F}_{\mathcal{R}}(z)$  is defined as

$$\mathcal{F}_{\mathcal{R}}(z) = \mathfrak{f}_{\mathcal{D}}(z) \cap \mathfrak{g}_{\mathcal{K}}(z), \tag{18}$$

where  $\cap$  is simply the  $q$ -ROF intersection between  $q$ -ROFSs  $\mathfrak{f}_{\mathcal{D}}(z)$  and  $\mathfrak{g}_{\mathcal{K}}(z)$ .

*Example 7.* Let  $(f, \mathcal{L})_{\mathcal{D}}$  and  $(g, \mathcal{W})_{\mathcal{K}}$  be two  $FP^4$  ROFSEs over the universe  $\mathcal{Y}$ , as taken in Example 6. Then, by using Definition 11, we obtain  $(f, \mathcal{L})_{\mathcal{D}} \bar{\cap} (g, \mathcal{W})_{\mathcal{K}} = (\mathcal{F}, \mathcal{Q})_{\mathcal{R}}$  where  $(\mathcal{F}, \mathcal{Q})_{\mathcal{R}}$  is a  $FP^4$  ROFSEs defined as

$$\begin{aligned}
 (\mathcal{F}, \mathcal{Q})_{\mathcal{R}} = & \left\langle \left\langle \left( \frac{0.8}{\mathfrak{s}_1}, e_1, 1 \right), \left\{ \frac{\eta_1}{(0.70, 0.60)}, \frac{\eta_2}{(0.30, 0.55)}, \frac{\eta_3}{(0.45, 0.56)} \right\} \right\rangle, \right. \\
 & \left\langle \left( \frac{0.6}{\mathfrak{s}_2}, e_1, 1 \right), \left\{ \frac{\eta_1}{(0.40, 0.50)}, \frac{\eta_2}{(0.52, 0.62)}, \frac{\eta_3}{(0.60, 0.42)} \right\} \right\rangle, \\
 & \left. \left\langle \left( \frac{0.8}{\mathfrak{s}_1}, e_2, 1 \right), \left\{ \frac{\eta_1}{(0.70, 0.40)}, \frac{\eta_2}{(0.43, 0.52)}, \frac{\eta_3}{(0.46, 0.78)} \right\} \right\rangle, \right.
 \end{aligned}$$

$$\begin{aligned} & \left\langle \left( \left( \frac{0.6}{s_2}, e_2, 1 \right), \left\{ \frac{\eta_1}{(0.36, 0.25)}, \frac{\eta_2}{(0.30, 0.80)}, \frac{\eta_3}{(0.45, 0.51)} \right\} \right) \right\rangle, \\ & \left\langle \left( \left( \frac{0.8}{s_1}, e_1, 0 \right), \left\{ \frac{\eta_1}{(0.28, 0.51)}, \frac{\eta_2}{(0.75, 0.60)}, \frac{\eta_3}{(0.60, 0.60)} \right\} \right) \right\rangle, \\ & \left\langle \left( \left( \frac{0.6}{s_2}, e_1, 0 \right), \left\{ \frac{\eta_1}{(0.50, 0.36)}, \frac{\eta_2}{(0.48, 0.66)}, \frac{\eta_3}{(0.55, 0.22)} \right\} \right) \right\rangle, \\ & \left\langle \left( \left( \frac{0.8}{s_1}, e_2, 0 \right), \left\{ \frac{\eta_1}{(0.44, 0.75)}, \frac{\eta_2}{(0.40, 0.25)}, \frac{\eta_3}{(0.22, 0.51)} \right\} \right) \right\rangle, \\ & \left\langle \left( \left( \frac{0.6}{s_2}, e_2, 0 \right), \left\{ \frac{\eta_1}{(0.66, 0.16)}, \frac{\eta_2}{(0.60, 0.50)}, \frac{\eta_3}{(0.28, 0.19)} \right\} \right) \right\rangle. \end{aligned} \tag{19}$$

**Proposition 3.** Let  $(f, \mathcal{L})_{\mathcal{D}}$ ,  $(g, \mathcal{W})_{\mathcal{K}}$ , and  $(h, \mathcal{T})_{\mathcal{F}}$  be an  $FP^q$  ROFSES over the universe  $\mathcal{Y}$ ; then, the following conditions hold:

- (1)  $(f, \mathcal{L})_{\mathcal{D}} \overline{\cap} (g, \mathcal{W})_{\mathcal{K}} = (g, \mathcal{W})_{\mathcal{K}} \overline{\cap} (f, \mathcal{L})_{\mathcal{D}}$
- (2)  $((f, \mathcal{L})_{\mathcal{D}} \overline{\cap} (g, \mathcal{W})_{\mathcal{K}}) \overline{\cap} (h, \mathcal{T})_{\mathcal{F}} = (f, \mathcal{L})_{\mathcal{D}} \overline{\cap} ((g, \mathcal{W})_{\mathcal{K}} \overline{\cap} (h, \mathcal{T})_{\mathcal{F}})$
- (3)  $(f, \mathcal{L})_{\mathcal{D}} \overline{\cap} (f, \mathcal{L})_{\mathcal{D}} = (f, \mathcal{L})_{\mathcal{D}}$

*Proof.* (1) Let  $(f, \mathcal{L})_{\mathcal{D}} \overline{\cap} (g, \mathcal{W})_{\mathcal{K}} = (\mathcal{J}, \mathcal{Q})_{\mathcal{R}}$ ; then,  $\forall z \in \mathcal{Q}$ , we have

$$\begin{aligned} \mathcal{R} &= \mathcal{D} \cap \mathcal{K} = \mathcal{K} \cap \mathcal{D}, \\ \mathcal{J}_{\mathcal{R}}(z) &= \underline{f}_{\mathcal{D}}(z) \cap \underline{g}_{\mathcal{K}}(z) = \underline{g}_{\mathcal{K}}(z) \cap \underline{f}_{\mathcal{D}}(z). \end{aligned} \tag{20}$$

This implies  $(\mathcal{J}, \mathcal{Q})_{\mathcal{R}} = (g, \mathcal{W})_{\mathcal{K}} \overline{\cap} (f, \mathcal{L})_{\mathcal{D}}$ . Hence,  $(f, \mathcal{L})_{\mathcal{D}} \overline{\cap} (g, \mathcal{W})_{\mathcal{K}} = (g, \mathcal{W})_{\mathcal{K}} \overline{\cap} (f, \mathcal{L})_{\mathcal{D}}$ .

The proof of the remaining parts is similar.  $\square$

**Proposition 4.** Let  $(f, \mathcal{L})_{\mathcal{D}}$ ,  $(g, \mathcal{W})_{\mathcal{K}}$ , and  $(h, \mathcal{T})_{\mathcal{F}}$  be  $FP^q$  ROFSESs over the universe  $\mathcal{Y}$ ; then, the following conditions hold:

- (1)  $(f, \mathcal{L})_{\mathcal{D}} \overline{\cap} ((g, \mathcal{W})_{\mathcal{K}} \cup (h, \mathcal{T})_{\mathcal{F}}) = ((f, \mathcal{L})_{\mathcal{D}} \overline{\cap} (g, \mathcal{W})_{\mathcal{K}}) \cup ((f, \mathcal{L})_{\mathcal{D}} \overline{\cap} (h, \mathcal{T})_{\mathcal{F}})$
- (2)  $(f, \mathcal{L})_{\mathcal{D}} \cup ((g, \mathcal{W})_{\mathcal{K}} \overline{\cap} (h, \mathcal{T})_{\mathcal{F}}) = ((f, \mathcal{L})_{\mathcal{D}} \cup (g, \mathcal{W})_{\mathcal{K}}) \overline{\cap} ((f, \mathcal{L})_{\mathcal{D}} \cup (h, \mathcal{T})_{\mathcal{F}})$

*Proof.* The proof is simple and is therefore omitted.  $\square$

**Proposition 5.** Let  $(f, \mathcal{L})_{\mathcal{D}}$  and  $(g, \mathcal{W})_{\mathcal{K}}$  be  $FP^q$  ROFSESs over the universe  $\mathcal{Y}$ . Then,

- (1)  $((f, \mathcal{L})_{\mathcal{D}} \cup (g, \mathcal{W})_{\mathcal{K}})^c = (f, \mathcal{L})_{\mathcal{D}}^c \overline{\cap} (g, \mathcal{W})_{\mathcal{K}}^c$
- (2)  $((f, \mathcal{L})_{\mathcal{D}} \overline{\cap} (g, \mathcal{W})_{\mathcal{K}})^c = (f, \mathcal{L})_{\mathcal{D}}^c \cup (g, \mathcal{W})_{\mathcal{K}}^c$

*Proof.* (1) Let  $(f, \mathcal{L})_{\mathcal{D}}$  and  $(g, \mathcal{W})_{\mathcal{K}}$  be two  $FP^q$  ROFSESs over the universe  $\mathcal{Y}$ ; then, we have

$$\underline{f}_{\mathcal{D}}^c(z) \cap \underline{g}_{\mathcal{K}}^c(z) = (\underline{f}_{\mathcal{D}}(z) \cup \underline{g}_{\mathcal{K}}(z))^c, \tag{21}$$

for all  $z \in \mathcal{D} \cap \mathcal{K}$ . Hence,  $((f, \mathcal{L})_{\mathcal{D}} \cup (g, \mathcal{W})_{\mathcal{K}})^c = (f, \mathcal{L})_{\mathcal{D}}^c \cap (g, \mathcal{W})_{\mathcal{K}}^c$ .

(2) Similar to Part 1.  $\square$

**Definition 12.** Let  $(f, \mathcal{L})_{\mathcal{D}}$  and  $(g, \mathcal{W})_{\mathcal{K}}$  be two  $FP^q$  ROFSESs over the universe  $\mathcal{Y}$ . Then, “ $((f, \mathcal{L})_{\mathcal{D}} \text{AND} (g, \mathcal{W})_{\mathcal{K}})$ ” represented by  $(f, \mathcal{L})_{\mathcal{D}} \wedge (g, \mathcal{W})_{\mathcal{K}} = (\mathfrak{F}, \mathcal{L} \times \mathcal{W})_{\mathcal{R}}$  is an  $FP^q$  ROFSES such that  $\mathcal{R} = \mathcal{D} \times \mathcal{K}$  and is given by

$$\mathfrak{F}_{\mathcal{R}}(\sigma, \delta) = (f_{\mathcal{D}}(\sigma) \cap g_{\mathcal{K}}(\delta)), \quad \forall (\sigma, \delta) \in \mathcal{L} \times \mathcal{W}. \tag{22}$$

**Definition 13.** Let  $(f, \mathcal{L})_{\mathcal{D}}$  and  $(g, \mathcal{W})_{\mathcal{K}}$  be two  $FP^q$  ROFSESs over the universe  $\mathcal{Y}$ . Then, “ $((f, \mathcal{L})_{\mathcal{D}} \text{OR} (g, \mathcal{W})_{\mathcal{K}})$ ” represented by  $(f, \mathcal{L})_{\mathcal{D}} \vee (g, \mathcal{W})_{\mathcal{K}} = (\mathfrak{P}, \mathcal{L} \times \mathcal{W})_{\mathcal{R}}$  is an  $FP^q$  ROFSES such that  $\mathcal{R} = \mathcal{D} \times \mathcal{K}$  and is given as

$$\mathfrak{P}_{\mathcal{R}}(\sigma, \delta) = (f_{\mathcal{D}}(\sigma) \cup g_{\mathcal{K}}(\delta)), \quad \forall (\sigma, \delta) \in \mathcal{L} \times \mathcal{W}. \tag{23}$$

**Proposition 6.** Let  $(f, \mathcal{L})_{\mathcal{D}}$  and  $(g, \mathcal{W})_{\mathcal{K}}$  be  $FP^q$  ROFSESs over the universe  $\mathcal{Y}$ . Then,

- (1)  $((f, \mathcal{L})_{\mathcal{D}} \wedge (g, \mathcal{W})_{\mathcal{K}})^c = (f, \mathcal{L})_{\mathcal{D}}^c \vee (g, \mathcal{W})_{\mathcal{K}}^c$
- (2)  $((f, \mathcal{L})_{\mathcal{D}} \vee (g, \mathcal{W})_{\mathcal{K}})^c = (f, \mathcal{L})_{\mathcal{D}}^c \wedge (g, \mathcal{W})_{\mathcal{K}}^c$

*Proof.* Its proof is directly followed from Proposition 5.  $\square$

### 3. Applications of $FP^q$ ROFSESs in Group Decision-Making

As a powerful extension to the existing fuzzy parameterized models,  $FP^q$  ROFSESs are highly applicable and can prove their efficiency in situations where other models failed. This section provides two MAGDM problems and their solutions under  $FP^q$  ROFSESs along with a developed algorithm.

Before going through the applications, some notions need to be reviewed as follows:

**Definition 14** (see [9]). Let  $\mathcal{Q} = (\alpha_f(z_i)(\eta_j), \beta_f(z_i)(\eta_j))$  be a  $q$ -ROFN. The score function of  $\mathcal{Q}$  is given by

$$s(\mathcal{Q}) = (\alpha_f(z_i)(\eta_j))^q - (\beta_f(z_i)(\eta_j))^q, \quad q \geq 1. \tag{24}$$



*Definition 15* (see [9]). Let  $\mathcal{Q} = (\alpha_f(z_i)(\eta_j), \beta_f(z_i)(\eta_j))$  be a  $q$ -ROFN. The accuracy function of  $\mathcal{Q}$  is given as

$$h(\mathcal{Q}) = (\alpha_f(z_i)(\eta_j))^q + (\beta_f(z_i)(\eta_j))^q, \quad q \geq 1. \quad (25)$$

*Definition 16* (see [9]). Let  $\mathcal{Q}_1 = (\alpha_{f_1}(z_i)(\eta_j), \beta_{f_1}(z_i)(\eta_j))$  and  $\mathcal{Q}_2 = (\alpha_{f_2}(z_i)(\eta_j), \beta_{f_2}(z_i)(\eta_j))$  be any two  $q$ -ROFNs, let  $s(\mathcal{Q}_1)$  and  $s(\mathcal{Q}_2)$  be the score functions of  $\mathcal{Q}_1$  and  $\mathcal{Q}_2$ , and let  $h(\mathcal{Q}_1)$  and  $h(\mathcal{Q}_2)$  be the accuracy functions of  $\mathcal{Q}_1$  and  $\mathcal{Q}_2$ ; then,

- (1) If  $s(\mathcal{Q}_1) > s(\mathcal{Q}_2)$ , then  $\mathcal{Q}_1 > \mathcal{Q}_2$
- (2) If  $s(\mathcal{Q}_1) = s(\mathcal{Q}_2)$ 
  - (i) If  $h(\mathcal{Q}_1) > h(\mathcal{Q}_2)$ , then  $\mathcal{Q}_1 > \mathcal{Q}_2$
  - (ii) If  $h(\mathcal{Q}_1) = h(\mathcal{Q}_2)$ , then  $\mathcal{Q}_1 = \mathcal{Q}_2$

*Definition 17.* For an agree- $FP^q$  ROFSES  $(\mathfrak{f}, \mathcal{X})_{\mathcal{D}}^1$ , its accumulated agree scores  $L_j$  are given as

$$L_j = \sum_i w_i X_{ij}, \quad (26)$$

where  $X_{ij}$ 's are entries of the score table for agree- $FP^q$  ROFSES and  $w_i$  represents weights for the parameters.

*Definition 18.* For a disagree- $FP^q$  ROFSES  $(\mathfrak{f}, \mathcal{X})_{\mathcal{D}}^0$ , its accumulated disagree scores  $C_j$  are given by

$$C_j = \sum_i w_i X_{ij}, \quad (27)$$

where  $X_{ij}$ 's are entries of the score table for disagree- $FP^q$  ROFSES and  $w_i$  represents weights for the parameters.

*Definition 19.* For a  $FP^q$  ROFSES  $(\mathfrak{f}, \mathcal{X})_{\mathcal{D}}$ , its final scores  $\mathfrak{R}_j$  are defined as

$$\mathfrak{R}_j = L_j - C_j. \quad (28)$$

We now present the applications of  $FP^q$  ROFSESs in the following.

### 3.1. Selection of an Appropriate Site for a Cafe Outlet.

Cafes are considered as places where one can meet up with his friends, sit away from home and work, or just simply grab a cup of coffee and let the laziness go away. Cafes are now present all over the world, and those owning these cafes are making huge profits all around. The cafe and restaurant business comprises a large part of the economy and is considered a catchy business to make a career with. Many cafe chains like McDonald's McCafe, Starbucks, Tim Hortons, etc., are well known for their worldwide business and reputation. Similarly, many small cafe chains are also reputable for the quality and services they provide.

The cafe chains keep on earning, growing, expanding, and again earning more. But many factors affect the cafe business, particularly where the cafe outlet is located. If the cafe is in a good place with many customers and less competition, then, it assures a good business if ran professionally. On the other hand, if the cafe is in a place with fewer customers or a high competition place, then, it can prove to be a challenge for the owners to make a good profit from it. In the example below, we are going to see how  $FP^q$  ROFSESs can help in finding the best location for a cafe outlet, so that the business gets profited instead of falling back.

Consider a cafe chain is willing to increase its business by opening a new outlet in the area of the city, where the chain has no prior outlets. To get the best choice, the chain considers experts' opinions in the selection process of an appropriate site for their new outlet. The cafe chain owner has five sites under consideration to extend their chain. Let  $\mathcal{Y} = \{\eta_1, \eta_2, \dots, \eta_5\}$  show the set of sites available. The experts consider  $\mathcal{S} = \{\mathfrak{s}_1, \mathfrak{s}_2, \mathfrak{s}_3\}$  as the set of important parameters for the analysis of the sites, where  $\mathfrak{s}_1$  is the competing cafes within the chosen area,  $\mathfrak{s}_2$  is the fraction of residents who visit one cafe for coffee or tea, and  $\mathfrak{s}_3$  is the cafe's accessibility which includes ample parking. Consider that  $\mathcal{E} = \{e_1, e_2, e_3, e_4\}$  is the set of experts and  $\mathcal{D} = \{(0.5/\mathfrak{s}_1), (0.3/\mathfrak{s}_2), (0.8/\mathfrak{s}_3)\}$  represents the weights for the parameters.

The experts visit and analyze the sites with respect to the indicated parameters and make their findings integrated into an  $FP^q$  ROFSES where  $q = 4$  as shown as follows:

$$\begin{aligned} (\mathfrak{f}, \mathcal{X})_{\mathcal{D}} = & \left\langle \left\langle \left( \frac{0.5}{\mathfrak{s}_1}, e_1, 1 \right) \left\{ \frac{\eta_1}{(0.90, 0.70)}, \frac{\eta_2}{(0.42, 0.38)}, \frac{\eta_3}{(0.11, 0.61)}, \frac{\eta_4}{(0.80, 0.70)}, \frac{\eta_5}{(0.58, 0.47)} \right\} \right\rangle, \right. \\ & \left\langle \left( \frac{0.3}{\mathfrak{s}_2}, e_1, 1 \right) \left\{ \frac{\eta_1}{(0.24, 0.39)}, \frac{\eta_2}{(0.19, 0.28)}, \frac{\eta_3}{(0.43, 0.16)}, \frac{\eta_4}{(0.53, 0.37)}, \frac{\eta_5}{(0.69, 0.36)} \right\} \right\rangle, \\ & \left\langle \left( \frac{0.8}{\mathfrak{s}_3}, e_1, 1 \right) \left\{ \frac{\eta_1}{(0.29, 0.37)}, \frac{\eta_2}{(0.89, 0.70)}, \frac{\eta_3}{(0.83, 0.20)}, \frac{\eta_4}{(0.14, 0.25)}, \frac{\eta_5}{(0.39, 0.75)} \right\} \right\rangle, \\ & \left. \left\langle \left( \frac{0.5}{\mathfrak{s}_1}, e_2, 1 \right) \left\{ \frac{\eta_1}{(0.51, 0.75)}, \frac{\eta_2}{(0.45, 0.65)}, \frac{\eta_3}{(0.12, 0.78)}, \frac{\eta_4}{(0.56, 0.72)}, \frac{\eta_5}{(0.90, 0.43)} \right\} \right\rangle, \right. \end{aligned}$$

$$\begin{aligned}
& \left\langle \left( \frac{0.3}{\mathfrak{s}_2}, e_2, 1 \right) \left\{ \frac{\eta_1}{(0.27, 0.45)}, \frac{\eta_2}{(0.21, 0.27)}, \frac{\eta_3}{(0.25, 0.27)}, \frac{\eta_4}{(0.69, 0.15)}, \frac{\eta_5}{(0.34, 0.13)} \right\} \right\rangle, \\
& \left\langle \left( \frac{0.8}{\mathfrak{s}_3}, e_2, 1 \right) \left\{ \frac{\eta_1}{(0.44, 0.81)}, \frac{\eta_2}{(0.45, 0.65)}, \frac{\eta_3}{(0.32, 0.41)}, \frac{\eta_4}{(0.29, 0.23)}, \frac{\eta_5}{(0.88, 0.34)} \right\} \right\rangle, \\
& \left\langle \left( \frac{0.5}{\mathfrak{s}_1}, e_3, 1 \right) \left\{ \frac{\eta_1}{(0.47, 0.62)}, \frac{\eta_2}{(0.32, 0.34)}, \frac{\eta_3}{(0.40, 0.36)}, \frac{\eta_4}{(0.28, 0.42)}, \frac{\eta_5}{(0.46, 0.16)} \right\} \right\rangle, \\
& \left\langle \left( \frac{0.3}{\mathfrak{s}_2}, e_3, 1 \right) \left\{ \frac{\eta_1}{(0.60, 0.80)}, \frac{\eta_2}{(0.24, 0.47)}, \frac{\eta_3}{(0.59, 0.37)}, \frac{\eta_4}{(0.11, 0.27)}, \frac{\eta_5}{(0.64, 0.20)} \right\} \right\rangle, \\
& \left\langle \left( \frac{0.8}{\mathfrak{s}_3}, e_3, 1 \right) \left\{ \frac{\eta_1}{(0.81, 0.52)}, \frac{\eta_2}{(0.56, 0.46)}, \frac{\eta_3}{(0.22, 0.65)}, \frac{\eta_4}{(0.92, 0.34)}, \frac{\eta_5}{(0.37, 0.56)} \right\} \right\rangle, \\
& \left\langle \left( \frac{0.5}{\mathfrak{s}_1}, e_4, 1 \right) \left\{ \frac{\eta_1}{(0.72, 0.44)}, \frac{\eta_2}{(0.56, 0.65)}, \frac{\eta_3}{(0.63, 0.36)}, \frac{\eta_4}{(0.43, 0.51)}, \frac{\eta_5}{(0.30, 0.80)} \right\} \right\rangle, \\
& \left\langle \left( \frac{0.3}{\mathfrak{s}_2}, e_4, 1 \right) \left\{ \frac{\eta_1}{(0.66, 0.36)}, \frac{\eta_2}{(0.44, 0.72)}, \frac{\eta_3}{(0.48, 0.52)}, \frac{\eta_4}{(0.45, 0.56)}, \frac{\eta_5}{(0.51, 0.42)} \right\} \right\rangle, \\
& \left\langle \left( \frac{0.8}{\mathfrak{s}_3}, e_4, 1 \right) \left\{ \frac{\eta_1}{(0.87, 0.45)}, \frac{\eta_2}{(0.62, 0.42)}, \frac{\eta_3}{(0.77, 0.63)}, \frac{\eta_4}{(0.30, 0.14)}, \frac{\eta_5}{(0.70, 0.21)} \right\} \right\rangle, \\
& \left\langle \left( \frac{0.5}{\mathfrak{s}_1}, e_1, 0 \right) \left\{ \frac{\eta_1}{(0.79, 0.50)}, \frac{\eta_2}{(0.81, 0.27)}, \frac{\eta_3}{(0.84, 0.50)}, \frac{\eta_4}{(0.86, 0.40)}, \frac{\eta_5}{(0.15, 0.22)} \right\} \right\rangle, \\
& \left\langle \left( \frac{0.3}{\mathfrak{s}_2}, e_1, 0 \right) \left\{ \frac{\eta_1}{(0.15, 0.22)}, \frac{\eta_2}{(0.17, 0.25)}, \frac{\eta_3}{(0.19, 0.22)}, \frac{\eta_4}{(0.17, 0.21)}, \frac{\eta_5}{(0.11, 0.24)} \right\} \right\rangle, \\
& \left\langle \left( \frac{0.8}{\mathfrak{s}_3}, e_1, 0 \right) \left\{ \frac{\eta_1}{(0.31, 0.42)}, \frac{\eta_2}{(0.12, 0.24)}, \frac{\eta_3}{(0.11, 0.23)}, \frac{\eta_4}{(0.10, 0.22)}, \frac{\eta_5}{(0.34, 0.46)} \right\} \right\rangle, \\
& \left\langle \left( \frac{0.5}{\mathfrak{s}_1}, e_2, 0 \right) \left\{ \frac{\eta_1}{(0.37, 0.39)}, \frac{\eta_2}{(0.18, 0.70)}, \frac{\eta_3}{(0.13, 0.25)}, \frac{\eta_4}{(0.38, 0.45)}, \frac{\eta_5}{(0.35, 0.45)} \right\} \right\rangle, \\
& \left\langle \left( \frac{0.3}{\mathfrak{s}_2}, e_2, 0 \right) \left\{ \frac{\eta_1}{(0.34, 0.40)}, \frac{\eta_2}{(0.39, 0.29)}, \frac{\eta_3}{(0.38, 0.27)}, \frac{\eta_4}{(0.15, 0.20)}, \frac{\eta_5}{(0.51, 0.36)} \right\} \right\rangle, \\
& \left\langle \left( \frac{0.8}{\mathfrak{s}_3}, e_2, 0 \right) \left\{ \frac{\eta_1}{(0.54, 0.22)}, \frac{\eta_2}{(0.13, 0.37)}, \frac{\eta_3}{(0.55, 0.15)}, \frac{\eta_4}{(0.62, 0.10)}, \frac{\eta_5}{(0.45, 0.16)} \right\} \right\rangle, \\
& \left\langle \left( \frac{0.5}{\mathfrak{s}_1}, e_3, 0 \right) \left\{ \frac{\eta_1}{(0.63, 0.45)}, \frac{\eta_2}{(0.39, 0.10)}, \frac{\eta_3}{(0.64, 0.19)}, \frac{\eta_4}{(0.63, 0.15)}, \frac{\eta_5}{(0.62, 0.17)} \right\} \right\rangle, \\
& \left\langle \left( \frac{0.3}{\mathfrak{s}_2}, e_3, 0 \right) \left\{ \frac{\eta_1}{(0.69, 0.21)}, \frac{\eta_2}{(0.71, 0.17)}, \frac{\eta_3}{(0.72, 0.32)}, \frac{\eta_4}{(0.73, 0.25)}, \frac{\eta_5}{(0.12, 0.30)} \right\} \right\rangle, \\
& \left\langle \left( \frac{0.8}{\mathfrak{s}_3}, e_3, 0 \right) \left\{ \frac{\eta_1}{(0.40, 0.36)}, \frac{\eta_2}{(0.29, 0.23)}, \frac{\eta_3}{(0.12, 0.28)}, \frac{\eta_4}{(0.45, 0.65)}, \frac{\eta_5}{(0.36, 0.55)} \right\} \right\rangle, \\
& \left\langle \left( \frac{0.5}{\mathfrak{s}_1}, e_4, 0 \right) \left\{ \frac{\eta_1}{(0.29, 0.37)}, \frac{\eta_2}{(0.81, 0.75)}, \frac{\eta_3}{(0.27, 0.43)}, \frac{\eta_4}{(0.47, 0.62)}, \frac{\eta_5}{(0.81, 0.52)} \right\} \right\rangle,
\end{aligned}$$

$$\left\langle \left\langle \left( \frac{0.3}{\mathfrak{s}_2}, e_4, 0 \right) \left\{ \frac{\eta_1}{(0.43, 0.16)}, \frac{\eta_2}{(0.83, 0.70)}, \frac{\eta_3}{(0.21, 0.27)}, \frac{\eta_4}{(0.40, 0.36)}, \frac{\eta_5}{(0.59, 0.37)} \right\} \right\rangle, \right. \\ \left. \left\langle \left( \frac{0.8}{\mathfrak{s}_3}, e_4, 0 \right) \left\{ \frac{\eta_1}{(0.32, 0.41)}, \frac{\eta_2}{(0.24, 0.47)}, \frac{\eta_3}{(0.27, 0.25)}, \frac{\eta_4}{(0.89, 0.60)}, \frac{\eta_5}{(0.92, 0.34)} \right\} \right\rangle \right\}. \tag{29}$$

For the selection of the best site based on the above data, the experts analyze the data under the decision-making method based on  $FP^q$  ROFSEs as given in Algorithm 1.

Table 1 represents the score table for the  $FP^4$  ROFSEs defined above. Tables 2 and 3 represent the score tables for agree- and disagree- $FP^4$  ROFSEs, respectively, along with the agree and disagree accumulated scores.

Using agree and disagree accumulated scores in Tables 2 and 3, Table 4 provides the final scores. From the final scores table, it can be seen that  $\mathfrak{R}_M = \max(\mathfrak{R}_j) = \mathfrak{R}_1$ ; hence, the site  $\eta_1$  is decided to be the most suitable site for the opening of a new cafe outlet.

To better understand Algorithm 1, its flowchart diagram is shown in Figure 2.

Now, we present the next application of  $FP^q$  ROFSEs.

**3.2. Selection of Best News Channel.** News channels and journalists all over the world keep us updated about the events in the world, the changes in policies, the crisis coverage, and a lot more. The main purposes, including informing, guiding, educating, and entertaining the audience, interpreting the news and facts, causing awareness for social issues, and forming value opinions about the policies and situations, etc., make these news channels and journalism a very important part of the society. With the advancements in technology, many changes have come to journalism too. First, we were informed with news in black and white and then came the radio tech and then the TV

networks, and now, the online services allow the availability of news in any place at any instant.

Although all the news channels try their best to keep their audience best updated and entertained, many factors like biased opinions, forced news, low quality, lack of factual material, and so on, can affect the quality of a news channel to a huge extent. For this, every year, many organizations (like AVTA, RTS, CNA, and CRN) award the channels by critical analysis of the channels in their respective domains, which helps to find the credibility of a news channel effectively. In this example, we model a problem where an award of “Best News Channel” is to be awarded on the basis of various criteria.

Consider that an organization announces an event for the award of “Best News Channel,” for which eight high-rated news channels are nominated. The nominated channels are presented in the set  $\mathcal{Y} = \{\eta_1, \eta_2, \dots, \eta_8\}$ . For the analysis of the channels, a committee of three experts as in the set  $\mathcal{E} = \{e_1, e_2, e_3\}$  is considered by the organization. These experts choose a favorable set of parameters given as  $\mathcal{S} = \{\mathfrak{s}_1, \mathfrak{s}_2, \mathfrak{s}_3, \mathfrak{s}_4, \mathfrak{s}_5\}$  for the judgments, where  $\mathfrak{s}_i$  ( $i = 1, 2, 3, 4, 5$ ) stand for “effective social awareness,” “quality entertainment,” “unbiased quality opinions,” “factual information,” and “quality guidance and education.” The weights assigned to the parameters by the experts are  $\mathcal{D} = \{(0.6/\mathfrak{s}_1), (0.2/\mathfrak{s}_2), (0.9/\mathfrak{s}_3), (0.7/\mathfrak{s}_4), (0.3/\mathfrak{s}_5)\}$ . After critically analyzing the channels, the committee provides the data, which is represented by an  $FP^q$  ROFSES  $(\mathfrak{f}, \mathcal{X})_{\mathcal{D}}$  with  $q = 5$  as follows:

$$(\mathfrak{f}, \mathcal{X})_{\mathcal{D}} = \left\{ \left\langle \left( \frac{0.6}{\mathfrak{s}_1}, e_1, 1 \right) \left\{ \frac{\eta_1}{(0.79, 0.91)}, \frac{\eta_2}{(0.58, 0.26)}, \frac{\eta_3}{(0.53, 0.48)}, \frac{\eta_4}{(0.85, 0.23)}, \frac{\eta_5}{(0.19, 0.37)}, \frac{\eta_6}{(0.49, 0.39)}, \frac{\eta_7}{(0.62, 0.87)}, \frac{\eta_8}{(0.13, 0.86)} \right\} \right\rangle, \right. \\ \left\langle \left( \frac{0.2}{\mathfrak{s}_2}, e_1, 1 \right) \left\{ \frac{\eta_1}{(0.17, 0.28)}, \frac{\eta_2}{(0.96, 0.36)}, \frac{\eta_3}{(0.17, 0.48)}, \frac{\eta_4}{(0.89, 0.13)}, \frac{\eta_5}{(0.25, 0.28)}, \frac{\eta_6}{(0.59, 0.49)}, \frac{\eta_7}{(0.81, 0.75)}, \frac{\eta_8}{(0.34, 0.13)} \right\} \right\rangle, \\ \left\langle \left( \frac{0.9}{\mathfrak{s}_3}, e_1, 1 \right) \left\{ \frac{\eta_1}{(0.25, 0.61)}, \frac{\eta_2}{(0.64, 0.88)}, \frac{\eta_3}{(0.85, 0.67)}, \frac{\eta_4}{(0.49, 0.20)}, \frac{\eta_5}{(0.41, 0.35)}, \frac{\eta_6}{(0.79, 0.69)}, \frac{\eta_7}{(0.65, 0.24)}, \frac{\eta_8}{(0.57, 0.12)} \right\} \right\rangle, \\ \left. \left\langle \left( \frac{0.7}{\mathfrak{s}_4}, e_1, 1 \right) \left\{ \frac{\eta_1}{(0.32, 0.31)}, \frac{\eta_2}{(0.73, 0.55)}, \frac{\eta_3}{(0.60, 0.75)}, \frac{\eta_4}{(0.26, 0.56)}, \frac{\eta_5}{(0.19, 0.90)}, \frac{\eta_6}{(0.28, 0.16)}, \frac{\eta_7}{(0.31, 0.54)}, \frac{\eta_8}{(0.39, 0.23)} \right\} \right\rangle \right\},$$

- (1) **Input**  
 $\mathcal{Y}$ , a universal set,  
 $\mathcal{S}$ , a universe of parameters,  
 $\mathcal{E}$ , a set of experts,  
 $\mathcal{D}$ , a set of weights for parameters,  
 $\mathcal{O}$ , a set of opinions,  
 $(\mathfrak{f}, \mathcal{X})_{\mathcal{D}}$ , an  $FP^q$  ROFSES.
- (2) Find the table of scores with entries  $X_{ij}$  by Definition 14.  
(3) Find the table of scores for agree- $FP^q$  ROFSES.  
(4) Find the table of scores for disagree- $FP^q$  ROFSES.  
(5) Input the accumulated agree scores  $L_j = \sum_i w_i X_{ij}$  in the last row of the score table of agree- $FP^q$  ROFSES.  
(6) Input the accumulated disagree scores  $C_j = \sum_i w_i X_{ij}$  in the last row of the score table of disagree- $FP^q$  ROFSES.  
(7) Find the values of final scores  $\mathfrak{R}_j = L_j - C_j$ .  
(8) Find  $m$ , for which  $\mathfrak{R}_m = \max \mathfrak{R}_j$ .  
(9) **Output**  
In step (8), the object  $\mathfrak{y}_m$  having maximum final score will be the most suitable choice. If there exist two or more objects with maximum final scores, then anyone can be chosen as a decision.

ALGORITHM 1: Decision-making method based on  $FP^q$  ROFSESs.

TABLE 1: Score table for  $FP^4$  ROFSES  $(\mathfrak{f}, \mathcal{X})_{\mathcal{D}}$ .

$\mathfrak{y}$	$\mathfrak{y}_1$	$\mathfrak{y}_2$	$\mathfrak{y}_3$	$\mathfrak{y}_4$	$\mathfrak{y}_5$
$((0.5/\mathfrak{s}_1), e_1, 1)$	0.4160	0.0103	-0.1383	0.1695	0.0644
$((0.3/\mathfrak{s}_2), e_1, 1)$	-0.0198	-0.0048	0.0335	0.0602	0.2099
$((0.8/\mathfrak{s}_3), e_1, 1)$	-0.0117	0.3873	0.4730	-0.0035	-0.2933
$((0.5/\mathfrak{s}_1), e_2, 1)$	-0.2488	-0.1375	-0.3699	-0.1704	0.6219
$((0.3/\mathfrak{s}_2), e_2, 1)$	-0.0357	-0.0034	-0.0014	0.2262	0.0131
$((0.8/\mathfrak{s}_3), e_2, 1)$	-0.3930	-0.1375	-0.0178	0.0043	0.5863
$((0.5/\mathfrak{s}_1), e_3, 1)$	-0.0990	-0.0029	0.0088	-0.0250	0.0441
$((0.3/\mathfrak{s}_2), e_3, 1)$	-0.2800	-0.0455	0.1024	-0.0052	0.1662
$((0.8/\mathfrak{s}_3), e_3, 1)$	0.3574	0.0536	-0.1762	0.7030	-0.0796
$((0.5/\mathfrak{s}_1), e_4, 1)$	0.2313	-0.0802	0.1407	-0.0335	-0.4015
$((0.3/\mathfrak{s}_2), e_4, 1)$	0.1730	-0.2313	-0.0200	-0.0573	0.0365
$((0.8/\mathfrak{s}_3), e_4, 1)$	0.5319	0.1166	0.1940	0.0077	0.2382
$((0.5/\mathfrak{s}_1), e_4, 0)$	0.3270	0.4252	0.4354	0.5214	-0.0018
$((0.3/\mathfrak{s}_2), e_1, 0)$	-0.0018	-0.0031	-0.0010	-0.0011	-0.0032
$((0.8/\mathfrak{s}_3), e_1, 0)$	-0.0219	-0.0031	-0.0027	-0.0022	-0.0314
$((0.5/\mathfrak{s}_1), e_2, 0)$	-0.0044	-0.2391	-0.0036	-0.0202	-0.0260
$((0.3/\mathfrak{s}_2), e_2, 0)$	-0.0122	0.0161	0.0155	-0.0011	0.0509
$((0.8/\mathfrak{s}_3), e_2, 0)$	0.0827	-0.0185	0.0910	0.1477	0.0404
$((0.5/\mathfrak{s}_1), e_3, 0)$	0.1165	0.0230	0.1665	0.1570	0.1469
$((0.3/\mathfrak{s}_2), e_3, 0)$	0.2247	0.2533	0.2583	0.2801	-0.0079
$((0.8/\mathfrak{s}_3), e_3, 0)$	0.0088	0.0043	-0.0059	-0.1375	-0.0747
$((0.5/\mathfrak{s}_1), e_4, 0)$	-0.0117	0.1141	-0.0289	-0.0990	0.3574
$((0.3/\mathfrak{s}_2), e_4, 0)$	0.0335	0.2345	-0.0034	0.0088	0.1024
$((0.8/\mathfrak{s}_3), e_4, 0)$	-0.0178	-0.0455	0.0014	0.4978	0.7030

TABLE 2: Accumulated score table for agree-FP<sup>4</sup> ROFSES (f, Z)<sub>D</sub><sup>1</sup>.

$\mathcal{Y}$	$\eta_1$	$\eta_2$	$\eta_3$	$\eta_4$	$\eta_5$
$((0.5/\mathfrak{s}_1), e_1, 1)$	0.4160	0.0103	-0.1383	0.1695	0.0644
$((0.3/\mathfrak{s}_2), e_1, 1)$	-0.0198	-0.0048	0.0335	0.0602	0.2099
$((0.8/\mathfrak{s}_3), e_1, 1)$	-0.0117	0.3873	0.4730	-0.0035	-0.2933
$((0.5/\mathfrak{s}_1), e_2, 1)$	-0.2488	-0.1375	-0.3699	-0.1704	0.6219
$((0.3/\mathfrak{s}_2), e_2, 1)$	-0.0357	-0.0034	-0.0014	0.2262	0.0131
$((0.8/\mathfrak{s}_3), e_2, 1)$	-0.3930	-0.1375	-0.0178	0.0043	0.5863
$((0.5/\mathfrak{s}_1), e_3, 1)$	-0.0990	-0.0029	0.0088	-0.0250	0.0441
$((0.3/\mathfrak{s}_2), e_3, 1)$	-0.2800	-0.0455	0.1024	-0.0052	0.1662
$((0.8/\mathfrak{s}_3), e_3, 1)$	0.3574	0.0536	-0.1762	0.7030	-0.0796
$((0.5/\mathfrak{s}_1), e_4, 1)$	0.2313	-0.0802	0.1407	-0.0335	-0.4015
$((0.3/\mathfrak{s}_2), e_4, 1)$	0.1730	-0.2313	-0.0200	-0.0573	0.0365
$((0.8/\mathfrak{s}_3), e_4, 1)$	0.5319	0.1166	0.1940	0.0077	0.2382
$L_j = \sum_i w_i X_{ij}$	$L_1 = 0.4887$	$L_2 = 0.1454$	$L_3 = 0.2334$	$L_4 = 0.6067$	$L_5 = 0.6534$

TABLE 3: Accumulated score table for disagree-FP<sup>4</sup> ROFSES (f, Z)<sub>D</sub><sup>0</sup>.

$\mathcal{Y}$	$\eta_1$	$\eta_2$	$\eta_3$	$\eta_4$	$\eta_5$
$((0.5/\mathfrak{s}_1), e_1, 0)$	0.3270	0.4252	0.4354	0.5214	-0.0018
$((0.3/\mathfrak{s}_2), e_1, 0)$	-0.0018	-0.0031	-0.0010	-0.0011	-0.0032
$((0.8/\mathfrak{s}_3), e_1, 0)$	-0.0219	-0.0031	-0.0027	-0.0022	-0.0314
$((0.5/\mathfrak{s}_1), e_2, 0)$	-0.0044	-0.2391	-0.0036	-0.0202	-0.0260
$((0.3/\mathfrak{s}_2), e_2, 0)$	-0.0122	0.0161	0.0155	-0.0011	0.0509
$((0.8/\mathfrak{s}_3), e_2, 0)$	0.0827	-0.0185	0.0910	0.1477	0.0404
$((0.5/\mathfrak{s}_1), e_3, 0)$	0.1165	0.0230	0.1665	0.1570	0.1469
$((0.3/\mathfrak{s}_2), e_3, 0)$	0.2247	0.2533	0.2583	0.2801	-0.0079
$((0.8/\mathfrak{s}_3), e_3, 0)$	0.0088	0.0043	-0.0059	-0.1375	-0.0747
$((0.5/\mathfrak{s}_1), e_4, 0)$	-0.0117	0.1141	-0.0289	-0.0990	0.3574
$((0.3/\mathfrak{s}_2), e_4, 0)$	0.0335	0.2345	-0.0034	0.0088	0.1024
$((0.8/\mathfrak{s}_3), e_4, 0)$	-0.0178	-0.0455	0.0014	0.4978	0.7030
$C_j = \sum_i w_i X_{ij}$	$C_1 = 0.3285$	$C_2 = 0.2616$	$C_3 = 0.4325$	$C_4 = 0.7703$	$C_5 = 0.7907$

TABLE 4: Final scores.

$L_j$	$C_j$	$\mathfrak{R}_j = L_j - C_j$
$L_1 = 0.4887$	$C_1 = 0.3285$	$\mathfrak{R}_1 = 0.1603$
$L_2 = 0.1454$	$C_2 = 0.2616$	$\mathfrak{R}_2 = -0.1162$
$L_3 = 0.2334$	$C_3 = 0.4325$	$\mathfrak{R}_3 = -0.1991$
$L_4 = 0.6067$	$C_4 = 0.7703$	$\mathfrak{R}_4 = -0.1636$
$L_5 = 0.6534$	$C_5 = 0.7909$	$\mathfrak{R}_5 = -0.1373$

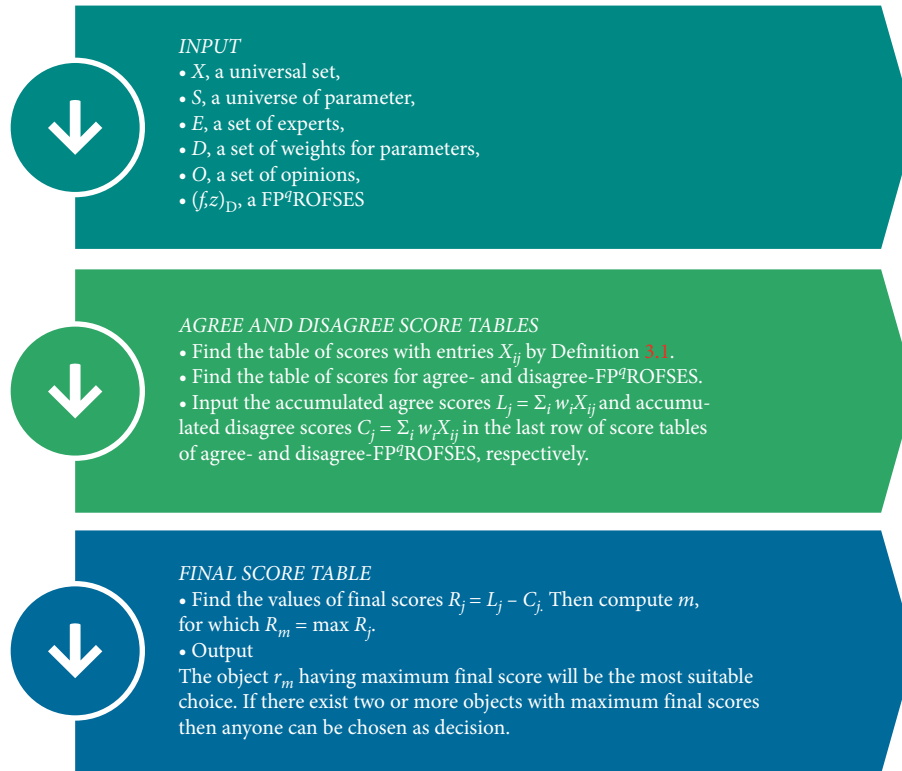


FIGURE 2: Flowchart diagram.

TABLE 5: Score table for  $FP^5$  ROFSSES  $(f, \mathcal{L})_{\mathcal{D}}$ .

$\mathcal{Y}$	$\eta_1$	$\eta_2$	$\eta_3$	$\eta_4$	$\eta_5$	$\eta_6$	$\eta_7$	$\eta_8$
$((0.6/\mathfrak{s}_1), e_1, 1)$	-0.3163	0.0644	0.0163	0.4431	-0.0067	0.0192	-0.2571	-0.4704
$((0.2/\mathfrak{s}_2), e_1, 1)$	-0.0016	0.8093	-0.0253	0.5584	-0.0007	0.0432	0.1114	0.0045
$((0.9/\mathfrak{s}_3), e_1, 1)$	-0.0835	-0.4204	0.3087	0.0279	0.0063	0.1513	0.1152	0.0601
$((0.7/\mathfrak{s}_4), e_1, 1)$	0.0005	0.1570	-0.1595	-0.0539	-0.5902	0.0016	-0.0431	0.0084
$((0.3/\mathfrak{s}_5), e_1, 1)$	0.0345	0.5515	0.0041	-0.1720	0.0070	-0.2203	0.0085	0.0019
$((0.6/\mathfrak{s}_1), e_2, 1)$	-0.1368	0.0082	-0.0049	-0.2028	-0.0133	0.0045	0.2499	-0.0687
$((0.2/\mathfrak{s}_2), e_2, 1)$	0.0051	-0.0015	0.4806	0.0976	0.0010	0.3322	0.0012	0.0221
$((0.9/\mathfrak{s}_3), e_2, 1)$	0.0844	0.0146	0.3925	0.2887	-0.0005	0.0014	0.3342	-0.0014
$((0.7/\mathfrak{s}_4), e_2, 1)$	-0.5803	0.0427	0.1504	-0.2283	0.5758	0.0714	-0.0668	0.0205
$((0.3/\mathfrak{s}_5), e_2, 1)$	0.1071	-0.0481	0.3107	0.0345	-0.1155	0.7294	-0.0012	-0.0010
$((0.6/\mathfrak{s}_1), e_3, 1)$	-0.0701	-0.0198	0.1770	0.0087	0.0210	0.3017	-0.0104	0.1192
$((0.2/\mathfrak{s}_2), e_3, 1)$	0.0312	0.2964	0.5127	0.1677	0.3277	0.0021	0.0309	-0.1578
$((0.9/\mathfrak{s}_3), e_3, 1)$	0.0003	0.1804	-0.0116	0.3483	0.1771	0.2642	0.3276	0.0102
$((0.7/\mathfrak{s}_4), e_3, 1)$	-0.1770	0.4800	0.0785	-0.0536	0.1714	0.0610	0.3253	0.0175
$((0.3/\mathfrak{s}_5), e_3, 1)$	-0.0014	0.0051	0.0932	-0.1683	0.0426	0.0214	0.0366	0.0125
$((0.6/\mathfrak{s}_1), e_1, 0)$	0.0024	0.5904	0.1596	0.1578	0.3253	0.0312	0.0844	0.0753
$((0.2/\mathfrak{s}_2), e_1, 0)$	0.5437	0.1525	-0.6498	-0.0584	0.2373	0.1681	0.1268	0.7337
$((0.9/\mathfrak{s}_3), e_1, 0)$	0.2964	0.0001	0.0003	0.0260	0.0144	-0.1222	0.1823	0.2765
$((0.7/\mathfrak{s}_4), e_1, 0)$	0.0004	0.0008	0.0020	0.0005	0.0021	0.0132	0.0065	0.0454
$((0.7/\mathfrak{s}_5), e_1, 0)$	0.1578	0.0465	-0.0768	0.0708	0.1516	-0.5303	0.1833	0.3484
$((0.3/\mathfrak{s}_1), e_2, 0)$	0.0008	0.0028	0.0102	0.0161	0.1679	0.0057	0.0002	0.0028
$((0.6/\mathfrak{s}_2), e_2, 0)$	0.5881	0.0024	0.0028	0.1601	0.0226	0.0841	0.1595	0.3870
$((0.2/\mathfrak{s}_3), e_2, 0)$	0.0012	0.0011	0.0008	0.0008	0.5901	-0.0009	0.0070	0.0266
$((0.9/\mathfrak{s}_4), e_2, 0)$	0.0309	0.0005	0.0001	0.0184	0.0243	0.2413	0.1634	0.4588
$((0.7/\mathfrak{s}_5), e_2, 0)$	0.0003	0.0009	-0.0005	-0.1677	0.0105	0.0156	0.0001	0.3472
$((0.3/\mathfrak{s}_1), e_3, 0)$	0.0916	0.0144	0.0184	0.1071	0.1560	0.1803	0.0992	0.0808
$((0.6/\mathfrak{s}_2), e_3, 0)$	0.0844	0.0183	0.0028	0.0503	0.0045	0.0045	0.0089	0.0915
$((0.2/\mathfrak{s}_3), e_3, 0)$	0.1901	0.2063	0.1368	0.0015	0.3936	0.0517	0.0714	0.2842
$((0.9/\mathfrak{s}_4), e_3, 0)$	0.0082	0.4806	-0.2887	0.0005	0.0014	0.0205	0.1071	-0.0481
$((0.7/\mathfrak{s}_5), e_3, 0)$	0.0427	0.0349	0.3936	0.0976	0.0133	-0.0045	-0.0505	0.3107

TABLE 6: Accumulated score table for agree-FP<sup>5</sup> ROFSES ( $\mathfrak{f}, \mathcal{F}$ )<sub>9</sub><sup>1</sup>.

$\mathcal{Y}$	$\eta_1$	$\eta_2$	$\eta_3$	$\eta_4$	$\eta_5$	$\eta_6$	$\eta_7$	$\eta_8$
$((0.6/\mathfrak{s}_1), e_1, 1)$	-0.3163	0.0644	0.0163	0.4431	-0.0067	0.0192	-0.2571	-0.4704
$((0.2/\mathfrak{s}_2), e_1, 1)$	-0.0016	0.8093	-0.0253	0.5584	-0.0007	0.0432	0.1114	0.0045
$((0.9/\mathfrak{s}_3), e_1, 1)$	-0.0835	-0.4204	0.3087	0.0279	0.0063	0.1513	0.1152	0.0601
$((0.7/\mathfrak{s}_4), e_1, 1)$	0.0005	0.1570	-0.1595	-0.0539	-0.5902	0.0016	-0.0431	0.0084
$((0.3/\mathfrak{s}_5), e_1, 1)$	0.0345	0.5515	0.0041	-0.1720	0.0070	-0.2203	0.0085	0.0019
$((0.6/\mathfrak{s}_1), e_2, 1)$	-0.1368	0.0082	-0.0049	-0.2028	-0.0133	0.0045	0.2499	-0.0687
$((0.2/\mathfrak{s}_2), e_2, 1)$	0.0051	-0.0015	0.4806	0.0976	0.0010	0.3322	0.0012	0.0221
$((0.9/\mathfrak{s}_3), e_2, 1)$	0.0844	0.0146	0.3925	0.2887	-0.0005	0.0014	0.3342	-0.0014
$((0.7/\mathfrak{s}_4), e_2, 1)$	-0.5803	0.0427	0.1504	-0.2283	0.5758	0.0714	-0.0668	0.0205
$((0.3/\mathfrak{s}_5), e_2, 1)$	0.1071	-0.0481	0.3107	0.0345	-0.1155	0.7294	-0.0012	-0.0010
$((0.6/\mathfrak{s}_1), e_3, 1)$	-0.0701	-0.0198	0.1770	0.0087	0.0210	0.3017	-0.0104	0.1192
$((0.2/\mathfrak{s}_2), e_3, 1)$	0.0312	0.2964	0.5127	0.1677	0.3277	0.0021	0.0309	-0.1578
$((0.9/\mathfrak{s}_3), e_3, 1)$	0.0003	0.1804	-0.0116	0.3483	0.1771	0.2642	0.3276	0.0102
$((0.7/\mathfrak{s}_4), e_3, 1)$	-0.1770	0.4800	0.0785	-0.0536	0.1714	0.0610	0.3253	0.0175
$((0.3/\mathfrak{s}_5), e_3, 1)$	-0.0014	0.0051	0.0932	-0.1683	0.0426	0.0214	0.0366	0.0125
$L_j = \sum_i w_i X_{ij}$	-0.7936	0.6780	1.0982	0.5857	0.3210	0.8989	0.8814	-0.1797

TABLE 7: Accumulated score table for disagree-FP<sup>5</sup> ROFSES ( $\mathfrak{f}, \mathcal{F}$ )<sub>9</sub><sup>0</sup>.

$\mathcal{Y}$	$\eta_1$	$\eta_2$	$\eta_3$	$\eta_4$	$\eta_5$	$\eta_6$	$\eta_7$	$\eta_8$
$((0.6/\mathfrak{s}_1), e_1, 0)$	0.0024	0.5904	0.1596	0.1578	0.3253	0.0312	0.0844	0.0753
$((0.2/\mathfrak{s}_2), e_1, 0)$	0.5437	0.1525	-0.6498	-0.0584	0.2373	0.1681	0.1268	0.7337
$((0.9/\mathfrak{s}_3), e_1, 0)$	0.2964	0.0001	0.0003	0.0260	0.0144	-0.1222	0.1823	0.2765
$((0.7/\mathfrak{s}_4), e_1, 0)$	0.0004	0.0008	0.0020	0.0005	0.0021	0.0132	0.0065	0.0454
$((0.7/\mathfrak{s}_5), e_1, 0)$	0.1578	0.0465	-0.0768	0.0708	0.1516	-0.5303	0.1833	0.3484
$((0.3/\mathfrak{s}_1), e_2, 0)$	0.0008	0.0028	0.0102	0.0161	0.1679	0.0057	0.0002	0.0028
$((0.6/\mathfrak{s}_2), e_2, 0)$	0.5881	0.0024	0.0028	0.1601	0.0226	0.0841	0.1595	0.3870
$((0.2/\mathfrak{s}_3), e_2, 0)$	0.0012	0.0011	0.0008	0.0008	0.5901	-0.0009	0.0070	0.0266
$((0.9/\mathfrak{s}_4), e_2, 0)$	0.0309	0.0005	0.0001	0.0184	0.0243	0.2413	0.1634	0.4588
$((0.7/\mathfrak{s}_5), e_2, 0)$	0.0003	0.0009	-0.0005	-0.1677	0.0105	0.0156	0.0001	0.3472
$((0.3/\mathfrak{s}_1), e_3, 0)$	0.0916	0.0144	0.0184	0.1071	0.1560	0.1803	0.0992	0.0808
$((0.6/\mathfrak{s}_2), e_3, 0)$	0.0844	0.0183	0.0028	0.0503	0.0045	0.0045	0.0089	0.0915
$((0.2/\mathfrak{s}_3), e_3, 0)$	0.1901	0.2063	0.1368	0.0015	0.3936	0.0517	0.0714	0.2842
$((0.9/\mathfrak{s}_4), e_3, 0)$	0.0082	0.4806	-0.2887	0.0005	0.0014	0.0205	0.1071	-0.0481
$((0.7/\mathfrak{s}_5), e_3, 0)$	0.0427	0.0349	0.3936	0.0976	0.0133	-0.0045	-0.0505	0.3107
$C_j = \sum_i w_i X_{ij}$	0.8271	0.9480	0.0026	0.2382	1.4126	0.1542	0.6377	1.4874

TABLE 8: Final scores.

$L_j$	$C_j$	$\mathfrak{R}_j = L_j - C_j$
$L_1 = -0.7936$	$C_1 = 0.8271$	$\mathfrak{R}_1 = -1.6206$
$L_2 = 0.6780$	$C_2 = 0.9480$	$\mathfrak{R}_2 = -0.2700$
$L_3 = 1.0982$	$C_3 = 0.0026$	$\mathfrak{R}_3 = 1.0957$
$L_4 = 0.5857$	$C_4 = 0.2382$	$\mathfrak{R}_4 = 0.3475$
$L_5 = 0.3210$	$C_5 = 1.4126$	$\mathfrak{R}_5 = -1.0917$
$L_6 = 0.8989$	$C_6 = 0.1542$	$\mathfrak{R}_6 = 0.7447$
$L_7 = 0.8814$	$C_7 = 0.6377$	$\mathfrak{R}_7 = 0.2438$
$L_8 = -0.1797$	$C_8 = 1.4874$	$\mathfrak{R}_8 = -1.6671$

TABLE 9: Comparison of final scores by applying proposed model on the application in [29].

Hybrid models	$u_1$	$u_2$	$u_3$	Ranking	Best option
FPIFSEs [29]	0.989	-0.937	4.039	$u_3 > u_1 > u_2$	$u_3$
FPPFSEs	0.844	-0.904	4.106	$u_3 > u_1 > u_2$	$u_3$
FPPFSEs	0.499	-0.633	4.089	$u_3 > u_1 > u_2$	$u_3$
Proposed FP <sup>q</sup> ROFSEs ( $q = 4$ )	0.184	-0.401	4.025	$u_3 > u_1 > u_2$	$u_3$
Proposed FP <sup>q</sup> ROFSEs ( $q = 5$ )	-0.082	-0.224	3.927	$u_3 > u_1 > u_2$	$u_3$

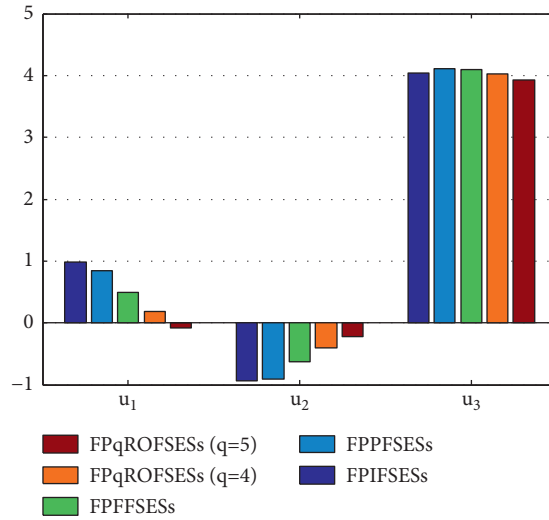


FIGURE 3: Comparison of final scores by applying the proposed model on the application in [29].

$$\begin{aligned}
 & \left\langle \left\langle \left( \frac{0.3}{s_5}, e_1, 1 \right) \left\{ \frac{\eta_1}{(0.51, 0.13)}, \frac{\eta_2}{(0.89, 0.37)}, \frac{\eta_3}{(0.35, 0.26)}, \frac{\eta_4}{(0.74, 0.83)}, \frac{\eta_5}{(0.39, 0.29)}, \frac{\eta_6}{(0.55, 0.77)}, \frac{\eta_7}{(0.42, 0.34)}, \frac{\eta_8}{(0.35, 0.32)} \right\} \right\rangle \right\rangle, \\
 & \left\langle \left\langle \left( \frac{0.6}{s_1}, e_2, 1 \right) \left\{ \frac{\eta_1}{(0.50, 0.70)}, \frac{\eta_2}{(0.39, 0.24)}, \frac{\eta_3}{(0.29, 0.37)}, \frac{\eta_4}{(0.511, 0.75)}, \frac{\eta_5}{(0.27, 0.43)}, \frac{\eta_6}{(0.34, 0.13)}, \frac{\eta_7}{(0.80, 0.60)}, \frac{\eta_8}{(0.47, 0.62)} \right\} \right\rangle \right\rangle, \\
 & \left\langle \left\langle \left( \frac{0.2}{s_2}, e_2, 1 \right) \left\{ \frac{\eta_1}{(0.42, 0.38)}, \frac{\eta_2}{(0.19, 0.28)}, \frac{\eta_3}{(0.89, 0.60)}, \frac{\eta_4}{(0.65, 0.45)}, \frac{\eta_5}{(0.27, 0.21)}, \frac{\eta_6}{(0.81, 0.44)}, \frac{\eta_7}{(0.34, 0.32)}, \frac{\eta_8}{(0.47, 0.24)} \right\} \right\rangle \right\rangle, \\
 & \left\langle \left\langle \left( \frac{0.9}{s_3}, e_2, 1 \right) \left\{ \frac{\eta_1}{(0.61, 0.11)}, \frac{\eta_2}{(0.43, 0.16)}, \frac{\eta_3}{(0.83, 0.27)}, \frac{\eta_4}{(0.78, 0.12)}, \frac{\eta_5}{(0.25, 0.27)}, \frac{\eta_6}{(0.29, 0.23)}, \frac{\eta_7}{(0.88, 0.72)}, \frac{\eta_8}{(0.11, 0.27)} \right\} \right\rangle \right\rangle, \\
 & \left\langle \left\langle \left( \frac{0.7}{s_4}, e_2, 1 \right) \left\{ \frac{\eta_1}{(0.40, 0.90)}, \frac{\eta_2}{(0.58, 0.47)}, \frac{\eta_3}{(0.69, 0.36)}, \frac{\eta_4}{(0.39, 0.75)}, \frac{\eta_5}{(0.90, 0.43)}, \frac{\eta_6}{(0.59, 0.15)}, \frac{\eta_7}{(0.74, 0.78)}, \frac{\eta_8}{(0.46, 0.16)} \right\} \right\rangle \right\rangle, \\
 & \left\langle \left\langle \left( \frac{0.3}{s_5}, e_2, 1 \right) \left\{ \frac{\eta_1}{(0.64, 0.20)}, \frac{\eta_2}{(0.37, 0.56)}, \frac{\eta_3}{(0.81, 0.52)}, \frac{\eta_4}{(0.56, 0.46)}, \frac{\eta_5}{(0.22, 0.65)}, \frac{\eta_6}{(0.94, 0.34)}, \frac{\eta_7}{(0.32, 0.34)}, \frac{\eta_8}{(0.21, 0.27)} \right\} \right\rangle \right\rangle, \\
 & \left\langle \left\langle \left( \frac{0.6}{s_1}, e_3, 1 \right) \left\{ \frac{\eta_1}{(0.54, 0.65)}, \frac{\eta_2}{(0.43, 0.51)}, \frac{\eta_3}{(0.72, 0.44)}, \frac{\eta_4}{(0.65, 0.64)}, \frac{\eta_5}{(0.50, 0.40)}, \frac{\eta_6}{(0.79, 0.36)}, \frac{\eta_7}{(0.36, 0.44)}, \frac{\eta_8}{(0.66, 0.36)} \right\} \right\rangle \right\rangle, \\
 & \left\langle \left\langle \left( \frac{0.2}{s_2}, e_3, 1 \right) \left\{ \frac{\eta_1}{(0.50, 0.15)}, \frac{\eta_2}{(0.80, 0.50)}, \frac{\eta_3}{(0.90, 0.60)}, \frac{\eta_4}{(0.70, 0.20)}, \frac{\eta_5}{(0.80, 0.10)}, \frac{\eta_6}{(0.30, 0.20)}, \frac{\eta_7}{(0.50, 0.20)}, \frac{\eta_8}{(0.40, 0.70)} \right\} \right\rangle \right\rangle, \\
 & \left\langle \left\langle \left( \frac{0.9}{s_3}, e_3, 1 \right) \left\{ \frac{\eta_1}{(0.20, 0.11)}, \frac{\eta_2}{(0.71, 0.12)}, \frac{\eta_3}{(0.10, 0.41)}, \frac{\eta_4}{(0.81, 0.21)}, \frac{\eta_5}{(0.71, 0.32)}, \frac{\eta_6}{(0.81, 0.61)}, \frac{\eta_7}{(0.80, 0.16)}, \frac{\eta_8}{(0.40, 0.14)} \right\} \right\rangle \right\rangle, \\
 & \left\langle \left\langle \left( \frac{0.7}{s_4}, e_3, 1 \right) \left\{ \frac{\eta_1}{(0.44, 0.72)}, \frac{\eta_2}{(0.87, 0.45)}, \frac{\eta_3}{(0.62, 0.42)}, \frac{\eta_4}{(0.52, 0.62)}, \frac{\eta_5}{(0.77, 0.63)}, \frac{\eta_6}{(0.65, 0.56)}, \frac{\eta_7}{(0.80, 0.30)}, \frac{\eta_8}{(0.45, 0.25)} \right\} \right\rangle \right\rangle, \\
 & \left\langle \left\langle \left( \frac{0.3}{s_5}, e_3, 1 \right) \left\{ \frac{\eta_1}{(0.27, 0.31)}, \frac{\eta_2}{(0.36, 0.25)}, \frac{\eta_3}{(0.63, 0.36)}, \frac{\eta_4}{(0.71, 0.81)}, \frac{\eta_5}{(0.61, 0.53)}, \frac{\eta_6}{(0.51, 0.42)}, \frac{\eta_7}{(0.56, 0.45)}, \frac{\eta_8}{(0.52, 0.48)} \right\} \right\rangle \right\rangle, \\
 & \left\langle \left\langle \left( \frac{0.6}{s_1}, e_1, 0 \right) \left\{ \frac{\eta_1}{(0.30, 0.14)}, \frac{\eta_2}{(0.90, 0.16)}, \frac{\eta_3}{(0.80, 0.70)}, \frac{\eta_4}{(0.70, 0.40)}, \frac{\eta_5}{(0.80, 0.30)}, \frac{\eta_6}{(0.50, 0.11)}, \frac{\eta_7}{(0.61, 0.12)}, \frac{\eta_8}{(0.60, 0.30)} \right\} \right\rangle \right\rangle, \\
 & \left\langle \left\langle \left( \frac{0.2}{s_2}, e_1, 0 \right) \left\{ \frac{\eta_1}{(0.89, 0.43)}, \frac{\eta_2}{(0.69, 0.33)}, \frac{\eta_3}{(0.54, 0.93)}, \frac{\eta_4}{(0.28, 0.57)}, \frac{\eta_5}{(0.75, 0.11)}, \frac{\eta_6}{(0.70, 0.11)}, \frac{\eta_7}{(0.81, 0.74)}, \frac{\eta_8}{(0.94, 0.19)} \right\} \right\rangle \right\rangle, \\
 & \left\langle \left\langle \left( \frac{0.9}{s_3}, e_1, 0 \right) \left\{ \frac{\eta_1}{(0.80, 0.50)}, \frac{\eta_2}{(0.20, 0.19)}, \frac{\eta_3}{(0.23, 0.20)}, \frac{\eta_4}{(0.50, 0.35)}, \frac{\eta_5}{(0.43, 0.20)}, \frac{\eta_6}{(0.54, 0.70)}, \frac{\eta_7}{(0.80, 0.68)}, \frac{\eta_8}{(0.79, 0.50)} \right\} \right\rangle \right\rangle,
 \end{aligned}$$



$$\left\langle \left( \frac{0.7}{\mathfrak{S}_4}, e_1, 0 \right) \left\{ \frac{\eta_1}{(0.22, 0.15)}, \frac{\eta_2}{(0.24, 0.11)}, \frac{\eta_3}{(0.29, 0.11)}, \frac{\eta_4}{(0.22, 0.10)}, \frac{\eta_5}{(0.39, 0.37)}, \frac{\eta_6}{(0.45, 0.35)}, \frac{\eta_7}{(0.38, 0.27)}, \frac{\eta_8}{(0.54, 0.22)} \right\} \right\rangle,$$

$$\left\langle \left( \frac{0.3}{\mathfrak{S}_5}, e_1, 0 \right) \left\{ \frac{\eta_1}{(0.70, 0.40)}, \frac{\eta_2}{(0.60, 0.50)}, \frac{\eta_3}{(0.25, 0.60)}, \frac{\eta_4}{(0.60, 0.37)}, \frac{\eta_5}{(0.70, 0.44)}, \frac{\eta_6}{(0.57, 0.90)}, \frac{\eta_7}{(0.72, 0.40)}, \frac{\eta_8}{(0.81, 0.20)} \right\} \right\rangle,$$

$$\left\langle \left( \frac{0.6}{\mathfrak{S}_1}, e_2, 0 \right) \left\{ \frac{\eta_1}{(0.25, 0.17)}, \frac{\eta_2}{(0.31, 0.13)}, \frac{\eta_3}{(0.42, 0.31)}, \frac{\eta_4}{(0.46, 0.34)}, \frac{\eta_5}{(0.70, 0.18)}, \frac{\eta_6}{(0.40, 0.34)}, \frac{\eta_7}{(0.20, 0.15)}, \frac{\eta_8}{(0.31, 0.13)} \right\} \right\rangle,$$

$$\left\langle \left( \frac{0.2}{\mathfrak{S}_2}, e_2, 0 \right) \left\{ \frac{\eta_1}{(0.90, 0.30)}, \frac{\eta_2}{(0.30, 0.12)}, \frac{\eta_3}{(0.31, 0.12)}, \frac{\eta_4}{(0.70, 0.38)}, \frac{\eta_5}{(0.48, 0.31)}, \frac{\eta_6}{(0.61, 0.20)}, \frac{\eta_7}{(0.75, 0.60)}, \frac{\eta_8}{(0.84, 0.50)} \right\} \right\rangle,$$

$$\left\langle \left( \frac{0.9}{\mathfrak{S}_3}, e_2, 0 \right) \left\{ \frac{\eta_1}{(0.27, 0.19)}, \frac{\eta_2}{(0.26, 0.14)}, \frac{\eta_3}{(0.24, 0.12)}, \frac{\eta_4}{(0.24, 0.12)}, \frac{\eta_5}{(0.90, 0.21)}, \frac{\eta_6}{(0.13, 0.25)}, \frac{\eta_7}{(0.39, 0.29)}, \frac{\eta_8}{(0.51, 0.38)} \right\} \right\rangle,$$

$$\left\langle \left( \frac{0.7}{\mathfrak{S}_4}, e_2, 0 \right) \left\{ \frac{\eta_1}{(0.50, 0.20)}, \frac{\eta_2}{(0.22, 0.10)}, \frac{\eta_3}{(0.23, 0.22)}, \frac{\eta_4}{(0.45, 0.11)}, \frac{\eta_5}{(0.51, 0.40)}, \frac{\eta_6}{(0.81, 0.64)}, \frac{\eta_7}{(0.82, 0.73)}, \frac{\eta_8}{(0.86, 0.41)} \right\} \right\rangle,$$

$$\left\langle \left( \frac{0.3}{\mathfrak{S}_5}, e_2, 0 \right) \left\{ \frac{\eta_1}{(0.21, 0.17)}, \frac{\eta_2}{(0.25, 0.16)}, \frac{\eta_3}{(0.11, 0.22)}, \frac{\eta_4}{(0.21, 0.70)}, \frac{\eta_5}{(0.45, 0.38)}, \frac{\eta_6}{(0.45, 0.31)}, \frac{\eta_7}{(0.17, 0.12)}, \frac{\eta_8}{(0.81, 0.27)} \right\} \right\rangle,$$

$$\left\langle \left( \frac{0.6}{\mathfrak{S}_1}, e_3, 0 \right) \left\{ \frac{\eta_1}{(0.62, 0.11)}, \frac{\eta_2}{(0.43, 0.20)}, \frac{\eta_3}{(0.45, 0.11)}, \frac{\eta_4}{(0.64, 0.19)}, \frac{\eta_5}{(0.69, 0.21)}, \frac{\eta_6}{(0.71, 0.17)}, \frac{\eta_7}{(0.63, 0.15)}, \frac{\eta_8}{(0.63, 0.45)} \right\} \right\rangle,$$

$$\left\langle \left( \frac{0.2}{\mathfrak{S}_2}, e_3, 0 \right) \left\{ \frac{\eta_1}{(0.61, 0.12)}, \frac{\eta_2}{(0.45, 0.16)}, \frac{\eta_3}{(0.31, 0.13)}, \frac{\eta_4}{(0.55, 0.15)}, \frac{\eta_5}{(0.34, 0.10)}, \frac{\eta_6}{(0.30, 0.12)}, \frac{\eta_7}{(0.39, 0.17)}, \frac{\eta_8}{(0.62, 0.17)} \right\} \right\rangle,$$

$$\left\langle \left( \frac{0.9}{\mathfrak{S}_3}, e_3, 0 \right) \left\{ \frac{\eta_1}{(0.72, 0.32)}, \frac{\eta_2}{(0.73, 0.25)}, \frac{\eta_3}{(0.70, 0.50)}, \frac{\eta_4}{(0.28, 0.19)}, \frac{\eta_5}{(0.83, 0.20)}, \frac{\eta_6}{(0.56, 0.32)}, \frac{\eta_7}{(0.59, 0.15)}, \frac{\eta_8}{(0.78, 0.34)} \right\} \right\rangle,$$

$$\left\langle \left( \frac{0.7}{\mathfrak{S}_4}, e_3, 0 \right) \left\{ \frac{\eta_1}{(0.39, 0.24)}, \frac{\eta_2}{(0.89, 0.60)}, \frac{\eta_3}{(0.12, 0.78)}, \frac{\eta_4}{(0.27, 0.25)}, \frac{\eta_5}{(0.29, 0.23)}, \frac{\eta_6}{(0.46, 0.16)}, \frac{\eta_7}{(0.64, 0.20)}, \frac{\eta_8}{(0.37, 0.56)} \right\} \right\rangle,$$

$$\left\langle \left( \frac{0.3}{\mathfrak{S}_5}, e_3, 0 \right) \left\{ \frac{\eta_1}{(0.58, 0.47)}, \frac{\eta_2}{(0.53, 0.37)}, \frac{\eta_3}{(0.83, 0.20)}, \frac{\eta_4}{(0.65, 0.45)}, \frac{\eta_5}{(0.43, 0.27)}, \frac{\eta_6}{(0.13, 0.34)}, \frac{\eta_7}{(0.34, 0.56)}, \frac{\eta_8}{(0.81, 0.52)} \right\} \right\rangle.$$

(30)

The committee uses Algorithm 1 for the selection of the “Best News Channel.”

Table 5 represents the score table for the FP<sup>5</sup> ROFSES defined above. Tables 6 and 7 represent the score tables for agree- and disagree-FP<sup>5</sup> ROFSESs, respectively, along with the agree and disagree accumulated scores.

Using agree and disagree accumulated scores in Tables 6 and 7, Table 8 provides the final scores. From the final scores table, it can be seen that  $\mathfrak{R}_m = \max(\mathfrak{R}_j) = \mathfrak{R}_3$ ; hence, the news channel  $\eta_3$  is awarded as the “Best News Channel” by the committee and the organization.

#### 4. Comparison

These days, experts believe that fuzzy parameterized extensions of the soft set model and its hybrid structures with other uncertainty theories are playing a crucial role in solving several daily-life decision-making problems. Till date, the mathematical tools considering above-mentioned topic in hand are FPFSSs [20], IFPFSSs [22], IFPIFSSs [24], IVIFP-IVIFSSs [25], FPFSESs [45], and FPIFSESs [29]. Inspection of researches completed in the last few decades proves the significance of uncertain hybrid models toward this topic. Clearly, our proposed hybrid model, FP<sup>q</sup> ROFSESs, generalized the FPIFSESs [29]. Note that FPIFSESs

[29], fuzzy parameterized Pythagorean FSESs (FPFSESs), and fuzzy parameterized Fermatean FSESs (FPFFSESs) are particular cases of our developed FP<sup>q</sup> ROFSES model for  $q = 1, 2$  and  $q = 3$ , respectively. One cannot apply the existing FPIFSES model to the proposed applications in Section 3. Thus, to clearly observe the advantages of the developed model and its comparative analysis with existing models, it is applied to the application in [29] and obtains similar results for different values of parameter “ $q$ ,” which are computed in Table 9 and displayed in Figure 3. In [29], the authors have not used weights in the group decision-making process, which was an essential part of their new construction. So, there is a flaw in their model. In our proposed method, we not only cover this issue (that is, we have utilized these weights in the developed group decision-making method, see Algorithm 1; Steps 5 and 6) but also provided its generalization. Thus, our proposed hybrid model applicability scope is wider than existing models, including FPIFSESs [29] and FPFSES [45].

*4.1. Advantages of the Initiated Model.* From the inspection of the recent decade, one can easily observe various developments in the hybrid models containing fuzzy parameterized soft sets as one of their components. All these

models are inefficient to tackle data in a  $q$ -ROF environment with  $n$  experts where  $n \geq 1$ . A generalized hybrid approach is currently required, which maintains the features of more than one existing model. With the motivation of these concerns, a new hybrid model called  $FP^q$  ROFSES is initiated. In our developed model, the estimations of all experts are examined in a  $q$ -ROF environment. The developed model's applicability scope is wider than various existing models, including FPFSSs [20], FPFSEs [45], and FPIFSEs [29] because it is an efficient extension of all these models. It can be easily seen that the existing MAGDM method, namely, FPIFSEs, cannot address the MADM situations as studied in Section 3. Thus, the developed model is very reliable and flexible for dealing with imprecise fuzzy parameterized  $q$ -ROF soft expert information, specifically, if the available information is collected from multiple experts in a  $q$ -ROF environment.

## 5. Conclusions

The theory of  $q$ -ROFSSs has proved to be a strong tool for dealing with high levels of uncertainties in many practical situations than IFSs, PFSs, and FFSs; thus, it is a basic component of many mathematical hybrid decision-making models for dealing with such complex decisive situations. The fuzzy parameterized soft sets and their extensions are more efficient in dealing with scenarios considering much preference of some of the parameters over the others, thus getting more precisely to the required decisions. Similarly, for MAGDM situations, SESs as an efficient model provide the facility of considering multiple experts' opinions in one place. This article extends the hybrid model FPIFSEs to a more generalized novel hybrid structure called  $FP^q$  ROFSEs, which is actually a combination of  $q$ -ROFSSs [5] and FPFSEs [46]. When  $q = 1$ , the proposed model reduces to the FPIFSE model [29], and when  $q = 2$  and  $q = 3$ , it degenerates into FPPFSEs and FPFSEs, respectively. Some essential basic notions including subset, complement, AND operation, OR operation, intersection, and union are studied coupled with illustrative examples. De Morgan's laws under  $FP^q$  ROFSEs are verified. Moreover, to show the applicability and efficiency of the proposed model, two real-life applications, including the selection of the best site for cafe outlet and Best News Channel, are provided and solved under  $FP^q$  ROFSEs with the help of a developed algorithm. Finally, a comparison of the developed group decision-making method under  $FP^q$  ROFSEs is studied with few existing approaches, including FPIFSEs [29]. This comparative analysis in Section 4 shows that the developed model's applicability and reliability scope is higher than existing models, including  $q$ -ROFSSs and FPIFSEs. During the construction of our initiated model, we observed that it has two major limitations. Firstly, the proposed model fails in a situation if weights are given in the form of an intuitionistic fuzzy environment. Secondly, it fails if experts provide their estimations in the form of an interval-valued  $q$ -ROF environment. In the future, to remove these drawbacks of our model, we are planning to expand our work with the following models: (a) intuitionistic fuzzy

parameterized  $q$ -rung orthopair fuzzy soft expert sets using the idea in [24], (b) fuzzy parameterized interval-valued  $q$ -rung orthopair fuzzy soft expert sets using the idea in [25], (c) fuzzy parameterized complex interval-valued  $q$ -rung orthopair fuzzy soft expert sets with aggregation operators using the concepts in [7], and (d) fuzzy parameterized complex  $q$ -rung orthopair fuzzy soft expert sets using [8].

## Data Availability

No supporting data are required for the results of the paper. All necessary details are available within the article.

## Ethical Approval

This article does not contain any studies with human participants or animals performed by any of the authors.

## Conflicts of Interest

The authors declare that they have no conflicts of interest regarding the publication of this article.

## References

- [1] L. A. Zadeh, "Fuzzy sets," *Information and Control*, vol. 8, no. 3, pp. 338–353, 1965.
- [2] K. T. Atanassov, "Intuitionistic fuzzy sets," *Fuzzy Sets and Systems*, vol. 20, no. 1, pp. 87–96, 1986.
- [3] R. R. Yager, "Pythagorean fuzzy subsets," in *Proceedings of the 2013 Joint IFSA World Congress and NAFIPS Annual Meeting (IFSA/NAFIPS)*, 2013.
- [4] T. Senapati and R. R. Yager, "Fermatean fuzzy sets," *Journal of Ambient Intelligence and Humanized Computing*, vol. 11, no. 2, pp. 663–674, 2020.
- [5] R. R. Yager, "Generalized orthopair fuzzy sets," *IEEE Transactions on Fuzzy Systems*, vol. 25, no. 5, pp. 1222–1230, 2016.
- [6] T. Shaheen, M. I. Ali, and H. Toor, "Why do we need  $q$ -rung orthopair fuzzy sets? Some evidence established via mass assignment," *International Journal of Intelligent Systems*, vol. 36, no. 10, pp. 5493–5505, 2021.
- [7] H. Garg, Z. Ali, and T. Mahmood, "Algorithms for complex interval-valued  $q$ -rung orthopair fuzzy sets in decision making based on aggregation operators, AHP, and TOPSIS," *Expert Systems*, vol. 38, no. 1, 2020.
- [8] H. Garg, "New exponential operation laws and operators for interval-valued  $q$ -rung orthopair fuzzy sets in group decision making process," *Neural Computing & Applications*, pp. 1–27, 2021.
- [9] P. Liu and P. Wang, "Some  $q$ -rung orthopair fuzzy aggregation operators and their applications to multiple-attribute decision making," *International Journal of Intelligent Systems*, vol. 33, no. 2, pp. 259–280, 2018.
- [10] X. Peng, H. Huang, and Z. Luo, " $q$ -rung orthopair fuzzy decision-making framework for integrating mobile edge caching scheme preferences," *International Journal of Intelligent Systems*, vol. 36, no. 5, pp. 2229–2266, 2021.
- [11] X. Peng, J. Dai, and H. Garg, "Exponential operation and aggregation operator for  $q$ -rung orthopair fuzzy set and their decision-making method with a new score function," *International Journal of Intelligent Systems*, vol. 33, no. 11, pp. 2255–2282, 2018.

- [12] D. Molodtsov, "Soft set theory-first results," *Computers and Mathematics with Applications*, vol. 37, no. 2, pp. 19–31, 1999.
- [13] P. K. Maji, A. R. Roy, and R. Biswas, "Soft set theory," *Computers and Mathematics with Applications*, vol. 54, no. 4–5, pp. 555–562, 2003.
- [14] P. K. Maji, A. R. Roy, and R. Biswas, "Fuzzy soft sets," *Journal of Fuzzy Mathematics*, vol. 9, no. 3, pp. 589–602, 2001.
- [15] P. K. Maji, R. Biswas, and A. R. Roy, "Intuitionistic fuzzy soft sets," *Journal of Fuzzy Mathematics*, vol. 9, no. 3, pp. 677–692, 2001.
- [16] M. T. Hamid, M. Riaz, and D. Afzal, "Novel MCGDM with  $q$ -rung orthopair fuzzy soft sets and TOPSIS approach under  $q$ -rung orthopair fuzzy soft topology," *Journal of Intelligent and Fuzzy Systems*, vol. 39, no. 3, pp. 3853–3871, 2020.
- [17] G. Ali, H. Alolaiyan, D. Pamucar, M. Asif, and N. Lateef, "A novel MADM framework under  $q$ -rung orthopair fuzzy bipolar soft sets," *Mathematics*, vol. 9, p. 2163, 2021.
- [18] N. Alkan and C. Kahraman, "Evaluation of government strategies against COVID-19 pandemic using  $q$ -rung orthopair fuzzy TOPSIS method," *Applied Soft Computing*, vol. 110, Article ID 107653, 2021.
- [19] N. Aman and S. Enginoglu, "FP-soft set theory and its applications," *Annals of Fuzzy Mathematics and Informatics*, vol. 2, no. 2, pp. 219–226, 2011.
- [20] N. aman, F. Çitak, and S. Enginoglu, "Fuzzy parameterized fuzzy soft set theory and its applications," *Turkish Journal of Fuzzy System*, vol. 1, no. 1, pp. 21–35, 2010.
- [21] I. Deli and N. Çağman, "Intuitionistic fuzzy parameterized soft set theory and its decision making," *Applied Soft Computing*, vol. 28, pp. 109–113, 2015.
- [22] E. E. Yagubi and A. R. Salleh, "Intuitionistic fuzzy parameterised fuzzy soft set," *Journal of Quality Measurement and Analysis*, vol. 9, no. 2, pp. 73–81, 2013.
- [23] S. Enginolu and B. Arslan, "Intuitionistic fuzzy parameterized intuitionistic fuzzy soft matrices and their application in decision-making," *Computational and Applied Mathematics*, vol. 39, no. 4, pp. 1–20, 2020.
- [24] F. Karaaslan, "Intuitionistic fuzzy parameterized intuitionistic fuzzy soft sets with applications in decision making," *Annals of Fuzzy Mathematics and Informatics*, vol. 11, no. 4, pp. 607–619, 2016.
- [25] T. Aydin and S. Enginolu, "Interval-valued intuitionistic fuzzy parameterized interval-valued intuitionistic fuzzy soft sets and their application in decision-making," *Journal of Ambient Intelligence and Humanized Computing*, vol. 12, no. 1, pp. 1541–1558, 2021.
- [26] S. Alkhazaleh and A. R. Salleh, "Soft expert sets," *Advances in Decision Sciences*, vol. 2011, Article ID 757868, 12 pages, 2011.
- [27] S. Alkhazaleh and A. R. Salleh, "Fuzzy soft expert set and its application," *Applied Mathematics*, vol. 5, no. 9, pp. 1349–1368, 2014.
- [28] G. Ali and M. Akram, "Decision-making method based on fuzzy  $N$ -soft expert sets," *Arabian Journal for Science and Engineering*, vol. 45, no. 12, pp. 10381–10400, 2020.
- [29] G. Selvachandran and A. R. Salleh, "Fuzzy parameterized intuitionistic fuzzy soft expert set theory and its application in decision making," *International Journal of Soft Computing*, vol. 11, pp. 52–63, 2016.
- [30] G. Ali, G. Muhiuddin, A. Adeel, and M. Zain Ul Abidin, "Ranking effectiveness of COVID-19 tests using fuzzy bipolar soft expert sets," *Mathematical Problems in Engineering*, vol. 2021, Article ID 5874216, 19 pages, 2021.
- [31] M. Sarwar, M. Akram, and S. Shahzadi, "Bipolar fuzzy soft information applied to hypergraphs," *Soft Computing*, vol. 25, no. 5, pp. 3417–3439, 2021.
- [32] M. Sarwar, M. Akram, and P. Liu, "An integrated rough ELECTRE II approach for risk evaluation and effects analysis in automatic manufacturing process," *Artificial Intelligence Review*, vol. 54, no. 6, pp. 4449–4481, 2021.
- [33] M. Sarwar, "Decision-making approaches based on color spectrum and D-TOPSIS method under rough environment," *Computational and Applied Mathematics*, vol. 39, no. 4, pp. 1–32, 2020.
- [34] M. Akram, G. Ali, M. A. Butt, and J. C. R. Alcantud, "Novel MCGDM analysis under  $m$ -polar fuzzy soft expert sets," *Neural Computing & Applications*, vol. 33, no. 18, pp. 12051–12071, 2021.
- [35] M. Akram, G. Ali, and J. C. R. Alcantud, "Parameter reduction analysis under interval-valued  $m$ -polar fuzzy soft information," *Artificial Intelligence Review*, vol. 54, pp. 5541–5582, 2021.
- [36] G. Ali and M. N. Ansari, "Multiattribute decision-making under Fermatean fuzzy bipolar soft framework," *Granular Computing*, 2021.
- [37] Z. Ali, T. Mahmood, T. Mahmood, K. Ullah, and Q. Khan, "Einstein geometric aggregation operators using a novel complex interval-valued Pythagorean fuzzy setting with application in green supplier chain management," *Reports in Mechanical Engineering*, vol. 2, no. 1, pp. 105–134, 2021.
- [38] A. Alost, O. Elmansuri, and I. Badi, "Resolving a location selection problem by means of an integrated AHP-RAFSI approach," *Reports in Mechanical Engineering*, vol. 2, no. 1, pp. 135–142, 2021.
- [39] F. Feng, H. Fujita, M. I. Ali, R. R. Yager, and X. Liu, "Another view on generalized intuitionistic fuzzy soft sets and related multi attribute decision making methods," *IEEE Transactions on Fuzzy Systems*, vol. 27, pp. 474–488, 2018.
- [40] H. Garg, A. Keikha, and H. Mishmast Nehi, "Multiple-attribute decision-making problem using TOPSIS and choquet integral with hesitant fuzzy number information," *Mathematical Problems in Engineering*, vol. 2020, Article ID 9874951, 12 pages, 2020.
- [41] D. Pamucar, D. Macura, M. Tavana, D. Božanić, and N. Knežević, "An integrated rough group multicriteria decision-making model for the ex-ante prioritization of infrastructure projects: the Serbian railways case," *Socio-Economic Planning Sciences*, 2021, In press, Article ID 101098.
- [42] D. Pamučar, "Multi-criteria model for the selection of construction materials: an approach based on fuzzy logic," *Tehnički Vjesnik*, vol. 27, no. 5, pp. 1531–1543, 2020.
- [43] G. Petrović, J. Mihajlović, Ž. Čojbašić, M. Madić, and D. Marinković, "Comparison of three fuzzy MCDM methods for solving the supplier selection problem," *Facta Universitatis Series: Mechanical Engineering*, vol. 17, no. 3, pp. 455–469, 2019.
- [44] K. R. Ramakrishnan and S. Chakraborty, "A cloud TOPSIS model for green supplier selection," *Facta Universitatis Series: Mechanical Engineering*, vol. 18, no. 3, pp. 375–397, 2020.
- [45] A. Hazaymeh, I. B. Abdullah, Z. Balkhi, and R. Ibrahim, "Fuzzy parameterized fuzzy soft expert set," *Applied Mathematical Sciences*, vol. 6, no. 112, pp. 5547–5564, 2012.
- [46] M. Bashir and A. R. Salleh, "Fuzzy parameterized soft expert set," *Abstract and Applied Analysis*, vol. 2012, Article ID 258361, 15 pages, 2012.

## Research Article

# Numerical Study of MHD Third-Grade Fluid Flow through an Inclined Channel with Ohmic Heating under Fuzzy Environment

Muhammad Nadeem,<sup>1</sup> Imran Siddique <sup>1</sup>, Fahd Jarad ,<sup>2,3</sup> and Raja Noshad Jamil <sup>1</sup>

<sup>1</sup>Department of Mathematics, University of Management and Technology, Lahore 54770, Pakistan

<sup>2</sup>Department of Mathematics, Cankaya University, Etimesgut, Ankara, Turkey

<sup>3</sup>Department of Medical Research, China Medical University Hospital, China Medical University, Taichung, Taiwan

Correspondence should be addressed to Imran Siddique; [imransmsrazi@gmail.com](mailto:imransmsrazi@gmail.com) and Fahd Jarad; [fahd@cankaya.edu.tr](mailto:fahd@cankaya.edu.tr)

Received 22 July 2021; Revised 30 August 2021; Accepted 2 September 2021; Published 23 September 2021

Academic Editor: Dragan Pamučar

Copyright © 2021 Muhammad Nadeem et al. This is an open access article distributed under the Creative Commons Attribution License, which permits unrestricted use, distribution, and reproduction in any medium, provided the original work is properly cited.

The uncertainties or fuzziness occurs due to insufficient knowledge, experimental error, operating conditions, and parameters that give the imprecise information. In this article, we discuss the combined effects of the gravitational and magnetic parameters for both crisp and fuzzy cases in the three basic flow problems (namely, Couette flow, Poiseuille flow, and Couette–Poiseuille flow) of a third-grade fluid over an inclined channel with heat transfer. The dimensionless governing equations with the boundary conditions are converted into coupled fuzzy differential equations (FDEs). The fuzzified forms of the governing equations along with the boundary conditions are solved by employing the numerical technique `bvp4c` built in MATLAB for both cases, which is very efficient and has a less computational cost. In the first case, proposed problems are analyzed in a crisp environment, while in the second case, they are discussed in a fuzzy environment with the help of  $\alpha$ -cut approach, which controls the fuzzy uncertainty. It is observed that the fuzzy gravitational and magnetic parameters are less sensitive for a better flow and heat situation. Using triangular fuzzy numbers (TFNs), the left, right, and mid values of the velocity and temperature profile are presented due to various values of the involved parameters in tabular form. For validation, the present results are compared with existing results for some special cases, viz., crisp case, and they are found to be in good agreement.

## 1. Introduction

The differential type fluids [1, 2] have gained considerable attention. The third-grade fluid is a subclass of differential type fluids, which has been examined successfully in different types of flow situations [3] and is known to capture the non-Newtonian effects such as shear thinning or shear thickening as well as normal stresses. The study of the flow of third-grade fluids through an inclined channel with heat transfer has important applications in engineering, technology, and science. Some of these applications can be found in materials manufactured by the extraction procedure particularly in polymer processing, the flow of synovial fluid in human joints, geological flows inside the earth's mantle, microfluids, drilling of oil and gas wells, etc. Heat transfer is important in industrial areas to launch transportation of

energy in the system. Generally, the flowing mixtures are made of solid particles in a fluid, so coal-based slurries show non-Newtonian features, which is why these mixtures are important in industrial applications. Also, heat transfer plays a vital role in processing and handling these mixtures. For example, it has been shown that substantial performance benefits can be obtained if the coal-water mixture is preheated [4, 5].

In fluid dynamics, the study of three fundamental flow problems (namely, Couette flow, Poiseuille flow, and Couette–Poiseuille flow) attracts the researchers because of their use in technology, engineering, and industry. The unidirectional flows are used in polymer engineering such as die flow, injection molding, extrusion, plastic forming, continuous casting, and asthenosphere flows [6–9]. Magnetohydrodynamics (MHD) deals with the study of the

motion of electrically conducting fluids in the presence of magnetic field. MHD flow has significant important applications in an inclined channel such as geophysical, astrophysical, metallurgical processing, MHD generators, pumps, geothermal reservoirs, polymer technology, and mineral industries. MHD fluid is used as a lubricant in industrial and other applications, for stopping the unexpected variation of lubricant viscosity with temperatures under certain norms. In this regard, there are a large number of works, such as Khan et al. [10], Hayat et al. [7, 11, 12], and Islam [13]. Kamran and Siddique [14] calculated the analytical solutions for MHD flow between infinite parallel plates. Siddiqui et al. [15] deliberated the flow of third-grade fluid between two inclined parallel plates with heat transfer using the homotopy perturbation method (HPM). Later on, Aiyesimi et al. [16] studied the solution of MHD Couette flow and Poiseuille flow problems of temperature and velocity profile by employing the perturbation method.

Fluid flow plays the main role in the field of science and engineering. There is a rise in an extensive range of problems such as chemical diffusion, magnetic effect, and heat transfer. After governing, these physical problems are converted into linear or nonlinear DEs. In general, the physical problems with involved geometry, coefficients, parameters, and initial and boundary conditions greatly affect the solutions of DEs. Then, the coefficients, parameters, and initial and boundary conditions are not crisp due to the mechanical defect, experimental error, measurement error, etc. Therefore, in this situation, fuzzy set theory is an effective tool for a better understanding of the considered phenomena, and it is more accurate than assuming the crisp or classical physical problems. More precisely, the FDEs play a major role in reducing the uncertainty and are a proper way to describe the physical problem which arises in uncertain parameters and initial and boundary conditions.

The fuzzy set theory (FST) was presented by Zadeh [17] in 1965. FST is a very valuable tool to define the situation in which information is imprecise, vague, or uncertain. FST is completely defined by its membership function or belongingness. In FST, the membership function describes each element of the universe of discourse by a number from  $[0, 1]$  interval. On the other hand, the degree of nonbelongingness is a complement to “one” of the membership degree or belongingness. Fuzzy number (FN) can be expected as a function whose range is specified from zero to one. Every numerical value in the range is allocated a definite grade of membership function, where 0 signifies the minimum possible grade and 1 is the maximum possible grade. FST is the generalization of crisp (classical) set theory, and similarly, FNs are the generalization of real intervals. Arithmetic operations on FNs were developed by Dubois and Prade [18]. Different types of FNs can be categorized into triangular, trapezoidal, and Gaussian fuzzy numbers. Here, we consider TFNs for the sake of completeness.

The information of dynamical systems modelled by partial or ordinary differential equations is commonly incomplete, vague, or uncertain, while fuzzy differential equations (FDEs) represent a proper way to model the dynamical systems under vagueness or uncertainty. This

impreciseness or vagueness can be defined mathematically using FNs or TFNs. In recent years, there have been many studies revolving around the concept of “FDEs.” Seikala [19] introduced the fuzzy differentiability concept. Later on, Kaleva [20] presented fuzzy differentiation and integration. Kandel and Byatt [21] introduced the FDEs in 1987. Buckley et al. [22] used two methods, extension principle and FNs, for the solution of FDEs. Nieto [23] studied the Cauchy problem for continuous FDEs. Lakshmikantham and Mohapatra studied the initial-value problems for FDEs [24]. Park and Hyo [25] used the successive approximation method for the existence and uniqueness solution of FDE. Gasilov et al. [26] developed the geometric method to solve the system of FDEs. Gasilov et al. [27] studied the system of FDEs with the help of TFNs. Salahsour et al. [28] studied the fuzzy logistic equation and alley effect using FDEs with the help of TFNs.

The fuzzy boundary value problems (FBVPs) depend on the concept of the solution of FDE. The scholars utilize the derivative in the FDE such as Hukuhara derivative (H-derivative) or generalized Hukuhara derivative (GH-derivative). Chalco-Cano et al. [29, 30] established the idea of fuzzy H-derivative. Bede and Gal [31] introduced the idea of the fuzzy generalized H-derivative. Khastan and Nieto [32, 33] proposed a new solution concept for a two-point FBVP for a second-order FDE using a generalized differentiability concept. Also, many scholars have applied FST to obtain well-known results in the field of commerce and science, such as in bank account model [34], HIV model [35], bacteria culture model [36], population dynamics model [37, 38], predator-prey model [39], computational biology [40], growth model [41], decay model [42], quantum optics and gravity [43], modeling hydraulic [44], model of friction [45], application in Laplace transform [46], civil engineering [47], integrodifferential equation [48], giving up smoking model [49], chemostat model [50], dengue virus model [51], and many others [52–55].

In the review of the literature, an attempt has been made to describe the three fundamental flow problems, namely, plane Couette, fully developed plane Poiseuille, and plane Couette–Poiseuille flow of a third-grade fluid through inclined parallel plates in an imprecise environment. Here, we discuss two cases: one is crisp and the other is fuzzy for a better flow situation. In this regard, the gravitational and magnetic parameters are taken as TFNs. The uncertainty of TFNs is controlled by  $\alpha$ -cut ( $0 \leq \alpha \leq 1$ ) with the help of the membership functions. The membership function provides a better understanding of uncertain parameters and flow situations. The basic purpose of this article is to show the uncertain flow mechanism through FDEs.

The rest of the article is structured as follows. Some basic definitions related to the fuzzy numbers, TFN, and fuzzy valued functions are discussed in Section 2, to convert the FDEs to parametric forms. In Section 3, the mathematical formulation of the problem is given. The FDEs of the considered problem have been presented in Section 4, which are solved by a numerical scheme `bvp4c` built in MATLAB. In Section 5, some fuzzy plots of velocity and temperature profiles are presented. Also, the present results have been

compared with the existing results for some special cases, viz., crisp case. Finally, in Section 6, conclusions have been made.

## 2. Preliminaries

In this section, some basic notations and definitions are given.

**Definition 1** (see [17]). Fuzzy set is defined as a set of ordered pairs such that  $\tilde{U} = \{(x, \mu_{\tilde{U}}(x)) : x \in X, \mu_{\tilde{U}}(x) \in [0, 1]\}$ , where  $X$  is the universal set and  $\mu_{\tilde{U}}(x)$  is the membership function of  $\tilde{U}$  and its mapping is defined as  $\mu_{\tilde{U}}(x) : X \rightarrow [0, 1]$ .

**Definition 2** (see [18]).  $\alpha$ -cut or  $\alpha$ -level of a fuzzy set  $\tilde{U}$  is a crisp set  $U_{\alpha}$  and defined by  $U_{\alpha} = \{x / \mu_{\tilde{U}}(x) \geq \alpha\}$ , where  $0 \leq \alpha \leq 1$ .

**Definition 3** (see [17]). Convex fuzzy set  $\tilde{U}$  is defined as  $\tilde{U} = \{x, \mu_{\tilde{U}}(x)\} \subseteq X$ . It is called convex fuzzy set if all  $U_{\alpha}$  for every  $\alpha \in [0, 1]$  are convex fuzzy set, i.e., for every  $y_1, y_2 \in U_{\alpha}$  and  $\alpha y_1 + (1 - \alpha)y_2 \in U_{\alpha}$  for all  $\alpha \in [0, 1]$ ; otherwise, it is a nonconvex fuzzy set.

**Definition 4** (see [17]). The fuzzy set  $\tilde{U}$  defined on the universal set of real number  $R$  is said to be an FN, which satisfies the following properties: (i)  $\mu_{\tilde{U}}(x)$  is piecewise continuous, (ii)  $\tilde{U}$  is convex, (iii)  $\tilde{U}$  is normal, i.e.,  $\exists x_0 \in R$  such that  $\mu_{\tilde{U}}(x_0) = 1$ , and (iv) support of  $\tilde{U}$  must be bounded.

$U_{\alpha}$  must be closed interval for every  $0 \leq \alpha \leq 1$ , where  $\alpha$  is called the level of credibility or presumption. Membership function or grade is also named as a grade of possibility or grade of credibility for a given number.

**Definition 5** (see [18]). Let  $\tilde{U} = (a_1, a_2, a_3)$  with membership function  $\mu_{\tilde{U}}(x)$  is called a TFN if

$$\mu_{\tilde{U}}(x) = \begin{cases} \frac{a_1 - x}{a_2 - a_1}, & \text{for } x \in [a_1, a_2], \\ \frac{x - a_3}{a_2 - a_3}, & \text{for } x \in [a_2, a_3], \\ 0, & \text{otherwise.} \end{cases} \quad (1)$$

The TFNs with peak (or centre)  $a_2$ , left width  $a_2 - a_1 > 0$ , and right width  $a_3 - a_2 > 0$  are transformed into interval numbers through  $\alpha$ -cut approach, which is written as  $\tilde{U} = [u(x; \alpha), v(x; \alpha)] = [a_1 + \alpha(a_2 - a_1), a_3 - \alpha(a_3 - a_2)]$ , where  $\alpha \in [0, 1]$ . A TFN  $\tilde{U} = (a_1, a_2, a_3)$  and  $\alpha$ -cut of membership function are shown in Figure 1. An arbitrary TFN satisfies the following conditions: (i)  $u(x; \alpha)$  is an increasing function on  $[0, 1]$ ; (ii)  $v(x; \alpha)$  is a decreasing function on  $[0, 1]$ ; (iii)  $u(x; \alpha) \leq v(x; \alpha)$  on  $[0, 1]$ ; (iv)  $u(x; \alpha)$  and  $v(x; \alpha)$  are bounded on left continuous and right

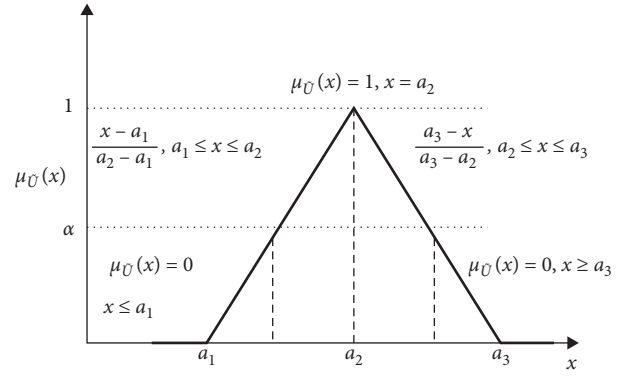


FIGURE 1: Membership functions of a TFN.

continuous at  $[0, 1]$  respectively; and (v)  $u(x; \alpha) = v(x; \alpha) = u(x)$ , where  $u(x)$  is the crisp number.

**Definition 6** (see [19–21]). Let  $I$  be a real interval. A mapping  $\tilde{u} : I \rightarrow F$  is called a fuzzy process, defined as  $\tilde{u}(x; \alpha) = [u(x; \alpha), v(x; \alpha)]$ ,  $x \in I$  and  $\alpha \in [0, 1]$ . The derivative  $d\tilde{u}(x; \alpha)/dx \in F$  of a fuzzy process  $\tilde{u}(x; \alpha)$  is defined by  $d\tilde{u}(x; \alpha)/dx = [du(x; \alpha)/dx, dv(x; \alpha)/dx]$ .

**Definition 7** (see [19–21]). Let  $I \subseteq R$ ,  $\tilde{u}$  be a fuzzy valued function defined on  $I$ . Let  $\tilde{u}(x; \alpha) = [u(x; \alpha), v(x; \alpha)]$  for all  $\alpha$ -cut. Assume that  $u(x; \alpha)$  and  $v(x; \alpha)$  have continuous derivatives or differentiable, for all  $x \in I$  and  $\alpha$ , then  $[d\tilde{u}(x; \alpha)/dx]_{\alpha} = [du(x; \alpha)/dx, dv(x; \alpha)/dx]_{\alpha}$ . Similarly, we can define higher-order ordinary derivatives in the same way. An FN by an ordered pair of functions  $[d\tilde{u}(x; \alpha)/dx]_{\alpha}$  satisfies the following conditions: (i)  $du(x; \alpha)/dx$  and  $dv(x; \alpha)/dx$  are continuous on  $[0, 1]$ ; (ii)  $du(x; \alpha)/dx$  is an increasing function on  $[0, 1]$ ; (iii)  $dv(x; \alpha)/dx$  is a decreasing function on  $[0, 1]$ ; and (iv)  $du(x; \alpha)/dx \leq dv(x; \alpha)/dx$  on  $[0, 1]$ .

## 3. Mathematical Formulation of the Problem

The basic equations which govern the MHD flow of an incompressible, third-grade electrically conducting fluid are as follows:

$$\text{div}V = 0, \quad (2)$$

$$\rho \frac{dV}{dt} = \text{div}\hat{S} - \nabla p + J \times B + \rho f, \quad (3)$$

where  $V$  is the velocity vector,  $\rho$  is the constant density,  $d/dt$  is the material derivative,  $p$  is the pressure,  $f$  is the external body force,  $B$  is the total magnetic field,  $B = B_0 + b$ , in which  $B_0$  represents the imposed magnetic field and  $b$  denotes the induced magnetic field, and

$$J = \sigma[V \times B + E], \quad (4)$$

which is the current density,  $\sigma$  is the electrical conductivity,  $E$  is the electric field which is not considered (i.e.,  $E = 0$ ), and  $\hat{S}$  is the Cauchy stress tensor which for a third-grade fluid satisfies the following constitutive equation:

$$\begin{aligned} \widehat{S} = & -pI + \mu A_1 + \alpha_1 A_2 + \alpha_2 A_1^2 + \beta_1 A_3 + \beta_2 (A_1 A_2 + A_2 A_1) \\ & + \beta_3 A_1 (\text{tr} A_2), \end{aligned} \quad (5)$$

$$A_n = \frac{dA_{n-1}}{dt} + A_{n-1} (\text{grad} V) + (\text{grad} V)^T A_{n-1}, \quad n \geq 1, \quad (6)$$

where  $pI$  is the isotropic stress due to constraint incompressibility,  $\mu$  is the dynamic viscosity,  $\alpha_1, \alpha_2, \beta_1, \beta_2,$  and  $\beta_3$  are material constants,  $T$  indicates the matrix transpose,  $A_1, A_2,$  and  $A_3$  are the first three Rivlin–Ericksen tensors, and  $A_0 = I$  is the identity tensor [13–16].

**3.1. Couette Flow.** Consider a steady MHD flow of a third-grade fluid between two infinite inclined horizontally parallel plates of distance  $2H$  apart, by angle  $\alpha$ . The upper and lower plates are at  $y = H$  and  $y = -H$  of a rectangular system with the  $x$ -axis as flow direction. The upper plate is moving with constant speed  $U$  while the lower plate is fixed as shown in Figure 2. The temperature of the lower plate is maintained at  $T_0$  and that of the upper plate at  $T_1$ . A homogeneous magnetic field  $B_0$  is applied in positive  $y$ -direction and is expected to be undisturbed as the induced magnetic field is neglected under the assumption of small magnetic Reynolds number. The ambient air is assumed stationary so that the flow is due to the movement of the upper plate and gravity alone.

Consider a velocity field of the form

$$V = [u(y), 0, 0]. \quad (7)$$

In the absence of modified pressure gradient, equations (2) and (3) along with equations (5)–(7), after introducing the following nondimensional parameters

$$\begin{aligned} u &= \bar{u}U, \\ y &= \bar{y}H, \\ \bar{\theta} &= \frac{T - T_0}{T_1 - T_0}, \end{aligned} \quad (8)$$

yield

$$\frac{d^2 u}{d\bar{y}^2} + 6\beta \left( \frac{du}{d\bar{y}} \right)^2 \frac{d^2 u}{d\bar{y}^2} - Mu + k = 0, \quad (9)$$

with boundary conditions

$$\begin{aligned} u(-1) &= 0, \\ u(1) &= 1. \end{aligned} \quad (10)$$

Also, the thermal boundary layer equation for the thermodynamically compatible third-grade fluid with viscous dissipation, work done due to deformation and Joule heating in a nondimensional form, is given as

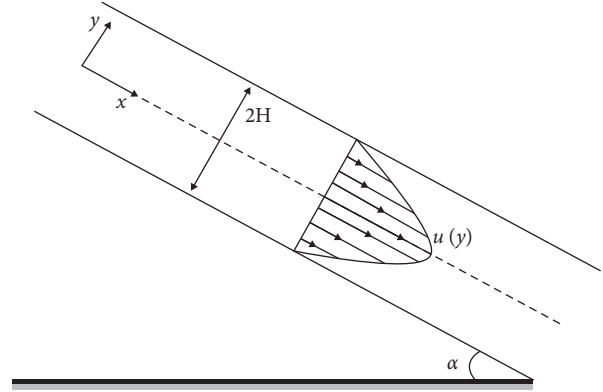


FIGURE 2: Geometry of the problem.

$$\frac{d^2 \theta}{d\bar{y}^2} + B_r \left( \frac{du}{d\bar{y}} \right)^2 + 2\beta B_r \left( \frac{du}{d\bar{y}} \right)^4 + B_r M u^2 = 0, \quad (11)$$

with boundary conditions

$$\begin{aligned} \theta(-1) &= 0, \\ \theta(1) &= 1, \end{aligned} \quad (12)$$

where  $\beta = (U/H)^2 (\beta_2 + \beta_3)/\mu$  is the third-grade fluid parameter,  $k = \rho g H^2 / \mu \sin \phi$  is the gravitational parameter,  $M = H^2 \sigma B_0^2 / \mu$  is the magnetic parameter, and  $B_r = \mu U^2 / k (T_1 - T_0)$  is the Brinkman number.

**3.2. Poiseuille Flow.** In this case, both the upper and lower plates are kept stationary and we assumed that the fluid motion is due to gravity alone. Consequently, in the absence of pressure gradient, equations (9) and (10) remain the same after scaling given by equation (8), while the boundary conditions (10) and (12) become

$$\begin{aligned} u(-1) &= 0, \\ u(1) &= 0, \end{aligned} \quad (13)$$

$$\begin{aligned} \theta(-1) &= 0, \\ \theta(1) &= 1. \end{aligned} \quad (14)$$

**3.3. Couette–Poiseuille Flow.** Because we considered that the flow is due to gravity and the movement of upper plate while the pressure gradient is neglected, the momentum and energy equations with their boundary conditions for Couette–Poiseuille flow will result to those of the Couette flow.

## 4. Fuzzification of the Problem

The velocity of fluid depends upon involved engineering parameters such as  $\beta, k,$  and  $M$ . Some researchers take fixed crisp values; the point is that the flow of fluid just depends on these fixed crisp values. Then, uncertainty arises due to the fixed crisp values of parameters. So, it is better to take these

parameters as an uncertain or fuzzy parameter. In this study, uncertain parameters  $k$  and  $M$  are taken as FN.

To handle this problem, we have taken TFN and discretization in the form of  $(a_1, a_2, a_3)$  (see Table 1). This discretization is used in fluid parameters for certain flow behaviour because these parameters are taken as FNs. Using the  $\alpha$ -cut approach, the fuzzy fluid parameters can be decomposed into an interval form regarding the  $\alpha$ -cut.

TABLE 1: TFNs of the fuzzy parameters.

Fuzzy parameters	Crisp value	TFN
$k$ (gravitational parameter)	3	[1, 3, 5]
$M$ (magnetic parameter)	15	[5, 14, 24]

Therefore, the governing equations (9) and (11) are converted into coupled FDEs:

$$\frac{d^2 \bar{u}(y; \alpha)}{dy^2} + 6\beta \frac{d^2 \bar{u}(y; \alpha)}{dy^2} \left( \frac{d\bar{u}(y; \alpha)}{dy} \right)^2 + \bar{k} - \bar{M}\bar{u}(y, \alpha) = 0, \tag{15}$$

$$\frac{d^2 \bar{\theta}(y, \alpha)}{dy^2} + B_r \left( \frac{d\bar{u}(y, \alpha)}{dy} \right)^2 + 2\beta B_r \left( \frac{d\bar{u}(y, \alpha)}{dy} \right)^4 + B_r \bar{M}\bar{u}^2(y, \alpha) = 0, \tag{16}$$

subject to boundary conditions

$$\begin{aligned} u(-1) &= 0, \\ u(1) &= 1, \end{aligned} \tag{17}$$

$$\begin{aligned} \theta(-1) &= 0, \\ \theta(1) &= 1, \end{aligned} \tag{18}$$

where “ $\bar{\cdot}$ ” stands for the fuzzy form and the lower and upper bounds of fuzzy velocity profiles are  $\bar{u}(y, \alpha) = [u_1(y, \alpha), u_2(y, \alpha)]$ ,  $0 \leq \alpha \leq 1$ . Similarly, the fuzzy temperature profiles are  $\bar{\theta}(y, \alpha) = [\theta_1(y, \alpha), \theta_2(y, \alpha)]$ ,  $0 \leq \alpha \leq 1$ .

The crisp values and TFNs of these parameters are listed in Table 1. The TFNs are used to describe the triangular

membership functions of the FNs. The investigated ranges are generally used to build up the aforesaid problem.

Now, we use a numerical method for boundary value problem solver MATLAB built-in function `bvp4c` in the governing crisp differential equations and FDEs (equations (15)–(17)) with boundary conditions. It is a finite difference algorithm that uses the three-stage Lobatto IIIA formula. It is a collocation polynomial, and the collocation formula yields a  $C1$ -continuous solution in  $[a, b]$  that is fourth-order accurate uniformly. The residual of the continuous solution is used for error control and mesh selection. To use this approach, transform the system of nonlinear ODEs and its boundary conditions to the system of the first-order ODEs and initial conditions as [56, 57].

Let

$$\begin{aligned} u(y) &= f(1), u'(y) = f'(1) = f(2), \text{ and } u'' = f'(2), \\ f'(2) &= \frac{Mf(1) - k}{1 + 6\beta(f(2))^2}, \\ \theta(y) &= f(3), \\ \theta'(y) &= f'(3) = f(4), \\ \theta''(y) &= f'(4), \\ f'(4) &= -Br(f(2))^2 - 2\beta Br(f(2))^4 - BrM(f(1))^2. \end{aligned} \tag{19}$$

And, boundary conditions are

$$\left. \begin{aligned} f_a(1) = 0, f_b(1) = 1, \quad \text{at } y = -1, \\ f_a(1) = 0, f_b(1) = 1, \quad \text{at } y = 1. \end{aligned} \right\} \tag{20}$$

All computations are performed with a tolerance of  $\varepsilon = 10^{-6}$  and a validated MATLAB code.

## 5. Results and Discussions

**5.1. Crisp Case.** In this section, we solve the proposed system of the crisp ODEs (9) and (11) together with the boundary conditions (10) and (12) numerically by MATLAB built-in technique `bvp4c`. Furthermore, we discuss the effects of gravitational parameter  $k$  and magnetic parameter  $M$  on the



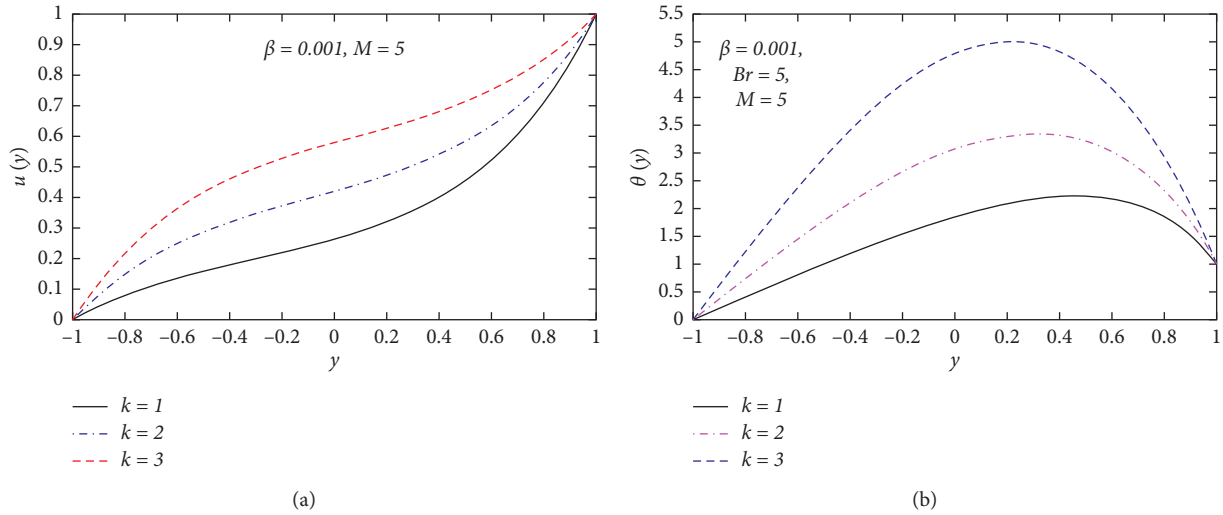


FIGURE 3: Effect of  $k$  on crisp velocity and temperature profiles of Couette flow.

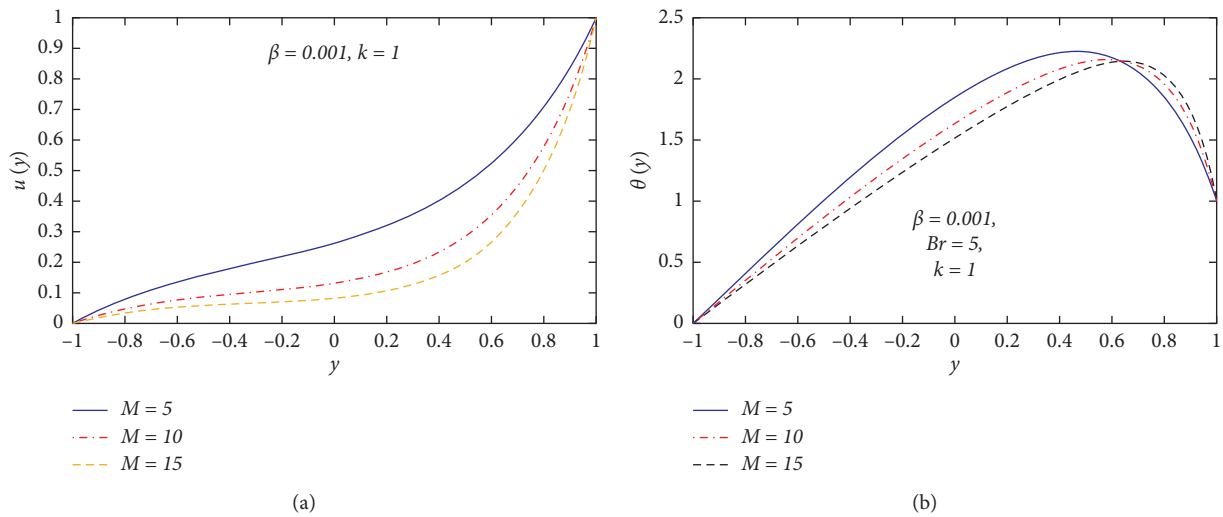


FIGURE 4: Effect of  $M$  on crisp velocity and temperature profiles of Couette flow.

TABLE 2: Comparison of numerical results with analytical results for the velocity of Couette flow when  $k=1$  and  $M=5$ .

$y$	Velocity at $\beta = 0.001$		Velocity at $\beta = 0.1$	
	Aiyesimi et al. [16] (PM)	Present result (bvp4c)	Aiyesimi et al. [16] (PM)	Present result (bvp4c)
-1	0	0	0	0
-0.8	0.0805992	0.080607	0.081260	0.083115
-0.6	0.136936	0.1369396	0.140203	0.142375
-0.4	0.180453	0.1804493	0.187494	0.189643
-0.2	0.219997	0.2199837	0.232351	0.233923
0	0.263605	0.263602	0.283677	0.283364
0.2	0.320143	0.320104	0.351506	0.347445
0.4	0.401095	0.400987	0.448301	0.436373
0.6	0.522872	0.522653	0.578833	0.563876
0.8	0.710055	0.709739	0.753411	0.746170
1	1	0.999997	1	1

TABLE 3: Comparison of numerical results with analytical results for the temperature of Couette flow when  $k=1$  and  $M=5$ .

$y$	Temperature at $\beta = 0.001$		Temperature at $\beta = 0.1$	
	Aiyesimi et al. [16] (PM)	Present result (bvp4c)	Aiyesimi et al. [16] (PM)	Present result (bvp4c)
-1	0	0	0	0
-0.8	1.22328	0.533675	1.402449	0.596488
-0.6	2.34181	1.037249	2.404120	1.159899
-0.4	3.31125	1.509760	3.151470	1.688806
-0.2	4.09503	1.941188	3.982890	2.171262
0	4.65215	2.315419	4.776961	2.587627
0.2	4.91100	2.606950	5.081522	2.906360
0.4	4.81112	2.770656	4.783381	3.072202
0.6	4.33810	2.718227	4.162820	2.980832
0.8	3.17165	2.264215	3.194671	2.426644
1	1	1	1	1

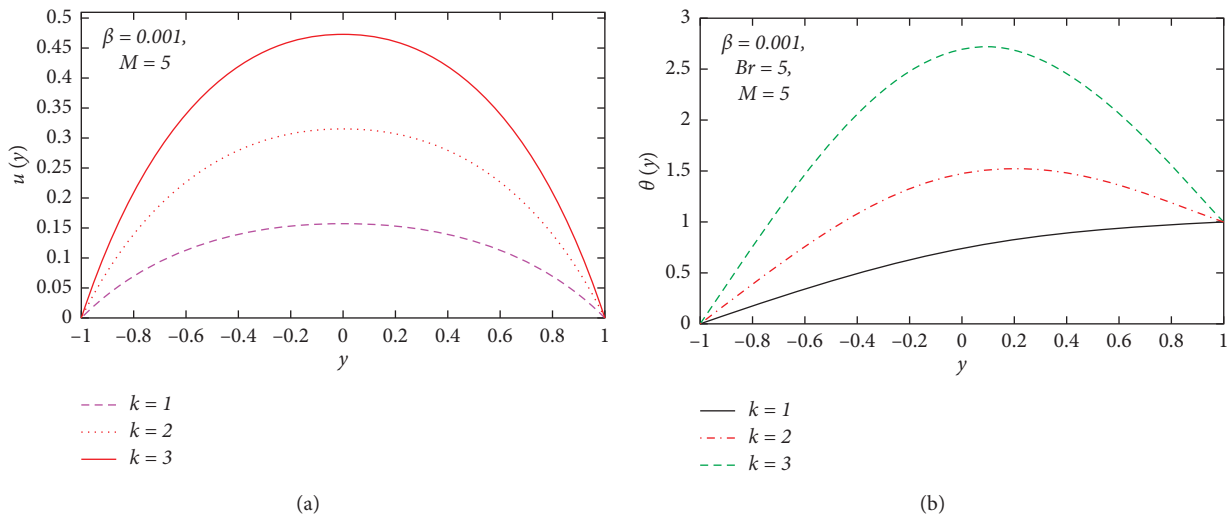


FIGURE 5: Effect of  $k$  on velocity and temperature profiles of Poiseuille flow.

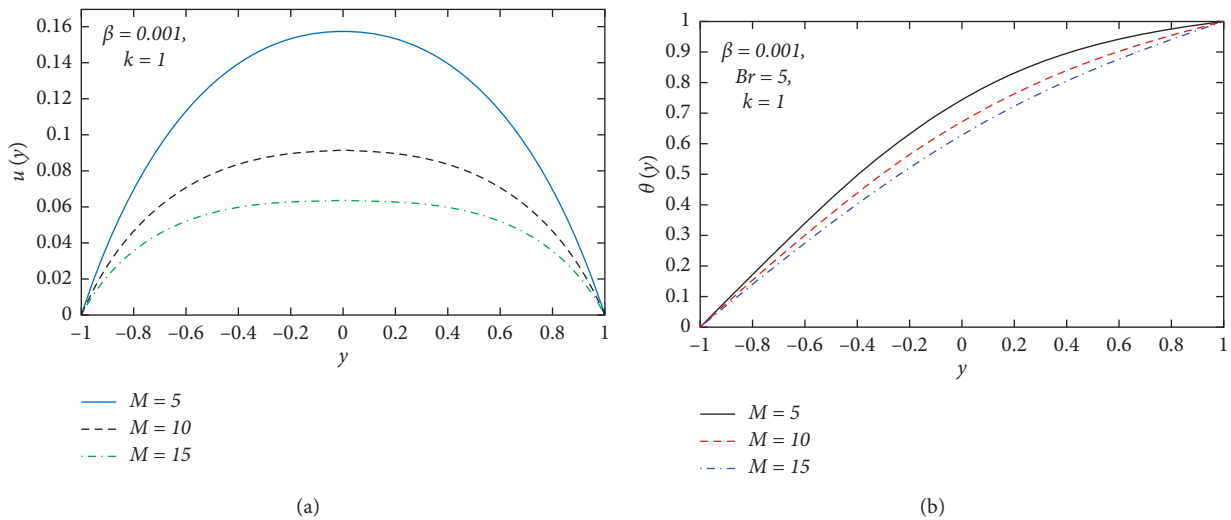


FIGURE 6: Effect of  $M$  on velocity and temperature profiles of Poiseuille flow.

TABLE 4: Comparison of numerical results with analytical results for the velocity of Poiseuille flow when  $k = 1$ ,  $Br = 5$ , and  $M = 5$ .

$y$	Velocity at $\beta = 0.001$		Velocity at $\beta = 0.1$	
	Aiyesimi et al. [16] (PM)	Present result (bvp4c)	Aiyesimi et al. [16] (PM)	Present result (bvp4c)
-1	0	0	0	0
-0.8	0.070019	0.069038	0.069009	0.068269
-0.6	0.113620	0.113095	0.112676	0.113143
-0.4	0.139659	0.139406	0.138934	0.139295
-0.2	0.153428	0.153341	0.152856	0.140774
0	0.157725	0.157745	0.157206	0.159183
0.2	0.153428	0.153517	0.152856	0.154794
0.4	0.139659	0.139493	0.138934	0.140774
0.6	0.113620	0.113072	0.112676	0.113143
0.8	0.0700194	0.069038	0.069009	0.068269
1	0	0	0	0

TABLE 5: Comparison of numerical results with analytical results for the temperature of Poiseuille flow when  $k = 1$ ,  $Br = 5$ , and  $M = 5$ .

$y$	Temperature at $\beta = 0.001$		Temperature at $\beta = 0.1$	
	Aiyesimi et al. [16] (PM)	Present result (bvp4c)	Aiyesimi et al. [16] (PM)	Present result (bvp4c)
-1	0	0	0	0
-0.8	0.67471	0.197694	0.67412	0.199630
-0.6	1.26537	0.374075	1.26427	0.377380
-0.4	1.73772	0.531557	1.73622	0.535884
-0.2	20.6938	0.667706	2.06763	0.672683
0	2.24792	0.780066	2.24609	0.785268
0.2	2.26938	0.867706	2.26763	0.872683
0.4	2.13772	0.931557	2.13622	0.935884
0.6	1.86537	0.974075	1.86427	0.977380
0.8	1.47471	0.997694	1.47412	0.999630
1	1	1	1	1

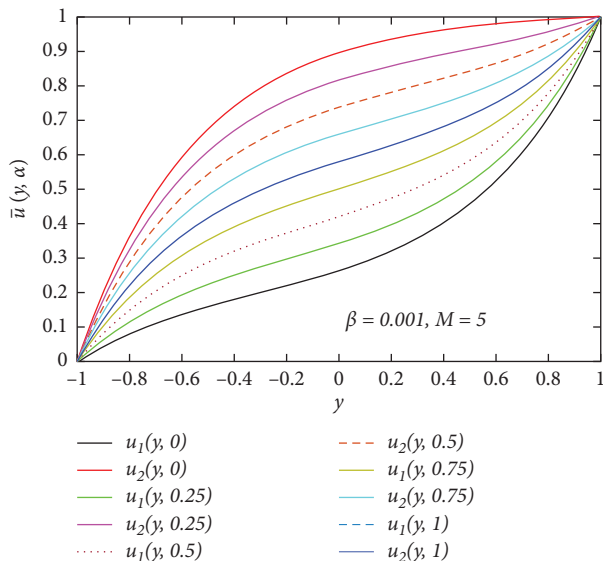


FIGURE 7: Effect of TFN  $k$  on fuzzy velocity profile of Couette flow.

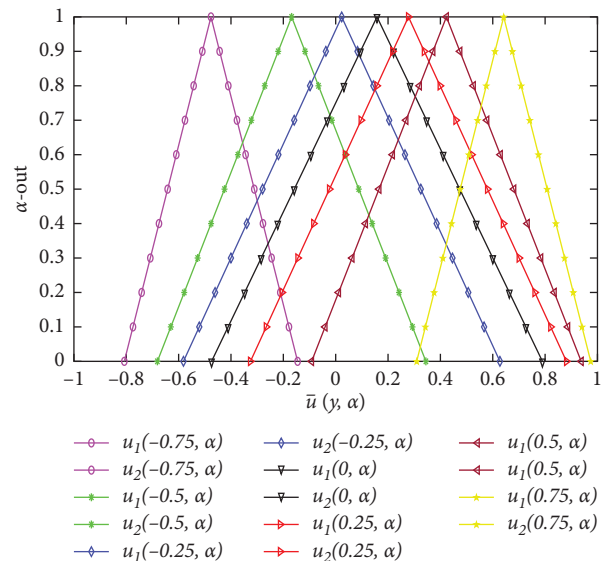


FIGURE 8: Membership functions of TFN if  $k$  is fuzzy (Couette flow).

velocity and temperature profiles of Couette and Poiseuille flow graphically. Furthermore, for validation, the present results are compared with the existing results in some special cases, viz., crisp case.

For Couette flow, Figures 3(a) and 3(b) show the effect of gravitational parameter  $k$  on crisp velocity and temperature profile with a fixed magnetic parameter  $M$ . It is seen that the

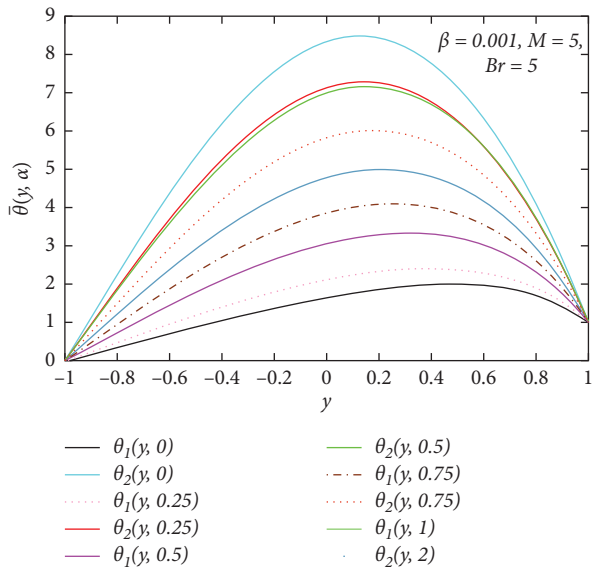


FIGURE 9: Effect of TFN  $k$  on fuzzy temperature profile of Couette flow.

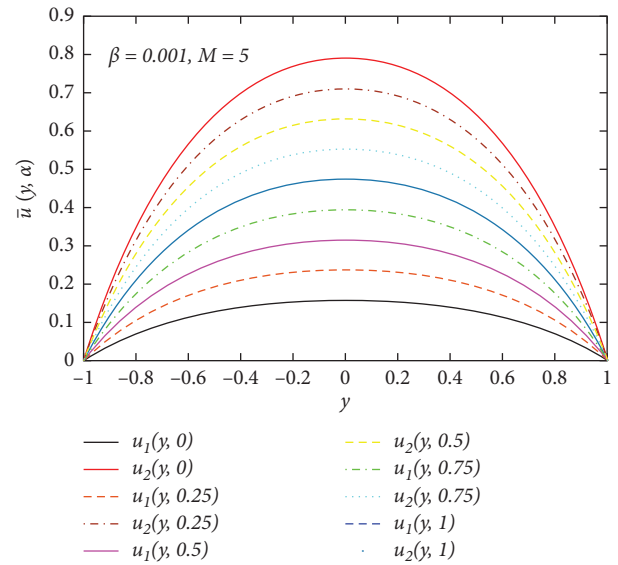


FIGURE 11: Effect of TFN  $k$  on fuzzy velocity profile of Poiseuille flow.

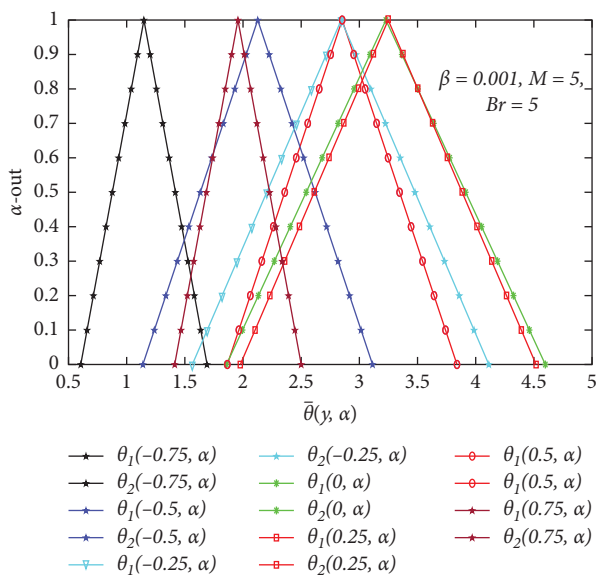


FIGURE 10: Membership functions of TFN if  $k$  is fuzzy (Couette flow).

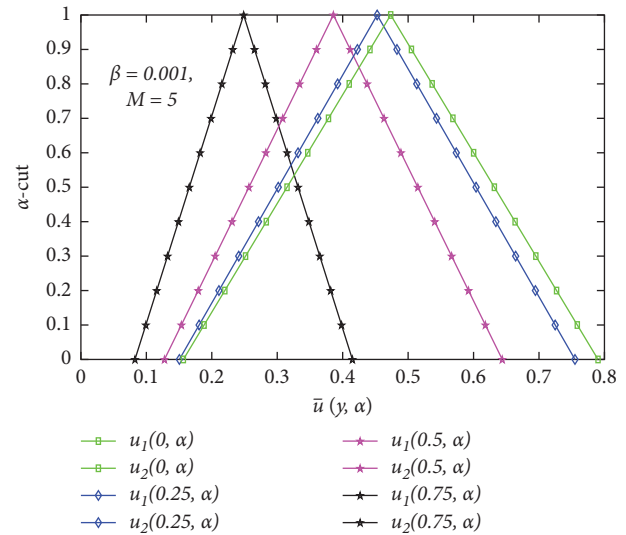


FIGURE 12: Membership functions of TFN if  $k$  is fuzzy (Poiseuille flow).

velocity and temperature profiles increase rapidly in the centre of the plates with increasing the values of  $k$ . Figures 4(a) and 4(b) show the effect of  $M$  on crisp velocity and temperature profiles with a fixed value of  $k$ . It is perceived that velocity and temperature profile decreases with increasing the value of  $k$ . Particularly in Figure 4(b), the temperature decreases in the region  $-1 < y \leq 0.6$  and it increases in region  $0.6 < y \leq 1$ . Tables 2 and 3 show the comparison of velocity and temperature profiles for different values of  $\beta$  with [16]. The validated results of the present study are found to be in excellent agreement.

For Poiseuille flow, Figures 5(a) and 5(b) show the effect of gravitational parameter  $k$  on crisp velocity and temperature profiles with fixed magnetic parameter  $M$ . It is observed that the velocity and temperature profile increase rapidly in the centre of the plates with increasing the values of  $k$ . Figures 6(a) and 6(b) show the effect of  $M$  on crisp velocity and temperature profile with a fixed value of  $k$ . It is noted that velocity and temperature profile decrease rapidly in the centre of the plates with increasing the value of  $k$ . Tables 4 and 5 show the comparison of velocity and temperature profiles for different values of  $\beta$  with [16]. The validated results of the present study are found to be in excellent agreement.

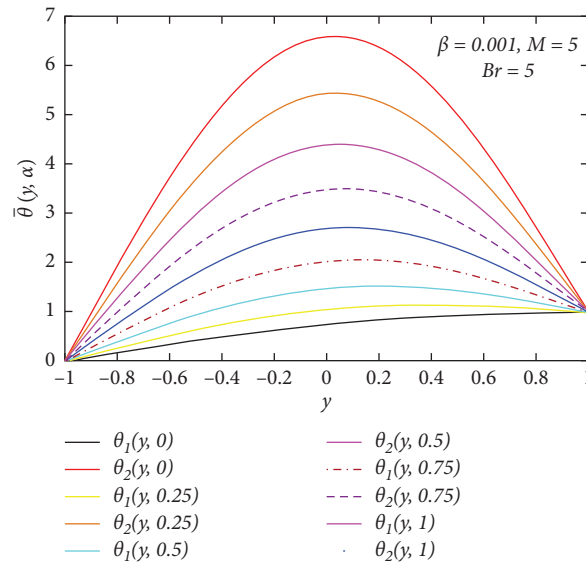


FIGURE 13: Effect of TFN  $k$  on fuzzy temperature profile of Poiseuille flow.

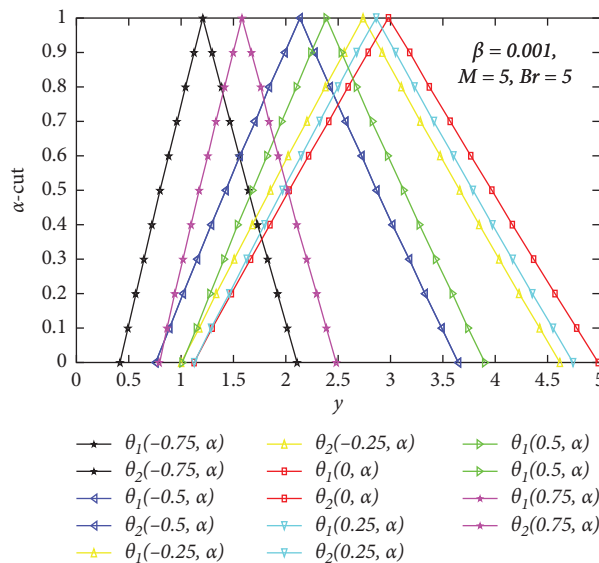


FIGURE 14: Membership functions of TFN if  $k$  is fuzzy (Poiseuille flow).

5.2. *Fuzzy Case.* In this section, we solve the proposed system of the fuzzy environmental problems (15) and (16) together with the boundary conditions (17) and (18) numerically by using MATLAB built-in technique `bvp4c`. Furthermore, we analyze the effects of the uncertain gravitational parameter  $k$  and uncertain magnetic parameter  $M$  through  $\alpha$ -cut approach ( $0 \leq \alpha \leq 1$ ) as discussed in detail in Section 4, on velocity and temperature profiles for Couette and Poiseuille flow graphically and tabularly. Here,  $\alpha$ -cut controls the fuzzy term, for example, if  $\alpha$ -cut = 0, it will cover the whole interval in the form of lower and upper bounds of fuzzy velocity or temperature profiles. If  $\alpha$ -cut increases from 0.05 to 0.95, the

lower and upper bound fuzzy velocity or temperature profiles decrease; when  $\alpha$ -cut = 1, the lower and upper bounds fuzzy velocity or temperature profiles cohere with each other, so they provide crisp results. It is important to note that if the width between lower and upper bounds of velocity or temperature profile is less, then the uncertainty is less. The fuzzy velocity and temperature profiles are plotted in Figures 7–22 for some particular values of  $\alpha$ -cut ( $\alpha = 0, 0.25, 0.5, 0.75, 1$ ) with different values of  $y$ . The triangular membership functions are depicted in Figures 8, 10, 12, 14, 16, 18, 20, and 22. In the triangular membership functions, if  $\alpha = 0$ , we can notice that the crisp solutions are limited by the lower and upper

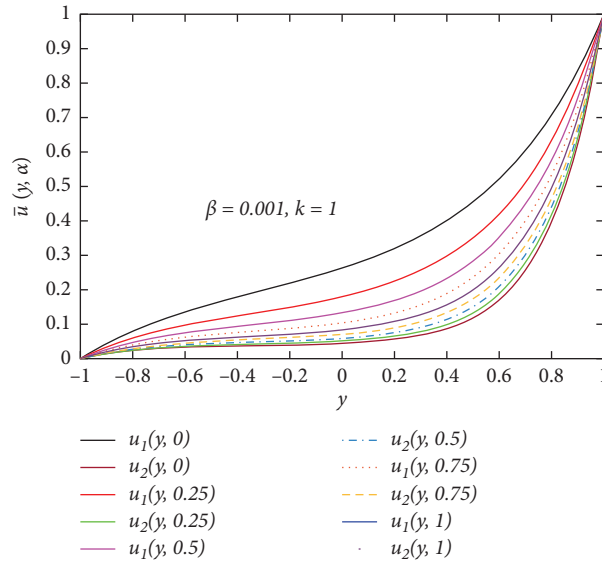


FIGURE 15: Effect of TFN  $M$  on fuzzy velocity profile of Couette flow.

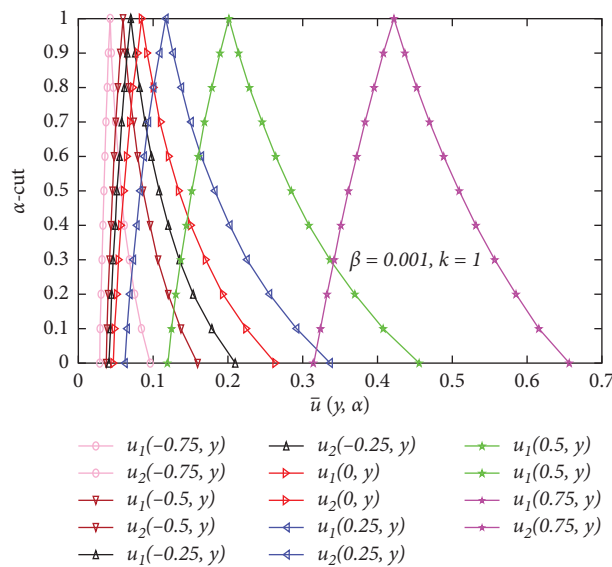


FIGURE 16: Membership functions of TFN if  $M$  is fuzzy (Couette flow).

outlets of the dependent parameters. Furthermore, if we take  $\alpha = 1$ , the projection of the peaks of the triangles coincides with the crisp solution.

In Figures 7–14, the gravitational parameter  $k$  is taken as a TFN (see Table 1), and the fuzzy velocity and temperature profiles are controlled by  $\alpha$  – cut. The crisp or classical solution lies among the fuzzy solutions; when  $\alpha$  increases, the width between lower and upper bounds of fuzzy velocity and temperature profiles decreases and when  $\alpha = 1$ , they cohere with one another (see Figures 7, 9, 11, and 13). Furthermore, crisp or classical solutions behave the single flow situation, while fuzzy solution behaves the lower and upper flow situation. Figures 8, 10, 12, and 14 represent the

membership functions of fuzzy velocity and temperature profiles when  $k$  is taken as TFN. In Figures 7 and 8, it is seen that the width of the fuzzy velocity profile at the centre of the plates is less, so uncertainty is less, while in Figures 9 and 10, the width of fuzzy temperature becomes more at the centre of the plates, therefore the uncertainty is maximum. In Figures 11 and 12, it is seen that triangular membership functions of fuzzy velocity show the same behaviour in the region  $-1 \leq y \leq 0$  and  $0 \leq y \leq 1$ . The width of the triangular membership functions is high, so the uncertainty is high, which means that the uncertain parameter  $k$  is sensitive. Now, in Figures 13 and 14, the width of fuzzy temperature from the centre value of each TFN is less, so there is

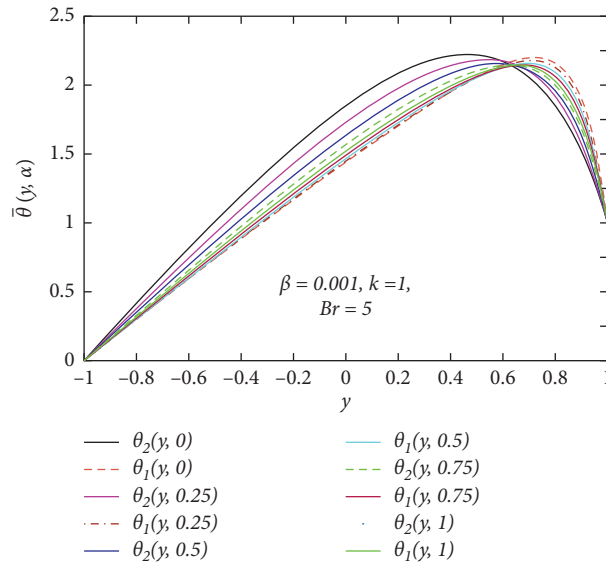


FIGURE 17: Effect of TFN  $M$  on the fuzzy temperature profile of Couette flow.

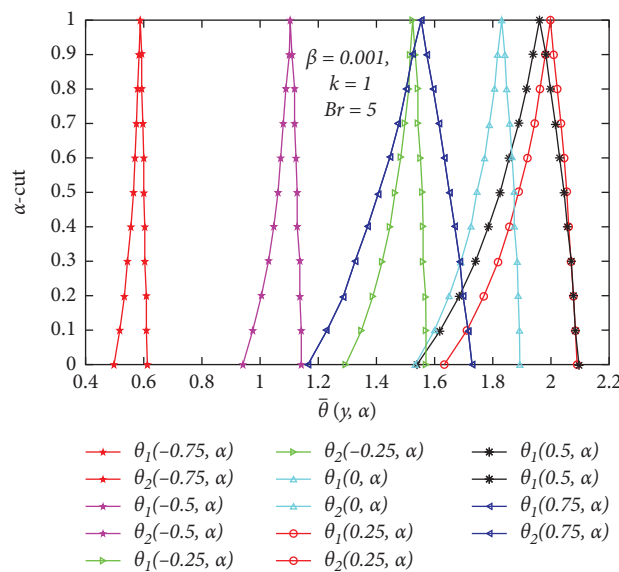


FIGURE 18: Membership functions of TFN if  $M$  is fuzzy (Couette flow).

minimum possibility of the uncertainty of fuzzy temperature.

In Figures 15–22, the magnetic parameter  $M$  is taken as a TFN (see Table 1), and the fuzzy velocity and temperature profiles are controlled by  $\alpha$ -cut. It is seen that  $\alpha$ -cut increases from 0 to 1, and the lower bound of fuzzy velocity and temperature is an increasing set-valued function whereas an upper bound is a decreasing one, which shows that the results are fuzzy numbers.

Figures 16, 18, 20, and 22 represent the triangular membership functions of fuzzy velocity and temperature profiles when  $M$  is taken as a TFN. In Figures 15 and 16, the widths of fuzzy velocity are less, so the uncertain parameter  $M$  is less sensitive, while in Figures 17 and 18, the width of fuzzy temperature is less at the centre of the plate, so the

uncertain parameter  $M$  is less sensitive. In Figures 19 and 20, it is seen that triangular membership functions of fuzzy velocity show the same behaviour in the region  $-1 \leq y \leq 0$  and  $0 \leq y \leq 1$ . The width of the triangular membership functions is very less, so uncertain parameter  $M$  is less sensitive. While in Figures 21 and 22, the width of fuzzy temperature from the centre value of each TFN is large, so there is maximum possibility of the uncertainty of fuzzy temperature and  $M$  is more sensitive.

The uncertain velocity and temperature values are presented in Tables 6–9. Using TFN, the lower, upper, and crisp or mid values of the uncertain velocity and temperature profiles are presented for different involved uncertain parameters. In Tables 6 and 7, the gravitational parameter  $k$  is taken as a TFN, and in Tables 8 and 9, the magnetic parameter  $M$  is taken as a

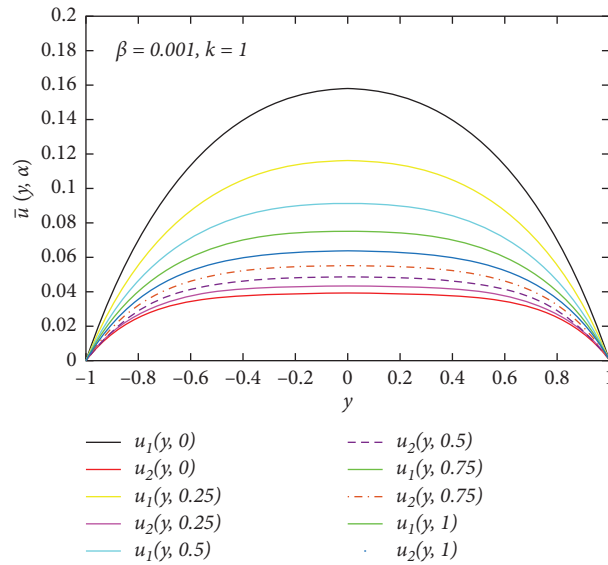


FIGURE 19: Effect of TFN  $M$  on fuzzy velocity profile of Poiseuille flow.

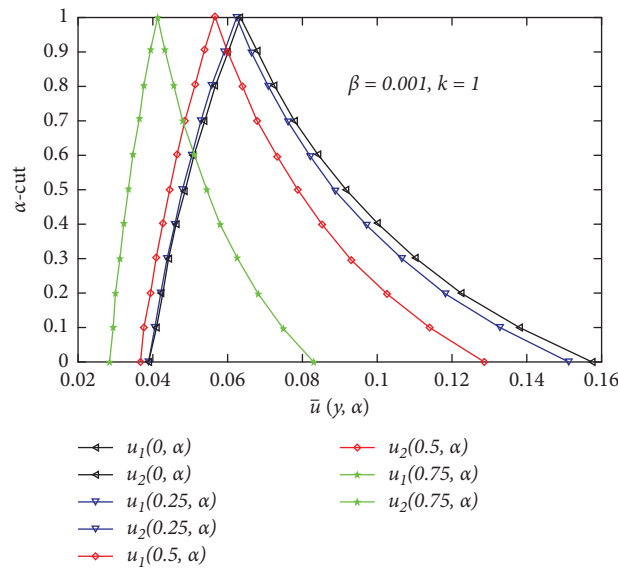


FIGURE 20: Membership functions of TFN plot if  $M$  is fuzzy (Poiseuille flow).

TFN. The lower and upper bounds of the uncertain velocity and temperature are calculated at  $\alpha - \text{cut} = 0$ . It is noted that the lower bound defines the minimum uncertain velocity and temperature while the upper bound defines the maximum uncertain velocity and temperature. The mid values of uncertain velocity and temperature are calculated at  $\alpha - \text{cut} = 1$ . It has been observed that the lower and upper uncertain velocity and temperature values coincide at  $\alpha - \text{cut} = 1$ . Here, it is observed that the uncertainties in physical parameters have nonnegligible effect on the fuzzy velocity and temperature

profiles. Also, it may be observed that, as  $\alpha$  increases from 0 to 1, we have a narrow width of fuzzy velocity and temperature profiles and uncertainty decreases drastically which finally provides crisp results for  $\alpha = 1$ . Finally, it can be seen that the fuzzy velocity and temperature profiles of the fluid are a better option as compared to the crisp or classical case. The crisp or classical velocity profile of fluid gives the single flow situation of the fluid, while the fuzzy velocity profile of fluid gives the interval flow situation like lower and upper bounds of the velocity profiles.



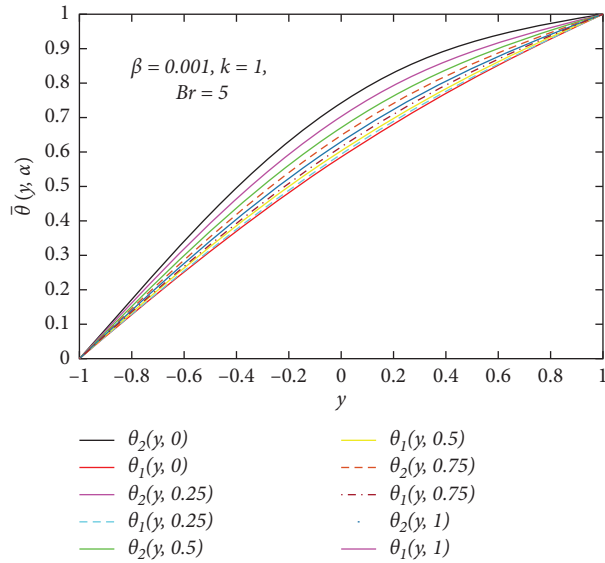


FIGURE 21: Effect of TFN  $M$  on the fuzzy temperature profile of Poiseuille flow.

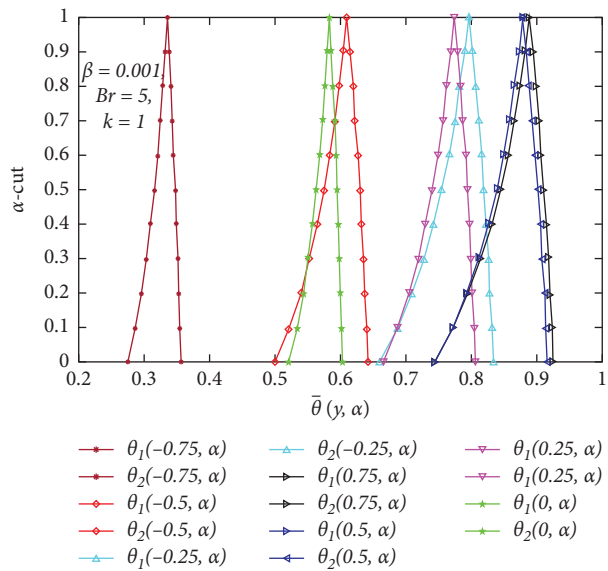


FIGURE 22: Membership functions of TFN plot if  $M$  is fuzzy (Poiseuille flow).

TABLE 6: Effect of fuzzy parameter  $k$  on fuzzy velocity and temperature of Couette flow when  $M=5$ ,  $Br=5$ , and  $\beta=0.001$ .

$y$	$u_1(y, \alpha)$	Crisp values	$u_2(y, \alpha)$	$\theta_1(y, \alpha)$	Crisp values	$\theta_2(y, \alpha)$
-1	0	0	0	0	0	0
-0.8	0.0793910383	0.2171491139	0.3541804031	0.3572109537	1.1940552414	2.1969200270
-0.6	0.1361377460	0.3620192484	0.5871865522	0.7159346247	2.3621707042	4.0864124256
-0.4	0.1798509668	0.4584108744	0.7364366065	1.0586808094	3.3992050827	6.1568171199
-0.2	0.2194526664	0.5259231666	0.8320410278	1.3735796018	4.2263529512	7.5284885661
0	0.2630274365	0.5783186895	0.8934076205	1.6468577300	4.7765309259	8.3100412353
0.2	0.3194707436	0.6262889631	0.9330297085	1.8600434054	4.9909331263	8.4100027173
0.4	0.4003009777	0.6796248866	0.9589849659	1.9840433370	4.8105538479	7.7656469133
0.6	0.5219955851	0.74920928316	0.9765685868	1.9670368365	4.1639897083	6.3343194207
0.8	0.7092930641	0.84922492764	0.9893692322	1.7084185223	2.9489067699	4.0864124256
1	1	1	1	1	1	1

TABLE 7: Effect of fuzzy parameter  $M$  on fuzzy velocity and temperature of Couette flow when  $k = 1$ ,  $Br = 5$ , and  $\beta = 0.001$ .

$y$	$u_1(y, \alpha)$	Mid values	$u_2(y, \alpha)$	$\theta_1(y, \alpha)$	Mid values	$\theta_2(y, \alpha)$
-1	0	0	0	0	0	0
-0.8	0.0251183255	0.0361886680	0.0794004671	0.2932734573	0.3145774346	0.4021269400
-0.6	0.0348150703	0.0541349796	0.1361596251	0.5894568242	0.6316208361	0.8056886060
-0.4	0.0388557462	0.0641457277	0.1798887488	0.8796771002	0.9399561571	1.1905214684
-0.2	0.0416481841	0.0725600838	0.2195125756	1.1623486661	1.2359097774	1.5427072376
0	0.0462385847	0.0847064491	0.2631194954	1.4362432704	1.5158252942	1.8460902450
0.2	0.0576344273	0.1082760594	0.3196093565	1.6991065685	1.7735086688	2.0789963435
0.4	0.0882654730	0.1581887046	0.4005032222	1.9440774756	1.9938534158	2.2072806878
0.6	0.1715120242	0.2659915363	0.5222692537	2.1437790808	2.1314185792	2.1701181990
0.8	0.3974990501	0.4993373042	0.7095850362	2.1577592359	2.0254091924	1.8493906825
1	1	1	1	1	1	1

TABLE 8: Effect of fuzzy parameter  $k$  on fuzzy velocity and temperature of Poiseuille flow when  $M = 5$ ,  $Br = 5$ , and  $\beta = 0.001$ .

$y$	$u_1(y, \alpha)$	Crisp/mid values	$u_2(y, \alpha)$	$\theta_1(y, \alpha)$	Crisp/mid values	$\theta_2(y, \alpha)$
-1	0	0	0	0	0	0
-0.8	0.0690238311	0.2068138971	0.3438429272	0.1697422956	0.7417557187	1.8870799070
-0.6	0.1130780838	0.3389955158	0.5642044944	0.3379379389	1.4534208777	3.6832778722
-0.4	0.1393877654	0.4179808104	0.6960314849	0.4934237771	2.0508411412	5.1627306592
-0.2	0.1533221660	0.4598230806	0.7658975816	0.6296208486	2.4748142954	6.1612132925
0	0.1577257957	0.4730473134	0.7879820816	0.7424429911	2.6885465757	6.5764285891
0.2	0.1534976786	0.4603501420	0.7667777480	0.8305122187	2.6796276828	6.3738573373
0.4	0.1397746217	0.4191423902	0.6979707849	0.8951523920	2.4599804768	5.5866630488
0.6	0.1137552488	0.3410281075	0.5675957317	0.9403959798	2.0659154647	4.3158009846
0.8	0.0701294721	0.2101298414	0.3493661793	0.9727790572	1.5562503437	2.7244461600
1	0	0	0	1	1	1

TABLE 9: Effect of fuzzy parameter  $M$  on fuzzy velocity and temperature of Poiseuille flow when  $k = 1$ ,  $Br = 5$ , and  $\beta = 0.001$ .

$y$	$u_1(y, \alpha)$	Crisp/mid values	$u_2(y, \alpha)$	$\theta_1(y, \alpha)$	Crisp/mid values	$\theta_2(y, \alpha)$
-1	0	0	0	0	0	0
-0.8	0.0690238311	0.0354590058	0.0250124563	0.1697422953	0.1379807796	0.1253350726
-0.6	0.1130780838	0.0521999379	0.0344859841	0.3379379385	0.2750045627	0.2501840381
-0.4	0.1393877654	0.0597798909	0.0379444484	0.4934237765	0.4039839461	0.3691961681
-0.2	0.1533221660	0.0629987330	0.0391605600	0.6296208481	0.5223124983	0.4810440916
0	0.1577257957	0.0638948132	0.0394609454	0.7424429906	0.6287559082	0.5852215968
0.2	0.1534976786	0.0630355833	0.0391732884	0.8305122181	0.7229570372	0.6816004849
0.4	0.1397746217	0.0598769275	0.0379837901	0.8951523915	0.8052584530	0.7703035479
0.6	0.1137552488	0.0524186091	0.0345948561	0.9403959794	0.8768729386	0.8518263495
0.8	0.0701294721	0.0359377764	0.0253096216	0.9727790569	0.9403737363	0.9274730619
1	0	0	0	1	1	1

### 6. Conclusion

In this work, we have studied the three fundamental flow problems that frequently arise in the field of fluid dynamics, namely, Couette flow, Poiseuille flow, and Couette–Poiseuille flow of a third-grade fluid through the inclined channel with heat transfer. The dimensionless nonlinear governing equations are converted into FDEs and then solved numerically by MATLAB built-in technique `bvp4c`. In the fuzzy case, the uncertain gravitational parameter  $k$  and magnetic parameter  $M$  are taken as the TFNs. Some findings of this work are given as follows:

- (i) The obtained results indicate that the ranges of calculated lower and upper velocity profiles depend upon  $\alpha$  – cut approach. Also, the obtained results are an envelope of solutions with a crisp solution, between the upper and lower solutions.
- (ii) Furthermore, it is observed that, in triangular membership functions, if the width of fuzzy or uncertain velocity and temperature becomes more, then the parameters are more sensitive, while for less width of fuzzy or uncertain velocity and temperature, the assumed uncertain parameters are less sensitive.

- (iii) Also, for validation, the present results are compared with the existing results in some special cases, viz., crisp case, which have good agreement.
- (iv) In future, the concept provided here can be simply applied to other fuzzy numbers as well.

## Data Availability

No data were used in this article.

## Conflicts of Interest

The authors declare that they have no conflicts of interest.

## References

- [1] C. Truesdell and W. Noll, *The Non-Linear Field's Theories of Mechanics*, Springer, Berlin, Germany, 3rd edition, 2004.
- [2] R. L. Fosdick and K. R. Rajagopal, "Thermodynamics and stability of fluids of third grade," *Proceedings of the Royal Society of London. A. Mathematical and Physical Sciences*, vol. 369, no. 1738, pp. 351–377, 1980.
- [3] K. R. Rajagopal, "On the stability of third-grade fluids," *Archives of Mechanics*, vol. 32, no. 6, pp. 867–875, 1980.
- [4] C. Y. Tsai, M. Novack, and G. Roffle, "Rheological and heat transfer characteristics of flowing coal-water mixtures," National Energy Technology Laboratory, Albany, OR, USA, DOE/MC/23255-2763, 1988.
- [5] S. I. Natarov and C. P. Conrad, "The role of poiseuille flow in creating depth-variation of asthenospheric shear," *Geophysical Journal International*, vol. 190, no. 3, pp. 1297–1310, 2012.
- [6] M. Massoudi and I. Christie, "Effects of variable viscosity and viscous dissipation on the flow of a third grade fluid in a pipe," *International Journal of Non-Linear Mechanics*, vol. 30, no. 5, pp. 687–699, 1995.
- [7] T. Hayat, M. Khan, and M. Ayub, "Couette and poiseuille flows of an oldroyd 6-constant fluid with magnetic field," *Journal of Mathematical Analysis and Applications*, vol. 298, no. 1, pp. 225–244, 2004.
- [8] T. Hayat, R. Naz, and M. Sajid, "On the homotopy solution for poiseuille flow of a fourth grade fluid," *Communications in Nonlinear Science and Numerical Simulation*, vol. 15, no. 3, pp. 581–589, 2010.
- [9] T. Chinyoka and O. D. Makinde, "Analysis of transient generalized couette flow of a reactive variable viscosity third-grade liquid with asymmetric convective cooling," *Mathematical and Computer Modelling*, vol. 54, no. 1, pp. 160–174, 2011.
- [10] M. Khan, C. Fetecau, and T. Hayat, "MHD transient flows in a channel of rectangular cross-section with porous medium," *Physics Letters A*, vol. 369, no. 1, pp. 44–54, 2007.
- [11] T. Hayat, T. Haroon, S. Asghar, and A. M. Siddiqui, "MHD flow of a third-grade fluid due to eccentric rotations of a porous disk and a fluid at infinity," *International Journal of Non-Linear Mechanics*, vol. 38, no. 4, pp. 501–511, 2003.
- [12] T. Hayat, K. Hutter, S. Asghar, and A. M. Siddiqui, "MHD flows of an oldroyd-B fluid," *Mathematical and Computer Modelling*, vol. 36, no. 9-10, pp. 987–995, 2002.
- [13] S. Islam, "Homotopy perturbations analysis of couette and poiseuille flows of a third-grade fluid with magnetic field," *Science International*, vol. 22, no. 3, 2010.
- [14] M. Kamran and I. Siddique, "MHD couette and poiseuille flow of a third grade fluid," *Open Journal of Mathematical Analysis*, vol. 1, no. 2, pp. 1–19, 2017.
- [15] A. M. Siddiqui, A. Zeb, Q. K. Ghorri, and A. M. Benhartbit, "Homotopy perturbation method for heat transfer flow of a third-grade fluid between parallel plate," *Chaos, Solitons & Fractals*, vol. 36, pp. 182–192, 2008.
- [16] Y. M. Aiyesimi, G. T. Okedayo, and O. W. Lawal, "Effects of magnetic field on the MHD flow of a third grade fluid through inclined channel with ohmic heating," *Journal of Applied & Computational Mathematics*, vol. 3, no. 2, pp. 1–6, 2014.
- [17] L. A. Zadeh, "Fuzzy sets," *Information and Control*, vol. 8, no. 3, pp. 338–353, 1965.
- [18] D. Dubois and H. Prade, "Operations on fuzzy numbers," *International Journal of Systems Science*, vol. 9, no. 6, pp. 613–626, 1978.
- [19] S. Seikala, "On the fuzzy initial value problem," *Fuzzy Sets and Systems*, vol. 24, no. 3, pp. 319–330, 1987.
- [20] O. Kaleva, "Fuzzy differential equations," *Fuzzy Sets and Systems*, vol. 24, no. 3, pp. 301–317, 1987.
- [21] A. Kandel and W. J. Byatt, "Fuzzy differential equations," in *Proceedings of International Conference Cybernetics and Society*, pp. 1213–1216, Tokyo, Japan, 1978.
- [22] J. J. Buckley, T. Feuring, and Y. Hayashi, "Linear systems of first order ordinary differential equations: fuzzy initial conditions," *Soft Computing*, vol. 6, pp. 415–421, 2002.
- [23] J. J. Nieto, "The cauchy problem for continuous fuzzy differential equations," *Fuzzy Sets and Systems*, vol. 102, pp. 259–262, 1999.
- [24] V. Lakshmikantham and R. N. Mohapatra, "Basic properties of solutions of fuzzy differential equations," *Nonlinear Studies*, vol. 8, pp. 113–124, 2000.
- [25] J. Y. Park and K. H. Hyo, "Existence and uniqueness theorem for a solution of fuzzy differential equations," *International Journal of Mathematics and Mathematical Sciences*, vol. 22, pp. 271–279, 1999.
- [26] N. Gasilov, S. E. Amrahov, and A. G. Fatullayev, "A geometric approach to solve fuzzy linear systems of differential equations," *Applied Mathematics and Information Sciences*, vol. 5, no. 3, pp. 484–499, 2011.
- [27] N. Gasilov, A. G. Fatullayev, and S. E. Amrahov, "Solution method for a non-homogeneous fuzzy linear system of differential equations," *Applied Soft Computing*, vol. 70, pp. 225–237, 2018.
- [28] S. Salahshour, A. Ahmadian, and A. Mahata, "The behavior of logistic equation with alley effect in fuzzy environment: fuzzy differential equation approach," *International Journal of Applied and Computational Mathematics*, vol. 4, p. 62, 2018.
- [29] Y. Chalco-Cano, R. Rodriguez-Lpez, and M. D. Jimnez-Gamero, "Characterizations of generalized differentiable fuzzy functions," *Fuzzy Sets and Systems*, vol. 295, pp. 37–56, 2016.
- [30] Y. Chalco-Cano and H. Rom'an-Flores, "On new solutions of fuzzy differential equations," *Chaos, Solitons & Fractals*, vol. 38, no. 1, pp. 112–119, 2008.
- [31] B. Bede and S. G. Gal, "Generalizations of the differentiability of fuzzy number valued functions with applications to fuzzy differential equations," *Fuzzy Sets and Systems*, vol. 151, pp. 581–599, 2005.
- [32] A. Khastan and J. J. Nieto, "A boundary value problem for second order fuzzy differential equations," *Nonlinear Analysis*, vol. 72, pp. 3583–3593, 2010.
- [33] A. Khastan, F. Bahrami, and K. Ivaz, "New results on multiple solutions for  $n$ th-order fuzzy differential equations under

- generalized differentiability,” *Boundary Value Problems*, vol. 2009, Article ID 395714, 13 pages, 2009.
- [34] S. P. Mondal and T. K. Roy, “First order linear homogeneous ordinary differential equation in fuzzy environment based on laplace transform,” *Journal of Fuzzy Set Valued Analysis*, vol. 2013, pp. 1–18, 2013.
- [35] H. Zarei, A. V. Kamyad, and A. A. Heydari, “Fuzzy modeling and control of HIV infection,” *Computational and Mathematical Methods in Medicine*, vol. 2012, Article ID 893474, 17 pages, 2012.
- [36] S. P. Mondal and T. K. Roy, “First order linear non-homogeneous ordinary differential equation in fuzzy environment,” *Mathematical Theory and Modeling*, vol. 3, no. 1, pp. 85–95, 2013.
- [37] M. Guo, X. Xue, and R. Li, “Impulsive functional differential inclusions and fuzzy population models,” *Fuzzy Sets and Systems*, vol. 138, pp. 601–615, 2003.
- [38] L. C. Barros, R. C. Bassanezi, and P. A. Tonelli, “Fuzzy modelling in population dynamics,” *Ecological Modelling*, vol. 128, pp. 27–33, 2000.
- [39] M. Z. Ahmad and B. De Baets, “A predator-prey model with fuzzy initial populations,” in *Proceedings of the Joint 2009 International Fuzzy Systems Association World Congress and 2009 European Society of Fuzzy Logic and Technology Conference, IFSA-EUSFLAT*, Lisbon, Portugal, July 2009.
- [40] J. Casasnovas and F. Rossell, “Averaging fuzzy bio-polymers,” *Fuzzy Sets and Systems*, vol. 152, pp. 139–158, 2005.
- [41] S. P. Mondal, S. Banerjee, and T. K. Roy, “First order linear homogeneous ordinary differential equation in fuzzy environment,” *International Journal of Pure and Applied Sciences and Technology*, vol. 14, no. 1, pp. 16–26, 2013.
- [42] G. L. Diniz, J. F. R. Fernandes, J. F. C. A. Meyer, and L. C. Barros, “A fuzzy cauchy problem modeling the decay of the biochemical oxygen demand in water,” vol. 1, pp. 512–516, in *Proceedings Joint 9th IFSA World Congress and 20th NAFIPS International Conference*, vol. 1, pp. 512–516, IEEE, Vancouver, BC, Canada, July 2001.
- [43] M. S. El Naschie, “From experimental quantum optics to quantum gravity via a fuzzy khler manifold,” *Chaos, Solitons and Fractals*, vol. 25, pp. 969–977, 2005.
- [44] A. Bencsik, B. Bede, J. Tar, and J. Fodor, “Fuzzy differential equations in modeling hydraulic differential servo cylinders,” in *Proceedings of the Third Romanian-Hungarian Joint Symposium on Applied Computational Intelligence (SACI)*, Timisoara, Romania, 2006.
- [45] B. Bede, I. J. Rudas, and J. Fodor, “Friction model by fuzzy differential equations,” *International Fuzzy Systems Association World Congress*, vol. 4529, pp. 23–32, Springer, Berlin, Germany, 2007.
- [46] T. Allahviranloo and S. Salahshour, “Applications of fuzzy laplace transforms,” *Soft Computing*, vol. 17, no. 1, pp. 145–158, 2013.
- [47] M. Oberguggenberger and S. Pittschmann, “Differential equations with fuzzy parameters,” *Mathematical Modelling of Systems*, vol. 5, pp. 181–202, 1999.
- [48] S. Hajighasemi, T. Allahviranloo, M. Khezerloo, M. Khorasany, and S. Salahshour, “Existence and uniqueness of solutions of fuzzy volterra integro-differential equations,” *Information Processing and Management of Uncertainty in Knowledge-Based*, vol. 81, pp. 491–500, 2010.
- [49] A. El Allaoui, S. Melliani, and L. S. Chadli, “A mathematical fuzzy model to giving up smoking,” in *Proceedings of the IEEE 6th International Conference on Optimization and Applications (ICOA)*, pp. 1–6, Beni Mellal, Morocco, April 2020.
- [50] H. C. Bhandari and K. Jha, “An analysis of microbial population of chemostat model in fuzzy environment,” *The Nepali Mathematical Sciences Report*, vol. 36, no. 1-2, 2019.
- [51] A. Rajkumar and C. Jesuraj, “Mathematical model for dengue virus infected populations with fuzzy differential equations,” *Advanced Informatics for Computing Research. Communications in Computer and Information Science*, vol. 955, pp. 206–217, 2018.
- [52] T. Todorov, R. Mitrev, and I. Penev, “Force analysis and kinematic optimization of a fluid valve driven by shape memory alloys,” *Reports in Mechanical Engineering*, vol. 1, no. 1, pp. 61–76, 2020.
- [53] M. R. Gharib, “Comparison of robust optimal QFT controller with TFC and MFC controller in a multi-input multi-output system,” *Reports in Mechanical Engineering*, vol. 1, no. 1, pp. 151–161, 2020.
- [54] O. F. Gorcun, S. Senthil, and H. Küçükönder, “Evaluation of tanker vehicle selection using a novel hybrid fuzzy MCDM technique,” *Decision Making: Applications in Management and Engineering*, vol. 4, no. 2, pp. 140–162, 2021.
- [55] R. Sahu, S. R. Dash, and S. Das, “Career selection of students using hybridized distance measure based on picture fuzzy set and rough set theory,” *Decision Making: Applications in Management and Engineering*, vol. 4, no. 1, pp. 104–126, 2021.
- [56] M. Bilal, S. Hussain, and M. Sagheer, “Boundary layer flow of magneto-micropolar nanofluid flow with hall and ion-slip effects using variable thermal diffusivity,” *Bulletin of the Polish Academy of Sciences, Technical Sciences*, vol. 65, no. 3, 2017.
- [57] D. C. Lu, M. Ramzan, M. Bilal, J. D. Chung, and U. Farooq, “A numerical investigation of 3D MHD rotating flow with binary chemical reaction, activation energy and non-fourier heat flux,” *Communications in Theoretical Physics*, vol. 70, p. 89, 2018.